In this Issue

Highlights from this issue of *A&R* | By Lara C. Pullen, PhD

Certolizumab Pegol Missing Primary End Point in Phase III RA Trial

In this issue, Weinblatt et al (p. 1937) report the results of the C-EARLY phase III study in patients with early rheumatoid arthritis (RA), which is the first reported randomized double-blind study with an anti–tumor necrosis factor biologic disease-modifying antirheumatic drug that compares 3 treatment strategies: continuation, tapering, and withdrawal of certolizumab pegol (CZP) after 1 year of therapy. This is a report on the second period of the C-EARLY study, during which patients with early RA who had achieved sustained low disease activity after 1 year of treatment with CZP plus methotrexate (MTX) were re-randomized 2:3:2 to receive CZP at a standard dose, CZP at a reduced frequency, or placebo, each in addition to MTX. The investigators noted that the first period of the study was underenrolled; thus, only 293 patients were randomized into the treatment groups in period 2.

p. 1937

The researchers found that, during this second period, treatment with CZP did not achieve the primary end point: percentage of patients who maintained low disease activity throughout weeks 52–104 without flares. They also found that there were no clinically meaningful differences between the standard and reduced frequency doses of CZP plus MTX and that both treatment regimens were able to control RA more effectively than stopping CZP. Although the trial did not achieve the primary end point, the investigators noted that a higher percentage of patients treated with the standard and reduced frequency regimens maintained low levels of disease activity as compared with those who stopped CZP. They observed similar trends for radiographic nonprogression and normative physical function. In addition, there were no deaths in the study, and all of the treatment groups had similar safety profiles. Reassuringly, the investigators did not detect any new safety signals in the patients who continued CZP to week 104.

Tofacitinib Plus Glucocorticoids May Increase the Risk of Developing Herpes Zoster

In this issue, Winthrop et al (p. 1960) write about their evaluation of the long-term risk of herpes zoster (HZ) within the tofacitinib clinical development program for rheumatoid arthritis. They evaluated data from all 19 studies in the database (6,192 patients and 16,839 patient-years). They found that patients who received concomitant treatment with tofacitinib and glucocorticoids (GCs) were at greater risk of developing HZ than were those who received tofacitinib monotherapy without GCs.

p. 1960

While 636 tofacitinib-treated patients experienced HZ, in most cases, the HZ was classified as nonserious, and only 1 dermatome was involved. The investigators found that the incident rates (IRs) of all HZ events per 100 patient-years varied across regions: 2.4 in Eastern Europe, 8.0 in Japan, and 8.4 in Korea. When they focused their attention on only the phase III studies in the database, they found that IRs for HZ varied according to tofacitinib dose, background conventional synthetic disease-modifying antirheumatic drug (csDMARD) treatment, and baseline use of GCs. Specifically, the IRs were numerically lowest for monotherapy with tofacitinib 5 mg twice daily without GCs (IR 0.56) and highest for tofacitinib 10 mg twice daily with csDMARDs and GCs (IR 5.44). In addition, they found that age, GC use, tofacitinib dose, and enrollment within Asia were all independent risk factors for HZ.

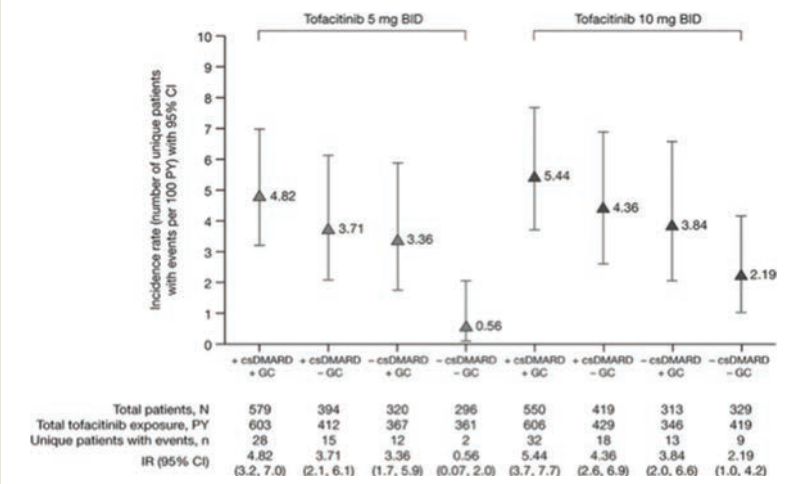

Figure 1. Crude incidence rates (IRs) of first herpes zoster (HZ) events within pooled phase III studies of tofacitinib, with or without conventional synthetic disease-modifying antirheumatic drugs (csDMARDs) and/or baseline glucocorticoid (GC) use. Patients from all regions were included. HZ IRs (with 95% confidence intervals [95% CIs]) are expressed per 100 patient-years (PYs) of exposure. BID = twice daily.

Live Zoster Vaccination Effective in Patients With RA

In this issue, Winthrop et al (p. 1969) report the results of a phase II trial of live zoster vaccination (LZV) in patients with rheumatoid arthritis (RA) prior to treatment with tofacitinib. This is the first study to directly assess the safety and immunogenicity of LZV in patients with RA. The investigators randomized 112 patients to receive tofacitinib or placebo postvaccination. At 6 weeks postvaccination, they measured the geometric mean fold rise (GMFR) in immune response in the 2 groups and found that the varicella zoster virus (VZV)–specific IgG levels were 2.11 in the tofacitinib group and 1.74 in the placebo group. The VZV-specific T cell GMFR was also similarly elevated in the 2 groups. Thus, patients who began tofacitinib treatment 2–3 weeks after receiving LZV had VZV-specific humoral and cell-mediated immune responses to LZV that were similar to those in placebo-treated controls.

p. 1969

Three serious adverse events occurred in the tofacitinib group and none in the placebo group. One patient who lacked preexisting VZV immunity and was technically not eligible for the vaccination developed a disseminated rash on day 16 postvaccination. The rash resolved when tofacitinib was discontinued and antiviral treatment was given. The researchers conclude that vaccination appears to be safe for most patients with RA who will be initiating treatment with tofacitinib. They note that patients receiving the vaccine should have a history of chicken pox or a serologic test showing exposure.

Adipsin Levels Associated With Pulmonary Arterial Hypertension

In this issue, Korman et al (p. 2062) describe data indicating that adipsin is a novel adipose tissue–derived marker of systemic sclerosis (SSc)–related pulmonary arterial hypertension (PAH). In addition, they report that patients with SSc generally have dysregulated levels of multiple adipokines. Specifically, the levels of adiponectin and adipsin were found to differ significantly between SSc patients and controls. Adipsin in particular was significantly elevated in patients with limited cutaneous SSc and PAH. This elevation was even more pronounced than that seen with B-type natriuretic peptide. Adipsin levels also were associated with serum autoantibody status, pulmonary function, and cardiovascular parameters. Patients with SSc who had adipsin gene single-nucleotide polymorphisms were more likely to have PAH. Transcriptome data set analysis reinforced this observation and demonstrated elevated adipsin expression in patients with SSc-related PAH.

p. 2062

The authors conclude by suggesting that adipsin might serve as a pathogenic link between adipocyte dysfunction and complement pathway activation. If this hypothesis proves to be true, then adipsin may be important in the pathogenesis of SSc-related PAH. Even absent a full understanding of the mechanism behind the association, however, circulating adipsin levels may be useful as a predictive biomarker in SSc.

Myeloperoxidase Is a Target for Autoantibodies in Microscopic Polyangiitis

In this issue, Hiwa et al (p. 2069) report that, in patients with microscopic polyangiitis (MPA), myeloperoxidase (MPO) complexed with HLA class II molecules is the target for MPO–antineutrophil cytoplasmic antibody (ANCA) and a driver of pathogenesis. Specifically, in individuals with an MPA-susceptible allele, intracellular MPO is transported to the surface by HLA class II molecules, such that MPO associated with HLA–DR expresses cryptic autoantibody epitopes for MPO-ANCA. When the investigators looked at autoantibodies in patients, they found that autoantibody binding to the MPO/HLA–DR complex correlated with the disease susceptibility conferred by each HLA–DR allele.

p. 2069

These findings suggest that the MPO/HLA–DR complex is involved in the pathogenicity of MPA. This conclusion was supported by the researchers' finding of MPO/HLA class II complexes in neutrophils from a patient with MPA as well as in cytokine-stimulated neutrophils from healthy donors. In addition, they found that MPO-ANCA was able to stimulate MPO/HLA–DR complex–expressing HL-60 cells.

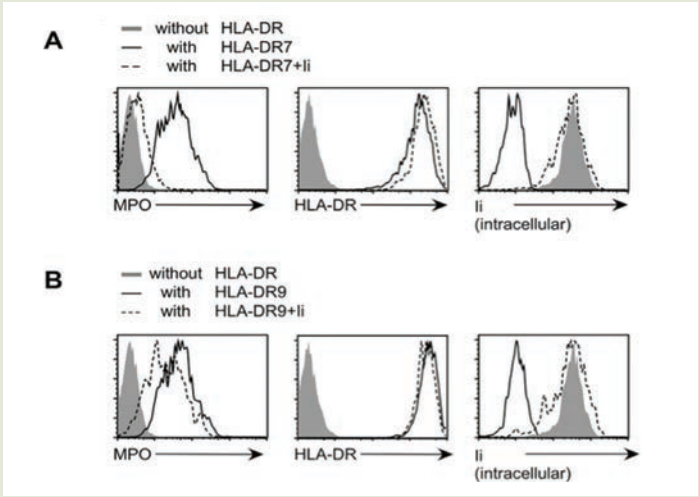

Figure 1. Cell surface expression of MPO induced by HLA–DR with an MPA-susceptible allele is less affected by the invariant chain (Ii) than by an MPA-nonsusceptible allele (HLA–DR7). MPO and green fluorescent protein (GFP) were cotransfected with HLA–DR into HEK 293T cells in the presence (broken lines) or absence (solid lines) of the invariant chain. Cell surface expression of HLA–DR and MPO on GFP-positive cells was analyzed. Cells transfected without HLA–DR were stained as a control (shaded histograms). Expression of the invariant chain was analyzed by intracellular staining. **A**, MPO was transfected with HLA–DR7. **B**, MPO was transfected with HLA–DR9. Results are representative of at least 3 independent experiments.

ACR ANNOUNCEMENTS

AMERICAN COLLEGE OF RHEUMATOLOGY
2200 Lake Boulevard NE, Atlanta, Georgia 30319-5312
www.rheumatology.org

ACR Meetings

Annual Meetings
November 3–8, 2017, San Diego
October 19–24, 2018, Chicago

Winter Rheumatology Symposium
January 20–26, 2018, Snowmass

State-of-the-Art Clinical Symposium
April 14–15, 2018, Chicago

For additional information, contact the ACR office.

2017 ACR/ARHP Annual Meeting: Advance Registration Ends Wednesday, October 18

Time is running out to register at advance rates for the 2017 ACR/ARHP Annual Meeting, to be held November 3–8 in San Diego, CA. Attendees will receive first-hand access to the latest innovations, research, and clinical applications transforming rheumatic disease care. Expand your knowledge into new areas of rheumatology, and register today at www.rheumatology.org/Annual-Meeting/Registration.

Maximize your meeting experience by taking advantage of the following resources:

- Mobile app: Create a personalized schedule, receive meeting alerts, search maps, and more.
- Session Tracker: You can use this printed resource to record your hours of participation as you go. The Session Tracker will be available on site and online.
- Searchable abstract site: Search and view accepted abstracts for the 2017 Annual Meeting at ACRabstracts.org.
- ACR Beyond: ACR Beyond allows you online access to sessions you missed. Experience education from the annual meeting at your own convenience and pace.

Education Programs

Eleventh International Congress on Autoimmunity. May 16–20, 2018, Lisbon, Portugal. The International Congress on Autoimmunity encompasses the most up-to-date clinical and basic research findings on more than 80 autoimmune diseases, with courses and lectures by some of the world's most distinguished experts. The deadline for submission of abstracts is November 22, 2017. The official language will be English. Registration fees are €620 (early; until March 6), €720 (March 7–May 8), and €820 (May 9–onsite) for full participants, and €380 (early; until March 6), €430 (March 7–May 8), and €480 (May 9–onsite) for trainees (students/fellows/residents) and nurses. Optional courses and functions are available for additional fees. For additional information, e-mail reg_autoimmunity18@kenes.com, phone +41 22 908 0488, or visit the web site http://autoimmunity.kenes.com/2018.

Arthritis & Rheumatology

An Official Journal of the American College of Rheumatology
www.arthritisrheum.org and wileyonlinelibrary.com

Cover design: Todd Machen

♾ This journal is printed on acid-free paper.

Arthritis & Rheumatology
An Official Journal of the American College of Rheumatology
www.arthritisrheum.org and wileyonlinelibrary.com

VOLUME 69 OCTOBER 2017 NO. 10

Cover image: The figure on the cover (from Peeters et al, page 1927) illustrates superenhancer-driven gene expression. Superenhancers are extremely large enhancers, characterized by increased histone acetylation (green ovals) and augmented protein binding, leading to increased gene expression. Superenhancers preferentially regulate genes associated with cell identity and disease, such as autoimmune arthritis, and are enriched for disease-associated single-nucleotide polymorphisms.

Clinical Connections

Induction of Matrix Metalloproteinase Expression by Synovial Wnt Signaling and Association With Disease Progression in Early Symptomatic Osteoarthritis

van den Bosch et al, *Arthritis Rheumatol* 2017;69:1978–1983.

CORRESPONDENCE
Arjen B. Blom, PhD: arjen.blom@radboudumc.nl

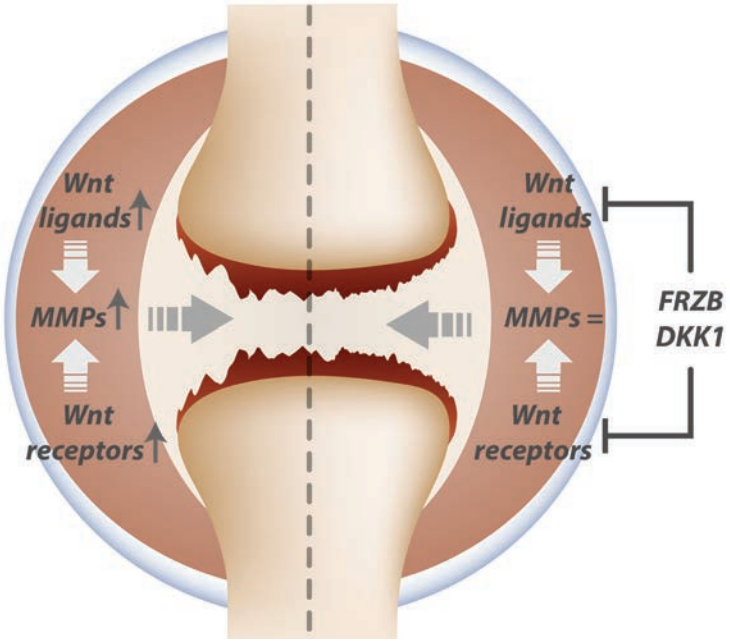

KEY POINTS

- Increased canonical Wnt signaling has been associated with the development of OA.
- Synovial Wnt signaling strongly correlates with matrix-degrading MMP expression in patients with early OA.
- Stimulation of human synovial explants with recombinant Wnt results in increased expression of various MMPs.
- Inhibition of (increased) endogenous Wnt signaling in the synovium of OA patients decreases the expression of matrix-degrading enzymes and may therefore prevent cartilage damage.

SUMMARY

Balanced canonical Wnt signaling is crucial for the development and homeostasis of joint tissues; therefore not surprisingly, excessive canonical Wnt signaling has been associated with the development of osteoarthritis (OA). While most previous studies focused on the effects of Wnt signaling in the articular cartilage, the study by van den Bosch and colleagues shows that increased synovial expression of Wnt ligands that activate canonical Wnt signaling results in an increased expression of matrix metalloproteinases (MMPs) that are relevant for the breakdown of cartilage during OA, such as MMP-3 and MMP-13. Furthermore, in synovial tissue from patients with early symptomatic OA, the expression of MMPs was found to be strongly associated with the expression of Wnt signaling receptors (Frizzled class receptors, or FZDs) and was inversely associated with the expression of a Wnt signaling inhibitor (FRZB). Patients with progression of pathology over 5 years had a higher expression of one FZD receptor but decreased expression of the inhibitor FRZB. Whereas recombinant Wnt protein stimulation of synovial biopsy tissues from patients with end-stage OA increased the production of MMPs, specific inhibition of endogenous Wnt signaling with either DKK1 or FRZB resulted in reduced production of these cartilage-degrading enzymes. These data demonstrate a novel link between increased Wnt signaling and the production of matrix-degrading enzymes in the synovium that might contribute to the breakdown of articular cartilage, the main hallmark of OA.

Plasmablasts With a Mucosal Phenotype Contribute to Plasmacytosis in Systemic Lupus Erythematosus

Mei et al, *Arthritis Rheumatology* 2017;69:2018–2028.

CORRESPONDENCE
Henrik E. Mei, PhD: mei@drfz.de

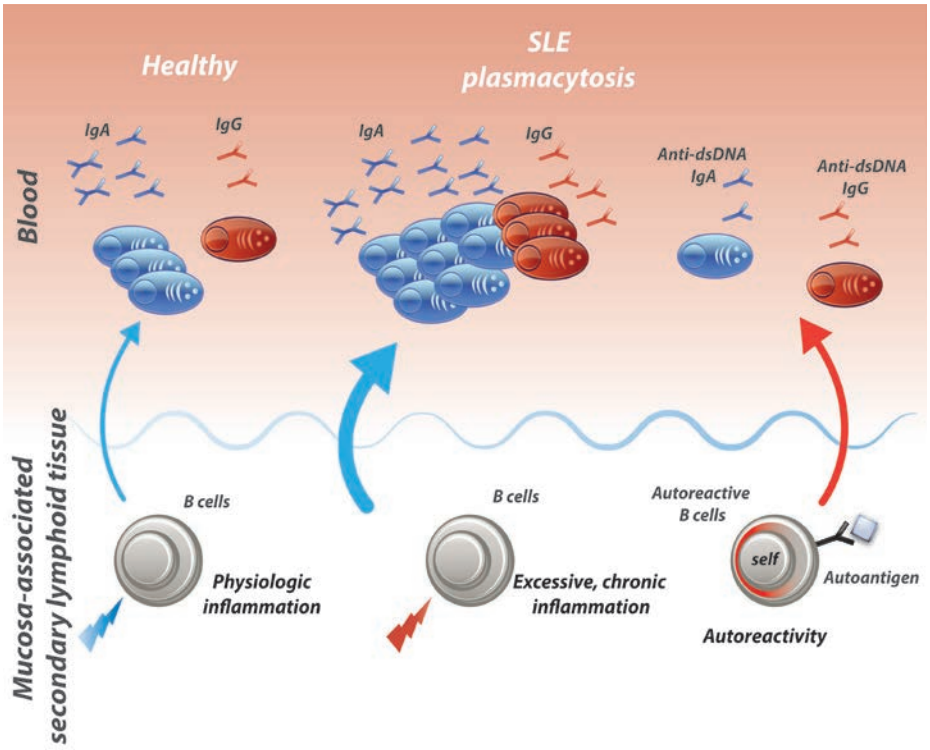

KEY POINTS

- Substantial fractions of the expanded plasmablast population in SLE express IgA, CCR10, or β7 integrin.
- Mucosal plasmablasts in blood are associated with serum cytokines and comprise autoreactive cells in SLE.
- Autoreactive anti–double-stranded DNA (anti–dsDNA)–secreting cells of IgA and IgG isotype are present in the circulation of SLE patients.
- Findings suggest an increased activity of mucosal immune compartments in SLE.

SUMMARY

In healthy individuals, mucosal immune activity maintains low-level plasmablast responses that reach a detectable concentration in the peripheral blood. In patients with active systemic lupus erythematosus (SLE), peripheral blood plasmablasts are expanded and correlate with lupus activity, but the underlying induction mechanisms are not well understood. By studying the antibody isotype and homing receptors of plasmablasts, Mei and colleagues show that plasmablasts carry either systemic or, most notably, mucosal characteristics. The latter express various combinations of IgA as well as the mucosal homing receptors CCR10 and β7 integrin and contribute substantially to the overall plasmablast expansion in active SLE. In contrast to systemically induced plasmablasts, only mucosal plasmablasts were found to be associated with distinct cytokines, which suggests that the cytokine environment is critical to their induction. Thus, plasmablast expansion in SLE appears to reflect a superimposed finding of systemic autoantigen-triggered plasmablasts and expansion of a population of mucosal plasmablasts that likely result from enhanced activity of mucosa-associated lymphoid tissues. Lupus activity scores (e.g., the SLE Disease Activity Index [SLEDAI]) are generally insensitive to gastrointestinal disease; however, this study focuses attention on the immunopathologic role of mucosal compartments in SLE.

ARTHRITIS & RHEUMATOLOGY
Vol. 69, No. 10, October 2017, pp 1917–1920
DOI 10.1002/art.40188

Arthritis & Rheumatology
An Official Journal of the American College of Rheumatology
www.arthritisrheum.org and wileyonlinelibrary.com

EDITORIAL

Herpes Zoster: Fear the Infection, Value the Solution

John J. Cush

Herpes zoster (HZ) is characterized by a blistering rash and painful neuritis that results from reactivation of the varicella zoster virus (VZV). HZ (also known as shingles) will affect one-third of adults in the US during their lifetime (1). In addition to the painful rash and the 20% risk of postherpetic neuralgia, shingles exacts substantial cost and a diminished quality of life in an aging populace.

Although the incidence of zoster is increasing, a Centers for Disease Control and Prevention (CDC) report states that only 28% of adults older than age 60 years have received preventive vaccination, despite the widespread availability of an approved, effective vaccine (2,3). Moreover, the risks are even higher in certain populations, especially in patients with autoimmune disease (4). The risk is further compounded by the therapeutic agents (e.g., corticosteroids, cytotoxic agents, biologic agents, and JAK inhibitors) used to treat such patients.

There is a imperative need to know who is at risk, when and how at-risk patients should be vaccinated, and what other risk-reduction measures should be considered. At a vaccine symposium held at the annual meeting of the American College of Rheumatology in 2015, Dr. William Schaffner stated, "if you don't fear the infection, you won't value the solution (vaccine)."

The solution

The live zoster vaccine (LZV) was approved by the Food and Drug Administration in 2006, based on the Shingles Prevention Trial that involved 38,546 subjects older than age 60 years who received either LZV or placebo (5). After nearly 3 years of follow-up, the VZV infection rate was 1.66% in those receiving LZV and 3.42% in the placebo group, with a 51% prevention rate in zoster and a two-thirds reduction in postherpetic neuralgia. It was also noted that efficacy decreased with age, with protection of 64% in the 60–69-year-old group, but only 18% in those older than age 80 years. Vaccine-related complications were rare and included zoster-like rashes in 1.6% of those receiving the vaccine and 1.1% of those receiving placebo. Disseminated infection (0.026% and 0.056%) and ophthalmic zoster (0.18% and 0.36%) were rarely observed in those treated with LZV and those in the placebo group, respectively.

Screening for zoster is unnecessary, because nearly everyone age 60 years and older is immune to varicella. Zoster vaccination should be offered regardless of a history of varicella infection or prior shingles, because HZ may recur. The duration of protection is at least 4 years and wanes thereafter, such that protection beyond 5 years is uncertain. This limited duration of protection is one of the reasons the vaccine is not offered to individuals in the 50–59-year age group. The LZV is not recommended for the treatment of acute zoster infection.

Who is at risk?

Most VZV infections are caused by reactivation of varicella virus. There are very few examples of VZV infection occurring in individuals not previously exposed, those with immature immune systems, or those who are highly immunosuppressed. Factors that influence eligibility for zoster vaccination in at-risk persons (1,6) may include the following:

1. Age older than 60 years. In individuals older than age 60 years and those with osteoarthritis, the HZ risk rate ranges from 0.6 per 100 patient-years to 1.0 per 100 patient-years (1).
2. Chronic medical conditions (e.g., renal failure, diabetes mellitus, rheumatoid arthritis [RA], or chronic pulmonary disease).
3. History of shingles.

John J. Cush, MD: Baylor Scott & White Research Institute and Baylor University Medical Center, Dallas, Texas.
Address correspondence to John J. Cush, MD, Arthritis Care and Research Center, 9900 North Central Expressway, Suite 550, Dallas, TX 75231. E-mail: john.cush@bswhealth.org.
Submitted for publication June 2, 2017; accepted in revised form June 20, 2017.

4. Long-term corticosteroid treatment. Most studies show a dose-dependent increase in the rate of HZ infection.
5. Treatment with recombinant biologic agents. Numerous population-based studies suggest that HZ infection rates may be increased in patients receiving tumor necrosis factor inhibitors compared with the rates in those receiving disease-modifying antirheumatic drugs, with rates ranging from 0.78 per 100 patient-years to 1.6 per 100 patient-years.
6. Treatment with JAK inhibitors. Tofacitinib drug development trials showed HZ infection rates of ~4.5 per 100 patient-years (7); this rate is ~3–7 times higher than that in patients with RA and the general population. Treatment with tofacitinib or other JAK inhibitors should prompt consideration of HZ vaccination prior to drug initiation and may not be limited to individuals older than age 60 years. The mechanisms underlying zoster infection in patients receiving JAK inhibitors are multifactorial and may include inhibition of JAK, lymphopenia, and reduced numbers of CD4 and natural killer cells.

Who is at greatest risk?

Warnings about the use of live virus vaccines (e.g., LZVs) in patients receiving biologic agents is not based on a body of evidence of known toxic events arising in patients receiving biologic agents. Instead, guidelines are based on hypothetical risks inferred from reports of disseminated viral infection following live virus vaccination, which usually is seen in patients with very immature, highly suppressed immune systems, such as children undergoing chemotherapy or transplantation.

Zhang et al analyzed a large Medicare population and identified 633 biologic agent–treated RA patients who inadvertently received the HZ vaccine; they observed that none of these patients developed HZ infection during the following 42-day period (8). Thus, for nearly all adults, vaccination with the LZV is a low-risk booster vaccination. Neoimmunization with VZV represents a greater risk, especially in patients who are very young, patients who are very immunosuppressed, and those without immunity to VZV.

Winthrop et al, whose article appears elsewhere in this issue of *Arthritis & Rheumatology* (9), report 1 case of disseminated multidermatomal zoster in a patient who had no detectable pretreatment immunity to VZV. The rash was noted 2 days after the start of treatment with tofacitinib (16 days postvaccination) and resolved after discontinuation of tofacitinib followed by 1 week of antiviral therapy. Molecular testing of an abdominal biopsy specimen obtained from this patient showed polymerase chain reaction positivity for VZV DNA from the vaccine (Oka strain). This event underscores the need to screen patients for prior VZV infection, preferably by eliciting a history of varicella infection. The reliability of testing for varicella titers has not been demonstrated.

Other than in the study by Winthrop et al (9), live virus vaccination in high-risk or immunosuppressed patients has seldom been investigated. Nonetheless, it should be noted that the LZV was developed largely in an elderly population in which the average age of participants was 69 years.

When to give zoster vaccination

Vaccination should be prescribed in accordance with risk and age. Nearly all published guidelines allow LZV to be given to patients receiving methotrexate or other disease-modifying drugs or corticosteroids (up to 20 mg/day prednisone or equivalent).

The most problematic patients are those with autoimmune disease who will be treated with recombinant biologic agents. For example, most patients with RA and most patients with psoriasis will receive biologic therapies during their lifetime; thus, zoster vaccination should occur at the earliest opportunity—specifically, when they are older than age 50 years, are not receiving treatment with a biologic agent, and have the financial means to receive it. Ideally, the zoster vaccine should be given before starting therapy with a biologic agent or when a suspension of biologic therapy affords a window of opportunity that would allow vaccination.

Timing of zoster vaccination. The timing of the antibody response mandates that initiation of treatment with biologic agents should be delayed for 2–4 weeks after administration of LZV. Hence, for biologic agent–naive patients, vaccination may be followed by the initiation of biologic agent treatment after a minimum of 2 weeks. The Advisory Committee on Immunization Practices (ACIP) guidelines state that patients being treated with a biologic agent should not be vaccinated until at least 4 weeks after discontinuation of that treatment, and that treatment with a biologic agent should not be initiated or restarted until 2–4 weeks after the vaccination (1,10).

In their study, Winthrop and colleagues (9) tested the safety and timing of LZV in 112 patients being treated with tofacitinib. Citing disparate recommendations by the CDC, the American College of Rheumatology, and the European League Against Rheumatism treatment guidelines and a lack of studies of LZV in patients with RA, they set out to study vaccine responses in patients with active RA being treated with methotrexate who were vaccinated 2–3 weeks prior to starting treatment with either tofacitinib or placebo. Twelve weeks after vaccination, patients vaccinated with LZV

had clinically adequate immunogenic responses that were not negatively affected by tofacitinib therapy.

This study was not designed to investigate the long-term effects of zoster vaccination in patients receiving tofacitinib but did show that a 2–3-week delay prior to tofacitinib initiation was effective in mounting zoster-specific titers. In patients receiving biologic agents or JAK inhibitors, it would be imprudent to interrupt effective therapy to administer the HZ vaccine. Instead, it would be pragmatic to defer HZ vaccination until the first interruption or suspension of therapy, e.g., for a change in therapy, loss of insurance, intercurrent illness, or surgery.

Future vaccine options. Clinicians treating patients with active disease may have to choose between initiating a biologic agent or JAK inhibitor immediately or waiting 2–4 weeks after administering LZV. Fortunately, non–live virus zoster vaccines will be commercially available in the near future, thereby allowing for simultaneous administration of a biologic agent and zoster vaccine.

The novel zoster subunit vaccine (HZ/su or Shingrix) is an inactive recombinant VZV glycoprotein adjuvant-based product administered as 2 intramuscular doses, 2 months apart (11). In the Zoster Efficacy Study in Adults 50 Years of Age or Older (ZOE-50) and the Zoster Efficacy Study in Adults 70 Years of Age or Older (ZOE-70) trials, the vaccine was 90% effective, even after 4 years, in adults older than age 70 years and 98% effective for HZ prevention in adults older than age 50 years. Moreover, postherpetic neuralgia did not occur in those younger than age 70 years, and the vaccine was 89% effective in preventing postherpetic neuralgia in individuals older than age 70 years. Unlike the LZV, efficacy and protection conferred by the zoster subunit vaccine were maintained and did not diminish with increasing age.

There may be disadvantages to this newer vaccine, including the need for 2 intramuscular injections and an 80% rate of muscle soreness at the injection site. Injection-site reactions/pain and myalgia were more frequent in the vaccine-treated patients, but serious adverse events were similar between groups.

Formal guidance for prevention of HZ. The ACIP issued its initial guidelines for zoster prevention in 2008 (10). The ACIP recommended routine live zoster vaccination in adults ages ≥60 years, ignoring use in those ages 50–59 years, citing lower infection rates in that group, initial vaccine shortages, and limited data on long-term protection in a younger cohort. The product labels for Xeljanz and Zostavax address prevention and vaccination, with a few instructive statements. Many of these statements represent cautious expert opinion and regulatory guidance based on the same.

JAK inhibitors (from the Xeljanz product label). 1) Zoster infection is one of the common serious and opportunistic infections seen with JAK inhibitor use; 2) Do not administer Xeljanz during an active or serious infection (including active VZV infection) and including localized infections. If a serious infection develops, interrupt Xeljanx until the infection is controlled; 3) Live vaccines should not be given concurrently with tofacitinib (or other JAK inhibitors).*

Zoster vaccine live (from the Zostavax product label). 1) LZV is contraindicated in individuals with immunodeficiency or those receiving immunosuppressive therapy;† 2) Defer vaccination in patients with active untreated tuberculosis; 3) Zostavax is a live, attenuated varicella zoster vaccine, and administration may result in disseminated disease in individuals who are immunosuppressed or immunodeficient.

Zoster vaccination uncertainties. Despite advances in our understanding, there are still some uncertainties regarding zoster vaccination, especially in autoimmune patients or patients receiving high-risk drugs (high-dose corticosteroids, biologic agents, and JAK inhibitors). These uncertainties include the following: 1) Once an individual is infected with shingles, when is the optimal time to vaccinate against recurrence of zoster infection? 2) Upon the onset of shingles, >90% of US rheumatologists will discontinue biologic or JAK therapy. It is unknown whether this practice is correct or when is the optimal time to restart treatment with biologic agents or JAK inhibitors. 3) Are there omissions in the current ACIP guidelines for HZ vaccination (which were used only in healthy elderly patients and have not been formally studied in high-risk patients and those with autoimmune or inflammatory disease)? 4) What are the advantages and disadvantages of the new zoster subunit vaccines that will likely be approved in late 2017? For each of these uncertainties, there is little or no evidence, which thus forms the basis for an ongoing research agenda in zoster vaccination studies.

AUTHOR CONTRIBUTIONS

Dr. Cush drafted the article, revised it critically for important intellectual content, and approved the final version to be published.

* Disappointingly, there are no recommendations on the label about screening for, monitoring, or treating zoster infections during treatment with JAK inhibitors.

† This was before the CDC and ACIP guidelines defined which therapies could and should not be used with the vaccine.

REFERENCES

1. Cush JJ, Calabrese L, Kavanaugh A. Prevention of herpes zoster (shingles) in immunosuppressed patients. Hotline. American College of Rheumatology; July 2008.
2. Hales CM, Harpaz R, Ortega-Sanchez I, Bialek SR, the Centers for Disease Control and Prevention. Update on recommendations for use of herpes zoster vaccine. MMWR Morb Mortal Wkly Rep 2014;63:729–31.
3. Varghese L, Standaert B, Olivieri A, Curran D. The temporal impact of aging on the burden of herpes zoster. BMC Geriatrics 2017;17:30.
4. Yun H, Yang S, Chen L, Xie F, Winthrop K, Baddley JW, et al. Risk of herpes zoster in autoimmune and inflammatory diseases: implications for vaccination. Arthritis Rheumatol 2016;68: 2328–37.
5. Oxman MN, Levin MJ, Johnson GR, Schmader KE, Straus SE, Gelb LD, et al. A vaccine to prevent herpes zoster and postherpetic neuralgia in older adults. N Engl J Med 2005;352:2271–84.
6. Forbes HJ, Thomas SL, Clayton T. Quantification of risk factors for herpes zoster: population based case-control study. BMJ 2014;348:g2911.
7. Winthrop KL, Yamanaka H, Valdez H, Mortensen E, Chew R, Krishnaswami S, et al. Herpes zoster and tofacitinib therapy in patients with rheumatoid arthritis. Arthritis Rheumatol 2014;66: 2675–84.
8. Zhang J, Delzell E, Xie F, Baddley JW, Spettell C, McMahan RM, et al. The use, safety, and effectiveness of herpes zoster vaccination in individuals with inflammatory and autoimmune diseases: a longitudinal observational study. Arthritis Res Ther 2011;13:R174.
9. Winthrop KL, Wouters AG, Choy EH, Soma K, Hodge JA, Nduaka CI, et al. The safety and immunogenicity of live zoster vaccination in patients with rheumatoid arthritis before starting tofacitinib: a randomized phase II trial. Arthritis Rheumatol 2017;69:1969–77.
10. Harpaz R, Ortega-Sanchez IR, Seward JF. Recommendations of the Advisory Committee on Immunization Practices (ACIP). MMWR 2008;57:1–30.
11. Lal H, Cunningham AL, Godeaux O, Chlibek R, Diez-Domingo J, Hwang SJ, et al. Efficacy of an adjuvanted herpes zoster subunit vaccine in older adults. N Engl J Med 2015;372: 2087–96.

ARTHRITIS & RHEUMATOLOGY
Vol. 69, No. 10, October 2017, pp 1921–1924
DOI 10.1002/art.40190

EDITORIAL

Lupus, the Chameleon: Many Disguises Difficult to Capture

Susan Manzi[1] and Joan Merrill[2]

Lupus is undeniably an enigmatic disease. The lack of a single diagnostic blood test, the subjective nature of common features, the appearance of good health in patients who may be critically ill, and the heterogeneity of organ manifestations in any given individual are some of its most puzzling characteristics. The poor outcomes when diagnosis is delayed underscores the urgency of these confusing problems, which may explain why the fictional Dr. House often considered lupus as a possible diagnosis for his most complex patients.

Challenges in reaching and treating lupus patients before serious organ damage occurs have fueled the quest to measure the burden of disease in the US and to identify populations at highest risk so that strategies for timely intervention can be developed. Impediments to reaching these goals include the inadequacy of self-reporting, the difficulty of defining lupus, ethnic disparities, and the lack of reliable case ascertainment. The confusing spectrum of lupus, both by organ involvement and severity of disease, means that some people may never seek medical attention or may be managed by primary care clinicians or single-organ specialists, depending on regional access to providers and cultural biases. The mere concept of accurately counting those living with lupus is daunting but necessary given the potentially fatal nature of the disease and the high frequency of disability and comorbidity that increases inexorably in relatively young people.

In 2002, the Centers for Disease Control and Prevention (CDC) published in *The Morbidity and Mortality Weekly Report* trends in deaths from systemic lupus erythematosus (SLE) from 1979 through 1998 (1). The report highlighted a 70% increase in death rates among black women ages 45–64 years during the study period. Of all lupus deaths, 36% occurred in persons ages 15–44 years. These shocking statistics resulted in a call to action by the CDC and the Lupus Foundation of America to develop a US population–based registry to monitor trends in lupus incidence and prevalence and to better characterize racial and ethnic disparities.

Starting in 2004, the CDC funded the creation of national lupus registries in several counties in Georgia (the Georgia Lupus Registry), Michigan (the Michigan Lupus Epidemiology and Surveillance Program), California (the California Lupus Surveillance Project), New York (the Manhattan Lupus Surveillance Program), and at select Indian Health Service (IHS) regions in Alaska, Phoenix, Arizona, and Oklahoma City.

The IHS, Michigan, and Georgia sites were the first of these registries and laid the groundwork and methodology for the later initiatives. They used similar case definitions, relying primarily on meeting ≥4 American College of Rheumatology (ACR) criteria or a renal biopsy of lupus nephritis/end-stage renal disease (ESRD) or a rheumatologist's diagnosis/consensus. The IHS study identified cases from a national data warehouse that requires mandatory reporting, while the Michigan and Georgia sites used similar case-finding sources: hospitals, specialists (rheumatology, dermatology, and nephrology), the US Renal Data System, and laboratory and pathology reports.

A number of lessons were learned from these registries, which were published in *Arthritis & Rheumatology* in 2014 (2–4). The Michigan and Georgia registries estimated lupus cases in nearly 3.9 million people living in 4 urban and rural counties, with a mix of primarily white (46–58%) and black residents (39–49%). Of note is that the race/ethnicity categories designated in the studies were white and black, which raises some limitations in terms of definition. They found an overall similar age-adjusted incidence of 5.5/100,000 persons and prevalence of 73/100,000 persons using ACR criteria as the primary definition of lupus. The incidence and prevalence rates increased to 6.9/100,000 and 92/100,000,

[1]Susan Manzi, MD, MPH: Allegheny Health Network, Pittsburgh, Pennsylvania; [2]Joan Merrill, MD: Oklahoma Medical Research Foundation, Oklahoma City.

Address correspondence to Susan Manzi, MD, MPH, Department of Medicine, Allegheny Health Network, Suite 295, South Tower, 320 East North Avenue, Pittsburgh, PA 15212. E-mail: susan.manzi@ahn.org.

Submitted for publication May 9, 2017; accepted in revised form June 22, 2017.

respectively, in the population from Georgia when lupus was also defined by a renal biopsy, ESRD, or 3 ACR criteria with a rheumatologist's diagnosis. Interestingly, the rates did not increase and in fact went down to 4.7/100,000 persons and 64/100,000 persons in Michigan when a consensus panel of rheumatologists weighed in on all cases, even those that met the ACR criteria, highlighting the discordance among rheumatologists of what constitutes lupus. Both studies showed a higher frequency of lupus in women (9–10-fold) and in black populations (2–3-fold). They also found that the mean age at diagnosis was ~10 years younger in black women. In addition, both groups noted that black patients had more renal involvement and ESRD. The IHS reported a high incidence and prevalence of lupus in American Indian and Alaska Native populations, comparable to that seen in US black residents. The IHS findings provided clarity on a frequently overlooked population at high risk of developing lupus.

The Michigan, Georgia, and IHS registries shed light on a number of important observations, but data on Asians and Hispanics were limited due to small numbers. To improve the reliability of incidence and prevalence estimates in these populations, the CDC supported the creation of 2 similar lupus registries in California and New York. In this issue of *Arthritis & Rheumatology*, the results of the California Lupus Surveillance Project (5) and the Manhattan Lupus Surveillance Program (6) are reported. The investigators from the University of California, San Francisco and New York University School of Medicine in conjunction with the California Department of Public Health and the New York City Department of Health and Mental Hygiene, respectively, sought to estimate the frequency of lupus in a combined 2.4 million residents living in San Francisco County and New York County (Manhattan), with greater representation of Asian or Pacific Islanders and Hispanics.

Using the same primary case definition (≥4 ACR criteria), the two studies found a similar overall age-adjusted incidence of 4.6/100,000 person-years, while the age-adjusted prevalence was slightly greater in California than Manhattan (84 versus 62/100,000 person-years). The reasons for this are unclear, but may reflect the case-finding efforts in San Francisco, focusing on the physicians and hospitals that care for minority residents, including but not limited to the community health network clinics. They also had access to the Veterans Affairs (VA) network. With a growing number of women and minorities in the military, the VA system will continue to be an important case-finding source. When the investigators broadened the case definition to include the recent Systemic Lupus International Collaborating Clinics (SLICC) criteria (Manhattan) or a rheumatologist's diagnosis or biopsy-proven lupus nephritis, the incidence and prevalence rates increased in both populations.

Like the Georgia and Michigan registries, the recent studies reported a higher frequency of lupus in women (~9–10-fold) and in blacks (~3–4-fold). In San Francisco and Manhattan, the prevalence of lupus in both Hispanics and Asians was greater than that in whites, but not as frequent as that in blacks. Interestingly, there was very little difference in prevalence estimates between Hispanics and Asian/Pacific Islanders in California, but not in Manhattan, where Hispanics had a higher prevalence of lupus than Asians. This may be due to differences in the racial subgroups comprising Hispanics or the methods of defining Hispanic ethnicity in both states. Neither study was able to differentiate between various Hispanic subgroups, although this distinction is relevant to outcomes, as highlighted in the LUpus in MInorities, NAture versus nurture (LUMINA) cohort (7). As previously reported, renal disease was more common in blacks, but it was also noted to be higher in Hispanics and Asians compared to white populations.

Throughout the years, there has been a nearly 10-fold difference in incidence rates and a 12-fold difference in prevalence rates of lupus reported in the published literature (2,8). This is likely due to the variability in study populations (regional and ethnic mix), case definitions (ACR criteria, self-report, International Classification of Diseases, Ninth Revision [ICD-9] codes, rheumatologist's diagnosis), and case ascertainment sources (hospitals, specialists, insurance claims data, laboratory and pathology reports, US renal databases, death certificates). Some of the highest prevalence estimates have been through Medicaid claims data (144/100,000 persons) (8). While insurance claims for a lupus diagnosis (having at least 2 or 3 claims several months apart) are thought to be sensitive (98%), they may be less specific (>72%). The value of these insurance databases rests in their large numbers (4-fold greater than the combined registries discussed here) of racially and ethnically diverse populations.

Together, the 5 CDC registries provide important information about lupus in populations totaling over 6.5 million from 4 states and 3 selected IHS regions, including mixed urban and rural areas. This is a major accomplishment, and the investigators should be congratulated. Studies of this magnitude hold great value, in that case definitions and case ascertainment methodologies have been standardized, with incorporation of capture–recapture analyses to estimate the completeness of case-finding (9). A critical premise of

capture–recapture is that the sources of ascertainment are independent. In reality, this assumption is hard to meet, and thus, capture–recapture may be helpful, but it has limited utility in epidemiologic studies of this nature. The investigators did recognize this limitation by using models that assessed the dependency of the different sources. Other limitations of the studies that were acknowledged by the authors include the retrospective chart review, which is subject to missing data, and illegibility of paper records. In addition, the assignment of race/ethnicity was ascertained from the records and not by self-identity, making it subject to misclassification.

Even with these limitations, this work provides new and confirmatory information about ethnic disparities in lupus. However, there are many reasons why we must use caution in extrapolating the number of people living with lupus in the US from the estimates of incidence and prevalence reported here. First, we have no gold standard for defining or diagnosing lupus. The ACR classification criteria were not designed for diagnosis, yet they were used as the primary definition in all of the registries (10,11). Even the recent SLICC classification criteria are not meant to be diagnostic, although they do increase sensitivity by including a broader range of features often seen in lupus (12). It should be noted that in all of the studies, when a different definition for lupus was applied, there were significant changes in the incidence and prevalence estimates, highlighting a lack of precision when there is no gold standard. The fact remains that there is discordance even among rheumatologists as to what constitutes a diagnosis of lupus (13).

While many refer to lupus as a heterogeneous disease, there has been growing interest in defining lupus as a disease spectrum with distinct phenotypes linked by genetic and molecular signatures. It should be noted that in the current CDC registries, the initial case-finding for lupus included ICD-9 diagnosis codes to capture unspecified connective tissue disease, other specified connective tissue disease, sicca syndrome, discoid lupus, and in some cases, antiphospholipid antibodies, highlighting the spectrum of conditions that could be considered lupus. By limiting the primary case definition to meeting $\geq$4 of the ACR criteria or having 3 ACR criteria with a rheumatologist's diagnosis, over one-half of the potential cases were eliminated. One could argue that the cases that were eliminated but living in the catchment areas may be the most interesting to study next.

Another phenotype in the spectrum of lupus that was surely underreported in these registries is chronic cutaneous lupus erythematosus (CLE), including classic discoid lupus, lupus panniculitis, bullous lupus, and subacute cutaneous lupus. A recent study from Olmsted County, Minnesota (primarily white population), found that the prevalence of CLE without systemic features was equal to that of SLE and 3 times more common in men (14). These findings suggest that we may be missing half of the cases of "lupus" by using only "SLE" classification criteria. Since CLE is more common in blacks, it is possible that even higher numbers of cases with only skin disease were not captured.

Recognizing that it may not be possible to determine the prevalence and incidence of lupus with absolute certainty, there is great value in the registries that have been developed through the support of the CDC and with the admirable efforts of the research teams. With better clarity around the definition of lupus that covers more of the spectrum without losing specificity for the pathology and a broader and refined approach to case ascertainment, our understanding of the real burden of disease in the US will only improve.

AUTHOR CONTRIBUTIONS

Drs. Manzi and Merrill drafted the article, revised it critically for important intellectual content, and approved the final version to be published.

REFERENCES

1. Sacks JJ, Helmick CG, Langmaid G, Sniezek JE. Trends in deaths from systemic lupus erythematosus — United States, 1979–1998. MMWR Morb Mortal Wkly Rep 2002;51:371–4.
2. Lim SS, Bayakly AR, Helmick CG, Gordon C, Easley KA, Drenkard C. The incidence and prevalence of systemic lupus erythematosus, 2002–2004: the Georgia Lupus Registry. Arthritis Rheumatol 2014;66:357–68.
3. Somers EC, Marder W, Cagnoli P, Lewis EE, DeGuire P, Gordon C, et al. Population-based incidence and prevalence of systemic lupus erythematosus: the Michigan Lupus Epidemiology and Surveillance program. Arthritis Rheumatol 2014;66:369–78.
4. Ferucci ED, Johnston JM, Gaddy JR, Sumner L, Posever JO, Choromanski TL, et al. Prevalence and incidence of systemic lupus erythematosus in a population-based registry of American Indian and Alaska Native people, 2007–2009. Arthritis Rheumatol 2014;66:2494–502.
5. Dall'Era M, Cisternas MG, Snipes K, Herrinton LJ, Gordon C, Helmick CG. The incidence and prevalence of systemic lupus erythematosus in San Francisco County, California: the California Lupus Surveillance Project. Arthritis Rheumatol 2017;69:1996–2005.
6. Izmirly PM, Wan I, Sahl S, Buyon JP, Belmont HM, Salmon JE, et al. The incidence and prevalence of systemic lupus erythematous in New York County (Manhattan), New York: the Manhattan Lupus Surveillance Program. Arthritis Rheumatol 2017;69:2006–17.
7. Vilá LM, Alarcón GS, McGwin G Jr, Friedman AW, Baethge BA, Bastian HM, et al, for the LUMINA Study Group. Early clinical manifestations, disease activity and damage of systemic lupus erythematosus among two distinct US Hispanic subpopulations. Rheumatology (Oxford) 2004;43:358–63.

8. Feldman CH, Hiraki LT, Liu J, Fischer MA, Solomon DH, Alarcón GS, et al. Epidemiology and sociodemographics of systemic lupus erythematosus and lupus nephritis among US adults with Medicaid coverage, 2000–2004. Arthritis Rheum 2013;65: 753–63.
9. Hook EB, Regal RR. Recommendations for presentation and evaluation of capture-recapture estimates in epidemiology. J Clin Epidemiol 1999;52:917–26.
10. Tan EM, Cohen AS, Fries JF, Masi AT, McShane DJ, Rothfield NF, et al. The 1982 revised criteria for the classification of systemic lupus erythematosus. Arthritis Rheum 1982;25: 1271–7.
11. Hochberg MC, for the Diagnostic and Therapeutic Criteria Committee of the American College of Rheumatology. Updating the American College of Rheumatology revised criteria for the classification of systemic lupus erythematosus [letter]. Arthritis Rheum 1997;40:1725.
12. Petri M, Orbai AM, Alarcón GS, Gordon C, Merrill JT, Fortin PR, et al. Derivation and validation of the Systemic Lupus International Collaborating Clinics classification criteria for systemic lupus erythematosus. Arthritis Rheum 2012;64:2677–86.
13. Narain S, Richards HB, Satoh M, Sarmiento M, Davidson R, Shuster J, et al. Diagnostic accuracy for lupus and other systemic autoimmune diseases in the community setting. Arch Intern Med 2004;164:2435–41.
14. Jarukitsopa S, Hoganson DD, Crowson CS, Sokumbi O, Davis MD, Michet CJ Jr, et al. Epidemiology of systemic lupus erythematosus and cutaneous lupus erythematosus in a predominantly white population in the United States. Arthritis Care Res (Hoboken) 2015;67:817–28.

ARTHRITIS & RHEUMATOLOGY
Vol. 69, No. 10, October 2017, pp 1925–1936
DOI 10.1002/art.40194

REVIEW

Enhancers in Autoimmune Arthritis

Implications and Therapeutic Potential

Janneke G. C. Peeters, Sebastiaan J. Vastert, Femke van Wijk, and Jorg van Loosdregt

Introduction

Genome-wide association studies (GWAS) have identified hundreds of single-nucleotide polymorphisms (SNPs) associated with autoimmune diseases, including autoimmune arthritis. So far, it has proven difficult to translate these findings into disease understanding and novel therapeutic approaches as the majority of these SNPs are not located in protein-coding regions. Recently, various studies found that a large number of autoimmune disease–associated SNPs affect DNA regulatory units, suggesting that altered epigenetic control of transcription is an important process in disease pathogenesis (1,2). Technical developments have allowed for detailed analysis of the epigenetic profile of disease-associated cells, creating new opportunities to study gene regulation in the context of disease. In this review, we will discuss these advances in the field of epigenetics, focusing on (super)enhancers associated with autoimmune arthritis. Furthermore, we will describe how enhancer profiling of disease-specific cells can contribute to better understanding of disease pathogenesis. Additionally, we will outline strategies that can target enhancer activity and discuss their potential use as therapeutic approaches in the treatment of autoimmune arthritis.

Supported by the Netherlands Organization for Scientific Research and the Dutch Arthritis Foundation.

Janneke G. C. Peeters, MSc, Sebastiaan J. Vastert, MD, PhD, Femke van Wijk, PhD, Jorg van Loosdregt, PhD: Laboratory of Translational Immunology, Wilhelmina Children's Hospital and University Medical Center Utrecht, Utrecht, The Netherlands.

Address correspondence to Jorg van Loosdregt, PhD, Division of Pediatrics, University Medical Center Utrecht, Lundlaan 6, 3584 EA Utrecht, The Netherlands. E-mail: J.vanloosdregt@umcutrecht.nl.

Submitted for publication March 14, 2017; accepted in revised form June 27, 2017.

Genetic basis of autoimmune arthritis

The genetic basis of autoimmune arthritis has been studied extensively, especially in the last decade. Advances using high-throughput genome sequencing have identified multiple risk variants associated with various rheumatic diseases, including rheumatoid arthritis (RA), juvenile idiopathic arthritis (JIA), systemic lupus erythematosus (SLE), ankylosing spondylitis (AS), and psoriatic arthritis (3–8). Although these studies provide some important clues about the biologic pathways that might be affected, novel insights regarding the molecular function and role in disease pathogenesis remain limited. For example, genome-wide significant loci, including the major histocompatibility complex (MHC) loci, and regions with suggestive associations can only explain 18% of the risk for JIA (4).

This is mainly because of 2 different reasons, the first being the difficulty to define which SNP is the disease-causal variant. Disease-associated loci identified by GWAS contain numerous SNPs. This is due to linkage disequilibrium (LD), the nonrandom association between 2 alleles of different loci. Therefore, disease-causal variants are often surrounded by neutral or other disease-causal variants, making it difficult to pinpoint the candidate disease-causal SNP(s) (9). Improvements in identifying disease-causal variants have recently been made by several groups by developing algorithms that take into account either cell type or tissue-specific epigenomic information (e.g., probabilistic identification of causal SNPs [PICS], EPIGWAS, Risk Variant Inference

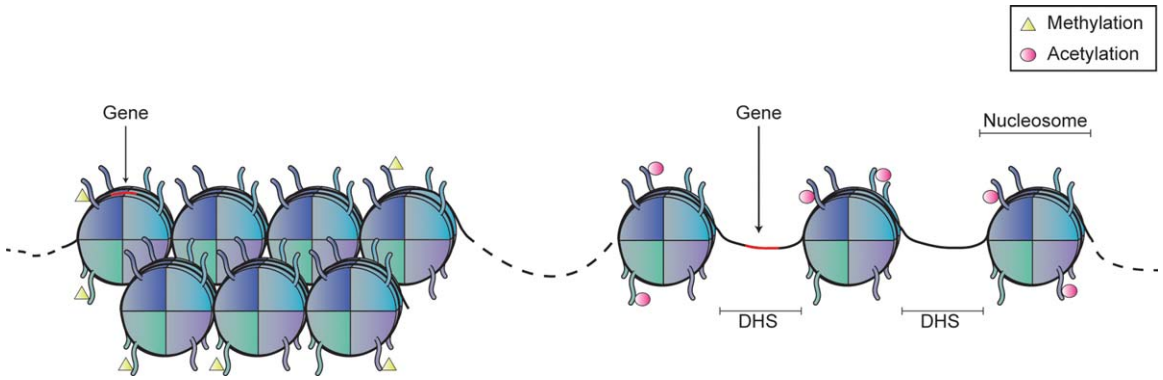

Figure 1. Schematic representation of chromatin structure. DNA is wrapped around an octamer of histone proteins, together forming a nucleosome. Nucleosomes can be tightly packed, rendering the DNA inaccessible (left), or can have a more loose structure, allowing transcription factors to bind (right). DHS = DNase I hypersensitivity site.

using Epigenomic Reference Annotation [RiVIERA], Robust Allele Specific QUAntitation and quality controL [RASQUAL]), (predicted) gene function and expression data (Data-driven Expression-Prioritized Integration for Complex Traits [DEPICT]), microRNA (miRNA)–target gene networks (miRNA–target gene enrichment analysis in GWAS [MIGWAS]), or genome-wide information from all SNPs, instead of a restricted SNP set, together with explicit modeling of LD (2,10–15). For example, the PICS algorithm demonstrates that only 5% of the SNPs that were originally thought to be disease-causing are actually assigned as being disease-causal variants (2). This indicates that genetic fine mapping of autoimmune disease variants will further unravel the genetic basis of autoimmunity.

The second reason that it has been difficult to translate GWAS findings into disease understanding is that ~90% of disease-associated SNPs are located outside of protein-coding regions, in regulatory DNA regions, making it difficult to understand which gene(s) is affected and how (1,2). As these regulatory DNA regions are epigenetically regulated, a better understanding of the epigenetic landscape is needed to understand the contribution of genetic variation to autoimmunity.

Enhancers and superenhancers

To fit the approximately 2-meter–long DNA strand in the nucleus, DNA is tightly packed. DNA is wrapped around the histone proteins H2A, H2B, H3, and H4, 2 of each type, thereby forming a nucleosome and creating the chromatin structure. The N-terminal tail of histones can be covalently modified. Generally, methylation allows tight packing of nucleosomes, rendering the DNA inaccessible. Acetylation reduces the positive charge of the histone tail, thereby reducing the interaction with the negatively charged DNA, allowing enzymes and transcription factors to bind (16) (Figure 1). Regulatory DNA regions are characterized by DNase I hypersensitivity sites, meaning that in these regions DNA can be cleaved by DNase I, indicating a loose chromatin structure. Of the SNPs located in regulatory DNA regions, the majority localize to so-called enhancers (10,17). Enhancers are *cis*-regulatory DNA elements to which transcription factors and cofactors can bind, and they are crucial for transcriptional regulation. By recruitment of RNA polymerase II and mediator complex to the promoter of their target gene, enhancer elements regulate gene expression (Figure 2A).

Enhancers are generally a few hundred basepairs in size, contain multiple transcription factor binding sites, and can be located up to 1,000 kb upstream or downstream of the promoter of their target gene (16). The dispersion of enhancers throughout the genome and the 3-dimensional chromatin conformation make it difficult to define which gene a certain enhancer is regulating. Generally, epigenomic studies assume that enhancers regulate the gene whose transcriptional start site is closest to the enhancer. For a more precise understanding of the gene regulated by a certain enhancer, chromosome conformation capture (3C) techniques (3C-based technologies) are available that enable capturing of the physical interactions between enhancers and promoters (18). These technologies indicate that 27–40% of the active enhancers indeed interact with their nearest promoter, suggesting that 3C-based technologies are pivotal for understanding the epigenetic landscape (19,20).

Enhancers that are permissive for transcriptional regulation but that are not active (i.e., inactive/poised enhancers) are characterized by monomethylation of histone H3 at lysine 4 (i.e., H3K4me), while active

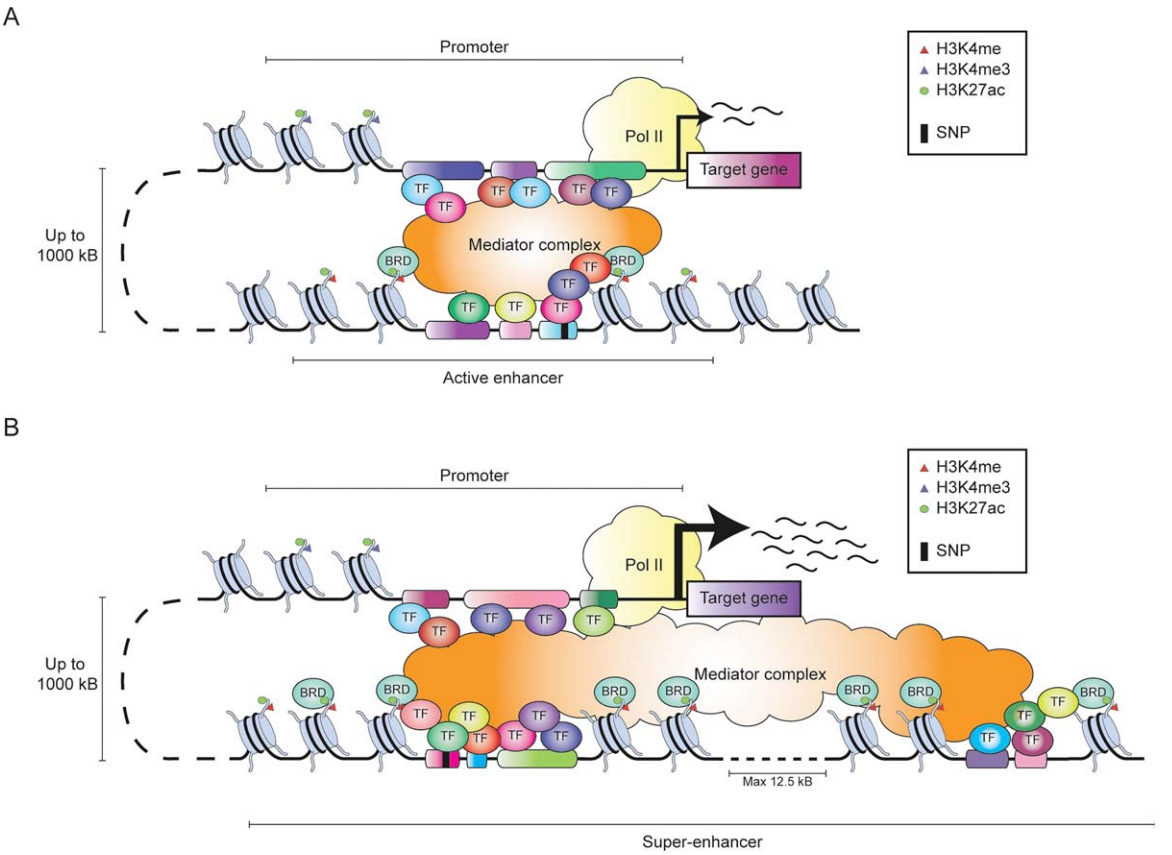

Figure 2. Schematic representation of transcriptional regulation by enhancers and superenhancers. **A,** Gene expression of a target gene driven by an active enhancer. Active enhancers are characterized by monomethylation of histone H3 at lysine 4 (H3K4me) and acetylation of histone H3 at lysine 27 (H3K27ac). Enhancers facilitate transcription by transcription factor (TF) binding, recruitment and binding of bromodomain and extraterminal proteins, consisting of bromodomain-containing proteins (BRDs), the mediator complex, looping of the DNA, and RNA polymerase II (Pol II) recruitment. Single-nucleotide polymorphisms (SNPs) are enriched in regulatory DNA regions, for example, enhancers. Enhancers can be located up to 1,000 kb from their target gene. **B,** Gene expression of a target gene driven by a superenhancer. Superenhancers are large enhancers characterized by extensive acetylation of histone H3 at lysine 27 and increased binding of the mediator complex and transcription factors. Active enhancers within 12.5 kb of each other can together form a superenhancer, leading to increased gene expression. Superenhancers are enriched for SNP localization compared to active enhancers. H3K4me3 = trimethylation of histone H3 at lysine 4.

enhancers contain both H3K4me and acetylation of histone H3 at lysine 27 (i.e., H3K27ac) (21,22). In any mammalian cell type, tens of thousands of enhancers can be found, exceeding the number of protein-coding genes (~20,000), indicating that a single gene can be regulated by multiple enhancers within one cell and that the enhancer(s) regulating a certain gene can differ between cells (19,23).

In addition, a number of studies have recently identified extremely large enhancer domains, containing clusters of individual enhancers, termed superenhancers or stretched enhancers (24–26). Active enhancers within 12.5 kb of each other can together form a superenhancer (Figure 2B). Superenhancers are identified by extensive H3K4me, H3K27ac, p300 binding, mediator complex occupancy, and increased DNase I hypersensitivity sites and are characterized by increased transcription factor binding. Superenhancer-regulated genes are expressed to a higher extent than genes driven by a regular enhancer (26). This increase in gene expression seems to be due to synergy between individual enhancer constituents within a superenhancer, rather than being the sum of individual enhancers (27–29). However, as some superenhancers are single enhancers, and enhancers within 12.5 kb of each other do not necessarily form a superenhancer, it remains questionable whether superenhancers are a novel concept in gene regulation, or whether they are more a reflection of the characteristics of their individual enhancer constituents, such as a different sequence composition leading to increased

transcription factor binding and increased transcriptional activity (30). Superenhancers preferentially regulate genes important for cell identity as well as genes associated with disease. For example, in multiple cancer subtypes, superenhancers are associated with tumor oncogenes (24,31). Taken together, this suggests that understanding the role of (super)enhancers in immune cell function will help in defining their function in disease pathogenesis. For autoimmune arthritis, it seems logical to analyze the importance of (super)enhancers in cells from both the adaptive and innate immune systems.

Enhancers in immune cell function

The diverse properties of different cell types within the immune system are reflected within their enhancer landscape, demonstrating that enhancers can be highly cell type specific. This is illustrated by the distinct enhancer landscape of naive CD4+ T cells versus differentiated T cell subsets (32,33). STAT proteins are pivotal for establishing subset-specific enhancers, with STAT-1 and STAT-4 being important for the generation of Th1 cell–specific enhancers, while STAT-6 shapes Th2 cell–specific enhancers (33). T cell superenhancers are preferentially associated with cytokines and cytokine receptors; for instance, the T cell subtype–specific genes *Ifng*, *Il13*, and *Il17a* are associated with a superenhancer in mouse Th1, Th2, and Th17 cells, respectively (34,35). The strongest superenhancer in CD4+ Th1, Th2, and Th17 cells is linked to *Bach2*, a suppressor of T effector cell differentiation. *Bach2* deletion reduces expression of other T cell superenhancer-associated genes, suggesting the presence of a key regulatory node in T cells driven by BACH2 (35). Also, in B cells BACH2 is associated with a superenhancer, highlighting the important role of this gene in adaptive immune cell regulation (24).

The innate immune response, with monocytes and macrophages being important mediators, is characterized by the rapid expression of a subset of genes 0.5–2 hours after stimulation (i.e., primary response genes) and by expression of another gene subset 2–8 hours after stimulation (i.e., secondary response genes) (36). These characteristics are reflected within the enhancer landscape of innate cells. Namely, Toll-like receptor 4 (TLR-4) stimulation leads to the acquisition of H3K27ac by some poised enhancers, reduction or complete loss of certain enhancers, and reduction of the strength of a subset of enhancers already present in unstimulated conditions (37,38). These epigenetic alterations are rapid and thus likely to be associated with expression of early primary response genes. TLR-4 stimulation also induces the formation of ~1,000 de novo enhancers. As de novo enhancer formation takes time and involves nucleosome remodeling, which is known to be required for secondary response gene expression, these enhancers are linked to secondary response genes (39).

In addition to lipopolysaccharide (LPS), the proinflammatory cytokine tumor necrosis factor (TNF), via activation of NF-κB, can shape the enhancer repertoire (40). This occurs mainly via de novo superenhancer formation and drives proinflammatory gene expression. Since some of these proinflammatory genes are cytokines, this implies a (positive) feedback loop whereby cytokines can affect the enhancer profile in an autocrine and paracrine manner. Similar effects of the (local) microenvironment on the enhancer landscape are described for tissue-resident macrophages. For example, transplantation of macrophages into distinct tissues of recipient mice leads to the acquisition of an enhancer profile comparable to that of recipient tissue-resident macrophages (41,42). Taken together, these studies illustrate that the microenvironment drives selection and function of enhancers and thereby regulates cellular identity and plasticity. This implies that it might be crucial to analyze the enhancer profile of cells directly after isolation from their tissue, as this reflects their enhancer landscape within the microenvironment. This is especially important to take into account for autoimmune arthritis, in which the microenvironment is one of the main drivers of the inflammatory cellular phenotype.

Enhancer regulation in autoimmune arthritis

Given the critical role of (super)enhancers for proper immune cell function, it is almost inevitable that they play a significant role in autoimmune arthritis as well. However, the role of enhancers in immune-related diseases has hardly been investigated. The importance of enhancers for autoimmunity is underscored by the enrichment of autoimmune disease–associated SNPs in enhancer regions of immune cells from healthy controls, with the highest enrichment in superenhancers compared to regular enhancers (2,24,25,35). For example, RA-associated noncoding SNPs are 3.2-fold more enriched in superenhancers and 2.2-fold more enriched in regular enhancers compared to other DNA regulatory regions. In addition, disease-associated variants preferentially map to (super)enhancers that are specific for disease-relevant cell types (24,25,35). For instance, the majority of RA-associated SNPs map to T cell, natural killer cell, and B cell (super)enhancers (43). For SLE, SNPs are predominantly located within B cell superenhancers, underscoring their important role in SLE pathogenesis (24). It might therefore be informative to

map disease-associated SNPs to the (super)enhancer profile of different immune cell (subsets) for not-so-well-characterized diseases, as this can reveal the cell type(s) involved in the disease.

Since ~90% of disease-associated SNPs are located in noncoding regions and 60% of these SNPs map to enhancers, disease-associated SNPs might affect gene transcription (1,2). Indeed, SNPs present in DNase I hypersensitivity sites are 4 times more likely to have an effect on gene expression compared to SNPs located outside DNase I hypersensitivity sites (44). Nonetheless, due to the presence of multiple SNPs in LD in a risk locus and because of the difficulty of defining which of these SNPs is causal for the disease, it is difficult to determine exactly the transcriptional effect of a SNP within a regulatory region. The effect of genetic enhancer variants on transcription is thought to be relatively small, with a reported 1.3–2-fold difference in target gene expression (45). Although modest, these differences can play important roles in disease pathogenesis.

For example, disease-associated SNPs are enriched at expression quantitative trait loci (eQTLs), which are genomic regions containing DNA variants that affect gene expression and that thus might alter the immunophenotype (46). A large proportion of eQTL SNPs are present around the transcription start site and are therefore likely to affect the promoter region (47). So far, eQTL studies have mostly been focused on promoter biology, but enhancer eQTL data are starting to emerge. For example, eQTL SNPs are enriched in DNase I hypersensitivity sites and regions characterized by active histone marks, with a strong enrichment for H3K27ac regions 5–100 kb upstream from the transcription start site, suggesting enrichment within enhancer regions (44). A more recent study (2), looking at SNPs associated with heritable differences in peripheral blood gene expression, shows that ~9% of the eQTL SNPs are located within promoters and ~14% within enhancers, suggesting that enhancer eQTL SNPs are important to take into account. However, considering that 60% of noncoding variants map to enhancers, this also suggests that a large proportion of enhancer SNPs do not map to eQTLs, and it remains to be investigated if and how these variants affect gene expression. There are some suggestions (e.g., for RA and SLE) that these diseases cannot be explained by one SNP, but that genetic variants within clusters of enhancers present at risk loci together affect gene expression and therefore confer disease susceptibility; however, this needs to be further investigated (48).

For autoimmune vitiligo, 3 SNPs are located within an MHC class II superenhancer, which also corresponds to an eQTL for HLA–DR and HLA–DQ expression. The presence of these SNPs correlates with increased HLA–DR and HLA–DQ surface expression and increased cytokine production, illustrating how SNP localization in a specific genomic region can contribute to the development of autoimmunity (49). Similarly, 2 SLE-associated SNPs are located in an enhancer element downstream of the *TNFAIP3* promoter (50). *TNFAIP3* encodes for A20, an inhibitor of NF-κB signaling. The presence of these 2 variants impairs NF-κB binding to the enhancer, thereby reducing promoter–enhancer interaction, leading to reduced A20 expression (50). This results in increased NF-κB signaling and thus supports a causal role for the SNP pair in SLE pathogenesis. For AS, a possible disease-causal SNP has been identified within an enhancer between *IL23R* and *IL12RB2* (51). The presence of this SNP corresponds to reduced H3K4me of the enhancer region in CD4+ T cells, impaired binding of nuclear proteins to the SNP-containing DNA region, and reduced reporter activity. However, expression of *IL23R* and *IL12RB2* is not affected, although the frequency of Th1 cells, which express *IL12RB2*, is altered. A possible explanation for this discrepancy could be that the SNP-containing enhancer is not regulating *IL23R* and *IL12RB2* expression but has another, yet unidentified, target gene affecting Th1 cell numbers. The 3C-based technologies could help in unraveling the biologic effect of this particular SNP and other disease-associated SNPs to which a molecular function has not so far been ascribed.

A confounding factor in linking GWAS data with epigenomics data is that the epigenetic data being used are predominantly based on cells from healthy controls and might not represent the epigenetic landscape of disease-relevant, patient-derived cells. Additionally, for most diseases it is more informative to profile cells from the affected tissue than cells from the peripheral circulation. Indeed, JIA (super)enhancer profiling of synovial-derived CD4+ T cells revealed a different profile compared to peripheral blood cells from healthy controls (52). Similar observations have been made in SLE-derived monocytes (53). Expression QTL mapping is generally also performed using samples from healthy controls; however, eQTLs were recently mapped using an RA cohort (54). This revealed that RA GWAS hits are enriched in RA-identified eQTLs compared to healthy control eQTLs and that RA eQTLs are enriched in enhancer regions. Furthermore, combination of these eQTL data with GWAS and epigenomics data identified novel disease-relevant genes (54).

Consistent with these observations, arthritis-associated SNPs are more enriched in JIA patient superenhancers compared to healthy control superenhancers (52).

These findings underscore the importance of using patient-derived cells and illustrate that integrating multiple data sets can be more informative than a single data set in identifying autoimmune arthritis–associated molecular mechanisms. In addition, comparing the enhancer profile of different autoimmune diseases can be useful in unraveling autoimmune disease pathogenesis. This is of particular interest since autoimmune disease–associated SNPs are profoundly enriched in T cell superenhancers in JIA, while this is not the case for non–autoimmune disease–associated SNPs (52). Correspondingly, it has been reported that autoimmune diseases have shared risk loci, suggesting overlap in disease pathogenesis (2). In addition, enhancer data may also define distinct pathogenic processes between diverse types of autoimmune arthritis. For example, RA synovial fibroblasts (RASFs) are distinguishable from osteoarthritis-derived synovial fibroblasts based on DNA methylation and transcriptome data (55). Furthermore, these data can also discriminate between RASFs isolated from different joints. These observations suggest that joint-specific epigenetic signatures exist, and they therefore indicate that molecular pathways affected in the disease might differ from one joint to another. Epigenetic profiling can be used to identify these differences, and, more importantly, these observations raise the question of whether epigenetic knowledge can be translated into novel therapeutic strategies for the treatment of autoimmune arthritis.

Inhibition of enhancer activity in relation to autoimmune arthritis

The observations that autoimmune arthritis–associated SNPs are preferentially located in enhancers and that superenhancers are associated with disease-relevant genes strongly suggest that enhancers contribute directly to disease pathogenesis. Therefore, there is a growing body of interest in the development of therapeutic strategies aimed at targeting (super)enhancer activity. Enhancer regions are critically dependent on chromatin regulators (e.g., reader proteins recognizing histone modifications), which recruit transcription factors and other proteins to facilitate transcription initiation and elongation. Important reader proteins at enhancers are bromodomain and extraterminal (BET) proteins, consisting of bromodomain-containing protein 2 (BRD-2), BRD-3, BRD-4, and bromodomain testis-specific protein, each containing 2 bromodomains (56) (Figure 2). The bromodomain allows BET proteins to bind to acetylated histone and nonhistone proteins. BRD-4 is most extensively studied and is present at promoters and active enhancers, with increased localization at superenhancers (31,57). Binding of BET proteins to acetylated transcription factors might contribute to their preferential localization in (super)enhancer regions (58).

Recently, a wide range of small-molecule inhibitors of BET proteins has been developed (59) (Table 1). The therapeutic potential of BET inhibitors has been demonstrated in numerous in vitro and in vivo tumor models, in which BET inhibitors inhibit the expression of different oncogenes, including c-*myc* (58,60). Inhibition of c-*myc* is linked to the disruption of c-*myc*–associated superenhancer activity (31). This is probably related to the high levels of BRD-4 present at superenhancers and the transcriptional dependency thereof and thus contributes to the preferential inhibition of superenhancer-driven gene expression by BET inhibitors.

BET inhibitors are highly effective in shaping the adaptive immune response. For example, the BET inhibitors JQ1 and I-BET762 significantly impair differentiation of naive CD4+ T cells into T effector cell subsets, both in vitro and in vivo (61,62). Furthermore, BET inhibition of differentiated CD4+ T cells has a profound effect on production of cytokines, such as interleukin-17 (IL-17). BET inhibition also impairs B cell function by inhibiting Ig class-switch recombination and B cell expansion and proliferation (63,64). Additionally, BET inhibitors can affect innate immune responses. For instance, JQ1, I-BET762, and I-BET151 all inhibit proinflammatory cytokine production by LPS-stimulated monocytes and macrophages in vitro and are effective in different in vivo animal models (65–69). Genes affected by I-BET762 in LPS-stimulated macrophages belong to the secondary response genes. Given the epigenetic differences underlying the expression of these genes, this suggests that I-BET762, and possibly other BET inhibitors as well, preferentially acts on de novo enhancers (68). This corresponds to the observation that de novo superenhancers, induced by TNF and LPS, are highly susceptible to BET inhibition, resulting in decreased superenhancer-mediated gene expression (37,40).

Inflammation-associated diseases are characterized by proinflammatory mediators present at the site of inflammation, suggesting that BET inhibition might be a way to specifically target cytokine-induced, and thus disease-associated, (super)enhancers. Indeed, JQ1 treatment of CD4+ T cells derived from synovium of JIA patients preferentially reduces expression of disease-associated genes, with the majority being involved in

Table 1. Overview of small molecules affecting enhancer activity*

Small molecule	Target	Effect on immune system (ref.)
CP1–0610	BRD-2, BRD-3, BRD-4, bromodomain testis-specific protein; targeted bromodomain: BD1	Not assessed
DRB	CDK-9	Inhibition of T cell priming under Th2 and Th17 conditions (62)
I-BET151	BRD-2, BRD-3, BRD-4, bromodomain testis-specific protein; targeted bromodomains: BD1 and BD2	Inhibition of proinflammatory gene expression in LPS-stimulated monocytes and macrophages (66,69); inhibition of inflammatory genes and matrix-degrading enzymes in RASFs (71); suppression of inflammation-induced arthritis, TNF-induced bone resorption, and EAE (66,74)
I-BET762	BRD-2, BRD-3, BRD-4, bromodomain testis-specific protein; targeted bromodomains: BD1 and BD2	Inhibition of macrophage and CD4+ T cell cytokine production (62,67,68); suppression of EAE (62)
JQ1	BRD-2, BRD-3, BRD-4, bromodomain testis-specific protein; targeted bromodomains: BD1 and BD2	Inhibition of proinflammatory cytokine production in macrophages and T cells (61,65,75); inhibition of DC maturation (86); inhibition of T cell differentiation (61); inhibition of Ig class-switch recombination and mitogenesis in B cells (63,64); inhibition of cytokine production in CD4+ T cells in JIA (52,70); suppression of CIA, EAE, psoriasis, and endotoxic shock in mouse models (61,65,72,73)
LY294002	BRD-2, BRD-3, BRD-4, bromodomain testis-specific protein; targeted bromodomain: BD1	Inhibition of inflammation in LPS-stimulated PBMCs (87)
MS417	BRD-2, BRD-3, BRD-4, bromodomain testis-specific protein; targeted bromodomains: BD1 and BD2	Inhibition of HIV-associated kidney disease (88)
Olinone	BRD-2, BRD-3, BRD-4, bromodomain testis-specific protein; targeted bromodomain: BD1	Not assessed
OTX015	BRD-2, BRD-3, BRD-4, bromodomain testis-specific protein; targeted bromodomains: BD1 and BD2	Disruption of HIV-1 latency (89)
PC579	CDK-9	Suppression of CIA (80)
PC585	CDK-9	Suppression of CIA (80)
PFI-1	BRD-2, BRD-3, BRD-4, bromodomain testis-specific protein; targeted bromodomains: BD1 and BD2	Inhibition of IL-1β–induced inflammation in airway epithelial cells (90)
RVX-208	BRD-2, BRD-3, BRD-4, bromodomain testis-specific protein; targeted bromodomain: BD2	Not assessed
RX-37	BRD-2, BRD-3, BRD-4, bromodomain testis-specific protein; targeted bromodomains: BD1 and BD2	Not assessed
TEN-010	BRD-2, BRD-3, BRD-4, bromodomain testis-specific protein; targeted bromodomains: BD1 and BD2	Not assessed
THZ1	CDK-7	Not assessed
Tofacitinib	JAK	Inhibition of RA-associated risk genes in CD4+ T cells from healthy controls (35); inhibition of TLR-induced cytokine gene expression in macrophages (67)

* BRD-2 = bromodomain-containing protein 2; CDK-9 = cyclin-dependent kinase 9; LPS = lipopolysaccharide; RASFs = rheumatoid arthritis synovial fibroblasts; TNF = tumor necrosis factor; EAE = experimental autoimmune encephalomyelitis; DC = dendritic cell; JIA = juvenile idiopathic arthritis; CIA = collagen-induced arthritis; PBMCs = peripheral blood mononuclear cells; IL-1β = interleukin-1β; TLR = Toll-like receptor.

proinflammatory and cytokine-related processes (52,70). Correspondingly, I-BET151 treatment of RASFs suppresses the production of matrix metalloproteinases and cytokines upon stimulation with TNF, IL-1β, or TLR ligands, resulting in reduced proliferation and chemoattractant properties (71). Similar observations are obtained by genetically silencing BET proteins in RASFs (72).

These findings indicate that BET inhibition can be a putative therapeutic approach for the treatment of autoimmune diseases. This has been tested using several in vivo autoimmune disease models. For instance, JQ1, I-BET151, or I-BET762 treatment of experimental autoimmune encephalomyelitis (EAE; an animal model of multiple sclerosis) and an in vivo model of psoriasis significantly reduces the onset and severity of disease symptoms (61,62,66,73). These results are associated with the preferential suppression of IL-6 and IL-17 production and Th17 cell numbers. The protective effect of BET inhibitors has also been explored in mouse models of autoimmune arthritis. For example, in serum-induced and collagen-induced arthritis (CIA) models, JQ1 and I-BET151 dramatically reduce disease progression and plasma and serum cytokine levels (61,72,74). Furthermore, I-BET151 inhibits the differentiation of monocytes toward osteoclasts in vitro and reduces TNF-induced bone resorption in vivo. This is consistent with observations that JQ1 inhibits RANKL-induced

up-regulation of osteoclast-associated genes (75). Since osteoclast formation and bone resorption are related to autoimmune arthritis, this implies a dual role for BET inhibitors in the treatment of autoimmune arthritis. As TNF and IL-6 can induce osteoclast differentiation, the effect of BET inhibition on osteoclast differentiation is likely to result from a combination of direct and indirect mechanisms of action, the latter via inhibition of TNF and IL-6 production by cells in the synovial compartment (76). Of note, 3 SNPs associated with RA are present in BRD-2 (77). It might be informative to study the effects of these SNPs on the regulation of gene transcription, disease, and susceptibility to BET inhibitors.

In addition to BET inhibitors, some other compounds could be used to inhibit enhancer activity, for instance, cyclin-dependent kinase (CDK) inhibitors specific for CDK-7 or CDK-9. CDK-7 and CDK-9 are both implicated in transcription initiation and elongation by phosphorylation of RNA polymerase II (78). CDK-7 inhibition, via the small molecule THZ1, affects superenhancer-driven gene expression in c-Myc–dependent tumor models (79). A recent study provides evidence for the use of CDK inhibitors in autoimmune diseases as well, as CDK-9 inhibition delays disease onset and reduces disease symptoms in a CIA model (80). Whether this effect is mediated via (preferential) inhibition of superenhancers has not been investigated and remains to be further explored. Comparison of the effect of CDK-9 inhibition and BET inhibition has revealed some differential effects on T cell priming, suggesting that different inhibitors of enhancer activity can have distinct properties (62). Therefore, the therapeutic potential of these compounds might differ between different disease types, probably reflecting differences in the underlying disease mechanisms.

The observed enrichment of STAT proteins at T cell (super)enhancers prompted researchers to investigate the effect of the JAK inhibitor tofacitinib, which is also approved for the treatment of RA as second-line therapy. In vitro treatment of T cells with tofacitinib dramatically alters gene expression, with a more drastic effect on genes driven by superenhancers compared to those driven by regular enhancers (35). Since the majority of RA-associated SNPs are located within T cell superenhancers, tofacitinib treatment of T cells in RA could result in selective targeting of RA-associated risk genes, underscoring its potential for the treatment of RA. Considering the (high) levels of acetylation and methylation associated with (super)enhancer activity, it could be speculated that targeting enzymes affecting acetylation and methylation of specific histone sites might be an alternative way to impair enhancer activity. For example, GSK-J4, an inhibitor of the H3K27me3 demethylases KDM6A and KDM6B, impairs the LPS-induced inflammatory response in macrophages derived from both healthy controls and RA patients (81). Furthermore, GSK-J4 suppresses in vitro Th17 cell differentiation and has been demonstrated to suppress EAE via the induction of tolerogenic dendritic cells (82,83). A possible explanation for this observation could be that decreased demethylation of H3K27 in enhancer regions renders these enhancers inactive, reducing the likelihood of acquiring acetylation and thus becoming active. Therefore, the immunomodulatory effect of GSK-J4 could be mediated via reduction of enhancer activity, but whether this is actually the case needs to be further explored.

Future perspective

In this review, we have discussed the recent advances in the field of epigenetics, focusing on enhancers and their implications for autoimmune arthritis. Epigenetic regulation of immune cells is essential for proper cell function and therefore crucial for mounting an appropriate immune response. It is becoming more and more evident that alterations related to (super)enhancers are linked to autoimmunity, including autoimmune arthritis.

For a better understanding of enhancers in the context of autoimmune arthritis, it is crucial to perform enhancer profiling of disease-relevant, patient-derived cells. As enhancers are highly cell type specific, it is pivotal that the enhancer landscape is defined in specific cell types and not in a mixed population of cells, as this will affect interpretation of the results. Since patient material is often limited, one of the challenges will be to obtain a sufficient number of cells. Another important factor to take into account is patient stratification, as distinct disease subtypes can have different enhancer landscapes. From another perspective, enhancer profiling could actually assist in classifying patients into existing disease subtypes and may be used for identifying novel disease subtypes. For example, this might be useful in the case of JIA, in which the designation of disease subtypes is still clinically based. Furthermore, it is important to know exactly what the target gene(s) of each enhancer is. Integration of chromosome conformation information with GWAS data will help in ascribing a molecular function to GWAS hits. This will contribute to better insight into the (shared) pathogenesis of autoimmune arthritis and might lead to the identification of novel therapeutic targets. In addition, enhancer profiling might reveal novel biomarkers that could be used to

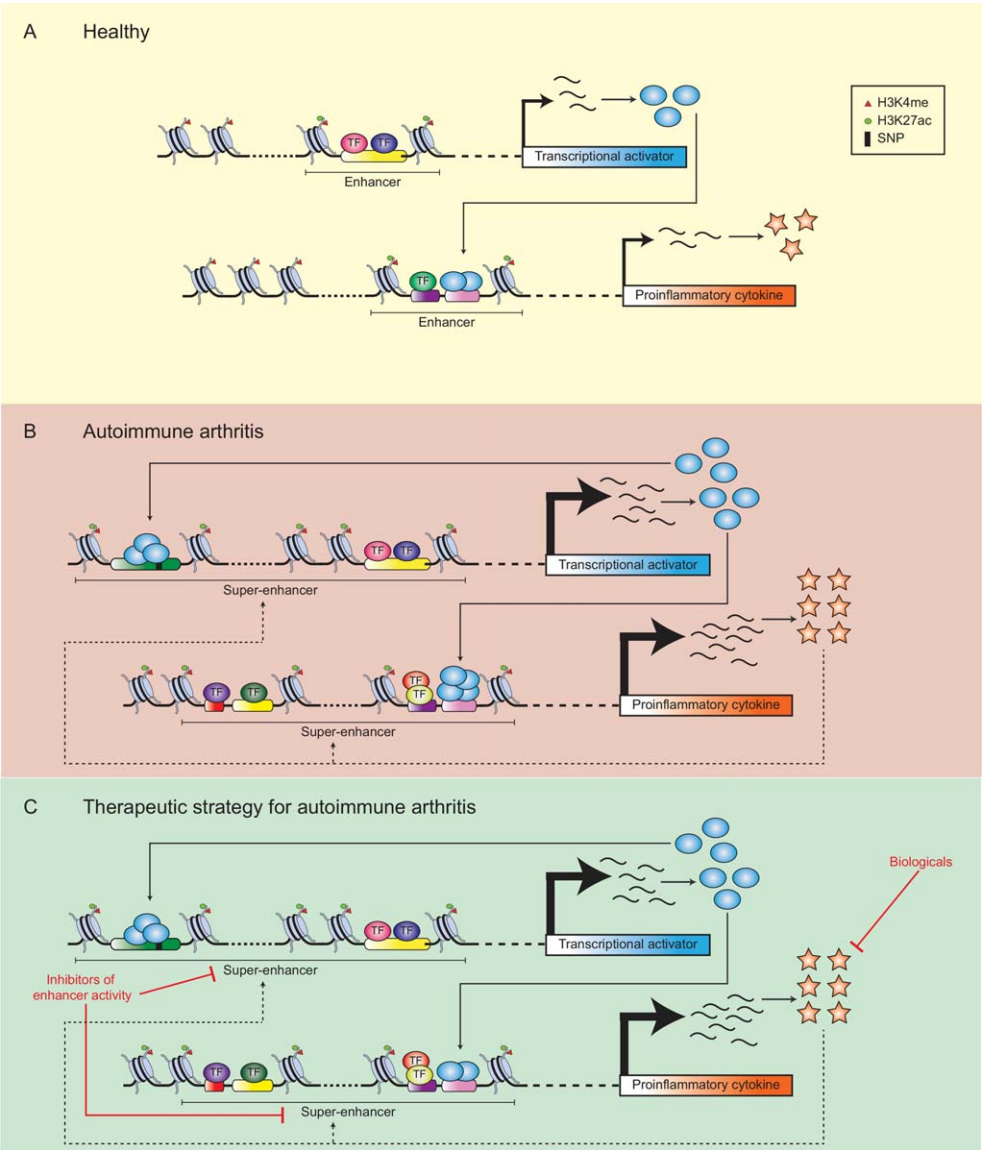

Figure 3. Schematic representation of the role of (super)enhancers in autoimmune arthritis. **A,** Under healthy conditions, enhancers regulate gene expression of proinflammatory cytokines and transcriptional activators, leading to controlled gene transcription. **B,** In autoimmune arthritis, superenhancers contribute to proinflammatory cytokine expression. Proinflammatory cytokines can shape the (super)enhancer repertoire, thereby creating self-regulatory loops and stimulating expression of transcriptional activators. Transcriptional activators can function in a regulatory feedback loop by regulating their own expression and that of proinflammatory cytokines. **C,** Inhibitors of enhancer activity can inhibit (super)enhancers, thereby reducing proinflammatory gene expression. Biologic agents can inhibit the mechanism of action of proinflammatory cytokines, thereby disrupting the regulatory feedback loop. See Figure 2 for definitions.

predict therapeutic responses. This information could be extremely relevant when aiming for more personalized or stratified treatment regimens for autoimmune arthritis.

The increased localization of SNPs in enhancer regions and the observations that proinflammatory cytokines can shape the enhancer repertoire suggest that autoimmune arthritis–associated enhancer alterations can be a cause as well as a consequence of the disease, and that it might be difficult to distinguish the one from the other. Furthermore, this indicates that (self)regulatory feedback loops can contribute to disease pathogenesis and thus suggests that it is important to disrupt these regulatory loops (Figure 3). This can be achieved by inhibiting (super)enhancer activity (e.g., by BET inhibitors). Compared to treatment with biologic agents, BET inhibitors might be favorable, as they preferentially inhibit

the expression of numerous disease-associated genes at once and inhibit the production of proinflammatory cytokines instead of inhibiting or blocking them after production. It could also be argued that combination therapy of BET inhibitors and biologic agents might be an even more powerful strategy, as biologic agents will prevent (super)enhancer formation by the inflammatory environment and thereby contribute to disruption of the regulatory feedback loop.

Although BET inhibitors seem highly effective in in vivo models of autoimmune arthritis, it remains to be established whether they will be as efficacious in a setting of autoimmune disease in humans. So far, the use of BET inhibitors in clinical trials for the treatment of severe cancers seems to be promising and to have limited side effects, such as thrombocytopenia, gastrointestinal adverse effects, and fatigue (84,85). However, it needs to be determined whether these side effects are acceptable for patients with autoimmune arthritis. Consistent with this, development of compounds with a higher selectivity for individual BET proteins, bromodomains, or novel targets will allow for more selective modulation of (super)-enhancer activity and thus for a more specific therapeutic application.

AUTHOR CONTRIBUTIONS

All authors were involved in drafting the article or revising it critically for important intellectual content, and all authors approved the final version to be published.

REFERENCES

1. Maurano MT, Humbert R, Rynes E, Thurman RE, Haugen E, Wang H, et al. Systematic localization of common disease-associated variation in regulatory DNA. Science 2012;337:1190–5.
2. Farh KK, Marson A, Zhu J, Kleinewietfeld M, Housley WJ, Beik S, et al. Genetic and epigenetic fine mapping of causal autoimmune disease variants. Nature 2014;518:337–43.
3. Stahl EA, Raychaudhuri S, Remmers EF, Xie G, Eyre S, Thomson BP, et al. Genome-wide association study meta-analysis identifies seven new rheumatoid arthritis risk loci. Nat Genet 2010;42:508–14.
4. Hinks A, Cobb J, Marion MC, Prahalad S, Sudman M, Bowes J, et al. Dense genotyping of immune-related disease regions identifies 14 new susceptibility loci for juvenile idiopathic arthritis. Nat Genet 2013;45:664–9.
5. Ombrello MJ, Remmers EF, Tachmazidou I, Grom A, Foell D, Haas JP, et al. HLA-DRB1*11 and variants of the MHC class II locus are strong risk factors for systemic juvenile idiopathic arthritis. Proc Natl Acad Sci U S A 2015;112:15970–5.
6. Cortes A, Hadler J, Pointon JP, Robinson PC, Karaderi T, Leo P, et al. Identification of multiple risk variants for ankylosing spondylitis through high-density genotyping of immune-related loci. Nat Genet 2013;45:730–8.
7. Bowes J, Budu-Aggrey A, Huffmeier U, Uebe S, Steel K, Hebert HL, et al. Dense genotyping of immune-related susceptibility loci reveals new insights into the genetics of psoriatic arthritis. Nat Commun 2015;6:6046.
8. Morris DL, Sheng Y, Zhang Y, Wang YF, Zhu Z, Tombleson P, et al. Genome-wide association meta-analysis in Chinese and European individuals identifies ten new loci associated with systemic lupus erythematosus. Nat Genet 2016;48:940–6.
9. Corradin O, Scacheri PC. Enhancer variants: evaluating functions in common disease. Genome Med 2014;6:85.
10. Trynka G, Sandor C, Han B, Xu H, Stranger BE, Liu XS, et al. Chromatin marks identify critical cell types for fine mapping complex trait variants. Nat Genet 2013;45:124–30.
11. Pers TH, Karjalainen JM, Chan Y, Westra HJ, Wood AR, Yang J, et al. Biological interpretation of genome-wide association studies using predicted gene functions. Nat Commun 2015;6:5890.
12. Li Y, Kellis M. Joint Bayesian inference of risk variants and tissue-specific epigenomic enrichments across multiple complex human diseases. Nucleic Acids Res 2016;44:e144.
13. Kumasaka N, Knights AJ, Gaffney DJ. Fine-mapping cellular QTLs with RASQUAL and ATAC-seq. Nat Genet 2016;48:206–13.
14. Okada Y, Muramatsu T, Suita N, Kanai M, Kawakami E, Iotchkova V, et al. Significant impact of miRNA–target gene networks on genetics of human complex traits. Sci Rep 2016;6:22223.
15. Finucane HK, Bulik-Sullivan B, Gusev A, Trynka G, Reshef Y, Loh PR, et al. Partitioning heritability by functional annotation using genome-wide association summary statistics. Nat Genet 2015;47:1228–35.
16. Alberts B, Johnson A, Lewis J, Raff M, Roberts K, Walter P. Molecular biology of the cell. 4th ed. New York: Garland Science; 2002.
17. Ernst J, Kheradpour P, Mikkelsen TS, Shoresh N, Ward LD, Epstein CB, et al. Mapping and analysis of chromatin state dynamics in nine human cell types. Nature 2011;473:43–9.
18. De Laat W, Dekker J. 3C-based technologies to study the shape of the genome. Methods 2012;58:189–91.
19. Andersson R, Gebhard C, Miguel-Escalada I, Hoof I, Bornholdt J, Boyd M, et al. An atlas of active enhancers across human cell types and tissues. Nature 2014;507:455–61.
20. Sanyal A, Lajoie BR, Jain G, Dekker J. The long-range interaction landscape of gene promoters. Nature 2012;489:109–13.
21. Heintzman ND, Stuart RK, Hon G, Fu Y, Ching CW, Hawkins RD, et al. Distinct and predictive chromatin signatures of transcriptional promoters and enhancers in the human genome. Nat Genet 2007;39:311–8.
22. Creyghton MP, Cheng AW, Welstead GG, Kooistra T, Carey BW, Steine EJ, et al. Histone H3K27ac separates active from poised enhancers and predicts developmental state. Proc Natl Acad Sci U S A 2010;107:21931–6.
23. Thurman RE, Rynes E, Humbert R, Vierstra J, Maurano MT, Haugen E, et al. The accessible chromatin landscape of the human genome. Nature 2012;489:75–82.
24. Hnisz D, Abraham BJ, Lee TI, Lau A, Saint-André V, Sigova AA, et al. Super-enhancers in the control of cell identity and disease. Cell 2013;155:934–47.
25. Parker SC, Stitzel ML, Taylor DL, Orozco JM, Erdos MR, Akiyama JA, et al. Chromatin stretch enhancer states drive cell-specific gene regulation and harbor human disease risk variants. Proc Natl Acad Sci U S A 2013;110:17921–6.
26. Whyte WA, Orlando DA, Hnisz D, Abraham BJ, Lin CY, Kagey MH, et al. Master transcription factors and mediator establish super-enhancers at key cell identity genes. Cell 2013;153:307–19.
27. Dukler N, Gulko B, Huang YF, Siepel A. Is a super-enhancer greater than the sum of its parts? Nat Genet 2016;49:2–3.
28. Shin HY, Willi M, Yoo KH, Zeng X, Wang C, Metser G, et al. Hierarchy within the mammary STAT5-driven Wap super-enhancer. Nat Genet 2016;48:904–11.
29. Hay D, Hughes JR, Babbs C, Davies JO, Graham BJ, Hanssen LL, et al. Genetic dissection of the α-globin super-enhancer in vivo. Nat Genet 2016;48:895–903.

30. Pott S, Lieb JD. What are super-enhancers? Nat Genet 2015;47: 8–12.
31. Lovén J, Hoke HA, Lin CY, Lau A, Orlando DA, Vakoc CR, et al. Selective inhibition of tumor oncogenes by disruption of super-enhancers. Cell 2013;153:320–34.
32. Schmidl C, Hansmann L, Lassmann T, Balwierz PJ, Kawaji H, Itoh M, et al. The enhancer and promoter landscape of human regulatory and conventional T-cell subpopulations. Blood 2014; 123:e68–78.
33. Vahedi G, Takahashi H, Nakayamada S, Sun H, Sartorelli V, Kanno Y, et al. STATs shape the active enhancer landscape of T cell populations. Cell 2012;151:981–93.
34. Fang Z, Hecklau K, Gross F, Bachmann I, Venzke M, Karl M, et al. Transcription factor co-occupied regions in the murine genome constitute T-helper-cell subtype-specific enhancers. Eur J Immunol 2015;45:3150–7.
35. Vahedi G, Kanno Y, Furumoto Y, Jiang K, Parker SC, Erdos MR, et al. Super-enhancers delineate disease-associated regulatory nodes in T cells. Nature 2015;520:558–62.
36. Medzhitov R, Horng T. Transcriptional control of the inflammatory response. Nat Rev Immunol 2009;9:692–703.
37. Kaikkonen MU, Spann NJ, Heinz S, Romanoski CE, Allison KA, Stender JD, et al. Remodeling of the enhancer landscape during macrophage activation is coupled to enhancer transcription. Mol Cell 2013;51:310–25.
38. Ostuni R, Piccolo V, Barozzi I, Polletti S, Termanini A, Bonifacio S, et al. Latent enhancers activated by stimulation in differentiated cells. Cell 2013;152:157–71.
39. Ramirez-Carrozzi VR, Nazarian AA, Li CC, Gore SL, Sridharan R, Imbalzano AN, et al. Selective and antagonistic functions of SWI/SNF and Mi-2β nucleosome remodeling complexes during an inflammatory response. Genes Dev 2006;20:282–96.
40. Brown JD, Lin CY, Duan Q, Griffin G, Federation AJ, Paranal RM, et al. NF-κB directs dynamic super enhancer formation in inflammation and atherogenesis. Mol Cell 2014;56:219–31.
41. Lavin Y, Winter D, Blecher-Gonen R, David E, Keren-Shaul H, Merad M, et al. Tissue-resident macrophage enhancer landscapes are shaped by the local microenvironment. Cell 2014;159: 1312–26.
42. Gosselin D, Link VM, Romanoski CE, Fonseca GJ, Eichenfield DZ, Spann NJ, et al. Environment drives selection and function of enhancers controlling tissue-specific macrophage identities. Cell 2014;159:1327–40.
43. Freudenberg J, Gregersen P, Li W. Enrichment of genetic variants for rheumatoid arthritis within T-cell and NK-cell enhancer regions. Mol Med 2015;21:180–4.
44. Gaffney DJ, Veyrieras JB, Degner JF, Pique-Regi R, Pai AA, Crawford GE, et al. Dissecting the regulatory architecture of gene expression QTLs. Genome Biol 2012;13:R7.
45. Patwardhan RP, Hiatt JB, Witten DM, Kim MJ, Smith RP, May D, et al. Massively parallel functional dissection of mammalian enhancers in vivo. Nat Biotechnol 2012;30:265–70.
46. Nicolae DL, Gamazon E, Zhang W, Duan S, Dolan ME, Cox NJ. Trait-associated SNPs are more likely to be eQTLs: annotation to enhance discovery from GWAS. PLoS Genet 2010;6: e1000888.
47. Veyrieras JB, Kudaravalli S, Kim SY, Dermitzakis ET, Gilad Y, Stephens M, et al. High-resolution mapping of expression-QTLs yields insight into human gene regulation. PLoS Genet 2008;4: e1000214.
48. Corradin O, Saiakhova A, Akhtar-Zaidi B, Myeroff L, Willis J, Cowper-Sal-lari R, et al. Combinatorial effects of multiple enhancer variants in linkage disequilibrium dictate levels of gene expression to confer susceptibility to common traits. Genome Res 2014;24:1–13.
49. Cavalli G, Hayashi M, Jin Y, Yorgov D, Santorico SA, Holcomb C, et al. MHC class II super-enhancer increases surface expression of HLA-DR and HLA-DQ and affects cytokine production in autoimmune vitiligo. Proc Natl Acad Sci U S A 2016;113:1363–8.
50. Wang S, Wen F, Tessneer KL, Gaffney PM. TALEN-mediated enhancer knockout influences TNFAIP3 gene expression and mimics a molecular phenotype associated with systemic lupus erythematosus. Genes Immun 2016;17:165–70.
51. Roberts AR, Vecellio M, Chen L, Ridley A, Cortes A, Knight JC, et al. An ankylosing spondylitis-associated genetic variant in the IL23R-IL12RB2 intergenic region modulates enhancer activity and is associated with increased Th1-cell differentiation. Ann Rheum Dis 2016;75:2150–6.
52. Peeters JG, Vervoort SJ, Tan SC, Mijnheer G, de Roock S, Vastert SJ, et al. Inhibition of super-enhancer activity in autoinflammatory site-derived T cells reduces disease-associated gene expression. Cell Rep 2015;12:1986–96.
53. Shi L, Zhang Z, Song L, Leung YT, Petri MA, Sullivan KE. Monocyte enhancers are highly altered in systemic lupus erythematosus. Epigenomics 2015;7:921–35.
54. Walsh AM, Whitaker JW, Huang CC, Cherkas Y, Lamberth SL, Brodmerkel C, et al. Integrative genomic deconvolution of rheumatoid arthritis GWAS loci into gene and cell type associations. Genome Biol 2016;17:79.
55. Ai R, Hammaker D, Boyle DL, Morgan R, Walsh AM, Fan S, et al. Joint-specific DNA methylation and transcriptome signatures in rheumatoid arthritis identify distinct pathogenic processes. Nat Commun 2016;7:11849.
56. Zeng L, Zhou MM. Bromodomain: an acetyl-lysine binding domain. FEBS Lett 2002;513:124–8.
57. Chapuy B, McKeown MR, Lin CY, Monti S, Roemer MG, Qi J, et al. Discovery and characterization of super-enhancer-associated dependencies in diffuse large B cell lymphoma. Cancer Cell 2013;24:777–90.
58. Delmore JE, Issa GC, Lemieux ME, Rahl PB, Shi J, Jacobs HM, et al. BET bromodomain inhibition as a therapeutic strategy to target c-Myc. Cell 2011;146:904–17.
59. Tough DF, Tak PP, Tarakhovsky A, Prinjha RK. Epigenetic drug discovery: breaking through the immune barrier. Nat Rev Drug Discov 2016;15:835–53.
60. Dawson MA, Prinjha RK, Dittmann A, Giotopoulos G, Bantscheff M, Chan WI, et al. Inhibition of BET recruitment to chromatin as an effective treatment for MLL-fusion leukaemia. Nature 2011;478:529–33.
61. Mele DA, Salmeron A, Ghosh S, Huang HR, Bryant BM, Lora JM. BET bromodomain inhibition suppresses TH17-mediated pathology. J Exp Med 2013;210:2181–90.
62. Bandukwala HS, Gagnon J, Togher S, Greenbaum JA, Lamperti ED, Parr NJ, et al. Selective inhibition of CD4+ T-cell cytokine production and autoimmunity by BET protein and c-Myc inhibitors. Proc Natl Acad Sci U S A 2012;109:14532–7.
63. Stanlie A, Yousif AS, Akiyama H, Honjo T, Begum NA. Chromatin reader Brd4 functions in Ig class switching as a repair complex adaptor of nonhomologous end-joining. Mol Cell 2014; 55:97–110.
64. Belkina AC, Blanton WP, Nikolajczyk BS, Denis GV. The double bromodomain protein Brd2 promotes B cell expansion and mitogenesis. J Leukoc Biol 2014;95:451–60.
65. Belkina AC, Nikolajczyk BS, Denis GV. BET protein function is required for inflammation: Brd2 genetic disruption and BET inhibitor JQ1 impair mouse macrophage inflammatory responses. J Immunol 2013;190:3670–8.
66. Barrett E, Brothers S, Wahlestedt C, Beurel E. I-BET151 selectively regulates IL-6 production. Biochim Biophys Acta 2014; 1842:1549–55.
67. Qiao Y, Giannopoulou EG, Chan CH, Park S, Gong S, Chen J, et al. Synergistic activation of inflammatory cytokine genes by interferon-γ-induced chromatin remodeling and Toll-like receptor signaling. Immunity 2013;39:454–69.
68. Nicodeme E, Jeffrey KL, Schaefer U, Beinke S, Dewell S, Chung CW, et al. Suppression of inflammation by a synthetic histone mimic. Nature 2010;468:1119–23.

69. Chan CH, Fang C, Qiao Y, Yarilina A, Prinjha RK, Ivashkiv LB. BET bromodomain inhibition suppresses transcriptional responses to cytokine-Jak-STAT signaling in a gene-specific manner in human monocytes. Eur J Immunol 2015;45:287–97.
70. Peeters J, Vervoort S, Mijnheer G, de Roock S, Vastert B, Nieuwenhuis E, et al. Autoimmune disease-associated gene expression is reduced by BET-inhibition. Genom Data 2015;7:14–7.
71. Klein K, Kabala PA, Grabiec AM, Gay RE, Kolling C, Lin LL, et al. The bromodomain protein inhibitor I-BET151 suppresses expression of inflammatory genes and matrix degrading enzymes in rheumatoid arthritis synovial fibroblasts. Ann Rheum Dis 2016;75:422–9.
72. Zhang Q, Qian J, Zhu Y. Targeting bromodomain-containing protein 4 (BRD4) benefits rheumatoid arthritis. Immunol Lett 2015;166:103–8.
73. Nadeem A, Al-Harbi NO, Al-Harbi MM, El-Sherbeeny AM, Ahmad SF, Siddiqui N, et al. Imiquimod-induced psoriasis-like skin inflammation is suppressed by BET bromodomain inhibitor in mice through RORC/IL-17A pathway modulation. Pharmacol Res 2015;99:248–57.
74. Park-Min KH, Lim E, Lee MJ, Park SH, Giannopoulou E, Yarilina A, et al. Inhibition of osteoclastogenesis and inflammatory bone resorption by targeting BET proteins and epigenetic regulation. Nat Commun 2014;5:5418.
75. Meng S, Zhang L, Tang Y, Tu Q, Zheng L, Yu L, et al. BET inhibitor JQ1 blocks inflammation and bone destruction. J Dent Res 2014;93:657–62.
76. O'Brien W, Fissel BM, Maeda Y, Yan J, Ge X, Gravallese EM, et al. RANK-independent osteoclast formation and bone erosion in inflammatory arthritis. Arthritis Rheumatol 2016;68:2889–900.
77. Mahdi H, Fisher BA, Källberg H, Plant D, Malmström V, Rönnelid J, et al. Specific interaction between genotype, smoking and autoimmunity to citrullinated α-enolase in the etiology of rheumatoid arthritis. Nat Genet 2009;41:1319–24.
78. Larochelle S, Amat R, Glover-Cutter K, Sansó M, Zhang C, Allen JJ, et al. Cyclin-dependent kinase control of the initiation-to-elongation switch of RNA polymerase II. Nat Struct Mol Biol 2012;19:1108–15.
79. Chipumuro E, Marco E, Christensen CL, Kwiatkowski N, Zhang T, Hatheway CM, et al. CDK7 inhibition suppresses super-enhancer-linked oncogenic transcription in MYCN-driven cancer. Cell 2014;159:1126–39.
80. Hellvard A, Zeitlmann L, Heiser U, Kehlen A, Niestroj A, Demuth HU, et al. Inhibition of CDK9 as a therapeutic strategy for inflammatory arthritis. Sci Rep 2016;6:31441.
81. Kruidenier L, Chung C, Cheng Z, Liddle J, Che K, Joberty G, et al. A selective jumonji H3K27 demethylase inhibitor modulates the proinflammatory macrophage response. Nature 2012;488:404–8.
82. Doñas C, Carrasco M, Fritz M, Prado C, Tejón G, Osorio-Barrios F, et al. The histone demethylase inhibitor GSK-J4 limits inflammation through the induction of a tolerogenic phenotype on DCs. J Autoimmun 2016;75:105–17.
83. Liu Z, Cao W, Xu L, Chen X, Zhan Y, Yang Q, et al. The histone H3 lysine-27 demethylase Jmjd3 plays a critical role in specific regulation of Th17 cell differentiation. J Mol Cell Biol 2015;7:505–16.
84. Berthon C, Raffoux E, Thomas X, Vey N, Gomez-Roca C, Yee K, et al. Bromodomain inhibitor OTX015 in patients with acute leukaemia: a dose-escalation, phase 1 study. Lancet Haematol 2016;3:e186–95.
85. Amorim S, Stathis A, Gleeson M, Iyengar S, Magarotto V, Leleu X, et al. Bromodomain inhibitor OTX015 in patients with lymphoma or multiple myeloma: a dose-escalation, open-label, pharmacokinetic, phase 1 study. Lancet Haematol 2016;3:e196–204.
86. Toniolo PA, Liu S, Yeh JE, Moraes-Vieira PM, Walker SR, Vafaizadeh V, et al. Inhibiting STAT5 by the BET bromodomain inhibitor JQ1 disrupts human dendritic cell maturation. J Immunol 2015;194:3180–90.
87. Dittmann A, Werner T, Chung CW, Savitski MM, Fälth Savitski M, Grandi P, et al. The commonly used PI3-kinase probe LY294002 is an inhibitor of BET bromodomains. ACS Chem Biol 2014;9:495–502.
88. Zhang G, Liu R, Zhong Y, Plotnikov AN, Zhang W, Zeng L, et al. Down-regulation of NF-κB transcriptional activity in HIV-associated kidney disease by BRD4 inhibition. J Biol Chem 2012;287:28840–51.
89. Lu P, Qu X, Shen Y, Jiang Z, Wang P, Zeng H, et al. The BET inhibitor OTX015 reactivates latent HIV-1 through P-TEFb. Sci Rep 2016;6:24100.
90. Khan YM, Kirkham P, Barnes PJ, Adcock IM. Brd4 is essential for IL-1β-induced inflammation in human airway epithelial cells. PLoS One 2014;9:e95051.

ARTHRITIS & RHEUMATOLOGY
Vol. 69, No. 10, October 2017, pp 1937–1948
DOI 10.1002/art.40196

A Phase III Study Evaluating Continuation, Tapering, and Withdrawal of Certolizumab Pegol After One Year of Therapy in Patients With Early Rheumatoid Arthritis

Michael E. Weinblatt,[1] Clifton O. Bingham III,[2] Gerd-Rüdiger Burmester,[3] Vivian P. Bykerk,[4] Daniel E. Furst,[5] Xavier Mariette,[6] Désirée van der Heijde,[7] Ronald van Vollenhoven,[8] Brenda VanLunen,[9] Cécile Ecoffet,[10] Christopher Cioffi,[9] and Paul Emery[11]

Objective. **In disease-modifying antirheumatic drug–naive patients with early rheumatoid arthritis (RA) who had achieved sustained low disease activity (a Disease Activity Score in 28 joints using the erythrocyte sedimentation rate of ≤3.2 at both week 40 and week 52) after 1 year of treatment with certolizumab pegol (CZP) at a standard dose (200 mg every 2 weeks plus optimized methotrexate [MTX]), we evaluated whether continuation of CZP treatment at a standard dose or at a reduced frequency (200 mg every 4 weeks plus MTX) was superior to stopping CZP (placebo plus MTX) in maintaining low disease activity for 1 additional year.**

Methods. **A total of 293 patients from period 1 of our study were re-randomized 2:3:2 in period 2 to CZP at a standard dose (n = 84), CZP at a reduced frequency (n = 127), or placebo plus MTX (CZP stopped) (n = 82). The primary end point was the percentage of patients who maintained low disease activity throughout weeks 52–104 without flares. We used a hierarchical testing scheme, comparing CZP at a standard dose with CZP stopped. If $P < 0.05$ was achieved, then CZP at a reduced frequency was compared with CZP stopped (nonresponder imputation).**

ClinicalTrials.gov identifier: NCT01521923.
Supported by UCB Pharma.

[1]Michael E. Weinblatt, MD: Brigham and Women's Hospital, Boston, Massachusetts; [2]Clifton O. Bingham III, MD: Johns Hopkins University, Baltimore, Maryland; [3]Gerd-Rüdiger Burmester, MD: Charité University Medicine Berlin, Berlin, Germany; [4]Vivian P. Bykerk, MD, FRCPC: Weill Cornell Medical College, New York, New York; [5]Daniel E. Furst, MD: David Geffen School of Medicine at University of California, Los Angeles; [6]Xavier Mariette, MD, PhD: Université Paris-Sud, AP-HP, Hôpitaux Universitaires Paris-Sud, INSERM U1184, Le Kremlin Bicêtre, France; [7]Désirée van der Heijde, MD, PhD: Leiden University Medical Center, Leiden, The Netherlands; [8]Ronald van Vollenhoven, MD, PhD: Amsterdam Rheumatology and Immunology Center, Amsterdam, The Netherlands; [9]Brenda VanLunen, MS, Christopher Cioffi, PhD: UCB Pharma, Raleigh, North Carolina; [10]Cécile Ecoffet, PharmD: UCB Pharma, Brussels, Belgium; [11]Paul Emery, MD, FRCP: University of Leeds and NIHR Leeds Musculoskeletal Biomedical Research Unit, Leeds Teaching Hospitals NHS Trust, Leeds, UK.

Dr. Weinblatt has received consulting fees, speaking fees, and/or honoraria from AbbVie, Amgen, Bristol-Myers Squibb, Roche (less than $10,000 each), Lilly, Pfizer, UCB Pharma, AstraZeneca, Merck, Novartis, Crescendo Bioscience, and MedImmune (more than $10,000 each). Dr. Bingham has received consulting fees, speaking fees, and/or honoraria from UCB Pharma (less than $10,000). Dr. Burmester has received consulting fees, speaking fees, and/or honoraria from AbbVie, Bristol-Myers Squibb, Celgene, MSD, UCB Pharma, Roche, Pfizer, and Lilly (less than $10,000 each). Dr. Bykerk has received consulting fees, speaking fees, and/or honoraria from Pfizer, AbbVie, Bristol-Myers Squibb, Sanofi, and UCB Pharma (less than $10,000 each). Dr. Furst has received consulting fees, speaking fees, and/or honoraria from Abbott, AbbVie, Amgen, Biogen, Bristol-Myers Squibb, Cytori, Gilead, GlaxoSmithKline, Janssen, NIH, Novartis, Pfizer, Roche/Genentech, and UCB Pharma (less than $10,000 each) and research grants from Abbott, Actelion, Amgen, Biogen, Bristol-Myers Squibb, GlaxoSmithKline, Novartis, Pfizer, Roche/Genentech, and UCB Pharma. Dr. Mariette has received consulting fees, speaking fees, and/or honoraria from Bristol-Myers Squibb, GlaxoSmithKline, Pfizer, and UCB Pharma (less than $10,000 each). Dr. van der Heijde has received consulting fees, speaking fees, and/or honoraria from AbbVie, Amgen, Astellas, AstraZeneca, Bristol-Myers Squibb, Boehringer Ingelheim, Celgene, Daiichi, Eli Lilly and Company, Galapagos, Gilead, Janssen, Merck, Novartis, Pfizer, Regeneron, Roche, Sanofi, and UCB Pharma (less than $10,000 each). Dr. van Vollenhoven has received consulting fees and/or honoraria from AbbVie, Biotest, Bristol-Myers Squibb, Celgene, Crescendo Bioscience, GlaxoSmithKline, Janssen, Lilly, Merck, Novartis, Pfizer, Roche, UCB Pharma, and Vertex (less than $10,000 each) and research grants from AbbVie, Amgen, Bristol-Myers Squibb, GlaxoSmithKline, Pfizer, Roche, and UCB Pharma. Ms VanLunen and Drs. Ecoffet and Cioffi own stock or stock options in UCB Pharma. Dr. Emery has received consulting fees and/or honoraria from Pfizer, MSD, AbbVie, Bristol-Myers Squibb, UCB Pharma, Roche, Novartis, Samsung, Sandoz, and Lilly (more than $10,000 each).

Results. **The 293 patients from period 1 represented 36% fewer patients than projected, yielding a smaller number of patients eligible for period 2. Higher proportions of patients treated with the standard and reduced frequency regimens maintained low disease activity than those who had stopped CZP (48.8% and 53.2%, respectively, versus 39.2% [$P = 0.112$ and $P = 0.041$, respectively; nominal P value, first hierarchical test not significant]). Similar trends were observed for radiographic nonprogression (change from baseline of ≤0.5 in modified Sharp/van der Heijde score; 79.2% and 77.9% of patients, respectively, versus 70.3%) and normative physical function (Health Assessment Questionnaire disability index score of ≤0.5; 71.4% and 70.6% of patients, respectively, versus 57.0%). Safety profiles were similar between all groups, with no new safety signals identified for continuing CZP to week 104. No deaths were reported.**

Conclusion. **The study failed to meet its primary end point. However, there were no clinically meaningful differences between the standard and reduced frequency doses of CZP plus MTX; both controlled RA more effectively than stopping CZP.**

With the current armamentarium of treatments for rheumatoid arthritis (RA), targeting achievement of low disease activity or disease remission is recommended and achievable in many patients. While there is agreement that the clinical response induced by biologic disease-modifying antirheumatic drugs (DMARDs) should ideally be sustained, there is currently no consensus regarding the length of time that defines a sustained response. Based on a state of enduring disease control, clinicians must also consider the possibility of successfully withdrawing or tapering therapy (i.e., decreasing dose or dosing frequency), a treatment concept referred to as the "induction-maintenance" approach.

Tapering therapies after achieving a desired treatment target has therefore become a topic of considerable interest; results of several recent trials have suggested that this may indeed be possible with several biologic agents, with some of these trials also focusing on patients with newly diagnosed RA (1). Applying such treatment strategies may confer significant benefits to individual patients through the reduction of medication dosage and the associated risks while maintaining a state of disease control, as well as through easing of the economic burden of the disease as a result of increased cost effectiveness of the treatment (2–5). Current recommendations issued by the American College of Rheumatology (ACR) and the European League Against Rheumatism (EULAR) (2,6) suggest continuation of therapy with only conditional recommendations for tapering, thereby implying that RA patients will thus spend long periods taking biologic agents.

The aim of the C-EARLY study was to advance potential care options with regard to the induction-maintenance concept by evaluating the early initiation of certolizumab pegol (CZP) in combination with optimized methotrexate (MTX), as well as subsequent continuation, tapering, or withdrawal of CZP, in a population of DMARD-naive patients with early RA at high risk of progressive disease. CZP is an Fc-free, PEGylated, anti–tumor necrosis factor (anti-TNF) biologic DMARD used to treat both established and early RA in combination with MTX (7–9). Period 1 of the C-EARLY study (NCT01519791) assessed the efficacy and safety of 1 year of CZP in combination with optimized MTX versus optimized MTX alone. Results from period 1 (9) showed that significantly higher proportions of patients treated with CZP plus MTX achieved clinical treatment targets such as sustained remission (28.9% had a Disease Activity Score in 28 joints [10] using the erythrocyte sedimentation rate [DAS28-ESR] of <2.6 at both week 40 and week 52; odds ratio [OR] 2.3 [95% confidence interval {95% CI} 1.50–3.47], $P < 0.001$) and sustained low disease activity (43.8% had a DAS28-ESR of ≤3.2 at both week 40 and week 52; OR 2.0 [95% CI 1.38–2.78], $P < 0.001$) than did their counterparts treated with placebo plus optimized MTX (15.0% had sustained remission and 28.6% had sustained low disease activity). There was also significant inhibition of the progression of articular structural damage and marked improvements in the physical function of the CZP-treated patients in comparison with the patients treated with optimized MTX alone (9).

Period 2 of the C-EARLY study (NCT01521923) was a continuation of period 1 for those patients who had achieved sustained low disease activity at both week 40 and week 52. We hypothesized that continuing the standard dose of CZP or reducing dosage frequency would be superior to withdrawal of CZP treatment in maintaining clinical response over an additional 52 weeks.

PATIENTS AND METHODS

Full details of patient eligibility and inclusion/exclusion criteria for the C-EARLY period 1 study (NCT01519791) have been reported previously (9). Briefly, eligible patients for the C-EARLY period 1 study had active RA according to the 2010

Address correspondence to Michael E. Weinblatt, MD, Division of Rheumatology, Immunology and Allergy, Brigham and Women's Hospital, Center for Arthritis and Joint Diseases, 75 Francis Street, PBB-B3, Boston, MA 02115. E-mail: mweinblatt@partners.org.

Submitted for publication December 20, 2016; accepted in revised form June 27, 2017.

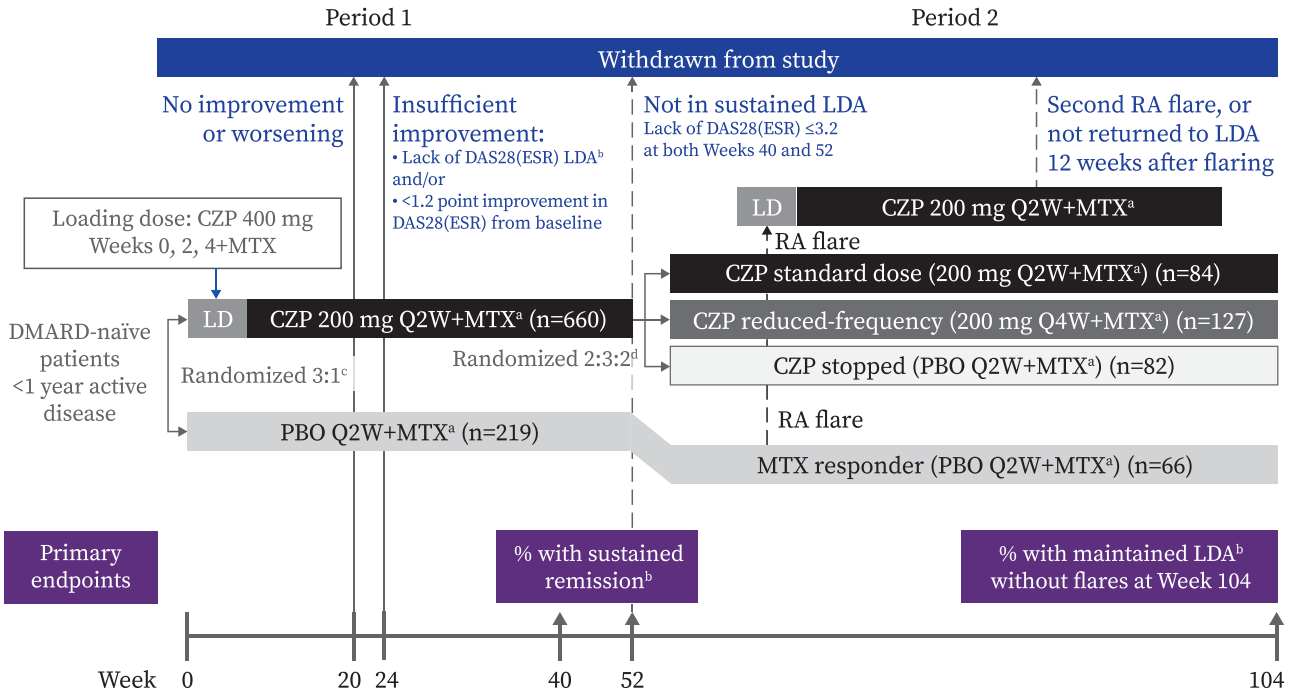

Figure 1. C-EARLY study design, showing set of enrolled patients. a = optimized methotrexate (MTX), defined as dose titrated from 10 mg/week (week 0) and increasing by 5 mg every 2 weeks (Q2W) to a maximum dose of 25 mg/week by weeks 6–8. Patients unable to tolerate ≥15 mg/week by week 8 were withdrawn from the study. b = low disease activity (LDA), defined as a Disease Activity Score in 28 joints using the erythrocyte sedimentation rate (DAS28-ESR) of ≤3.2. Low disease activity was considered to be maintained if continued throughout weeks 52–104 without disease flares. Patients reporting a flare had to meet the following 3 criteria at 2 consecutive visits 2 weeks apart: 1) an increase in the DAS28-ESR of ≥0.6 above the DAS28-ESR at week 52; 2) a DAS28-ESR of >3.2; and 3) in the investigator's judgment, an increase in the patient's rheumatoid arthritis (RA) activity. Sustained remission was defined as a DAS28-ESR of <2.6 at both week 40 and week 52. c = randomization stratified by time since RA diagnosis at baseline (≤4 months or >4 months). d = randomization stratified by time since RA diagnosis at baseline and by sustained remission status at week 52. CZP = certolizumab pegol; LD = loading dose; DMARD = disease-modifying antirheumatic drug; PBO = placebo; Q4W = every 4 weeks. See Patients and Methods for descriptions of groups.

ACR/EULAR classification criteria (11), were DMARD-naive with early disease (diagnosis <1 year prior to randomization, with 76% of patients randomized within 4 months of their diagnosis), and had poor prognostic factors for severe disease progression (positive at screening for rheumatoid factor or anti–citrullinated protein antibody). Use of intraarticular, intramuscular, or intravenous corticosteroids at any dose was prohibited in the C-EARLY study. Patients who had used intraarticular corticosteroids within 28 days of baseline (in C-EARLY period 1) were excluded from study enrollment. The maximum allowed dose of oral corticosteroids during the study was ≤10 mg/day prednisone or equivalent, with changes in dose allowed only between weeks 4 and 14 and between weeks 24 and 34 in period 1 of the study. Therefore, patients taking oral corticosteroids were to maintain their dosage during period 2.

Patients in C-EARLY period 1 who had achieved sustained low disease activity at weeks 40 and 52 (a key secondary end point of period 1) after 52 weeks of CZP plus optimized MTX treatment were eligible for enrollment into C-EARLY period 2. Sustained low disease activity was chosen as the entry criterion for period 2 as a clinically relevant criterion that can be used to identify patients who are proven responders to treatment.

Study design. C-EARLY period 2 was a phase III, multicenter, double-blind, placebo-controlled, randomized study conducted in Europe, Australia, North America, and Latin America at 103 participating sites (of the 181 that participated in C-EARLY period 1) from February 2013 to July 2015. Eligible patients from period 1 treated with 200 mg CZP every 2 weeks plus MTX were re-randomized at week 52 at a ratio of 2:3:2 to receive the standard CZP dose of 200 mg every 2 weeks plus MTX (CZP standard group), the reduced frequency regimen of 200 mg CZP every 4 weeks plus MTX (reduced frequency group), or CZP stopped (placebo every 2 weeks plus MTX) (CZP stopped group) (Figure 1). Re-randomization at week 52 was performed centrally using an Interactive Voice/Web Response System (IXRS) and stratified by time since RA diagnosis at baseline (≤4 months or >4 months) and week 52 sustained remission status. Week 0 (period 1) was considered the study baseline. Placebo plus MTX–treated patients from period 1 who had sustained low disease activity at both week 40 and week 52 entered period 2 as a separate group ("MTX responder" group), continued to receive placebo plus MTX only, and were not re-randomized. These patients were analyzed post hoc as a descriptive arm only.

The primary efficacy end point was the proportion of patients with sustained low disease activity (DAS28-ESR of ≤3.2 at both week 40 and week 52) who maintained low disease activity (DAS28-ESR of ≤3.2) for all 5 consecutive study visits to week 104 without flares. The key secondary end point was the proportion of patients with sustained remission (DAS28-ESR of <2.6 at both week 40 and week 52) who maintained remission (DAS28-

ESR of <2.6) for all 5 consecutive study visits to week 104 without flares. Additional secondary end points included the overall proportions of patients with low disease activity (DAS28-ESR of ≤3.2), remission (DAS28-ESR of <2.6), and normative physical function (defined as a Health Assessment Questionnaire disability index [HAQ DI] score [12] of ≤0.5), as well as the proportion of patients achieving radiographic nonprogression during period 2 (defined as a change in the modified Sharp/van der Heijde score [SHS] [13] of ≤0.5 from week 52 to week 104) and over the 2 years of the study (defined as a change from baseline in the SHS of ≤0.5 at week 104).

Time to flare was also explored as a secondary end point. An exploratory end point was the proportion of patients with disease flares who underwent reinduction with CZP treatment and subsequently re-achieved low disease activity. In this study, disease flares had to be self-reported by the patient at a study visit; solicitation by the study investigators was not mandated by the protocol. In addition, patients reporting a flare also had to meet the following 3 criteria at 2 consecutive visits 2 weeks apart: 1) an increase in the DAS28-ESR of ≥0.6 above the DAS28-ESR at week 52; 2) a DAS28-ESR of >3.2; and 3) in the investigator's judgment, an increase in the patient's RA activity. In the event of a confirmed disease flare, patients received a loading dose of CZP (400 mg at 3 subsequent visits) followed by the standard dose (200 mg every 2 weeks) until the end of the study. Patients who experienced flares twice or who did not re-achieve low disease activity within 12 weeks after reintroduction of CZP were withdrawn from the study.

Study drug. Placebo was supplied as 0.9% saline, and CZP was supplied as a 200 mg solution. Both were in prefilled syringes for subcutaneous injection and were administered up to week 102. Additional details regarding the initiating CZP dose have been described previously (9).

Oral MTX was dose-optimized throughout the study. MTX was initiated during period 1 (9) at 10 mg/week and escalated by 5 mg every 2 weeks to a maximum of 25 mg/week (with a minimum of 15 mg/week) by week 8, if tolerated. This maximum tolerated ("optimized") dose was maintained and continued to be administered every week from week 52 to week 103.

Study procedures and evaluations. In period 2, patients were assessed every 8–12 weeks at weeks 52, 64, 76, 84, 92, and 104. All study personnel were blinded with regard to treatment, except for a separate group who supervised and administered the study medication and determined ESR but who otherwise had no involvement in the study. Safety analyses included all treatment-emergent adverse events (AEs), serious AEs (SAEs), and severe treatment-emergent AEs, as well as clinical laboratory measurements.

Ethical approval. This study was conducted in accordance with the current version of the applicable regulatory and International Conference on Harmonisation Guidelines for Good Clinical Practice, the ethical principles that have their origin in the principles of the Declaration of Helsinki, and the local laws of the countries involved.

Statistical analysis. Based on a priori assumptions of response during period 1, 455 CZP-treated patients from period 1 were expected to be eligible for period 2, with 130, 195, and 130 patients randomly assigned to the CZP standard, reduced frequency, and CZP stopped groups, respectively. Given this sample size, power was calculated to be 99% and 92% to detect a statistically significant difference in maintaining low disease activity between the CZP standard and reduced frequency groups, respectively, compared with the CZP stopped group at a given $\alpha = 0.05$. Response rates of 95%, 90%, and 75% were assumed for the CZP standard, reduced frequency, and CZP stopped groups, respectively.

Statistical testing for the primary and key secondary end points was performed in a hierarchical manner. CZP standard versus CZP stopped was tested first. If the difference was significant at the $\alpha = 0.05$ level, then reduced frequency versus CZP stopped was tested. The full analysis set (those with sustained low disease activity at both week 40 and week 52 [per the IXRS] with valid post–week 52 efficacy measurements for DAS28-ESR) was used for all efficacy data except for radiographic data, which used the radiographic data set (those with valid radiographs at baseline, week 52, and week 104/withdrawal visit). Where reported in radiographic analyses, the MTX responder patients treated with placebo plus MTX throughout the study fulfilled the same criteria for the radiographic data set. The safety set comprised all patients who received at least 1 dose of study medication, and was used for the safety data.

A logistic regression model with factors for treatment, region, time since RA diagnosis at baseline, and week 52 sustained remission status was used for the primary and key secondary end points, as well as for the proportions of patients achieving low disease activity, remission, normative physical function, and radiographic nonprogression during period 2. The Clopper-Pearson method was used to generate 95% CIs for the logistic regression models.

Missing data from patients who entered period 2 but withdrew before the end of the study were imputed using nonresponder imputation for the primary and key secondary end points. Radiographic analyses used linear extrapolation. In post hoc analyses, last observation carried forward (LOCF) imputation was used for the proportions of patients achieving low disease activity, remission, and normative physical function.

RESULTS

Patient disposition and baseline characteristics. A total of 293 CZP-treated patients from period 1 were re-randomized at week 52 and enrolled in this study, with 84 patients in the CZP standard group, 127 patients in the reduced frequency group, and 82 patients in the CZP stopped group. These patients represent 44% of the 660 CZP-treated patients in period 1. However, this was 36% fewer than the planned randomizations of 130, 195, and 130 patients, respectively, due to fewer patients than projected with sustained low disease activity at the end of period 1. Of those who were re-randomized, 84, 126, and 79 patients comprised the full analysis set; 72, 113, and 75 patients comprised the radiographic set (see Supplementary Figure 1, available on the *Arthritis & Rheumatology* web site at http://onlinelibrary.wiley.com/doi/10.1002/art.40196/abstract).

In period 2, 14 of 84 patients (16.7%) in the CZP standard group, 15 of 127 patients (11.8%) in the reduced frequency group, 10 of 82 patients (12.2%) in the CZP

Table 1. Demographic and clinical characteristics of patients enrolled in C-EARLY period 2 at study baseline (entry to period 1) and week 52*

	CZP standard dose (n = 84)†	CZP reduced frequency (n = 126)†	CZP stopped (n = 79)†	MTX responders (n = 66)‡
Baseline demographics				
Age, mean ± SD years	49.1 ± 13.1	49.2 ± 12.5	47.6 ± 14.0	51.2 ± 13.7
Women, no. (%)	66 (78.6)	86 (68.3)	58 (73.4)	54 (81.8)
BMI, mean ± SD kg/m^2	28 ± 5.6§	27 ± 6.0	26 ± 4.5	28 ± 5.0
Time since RA diagnosis, mean ± SD months	2.5 ± 2.5	2.6 ± 2.8	2.9 ± 3.1	2.7 ± 2.8
Region, no. (%)				
Europe and Australia	57 (67.9)	85 (67.5)	59 (74.7)	42 (63.6)
Latin America and North America	27 (32.1)	41 (32.5)	20 (25.3)	24 (36.4)
Patient characteristics				
Oral corticosteroids, mean ± SD/median (range) mg/day				
Baseline	1.9 ± 3.5/0 (0–10.0)	1.6 ± 3.2/0 (0–10.0)	2.0 ± 3.5/0 (0–10.0)	1.4 ± 3.0/0 (0–10.0)
Taking oral corticosteroids, no. (%)	22 (26.2)	30 (23.8)	22 (27.8)	13 (19.7)
Week 52	1.3 ± 3.1/0 (0–10.0)	1.3 ± 2.9/0 (0–10.0)	1.5 ± 3.1/0 (0–10.0)	1.0 ± 2.5/0 (0–10.0)
Taking oral corticosteroids, no. (%)	13 (15.5)	25 (19.8)	18 (22.8)	11 (16.7)
Oral MTX dose, mean ± SD/median (range) mg/week‡	21.3 ± 4.3/24.1 (10.5–25.0)§	20.3 ± 4.4/20.0 (10.0–25.0)	20.9 ± 4.5/20.0 (10.0–25.0)¶	22.0 ± 3.9/25.0 (15.0–25.0)
Concomitant use of NSAIDs, no. (%)‡	52 (62.7)§	77 (60.6)#	46 (56.8)¶	43 (65.2)
RF positive (≥14 IU/ml) at baseline, no. (%)	82 (97.6)	120 (95.2)	79 (100.0)	63 (95.5)
ACPA positive (≥7 IU/ml) at baseline, no. (%)	77 (91.7)	112 (88.9)	68 (86.1)	59 (89.4)
TJC28, mean ± SD				
Baseline	13.0 ± 6.0	15.4 ± 5.7	14.1 ± 6.3	15.5 ± 6.6
Week 52	0.4 ± 0.7§	0.7 ± 1.3	0.4 ± 0.8	0.6 ± 1.3**
SJC28, mean ± SD				
Baseline	11.3 ± 5.3	12.4 ± 5.1	11.3 ± 4.8	11.9 ± 4.8
Week 52	0.3 ± 1.2§	0.5 ± 1.4	0.3 ± 0.7	0.7 ± 1.6**
ESR, mean ± SD mm/hour				
Baseline	47.9 ± 23.6	46.6 ± 21.7	46.1 ± 19.3	43.5 ± 18.6
Week 52	15.1 ± 13.2§	12.3 ± 8.4	13.2 ± 9.4	15.7 ± 11.0**
High-sensitivity CRP, mean ± SD/median (range) mg/liter				
Baseline	20.8 ± 23.8/11.9 (0.2–131.9)	21.0 ± 30.0/8.6 (0.2–171.0)	17.3 ± 25.6/7.9 (0.4–156.7)	16.0 ± 20.6/8.0 (0.3–97.2)
Week 52	3.1 ± 5.7/1.6 (0.2–41.3)§	2.5 ± 4.7/1.3 (0.2–43.4)	3.6 ± 9.5/1.6 (0.2–75.2)	4.0 ± 7.2/1.6 (0.2–50.4)**
DAS28-ESR, mean ± SD				
Baseline	6.4 ± 1.0	6.6 ± 0.8	6.5 ± 0.8	6.6 ± 0.9
Week 52	2.0 ± 0.7§	2.0 ± 0.6	1.9 ± 0.7	2.2 ± 0.7**
SHS, mean ± SD/median (range)				
Baseline	3.1 ± 5.4/1 (0–34)	4.5 ± 9.2/1.5 (0–64)	5.1 ± 8.5/1.5 (0–40)	6.0 ± 12.4/2.0 (0–70)
Week 52	3.3 ± 5.1/1.8 (0–34)	4.5 ± 8.9/1.5 (0–64)††	5.0 ± 7.4/2.5 (0–38)	6.8 ± 12.7/2.5 (0–70)
HAQ DI score, mean ± SD/median (range)				
Baseline	1.6 ± 0.6/1.6 (0.0–2.9)	1.6 ± 0.6/1.6 (0.1–3.0)	1.5 ± 0.5/1.5 (0.4–2.5)	1.5 ± 0.6/1.6 (0.0–2.6)
Week 52	0.3 ± 0.4/0.1 (0.0–1.6)§	0.3 ± 0.5/0.1 (0.0–2.0)	0.3 ± 0.5/0.1 (0.0–1.6)	0.4 ± 0.5/0.1 (0.0–1.4)**

* Nonsteroidal antiinflammatory drugs (NSAIDs) were defined by the preferred term M01A from the World Health Organization Drug Dictionary. CZP = certolizumab pegol; MTX = methotrexate; BMI = body mass index; RA = rheumatoid arthritis; RF = rheumatoid factor; ACPA = anti–citrullinated protein antibody; TJC28 = tender joint count in 28 joints; SJC28 = swollen joint count in 28 joints; ESR = erythrocyte sedimentation rate; CRP = C-reactive protein; DAS28-ESR = Disease Activity Score in 28 joints using the ESR; SHS = modified Sharp/van der Heijde score; HAQ DI = Health Assessment Questionnaire disability index.
† Full analysis set.
‡ Safety set.
§ n = 83.
¶ n = 81.
# n = 127.
** n = 65.
†† n = 123.

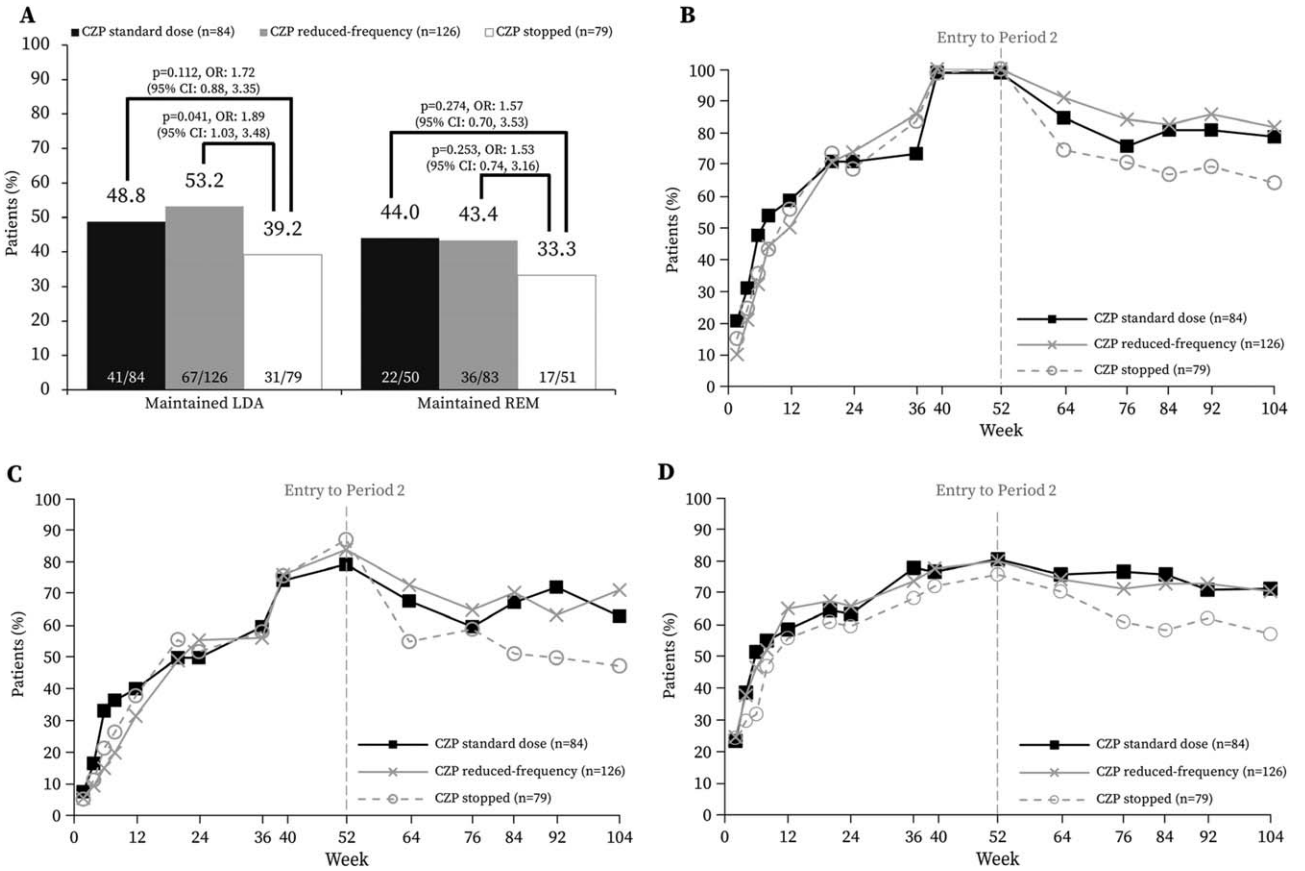

Figure 2. Clinical response in period 2 of the C-EARLY study, showing the full analysis set. **A,** Proportion of patients in whom low disease activity (LDA) was maintained, and proportion in whom remission (REM) was maintained, at week 104. Odds ratios (ORs) with 95% confidence intervals (95% CIs) and corresponding *P* values are from a logistic regression model with factors for treatment, region, time since rheumatoid arthritis (RA) diagnosis, and sustained remission status at week 52. Only patients with disease in sustained remission at week 52 were included in the analysis for maintained remission at week 104. Nonresponder imputation was used for missing data. **B,** Proportion of patients with low disease activity, defined as a Disease Activity Score in 28 joints using the erythrocyte sedimentation rate (DAS28-ESR) of ≤3.2. **C,** Proportion of patients with disease in remission, defined as a DAS28-ESR of <2.6. **D,** Proportion of patients with normative physical function, defined as a Health Assessment Questionnaire disability index score of ≤0.5. **B–D** show results of post hoc analyses. The last observation carried forward approach was used to impute missing data. CZP = certolizumab pegol. See Patients and Methods for descriptions of groups.

stopped group, and 7 of 66 MTX responder patients (10.6%) discontinued treatment by week 104. The most common reason for discontinuation was treatment-emergent AEs, in 4 of 84 patients (4.8%), 8 of 127 patients (6.3%), 7 of 82 patients (8.5%), and 2 of 66 patients (3.0%), respectively (see Supplementary Figure 1, http://onlinelibrary.wiley.com/doi/10.1002/art.40196/abstract). Patient demographic characteristics were generally well balanced across all treatment groups (Table 1) except for sex, with a higher percentage of women in the CZP standard group (66 of 84 [78.6%]) than in the reduced frequency group (86 of 126 [68.3%]) and CZP stopped group (58 of 79 [73.4%]). Disease characteristics at both baseline and week 52 (Table 1; also see Supplementary Table 1, http://onlinelibrary.wiley.com/doi/10.1002/art.40196/abstract) were also reasonably well balanced across all groups. The mean weekly optimized MTX dose was similar across all groups (mean 20–22 mg/week), with a maximum of 25 mg/week.

Efficacy. At week 104, 41 of 84 patients (48.8%) in the CZP standard group and 67 of 126 patients (53.2%) in the reduced frequency group had maintained low disease activity without flares, compared with 31 of 79 patients (39.2%) in the CZP stopped group ($P = 0.112$ and $P = 0.041$, respectively; nominal *P* value due to lack of significance in first hierarchical test). Of patients with sustained remission, 22 of 50 (44.0%) in the CZP standard group and 36 of 83 (43.4%) in the reduced frequency group maintained remission to week 104 without flares, compared with 17 of 51 patients

(33.3%) in the CZP stopped group ($P = 0.274$ and $P = 0.253$, respectively) (Figure 2A).

Despite the failure to achieve the primary end point, the overall data demonstrate that patients continuing CZP at either the standard or reduced frequency doses were better able to maintain clinical response compared with those who stopped CZP, as illustrated by low disease activity, remission, and normative physical function. In post hoc analyses using LOCF imputation, higher proportions of patients in the CZP standard and reduced frequency groups achieved low disease activity (66 of 84 [78.6%] and 103 of 126 [81.7%], respectively), remission (53 of 84 [63.1%] and 90 of 126 [71.4%], respectively), and normative physical function (60 of 84 [71.4%] and 89 of 126 [70.6%], respectively) at week 104 compared with those who stopped CZP (50 of 78 [64.1%; 1 patient's data missing] achieved low disease activity, 37 of 78 [47.4%; 1 patient's data missing] achieved remission, and 45 of 79 [57.0%] achieved normative physical function) (Figures 2B–D). Furthermore, mean DAS28-ESR and HAQ DI score values were also numerically lower throughout period 2 for patients continuing CZP treatment compared with those who stopped (see Supplementary Figure 2, http://onlinelibrary.wiley.com/doi/10.1002/art.40196/abstract).

Few patients exhibited radiographic progression in period 2 (change in SHS of >0.5 from week 52); these included 7 of 72 patients (9.7%) in the CZP standard group and 18 of 113 patients (15.9%) in the reduced frequency group, compared with 14 of 74 patients (18.9%) in the CZP stopped group. Over the 2 years of the study, patients continuing CZP treatment (in the CZP standard and reduced frequency groups) exhibited stabilization of structural damage, with numerically fewer patients (15 of 72 [20.8%] and 25 of 113 [22.1%], respectively) experiencing radiographic progression at week 104 (change in SHS of >0.5 from baseline) in comparison with patients who stopped CZP (22 of 74 [29.7%]) after week 52 (Figure 3).

Relatively few disease flares were recorded in patients during this study, which was possibly due to the limitation of the patients having to self-report flares to the investigator. Patients self-reporting flares included 7 of 84 (8.3%) in the CZP standard group, 3 of 126 (2.4%) in the reduced frequency group, and 10 of 79 (12.7%) in the CZP stopped group. Most flares occurred in these patients by week 64 (i.e., 12 weeks after the change in treatment dosing) (Figure 4). Patients with flares underwent re-induction with the standard dose of CZP (including a loading dose), and 80% of them (16 of 20; 7 in the CZP standard group, 1 in the reduced frequency group, and 8 in the CZP stopped group) subsequently achieved low disease activity again within 12 weeks.

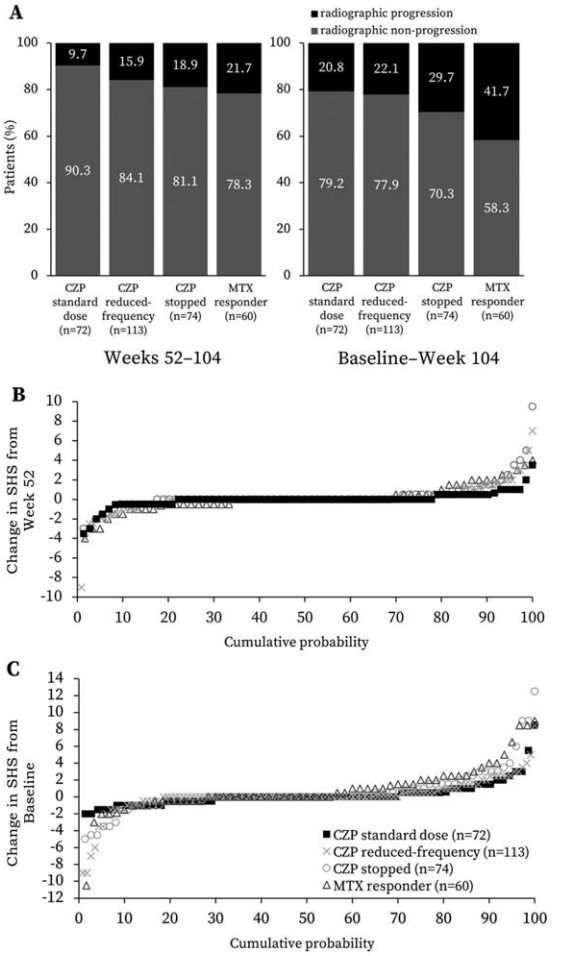

Figure 3. Radiographic progression in the C-EARLY study. Shown is the radiographic data set with methotrexate (MTX) responder patients meeting the same criteria (those who had valid radiographs at baseline, week 52, and week 104/withdrawal visit). **A,** Radiographic progression and nonprogression rates. **B,** Cumulative probability of change in modified Sharp/van der Heijde score (SHS) from week 52 to week 104. **C,** Cumulative probability of change in SHS from baseline to week 104. Results for MTX responder patients were obtained using post hoc analyses. Radiographic nonprogression was defined as a change in the SHS of ≤0.5 from baseline or week 52. Radiographic progression was defined as a change in the SHS of >0.5 from baseline or week 52. One outlier in the certolizumab pegol (CZP) stopped group was excluded. Linear extrapolation was used for missing data. Symbols in **B** and **C** represent values for each patient. See Patients and Methods for descriptions of groups.

MTX responders. Compared with the 44% of patients (293 of 660) in whom CZP treatment was initiated, a smaller proportion of patients who were only started on optimized MTX achieved sustained low disease activity at both week 40 and week 52 and continued to period 2, representing 30% (66 of 219) of the patients

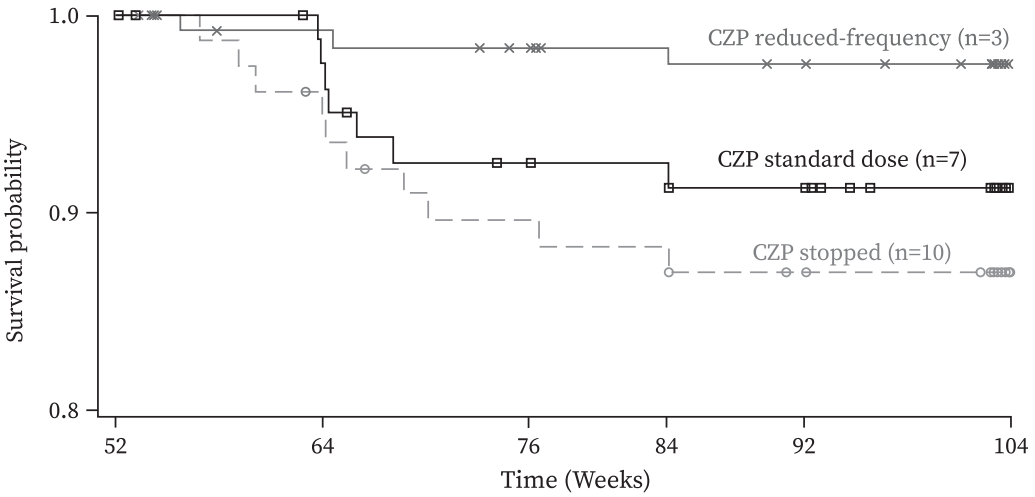

Figure 4. Kaplan-Meier plot of time to rheumatoid arthritis (RA) disease flare, showing the full analysis set. Disease flares had to be self-reported by the patient to the investigator at a study visit; solicitation by the study investigators was not mandated by the protocol. Patients reporting a flare had to meet the following 3 criteria at 2 consecutive visits 2 weeks apart: 1) an increase in the Disease Activity Score in 28 joints using the erythrocyte sedimentation rate (DAS28-ESR) of ≥0.6 above the DAS28-ESR at week 52; 2) a DAS28-ESR of >3.2; and 3) in the investigator's judgment, an increase in the patient's RA activity. Time to flare was defined as the time from the date of the week 52 injection of study medication to the date of the first flare visit for a confirmed flare. Patients who did not have a flare were censored at the date of the latest assessment of the DAS28-ESR. CZP = certolizumab pegol. See Patients and Methods for descriptions of groups.

treated with placebo plus MTX. Sixty patients were included in the radiographic analyses as a separate group. The safety set included 83 patients in the CZP standard group, 127 in the reduced frequency group, 81 in the CZP stopped group, and 66 MTX responder patients.

In this group of patients with an enhanced response to MTX therapy, exploratory, descriptive post hoc analyses were performed with LOCF imputation. At week 104, 81.3% (52 of 64; 2 patients' data missing), 59.4% (38 of 64; 2 patients' data missing), and 59.4% (38 of 64; 2 patients' data missing) of these patients had achieved good clinical response—low disease activity, remission, and normative physical function, respectively (see Supplementary Figure 3, http://onlinelibrary.wiley.com/doi/10.1002/art.40196/abstract). However, a higher proportion of MTX responders experienced radiographic progression over the 2 years of the study (41.7% [25 of 60]) compared with the 3 groups initially treated with CZP (Figure 3).

Safety. The incidence of treatment-emergent AEs in period 2 was similar across all 3 re-randomized groups: 63.9% of patients (53 of 83) in the CZP standard group, 63.8% (81 of 127) in the reduced frequency group, and 59.3% (48 of 81) in the CZP stopped group experienced treatment-emergent AEs, with a lower rate observed in the MTX responder group (50.0% [33 of 66]). Infections were the most frequent treatment-emergent AEs, with a higher proportion of patients continuing CZP treatment reporting infections (31.3% [26 of 83] in the CZP standard group and 38.6% [49 of 127] in the reduced frequency group), compared with 27.2% (22 of 81) of those who stopped CZP and 15.2% (10 of 66) of MTX responders. Serious infections and infestations were experienced by 1.2% of patients (1 of 83) in the CZP standard group, 0.8% (1 of 127) in the reduced frequency group, 2.5% (2 of 81) in the CZP stopped group, and 1.5% (1 of 66) of MTX responders. For patients exposed to CZP treatment at any time in period 2 (patients in the CZP standard and reduced frequency groups and any patients who received CZP after disease flares), the incidence rate of infections was 45.1 per 100 patient-years. The rate of SAEs was similar between all groups (4.8% of patients [4 of 83] in the CZP standard group, 7.1% [9 of 127] in the reduced frequency group, 7.4% [6 of 81] in the CZP stopped group, and 6.1% [4 of 66] of MTX responders).

There were higher rates of drug-related treatment-emergent AEs in the CZP-treated patients: 30.1% of patients (25 of 83) in the CZP standard group and 23.6% (30 of 127) in the reduced frequency group, compared with 17.3% (14 of 81) in the CZP stopped group and 15.2% (10 of 66) of MTX responders. Discontinuations due to treatment-emergent AEs followed a similar pattern, being observed in 2.4% of patients (2 of 83) in the CZP standard group and 5.5% (7 of 127) in the reduced frequency group, compared with 4.9% (4 of 81) in the CZP stopped group and 1.5% (1 of 66) of MTX responders.

Table 2. Summary of AEs*

	CZP standard dose (n = 83), no. (%)	CZP reduced frequency (n = 127), no. (%)	CZP stopped (n = 81), no. (%)	MTX responders (n = 66), no. (%)	CZP at any time (n = 223), no. (%)/ event rate†
Any treatment-emergent AEs (≥5% in any system organ class)	53 (63.9)	81 (63.8)	48 (59.3)	33 (50.0)	145 (65.0)/163.5
Gastrointestinal disorders	5 (6.0)	6 (4.7)	8 (9.9)	7 (10.6)	13 (5.8)/6.9
General disorders and administration site conditions	4 (4.8)	10 (7.9)	4 (4.9)	5 (7.6)	16 (7.2)/6.9
Infections and infestations	26 (31.3)	49 (38.6)	22 (27.2)	10 (15.2)	82 (36.8)/57.8
Injury, poisoning, and procedural complications	5 (6.0)	14 (11.0)	7 (8.6)	1 (1.5)	20 (9.0)/9.0
Investigations	11 (13.3)	12 (9.4)	8 (9.9)	8 (12.1)	23 (10.3)/13.3
Metabolism and nutrition disorders	3 (3.6)	14 (11.0)	6 (7.4)	5 (7.6)	17 (7.6)/9.0
Musculoskeletal and connective tissue disorders	8 (9.6)	12 (9.4)	12 (14.8)	6 (9.1)	23 (10.3)/12.0
Nervous system disorders	6 (7.2)	7 (5.5)	1 (1.2)	1 (1.5)	15 (6.7)/14.1
Renal and urinary disorders	5 (6.0)	2 (1.6)	0	1 (1.5)	8 (3.6)/3.9
Respiratory, thoracic, and mediastinal disorders	5 (6.0)	8 (6.3)	3 (3.7)	1 (1.5)	13 (5.8)/6.9
Skin and subcutaneous tissue disorders	8 (9.6)	9 (7.1)	3 (3.7)	2 (3.0)	17 (7.6)/8.6
Any malignant tumor	0	3 (2.4)	2 (2.5)	0	4 (1.8)/1.7
Serious treatment-emergent AEs	4 (4.8)	9 (7.1)	6 (7.4)	4 (6.1)	16 (7.2)/6.9
Serious infections and infestations	1 (1.2)	1 (0.8)	2 (2.5)	1 (1.5)	2 (0.9)/0.9
Discontinuation due to treatment-emergent AEs	2 (2.4)	7 (5.5)	4 (4.9)	1 (1.5)	10 (4.5)/NA
Treatment-emergent AEs requiring MTX reduction	0	5 (3.9)	1 (1.2)	1 (1.5)	NA
Drug-related treatment-emergent AEs	25 (30.1)	30 (23.6)	14 (17.3)	10 (15.2)	60 (26.9)/NA
Severe treatment-emergent AEs	1 (1.2)	4 (3.1)	2 (2.5)	3 (4.5)	5 (2.2)/NA
Deaths (treatment-emergent AEs leading to death)	0	0	0	1 (1.5)	0

* Safety set, comprising all patients who received at least 1 dose of study medication. Terms are from Medical Dictionary for Regulatory Activities, version 17.0. NA = not available.
† Includes adverse events (AEs) occurring in period 2 in any group after receiving certolizumab pegol (CZP) in period 2, including treatment-emergent AEs occurring after induction/reinduction with CZP for patients in the methotrexate (MTX) responder and CZP stopped groups. The total number of patients exposed to CZP in period 2 was used as the denominator; event rates are per 100 patient-years.

Continuing treatment at the standard dose was not associated with an increased risk of malignancies compared with that in the reduced frequency or CZP stopped groups. The overall incidence of malignant tumors was low, with 2.4% of patients (3 of 127) in the reduced frequency group (1 with breast cancer, 1 with lip squamous cell carcinoma, and 1 with myxoid liposarcoma) and 2.5% of patients (2 of 81) in the CZP stopped group (both with prostate cancer) reporting any malignant tumors. No patients developed malignancies in the CZP standard or MTX responder groups (Table 2), nor were there any reports of hematologic reactions or demyelinating disorders. No deaths were reported in the re-randomized treatment groups. There was 1 death due to cardiac failure in the MTX responder group 11 days after the final dose of study medication. The event was not considered to be related to study medication. The safety profile of MTX responder patients was comparable to that of the patients who were re-randomized.

DISCUSSION

C-EARLY is the first reported randomized, double-blind study with an anti-TNF biologic DMARD that compares the following 3 treatment strategies: continuation at full dose, tapering, or withdrawal of biologic therapy, in combination with optimized MTX, in maintaining low disease activity after 1 year of anti-TNF treatment in DMARD-naive patients with early and progressive, active RA. Previous studies, such as the Productivity and Remission in a Randomized Controlled Trial of Etanercept vs. Standard of Care in Early Rheumatoid Arthritis (PRIZE) study (14), compared the effect of tapering to a half dose (25 mg/week) of etanercept in combination with MTX with the effects of etanercept withdrawal (with MTX) and treatment with placebo alone. The Optimal Protocol for Methotrexate and Adalimumab Combination Therapy in Early Rheumatoid Arthritis (OPTIMA) study (15) compared the effect of continuing the full dose of adalimumab with the effects of biologic therapy withdrawal (with MTX) and MTX monotherapy.

The primary end point of the present study was not achieved. Fewer patients than projected from period 1 were eligible to enter period 2 (i.e., achieved sustained low disease activity), which may have resulted in an underpowered study. The use of sustained low disease activity at 2 consecutive study visits (both week 40 and week 52) as the entry criterion for period 2 was more difficult to achieve

than a single-visit criterion. The primary end point of period 2 was stringent, as patients were required to have maintained low disease activity throughout the entirety of the second year for 5 consecutive visits rather than just at a single study visit. The expected 20% and 15% differences between the CZP standard and reduced frequency groups versus the CZP stopped group in the maintenance of low disease activity to week 104 were also not realized. It should be noted that the study protocol design was undertaken in 2010, prior to the issuance of the 2011 ACR/EULAR guidelines (16), in which the Simplified Disease Activity Index (17) and Boolean-based definitions of low disease activity and remission superseded DAS28-ESR–based definitions as the closest reflection of "deep" disease control.

Nevertheless, results from period 2 of C-EARLY may still be of value to rheumatologists and patients, and could inform care options, since the data suggest that after 1 year of CZP treatment at the standard dose (200 mg every 2 weeks plus MTX), continuing treatment for an additional year at a reduced frequency dosage (200 mg every 4 weeks plus MTX) provided control of disease activity comparable to continuing treatment at the standard dose. A numerically higher proportion of patients continuing CZP at both dosages maintained clinical response and improvements in physical function in comparison with patients who stopped CZP treatment after 1 year.

Unexpectedly, a slightly higher proportion of patients continuing treatment at the reduced frequency dose achieved low disease activity, remission, and normative physical function compared with patients continuing a standard dose of CZP. This could have been due to the smaller-than-expected sample size, which led to more variability in the results. However, the numerical differences between the CZP standard dose and reduced frequency groups are small and not considered clinically meaningful.

Treatment of patients very early in the course of RA is associated with inhibition of the progression of joint damage as well as with better clinical outcomes. The 52-week data from C-EARLY period 1 revealed that early initiation of CZP plus MTX significantly inhibited joint destruction compared with no CZP treatment (9). The results of exploratory analyses from period 2 suggest that early initiation of CZP treatment can provide better and continued protection against progression of structural damage over a 2-year period, regardless of whether CZP was continued after 1 year. This difference was larger when compared with the descriptive arm of the MTX responders, even though those patients had a good clinical response with 2 years of therapy with optimized MTX alone. We note that our study was not powered to detect differences in radiographic progression rates; however, our findings are consistent with previous data from Japanese MTX-naive patients with early RA in the Certolizumab-Optimal Prevention of joint damage for Early RA (C-OPERA) trial, in which patients who had been treated with CZP plus MTX for 1 year exhibited lower rates of radiographic progression for 1 additional year after stopping CZP, in comparison with patients who had been receiving 2 years of MTX monotherapy (7,18). Similar results were also reported in DMARD-naive patients started on adalimumab plus MTX in the High Induction Therapy with Anti-Rheumatic Drugs (HIT HARD) study (19), although with a shorter (24-week) treatment duration.

In addition to the clinical efficacy described above, early initiation of CZP plus MTX has demonstrated benefits over optimized MTX alone in patient-reported measures such as workplace and household productivity (20). More patients who continued the standard or reduced frequency doses were able to maintain the initial 52-week improvements up to week 104 in comparison with patients who stopped CZP (21).

MTX therapy in this study was optimized by week 8 (i.e., patients were given the maximum tolerated dose, between 15 mg and 25 mg) (9). To our knowledge, the Dutch U-Act-Early study (22) and our international C-EARLY study are the only trials to mandate per-protocol optimization of MTX to achieve high levels of MTX dosage in DMARD- and MTX-naive patients with early RA. This optimization may in part explain the good clinical responses achieved by the MTX responders over the course of the 2 years.

There were low numbers of flares reported in this study, a limitation which was likely due to the requirement that flares be self-reported by the patient. The physicians involved in this study did not have a systematic evaluation method and were not mandated to formally assess disease flares. Although DAS components were measured at each study visit, the investigator remained blinded with regard to the DAS score. The low number of flares is not reflected by the relatively high proportion of patients (~50%) who did not maintain low disease activity. Of those who had disease flares, most (80%) achieved low disease activity again, and no safety issues were identified in those patients. However, because too few patients were identified as having a disease flare, no formal conclusions can be drawn about the safety and efficacy of reintroduction of the CZP standard dose in restoring low disease activity. Further evaluation of flares among the patients in this study is warranted. No new safety signals were identified for an additional 52 weeks of CZP plus MTX treatment, and the safety profile was consistent between all groups, including the MTX responder patients, who had been treated with placebo

plus optimized MTX for 2 years and had never received CZP.

Overall, the data from the first 52 weeks of the C-EARLY study demonstrated a favorable benefit-to-risk ratio for early initiation of CZP plus MTX therapy in DMARD-naive patients within 1 year of receiving their diagnosis of active RA with poor prognostic factors for disease progression (9). Clinical improvements achieved by the early initiation of CZP therapy during period 1 of the study were maintained in numerically more patients who continued at the standard or reduced frequency doses, thus providing support for the "induction-maintenance" approach for this specific population of patients with early RA who had never been exposed to either synthetic or biologic DMARDs. Exploratory analyses of radiographic data reported from period 2 suggested that early CZP initiation could be a better option for avoiding structural damage in this patient population compared with treatment with MTX alone, supporting the results reported from other studies (18). Further research would be needed to identify the characteristics of patients who would be able to stop CZP therapy successfully. By investigating the effect of continuing or tapering biologic DMARD therapy after reaching a disease target, our study contributes to the body of knowledge supporting the induction-maintenance treatment approach, and our results inform the evolving paradigms of disease management in RA while also highlighting the need for further clinical trial evidence.

ACKNOWLEDGMENTS

The authors thank the patients and their caregivers in addition to the investigators and their teams who contributed to this study. The authors acknowledge Simone E. Auteri, MSc (UCB Pharma, Brussels, Belgium) for publication coordination, and Lisa Wulund, PhD (Costello Medical Consulting Ltd, Cambridge, UK) for medical writing and editorial assistance in preparing the manuscript for publication based on the authors' input and direction.

AUTHOR CONTRIBUTIONS

All authors were involved in drafting the article or revising it critically for important intellectual content, and all authors approved the final version to be published. Dr. Weinblatt had full access to all of the data in the study and takes responsibility for the integrity of the data and the accuracy of the data analysis.

Study conception and design. Weinblatt, Bingham, Burmester, Bykerk, Furst, Mariette, van der Heijde, van Vollenhoven, VanLunen, Ecoffet, Cioffi, Emery.

Acquisition of data. Weinblatt, Bingham, Burmester, Bykerk, Furst, Mariette, van der Heijde, van Vollenhoven, VanLunen, Ecoffet, Cioffi, Emery.

Analysis and interpretation of data. Weinblatt, Bingham, Burmester, Bykerk, Furst, Mariette, van der Heijde, van Vollenhoven, VanLunen, Ecoffet, Cioffi, Emery.

ROLE OF THE STUDY SPONSOR

UCB Pharma sponsored the study, and all costs associated with the development of the manuscript were funded by UCB Pharma, including the funding of medical writing and editorial assistance by Costello Medical Consulting Ltd. UCB Pharma performed a full review to ensure that the data presented in the publication are scientifically, technically, and medically supportable and in compliance with the intellectual property rights of UCB Pharma. Furthermore, UCB Pharma ensured that the publication complies with applicable laws, regulations, guidelines, and good industry practice.

REFERENCES

1. Emamikia S, Arkema EV, Gyori N, Detert J, Chatzidionysiou K, Dougados M, et al. Induction maintenance with tumour necrosis factor-inhibitor combination therapy with discontinuation versus methotrexate monotherapy in early rheumatoid arthritis: a systematic review and meta-analysis of efficacy in randomised controlled trials. RMD Open 2016;2:e000323.
2. Singh JA, Saag KG, Bridges SL Jr, Akl EA, Bannuru RR, Sullivan MC, et al. 2015 American College of Rheumatology guideline for the treatment of rheumatoid arthritis. Arthritis Care Res (Hoboken) 2016;68:1–25.
3. Van Vollenhoven RF, Nagy G, Tak PP. Early start and stop of biologics: has the time come? BMC Med 2014;12:25.
4. Nagy G, van Vollenhoven RF. Sustained biologic-free and drug-free remission in rheumatoid arthritis, where are we now? Arthritis Res Ther 2015;17:181.
5. Schett G, Emery P, Tanaka Y, Burmester G, Pisetsky DS, Naredo E, et al. Tapering biologic and conventional DMARD therapy in rheumatoid arthritis: current evidence and future directions. Ann Rheum Dis 2016;75:1428–37.
6. Smolen JS, Landewe R, Bijlsma J, Burmester G, Chatzidionysiou K, Dougados M, et al. EULAR recommendations for the management of rheumatoid arthritis with synthetic and biological disease-modifying antirheumatic drugs: 2016 update. Ann Rheum Dis 2017;76:960–77.
7. Atsumi T, Yamamoto K, Takeuchi T, Yamanaka H, Ishiguro N, Tanaka Y, et al. The first double-blind, randomised, parallel-group certolizumab pegol study in methotrexate-naive early rheumatoid arthritis patients with poor prognostic factors, C-OPERA, shows inhibition of radiographic progression. Ann Rheum Dis 2016;75:75–83.
8. Smolen J, Landewe RB, Mease P, Brzezicki J, Mason D, Luijtens K, et al. Efficacy and safety of certolizumab pegol plus methotrexate in active rheumatoid arthritis: the RAPID 2 study. A randomised controlled trial. Ann Rheum Dis 2009;68:797–804.
9. Emery P, Bingham CO, Burmester GR, Bykerk VP, Furst DE, Mariette X, et al. Certolizumab pegol in combination with dose-optimised methotrexate in DMARD-naive patients with early, active rheumatoid arthritis with poor prognostic factors: 1-year results from C-EARLY, a randomised, double-blind, placebo-controlled phase III study. Ann Rheum Dis 2017;76:96–104.
10. Prevoo ML, van't Hof MA, Kuper HH, van Leeuwen MA, van de Putte LB, van Riel PL. Modified disease activity scores that include twenty-eight–joint counts: development and validation in a prospective longitudinal study of patients with rheumatoid arthritis. Arthritis Rheum 1995;38:44–8.
11. Aletaha D, Neogi T, Silman AJ, Funovits J, Felson DT, Bingham CO III, et al. 2010 rheumatoid arthritis classification criteria: an American College of Rheumatology/European League Against Rheumatism collaborative initiative. Arthritis Rheum 2010;62:2569–81.
12. Fries JF, Spitz P, Kraines RG, Holman HR. Measurement of patient outcome in arthritis. Arthritis Rheum 1980;23:137–45.

13. Van der Heijde DM, van Riel PL, Gribnau FW, Nuver-Zwart IH, van de Putte LB. Effects of hydroxychloroquine and sulphasalazine on progression of joint damage in rheumatoid arthritis. Lancet 1989;1:1036–8.
14. Emery P, Hammoudeh M, FitzGerald O, Combe B, Martin-Mola E, Buch MH, et al. Sustained remission with etanercept tapering in early rheumatoid arthritis. N Engl J Med 2014;371: 1781–92.
15. Smolen JS, Emery P, Fleischmann R, van Vollenhoven RF, Pavelka K, Durez P, et al. Adjustment of therapy in rheumatoid arthritis on the basis of achievement of stable low disease activity with adalimumab plus methotrexate or methotrexate alone: the randomised controlled OPTIMA trial. Lancet 2014; 383:321–32.
16. Felson DT, Smolen JS, Wells G, Zhang B, van Tuyl LH, Funovits J, et al. American College of Rheumatology/European League Against Rheumatism provisional definition of remission in rheumatoid arthritis for clinical trials. Arthritis Rheum 2011; 63:573–86.
17. Smolen JS, Breedveld FC, Schiff MH, Kalden JR, Emery P, Eberl G, et al. A Simplified Disease Activity Index for rheumatoid arthritis for use in clinical practice. Rheumatology (Oxford) 2003;42:244–57.
18. Atsumi T, Tanaka Y, Yamamoto K, Takeuchi T, Yamanaka H, Ishiguro N, et al. Clinical benefit of 1-year certolizumab pegol (CZP) add-on therapy to methotrexate treatment in patients with early rheumatoid arthritis was observed following CZP discontinuation: 2-year results of the C-OPERA study, a phase III randomised trial. Ann Rheum Dis 2017;76:1348–56.
19. Detert J, Bastian H, Listing J, Weiss A, Wassenberg S, Liebhaber A, et al. Induction therapy with adalimumab plus methotrexate for 24 weeks followed by methotrexate monotherapy up to week 48 versus methotrexate therapy alone for DMARD-naive patients with early rheumatoid arthritis: HIT HARD, an investigator-initiated study. Ann Rheum Dis 2013;72:844–50.
20. Emery P, Bingham CO, Bykerk VP, Furst DE, Mariette X, Purcaru O, et al. Improvements in patient-reported outcomes and workplace and household productivity following 52 weeks of treatment with certolizumab pegol in combination with methotrexate in DMARD-naïve early rheumatoid arthritis patients: results from the C-EARLY randomized, double-blind, controlled phase 3 study. Ann Rheum Dis 2015;74 Suppl 2:712.
21. Bingham CO, Emery P, Weinblatt M, Burmester GR, Furst DE, Mariette X, et al. Maintenance of improvements in workplace and household productivity and physical function at 2 years in early RA patients with severe progressive disease who achieved sustained low disease activity following 1 year of initial therapy, with two dosing frequencies of certolizumab pegol. Ann Rheum Dis 2016;75 Suppl 2:226.
22. Bijlsma JW, Welsing PM, Woodworth TG, Middelink LM, Petho-Schramm A, Bernasconi C, et al. Early rheumatoid arthritis treated with tocilizumab, methotrexate, or their combination (U-Act-Early): a multicentre, randomised, double-blind, double-dummy, strategy trial. Lancet 2016;388:343–55.

ARTHRITIS & RHEUMATOLOGY
Vol. 69, No. 10, October 2017, pp 1949–1959
DOI 10.1002/art.40186

Efficacy, Safety, Pharmacokinetics, and Pharmacodynamics of Filgotinib, a Selective JAK-1 Inhibitor, After Short-Term Treatment of Rheumatoid Arthritis

Results of Two Randomized Phase IIa Trials

Frédéric Vanhoutte,[1] Minodora Mazur,[2] Oleksandr Voloshyn,[3] Mykola Stanislavchuk,[4] Annegret Van der Aa,[1] Florence Namour,[5] René Galien,[5] Luc Meuleners,[1] and Gerben van 't Klooster[1]

Objective. **JAK inhibitors have shown efficacy in rheumatoid arthritis (RA). We undertook this study to test our hypothesis that selective inhibition of JAK-1 would combine good efficacy with a better safety profile compared with less selective JAK inhibitors.**

Methods. **In two 4-week exploratory, double-blind, placebo-controlled phase IIa trials, 127 RA patients with an insufficient response to methotrexate (MTX) received filgotinib (GLPG0634, GS-6034) oral capsules (100 mg twice daily or 30, 75, 150, 200, or 300 mg once daily) or placebo, added onto a stable regimen of MTX, to evaluate safety, efficacy, pharmacokinetics (PK), and pharmacodynamics (PD) of filgotinib. The primary efficacy end point was the number and percentage of patients in each treatment group meeting the American College of Rheumatology 20% improvement criteria (achieving an ACR20 response) at week 4.**

Results. **Treatment with filgotinib at 75–300 mg met the primary end point and showed early onset of efficacy. ACR20 response rates progressively increased to week 4, and the Disease Activity Score in 28 joints using the C-reactive protein (CRP) level decreased. Marked and sustained improvements were observed in serum CRP level and other PD markers. The PK of filgotinib and its major metabolite was dose proportional over the 30–300 mg range. Early side effects seen with other less selective JAK inhibitors were not observed (e.g., there was no worsening of anemia [JAK-2 inhibition related], no effects on liver transaminases, and no increase in low-density lipoprotein or total cholesterol). A limited decrease in neutrophils without neutropenia was consistent with immunomodulatory effects through JAK-1 inhibition. There were no infections. Overall, filgotinib was well tolerated. Events related to study drug were mild or moderate and transient during therapy, and the most common such event was nausea.**

Conclusion. **Selective inhibition of JAK-1 with filgotinib shows initial efficacy in RA with an encouraging safety profile in these exploratory studies.**

Rheumatoid arthritis (RA) is a chronic autoimmune inflammatory and degenerative joint disease that affects almost 1% of the adult population worldwide, with onset classically between ages 30 and 50 years and a higher prevalence in women (1,2). Current therapeutic approaches rely on disease-modifying antirheumatic drugs (DMARDs), such as methotrexate (MTX), as well as on biologic therapeutics that target tumor

ClinicalTrials.gov identifiers: NCT01384422; NCT01668641.
Supported by Galápagos.
[1]Frédéric Vanhoutte, MD, Annegret Van der Aa, PhD, Luc Meuleners, MSc, Gerben van 't Klooster, PhD: Galápagos NV, Mechelen, Belgium; [2]Minodora Mazur, MD: University Hospital, Chisinau, Moldova; [3]Oleksandr Voloshyn, MD: Chernivtsi Regional Clinical Hospital, Chernivtsi, Ukraine; [4]Mykola Stanislavchuk, MD: Vinnytsia Regional Clinical Hospital, Vinnytsia, Ukraine; [5]Florence Namour, MSc, René Galien, PhD: Galápagos SASU, Romainville, France.

Drs. Vanhoutte, Van der Aa, Galien, and van 't Klooster and Ms Namour and Mr. Meuleners own stock or stock options in Galápagos NV/SASU.

Address correspondence to Gerben van 't Klooster, PhD, Galápagos NV, Generaal de Wittelaan, L11 A3 Mechelen, Antwerp 2800, Belgium. E-mail: gerben.vantklooster@glpg.com.

Submitted for publication July 8, 2016; accepted in revised form June 15, 2017.

necrosis factor, interleukin-6 (IL-6), and T cell activation (abatacept, a CTLA-4Ig fusion protein) or that eliminate CD20+ B cells (rituximab) (3). Limitations with these treatments, such as waning efficacy over time, are observed in a proportion of patients and are associated with side effects (e.g., with MTX or steroids) and dosing inconvenience (injected biologic therapeutics). This has led to the exploration of alternative oral treatments. In the past decade, small-molecule inhibitors targeting kinases involved in disease-relevant signal transduction pathways such as p38 MAPK, Syk, and JAK have been evaluated in RA patients (4). In 2012, tofacitinib became the first JAK inhibitor approved by the US Food and Drug Administration for the treatment of RA.

JAKs are intracellular cytoplasmic tyrosine kinases, which signal in pairs and transduce cytokine signaling from membrane receptors via the STAT factors to the cell nucleus (5). JAK inhibitors block the signaling of various cytokines, growth factors, and hormones, including IL-6. Four different types of JAKs are known: JAK-1, JAK-2, JAK-3, and Tyk-2. JAK-1 is a novel target for inflammatory diseases, transducing cytokine-driven proinflammatory signaling, and for other diseases driven by JAK-mediated signal transduction. JAK-2 signals for a range of cytokines, often pairing with JAK-1, but only JAK-2 is downstream of a number of growth factors involved in hematopoiesis, such as erythropoietin (EPO) and thrombopoietin (TPO). JAK-3 is considered a prime target for immunosuppression, being downstream of proinflammatory cytokines, and also for immunoinflammatory diseases. While JAK-1, JAK-2, and Tyk-2 are expressed in many cell types and tissues, JAK-3 expression is restricted to the lymphoid lineage.

The first marketed JAK inhibitor, tofacitinib, inhibits JAK-3, JAK-1, and JAK-2 in descending order of potency. It is efficacious in treating the signs and symptoms of RA with a rapid onset of action. The most common adverse events (AEs) are infections and infestations, increases in serum creatinine, and a decrease in neutrophil counts (6,7). Tofacitinib also increases total cholesterol levels, with low-density lipoprotein (LDL) increases typically exceeding those for high-density lipoprotein (HDL). At doses exceeding the approved regimen of 5 mg twice daily, tofacitinib treatment was associated with anemia, which is thought to be linked to inhibition of JAK-2. Several other JAK inhibitors with varying selectivity profiles are in development for RA, including baricitinib (JAK-1/JAK-2 inhibitor), peficitinib (JAK-3/JAK-1/JAK-2 inhibitor), and ABT-494 (JAK-1 inhibitor) (8).

It has been hypothesized that inhibition of JAK-1 in particular is beneficial in RA treatment. While inhibition of JAK-2 and β-chain receptor–interacting family cytokines may contribute to the efficacy, it could also cause anemia, thrombocytopenia, and neutropenia by interfering with EPO signaling and with colony-stimulating factors (9,10).

We present the first data in RA patients for filgotinib (GLPG0634, GS-6034), a highly selective orally available JAK-1 inhibitor with ~30-fold selectivity for inhibition of JAK-1 relative to JAK-2 in human whole blood assays (11). Filgotinib is metabolized to form one major metabolite, which also exhibits selective JAK-1 inhibition, although with ~10-fold lower potency. As the overall exposure of this metabolite in humans is ~15-fold higher than that of filgotinib, the clinical activity likely results from the combination of the parent molecule and the major metabolite (12).

Filgotinib treatment of healthy volunteers for up to 10 days with doses up to 450 mg once daily was well tolerated and safe (13). Significant inhibition of JAK-1 pathways but not JAK-2 was found in pharmacodynamic (PD) assays at daily doses of ≥100 mg. In healthy volunteers, the exposure of filgotinib was well in excess of that showing efficacy in animal models of RA.

We present data obtained in two 4-week trials with filgotinib, one proof-of-concept study and one dose-ranging study. The observed safety and efficacy in RA patients provide initial evidence that selective inhibition of JAK-1 may represent a future way to treat RA.

PATIENTS AND METHODS

Study design and treatments. Two 4-week exploratory, randomized, double-blind, placebo-controlled studies were performed in RA patients who had an inadequate response to MTX. Both studies aimed to evaluate the preliminary safety, efficacy, pharmacokinetics (PK), and PD of filgotinib added onto a stable regimen of MTX. Study 1 (GLPG0634-CL-201; NCT01384422) was a phase IIa proof-of-concept study enrolling 36 patients and evaluating daily doses of 200 mg of filgotinib, given at 200 mg once daily or 100 mg twice daily, versus placebo. The study was conducted at a single site in the Republic of Moldova. Study 2 (GLPG0634-CL-202; NCT01668641) was a phase IIa dose-ranging study in which 91 patients were enrolled to receive filgotinib once daily at 30 mg, 75 mg, 150 mg, or 300 mg versus placebo. The study was conducted at 19 sites in 4 countries (Republic of Moldova, Ukraine, Russia, and Hungary). Eligible patients were randomly assigned to receive filgotinib or matching placebo as capsules for 4 weeks, with a 7–10-day follow-up period. For both studies, local ethics committees approved the protocol. All patients gave informed consent, and the studies were conducted in accordance with the Declaration of Helsinki.

Patients. Eligible patients fulfilled the American College of Rheumatology (ACR) 1987 revised criteria for the classification of RA (14), were ages 18–70 years, had ≥5 swollen joints and ≥5 tender joints, and had a serum C-reactive protein (CRP) level of ≥10 mg/liter at screening. Prior to screening, patients had to have received MTX for at least 12 weeks (study 2) or at least 6 months (study 1) and had to have been receiving a stable dose of 7.5–25 mg/week for at least 4 weeks. Oral steroids at a stable dose (≤10 mg once daily) for at least 4 weeks prior to screening and nonsteroidal antiinflammatory drugs at a stable dose for at least 2 weeks prior to screening were allowed. Major exclusion criteria were having received DMARDs other than MTX within the 8 weeks prior to screening or having received treatment with a biologic agent, with the exception of a biologic agent administered in a single clinical study setting >6 months prior to screening (>12 months prior to screening for rituximab or other cell-depleting agents).

Efficacy assessments. In both studies, the primary efficacy end point was the number and percentage of patients in each treatment group meeting the ACR 20% improvement criteria (achieving an ACR20 response) (15) at week 4. Secondary efficacy end points included the number and percentage of patients achieving an ACR20/ACR50/ACR70 response in each treatment group at weeks 1 and 2, and at week 4 for an ACR50/ACR70 response; the Disease Activity Score in 28 joints (16) using the CRP level (DAS28-CRP) at weeks 1, 2, and 4 and change from baseline in the DAS28-CRP at weeks 1, 2, and 4; and change from baseline and percentage of change from baseline at each visit in the individual components of the ACR core set of disease activity measures (17) (swollen joint count in 66 joints [SJC66], tender joint count in 68 joints [TJC68], physician's and patient's global assessments of disease activity and patient's assessment of pain on a visual analog scale, Health Assessment Questionnaire disability index [HAQ DI] score [18], and serum CRP level).

Safety assessments. AEs, vital signs, concomitant medications, routine hematology, serum biochemistry, coagulation, urinalysis, and other clinical laboratory test results were collected at each visit. A 12-lead electrocardiogram (EKG) was carried out at baseline and follow-up, and also at week 4 for study 1. A physical examination was performed at screening and follow-up. Data were summarized in a descriptive manner. No formal statistical comparisons of safety data were performed.

PK. Plasma concentrations of filgotinib and its major metabolite were measured in samples collected from a subset of patients in both studies (12 patients in study 1 and 15 patients in study 2) to assess individual steady-state PK of filgotinib and its major metabolite. Blood samples were collected before the morning dose and 1, 2, 3, 5, and 8 hours after the morning dose at either the week 2 or week 4 visit.

PD. In plasma samples collected at the baseline and week 4 visits from all participants in study 2, levels of various marker proteins were assessed using 2 different technologies. The measurement of the concentration of the YKL-40 factor (chitinase 3–like protein 1) was performed using an enzyme-linked immunosorbent assay from R&D Systems. The other markers (vascular cell adhesion molecule 1 [VCAM-1], intercellular adhesion molecule 1 [ICAM-1], matrix metalloproteinase 3 [MMP-3], haptoglobin, IL-18) were quantified at Myriad RBM. Data were normalized to the baseline value for each patient and plotted as the percentage of change from baseline.

Statistical analysis. No formal statistical power calculation was used to determine sample sizes, as the studies were purely exploratory. All randomized patients who received at least one dose of study drug and had at least one postbaseline efficacy assessment (intent-to-treat population) were included in the efficacy analyses. Descriptive statistics were calculated by dose for each of the PK parameters for filgotinib and its major metabolite. Exploratory between-group comparisons were also performed.

Safety data were summarized for all randomized patients who received at least one dose of study drug (safety population). Descriptive statistics were calculated for each parameter at every time point and in each treatment group. A treatment-emergent AE analysis was performed.

PD data are expressed as the mean ± SEM. Comparisons of PD marker levels among the groups were made using a nonparametric Kruskal-Wallis test followed by Dunn's post hoc test.

RESULTS

Patient disposition and baseline demographics. A total of 127 RA patients, 36 in study 1 and 91 in study 2, were randomly assigned to receive the study treatment. All randomized patients completed the studies, except for 1 patient in the placebo group of study 2 who discontinued for safety reasons (sponsor request) due to initial positive HIV test results and before negative confirmatory test results became available.

Of the 98 patients screened for study 1, 36 met the inclusion/exclusion criteria and were randomly assigned in a 1:1:1 ratio to receive 100 mg GLPG0634 twice daily, 200 mg GLPG0634 once daily, or placebo. All randomized subjects completed the study. While some differences in various parameters were apparent among the 3 treatment groups at baseline, DAS28-CRP scores reflecting overall RA activity status were very similar (see Supplementary Table 1, available on the *Arthritis & Rheumatology* web site at http://onlinelibrary.wiley.com/doi/10.1002/art.40186/abstract).

For study 2, 214 patients were screened, 91 of whom were randomly assigned in a 1:1:1:1:1 allocation ratio to receive treatment during 4 weeks with 30 mg GLPG0634, 75 mg GLPG0634, 150 mg GLPG0634, 300 mg GLPG0634, or placebo. The patients in the placebo group in study 2 were comparatively younger and had shorter disease duration than those in the filgotinib treatment groups; the group receiving 150 mg filgotinib showed more severe disease at baseline, with consistently higher values in DAS28-CRP, SJC66, TJC68, HAQ DI score, and CRP level (see Supplementary Table 1, http://onlinelibrary.wiley.com/doi/10.1002/art.

Table 1. Efficacy parameters at week 4*

	Study 1			Study 2				
	Placebo (n = 12)	Filgotinib 200 mg once daily (n = 12)	Filgotinib 100 mg twice daily (n = 12)	Placebo (n = 17)	Filgotinib 30 mg once daily (n = 17)	Filgotinib 75 mg once daily (n = 22)	Filgotinib 150 mg once daily (n = 15)	Filgotinib 300 mg once daily (n = 20)
ACR responders, no. (%)†								
ACR20	4 (33.3)	9 (75.0)	11 (91.7)	7 (41.2)	6 (35.3)	12 (54.5)	6 (40.0)	13 (65.0)
P vs. placebo	–	0.0995	0.0094	–	0.736	0.456	0.834	0.111
ACR50	1 (8.3)	2 (16.7)	4 (33.3)	1 (5.9)	2 (11.8)	6 (27.3)	0	9 (45.0)
P vs. placebo	–	>0.9999	0.3168	–	0.386	0.072	0.414	0.010
Secondary efficacy parameters, mean change from baseline								
Serum CRP, mg/liter	21.87	−35.05	−13.84	−5.74	−13.28	−15.09	−20.50	−20.98
P vs. placebo	–	<0.0001	<0.0001	–	0.121	0.006	0.012	<0.001
DAS28-CRP	−0.30	−2.23	−2.81	−1.20	−1.08	−1.72	−1.80	−2.25
P vs. placebo	–	<0.0001	<0.0001	–	0.893	0.119	0.278	0.005
SJC66	−4.6	−12.8	−15.4	−7.76	−6.24	−8.42	−10.52	−8.48
P vs. placebo	–	0.0365	0.0920	–	0.749	0.427	0.558	0.496
TJC68	−13.7	−23.1	−36.3	−9.71	−10.18	−13.72	−14.85	−14.68
P vs. placebo	–	0.2031	0.0080	–	0.886	0.161	0.492	0.225
Physician's global assessment of disease activity, 0–10-cm VAS	−5.8	−26.7	−35.0	−19.65	−9.76	−27.09	−24.87	−29.20
P vs. placebo	–	0.0043	0.0004	–	0.463	0.089	0.431	0.057
Patient's global assessment of disease activity, 0–10-cm VAS	−13.6	−23.8	−25.8	−17.82	−11.88	−21.00	−12.33	−25.85
P vs. placebo	–	0.1176	0.0918	–	0.563	0.364	0.681	0.122
Patient's assessment of pain, 0–10-cm VAS	−8.8	−24.3	−29.8	−11.65	−7.41	−21.27	−14.07	−29.85
P vs. placebo	–	0.0458	0.0167	–	0.596	0.089	0.727	0.015
HAQ DI score	−0.11	−0.57	−0.52	−0.31	−0.15	−0.47	−0.26	−0.68
P vs. placebo	–	0.0283	0.0272	–	0.540	0.065	0.596	0.014
EULAR cumulative score, good/moderate, %	NA	NA	NA	58.8	58.8	68.2	66.7	80.0
Remission rate, no. (%)‡	0	2 (16.7)	3 (25.0)	1 (5.9)	2 (11.8)	3 (13.6)	0	5 (25.0)

* Percentages are calculated based on the number of patients in the intent-to-treat population in each treatment group. SJC66 = swollen joint count in 66 joints; TJC68 = tender joint count in 68 joints; VAS = visual analog scale; HAQ DI = Health Assessment Questionnaire disability index; EULAR = European League Against Rheumatism; NA = not available.

† The last observation carried forward rule is applied to each component variable used to calculate the number and percentage of patients in each treatment group meeting the American College of Rheumatology 20% or 50% improvement criteria (achieving an ACR20 or ACR50 response).

‡ A Disease Activity Score in 28 joints using the C-reactive protein level (DAS28-CRP) of <2.6.

40186/abstract). In both studies, all participants were Caucasian and the majority were women.

Efficacy findings. In study 1 at the end of 4 weeks of treatment, >83% of the filgotinib-treated patients achieved an ACR20 response, which was statistically significantly different compared to placebo. In study 2 at week 4 of treatment, the majority of patients receiving 300 mg filgotinib (65%) achieved an ACR20 response, but the difference from the placebo group was not statistically significant (Table 1). In all treatment groups for both studies, the ACR20 response rate tended to increase progressively from week 1 to week 4, although in the 300 mg group the peak response was already reached at week 2, and it was maintained at week 4 (Figure 1). Within the filgotinib treatment groups, an increasing ACR20 response rate with increasing dose was observed with the exception of the 150 mg dose.

The antiinflammatory effect of filgotinib was confirmed by changes in secondary efficacy parameters by week 4 (Table 1). In both studies, within 1 week of treatment, mean serum CRP levels progressively and consistently decreased from baseline in all filgotinib dose groups, and these lower CRP levels were sustained throughout the remaining study treatment period. In both studies, dose-dependent decreases in DAS28-CRP scores were apparent within 1 week and became more pronounced from week 1 to week 4 for the filgotinib-treated groups. Within the 4-week treatment duration, a proportion of patients (up to 25% in the 300 mg group)

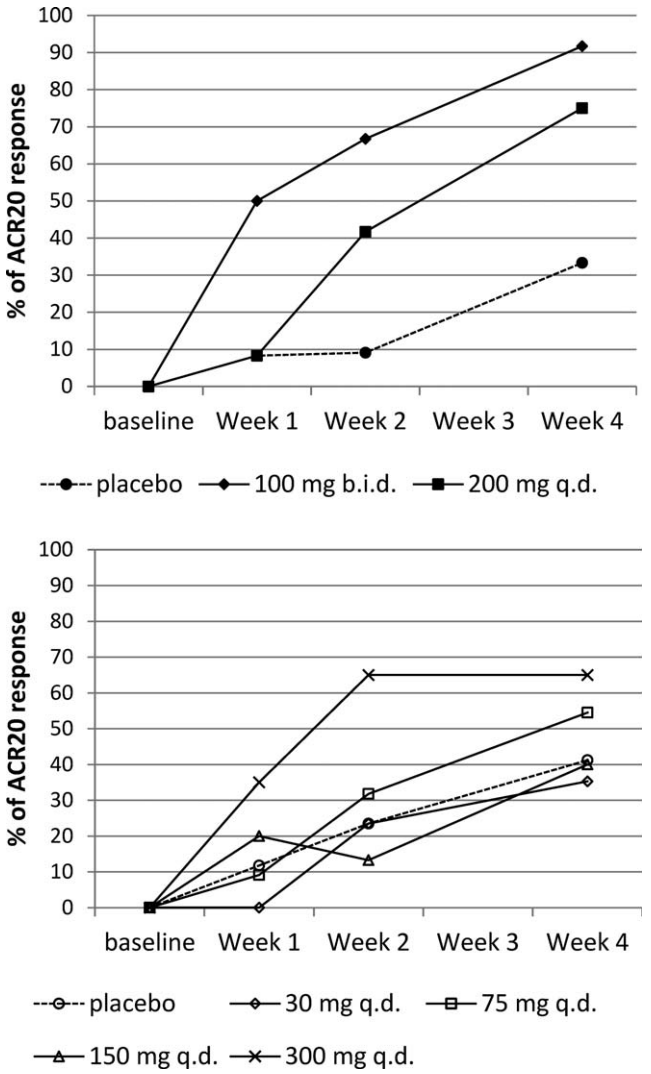

Figure 1. Percentage of patients in each treatment group in study 1 (top) and study 2 (bottom) meeting the American College of Rheumatology 20% improvement criteria (achieving an ACR20 response) at each visit. bid = twice daily; qd = once daily.

achieved remission (DAS28-CRP <2.6). In the 150 mg filgotinib group, which had the highest level of disease activity at baseline, relevant improvements in patient's global assessment of disease activity, patient's assessment of pain, and HAQ DI score were not achieved after 4 weeks of treatment, while numerical improvements were found in serum CRP levels, physician's global assessment of disease activity, TJC68, and SJC66.

Safety findings. Filgotinib was generally well tolerated. All reported treatment-emergent AEs were mild or moderate and transient during therapy. No study participant permanently discontinued treatment due to treatment-emergent AEs. One patient in the 300 mg group (study 2) had a 1-day treatment interruption because of nausea, and 1 patient receiving placebo in study 1 was reported as having an insect bite (serious AE), resulting in a temporary treatment interruption.

Of the patients in study 1, 16 (44.4%) had at least 1 treatment-emergent AE, while in study 2, 30 patients (33.0%) experienced at least 1 treatment-emergent AE (see Supplementary Table 2, http://onlinelibrary.wiley.com/doi/10.1002/art.40186/abstract). Although no notable dose relationship trends were observed in the incidences of treatment-emergent AEs, the highest incidence of treatment-emergent AEs in study 2 was observed at a dose of 300 mg (45.0%). In study 1, treatment-emergent AEs considered by the investigator to be at least possibly related to study drug were reported in 9 patients (25.0%) (Table 2). All drug-related treatment-emergent AEs were reported in 1 patient at most, except for nausea (n = 4) and asthenia (n = 2). In study 2, treatment-emergent AEs considered to be at least possibly related to study drug were reported in 11 patients (12.1%) (Table 2). The only drug-related treatment-emergent AE reported by >1 patient was nausea (n = 2). One case of cystitis, which resolved during the study, was reported in the 300 mg group.

Hematologic evaluation during filgotinib treatment showed a mild mean decrease in platelets and in neutrophils but no neutropenia (Table 3). Lymphocytes and lymphocyte subpopulations were unaffected. Mean hemoglobin levels increased slightly with filgotinib treatment.

No relevant abnormalities in serum biochemistry were reported, and there were no trends indicating a difference between placebo and filgotinib treatment. Importantly, this included a lack of changes on liver function tests (transaminases). Slight variations were observed in total cholesterol and LDL levels (Table 3). Increases in LDL or total cholesterol observed at week 4 were generally similar for placebo and filgotinib treatment groups. An apparent dose response was observed for increase in HDL levels. HDL tended to increase more in filgotinib-treated patients than in placebo-treated patients (2% on average at week 4 versus baseline), with an ~15% increase at 200 mg and a >30% increase at 300 mg.

Incidental laboratory abnormalities were reported as treatment-emergent AEs without apparent relationship to dose, including a single case of anemia at 75 mg and a single case of increased aspartate aminotransferase at 30 mg; the latter normalized during treatment. Hypercholesterolemia was reported once in the 75 mg group and once in the placebo group.

Table 2. Incidence of treatment-related treatment-emergent AEs by system organ class and preferred term (regardless of intensity)*

	Study 1			Study 2				
System organ class, preferred term	Placebo (n = 12)	Filgotinib 200 mg once daily (n = 12)	Filgotinib 100 mg twice daily (n = 12)	Placebo (n = 17)	Filgotinib 30 mg once daily (n = 17)	Filgotinib 75 mg once daily (n = 22)	Filgotinib 150 mg once daily (n = 15)	Filgotinib 300 mg once daily (n = 20)
Any AE	4 (33.3)	2 (16.7)	3 (25.0)	1 (5.9)	3 (17.6)	3 (13.6)	1 (6.7)	3 (15.0)
Blood and lymphatic system disorders	1 (8.3)	0	0	0	0	1 (4.5)	0	0
Thrombocytopenia	1 (8.3)	0	0	0	0	0	0	0
Anemia	0	0	0	0	0	1 (4.5)	0	0
Ear and labyrinth disorders	1 (8.3)	0	0	0	0	0	0	0
Vertigo	1 (8.3)	0	0	0	0	0	0	0
Gastrointestinal disorders	0	2 (16.7)	2 (16.7)	1 (5.9)	1 (5.9)	2 (9.1)	1 (6.7)	2 (10.0)
Nausea	0	2 (16.7)	2 (16.7)	0	0	0	1 (6.7)	1 (5.0)
Abdominal pain, upper	0	1 (8.3)	0	1 (5.9)	0	0	0	0
Abdominal discomfort	0	0	1 (8.3)	0	0	0	0	0
Duodenogastric reflux	0	0	0	0	0	1 (4.5)	0	0
Gastritis	0	0	0	0	1 (5.9)	0	0	0
Gastrointestinal pain	0	0	0	0	0	0	0	1 (5.0)
Gingival bleeding	0	0	0	0	0	1 (4.5)	0	0
General disorders and administration site reactions	2 (16.7)	0	0	0	0	0	0	0
Asthenia	2 (16.7)	0	0	0	0	0	0	0
Infections and infestations	0	0	0	0	0	0	0	1 (5.0)
Cystitis	0	0	0	0	0	0	0	1 (5.0)
Laboratory findings	2 (16.7)	0	1 (8.3)	0	2 (11.8)	0	0	0
Lipase increased	1 (8.3)	0	1 (8.3)	0	0	0	0	0
Aspartate aminotransferase increased	0	0	0	0	1 (5.9)	0	0	0
Blood amylase increased	1 (8.3)	0	0	0	0	0	0	0
Blood triglycerides increased	0	0	0	0	1 (5.9)	0	0	0
Musculoskeletal and connective tissue disorders	1 (8.3)	0	0	0	0	0	0	0
Arthralgia	1 (8.3)	0	0	0	0	0	0	0
Nervous system disorders	1 (8.3)	1 (8.3)	1 (8.3)	0	0	0	0	0
Headache	1 (8.3)	1 (8.3)	0	0	0	0	0	0
Dysgeusia	0	0	1 (8.3)	0	0	0	0	0
Somnolence	0	0	1 (8.3)	0	0	0	0	0
Renal and urinary disorders	0	0	0	0	0	0	0	1 (5.0)
Cystitis, noninfectious	0	0	0	0	0	0	0	1 (5.0)

* Adverse events (AEs) were classified as treatment-emergent if they started on or after the date of the first dose of study treatment. AEs with partial or missing start dates were classified as treatment-emergent unless the nonmissing components of the start date confirmed otherwise. A patient with >1 treatment-emergent AE with the same preferred term was counted once for that term. A patient with >1 treatment-emergent AE under a system organ class was counted once for that class. Values are the number (%) of patients.

No clinically relevant trends or changes were observed over time in vital signs values and EKG parameters. Both angina pectoris and hypertension were reported once. These were reported as not being drug related. No clinically relevant treatment-emergent urinalysis abnormalities or clinically significant physical examination findings were observed during the treatment phase.

PK findings. Steady-state PK of filgotinib and its major metabolite was investigated in a subset of 27 patients included in study 1 or study 2 (Table 4). Exposure to filgotinib and its major metabolite increased essentially in proportion to the dose within the 30–300 mg dose range. Given the low number of patients per treatment group (n = 2 to n = 6) and the variability observed in filgotinib PK parameters, these results should be interpreted with caution. At steady state, attained within 2 days and 4 days of dosing for filgotinib and its metabolite, respectively, exposure to the major metabolite was 13-fold higher than exposure to the parent filgotinib within the 75–300 mg dose range.

PD findings. The concentration of several known markers of RA and of inflammation was measured in plasma from participants in study 2 treated with filgotinib at 75, 150, or 300 mg or treated with placebo. Data presented in Figure 2 demonstrate a dose-dependent effect of filgotinib on levels of these circulating markers after 4 weeks of treatment.

Table 3. Selected laboratory safety and hematologic findings during 4 weeks of filgotinib treatment*

	Placebo (n = 28)†	Filgotinib 30 mg once daily (n = 17)	Filgotinib 75 mg once daily (n = 21)	Filgotinib 150 mg once daily (n = 14)	Filgotinib 200 mg once daily (n = 12)	Filgotinib 100 mg twice daily (n = 12)	Filgotinib 300 mg once daily (n = 20)
Hemoglobin, gm/liter							
Baseline	114	124	122	125	113	112	125
Change, day 28	−0.6	−0.3	2.0	−1.0	7.8	3.0	4.4
Neutrophils, $\times 10^9$/liter							
Baseline	5.42	4.85	5.41	5.59	5.10	4.94	5.00
Change, day 28	0.17	−0.65	−0.74	−1.37	−1.21	−1.45	−1.13
Platelets, $\times 10^9$/liter							
Baseline	307	279	294	289	295	287	304
Change, day 28	−19	−18	−35	−32	−33	−35	−58
Creatinine, μmoles/liter							
Baseline	58.1	65.1	64.4	61.3	68.7	70.8	60.1
Change, day 28	−2.32	1.47	5.18	4.50	5.47	−6.98	6.90
LDL cholesterol, mmoles/liter							
Baseline	2.70	3.39	3.22	3.01	3.06	2.77	2.82
Change, day 28	0.05	0.25	0.14	0.01	−0.25	0.07	0.37
HDL cholesterol, mmoles/liter							
Baseline	1.41	1.40	1.46	1.46	1.54	1.52	1.36
Change, day 28	0.01	0.03	0.11	0.07	0.16	0.20	0.48

* Values are the mean. LDL = low-density lipoprotein; HDL = high-density lipoprotein.
† Pooled placebo-treated patients from study 1 and study 2.

DISCUSSION

Less selective JAK inhibitors like tofacitinib have shown an early onset of action and long-term efficacy in RA; however, dose levels were limited by side effects. We have targeted JAK-1 with selective inhibition based on the hypothesis that JAK-1 is the predominant JAK family member in inflammatory pathways and autoimmune pathology, while a cleaner safety profile may be achieved by avoiding inhibition of other JAK types.

We have described a 4-week proof-of-concept study testing the hypothesis of the efficacy of selective JAK-1 inhibition in the treatment of RA, followed by a study further exploring the preliminary efficacy, safety, PK, and PD of the compound over a 30–300 mg dose range. Both phase IIa trials were exploratory, randomized, double-blind, placebo-controlled studies in patients with active RA with an inadequate response to MTX who continued their stable dose of MTX for the duration of the study. As the same population has been studied in initial explorations of other JAK inhibitors in RA, a global comparison of results after 4 weeks of treatment was possible.

While we recognized that the small number of patients treated for a short period of time was insufficient to reach maximal efficacy levels or to obtain a full safety picture, we envisioned that the rapid onset of action of JAK inhibitors would enable a rapid

Table 4. Steady-state pharmacokinetic parameters of filgotinib and its major metabolite after once-daily and twice-daily dosing with filgotinib*

	Filgotinib 30 mg once daily (study 2) (n = 3)	Filgotinib 75 mg once daily (study 2) (n = 2)	Filgotinib 100 mg twice daily (study 1) (n = 6)	Filgotinib 150 mg once daily (study 2) (n = 5)	Filgotinib 200 mg once daily (study 1) (n = 6)	Filgotinib 300 mg once daily (study 2) (n = 5)
Filgotinib parameters						
C_{max}, μg/ml	0.0716 (112)	0.492	0.730 (43.2)	1.16 (29.8)	1.43 (54.4)	1.34 (38.2)
T_{max}, median (range) hours	1 (0–5)	1.5 (1–2)	2.0 (1–3)	1 (1–2)	2 (1–3)	1.5 (1–2)
AUC_{tau}, μg.hour/ml	1.34 (155)	2.12	2.47 (23.4)	6.44 (60.4)†	5.38 (34.6)	7.71 (73.8)
Major metabolite parameters						
C_{max}, μg/ml	0.582 (48.5)	1.46	3.18 (25.0)	3.79 (26.5)	3.77 (23.6)	4.62 (9.98)
T_{max}, median (range) hours	5 (1–8)	5.5 (3–8)	2 (0–5)	3 (2–5)	3 (1–5)	3 (3–8)
AUC_{tau}, μg.hour/ml	11.2 (52.2)	26.0	33.1 (26.3)	75.9 (31.0)	71.8 (31.3)	93.9 (20.4)

* Except where indicated otherwise, values are the arithmetic mean (coefficient of variation). C_{max} = maximum plasma concentration; T_{max} = time to C_{max}; AUC_{tau} = area under the plasma drug concentration–time curve of a dosing interval.
† One outlier with higher exposure (AUC_{tau} 13.3 μg.hour/ml) compared to the other 4 patients (AUC_{tau} 4.79–5.29 μg.hour/ml).

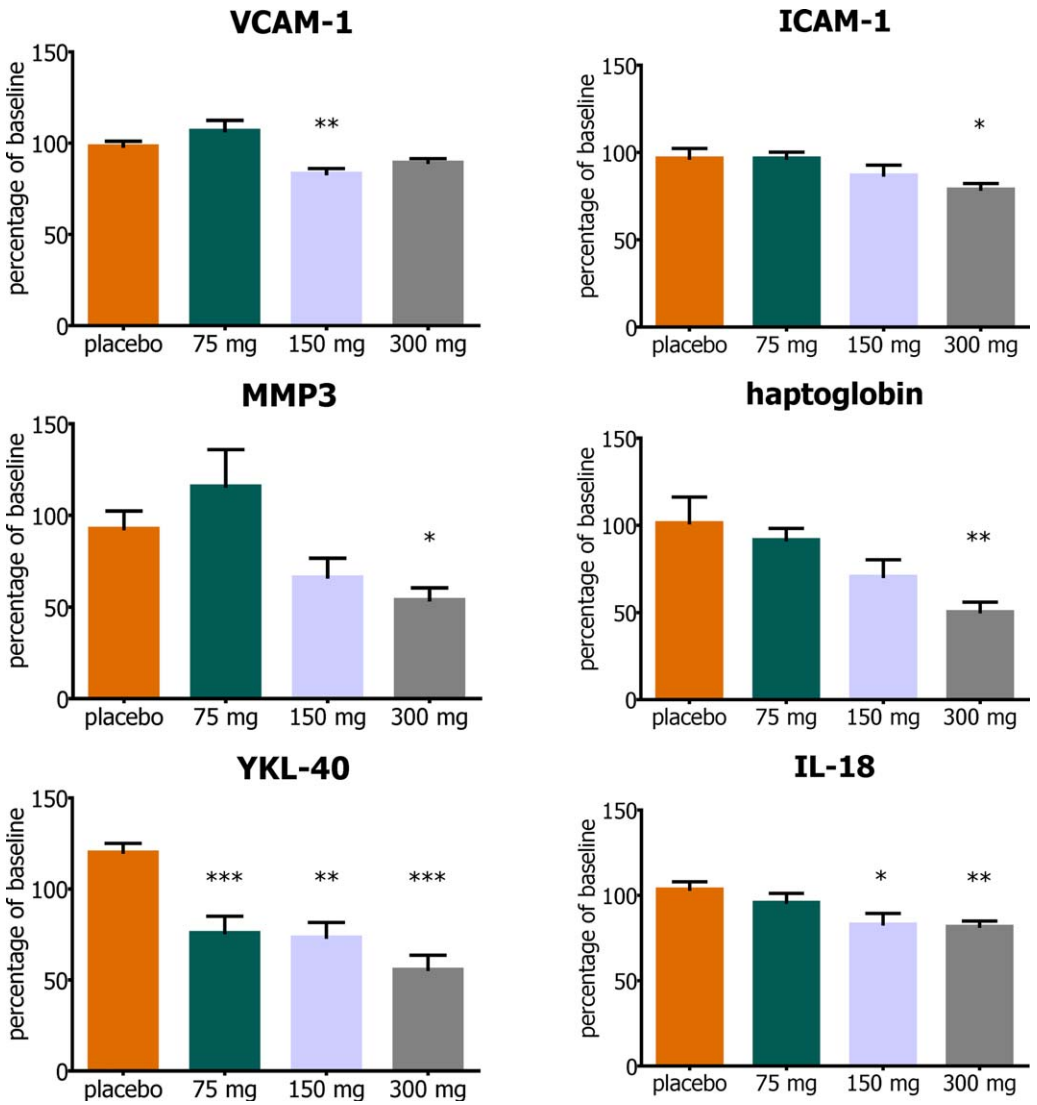

Figure 2. Plasma levels of biomarkers for rheumatoid arthritis and inflammation after 4 weeks of filgotinib or placebo treatment, assessed in plasma from patients in study 2. Values are the mean ± SEM. * = $P < 0.05$; ** = $P < 0.01$; *** = $P < 0.001$ versus placebo. VCAM-1 = vascular cell adhesion molecule 1; ICAM-1 = intercellular adhesion molecule 1; MMP-3 = matrix metalloproteinase 3; IL-18 = interleukin-18.

evaluation of JAK-1 inhibition with a minimal burden to patients. For previously studied JAK inhibitors, achieving maximal ACR20 response rates took 12 weeks, but roughly 70–80% of the achievable rates were reached within the first 4 weeks (19,20). However, a 4-week treatment period is deemed insufficient to make an estimate of the ACR50 response rate and, even more so, of the ACR70 response rate, as these were only stable after 6–9 months. For short-term treatment, inflammation markers such as serum CRP level or continuous patient efficacy scores (e.g., the DAS28-CRP) are clearly more helpful than the binary ACR scores.

In the current studies, filgotinib treatment showed signs of early efficacy, while the duration of treatment and limited group size did not allow clear differentiation among daily oral doses from 75 mg to 300 mg. In all treatment groups, the ACR20 response rate increased and the DAS28-CRP decreased progressively from week 1 to week 4 at doses of ≥75 mg, while the 30 mg dose was suboptimal. However, even at this low dose, filgotinib induced a marked and maintained improvement in serum CRP level. The results achieved at 300 mg were similar to those at 200 mg in the initial proof-of-concept study.

It was remarkable that in the absence of a maintained effect on CRP level, the clinical response in the placebo group of the dose-ranging study exceeded that in the 30 mg filgotinib group. The relatively high response in this placebo group may have been influenced by some imbalance in baseline patient characteristics (i.e., a lower disease activity at baseline). Somewhat unexpected and apparently contradictory results were also observed in the 150 mg group, which had more pronounced disease activity at baseline than did other groups. The results suggest that for this dose group, 4 weeks of treatment was too short to obtain good patient-reported outcomes, probably because the measured improvements in physician's global assessment of disease activity, serum CRP level, TJC68, and SJC66 were not large enough to translate into relevant patient-reported improvements in pain, global disease activity, and HAQ DI score.

Filgotinib had a PK half-life of ~7 hours, and it was metabolized to form a major active metabolite with a half-life of ~1 day (13). Therefore, the proof-of-concept study was designed to evaluate both once- and twice-daily dosing, with an equal daily dose of 200 mg, thus comparing 200 mg once daily and 100 mg twice daily. Both regimens showed encouraging early efficacy rates, with normalization of serum CRP level within 1 week and similar safety; therefore, only once-daily regimens were selected for evaluation in the subsequent dose-ranging study.

The PK of filgotinib and its major metabolite was essentially dose proportional over the 30–300 mg range, with ~13-fold higher plasma concentrations of the major metabolite compared to those of its parent filgotinib. These results were highly similar to previous results in healthy volunteers (13), indicating that neither the disease status nor the coadministered drugs, in particular MTX, had a relevant impact on the PK of filgotinib.

While the treatment duration of 4 weeks limits the safety assessment of filgotinib, several of the safety observations with other JAK inhibitors relate to events occurring early in treatment. Reduced hemoglobin and induction of anemia have been observed within 2 weeks and are thought to be linked to inhibition of JAK-2 (21). Similarly, effects on liver transaminases and cholesterol appear early on with other JAK inhibitors.

A dose-dependent increase in HDL was found relative to placebo, without a corresponding increase in LDL or total cholesterol. This was an unexpected finding, as it has been suggested that interference with the IL-6 pathway may be associated with generalized changes in blood lipids (22). Increases in LDL and total cholesterol were reported with anti–IL-6 monoclonal antibodies as well as with JAK inhibitors (19,23). Since JAK-1 is dominant in signaling for IL-6 (24), the limited effects on LDL with more clear effects on HDL following filgotinib treatment cannot readily be explained. Larger and longer-term studies are needed to determine if these are transient or long-term effects of filgotinib on HDL and LDL levels.

Similarly, the very low incidence of filgotinib-related infections is encouraging, but the short treatment duration in a limited number of patients does not allow assessment of a potential benefit of selective JAK-1 inhibition as related to immunomodulatory effects. It has been suggested that avoiding inhibition of JAK-3 may lead to less immunosuppression through a differential effect of JAK inhibition (24). This hypothesis needs further clinical substantiation in larger, longer clinical studies.

Hematologic evaluations in filgotinib-treated patients showed a limited decrease in neutrophils (an ~14–24% decrease from baseline for doses of ≥75 mg), consistent with immunomodulatory effects through inhibition of JAK-1, but it did not lead to neutropenia. Based on experience with other RA therapies, a decline in the first month with stabilization of neutrophils thereafter is typically observed and has been suggested to be an early sign of efficacy (25). In addition, the decrease observed in some plasma biomarkers such as ICAM-1 or VCAM-1 (chemoattractant molecules for leukocytes like neutrophils) may further explain this decrease in circulating neutrophils (25). Similarly, the slight decrease in platelets is deemed indicative of the antiinflammatory effects of the compound.

In contrast to observations with inhibitors of JAK-2 that interfere with signaling for EPO and TPO, no anemia or decline in hemoglobin was observed, but instead a modest increase in hemoglobin was induced. The absence of effects on reticulocytes also supports the conclusion that filgotinib does not cause a clinically relevant inhibition of JAK-2.

Genovese et al recently reported results from a phase IIb study with the selective JAK-1 inhibitor ABT-494 combined with MTX in patients with RA who had had an insufficient response to MTX (26). Within 4 weeks, the middle and higher doses of ABT-494 led to a decline in hemoglobin. Natural killer (NK) cells also decreased. Both observations are not consistent with what was observed in filgotinib-treated patients, up to the highest doses. The authors suggest that less selectiveness of ABT-494 for JAK at higher doses may explain the findings. Reductions in hemoglobin and NK cells have also been reported with tofacitinib, and these are deemed to be associated with inhibition of JAK-2

and JAK-3, respectively. Tofacitinib potently inhibits JAK-3 and has a functional selectivity for JAK-1 over JAK-2; consequently, JAK-1, JAK-2, and JAK-3 are inhibited at high doses (5). Clinical findings with ABT-494 suggest a similar dose dependency for signs of JAK-2 and JAK-3 inhibition and are consistent with patent data for ABT-494 showing a similar JAK inhibition profile as tofacitinib, with hematologic findings in ABT-494 animal studies resembling those observed in clinical studies.

Filgotinib was generally well tolerated. No AEs were considered to be related to treatment in the majority of RA patients treated in both phase IIa studies (107 of 127 patients [84.3%]) (98 patients received filgotinib). All events reported as potentially related to study drug were mild or moderate and transient during therapy. The most commonly reported event was nausea (in 9 patients [7%]).

Several plasma proteins proposed as markers of inflammation or RA were evaluated in study 2. ICAM-1 and VCAM-1 are involved in adhesion of immune cells facilitating their invasion into inflamed tissue (27). MMP-3 is a protease involved in arthritis pathology that has been shown to be increased in the plasma of RA patients (28). Gene expression of the acute-phase proteins CRP and haptoglobin, as well as YKL-40, which plays a role in inflammation and tissue remodeling (29), is under the control of the JAK/STAT pathway (30,31). IL-18 is well known as a proinflammatory cytokine (32). The observed decrease of the levels of these 7 proteins in the plasma of RA patients after 4 weeks of filgotinib treatment was paralleled by the improvement in their disease status. Several of these proteins have been reported to be affected by treatments used in RA patients (33–36). Declines in plasma levels of VCAM-1, MMP-3, and YKL-40 are similar to those reported for the JAK inhibitor tofacitinib (37) and the anti–IL-6 monoclonal antibody tocilizumab (38).

From these two 4-week phase IIa studies of filgotinib in RA patients with an insufficient response to MTX, we conclude that selective inhibition of JAK-1 demonstrated early efficacy. With a mild increase in hemoglobin and no change in reticulocytes, treatment with filgotinib did not show signs of inhibition of JAK-2. Four-week treatment had an encouraging safety profile. These promising results warrant further development of filgotinib in larger studies of longer duration.

ACKNOWLEDGMENTS

The authors would like to thank T. Rotaru (RTL SM Ltd), L. Fagard (SGS), M. De Weer (Galapagos NV), O. Boyarskaya (Pharmanet-i3), and A. La Noce (Pharmanet-i3) for their contribution to the successful conduct of the studies.

AUTHOR CONTRIBUTIONS

All authors were involved in drafting the article or revising it critically for important intellectual content, and all authors approved the final version to be published. Dr. van 't Klooster had full access to all of the data in the study and takes responsibility for the integrity of the data and the accuracy of the data analysis.

Study conception and design. Vanhoutte, Van der Aa, Namour, Galien, Meuleners, van 't Klooster.

Acquisition of data. Mazur, Voloshyn, Stanislavchuk.

Analysis and interpretation of data. Vanhoutte, Van der Aa, Namour, Galien, Meuleners, van 't Klooster.

ROLE OF THE STUDY SPONSORS

These studies were supported by Galápagos, which was involved in design of the study, interpretation of the data, and writing of the manuscript. AbbVie provided funding to Galápagos for phase II development of filgotinib. SGS, Innophar, and Pharmanet-i3 were responsible for operational management of the clinical studies and for data collection and data analysis but were not involved in preparation of the manuscript. The authors had the final decision to submit the manuscript for publication. Publication of this article was not contingent upon approval by Galápagos, AbbVie, SGS, Innophar, or Pharmanet-i3.

REFERENCES

1. Firestein GS. Evolving concepts of rheumatoid arthritis. Nature 2003;423:356–61.
2. Smolen JS, Steiner G. Therapeutic strategies for rheumatoid arthritis. Nat Rev Drug Discov 2003;2:473–88.
3. Koenders MI, van den Berg WB. Novel therapeutic targets in rheumatoid arthritis. Trends Pharmacol Sci 2015;36:189–95.
4. Kyttaris VC. Kinase inhibitors: a new class of antirheumatic drugs. Drug Des Devel Ther 2012;6:245–50.
5. O'Shea JJ, Schwartz DM, Villarino AV, Gadina M, McInnes IB, Laurence A. The JAK-STAT pathway: impact on human disease and therapeutic intervention. Ann Rev Med 2015;66:311–28.
6. Kaur K, Kalra S, Kaushal S. Systematic review of tofacitinib: a new drug for the management of rheumatoid arthritis. Clin Ther 2014;36:1074–86.
7. Vyas D, O'Dell KM, Bandy JL, Boyce EG. Tofacitinib: the first janus kinase (JAK) inhibitor for the treatment of rheumatoid arthritis. Ann Pharmacother 2013;47:1524–31.
8. Norman P. Selective JAK inhibitors in development for rheumatoid arthritis. Expert Opin Investig Drugs 2014;23:1067–77.
9. Grisouard J, Hao-Shen H, Dirnhofer S, Wagner KU, Skoda RC. Selective deletion of Jak2 in adult mouse hematopoietic cells leads to lethal anemia and thrombocytopenia. Haematologica 2014;99:e52–4.
10. Neubauer H, Cumano A, Müller M, Wu H, Huffstadt U, Pfeffer K. JAK2 deficiency defines an essential developmental checkpoint in definitive hematopoiesis. Cell 1998;93:397–409.
11. Van Rompaey L, Galien R, van der Aar EM, Clement-Lacroix P, Nelles L, Smets B, et al. Preclinical characterization of GLPG0634, a selective inhibitor of JAK1, for the treatment of inflammatory diseases. J Immunol 2013;191:3568–77.
12. Namour F, Diderichsen PM, Cox E, Vayssière B, van der Aa A, Tasset C, et al. Pharmacokinetics and pharmacokinetic/pharmacodynamic modeling of filgotinib (GLPG0634), a selective JAK1 inhibitor, in support of phase IIB dose selection. Clin Pharmacokinet 2015;54:859–74.

13. Namour F, Galien R, Gheyle L, Vanhoutte F, Vayssiere B, van der Aa A, et al. Once daily high dose regimens of GLPG0634 in healthy volunteers are safe and provide continuous inhibition of JAK1 but not JAK2 [abstract]. Arthritis Rheum 2012;64 Suppl: S573.
14. Arnett FC, Edworthy SM, Bloch DA, McShane DJ, Fries JF, Cooper NS, et al. The American Rheumatism Association 1987 revised criteria for the classification of rheumatoid arthritis. Arthritis Rheum 1988;31:315–24.
15. Felson DT, Anderson JJ, Boers M, Bombardier C, Furst D, Goldsmith C, et al. American College of Rheumatology preliminary definition of improvement in rheumatoid arthritis. Arthritis Rheum 1995;38:727–35.
16. Prevoo ML, van 't Hof MA, Kuper HH, van Leeuwen MA, van de Putte LB, van Riel PL. Modified disease activity scores that include twenty-eight–joint counts: development and validation in a prospective longitudinal study of patients with rheumatoid arthritis. Arthritis Rheum 1995;38:44–8.
17. Felson DT, Anderson JJ, Boers M, Bombardier C, Chernoff M, Fried B, et al. The American College of Rheumatology preliminary core set of disease activity measures for rheumatoid arthritis clinical trials. Arthritis Rheum 1993;36:729–40.
18. Fries JF, Spitz P, Kraines RG, Holman HR. Measurement of patient outcome in arthritis. Arthritis Rheum 1980;23:137–45.
19. Kremer JM, Cohen S, Wilkinson BE, Connell CA, French JL, Gomez-Reino J, et al. A phase IIb dose-ranging study of the oral JAK inhibitor tofacitinib (CP-690,550) versus placebo in combination with background methotrexate in patients with active rheumatoid arthritis and an inadequate response to methotrexate alone. Arthritis Rheum 2012;64:970–81.
20. Keystone E, Taylor P, Genovese M, Schlichting D, Beattie S, Gaich C, et al. 12-week results of a phase 2B dose-ranging study of LY3009104 (INCB028050), an oral JAK1/JAK2 inhibitor, in combination with traditional DMARDS in patients with rheumatoid arthritis [abstract]. Ann Rheum Dis 2012;71 Suppl 3:152.
21. Kremer JM, Bloom BJ, Breedveld FC, Coombs JH, Fletcher MP, Gruben D, et al. The safety and efficacy of a JAK inhibitor in patients with active rheumatoid arthritis: results of a double-blind, placebo-controlled phase IIa trial of three dosage levels of CP-690,550 versus placebo [published erratum appears in Arthritis Rheum 2012;64:1487]. Arthritis Rheum 2009;60:1895–905.
22. Popa CD, Arts E, Fransen J, van Riel PL. Atherogenic index and high-density lipoprotein cholesterol as cardiovascular risk determinants in rheumatoid arthritis: the impact of therapy with biologicals. Mediators Inflamm 2012;2012:785946.
23. McInnes IB, Thompson L, Giles JT, Bathon JM, Salmon JE, Beaulieu AD, et al. Effect of interleukin-6 receptor blockade on surrogates of vascular risk in rheumatoid arthritis: MEASURE, a randomised, placebo-controlled study. Ann Rheum Dis. In Press.
24. Rodig SJ, Meraz MA, White JM, Lampe PA, Riley JK, Arthur CD, et al. Disruption of the Jak1 gene demonstrates obligatory and nonredundant roles of the Jaks in cytokine-induced biologic responses. Cell 1998;93:373–83.
25. Schnoor M, Alcaide P, Voisin MB, van Buul JD. Crossing the vascular wall: common and unique mechanisms exploited by different leukocyte subsets during extravasation. Mediators Inflamm 2015;2015:946509.
26. Genovese MC, Smolen JS, Weinblatt ME, Burmester GR, Meerwein S, Camp HS, et al. Efficacy and safety of ABT-494, a selective JAK-1 inhibitor, in a phase IIb study in patients with rheumatoid arthritis and an inadequate response to methotrexate. Arthritis Rheumatol 2016;68:2857–66.
27. Navarro-Hernández RE, Oregon-Romero E, Vázquez-Del Mercado M, Rangel-Villalobos H, Palafox-Sánchez CA, Muñoz-Valle JF. Expression of ICAM1 and VCAM1 serum levels in rheumatoid arthritis clinical activity: association with genetic polymorphisms. Dis Markers 2009;26:119–26.
28. Ally MM, Hodkinson B, Meyer PW, Musenge E, Tikly M, Anderson R. Serum matrix metalloproteinase-3 in comparison with acute phase proteins as a marker of disease activity and radiographic damage in early rheumatoid arthritis. Mediators Inflamm 2013;2013:183653.
29. Väänänen T, Koskinen A, Paukkeri EL, Hämäläinen M, Moilanen T, Moilanen E, et al. YKL-40 as a novel factor associated with inflammation and catabolic mechanisms in osteoarthritic joints. Mediators Inflamm 2014;2014:215140.
30. Kim H, Hawley TS, Hawley RG, Baumann H. Protein tyrosine phosphatase 2 (SHP-2) moderates signaling by gp130 but is not required for the induction of acute-phase plasma protein genes in hepatic cells. Mol Cell Biol 1998;18:1525–33.
31. Singh SK, Bhardwaj R, Wilczynska KM, Dumur CI, Kordula T. A complex of nuclear factor I-X3 and STAT3 regulates astrocyte and glioma migration through the secreted glycoprotein YKL-40. J Biol Chem 2011;286:39893–903.
32. Sivalingam SP, Thumboo J, Vasoo S, Thio ST, Tse C, Fong KY. In vivo pro- and anti-inflammatory cytokines in normal and patients with rheumatoid arthritis. Ann Acad Med Singapore 2007;36:96–9.
33. Visvanathan S, Rahman MU, Keystone E, Genovese M, Klareskog L, Hsia E, et al. Association of serum markers with improvement in clinical response measures after treatment with golimumab in patients with active rheumatoid arthritis despite receiving methotrexate: results from the GO-FORWARD study. Arthritis Res Ther 2010;12:R211.
34. Wagner C, Chen D, Fan H, Hsia EC, Mack M, Emery P, et al. Evaluation of serum biomarkers associated with radiographic progression in methotrexate-naive rheumatoid arthritis patients treated with methotrexate or golimumab. J Rheumatol 2013;40: 590–8.
35. Yanagida M, Kawasaki M, Fujishiro M, Miura M, Ikeda K, Nozawa K, et al. Serum proteome analysis in patients with rheumatoid arthritis receiving therapy with tocilizumab: an anti-interleukin-6 receptor antibody. Biomed Res Int 2013;2013: 607137.
36. Kirkham BW, Wasko MC, Hsia EC, Fleischmann RM, Genovese MC, Matteson EL, et al. Effects of golimumab, an anti-tumour necrosis factor-α human monoclonal antibody, on lipids and markers of inflammation. Ann Rheum Dis 2014;73:161–9.
37. Yamaoka K, Kubo S, Li W, Sonomoto K, Hirata S, Sasso EH, et al. Effects of tofacitinib treatment on leptin and other components of the multi-biomarker disease activity score in patients with rheumatoid arthritis [abstract]. Ann Rheum Dis 2014;73 Suppl 2:FRI0333.
38. Tanaka Y, Hanami K, Tasaka H, Fukuyo S, Haney DJ, Bolce R, et al. A multi-biomarker disease activity (VECTRA DA algorithm) score reflects clinical disease activity and structural changes in rheumatoid arthritis patients treated with tocilizumab [abstract]. Arthritis Rheum 2012;64 Suppl:S897.

ARTHRITIS & RHEUMATOLOGY
Vol. 69, No. 10, October 2017, pp 1960–1968
DOI 10.1002/art.40189

Herpes Zoster and Tofacitinib

Clinical Outcomes and the Risk of Concomitant Therapy

Kevin L. Winthrop,[1] Jeffrey R. Curtis,[2] Stephen Lindsey,[3] Yoshiya Tanaka,[4] Kunihiro Yamaoka,[5] Hernan Valdez,[6] Tomohiro Hirose,[7] Chudy I. Nduaka,[8] Lisy Wang,[9] Alan M. Mendelsohn,[8] Haiyun Fan,[8] Connie Chen,[6] and Eustratios Bananis[8]

Objective. **Patients with rheumatoid arthritis (RA) are at increased risk of herpes zoster (HZ), and the risk appears to be increased in patients treated with tofacitinib. The aim of this study was to evaluate whether concomitant treatment with conventional synthetic disease-modifying antirheumatic drugs (csDMARDs) or glucocorticoids (GCs) contributes to the increased risk of HZ in RA patients treated with tofacitinib.**

Methods. **HZ cases were identified from the databases of 2 phase I, 9 phase II, 6 phase III, and 2 long-term extension studies of tofacitinib in RA patients. Crude incidence rates (IRs) of all HZ events (serious and nonserious) per 100 patient-years (with 95% confidence intervals [95% CIs]) were calculated for unique patients. Within phase III studies, we described HZ rates according to concomitant csDMARD treatment and baseline GC use. A multivariable Cox proportional hazards regression model was used to evaluate HZ risk factors across studies.**

Results. **Across all studies (6,192 patients; 16,839 patient-years), HZ was reported in 636 tofacitinib-treated patients (IR 4.0, 95% CI 3.7–4.4). In most cases (93%), HZ was classified as nonserious, and the majority of patients (94%) had involvement of only 1 dermatome. HZ IRs varied across regions, from 2.4 (95% CI 2.0–2.9) in Eastern Europe to 8.0 (95% CI 6.6–9.6) in Japan and 8.4 (95% CI 6.4–10.9) in Korea. Within phase III studies, HZ IRs varied according to tofacitinib dose, background csDMARD treatment, and baseline use of GCs. The IRs were numerically lowest for monotherapy with tofacitinib 5 mg twice daily without GCs (IR 0.56 [95% CI 0.07–2.01]) and highest for tofacitinib 10 mg twice daily with csDMARDs and GCs (IR 5.44 [95% CI 3.72–7.68]). Age, GC use, tofacitinib dose, and enrollment within Asia were independent risk factors for HZ.**

Conclusion. **Patients receiving treatment with tofacitinib and GCs appear to have a greater risk of developing HZ compared with patients receiving tofacitinib monotherapy without GCs.**

Shingles, also known as herpes zoster (HZ), is caused by the reactivation of varicella zoster virus (VZV) and is a common and potentially debilitating illness (1,2).

Supported by Pfizer.

[1]Kevin L. Winthrop, MD, MPH: Oregon Health and Science University, Portland; [2]Jeffrey R. Curtis, MD, MS, MPH: University of Alabama at Birmingham; [3]Stephen Lindsey, MD: Ochsner Medical Center, Baton Rouge, Louisiana; [4]Yoshiya Tanaka, MD, PhD: University of Occupational and Environmental Health Japan, Kitakyushu, Japan; [5]Kunihiro Yamaoka, MD, PhD: Keio University School of Medicine, Tokyo, Japan; [6]Hernan Valdez, MD, Connie Chen, PharmD: Pfizer, New York, New York; [7]Tomohiro Hirose, MSci: Pfizer Japan, Tokyo, Japan; [8]Chudy I. Nduaka, DVM, PhD, Alan M. Mendelsohn, MD, Haiyun Fan, MS, Eustratios Bananis, PhD: Pfizer Inc., Collegeville, Pennsylvania; [9]Lisy Wang, MD: Pfizer, Groton, Connecticut.

Dr. Winthrop has received consulting fees (more than $10,000) and research grants from Pfizer. Dr. Curtis has received consulting fees (more than $10,000) and research grants from Pfizer. Dr. Lindsey has received speaking fees (less than $10,000) from Pfizer. Dr. Tanaka has received consulting fees, speaking fees, and/or honoraria (less than $10,000) from Pfizer. Dr. Yamaoka has received consulting fees and speaking fees (more than $10,000) from Pfizer. Drs. Valdez, Nduaka, Wang, Mendelsohn, Chen, and Bananis, and Mr. Hirose and Ms Fan own stock or stock options in Pfizer Inc.

Address correspondence to Kevin L. Winthrop, MD, MPH, Casey Eye Institute, Oregon Health and Science University, 3375 SW Terwilliger Boulevard, Portland, OR 97239. E-mail: Winthrop@ohsu.edu.

Submitted for publication November 1, 2016; accepted in revised form June 20, 2017.

Approximately one-third of the general population will develop HZ within their lifetime (1), and ~10% of these patients develop postherpetic neuralgia, which can last for months to years and cause significant pain and morbidity (3). Rarely, but especially in immunosuppressed patients, reactivation can result in disseminated or visceral disease, such as encephalitis, or other complications (1). Patients with rheumatoid arthritis (RA) have a 1.5-fold to 2-fold higher risk of HZ compared with similarly aged individuals in the general population (4,5). This risk is related in part to the disease itself but can be further increased by RA treatments (4).

Glucocorticoids (GCs), including prednisone, are well-documented risk factors for HZ (6,7), and more recently, use of JAK inhibitors, including both tofacitinib and baricitinib, has been associated with a higher rate of HZ (8–10). In addition, although not all studies have documented an increased risk attributable to biologic therapies (11,12), a recent systematic review suggested an increased risk of HZ associated with tumor necrosis factor (TNF) antagonist treatment (13), and a theoretical risk is associated with various conventional synthetic disease-modifying antirheumatic drugs (csDMARDs) such as methotrexate (MTX) and chloroquine (14,15). Given the increased risk of HZ observed among patients with RA compared with the general population and the risk associated with RA therapies, it is possible that the risk of HZ may be further increased when such therapies are combined.

Tofacitinib is an oral JAK inhibitor for the treatment of RA. We recently reported an increased risk of HZ with tofacitinib therapy compared with placebo during the tofacitinib global clinical development program for RA (8). Although the risk of HZ was increased throughout the global program, this risk varied by geographic region, with significantly higher rates reported in Japan and Korea. Many of the patients in the phase III program also used concomitant csDMARDs as well as GCs (8). We undertook the current analysis to better characterize the clinical aspects of HZ events with longer periods of follow-up and exposure, and to evaluate whether the risk of HZ is greater in patients receiving tofacitinib and concomitant MTX and GCs.

PATIENTS AND METHODS

The global tofacitinib RA development program consisted of 2 phase I, 9 phase II, 6 phase III, and 2 open-label long-term extension (LTE) studies and included a total of 6,192 tofacitinib-treated patients with 16,839 patient-years of tofacitinib exposure at the time of the datacut (April 2014). LTE study A3921024 data collection and analyses were still ongoing at the time of this analysis; because the study database had not yet been locked, some values may change in the final locked study database. Details of these trials with regard to tofacitinib dosing and study conduct have previously been published (16–33). Patients with a history of recurrent HZ (>1 episode), disseminated HZ (single episode), or disseminated herpes simplex (single episode) were excluded from these trials. Patients who had previously experienced an HZ event involving a single dermatome were eligible to participate.

All studies were conducted in compliance with the Declaration of Helsinki, the International Conference on Harmonisation Guidelines for Good Clinical Practice, and the regulations of the relevant local countries. All enrolled patients provided written informed consent, and all participating institutions provided institutional review board or ethics committee approval prior to participation.

HZ reporting and adjudication. For each study, adverse event (AE) data were reported by site investigators and entered into the Pfizer clinical database. Standard Medical Dictionary for Regulatory Activities codes were used to categorize AEs, and infectious AEs, such as HZ, were graded as "serious" if they were associated with hospitalization or death, were medically important, or required treatment with parenteral therapy. All patients with serious HZ events discontinued tofacitinib treatment, according to the study protocols, but patients with nonserious HZ were permitted to continue in the trial. All cases of HZ reported to involve >1 dermatome were evaluated by an independent adjudication committee and designated as multidermatomal (nonadjacent or >2 adjacent dermatomes) or disseminated. Dermatome maps completed by investigators at the study sites were used during the adjudication process.

Incidence rate (IR) calculation. Across the global tofacitinib RA development program, HZ events in tofacitinib-treated patients were captured. We calculated crude IRs of the number of unique patients with HZ events per 100 patient-years (with 95% confidence intervals [95% CIs]), and stratified the data by race, age, baseline DMARD use, baseline GC use, and other factors. Patients were censored at the time of the first HZ event, death, or study withdrawal, whichever came first. Crude HZ IRs of the first HZ event over the entire phase I, phase II, phase III, and LTE study time period were calculated. Due to variability within this pooled data set with respect to concomitant DMARD treatment and tofacitinib dose, only phase III data (for which concomitant therapies and tofacitinib dose were held constant) were used to examine IRs stratified with regard to these factors.

Cox proportional hazards regression analysis of risk factors for HZ. To evaluate risk factors for HZ among tofacitinib-treated patients, we used pooled data from the phase I, phase II, phase III, and LTE studies. Univariate analysis using a Cox proportional hazards regression model was performed on known risk factors for HZ and those of potential interest based on clinical considerations (see Supplementary Table 1, available on the *Arthritis & Rheumatology* web site at http://onlinelibrary.wiley.com/doi/10.1002/art.40189/abstract). A pool of factors was then formed to select the final multivariable Cox proportional hazards regression model for the analysis of the time to HZ event from the first dose of tofacitinib, including age, sex, disease duration, baseline 4-variable Disease Activity Score in 28 joints (34) using the C-reactive protein level (DAS28-CRP), baseline absolute lymphocyte count, baseline diabetes mellitus, baseline Health Assessment Questionnaire

Table 1. Crude IRs of HZ in patients with RA treated with tofacitinib during phase I, phase II, phase III, and long-term extension studies, by region of enrollment*

	Unique patients with HZ events	Total patient-years of drug exposure	Crude IR (95% CI)†
Global RA program	636	16,839	4.0 (3.7–4.4)
By region			
US/Canada/Australia/New Zealand	159	3,910	4.3 (3.7–5.1)
Western Europe	43	1,395	3.3 (2.4–4.4)
Eastern Europe	105	4,509	2.4 (2.0–2.9)
Latin America	96	2,802	3.6 (3.0–4.5)
Asia	233	4,223	6.1 (5.4–7.0)
Japan	120	1,705	8.0 (6.6–9.6)
Korea	56	779	8.4 (6.4–10.9)
India	16	435	3.9 (2.2–6.3)
Thailand/Malaysia/Philippines	18	479	4.0 (2.4–6.3)
China/Taiwan	23	822	3.0 (1.9–4.5)

* HZ = herpes zoster; RA = rheumatoid arthritis; 95% CI = 95% confidence interval.
† Crude incidence rates (IRs) of an HZ event per 100 patient-years in unique patients (data as of April 2014, for all tofacitinib doses).

score (35), background therapy (any DMARD versus monotherapy), body mass index (BMI), baseline chronic obstructive pulmonary disease, smoking status (former or nonsmoker versus current smoker), baseline oral GC use, and geographic region. A backward selection process with the criterion to stay in the model fixed at 10% was used to screen and select the risk factors. The final Cox proportional hazards regression model included all of the risk factors that were selected using the backward procedure. The tofacitinib group was added in a time-varying format; any other risk factors that were not selected by the procedure but were considered as being clinically relevant would be forced back into the final model. Age, BMI, 4-variable DAS28-CRP, disease duration, and baseline absolute lymphocyte count were evaluated as continuous variables. All analyses were conducted using SAS software.

Table 2. Baseline characteristics of the patients with rheumatoid arthritis in phase III tofacitinib trials, by treatment group*

Characteristic	Tofacitinib 5 mg BID + csDMARDs (n = 973)	Tofacitinib 5 mg BID monotherapy (n = 616)	Tofacitinib 10 mg BID + csDMARDs (n = 969)	Tofacitinib 10 mg BID monotherapy (n = 642)
Age, mean ± SD years	53.4 ± 11.7	51.1 ± 12.0	52.6 ± 11.6	50.5 ± 12.4
Female	820 (84.3)	493 (80.0)	814 (84.0)	543 (84.6)
BMI, mean ± SD kg/m^2	27.0 ± 6.8	26.7 ± 5.9	27.0 ± 6.4	27.1 ± 6.3
Diabetes mellitus	83 (8.5)	47 (7.6)	81 (8.4)	46 (7.2)
COPD	78 (8.0)	47 (7.6)	83 (8.6)	51 (7.9)
RA disease duration, mean ± SD years	8.9 ± 8.0	4.9 ± 7.0	9.2 ± 8.2	5.4 ± 7.3
DAS28-ESR, mean ± SD	6.4 ± 1.0	6.7 ± 1.0	6.4 ± 1.0	6.6 ± 1.0
Baseline GC use	579 (59.5)	320 (51.9)	550 (56.8)	313 (48.8)
GC dose, mean (median) mg	6.3 (5.0)	7.3 (6.3)	6.3 (5.0)	7.4 (5.0)
Concomitant DMARDs				
Methotrexate	896 (92.1)	1 (0.2)	895 (92.4)	0 (0.0)
Leflunomide	90 (9.2)	0 (0.0)	84 (8.7)	0 (0.0)
Chloroquine	68 (7.0)	87 (14.1)	63 (6.5)	99 (15.4)
Race				
White	584 (60.0)	392 (63.6)	573 (59.1)	434 (67.6)
Black	33 (3.4)	25 (4.1)	25 (2.6)	22 (3.4)
Asian	286 (29.4)	109 (17.7)	282 (29.1)	95 (14.8)
Other	70 (7.2)	90 (14.6)	89 (9.2)	91 (14.2)
Smoking history				
Never smoker	644 (66.2)	410 (66.6)	647 (66.8)	444 (69.2)
Current smoker	136 (14.0)	97 (15.7)	168 (17.3)	114 (17.8)
Former smoker	193 (19.8)	109 (17.7)	154 (15.9)	84 (13.1)

* Except where indicated otherwise, values are the number (%). BID = twice daily; csDMARDs = conventional synthetic disease-modifying antirheumatic drugs; BMI = body mass index; COPD = chronic obstructive pulmonary disease; RA = rheumatoid arthritis; DAS28-ESR = 4-variable Disease Activity Score in 28 joints using the erythrocyte sedimentation rate; GC = glucocorticoid.

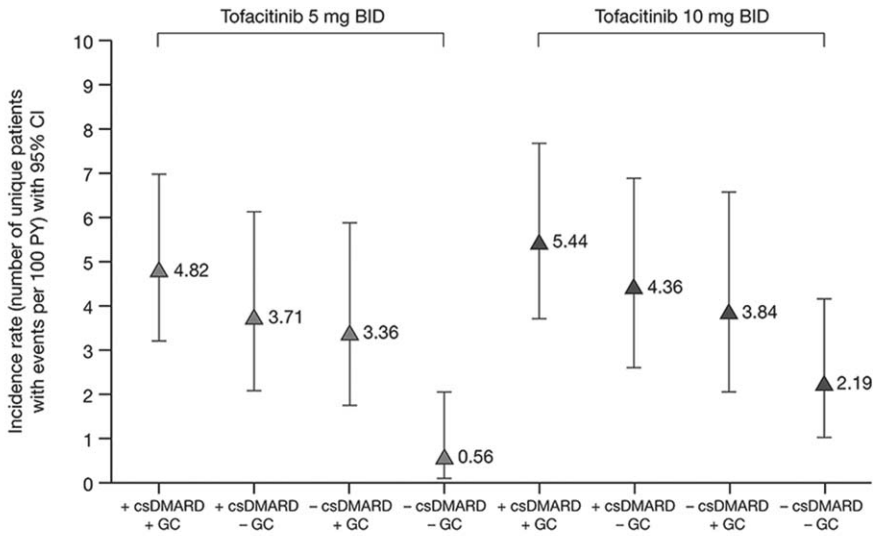

	+ csDMARD + GC	+ csDMARD − GC	− csDMARD + GC	− csDMARD − GC	+ csDMARD + GC	+ csDMARD − GC	− csDMARD + GC	− csDMARD − GC
Total patients, N	579	394	320	296	550	419	313	329
Total tofacitinib exposure, PY	603	412	367	361	606	429	346	419
Unique patients with events, n	28	15	12	2	32	18	13	9
IR (95% CI)	4.82 (3.2, 7.0)	3.71 (2.1, 6.1)	3.36 (1.7, 5.9)	0.56 (0.07, 2.0)	5.44 (3.7, 7.7)	4.36 (2.6, 6.9)	3.84 (2.0, 6.6)	2.19 (1.0, 4.2)

Figure 1. Crude incidence rates (IRs) of first herpes zoster (HZ) events within pooled phase III studies of tofacitinib, with or without conventional synthetic disease-modifying antirheumatic drugs (csDMARDs) and/or baseline glucocorticoid (GC) use. Patients from all regions were included. HZ IRs (with 95% confidence intervals [95% CIs]) are expressed as the number of unique patients with an HZ event per 100 patient-years (PYs) of exposure. BID = twice daily.

RESULTS

Summary of HZ events during phase I, phase II, phase III, and LTE studies. Among 6,192 patients with 16,839 patient-years of tofacitinib exposure, we identified 636 patients (10%) who developed HZ over a median follow-up period of 3.0 years of tofacitinib exposure and in whom the median time to first HZ event was 1.6 years. The overall crude IR for the first HZ event in tofacitinib-treated patients was 4.0 (95% CI 3.7–4.4). Similar to a previous study by our group (8), the crude IRs varied widely across regions of enrollment and were numerically lowest in Eastern Europe (2.4 [95% CI 2.0–2.9]) and Western Europe (3.3 [95% CI 2.4–4.4]) and highest in Asia, particularly in Japan (8.0 [95% CI 6.6–9.6]) and Korea (8.4 [95% CI 6.4–10.9]) (Table 1).

For the first HZ event, the majority of patients (597 [93.9%]) had single-dermatome involvement, 46 patients (7.2%) were classified as having a serious HZ event, and no case resulted in death. Most patients (570 [89.6%]) received antiviral therapy while being treated with tofacitinib. After the first HZ event, tofacitinib treatment was continued in 274 patients (43.1%), while 267 patients (42.0%) temporarily stopped receiving tofacitinib, 5 patients (0.8%) reduced the tofacitinib dose during the event, 51 patients (8.0%) permanently discontinued tofacitinib treatment, and treatment changes were not reported in 39 patients (6.1%). Of the first HZ events, 602 cases had resolved at the time of the current analysis, with a median time to resolution of 21 days (range 1–733). The clinical study investigators reported that 47 (7.4%) of the initial patients developed postherpetic neuralgia.

Similar outcomes were reported for subsequent HZ events. Forty-seven patients (0.8% of all patients; 7.4% of patients in whom HZ developed) reported having at least 1 additional HZ event later during the study. None of the patients with a second HZ event had multiple dermatomes or visceral dissemination; 2 patients (4.3%) were graded as having serious AEs, and these patients were withdrawn from the study. Among the patients with a second HZ event, 19 (40.4%) continued to receive therapy during the event, 22 (46.8%) stopped tofacitinib temporarily during the event, and 4 (8.5%) permanently discontinued tofacitinib. The median time to resolution of a second HZ event was 20 days (range 4–122). Eight patients reported a third HZ event, and 1 patient experienced a total of 6 separate HZ events.

Examination of the effect of concomitant DMARD or GC therapy in phase III studies. With the exception of mean disease duration (for combination therapy, range 8.9–9.2 years; for monotherapy, range

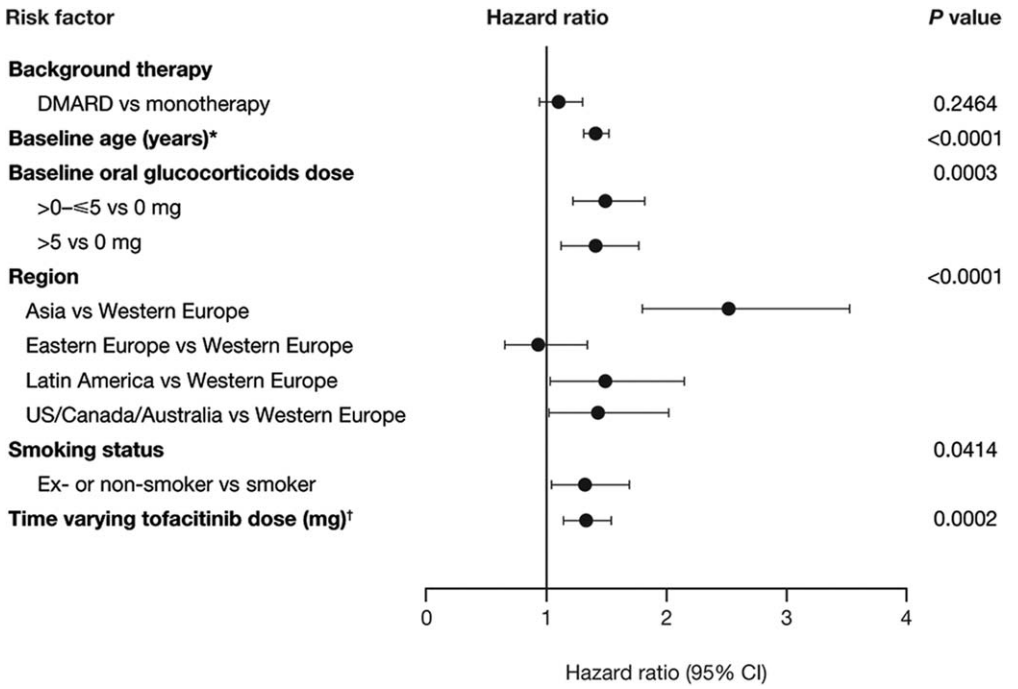

Figure 2. Cox proportional hazards regression model for the risk of herpes zoster with baseline factors among patients treated with tofacitinib in pooled phase I, II, III, and long-term extension studies. * = unit = 10 years. † = unit = 5 years. DMARD = disease-modifying antirheumatic drug; 95% CI = 95% confidence interval.

4.9–5.4 years), baseline characteristics in phase III studies were similar between patients receiving concomitant DMARDs and those receiving tofacitinib monotherapy (Table 2). For patients receiving concomitant DMARDs, most (92.2%) were receiving MTX. GC use was similar (~50%) between patients receiving either dose of tofacitinib with or without concomitant csDMARDs.

Although 681 patients received placebo in the phase III studies, the exposure time was very limited (202.7 patient-years), and only 3 patients were reported as having HZ during their exposure to placebo, with a crude IR of 1.5 (95% CI 0.3–4.3). As such, placebo data were not included in this stratified analysis. Details of these events in placebo-treated patients have previously been reported (8). All placebo-treated patients who reported HZ received concomitant csDMARDs, and 1 patient also received background GCs.

Crude IRs varied according to tofacitinib dose as well as treatment with background GCs and csDMARDs. Overall, the crude HZ IR among patients receiving tofacitinib 10 mg was numerically higher than that among those receiving 5 mg twice daily (4.1 [95% CI 3.3–5.2] versus 3.3 [95% CI 2.6–4.3]). Trends were seen for both the 5 mg twice daily and 10 mg twice daily dosage groups, in which the HZ IR was numerically lower in the absence of either background csDMARD or GC treatment (Figure 1). Numerically, the highest crude IR was observed in patients receiving tofacitinib 10 mg twice daily and both background DMARDs and GCs (5.4 [95% CI 3.7–7.7], based on 32 unique patients with events from among 550 patients with 606 patient-years of exposure) and the lowest crude IR was observed among patients receiving tofacitinib 5 mg twice daily as monotherapy without GCs (0.56 [95% CI 0.07–2.0], based on 2 unique patients with events among 296 patients with 361 patient-years of exposure).

Univariate and multivariable Cox proportional hazards regression analysis of HZ risk factors among patients treated with tofacitinib in pooled phase I, phase II, phase III, and LTE studies. In the Cox univariate analysis, a number of factors showed an association with an increased risk of HZ (see Supplementary Table 1, available on the *Arthritis & Rheumatology* web site at http://onlinelibrary.wiley.com/doi/10.1002/art.40189/abstract). Using the pool of risk factors identified by the univariate analysis and based on clinical consideration, after applying the backward selection procedure, 4 factors were selected for the final Cox proportional hazards regression model (Figure 2). These factors included baseline age (hazard ratio [HR] 1.41, 95% CI 1.31–1.52; unit = 10 years), baseline GC use (for >0 to ≤5 mg/day versus 0 mg/day, HR 1.49, 95% CI 1.22–

1.82; for >5 mg/day versus 0 mg/day, HR 1.41, 95% CI 1.12–1.77); region (for Asia versus Western Europe, HR 2.52, 95% CI 1.80–3.53; for Latin America versus Western Europe, HR 1.49, 95% CI 1.03–2.15; for US/Canada/Australia versus Western Europe, HR 1.43, 95% CI 1.02–2.02), and smoking status (former smoker or nonsmoker versus smoker, HR 1.32, 95% CI 1.04–1.69). The time-varying tofacitinib dose, which was added to the final model, also appeared to be a risk factor for HZ (HR 1.33, 95% CI 1.14–1.54; unit = 5 mg, e.g., an increase from 5 mg to 10 mg). Background csDMARD treatment was considered to be clinically relevant and was forced back into the final model, although it was not selected using the backward selection procedure. This factor did not appear to show an association with an increased risk of HZ (background DMARDs versus monotherapy, HR 1.10 [95% CI 0.94–1.30]).

DISCUSSION

We evaluated the long-term risk of HZ within the tofacitinib clinical development program for RA, with specific attention to the contribution of concomitant csDMARD therapy and GCs to the development of HZ. This analysis was performed following our preliminary evaluation of this question, in which we noted high rates of HZ among tofacitinib-treated patients compared with the expected rates in other studies in RA patients receiving TNF inhibitor (TNFi) therapy (8). Our current analysis includes a greater number of patients and longer exposure to tofacitinib than in the preliminary study. Analysis of this RA cohort, with almost 17,000 patient-years of tofacitinib exposure, suggests that use of concomitant GCs and age contribute to the risk of HZ, and that patients receiving tofacitinib at a dosage of 10 mg twice daily may be at higher risk than those using 5 mg twice daily. Data from phase III studies also indicated a trend toward higher rates of HZ in patients receiving background csDMARDs, particularly when combined with GCs. Our findings suggest that the use of the Food and Drug Administration–approved 5 mg twice daily dosage, and elimination of concomitant therapies, may represent potential risk-reduction strategies for physicians and patients, provided disease activity remains controlled. Overall, the HZ events seemed to be clinically manageable and resolved in the majority of cases. Regardless of concomitant therapy or tofacitinib dose, patients from Japan and Korea have the highest risk of HZ compared with that in other regions. It has also previously been reported that the HZ incidence is consistent over time in tofacitinib-treated patients, suggesting no increased risk for HZ with longer exposure to tofacitinib (10).

In our analysis of phase III studies, we observed that patients receiving tofacitinib at a dosage of 5 mg twice daily as monotherapy without GCs had a numerically 10-fold lower incidence of HZ compared with the patients receiving tofacitinib at a dosage of 10 mg twice daily with concomitant csDMARDs and GCs (exposure time was lower in the former group, which may increase variance). The incidence of HZ in patients receiving tofacitinib 5 mg twice daily as monotherapy without GCs (crude IR 0.56 [95% CI 0.07–2.01]) was similar to the incidence reported in those receiving biologic therapies, including patients who were and those who were not receiving concomitant MTX and GCs (6,12). GCs are a well-described dose-dependent risk factor for HZ worldwide (6,7).

Several studies have also shown an increased risk of HZ in association with biologic therapies, with similar risk factors for HZ identified, including the use of GCs (6,11–13). There are limited data, however, showing that MTX itself increases the risk of HZ in patients with RA (4). A prior meta-analysis of observational studies in RA failed to identify an association (14), and a subsequent population-based study in Minnesota also demonstrated no increased risk with MTX (36). A study in patients with psoriasis showed no increased risk of HZ in patients treated with MTX but did document an increased risk when MTX was combined with TNF blockers (37), and an analysis of psoriatic arthritis had similar findings, in that MTX was a risk only when it was administered in combination with biologic agents (38). We could not evaluate whether MTX alone causes HZ, and although concomitant csDMARD treatment appeared to increase the incidence of HZ in phase III studies, csDMARD treatment was not identified as an independent risk factor for HZ based on the Cox proportional hazards regression model used to evaluate HZ risk factors across all phases of the tofacitinib program.

The mechanism by which tofacitinib increases the risk of HZ is not well understood but may be related to inhibition of interferon (IFN) signaling. Antiviral defenses rely on type I and II IFN signaling via the JAK/STAT pathway (39), which is inhibited by tofacitinib (40,41). This hypothesis is supported by results from studies of sifalimumab, an anti-IFNα monoclonal antibody, which showed a substantial dose-dependent increase in the incidence of HZ following antibody treatment in patients with systemic lupus erythematosus (SLE) (42). An increase in the incidence of HZ was also observed in patients with SLE in a phase II

study of the anti-IFN inhibitor anifrolumab (43) and in a phase I study of rontalizumab (44). The association between MTX treatment, GC treatment, and an increased risk of HZ may also be explained by changes in IFN signaling, because concomitant GC and/or MTX treatment has been shown to suppress IFN signaling in patients with RA (45,46). Other mechanisms, including T cell alterations and cytokine inhibition, may also be involved.

Similar to the observations in our prior analysis (8), these data showed the risk of HZ to be substantially higher in certain areas of Asia. The IRs were shown to be highest in Japan and Korea, whereas rates elsewhere in Asia were comparable to those seen in Western Europe or North America. This raises the possibility that a genetic predisposition toward HZ under the condition of JAK inhibition might exist in some of these populations. However, regional differences in HZ reporting due to different access to health care professionals may also contribute. Bing et al reported 2 polymorphisms that were suggested to be associated with a higher risk of HZ in tofacitinib-treated patients, although these polymorphisms were relatively rare and explained only a fraction of the increased risk observed in the Japanese patients (47). It is possible that other genetic factors could explain this. However, it is unlikely that this is attributable to a difference in background varicella rates, because the seroprevalence of varicella in these Asian regions is similar to that in North America (48).

Although we are uncertain how many of the patients enrolled in this program in North America or elsewhere received shingles vaccination, because we did not collect a vaccination history prior to study entry, it is likely that very few or no patients received the vaccination prior to entering these studies. Population-based studies suggested that vaccine uptake during the period in which these studies were conducted was very poor among patients with RA in the US (49), and the vaccine was not available for use in some countries where enrollment took place (e.g., Japan). Furthermore, the vaccine is currently contraindicated for use during tofacitinib or biologic therapy, so it is unlikely that any patients were vaccinated during the LTE studies. However, studies are ongoing to evaluate the safety and immunogenicity of this vaccine when it is given before starting tofacitinib treatment (50).

Tofacitinib appears to be associated with an increased risk of HZ compared with TNFi therapy, and other JAK inhibitors, such as baricitinib, have also been associated with higher rates of HZ (9,51). However, direct comparisons with baricitinib are limited by the considerably shorter follow-up period and number of patient-years of exposure to baricitinib compared with tofacitinib. A large proportion of patients continued or only temporarily discontinued tofacitinib treatment during their HZ event, although almost all patients received antiviral therapy while receiving tofacitinib, which could potentially have protected against dissemination. According to the tofacitinib product label, treatment should be temporarily withdrawn during any serious infection, including HZ, until the infection is resolving, and patients should be closely monitored during any infection (52).

A recent analysis showed that postherpetic neuralgia occurred in 9.1% of patients with RA in whom HZ developed, with the incidence of postherpetic neuralgia increasing with age (53). In the tofacitinib development program, 7.4% of patients developed postherpetic neuralgia following their first HZ event. However, because reports of postherpetic neuralgia were not systematically requested, our findings may represent an underestimation of this complication. Interestingly, our study showed that current smoking was protective against HZ. There is some evidence that smoking can influence IFN signaling in mice (54). However, to our knowledge, our study is the first to demonstrate that smoking is protective against HZ. This finding is in contrast to at least 1 study of zoster ophthalmicus, in which smokers had a much earlier onset of HZ compared with nonsmokers (55).

In this analysis, our ability to evaluate the influence of GC dosage on the risk of HZ was limited. The exact dose of GCs and the total duration of GC use was not reported for many patients. In addition, we were unable to evaluate the influence of MTX dosage on the risk of HZ. Another limitation of this analysis was the substantially smaller number of patient-years of tofacitinib exposure in the monotherapy group compared with the combination therapy groups, leading to less robust incidence estimates for the monotherapy group.

In summary, we have described the long-term risk of HZ among patients treated with tofacitinib. Importantly, we found that the risk of HZ is likely to be greater in patients receiving tofacitinib in combination with GCs compared with those receiving monotherapy without GCs. Given that similar efficacy has been observed with tofacitinib in phase III clinical studies regardless of whether it is administered as monotherapy or in combination with csDMARDs and/or GCs (56), the use of tofacitinib monotherapy without GCs could represent a risk-reduction strategy for physicians and patients with regard to HZ and provide an effective

treatment strategy for reduction of the signs and symptoms of RA, provided the patient's RA remains controlled. It is also notable that HZ events were mostly nonserious and resolved with standard antiviral treatment. Furthermore, physicians should continue to consider shingles vaccination prior to starting tofacitinib or biologic therapy. Further research is necessary to understand why Japanese and Korean patients are at increased risk, as well as to understand the mechanism by which JAK inhibition combined with GCs leads to higher rates of VZV reactivation.

AUTHOR CONTRIBUTIONS

All authors were involved in drafting the article or revising it critically for important intellectual content, and all authors approved the final version to be published. Dr. Winthrop had full access to all of the data in the study and takes responsibility for the integrity of the data and the accuracy of the data analysis.

Study conception and design. Winthrop, Curtis, Fan, Chen, Bananis.

Acquisition of data. Winthrop, Fan, Chen, Bananis.

Analysis and interpretation of data. Winthrop, Curtis, Lindsey, Tanaka, Yamaoka, Valdez, Hirose, Nduaka, Wang, Mendelsohn, Fan, Chen, Bananis.

ROLE OF THE STUDY SPONSOR

This study was sponsored by Pfizer Inc. The manuscript was drafted, under direction from the authors, by Alice MacLachlan at Complete Medical Communications, funded by Pfizer Inc., with all authors providing subsequent critical revision. All authors interpreted the results, approved the final draft, and had the final decision to submit the manuscript for publication. Pfizer Inc. did not control the analysis or interpretation of the study results. Publication of this article was not contingent upon approval by Pfizer Inc.

REFERENCES

1. Harpaz R, Ortega-Sanchez IR, Seward JF. Prevention of herpes zoster: recommendations of the Advisory Committee on Immunization Practices (ACIP). MMWR Recomm Rep 2008;57(RR–5): 1–30.
2. Schmader KE. Epidemiology and impact on quality of life of postherpetic neuralgia and painful diabetic neuropathy. Clin J Pain 2002;18:350–4.
3. Watson PN. Postherpetic neuralgia. BMJ Clin Evid 2010;2010.
4. Smitten AL, Choi HK, Hochberg MC, Suissa S, Simon TA, Testa MA, et al. The risk of herpes zoster in patients with rheumatoid arthritis in the United States and the United Kingdom. Arthritis Rheum 2007;57:1431–8.
5. Yun H, Yang S, Chen L, Xie F, Winthrop K, Baddley JW, et al. Risk of herpes zoster in autoimmune and inflammatory diseases: implications for vaccination. Arthritis Rheumatol 2016;68:2328–37.
6. Yun H, Xie F, Delzell E, Chen L, Levitan EB, Lewis JD, et al. Risks of herpes zoster in patients with rheumatoid arthritis according to biologic disease-modifying therapy. Arthritis Care Res (Hoboken) 2015;67:731–6.
7. Pappas DA, Hooper MM, Kremer JM, Reed G, Shan Y, Wenkert D, et al. Herpes zoster reactivation in patients with rheumatoid arthritis: analysis of disease characteristics and disease-modifying antirheumatic drugs. Arthritis Care Res (Hoboken) 2015;67:1671–8.
8. Winthrop K, Yamanaka H, Valdez H, Mortensen E, Chew R, Krishnaswami S, et al. Herpes zoster and tofacitinib therapy in patients with rheumatoid arthritis. Arthritis Rheumatol 2014;66: 2675–84.
9. Genovese MC, Kremer J, Zamani O, Ludivico C, Krogulec M, Xie L, et al. Baricitinib in patients with refractory rheumatoid arthritis. N Engl J Med 2016;374:1243–52.
10. Cohen SB, Tanaka Y, Mariette X, Curtis JR, Lee EB, Nash P, et al. Long-term safety of tofacitinib for the treatment of rheumatoid arthritis up to 8.5 years: integrated analysis of data from the global clinical trials. Ann Rheum Dis 2017;76:1253–62.
11. Winthrop KL, Novosad SA, Baddley JW, Calabrese L, Chiller T, Polgreen P, et al. Opportunistic infections and biologic therapies in immune-mediated inflammatory diseases: consensus recommendations for infection reporting during clinical trials and postmarketing surveillance. Ann Rheum Dis 2015;74:2107–16.
12. Strangfeld A, Listing J, Herzer P, Liebhaber A, Rockwitz K, Richter C, et al. Risk of herpes zoster in patients with rheumatoid arthritis treated with anti-TNF-α agents. JAMA 2009;301:737–44.
13. Che H, Lukas C, Morel J, Combe B. Risk of herpes/herpes zoster during anti-tumor necrosis factor therapy in patients with rheumatoid arthritis: systematic review and meta-analysis. Joint Bone Spine 2014;81:215–21.
14. Zhang N, Wilkinson S, Riaz M, Ostor AJ, Nisar MK. Does methotrexate increase the risk of varicella or herpes zoster infection in patients with rheumatoid arthritis? A systematic literature review. Clin Exp Rheumatol 2012;30:962–71.
15. Cook IF. Herpes zoster in children following malaria. J Trop Med Hyg 1985;88:261–4.
16. Charles-Schoeman C, Fleischmann R, Davignon J, Schwartz H, Turner SM, Beysen C, et al. Potential mechanisms leading to the abnormal lipid profile in patients with rheumatoid arthritis versus healthy volunteers and reversal by tofacitinib. Arthritis Rheumatol 2015;67:616–25.
17. Kremer JM, Kivitz AJ, Simon-Campos JA, Nasonov EL, Tony H, Lee SK, et al. Evaluation of the effect of tofacitinib on measured glomerular filtration rate in patients with active rheumatoid arthritis: results from a randomised controlled trial. Arthritis Res Ther 2015;17:95.
18. Kremer JM, Bloom BJ, Breedveld FC, Coombs JH, Fletcher MP, Gruben D, et al. The safety and efficacy of a JAK inhibitor in patients with active rheumatoid arthritis: results of a double-blind, placebo-controlled phase IIa trial of three dosage levels of CP-690,550 versus placebo [published erratum appears in Arthritis Rheum 2012;64:1487]. Arthritis Rheum 2009;60:1895–905.
19. Kremer JM, Cohen S, Wilkinson BE, Connell CA, French JL, Gomez-Reino J, et al. A phase IIb dose-ranging study of the oral JAK inhibitor tofacitinib (CP-690,550) versus placebo in combination with background methotrexate in patients with active rheumatoid arthritis and an inadequate response to methotrexate alone. Arthritis Rheum 2012;64:970–81.
20. Fleischmann R, Cutolo M, Genovese MC, Lee EB, Kanik KS, Sadis S, et al. Phase IIb dose-ranging study of the oral JAK inhibitor tofacitinib (CP-690,550) or adalimumab monotherapy versus placebo in patients with active rheumatoid arthritis with an inadequate response to disease-modifying antirheumatic drugs. Arthritis Rheum 2012;64:617–29.
21. Tanaka Y, Suzuki M, Nakamura H, Toyoizumi S, Zwillich SH, Tofacitinib Study Investigators. Phase II study of tofacitinib (CP-690,550) combined with methotrexate in patients with rheumatoid arthritis and an inadequate response to methotrexate. Arthritis Care Res (Hoboken) 2011;63:1150–8.
22. Tanaka Y, Takeuchi T, Yamanaka H, Nakamura H, Toyoizumi S, Zwillich S. Efficacy and safety of tofacitinib as monotherapy in Japanese patients with active rheumatoid arthritis: a 12-week, randomized, phase 2 study. Mod Rheumatol 2015;25:514–21.
23. Conaghan PG, Østergaard M, Bowes MA, Wu C, Fuerst T, van der Heijde D, et al. Comparing the effects of tofacitinib, methotrexate and the combination, on bone marrow oedema, synovitis

and bone erosion in methotrexate-naive, early active rheumatoid arthritis: results of an exploratory randomised MRI study incorporating semiquantitative and quantitative techniques. Ann Rheum Dis 2016;75:1024–33.
24. Boyle DL, Soma K, Hodge J, Kavanaugh A, Mandel D, Mease P, et al. The JAK inhibitor tofacitinib suppresses synovial JAK1-STAT signalling in rheumatoid arthritis. Ann Rheum Dis 2015; 74:1311–6.
25. McInnes IB, Kim HY, Lee SH, Mandel D, Song YW, Connell CA, et al. Open-label tofacitinib and double-blind atorvastatin in rheumatoid arthritis patients: a randomised study. Ann Rheum Dis 2014;73:124–31.
26. Burmester GR, Blanco R, Charles-Schoeman C, Wollenhaupt J, Zerbini C, Benda B, et al. Tofacitinib (CP-690,550) in combination with methotrexate in patients with active rheumatoid arthritis with an inadequate response to tumour necrosis factor inhibitors: a randomised phase 3 trial. Lancet 2013;381:451–60.
27. Van der Heijde D, Tanaka Y, Fleischmann R, Keystone E, Kremer J, Zerbini C, et al. Tofacitinib (CP-690,550) in patients with rheumatoid arthritis receiving methotrexate: twelve-month data from a twenty-four–month phase III randomized radiographic study. Arthritis Rheum 2013;65:559–70.
28. Fleischmann R, Kremer J, Cush J, Schulze-Koops H, Connell CA, Bradley JD, et al. Placebo-controlled trial of tofacitinib monotherapy in rheumatoid arthritis. N Engl J Med 2012;367:495–507.
29. Kremer J, Li ZG, Hall S, Fleischmann R, Genovese M, Martin-Mola E, et al. Tofacitinib in combination with nonbiologic disease-modifying antirheumatic drugs in patients with active rheumatoid arthritis: a randomized trial. Ann Intern Med 2013;159:253–61.
30. Van Vollenhoven RF, Fleischmann R, Cohen S, Lee EB, García Meijide JA, Wagner S, et al. Tofacitinib or adalimumab versus placebo in rheumatoid arthritis. N Engl J Med 2012;367:508–19.
31. Lee EB, Fleischmann R, Hall S, Wilkinson B, Bradley J, Gruben D, et al. Tofacitinib versus methotrexate in rheumatoid arthritis. N Engl J Med 2014;370:2377–86.
32. Wollenhaupt J, Silverfield J, Lee EB, Curtis JR, Wood SP, Soma K, et al. Safety and efficacy of tofacitinib, an oral Janus kinase inhibitor, for the treatment of rheumatoid arthritis in open-label, longterm extension studies. J Rheumatol 2014;41:837–52.
33. Winthrop KL, Silverfield J, Racewicz A, Neal J, Lee EB, Hrycaj P, et al. The effect of tofacitinib on pneumococcal and influenza vaccine responses in rheumatoid arthritis. Ann Rheum Dis 2016;75:687–95.
34. Prevoo ML, van 't Hof MA, Kuper HH, van Leeuwen MA, van de Putte LB, van Riel PL. Modified disease activity scores that include twenty-eight–joint counts: development and validation in a prospective longitudinal study of patients with rheumatoid arthritis. Arthritis Rheum 1995;38:44–8.
35. Fries JF, Spitz P, Kraines RG, Holman HR. Measurement of patient outcome in arthritis. Arthritis Rheum 1980;23:137–45.
36. Veetil BM, Myasoedova E, Matteson EL, Gabriel SE, Green AB, Crowson CS. Incidence and time trends of herpes zoster in rheumatoid arthritis: a population-based cohort study. Arthritis Care Res (Hoboken) 2013;65:854–61.
37. Shalom G, Zisman D, Bitterman H, Harman-Boehm I, Greenberg-Dotan S, Dreiher J, et al. Systemic therapy for psoriasis and the risk of herpes zoster: a 500,000 person-year study. JAMA Dermatol 2015;151:533–8.
38. Zisman D, Bitterman H, Shalom G, Feldhamer I, Comanesther D, Batat E, et al. Psoriatic arthritis treatment and the risk of herpes zoster. Ann Rheum Dis 2016;75:131–5.
39. Malmgaard L. Induction and regulation of IFNs during viral infections. J Interferon Cytokine Res 2004;24:439–54.
40. Meyer D, Head R, Thompson J, Ghosh S, LaBranche T, Storer C, et al. Mechanism of action of the JAK inhibitor, CP-690550, in rheumatoid arthritis. Presented at the 8th Cytokines and Inflammation Conference; 2010 January 28; San Diego, California.
41. Konig N, Fiehn C, Wolf C, Schuster M, Cura Costa E, Tungler V, et al. Familial chilblain lupus due to a gain-of-function mutation in STING. Ann Rheum Dis 2017;76:468–72.
42. Khamashta M, Merrill JT, Werth VP, Furie R, Kalunian K, Illei GG, et al. Sifalimumab, an anti-interferon-α monoclonal antibody, in moderate to severe systemic lupus erythematosus: a randomised, double-blind, placebo-controlled study. Ann Rheum Dis 2016;75:1909–16.
43. Narain S, Furie R. Update on clinical trials in systemic lupus erythematosus. Curr Opin Rheumatol 2016;28:477–87.
44. McBride JM, Jiang J, Abbas AR, Morimoto A, Li J, Maciuca R, et al. Safety and pharmacodynamics of rontalizumab in patients with systemic lupus erythematosus: results of a phase I, placebo-controlled, double-blind, dose-escalation study. Arthritis Rheum 2012;64:3666–76.
45. De Jong TD, Vosslamber S, Blits M, Wolbink G, Nurmohamed MT, van der Laken CJ, et al. Effect of prednisone on type I interferon signature in rheumatoid arthritis: consequences for response prediction to rituximab. Arthritis Res Ther 2015;17:78.
46. Haroon N, Srivastava R, Misra R, Aggarwal A. A novel predictor of clinical response to methotrexate in patients with rheumatoid arthritis: a pilot study of in vitro T cell cytokine suppression. J Rheumatol 2008;35:975–8.
47. Bing N, Zhou H, Zhang B, Bradley JD, Nagaoka M, Valdez H, et al. Genome-wide trans-ancestry meta-analysis of herpes zoster in RA and Pso patients treated with tofacitinib [abstract]. Arthritis Rheumatol 2015;67 Suppl 10. URL: http://acrabstracts.org/abstract/genome-wide-trans-ancestry-meta-analysis-of-herpes-zoster-in-ra-and-pso-patients-treated-with-tofacitinib/.
48. Takao Y, Miyazaki Y, Okeda M, Onishi F, Yano S, Gomi Y, et al. Incidences of herpes zoster and postherpetic neuralgia in Japanese adults aged 50 years and older from a community-based prospective cohort study: the SHEZ study. J Epidemiol 2015;25:617–25.
49. Zhang J, Xie F, Delzell E, Chen L, Winthrop KL, Lewis JD, et al. Association between vaccination for herpes zoster and risk of herpes zoster infection among older patients with selected immune-mediated diseases. JAMA 2012;308:43–9.
50. Winthrop K, Wouters A, Choy E, Soma K, Hodge J, Nduaka C, et al. Assessment of immunogenicity of live zoster vaccination (Zostavax®) in rheumatoid arthritis patients on background methotrexate before and after initiating tofacitinib or placebo [abstract]. Arthritis Rheumatol 2015;67 Suppl 10. URL: http://acrabstracts.org/abstract/assessment-of-immunogenicity-of-live-zoster-vaccination-zostavax-in-rheumatoid-arthritis-patients-on-background-methotrexate-before-and-after-initiating-tofacitinib-or-placebo/.
51. Dougados M, van der Heijde D, Chen YC, Greenwald M, Drescher E, Liu J, et al. Baricitinib, an oral Janus kinase (JAK)1/JAK2 inhibitor, in patients with active rheumatoid arthritis (RA) and an inadequate response to cDMARD therapy: results of the phase 3 RA-BUILD study. Ann Rheum Dis 2015;74 Suppl 2:79.
52. XELJANZ prescribing information. New York: Pfizer; 2016. URL: http://labeling.pfizer.com/ShowLabeling.aspx?id=959.
53. Forbes HJ, Bhaskaran K, Thomas SL, Smeeth L, Clayton T, Mansfield K, et al. Quantification of risk factors for postherpetic neuralgia in herpes zoster patients: a cohort study. Neurology 2016;87:94–102.
54. Bidkar M, Vassallo R, Luckey D, Smart M, Mouapi K, Taneja V. Cigarette smoke induces immune responses to vimentin in both, arthritis-susceptible and -resistant humanized mice. PLoS One 2016;11:e0162341.
55. Chan AY, Conrady CD, Ding K, Dvorak JD, Stone DU. Factors associated with age of onset of herpes zoster ophthalmicus. Cornea 2015;34:535–40.
56. Fleischmann R, Charles-Schoeman C, Burmester G, Zerbini C, Nash P, Kwok K, et al. The effects of glucocorticoids on the efficacy of tofacitinib as monotherapy and in combination therapy with nonbiologic Dmards: an analysis of data from six phase 3 studies [abstract]. Arthritis Rheumatol 2015;67 Suppl 10. URL: http://acrabstracts.org/abstract/the-effects-of-glucocorticoids-on-the-efficacy-of-tofacitinib-as-monotherapy-and-in-combination-therapy-with-nonbiologic-dmards-an-analysis-of-data-from-six-phase-3-studies/.

ARTHRITIS & RHEUMATOLOGY
Vol. 69, No. 10, October 2017, pp 1969–1977
DOI 10.1002/art.40187

The Safety and Immunogenicity of Live Zoster Vaccination in Patients With Rheumatoid Arthritis Before Starting Tofacitinib

A Randomized Phase II Trial

Kevin L. Winthrop,[1] Ann G. Wouters,[2] Ernest H. Choy,[3] Koshika Soma,[2] Jennifer A. Hodge,[2] Chudy I. Nduaka,[4] Pinaki Biswas,[2] Elie Needle,[5] Sherry Passador,[2] Christopher F. Mojcik,[2] and William F. Rigby[6]

Objective. **Patients with rheumatoid arthritis (RA) are at increased risk of herpes zoster, and vaccination is recommended for patients ages 50 years and older, prior to starting treatment with biologic agents or tofacitinib. Tofacitinib is an oral JAK inhibitor for the treatment of RA. We evaluated its effect on the immune response and safety of live zoster vaccine (LZV).**

Methods. **In this phase II, 14-week, placebo-controlled trial, patients ages 50 years and older who had active RA and were receiving background methotrexate were given LZV and randomized to receive tofacitinib 5 mg twice daily or placebo 2–3 weeks postvaccination. We measured humoral responses (varicella zoster virus [VZV]–specific IgG level as determined by glycoprotein enzyme-linked immunosorbent assay) and cell-mediated responses (VZV-specific T cell enumeration, as determined by enzyme-linked immunospot assay) at baseline and 2 weeks, 6 weeks, and 14 weeks postvaccination. End points included the geometric mean fold rise (GMFR) in VZV-specific IgG levels (primary end point) and T cells (number of spot-forming cells/10^6 peripheral blood mononuclear cells) at 6 weeks postvaccination.**

Results. **One hundred twelve patients were randomized to receive tofacitinib (n = 55) or placebo (n = 57). Six weeks postvaccination, the GMFR in VZV-specific IgG levels was 2.11 in the tofacitinib group and 1.74 in the placebo group, and the VZV-specific T cell GMFR was similar in the tofacitinib group and the placebo group (1.50 and 1.29, respectively). Serious adverse events occurred in 3 patients in the tofacitinib group (5.5%) and 0 patients (0.0%) in the placebo group. One patient, who lacked preexisting VZV immunity, developed cutaneous vaccine dissemination 2 days after starting tofacitinib (16 days postvaccination). This resolved after tofacitinib was discontinued and the patient received antiviral treatment.**

Conclusion. **Patients who began treatment with tofacitinib 2–3 weeks after receiving LZV had VZV-specific humoral and cell-mediated immune responses to LZV similar to those in placebo-treated patients. Vaccination appeared to be safe in all of the patients except 1 patient who lacked preexisting VZV immunity.**

Herpes zoster (HZ), or shingles, is a common and sometimes debilitating disease that disproportionately affects elderly individuals and those who are immunocompromised (1). Patients with rheumatoid arthritis (RA) have a 1.5–2-fold higher risk of developing HZ compared with healthy adults (2), and treatment with some disease-

ClinicalTrials.gov identifier: NCT02147587.
Supported by Pfizer.
[1]Kevin L. Winthrop, MD, MPH: Oregon Health and Science University, Portland; [2]Ann G. Wouters, MS, Koshika Soma, MD, Jennifer A. Hodge, PhD, Pinaki Biswas, PhD, Sherry Passador, MS, Christopher F. Mojcik, MD, PhD: Pfizer Inc, New York, New York; [3]Ernest H. Choy, MD: Cardiff University School of Medicine, Cardiff, UK; [4]Chudy I. Nduaka, DVM, PhD: Pfizer Inc, Collegeville, Pennsylvania; [5]Elie Needle, BS: Pfizer Inc, Pearl River, New York; [6]William F. Rigby, MD: Geisel School of Medicine at Dartmouth, Lebanon, New Hampshire.
Dr. Winthrop has received consulting fees (more than $10,000) and research grants from Pfizer. Dr. Choy has received consulting fees and speaking fees (less than $10,000) and research grants from Pfizer. Drs. Soma, Hodge, Nduaka, Biswas, and Mojcik, and Ms Wouters, Mr. Needle, and Ms Passador own stock or stock options in Pfizer. Dr. Rigby has received consulting fees from Pfizer (less than $10,000).
Address correspondence to Kevin L. Winthrop, MD, MPH, Casey Eye Institute, Oregon Health and Science University, 3375 SW Terwilliger Boulevard, Portland, OR 97239. E-mail: Winthrop@ohsu.edu.
Submitted for publication October 31, 2016; accepted in revised form June 20, 2017.

modifying antirheumatic drugs (DMARDs) has been shown to further increase this risk (3,4). Tofacitinib is an oral JAK inhibitor for the treatment of RA. The efficacy and safety of tofacitinib at dosages of 5 mg twice daily and 10 mg twice daily, administered as monotherapy or in combination with DMARDs, in patients with active RA have been demonstrated in phase II, phase III, and long-term extension (LTE) studies (5–13). Tofacitinib has been shown to increase the risk of developing HZ, particularly when it is given in combination with methotrexate (MTX) or prednisone (14–16).

Given the preventable nature of HZ, the American College of Rheumatology (ACR), the European League Against Rheumatism (EULAR), and other committees, such as the Advisory Committee on Immunization Practices (ACIP), recommend vaccinating patients with RA (1,17–19). Due to the live nature of the zoster vaccine, there is a theoretical risk of dissemination in immunosuppressed patients, and it is recommended that treatment with a biologic agent or tofacitinib should not be started until 2–4 weeks after the vaccination (1,20). However, guidelines for the timing of the vaccination relative to the start of immunosuppressive therapy are conflicting. According to the ACR guidelines, RA patients ages ≥50 years should be vaccinated with the live zoster vaccine (LZV) at least 2 weeks prior to starting therapy with a biologic agent or tofacitinib (18,21). The 2011 EULAR guidelines suggest general avoidance of this vaccine in immunosuppressed patients but emphasize the potential importance of the vaccine and the need to give it to those with positive findings on serologic tests for varicella zoster virus in combination with temporary cessation of immunosuppressive drug therapy (19). The ACIP recommends administration of the vaccine to persons ages ≥60 years, including those with chronic medical conditions such as RA (1).

Previous studies have shown that in immunocompetent individuals, the efficacy of LZV for protection against HZ was 51% in those ages ≥60 years over a follow-up period of 4.9 years and 70% in those ages 50–59 years over a follow-up period of 1.3 years (17). Despite the higher risk of HZ in patients with RA, there has been no large interventional clinical study of LZV in the setting of RA. The immunogenicity and safety of LZV in patients receiving DMARDs (including tofacitinib) are unknown. Accordingly, we sought to evaluate the safety and immunogenicity of LZV in a group of patients with RA, prior to starting tofacitinib therapy.

PATIENTS AND METHODS

We enrolled patients with active RA who were receiving stable background doses of MTX into a phase II, 14-week, randomized, double-blind, parallel-arm, placebo-controlled trial (study A3921237; ClinicalTrials.gov identifier: NCT02147587). Patients were randomized (1:1) to receive tofacitinib at a dosage of 5 mg twice daily or placebo 2–3 weeks after vaccination with LZV, to specifically assess the effect of tofacitinib 5 mg twice daily on the safety and immunogenicity of LZV. The study was conducted at 27 centers across the US, between June 2014 and July 2015 (see Supplementary Information, available on the *Arthritis & Rheumatology* web site at http://onlinelibrary.wiley.com/doi/10.1002/art.40187/abstract). RA patients ages 50 years and older were eligible if they had at least 4 tender/painful joints and ≥4 swollen joints (28 assessed) at the time of screening or at baseline (before vaccination), and a C-reactive protein level of >3 mg/liter or a Clinical Disease Activity Index (22) score of >10 at the time of screening or at baseline. Patients were enrolled if they met the 2010 ACR/EULAR criteria for an RA score of ≥6 (23). Prior to screening, patients must have received continuous treatment with MTX at a dosage of 15–25 mg/week for at least 4 months. Exclusion criteria were any of the following: recent history of serious infection (within 6 months), recent infection requiring treatment (within 2 weeks), active hepatitis B or hepatitis C virus infection, untreated latent tuberculosis, any history of malignancy (except nonmelanoma or squamous cell skin cancer or cervical carcinoma in situ), a history of recurrent (>1 episode) or disseminated HZ, prior exposure to LZV, or a history of any other vaccination in the past 6 weeks (see inclusion/exclusion criteria, available on the *Arthritis & Rheumatology* web site at http://onlinelibrary.wiley.com/doi/10.1002/art.40187/abstract).

Study conduct. Eligible patients were vaccinated and then randomized (1:1) to receive either tofacitinib 5 mg twice daily or placebo, initiated 2–3 weeks postvaccination (see Supplementary Figure 1, available on the *Arthritis & Rheumatology* web site at http://onlinelibrary.wiley.com/doi/10.1002/art.40187/abstract). Patients continued to receive their current dose of MTX. Concomitant treatment with prednisone or equivalent at a dosage of ≤10 mg/day was allowed. A history of varicella was not investigated, and patients were not screened for VZV antibodies. RA disease activity was measured only at baseline, prior to vaccination. Other demographic, comorbidity, and other clinical data for the participants were collected at baseline. The study concluded after 12 weeks of treatment with tofacitinib or placebo (14 weeks postvaccination), and the patients were given the option of joining a separate LTE study at that time (see Supplementary Figure 2, available on the *Arthritis & Rheumatology* web site at http://onlinelibrary.wiley.com/doi/10.1002/art.40187/abstract). These studies were approved by the institutional review board and/or independent ethics committee at each center and were carried out in accordance with the Declaration of Helsinki and in compliance with all International Conference on Harmonisation Good Clinical Practice guidelines.

Immunogenicity analyses. We evaluated both humoral and cell-mediated responses at baseline (just prior to vaccination) and at 2, 6, and 14 weeks after vaccination (day 1, week 4, and week 12 of treatment with tofacitinib or placebo). Measures included VZV-specific IgG levels, as determined by purified glycoprotein enzyme-linked immunosorbent assay (gpELISA), and VZV-specific T cell responses, as determined by enumeration of interferon-γ (IFNγ) spot-forming cells (SFCs) using an enzyme-linked immunospot (ELISpot) assay.

The primary end point of the trial was the geometric mean fold rise (GMFR) in VZV-specific IgG levels at 6 weeks postvaccination. Secondary and additional end points included

Table 1. Characteristics of the patients, including measures of VZV immunity on the day of LZV immunization*

	Placebo	Tofacitinib 5 mg BID
Baseline demographics		
Age, mean ± SD years	62.0 ± 8.7	61.7 ± 6.2
Female	38 (66.7)	42 (76.4)
BMI, mean ± SD kg/m^2	30.7 ± 6.1	31.4 ± 7.1
Background MTX	57 (100.0)	54 (98.2)
MTX dose, mean ± SD mg/week	16.9 ± 4.3	17.1 ± 4.7
Prednisone daily equivalent	21 (36.8)	26 (47.3)
Prednisone, or equivalent, dose, mean ± SD mg/day	7.1 ± 4.8	5.9 ± 2.2
No prior biologic DMARD exposure	20 (35.1)	29 (52.7)
Inadequate response to prior biologic DMARD	37 (64.9)	26 (47.3)
More than 1 biologic DMARD failure	12 (21.1)	8 (14.5)
RA assessments at screening		
CRP, mean ± SD mg/liter	1.3 ± 1.3	1.6 ± 2.9
ESR, mean ± SD mm/hour	41.1 ± 22.9	47.1 ± 29.3
Tender/painful joint count (28 assessed), mean ± SD	14.6 ± 6.6	14.5 ± 6.5
Swollen joint count (28 assessed), mean ± SD	10.8 ± 5.8	11.0 ± 5.6
Measurement of immunity to VZV at baseline		
VZV-specific IgG level, GMT (80% CI) [range]	182.3 (151.3–219.8) [8.3–1,176.9]	201.0 (166.0–243.2) [0.32–2,370.8]
VZV-specific T cell response, GMC (80% CI) [range]†	43.2 (36.4–51.3) [25–559]	48.4 (40.6–57.7) [25–309]

* The numbers of patients in the placebo and tofacitinib groups are as follows: for baseline demographics, n = 57 and n = 55, respectively; for rheumatoid arthritis (RA) assessments at screening, n = 57 and n = 55, respectively; for measurement of immunity to varicella zoster virus (VZV), n = 53 and n = 54, respectively. Except where indicated otherwise, values are the number (%). LZV = live zoster vaccine; BID = twice daily; BMI = body mass index; MTX = methotrexate; DMARD = disease-modifying antirheumatic drug; CRP = C-reactive protein; ESR = erythrocyte sedimentation rate; GMT = geometric mean titer; 80% CI = 80% confidence interval; GMC = geometric mean count.

† Measured by enumeration of interferon-γ spot-forming cells, using enzyme-linked immunospot assay.

the proportion of patients achieving a ≥1.5-fold increase in VZV-specific IgG levels, the absolute VZV-specific IgG levels, the absolute numbers of VZV-specific reactive T cells, and the GMFR in VZV-specific reactive T cells between baseline and 2, 6, and 14 weeks postvaccination.

For gpELISA measures, we used a validated assay (PPD Vaccines and Biologics) used for licensure of Zostavax and widely used in research settings. For gpELISA output, the geometric mean titer was defined as the geometric mean of 3 independent assay measurements of each blood sample.

ELISpot results were obtained using an assay qualified to quantify the number of IFNγ-secreting cells (performed at the Pfizer Inc Vaccine Research Unit, Pearl River, NY). Four hundred thousand peripheral blood mononuclear cells (PBMCs) isolated from whole blood samples obtained from the patients were plated on 96-well plates in triplicate. After a mean ± SD of 18 ± 2 hours of incubation (37°C in 5% CO_2) with processed VZV from Oka vaccine strain, reactive T lymphocytes were enumerated. The number of SFCs/10^6 PBMCs was recorded (24).

Safety assessments. The safety end points were evaluated for 12 weeks after randomization and included adverse events (AEs), serious AEs (SAEs), clinically significant laboratory abnormalities, vaccine-related AEs (including injection-site reactions and HZ-like lesions), and clinical HZ events. Patients who developed rashes during this time period were instructed to be seen by their study physician, and a biopsy specimen of the involved skin was to be obtained if the rash was clinically suggestive of VZV infection. For any patients needing a biopsy, specimens were to be transferred in viral transport media and then sent to the Centers for Disease Control and Prevention (CDC) for VZV testing. Real-time Förster Resonance Energy Transfer–based polymerase chain reaction (PCR) analysis using a LightCycler platform was performed to target different vaccine-associated single-nucleotide markers in the VZV genome. If VZV infection was identified, samples were tested for markers in open-reading frame 38 (ORF 38) and ORF 54 (to discriminate the Oka vaccine strain from other wild-type strains) and for 2 vaccine strain–specific markers in ORF 62, to confirm VZV infection and to robustly discriminate the vaccine strain from wild-type strains.

Sample size determination. The number of patients (up to ~70 in each treatment group) was selected based on a literature review and clinical considerations (25). Specifically, for the primary end point of fold increase from baseline in VZV-specific IgG antibodies at 6 weeks postvaccination (week 4 of treatment with the study drug), assuming a common SD of 1.33 on the logarithmic scale (~3.8-fold on the original scale), a sample size of up to 70 patients in each group would yield a halfwidth of ~0.288 on the logarithmic scale for a 2-sided 80% confidence interval (80% CI) of the ratio of the GMFRs between the tofacitinib 5 mg twice daily group and the placebo group (tofacitinib/placebo), ensuring that the GMFR is estimated with reasonable precision.

Statistical analysis. The final analysis included only patients who were deemed "evaluable" and had a complete set of assay results for gpELISA at both baseline and 6 weeks postvaccination, had started the study drug according to the protocol 2–3 weeks postvaccination, and had been ≥80% compliant with the

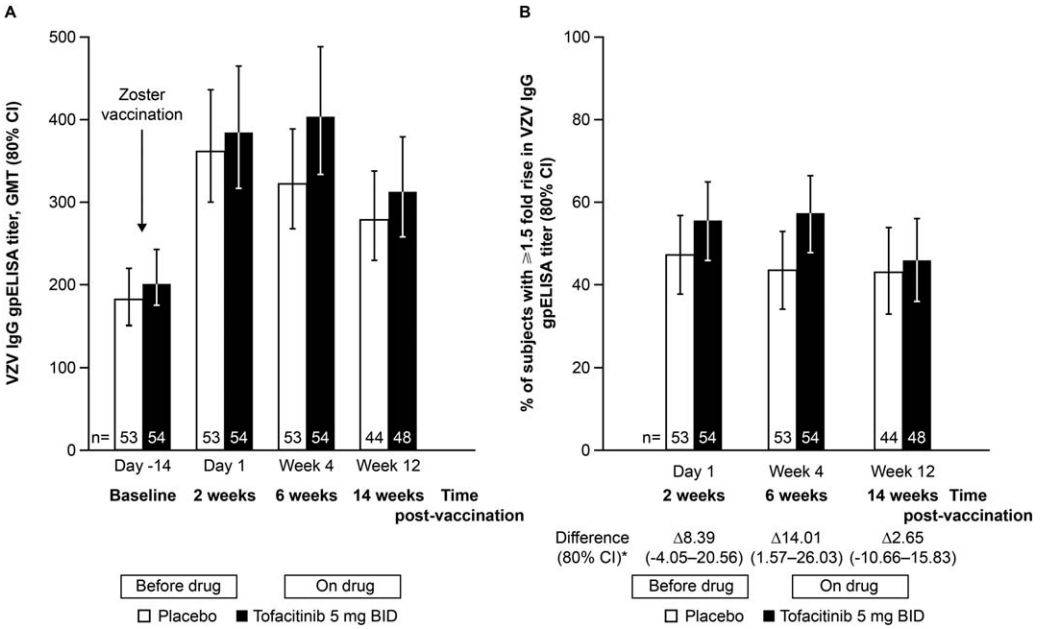

Figure 1. Analyses of varicella zoster virus (VZV)–specific IgG levels. Live zoster vaccine was given on day −14; a blood sample from each subject was obtained at that time to evaluate the baseline immune response to VZV immediately before vaccination. **A,** Mean absolute VZV-specific IgG levels (glycoprotein enzyme-linked immunosorbent assay [gpELISA] titer) in the tofacitinib group and the placebo group at baseline (day −14, before vaccination) and 2, 6, and 12 weeks postvaccination. **B,** Proportion of patients with a ≥1.5-fold change in VZV-specific IgG levels (gpELISA titer) in the tofacitinib group and the placebo group at 2, 6, and 12 weeks postvaccination. * = The 80% confidence intervals (80% CIs) were calculated using the Clopper-Pearson exact method. GMT = geometric mean titer; BID = twice daily.

study drug until 6 weeks postvaccination. The study was not designed to test any statistical hypotheses; therefore, all comparisons described herein are based on the observed magnitudes of the estimates only. For the primary outcome in this group, we compared measures at baseline with those obtained at week 6 postvaccination. We calculated an adjusted estimation of the GMFR ratios (tofacitinib/placebo) using a linear mixed model (analysis of covariance) with repeated measures that included age, sex, randomization stratum (biologic agent–naive versus prior biologic nonresponder) and baseline value as covariates, and study treatment, visit after vaccination, and treatment-by-visit interaction as fixed effects. The GMFR ratios (tofacitinib/placebo) from baseline were computed. The 2-sided 80% CI of this ratio was obtained from this model (back-transformation).

Additionally, the primary end point was analyzed using descriptive methods (GMFR, geometric SD, minimum, and maximum, according to treatment group and visit following vaccination). Two-sided 80% CIs for the geometric mean constructed by back-transformation of the CI for the mean of the logarithmically transformed end point (computed using Student's *t*-distribution) were calculated.

RESULTS

Baseline characteristics of the patients. One hundred twelve patients were randomized to receive placebo (n = 57) or tofacitinib (n = 55). Overall, patients in both treatment groups were similar with regard to sex, age, baseline disease activity, and baseline VZV immune measures (Table 1). Among the 112 patients vaccinated and subsequently randomized, 16 discontinued because of AEs not related to the study drug (2 patients in the tofacitinib group and 7 patients in the placebo group), AEs related to the study drug (2 patients in the tofacitinib group and 2 patients in the placebo group), or an insufficient clinical response (1 patient in the tofacitinib group and 2 patients in the placebo group) (see Supplementary Figure 3, available on the *Arthritis & Rheumatology* web site at http://onlinelibrary.wiley.com/doi/10.1002/art.40187/abstract).

Immunogenicity. Most patients (53 [93%] of those in the placebo group and 54 [98%] of those in the tofacitinib group) were evaluable for the immune response end points. Among these individuals, the GMFR for VZV-specific IgG levels at 6 weeks postvaccination was similar between the tofacitinib-treated and placebo-treated patients.

The mean VZV-specific IgG levels at 6 weeks postvaccination (4 weeks after treatment initiation) were 403.42 units/ml and 322.49 units/ml in tofacitinib-treated and placebo-treated patients, respectively (Figure 1A), and the GMFRs from baseline at this time point were 2.11 (80% CI 1.87–2.37) and 1.74 (80% CI 1.55–1.95), respectively. VZV-specific IgG levels were also evaluated on day 1 (2 weeks postvaccination) and after 3 months (14 weeks

Table 2. GMFR in VZV-specific IgG levels from baseline over the 12-week treatment period*

Visit, treatment	GMFR (80% CI)	GMFR ratios (tofacitinib/placebo) (80% CI)
Day 1 (2 weeks postvaccination)		
Tofacitinib 5 mg BID (n = 54)	2.01 (1.78–2.26)	1.03 (0.88–1.21)
Placebo (n = 53)	1.95 (1.73–2.19)	
Week 4 (6 weeks postvaccination)		
Tofacitinib 5 mg BID (n = 54)	2.11 (1.87–2.37)	1.21 (1.03–1.42)
Placebo (n = 53)	1.74 (1.55–1.95)	
Week 12 (14 weeks postvaccination)		
Tofacitinib 5 mg BID (n = 48)	1.64 (1.45–1.85)	1.09 (0.92–1.29)
Placebo (n = 44)	1.50 (1.32–1.69)	

* GMFR = geometric mean fold rise; VZV = varicella zoster virus; 80% CI = 80% confidence interval; BID = twice daily.

postvaccination) of tofacitinib or placebo treatment. At all postvaccination time points, there was a trend toward numerically higher GMFRs in tofacitinib-treated patients (Table 2), but the differences were small and not statistically significant. Furthermore, the proportion of patients developing a ≥1.5-fold postvaccination increase in IgG levels at 6 weeks postvaccination trended higher for those receiving tofacitinib (57.4%) compared with those receiving placebo (43.4%) (Figure 1B). Similar results were observed in a subpopulation of patients who were not treated with corticosteroids and with data stratified according to age (see Supplementary Table 1, available on the *Arthritis & Rheumatology* web site at http://onlinelibrary.wiley.com/doi/10.1002/art.40187/abstract).

An ELISpot assay to enumerate VZV-specific IFNγ-secreting T cells was performed. For this cell-mediated immune response, the absolute VZV-specific reactive cell counts were 69.97 and 56.39 SFCs/10^6 PBMCs 6 weeks postvaccination in the tofacitinib group and the placebo group, respectively (Figure 2). The GMFR in VZV-specific T cell responses at 6 weeks was similar in tofacitinib-treated patients (1.50; 80% CI

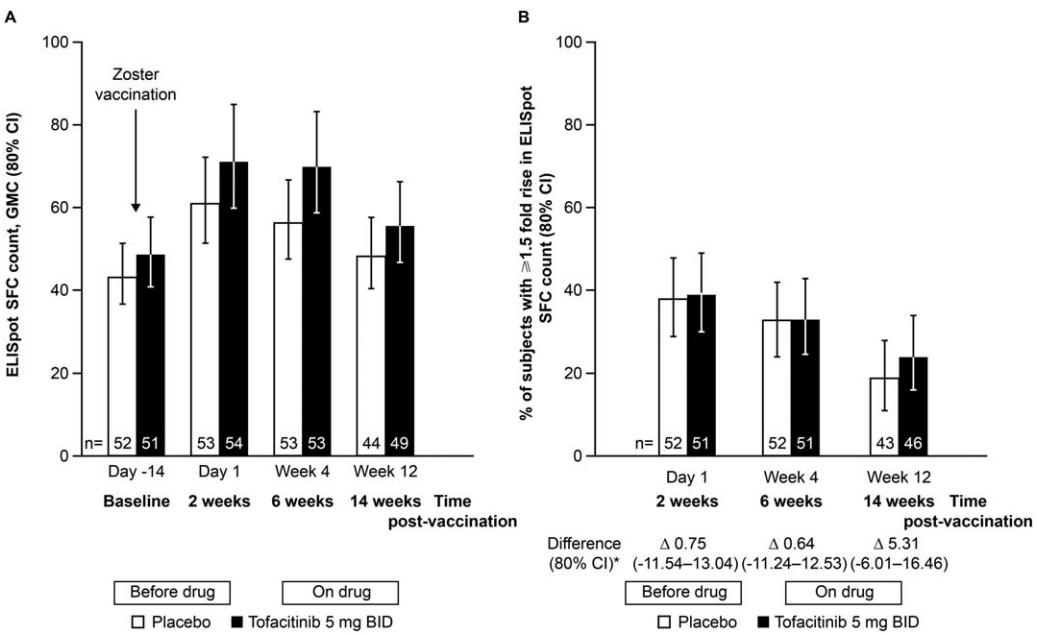

Figure 2. Analyses of VZV-specific T cell responses, measured by enumeration of interferon-γ spot-forming cells (SFCs) using enzyme-linked immunospot (ELISpot) assay. Live zoster vaccine was given on day −14; a blood sample from each subject was obtained at that time to evaluate the baseline immune response to VZV immediately before vaccination. **A,** Mean absolute values of VZV-specific reactive T cells, as determined by ELISpot assay, in the tofacitinib group and the placebo group at baseline (day −14, before vaccination) and 2, 6, and 12 weeks postvaccination. **B,** Proportion of patients with a ≥1.5-fold change in the VZV-specific T cell response, as determined by ELISpot assay, in the tofacitinib group and the placebo group at 2, 6, and 12 weeks postvaccination. * = The 80% confidence intervals (80% CIs) were calculated using the Clopper-Pearson exact method. GMC = geometric mean count (see Figure 1 for other definitions).

Table 3. GMFR in VZV-specific T cell responses over the 12-week treatment period*

Visit, treatment	GMFR (80% CI)	Ratio of GMFRs tofacitinib/placebo (80% CI)
Day 1 (2 weeks postvaccination)		
Tofacitinib 5 mg BID (n = 51)	1.54 (1.35–1.75)	1.10 (0.92–1.31)
Placebo (n = 52)	1.40 (1.23–1.58)	
Week 4 (6 weeks postvaccination)		
Tofacitinib 5 mg BID (n = 51)	1.50 (1.31–1.70)	1.16 (0.97–1.38)
Placebo (n = 52)	1.29 (1.14–1.46)	
Week 12 (14 weeks postvaccination)		
Tofacitinib 5 mg BID (n = 46)	1.17 (1.02–1.34)	1.05 (0.88–1.27)
Placebo (n = 43)	1.11 (0.97–1.27)	

* GMFR = geometric mean fold rise; VZV = varicella zoster virus; 80% CI = 80% confidence interval; BID = twice daily.

1.31–1.70) and placebo-treated patients (1.29; 80% CI 1.14–1.46) (Table 3). This increase was also similar at weeks 2 and 14 postvaccination. The proportion of patients developing a ≥1.5-fold postvaccination increase in the T cell response was similar between groups at 6 weeks postvaccination (33.3% in the tofacitinib group and 32.7% in the placebo group), as well as other postvaccination time points (Figure 2B). Similar results were observed when we analyzed a subgroup of patients who did not receive concomitant glucocorticoids (see Supplementary Table 2, available on the *Arthritis & Rheumatology* web site at http://onlinelibrary.wiley.com/doi/10.1002/art.40187/abstract).

Safety. One patient in the placebo group discontinued treatment following abnormal results for the absolute neutrophil count; other nonserious vaccine-related AEs were identified in 7 patients in the tofacitinib group and 5 patients in the placebo group (see Supplementary Table 3, available on the *Arthritis & Rheumatology* web site at http://onlinelibrary.wiley.com/doi/10.1002/art.40187/abstract). These AEs included mild injection-site swelling, redness, or itching.

SAEs occurred in 3 patients in the tofacitinib group (5.5%) and 0 patients in the placebo group (0%). The 3 SAEs included 1 case each of cholangitis and bronchitis, and 1 case of disseminated primary varicella. Onset of the disseminated rash occurred 16 days postvaccination (2 days after starting tofacitinib), on the patient's trunk (back and abdomen) and right ipsilateral arm. The patient discontinued tofacitinib and was treated with antiviral (valcyclovir) therapy for 7 days, and the rash resolved. She was not hospitalized and continued to receive background oral MTX (15 mg/week) and oral prednisone (4 mg/day) for RA, as per prior and upon vaccination. Biopsy specimens from both her abdomen and forearm showed mixed deep granulomatous perivascular inflammation with fibrinoid degeneration of vessel walls, which was morphologically compatible with VZV infection. Molecular testing in the abdominal specimen showed PCR positivity for VZV DNA, with subsequent genomic work-up at the CDC confirming that VZV was the Oka vaccine strain.

Subsequent evaluation of this patient's baseline blood specimens showed that she lacked preexisting immunity to VZV. Unlike any other patient in the study, she had no measurable VZV-specific T cell response and a negative gpELISA titer at baseline (Table 4). Interestingly, at 2 weeks after vaccination (and just prior to starting tofacitinib treatment), this patient had no measurable

Table 4. VZV-specific immune response evaluations in the patient with disseminated HZ*

Immune response, assay	Day −14, before vaccination (1/13/15)	Day 1, 2 weeks after vaccination (1/27/15)	Early termination, 6 weeks after vaccination (2/24/15)	Notes
VZV IgG, gpELISA	Undetectable	Undetectable	96.64 gpELISA units/ml	None
IFNγ response to VZV antigen, ELISpot	25 SFCs/10^6 PBMCs†	25 SFCs/10^6 PBMCs	566 SFCs/10^6 PBMCs	25 SFCs: negative response (no VZV-specific T cells)
VZV IgM, ELISA	0.54 units/ml	0.55 units/ml	>5.00 units/ml	≤0.90 units/ml: negative response (no VZV-specific IgM)

* VZV = varicella zoster virus; HZ = herpes zoster; gpELISA = glycoprotein enzyme-linked immunosorbent assay; IFNγ = interferon-γ; ELISpot = enzyme-linked immunospot.
† Limit of detection = 25 spot-forming cells (SFCs)/10^6 peripheral blood mononuclear cells (PBMCs).

response to vaccination, since the results of both the gpELISA and ELISpot assay remained negative. After developing disseminated vaccine-strain varicella, the patient developed robust immunity, as evidenced by 6-week postvaccination assessments in which the gpELISA titer was 96.6 units/ml and the ELISpot count was 566 SFCs/10^6 PBMCs. Additional VZV-specific IgM and IgG avidity testing also showed negative responses at baseline and 2 weeks after zoster vaccination, followed by robust responses at week 6. These findings are consistent with a primary VZV infection.

DISCUSSION

To our knowledge, this study is the first to directly assess the safety and immunogenicity of the LZV in patients with RA. We observed that patients with active RA developed robust immune responses to this vaccine, and that starting tofacitinib treatment 2–3 weeks after vaccination had no negative impact on the established immune response. Patients treated with tofacitinib had similar or even numerically higher VZV-specific humoral and cell-mediated immune responses to the vaccine compared with placebo-treated patients. Importantly, although our results suggest that the vaccine is safe for RA patients with prior VZV exposure, they also indicate the potential need to either screen for prior exposure before giving this vaccine or waiting longer than 2–3 weeks before starting immunosuppression with tofacitinib.

Patients with RA are known to respond less robustly to certain vaccines (26,27). This is likely attributable to disease activity as well as, potentially, DMARD and corticosteroid use. LZV is currently contraindicated in patients receiving high-dose steroids (>20 mg/day prednisone or equivalent) or MTX at a dosage of >25 mg/week. Below these dosing thresholds, the vaccine is thought to be safe and effective, although this recommendation has been based on expert opinion in the absence of data (1). Importantly, the current study provides data for this recommendation, because the vaccine appeared to be adequately immunogenic as well as safe in patients receiving standard doses of MTX and/or lower doses of steroids. Although we did not enroll patients without RA in our study, for context it is useful to compare the magnitude of response observed in our study with that observed in studies in healthy individuals—the Shingles Prevention Study (SPS) (28) and the Zostavax Efficacy and Safety Trial (ZEST) (29). The SPS study enrolled more than 38,000 individuals ages ≥60 years, none of whom had RA. In the SPS Immunology Substudy, 1,395 individuals were evaluated using the same outcomes measures used in our study. They observed an average increase in VZV-specific IgG levels (gpELISA titer) between baseline and 6 weeks postvaccination of 1.7-fold, and an ~2.0-fold increase was observed for the VZV-specific ELISpot measures (1,24,28,29). In the ZEST study, 2,269 healthy volunteers ages 50–59 years had a VZV-specific IgG increase of 2.3 at 6 weeks postvaccination (25). This magnitude of IgG responses in immunocompetent individuals was similar to what we observed. Although the magnitude of cell-mediated responses was slightly less than that observed in healthy individuals within the ZEST study, it is possible that this could be attributable to the older age of our study population, the impact of RA, or the therapies being used for these patients.

Our study provides the first data regarding use of LZV in patients with RA and suggests that these patients, even those being treated with nonbiologic DMARDs at the time of vaccination, are capable of mounting adequate immune responses to this vaccine. Furthermore, our data suggest that the use of tofacitinib following VZV vaccination in patients with RA did not negatively impact the vaccine immunogenicity or the time course of the immune response to the vaccine. Interestingly, immune responses in RA patients receiving tofacitinib 5 mg twice daily or placebo were comparable with those expected in healthy individuals (24,25). From a safety standpoint, our study highlights the potential for vaccine dissemination in an immunocompromised host. In the SPS trial, in which >19,000 patients received the vaccine, no cases of local or disseminated HZ with this vaccine strain occurred in the first 42 days after vaccination (28). Although we observed only 1 such case in a study of 112 patients, it is notable given the lack of such cases in a study as large as SPS. The SPS study did not check for preexisting VZV immunity before administering the vaccine (similar to our study design); however, it is highly likely that at least a handful of such individuals were entered into the study but did not develop vaccine dissemination. Interestingly, 100% of the 1,395 individuals analyzed in an immunology substudy had serologic evidence of prior VZV exposure, suggesting that the number of individuals lacking prior exposure within the SPS study was likely small (25). Based on the SPS experience, the vaccine is licensed and approved for patients ages 50 or older regardless of a history of VZV (30). In our 1 case of disseminated primary varicella, the patient developed an injection-site reaction the day she started receiving tofacitinib and a disseminated rash on day 16 after vaccination, just 2 days after starting tofacitinib. It is known that patients can have circulating virus for several weeks after vaccination, and a small number of individuals may shed virus in saliva for up to 4 weeks postvaccination (31). Given this temporal sequence, it is possible that tofacitinib may have played a role in vaccine dissemination. Because of this potential for prolonged viremia, some time lag between

vaccination and the start of immunosupression makes theoretical sense, in order to further decrease the possibility of dissemination. Current recommendations suggest that this time lag should be 2–4 weeks (1,20), but our data would suggest that 4 weeks might be preferable. Alternatively, testing patients who do not recollect a history of chickenpox, to ensure prior exposure to VZV before vaccinating them, would also potentially mitigate this risk. In this case, our patient who lacked preexisting immunity would not have been a candidate for LZV.

A limitation of the current study is that the long-term effectiveness of the vaccine in RA patients was not investigated. However, this point is being investigated in the patients who joined an open-label LTE study of tofacitinib. In addition, because this study was conducted specifically to assess vaccine responses and not the efficacy of tofacitinib, further RA disease activity measures were not obtained. Last, our study was small in nature such that our conclusions regarding the safety of this vaccine and in RA patients in general are limited. Although only 1 case of vaccine dissemination occurred, in a patient lacking preexisting immunity, it is possible that other such cases could occur in the RA setting. Larger studies should be conducted to better understand the risk of this complication in RA patients in general.

In summary, we have conducted the first clinical study evaluating the use of LZV in patients with RA who are receiving nonbiologic DMARDs. In accordance with guidelines, our patients were vaccinated 2–3 weeks prior to starting tofacitinib therapy. Importantly, our data suggest that starting tofacitinib according to these guidelines does not hinder the immunogenicity of this vaccine, and that these patients were able to mount humoral and cell-mediated responses similar to those seen in other studies in healthy volunteers who do not have RA.

From a safety standpoint, the single event of disseminated shingles vaccine (Oka) virus in a patient without prior immunity suggests that patients should be screened for prior immunity (i.e., by eliciting a history of chickenpox or testing with commercially available VZV serologic tests) before receiving this vaccine, or that the time periods between vaccination and initiation of tofacitinib treatment should be longer (e.g., 4 weeks). Further research is necessary to understand the risk of this complication as well as the long-term effectiveness of this LZV to prevent HZ in this high-risk population.

ACKNOWLEDGMENTS

The authors would like to thank the patients, investigators, and study team involved in the trial, and Lisa McNeil, former employee of Pfizer Inc for her input on the study.

AUTHOR CONTRIBUTIONS

All authors were involved in drafting the article or revising it critically for important intellectual content, and all authors approved the final version to be published. Dr. Winthrop had full access to all of the data in the study and takes responsibility for the integrity of the data and the accuracy of the data analysis.

Study conception and design. Winthrop, Wouters, Soma, Biswas, Passador, Mojcik.

Acquisition of data. Winthrop, Wouters, Soma, Biswas, Passador, Mojcik.

Analysis and interpretation of data. Winthrop, Wouters, Choy, Soma, Hodge, Nduaka, Biswas, Needle, Passador, Mojcik, Rigby.

ROLE OF THE STUDY SPONSOR

The manuscript was drafted by Dr. Winthrop, with all authors providing subsequent critical revision. All authors interpreted the results, approved the final draft, and made the final decision to submit the manuscript for publication. Pfizer Inc did not control the analysis or interpretation of the study results. Pfizer Inc provided editorial assistance, performed by Sandrine M. Dupré, PhD, at Complete Medical Communications, funded by Pfizer Inc. Publication of this article was not contingent upon approval by Pfizer Inc.

REFERENCES

1. Harpaz R, Ortega-Sanchez IR, Seward JF. Prevention of herpes zoster: recommendations of the Advisory Committee on Immunization Practices (ACIP). MMWR Recomm Rep 2008;57(RR-5): 1–30.
2. Yun H, Yang S, Chen L, Xie F, Winthrop K, Baddley JW, et al. Risk of herpes zoster in autoimmune and inflammatory diseases: implications for vaccination. Arthritis Rheumatol 2016;68:2328–37.
3. Smolen J, Genovese M, Takeuchi T, Hyslop D, Macias WL, Rooney TP, et al. Safety profile of baricitinib in patients with active RA: integrated analysis [abstract]. Ann Rheum Dis 2016; 75:THU0166.
4. Jung CW, Shih LY, Xiao Z, Jie J, Hou HA, Du X, et al. Efficacy and safety of ruxolitinib in Asian patients with myelofibrosis. Leuk Lymphoma 2015;56:2067–74.
5. Fleischmann R, Kremer J, Tanaka Y, Gruben D, Kanik K, Koncz T, et al. Efficacy and safety of tofacitinib in patients with active rheumatoid arthritis: review of key Phase 2 studies. Int J Rheum Dis 2016;19:1216–25.
6. Van Vollenhoven RF, Fleischmann R, Cohen S, Lee EB, García Meijide JA, Wagner S, et al. Tofacitinib or adalimumab versus placebo in rheumatoid arthritis. N Engl J Med 2012;367:508–19.
7. Fleischmann R, Kremer J, Cush J, Schulze-Koops H, Connell CA, Bradley JD, et al. Placebo-controlled trial of tofacitinib monotherapy in rheumatoid arthritis. N Engl J Med 2012;367: 495–507.
8. Burmester GR, Blanco R, Charles-Schoeman C, Wollenhaupt J, Zerbini C, Benda B, et al. Tofacitinib (CP-690,550) in combination with methotrexate in patients with active rheumatoid arthritis with an inadequate response to tumour necrosis factor inhibitors: a randomised phase 3 trial. Lancet 2013;381:451–60.
9. Van der Heijde D, Tanaka Y, Fleischmann R, Keystone E, Kremer J, Zerbini C, et al. Tofacitinib (CP-690,550) in patients with rheumatoid arthritis receiving methotrexate: twelve-month data from a twenty-four–month phase III randomized radiographic study. Arthritis Rheum 2013;65:559–70.
10. Kremer J, Li ZG, Hall S, Fleischmann R, Genovese M, Martin-Mola E, et al. Tofacitinib in combination with nonbiologic disease-modifying antirheumatic drugs in patients with active rheumatoid arthritis: a randomized trial. Ann Intern Med 2013; 159:253–61.

11. Lee EB, Fleischmann R, Hall S, Wilkinson B, Bradley J, Gruben D, et al. Tofacitinib versus methotrexate in rheumatoid arthritis. N Engl J Med 2014;370:2377–86.
12. Wollenhaupt J, Silverfield J, Lee EB, Curtis JR, Wood SP, Soma K, et al. Safety and efficacy of tofacitinib, an oral Janus kinase inhibitor, for the treatment of rheumatoid arthritis in open-label, longterm extension studies. J Rheumatol 2014;41:837–52.
13. Wollenhaupt J, Silverfield J, Lee EB, Wood SP, Terry K, Nakamura H, et al. Tofacitinib, an oral janus kinase inhibitor, for the treatment of rheumatoid arthritis: safety and efficacy in open-label, long-term extension over 6 years [abstract]. Ann Rheum Dis 2015;74:259.
14. Ruderman EM. Overview of safety of non-biologic and biologic DMARDs. Rheumatology (Oxford) 2012;51 Suppl 6:vi37–43.
15. Curtis JR, Xie F, Yun H, Bernatsky S, Winthrop KL. Real-world comparative risks of herpes virus infections in tofacitinib and biologic-treated patients with rheumatoid arthritis. Ann Rheum Dis 2016;75:1843–7.
16. Winthrop KL, Curtis JR, Lindsey S, Valdez H, Fan H, Wang L, et al. Herpes zoster and tofacitinib: the risk of concomitant nonbiologic therapy [abstract]. Arthritis Rheumatol 2015;67 Suppl 10. URL: http://acrabstracts.org/abstract/herpes-zoster-and-tofacitinib-the-risk-of-concomitant-nonbiologic-therapy.
17. Hales CM, Harpaz R, Ortega-Sanchez I, Bialek SR. Update on recommendations for use of herpes zoster vaccine. MMWR Morb Mortal Wkly Rep 2014;63:729–31.
18. Singh JA, Saag KG, Bridges SL Jr, Akl EA, Bannuru RR, Sullivan MC, et al. 2015 American College of Rheumatology guideline for the treatment of rheumatoid arthritis. Arthritis Rheumatol 2016; 68:1–26.
19. Van Assen S, Agmon-Levin N, Elkayam O, Cervera R, Doran MF, Dougados M, et al. EULAR recommendations for vaccination in adult patients with autoimmune inflammatory rheumatic diseases. Ann Rheum Dis 2011;70:414–22.
20. Rubin LG, Levin MJ, Ljungman P, Davies EG, Avery R, Tomblyn M, et al. 2013 IDSA clinical practice guideline for vaccination of the immunocompromised host. Clin Infect Dis 2014;58:309–18.
21. Singh JA, Furst DE, Bharat A, Curtis JR, Kavanaugh AF, Kremer JM, et al. 2012 update of the 2008 American College of Rheumatology recommendations for the use of disease-modifying antirheumatic drugs and biologic agents in the treatment of rheumatoid arthritis. Arthritis Care Res (Hoboken) 2012;64:625–39.
22. Aletaha D, Nell VP, Stamm T, Uffmann M, Pflugbeil S, Machold K, et al. Acute phase reactants add little to composite disease activity indices for rheumatoid arthritis: validation of a clinical activity score. Arthritis Res Ther 2005;7:R796–806.
23. Aletaha D, Neogi T, Silman AJ, Funovits J, Felson DT, Bingham CO III, et al. 2010 rheumatoid arthritis classification criteria: an American College of Rheumatology/European League Against Rheumatism collaborative initiative. Arthritis Rheum 2010;62: 2569–81.
24. Levin MJ, Schmader KE, Gnann JW, McNeil SA, Vesikari T, Betts RF, et al. Varicella-zoster virus-specific antibody responses in 50–59-year-old recipients of zoster vaccine. J Infect Dis 2013; 208:1386–90.
25. Levin MJ, Oxman MN, Zhang JH, Johnson GR, Stanley H, Hayward AR, et al. Varicella-zoster virus-specific immune responses in elderly recipients of a herpes zoster vaccine. J Infect Dis 2008;197:825–35.
26. Friedman MA, Winthrop K. Vaccinations for rheumatoid arthritis. Curr Opin Rheumatol 2016;28:330–6.
27. Perry LM, Winthrop KL, Curtis JR. Vaccinations for rheumatoid arthritis. Curr Rheumatol Rep 2014;16:431.
28. Oxman MN, Levin MJ, Johnson GR, Schmader KE, Straus SE, Gelb LD, et al. A vaccine to prevent herpes zoster and postherpetic neuralgia in older adults. N Engl J Med 2005;352: 2271–84.
29. Schmader KE, Levin MJ, Gnann JW Jr, McNeil SA, Vesikari T, Betts RF, et al. Efficacy, safety, and tolerability of herpes zoster vaccine in persons aged 50–59 years. Clin Infect Dis 2012;54: 922–8.
30. US Food and Drug Administration. Zostavax® (Zoster vaccine live) suspension for subcutaneous injection, highlights of prescribing information. 2016. URL: http://www.fda.gov/downloads/BiologicsBloodVaccines/Vaccines/ApprovedProducts/UCM132831.pdf.
31. Pierson DL, Mehta SK, Gilden D, Cohrs RJ, Nagel MA, Schmid DS, et al. Varicella zoster virus DNA at inoculation sites and in saliva after Zostavax immunization. J Infect Dis 2011;203: 1542–5.

ARTHRITIS & RHEUMATOLOGY
Vol. 69, No. 10, October 2017, pp 1978–1983
DOI 10.1002/art.40206

BRIEF REPORT

Induction of Matrix Metalloproteinase Expression by Synovial Wnt Signaling and Association With Disease Progression in Early Symptomatic Osteoarthritis

Martijn H. van den Bosch,[1] Arjen B. Blom,[1] Fons A. van de Loo,[1] Marije I. Koenders,[1] Floris P. Lafeber,[2] Wim B. van den Berg,[1] Peter M. van der Kraan,[1] and Peter L. van Lent[1]

Objective. **Increased Wnt signaling in chondrocytes is associated with development of osteoarthritis (OA). However, OA is considered a disease of the entire joint, where the synovium has been attributed an important role in disease pathogenesis and progression. This study was undertaken to determine whether Wnt signaling in synovial tissue could contribute to pathologic development of OA through the production of matrix metalloproteinases (MMPs), and to assess the relationship of synovial expression of Frizzled (*FZD*) receptors and the Wnt inhibitor *FRZB* to MMP expression and disease progression in patients with early OA in the Dutch Cohort Hip and Cohort Knee (CHECK) study cohort.**

Methods. **In mouse knee joints, human WNT8A and mouse Wnt16 were overexpressed using adenoviral vectors, and expression of messenger RNA (mRNA) for MMPs in the synovium was determined by reverse transcription–polymerase chain reaction or Luminex assay. In human synovial tissue from a subgroup of patients with early OA with knee pain enrolled in the CHECK cohort, levels of Wnt family members were assessed for linkage to MMP expression and disease progression. In addition, MMP production in human synovium from patients with end-stage OA was determined after stimulation of Wnt signaling with WNT3A or inhibition with FRZB or DKK1 in the synovium.**

Results. **Overexpression of WNT8A and Wnt16 in mouse knee joints induced MMP expression in vivo. Expression of MMPs relevant to human OA in the synovium from CHECK study participants significantly correlated with expression of *FZD1*, *FZD10,* and *FRZB* mRNA. Moreover, increased *FZD1* mRNA expression and decreased *FRZB* mRNA expression were observed in CHECK study patients who experienced disease progression compared to those who were nonprogressors. Stimulation of human OA synovium with WNT3A induced the production of various MMPs, whereas inhibition of Wnt signaling with FRZB or DKK1 reduced the production of MMPs.**

Conclusion. **Wnt signaling in the synovium may potently induce progression of OA via increased production of MMPs.**

Osteoarthritis (OA) is one of the most common debilitating diseases worldwide. However, no curative treatment is available. It is now accepted that OA involves all tissues in the joint (1). Synovial activation, which is present in >50% of OA patients, is involved in cartilage degeneration (2,3).

We previously described strongly increased synovial expression of members of the Wnt signaling pathway in experimental models of OA (4). Wnt proteins are lipid-modified glycoproteins that bind to Frizzled (FZD) receptors. Binding to both an FZD receptor and the coreceptor low-density lipoprotein receptor–related protein 5 (LRP-5)/LRP-6 activates the β-catenin–dependent canonical Wnt signaling pathway, whereas binding to FZD alone results in noncanonical Wnt signaling (5).

Various studies have linked aberrant Wnt signaling to the development of OA (6,7). A polymorphism in the Wnt inhibitor gene *FRZB* that decreases its inhibitory activity against Wnt signaling is associated with a higher incidence of OA (8). Consistent with this observation, absence of *Frzb* in experimental mouse models increases the level of disease activity during OA (9). A possible

Supported by the Dutch Arthritis Foundation (grants 08-1-309 and 07-2-301).

[1]Martijn H. van den Bosch, PhD, Arjen B. Blom, PhD, Fons A. van de Loo, PhD, Marije I. Koenders, PhD, Wim B. van den Berg, PhD, Peter M. van der Kraan, PhD, Peter L. van Lent, PhD: Radboud University Medical Center, Nijmegen, The Netherlands; [2]Floris P. Lafeber, PhD: University Medical Center Utrecht, Utrecht, The Netherlands.

Address correspondence to Arjen B. Blom, PhD, Radboud University Medical Center, Geert Grooteplein 28, 6525 GA Nijmegen, The Netherlands. E-mail: arjen.blom@radboudumc.nl.

Submitted for publication January 11, 2017; accepted in revised form June 29, 2017.

mechanism of action of this increased disease activity might be elevated production of matrix metalloproteinases (MMPs) induced by active Wnt signaling, as has been described in various other diseases (10,11).

Whereas most previous studies focused on the relationship between Wnt signaling in the cartilage and the development of OA, in this concise study we investigated whether active Wnt signaling in the synovial tissue results in increased expression of MMPs. Furthermore, we studied the relationship between the expression of members of the Wnt signaling pathway and disease progression in patients with early symptomatic OA from the Dutch Cohort Hip and Cohort Knee (CHECK) study.

MATERIALS AND METHODS

Patients with early OA. Synovial biopsy tissue was obtained arthroscopically from a subgroup of participants with knee pain who were enrolled in the CHECK study, which was initiated to follow up patients with early symptomatic OA. Standardized radiographs were obtained from each patient to determine measurements of joint space width narrowing and osteophyte size, carried out using Knee Images Digital Analysis (12). At baseline, participants reported having pain and/or stiffness of the knee or hip, were ages 45–65 years, and had not consulted their physician for these symptoms during the 6 months before study entry. Participants with other pathologic conditions that could explain the symptoms were excluded. We determined whether the CHECK study participants showed progression in joint space width narrowing and osteophyte size between the baseline and 5-year follow-up measurements, and participants were accordingly classified as either progressors or nonprogressors. Progression was defined as a decrease in joint space width of $\geq$1 mm and an increase in osteophyte size of $\geq$4 times. All patients (n = 5 female patients, mean $\pm$ SD age 60.9 $\pm$ 4.1 years, 2 progressors and 3 nonprogressors; n = 4 male patients, mean $\pm$ SD age 55.8 $\pm$ 2.3 years, 2 progressors and 2 nonprogressors) signed written informed consent to participate in the study. All study protocols involving human tissue were approved by the local ethics committee (CMO Arnhem–Nijmegen; approval no. 2004–009).

Patients with established OA, and tissue culture. Anonymized synovial tissue specimens were obtained from patients with end-stage OA who were undergoing joint replacement. Punch biopsy specimens were randomly allocated to wells, and 2 punches per well were stimulated in quadruplicate with 300 ng/ml WNT3A (R&D Systems), which is one of the few recombinant canonical Wnt signaling inducers with sufficient bioactivity, or with 10 ng/ml interleukin-1 (IL-1) (R&D Systems). Alternatively, biopsy specimens were incubated with 100 ng/ml FRZB (R&D Systems), 500 ng/ml DKK1 (PeproTech), or IL-1 receptor antagonist (Sobi). All cultures were performed in RPMI 1640 medium, supplemented with 10% fetal calf serum, sodium pyruvate, 100 units/ml penicillin, and 100 μg/ml streptomycin, for 24 hours.

Animals and adenoviral vectors. Adenoviral vectors for human WNT8A and murine Wnt16 were made as previously described (13). First, 1×10^7 plaque-forming units of adenoviral vector was injected into the naive knee joints of 12-week-old male C57BL/6J mice (supplied by Janvier). Mice were housed in filter-topped cages, and water and food were provided ad libitum. The mice were killed 3 days after

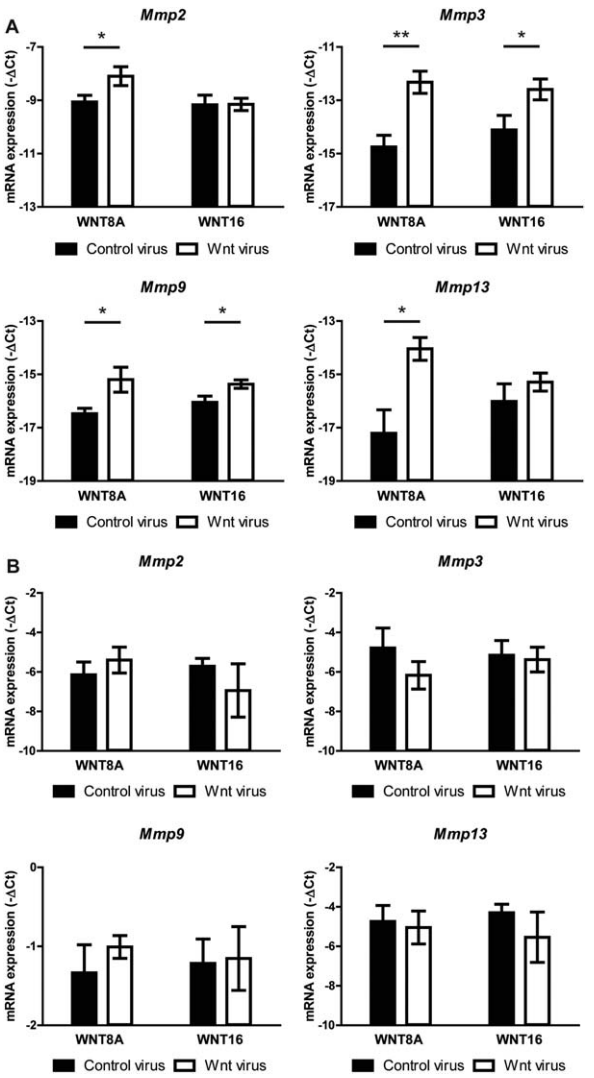

Figure 1. Synovial overexpression of Wnt ligands results in increased expression of matrix metalloproteinases (MMPs). WNT8A, a classic example of a Wnt ligand that activates the canonical Wnt signaling pathway, and Wnt16, known to be strongly up-regulated in the joint during experimental osteoarthritis, were overexpressed in mouse synovium by intraarticular injection of 1×10^7 plaque-forming units of adenoviral vectors containing human WNT8A or mouse Wnt16; a luciferase adenoviral vector was used as a control. Expression of mRNA for MMPs 2, 3, 9, and 13 was assessed by quantitative real-time reverse transcription–polymerase chain reaction in the synovial tissue **(A)** and articular cartilage **(B)** from mice 3 days after overexpression of WNT8A and Wnt16. Bars show the mean $\pm$ SEM relative levels of expression (corrected for the expression of the reference gene GAPDH [$-\Delta C_t$]) in 6 samples per group. $* = P < 0.05$; $** = P < 0.01$.

adenoviral overexpression. As a control, we used an adenoviral vector for luciferase. Animal studies were approved by the local animal experimentation committee (RU-DEC approval no. 2011–226).

RNA isolation and quantitative real-time reverse transcription–polymerase chain reaction (RT-PCR). Gene expression was determined using quantitative real-time RT-PCR. Total RNA was isolated using TRIzol reagent (Invitrogen), according to the manufacturer's protocol, after homogenizing the cartilage or synovial tissue with a MagNA Lyser Instrument (Roche). RT-PCR was performed with specific primers and SYBR Green Master Mix, using a StepOnePlus real-time PCR system (Applied Biosystems). Expression levels are presented as ΔC_t values, normalized to the expression values for the reference gene GAPDH.

Protein measurement using Luminex technology. Protein levels in culture supernatants were determined using Luminex multianalyte technology on a Bio-Plex system, in combination with multiplex kits (Millipore). The supernatants in each well were adjusted for the weight of the synovial biopsy tissue, which was determined after cell culture.

Statistical analysis. Statistical analyses were performed using GraphPad Prism software (version 5). For every analysis, data were checked for normality using the D'Agostino-Pearson test. Differences between groups were tested using Student's *t*-test or 1-sample *t*-test. The number of repeats conducted in each experiment varied (as reported in the Figure legends). *P* values less than 0.05 were considered significant. Correlations were tested with Pearson's correlation coefficients, at a significance level of $P < 0.05$.

RESULTS

Increased expression of MMPs after overexpression of Wnts in vivo in the synovial tissue. We previously showed that in vivo targeting of the synovium by intraarticular injection of adenoviral vectors for prolonged periods in vivo leads to overexpression of WNT8A, a classic model used to achieve activation of canonical Wnt signaling, and overexpression of WNT16, the levels of which we previously found to be strongly increased in the joint during experimental OA. Adenoviral injection leads to strong overexpression of both Wnt ligands in the synovium, as well as activation of canonical Wnt signaling in the joint and induction of cartilage damage, within 7 days after overexpression (14). Because the resulting cartilage damage was observed to be associated with formation of neoepitopes linked to cartilage-degrading enzymes, we assessed samples of mouse synovium and articular cartilage to determine whether the overexpression of both Wnt ligands could result in increased expression of MMPs.

The expression levels of messenger RNA (mRNA) for *Mmp2*, *Mmp3*, *Mmp9*, and *Mmp13* were significantly increased in the synovium of mice 3 days after overexpression of WNT8A, whereas after overexpression of Wnt16, the levels of mRNA for *Mmp3* and *Mmp9* were increased (Figure 1A). In contrast, no differential expression of *Mmp* mRNAs was observed in the articular cartilage from mice (Figure 1B).

Correlation of expression levels between relevant MMPs and members of the Wnt signaling pathway in human OA. Human synovial biopsy tissue donated by a subgroup of 9 participants with early symptomatic OA in the CHECK study who were followed up over time was assessed to determine whether baseline mRNA levels of relevant MMPs for OA development correlated with the expression of a set of members of the Wnt signaling pathway; these members were selected because they were found to be differentially expressed between disease progressors and nonprogressors in a microarray analysis of the synovial biopsy specimens. We observed that the expression levels of mRNA for *MMP1*, *MMP2*, *MMP3*, and *MMP13* correlated inversely with expression of the Wnt inhibitor *FRZB*, and correlated positively with the expression of the Wnt receptors *FZD1* and *FZD10*, but not *FZD8*. In addition, *FZD1* mRNA expression correlated positively with *AXIN2* expression, while *FRZB* mRNA expression correlated inversely with *AXIN2* expression, the latter acting as an indicator of active canonical Wnt signaling. In contrast, *MMP9* mRNA levels were not correlated with any of these members of the Wnt signaling pathway (Figure 2A).

Increased expression of *FZD* receptors, but decreased expression of the Wnt inhibitor *FRZB*, in patients with early OA showing disease progression. Subsequently, we investigated the relationship between the expression of members of the Wnt signaling pathway and progression of OA. We observed significantly increased expression of the Wnt receptor *FZD1* and significantly decreased expression of the Wnt inhibitor *FRZB* in patients who were disease progressors, as compared to those who were nonprogressors (Figure 2B), which is consistent with the correlation data reported above.

Increased MMP production as a result of Wnt signaling in human synovial tissue from patients with end-stage OA. We next determined whether stimulation of the synovium from patients with end-stage OA with recombinant WNT3A would increase the production of MMPs. For these relatively short-term experiments, we used recombinant WNT3A, as opposed to adenoviral overexpression, in order to better control the dosage and timing. Following WNT3A stimulation of the synovium from patients with end-stage OA, we observed significantly increased concentrations of MMP-1 and MMP-9 proteins, whereas MMP-2 and

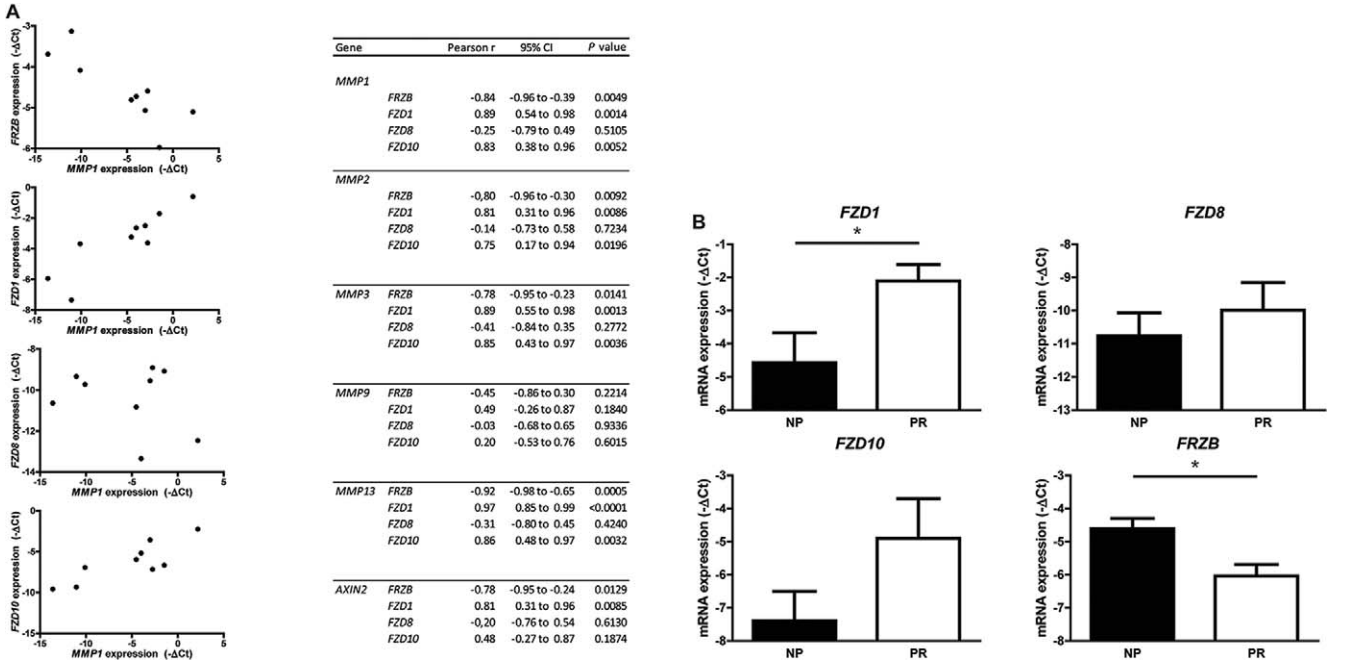

Gene		Pearson r	95% CI	*P* value
MMP1				
	FRZB	-0.84	-0.96 to -0.39	0.0049
	FZD1	0.89	0.54 to 0.98	0.0014
	FZD8	-0.25	-0.79 to 0.49	0.5105
	FZD10	0.83	0.38 to 0.96	0.0052
MMP2				
	FRZB	-0.80	-0.96 to -0.30	0.0092
	FZD1	0.81	0.31 to 0.96	0.0086
	FZD8	-0.14	-0.73 to 0.58	0.7234
	FZD10	0.75	0.17 to 0.94	0.0196
MMP3	*FRZB*	-0.78	-0.95 to -0.23	0.0141
	FZD1	0.89	0.55 to 0.98	0.0013
	FZD8	-0.41	-0.84 to 0.35	0.2772
	FZD10	0.85	0.43 to 0.97	0.0036
MMP9	*FRZB*	-0.45	-0.86 to 0.30	0.2214
	FZD1	0.49	-0.26 to 0.87	0.1840
	FZD8	-0.03	-0.68 to 0.65	0.9336
	FZD10	0.20	-0.53 to 0.76	0.6015
MMP13	*FRZB*	-0.92	-0.98 to -0.65	0.0005
	FZD1	0.97	0.85 to 0.99	<0.0001
	FZD8	-0.31	-0.80 to 0.45	0.4240
	FZD10	0.86	0.48 to 0.97	0.0032
AXIN2	*FRZB*	-0.78	-0.95 to -0.24	0.0129
	FZD1	0.81	0.31 to 0.96	0.0085
	FZD8	-0.20	-0.76 to 0.54	0.6130
	FZD10	0.48	-0.27 to 0.87	0.1874

Figure 2. Correlation between expression of matrix metalloproteinases (MMPs) relevant to human osteoarthritis (OA) and expression of various Wnt signaling members. **A,** Gene expression analysis by reverse transcription–polymerase chain reaction was performed in freshly isolated synovial tissue from patients with early symptomatic OA enrolled in the Cohort Hip and Cohort Knee (CHECK) study. The relative mRNA expression levels of the Wnt receptors *FZD1*, *FZD8*, and *FZD10* and the Wnt inhibitor *FRZB* were assessed for associations with disease progression as measured by *MMP1* expression (left), and for correlations with the expression of *MMP1*, *MMP2*, *MMP3*, *MMP9*, *MMP13*, and *AXIN2* (right). Correlations were determined using the Pearson's correlation coefficient with 95% confidence interval (95% CI). **B,** Expression of the Wnt receptors *FZD1*, *FZD8*, and *FZD10* and the Wnt inhibitor *FRZB* at baseline in synovial tissue from CHECK study participants was compared between patients who showed progression of OA (PR) (n = 4) and those who were nonprogressors (NP) (n = 5). Disease progression was defined as an increase in joint space width narrowing of ≥1 mm and an increase in osteophyte size of ≥4 times between baseline and the 5-year follow-up measurement. The MMPs in **A** were chosen because of the relevance for development of OA. The Wnt signaling members in **A** and **B** were selected from microarray analysis of the same synovia, in which the expression of these markers was different between progressors and nonprogressors. Circles in **A** represent individual donors. Bars in **B** show the mean ± SEM relative levels of expression (corrected for the expression of the reference gene GAPDH [$-\Delta C_t$]). $* = P < 0.05$.

MMP-3 proteins showed a trend toward increased production (Figure 3A).

To test the hypothesis that endogenous Wnt signaling in OA synovium drives the production of MMPs, we incubated human OA synovium with recombinant FRZB (an inhibitor of all Wnt pathways). Following incubation of the synovium with FRZB, we observed significantly decreased production of MMP-2 and MMP-3 (Figure 3B). To determine whether this decreased MMP production was the result of inhibition of canonical Wnt signaling, we blocked human OA synovium with recombinant DKK1, which specifically inhibits β-catenin/canonical signaling. This led to decreased protein production of MMP-1 and MMP-3, but not MMP-2 and MMP-9 (Figure 3C).

DISCUSSION

The findings from the study reported herein are the first to show that activated Wnt signaling in OA synovial tissue results in increased MMP production, a process that might contribute to cartilage damage. Furthermore, we show that synovial expression of various Wnt receptors and the Wnt inhibitor *FRZB* is correlated with MMP expression, and that increased *FZD1* expression and decreased *FRZB* expression are associated with disease progression in a cohort of patients with early symptomatic OA.

Until now, research on the relationship between Wnt signaling and OA has mainly focused on the cartilage (6,7,9). In this study, we add to this knowledge by studying synovial Wnt signaling in the context of OA. We previously showed that induction of canonical Wnt signaling by synovial overexpression of WNT8A and Wnt16 resulted in OA-like cartilage lesions in mice, associated with formation of protease neoepitopes (14). In the present study, we show that overexpression of WNT8A and Wnt16 increased the synovial expression of MMPs that are able to enhance cartilage matrix breakdown. The different extent of MMP regulation by

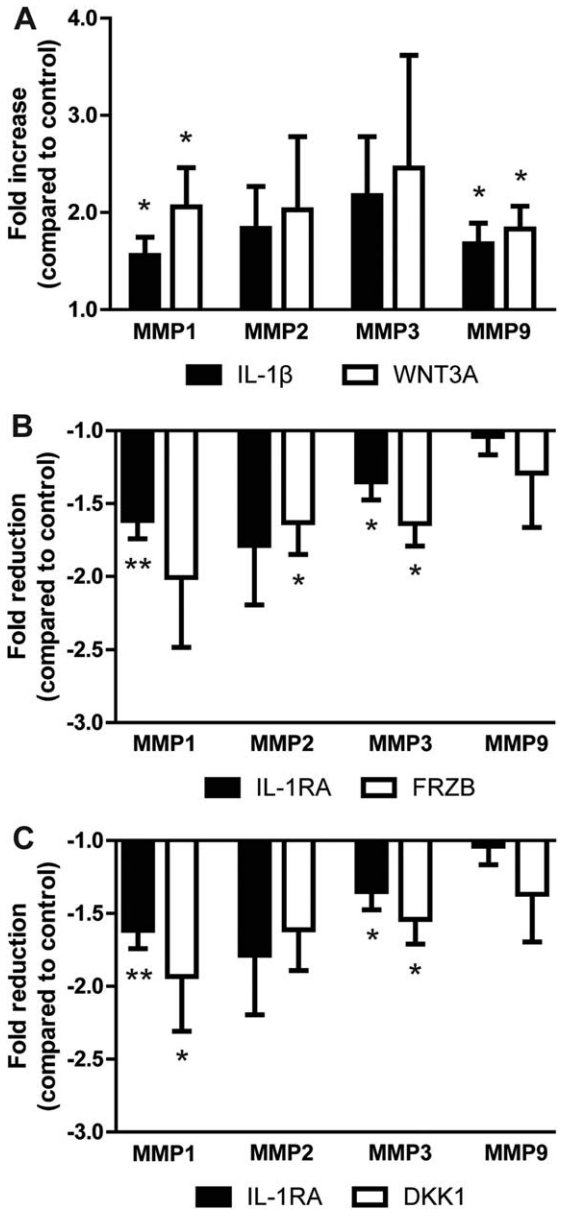

Figure 3. Increased synovial Wnt signaling induces the production of matrix-degrading matrix metalloproteinases (MMPs) in human osteoarthritis (OA) synovium. **A,** Synovial biopsy tissue was obtained from patients with end-stage OA undergoing joint replacement. The synovial samples were stimulated with 300 ng/ml recombinant human WNT3A (or interleukin-1β [IL-1β] as a treatment control) for 24 hours, and the fold change in protein levels of MMPs 1, 2, 3, and 9, relative to the untreated control, were measured in the supernatants. **B** and **C,** Based on the hypothesis that increased Wnt signaling, and thus increased production of MMPs, is present in OA synovial tissue, the synovial biopsy samples from patients with end-stage OA were incubated with 100 ng/ml recombinant human FRZB (an inhibitor of all Wnt signaling) **(B)** or 500 ng/ml recombinant human DKK1 (a specific inhibitor of canonical Wnt signaling) **(C)**, and the fold change in levels of MMPs 1, 2, 3, and 9, relative to the untreated control, were assessed 24 hours after the start of the experiment. IL-1 receptor antagonist (IL-1RA) was used as a treatment control. Bars show the mean ± SEM of 6 samples per experiment. $* = P < 0.05$; $** = P < 0.01$, versus unstimulated samples.

WNT8A overexpression as compared to Wnt16 overexpression might be the result of either differences in signaling by the individual Wnts or differences in the efficiency of these adenoviral vectors that might arise during overexpression of the Wnt ligands.

Preferably, we would have used the same Wnt ligand for all experiments. However, we used adenoviral vectors for relatively prolonged in vivo overexpression, since injection of recombinant proteins would result in quick clearance from the joint, whereas recombinant proteins were chosen for the relatively short-term in vitro tissue cultures, allowing tightly controlled dosages and timing. Moreover, tissue specimens are relatively difficult to target with adenoviruses in vitro. We used recombinant WNT3A because this is one of the few recombinant inducers of canonical Wnt signaling that has sufficient bioactivity. Although all of the Wnt ligands used in this study preferentially signal via the β-catenin–dependent canonical Wnt signaling route, the unique characteristics of the individual Wnt ligands and their signaling remain a matter of debate in the field of research on Wnt signaling pathways. Our data show that synovial Wnt signaling increases the production of various MMPs that are relevant for OA development, a finding that is consistent with a study that showed an increase in MMP expression in rheumatoid arthritis fibroblasts upon stimulation with Wnt1 (15). The discrepancy in regulation of MMP production that was observed after stimulation of Wnt signaling as compared to inhibition of Wnt signaling might derive from the use of synovium from patients with end-stage OA, in whom the expression of various MMPs, such as MMP-3, is likely to be strongly increased. This might also account for the relatively high variation between the separate donors, both in basal MMP expression levels and in the observed effects of the WNT3A, FRZB, or DKK1 proteins.

Whereas Wnt signaling in multiple joint tissues has been studied in the context of OA, this study using synovial tissue from patients in the CHECK study is the first that links synovial expression of *FZD1* and *FRZB* to OA disease progression. This cohort study provides unique opportunities to study disease progression, starting from the initial phases of the disease. Our findings support those of other studies that show continuous β-catenin signaling in fibroblast-like synoviocytes from rheumatoid arthritis patients (15,16). Moreover, we show that the expression of various MMPs in the synovium of patients with early symptomatic OA is correlated with expression of members of the Wnt signaling pathway, some of which showed an altered expression in microarray analysis of these synovial samples. Nonetheless,

the number of synovium donors was limited, although the nature of the samples, collected at the initial phases of OA, was highly unique. Therefore, further studies with comparable designs would greatly improve insight into the early events that promote OA development. Moreover, these studies should aim to provide more evidence at the protein level, which was not feasible in this study due to the relatively small number of biopsy samples obtained. Moreover, although the results obtained in the various experiments in this study are consistent with each other, we have to mention a possible inflation of the Type I error, since no correction for multiple comparisons has been applied.

In conclusion, in the current study we show for the first time that Wnt signaling, at least partially via the canonical Wnt signaling pathway, in synovial tissue induces the expression of various MMPs that are relevant to the development of OA. Furthermore, we show that increased synovial expression of the *FZD1* receptor and decreased expression of the Wnt inhibitor *FRZB* are associated with disease progression in patients with early symptomatic OA.

ACKNOWLEDGMENTS

The authors would like to thank Annet Sloetjes, Anke van Erp, and Sylvia Suen for their excellent technical assistance.

AUTHOR CONTRIBUTIONS

All authors were involved in drafting the article or revising it critically for important intellectual content, and all authors approved the final version to be published. Dr. Blom had full access to all of the data in the study and takes responsibility for the integrity of the data and the accuracy of the data analysis.

Study conception and design. Van den Bosch, Blom, van de Loo, Koenders, Lafeber, van den Berg, van der Kraan, van Lent.

Acquisition of data. Van den Bosch, Blom.

Analysis and interpretation of data. Van den Bosch, Blom, van de Loo, Koenders, Lafeber, van den Berg, van der Kraan, van Lent.

REFERENCES

1. Samuels J, Krasnokutsky S, Abramson SB. Osteoarthritis: a tale of three tissues. Bull NYU Hosp Jt Dis 2008;66:244–50.
2. Ayral X, Pickering EH, Woodworth TG, Mackillop N, Dougados M. Synovitis: a potential predictive factor of structural progression of medial tibiofemoral knee osteoarthritis: results of a 1 year longitudinal arthroscopic study in 422 patients. Osteoarthritis Cartilage 2005;13:361–7.
3. Kortekaas MC, Kwok WY, Reijnierse M, Stijnen T, Kloppenburg M. Association of inflammation with development of erosions in patients with hand osteoarthritis: a prospective ultrasonography study. Arthritis Rheumatol 2016;68:392–7.
4. Blom AB, Brockbank SM, van Lent PL, van Beuningen HM, Geurts J, Takahashi N, et al. Involvement of the Wnt signaling pathway in experimental and human osteoarthritis: prominent role of Wnt-induced signaling protein 1. Arthritis Rheum 2009; 60:501–12.
5. Clevers H, Nusse R. Wnt/β-catenin signaling and disease. Cell 2012;149:1192–205.
6. Zhu M, Tang D, Wu Q, Hao S, Chen M, Xie C, et al. Activation of β-catenin signaling in articular chondrocytes leads to osteoarthritis-like phenotype in adult β-catenin conditional activation mice. J Bone Miner Res 2009;24:12–21.
7. Zhu M, Chen M, Zuscik M, Wu Q, Wang YJ, Rosier RN, et al. Inhibition of β-catenin signaling in articular chondrocytes results in articular cartilage destruction. Arthritis Rheum 2008;58:2053–64.
8. Min JL, Meulenbelt I, Riyazi N, Kloppenburg M, Houwing-Duistermaat JJ, Seymour AB, et al. Association of the frizzled-related protein gene with symptomatic osteoarthritis at multiple sites. Arthritis Rheum 2005;52:1077–80.
9. Lories RJ, Peeters J, Bakker A, Tylzanowski P, Derese I, Schrooten J, et al. Articular cartilage and biomechanical properties of the long bones in Frzb-knockout mice. Arthritis Rheum 2007;56:4095–103.
10. Lee MA, Park JH, Rhyu SY, Oh ST, Kang WK, Kim HN. Wnt3a expression is associated with MMP-9 expression in primary tumor and metastatic site in recurrent or stage IV colorectal cancer. BMC Cancer 2014;14:125.
11. Zhao C, Bu X, Zhang N, Wang W. Downregulation of SFRP5 expression and its inverse correlation with those of MMP-7 and MT1-MMP in gastric cancer. BMC Cancer 2009;9:224.
12. Marijnissen AC, Vincken KL, Vos PA, Saris DB, Viergever MA, Bijlsma JW, et al. Knee Images Digital Analysis (KIDA): a novel method to quantify individual radiographic features of knee osteoarthritis in detail. Osteoarthritis Cartilage 2008;16:234–43.
13. Smeets RL, Veenbergen S, Arntz OJ, Bennink MB, Joosten LA, van den Berg WB, et al. A novel role for suppressor of cytokine signaling 3 in cartilage destruction via induction of chondrocyte desensitization toward insulin-like growth factor. Arthritis Rheum 2006;54:1518–28.
14. Van den Bosch MH, Blom AB, Sloetjes AW, Koenders MI, van de Loo FA, van den Berg WB, et al. Induction of canonical Wnt signaling by synovial overexpression of selected Wnts leads to protease activity and early osteoarthritis-like cartilage damage. Am J Pathol 2015;185:1970–80.
15. Sen M, Reifert J, Lauterbach K, Wolf V, Rubin JS, Corr M, et al. Regulation of fibronectin and metalloproteinase expression by Wnt signaling in rheumatoid arthritis synoviocytes. Arthritis Rheum 2002;46:2867–77.
16. Xiao CY, Pan YF, Guo XH, Wu YQ, Gu JR, Cai DZ. Expression of β-catenin in rheumatoid arthritis fibroblast-like synoviocytes. Scand J Rheumatol 2011;40:26–33.

ARTHRITIS & RHEUMATOLOGY
Vol. 69, No. 10, October 2017, pp 1984–1995
DOI 10.1002/art.40183

Intestinal Metabolites Are Profoundly Altered in the Context of HLA–B27 Expression and Functionally Modulate Disease in a Rat Model of Spondyloarthritis

Mark Asquith,[1] Sean Davin,[1] Patrick Stauffer,[1] Claire Michell,[1] Cathleen Janowitz,[1] Phoebe Lin,[1] Joe Ensign-Lewis,[2] Jason M. Kinchen,[3] Dennis R. Koop,[1] and James T. Rosenbaum[4]

Objective. **HLA–B27–associated spondyloarthritides are associated with an altered intestinal microbiota and bowel inflammation. We undertook this study to identify HLA–B27–dependent changes in both host and microbial metabolites in the HLA–B27/β_2-microglobulin (β_2m)–transgenic rat and to determine whether microbiota-derived metabolites could impact disease in this major model of spondyloarthritis.**

Methods. **Cecal contents were collected from Fischer 344 33–3 HLA–B27/β_2m–transgenic rats and wild-type controls at 6 weeks (before disease) and 16 weeks (with active bowel inflammation). Metabolomic profiling was performed by high-throughput gas and liquid chromatography–based mass spectrometry. HLA–B27/β_2m–transgenic rats were treated with the microbial metabolites propionate or butyrate in drinking water for 10 weeks, and disease activity was subsequently assessed.**

Results. **Our screen identified 582 metabolites, of which more than half were significantly altered by HLA–B27 expression at 16 weeks. Both microbial and host metabolites were altered, with multiple pathways affected, including those for amino acid, carbohydrate, xenobiotic, and medium-chain fatty acid metabolism. Differences were even observed at 6 weeks, with upregulation of histidine, tyrosine, spermidine, *N*-acetylmuramate, and glycerate in HLA–B27/β_2m–transgenic rats. Administration of the short-chain fatty acid propionate significantly attenuated HLA–B27–associated inflammatory disease, although this was not associated with increased FoxP3+ T cell induction or with altered expression of the immunomodulatory cytokines interleukin-10 (IL-10) or IL-33 or of the tight junction protein zonula occludens 1. HLA–B27 expression was also associated with altered host expression of messenger RNA for the microbial metabolite receptors free fatty acid receptor 2 (FFAR2), FFAR3, and niacin receptor 1.**

Conclusion. **HLA–B27 expression profoundly impacts the intestinal metabolome, with changes evident in rats even at age 6 weeks. Critically, we demonstrate that a microbial metabolite, propionate, attenuates development of HLA–B27–associated inflammatory disease. These and other microbiota-derived bioactive mediators may provide novel treatment modalities in HLA–B27–associated spondyloarthritides.**

The intestinal microbiota mediates several core functions essential to host fitness, including digestion and metabolite provision, resistance to colonization by gut pathogens, and signals that promote immune function. A disturbed, or "dysbiotic," gut microbiota is implicated in the pathogenesis of local inflammatory diseases of the intestine, including Crohn's disease

Supported by the Collins Medical Trust and the Medical Research Foundation of Oregon (grants to Dr. Asquith) and the Spondylitis Association of America (Jane Bruckel Award to Dr. Asquith). Dr. Lin's work was supported by the NIH (grant K08-EY-022948) and an individual Research to Prevent Blindness Career Development Award. Dr. Rosenbaum's work was supported by the Stan and Madelle Rosenfeld Family Trust and the William and Mary Bauman Foundation.

[1]Mark Asquith, PhD, Sean Davin, BS, Patrick Stauffer, BS, Claire Michell, BS, Cathleen Janowitz, BS, Phoebe Lin, MD, PhD, Dennis R. Koop, PhD: Oregon Health and Science University, Portland; [2]Joe Ensign-Lewis, MD: University of Pennsylvania, Philadelphia; [3]Jason M. Kinchen, PhD: Metabolon, Inc., Durham, North Carolina; [4]James T. Rosenbaum, MD: Oregon Health and Science University and Devers Eye Institute, Portland, Oregon.

Address correspondence to Mark Asquith, PhD, Division of Arthritis and Rheumatic Diseases, Oregon Health and Science University, 3181 SW Sam Jackson Park Road, Portland, OR 97239-3098. E-mail: asquith@ohsu.edu.

Submitted for publication August 24, 2016; accepted in revised form June 13, 2017.

(CD) and ulcerative colitis, as well as in extraintestinal inflammatory diseases, including arthritis, diabetes mellitus, and multiple sclerosis (for review, see refs. 1 and 2). Recently, it has been established that dysbiosis may be accompanied by a profound change to the metabolic profile of the gut, including alterations in microbial metabolites such as short-chain fatty acids (SCFAs) and trimethylamine *N*-oxide, which are bioactive mediators that modulate host physiology (for review, see ref. 3).

The HLA–B27/β_2-microglobulin (β_2m)–transgenic rat is the foremost translational model of spondyloarthritis (SpA). These animals express multiple copies of human HLA–B27 in association with the β_2m heavy chain (4). HLA–B27 is the gene with the strongest known genetic association with SpA. These animals model human SpA, with the development of peripheral arthritis, psoriasis, and bowel inflammation to varying degrees contingent on the copy number of this transgene in addition to rat background (5). We have shown previously that HLA–B27 expression significantly alters the intestinal microbiota in this model (6,7), mirroring parallel reports that SpA patient populations exhibit a dysbiotic gut phenotype (8–10). These findings complement prior animal and clinical studies that strongly implicate the intestinal microbiota in SpA pathogenesis (for review, see ref. 11).

In the present study, we assessed the impact of HLA–B27 expression on the gut metabolome in this rat model of SpA. We found that multiple metabolite families were significantly altered by HLA–B27 expression, including amino acids, lipids, carbohydrates, and xenobiotics. Among the most significantly altered were medium-chain fatty acids (MCFAs) and SCFAs. Strikingly, treatment of HLA–B27/β_2m–transgenic rats with the SCFA propionate significantly attenuated HLA–B27–associated inflammatory disease. These findings establish a functional link between HLA–B27 expression, an altered gut metabolome, and the pathogenesis of SpA-like disease.

MATERIALS AND METHODS

Ethics statement. All animal experiments were performed according to the experimental and ethical standards of the Association for Assessment and Accreditation of Laboratory Animal Care International and the Oregon Health and Science University (OHSU) Institutional Animal Care and Use Committee.

Animals. We maintained a colony of Fischer 33–3 HLA–B27/β_2m hemizygous rats as described previously (7). Briefly, hemizygous female rats were crossed with wild-type (WT) Fischer 344 male rats to produce HLA–B27/β_2m–transgenic rats and littermate controls. Animals were singly housed and maintained under specific pathogen–free conditions. All animals were fed a diet of standard laboratory chow (LabDiet). All animal groups included males and females, with age/sex matching between groups.

Sample collection. Animals were euthanized at the indicated ages/time points by CO_2 asphyxiation and cervical dislocation. Cecal contents (~1 ml) and cecal and colonic tissue (~50 mg) were snap-frozen and stored at −80°C prior to subsequent analysis. Snap-frozen colonic tissue was collected from mid colon. For cell isolation experiments, intestinal tissue, mesenteric lymph nodes (MLNs), and spleen were collected into phosphate buffered saline/0.1% bovine serum albumin and stored on ice prior to subsequent processing. For histology, longitudinal sections of cecum and ~1-cm cross-sections of proximal, mid, and distal colon were fixed in 10% neutral buffered formalin.

Metabolomic profiling of the gut. Cecal content samples were analyzed using an HD4 platform (Metabolon). Briefly, samples were prepared using an automated Microlab STAR system from Hamilton (for further details, see Supplementary Methods, available on the *Arthritis & Rheumatology* web site at http://onlinelibrary.wiley.com/doi/10.1002/art.40183/abstract). To remove protein and dissociate small molecules bound to protein, samples were precipitated with methanol and centrifuged, and extract was divided for ultra-performance liquid chromatography tandem mass spectrometry (MS) analysis and gas chromatography (GC)–MS analysis.

The GC-MS metabolite screen was performed using a Thermo-Finnigan Trace DSQ fast-scanning single-quadrupole mass spectrometer (Thermo Electron Corporation) using electron impact ionization and operated at unit mass resolving power. The instrument had a mass/charge scan range of 50–750.

SCFA analysis. SCFAs were measured by GC-MS at the Bioanalytical Shared Resource/Pharmacokinetics Core facility at OHSU (see Supplementary Methods).

SCFA treatment. Six-week-old HLA–B27/β_2m–transgenic rats or WT controls were administered either sodium propionate (150 m*M*) or sodium butyrate (150 m*M*) ad libitum in drinking water throughout the experiment. Animals were necropsied at age 16 weeks. These doses and this route of administration were selected based on previously reported in vivo studies (12,13).

Histology and disease scoring. Formalin-fixed intestinal tissues were embedded in paraffin, sectioned to 5 μm, and stained with hematoxylin and eosin. Scoring of intestinal inflammation was performed using a semiquantitative scoring system (0–12) as described previously (7). Briefly, this 4-parameter scoring system includes epithelial hyperplasia, goblet cell numbers, leukocytic infiltrate, and markers of severe inflammation (e.g., submucosal inflammation, abscesses, or ulceration). Each parameter is scored 0–3, with the total cecum score and mean colon score (for the 3 colon sections collected) shown for each animal. By the final time point of 16 weeks used in our study, animals had not presented with either psoriasis or arthritis, which typically develops at >20 weeks in the Fischer 344 33–3 HLA–B27/β_2m–transgenic line.

Analysis of intestinal gene expression. Briefly, RNA was extracted from intestinal tissue using TRIzol reagent (Ambion) and reverse transcribed into complementary DNA (cDNA) using a High Capacity cDNA Reverse Transcription kit (Life Technologies). For quantitative reverse transcription–polymerase chain reaction (qRT-PCR) analysis of interleukin-17A (IL-17A),

interferon-γ (IFNγ), and IL-1β, we used published primer sequences and RT^2 SYBR Green qPCR Master Mix (Qiagen) as described previously (7). For all other qRT-PCR analyses, we used TaqMan Gene Expression Assays (Life Technologies) in conjunction with Maxima Probe qPCR Master Mix (Thermo Scientific). Samples' hypoxanthine guanine phosphoribosyltransferase controls were prepared for both qRT-PCR chemistries for the purpose of normalization. For further details (including primer details), (see Supplementary Methods).

Analysis of immune cells by flow cytometry. Suspensions of spleen and MLN cells were prepared as described previously (14). Cecal and colonic lamina propria lymphocytes were isolated by EDTA digestion, collagenase/DNase treatment, and Percoll gradient as described previously (7). Cells were then surface-stained for 20 minutes on ice with AQUA Live/Dead stain (Invitrogen), PerCP–Cy5.5–conjugated anti-rat CD4 (BioLegend), and phycoerythrin-conjugated anti-rat T cell receptor β (BD Biosciences), and then FoxP3 staining was performed using a FoxP3 staining kit (eBioscience) in accordance with the manufacturer's instructions using allophycocyanin-conjugated anti-rat/mouse FoxP3 (eBioscience). Cells were acquired on a BD Fortessa instrument (BD Biosciences) and analyzed using FlowJo software.

Statistical analysis. Details of the statistical analysis used for our metabolomic screen, see Supplementary Methods, available online at http://onlinelibrary.wiley.com/doi/10.1002/art.40183/abstract. For analysis of individual metabolite levels from our screen, data were normalized to an equivalent of 2 mg dry weight of cecal material per sample and log-transformed prior to application of Welch's unpaired *t*-test (which does not assume equal variances) with subsequent Benjamini-Hochberg correction to account for multiple comparisons, and a false discovery rate of 0.2 was applied. For samples obtained from 6-week-old animals, the least abundant 20% of metabolites (median abundance for each metabolite across the data set, irrespective of genotype or fold difference) were removed prior to this analysis. For comparison of histologic scores, gene expression, immune cell frequencies, and cecal SCFA concentrations between untreated and SCFA-treated animals or between WT and HLA–B27/β_2m–transgenic animals, the nonparametric Mann-Whitney U test was used unless specified otherwise. All statistical analysis was performed using the R package (www.r-project.org) or GraphPad Prism software.

RESULTS

Significant alteration of the intestinal metabolome by HLA–B27 expression. To establish the impact of HLA–B27 expression on the intestinal metabolome, we performed metabolomic profiling of cecal contents from HLA–B27/β_2m–transgenic rats and WT controls at age 6 weeks and at age 16 weeks, representing animals before disease and those with established disease, respectively. Our metabolite screen identified 582 named biochemicals in cecal contents. Using analysis of variance with a *P* value threshold of 0.05 to initially compare groups, we found that 188 metabolites were up-regulated in 16-week-old HLA–B27/β_2m–transgenic animals relative to WT littermate controls, and 66 were down-regulated (see Supplementary Data, available at http://onlinelibrary.wiley.com/doi/10.1002/art.40183/abstract), indicating that HLA–B27/β_2m–transgenic rats have a profoundly altered intestinal metabolome. In addition to these changes in rats with established disease, 52 metabolites were up-regulated and 11 were down-regulated in 6-week-old transgenic rats relative to age-matched controls. These differences were visualized by hierarchical cluster analysis (Figure 1A), which demonstrated the global metabolic shifts in 16-week-old HLA–B27/β_2m–transgenic animals in addition to more moderate changes in 6-week-old animals (before disease).

To further examine metabolic shifts driven by HLA–B27 expression, we also performed pathway enrichment analysis (15) to identify biochemical pathways that were strongly influenced by HLA–B27 expression (Figures 1B and C). Notably, HLA–B27 expression impacted metabolites involved in numerous biochemical pathways, including those associated with amino acid, carbohydrate, lipid, and xenobiotic metabolism. When we examined both 6-week (Figure 1B) and 16-week (Figure 1C) time points, a number of these enriched pathways were shared at both time points, including glycine, serine, and threonine metabolism; aminosugar metabolism; MCFA metabolism; fructose, mannose, and galactose metabolism; and phenylalanine and tyrosine metabolism. We noted, however, that some affected metabolite pathways were only observed at 1 time point, for instance, gamma glutamyl amino acids at the 6-week time point (Figure 1B; also see Supplementary Figure 1, available at http://onlinelibrary.wiley.com/doi/10.1002/art.40183/abstract) or food component/plant and secondary bile acid metabolism at the 16-week time point (Figure 1C). These may point to evolving disturbances of the intestinal metabolome over time induced by HLA–B27 expression.

Microbial fermentation products significantly impacted by HLA–B27 expression. In light of the large number of metabolites detected in our screen of cecal contents, and given our relatively restricted sample size (n = 8 animals per genotype per age group), we were unable to identify any individual metabolites that exhibited differential abundance in 6-week-old animals that attained statistical significance when we adjusted stringently for multiple comparisons across the entire data set. However, after removal of low-abundance metabolites (the lowest 20%), we observed 5 metabolites that exhibited a significantly higher abundance in HLA–B27/β_2m–transgenic animals than in WT controls (Figure 2A). We did not observe any significantly down-regulated individual metabolites at this time point. The

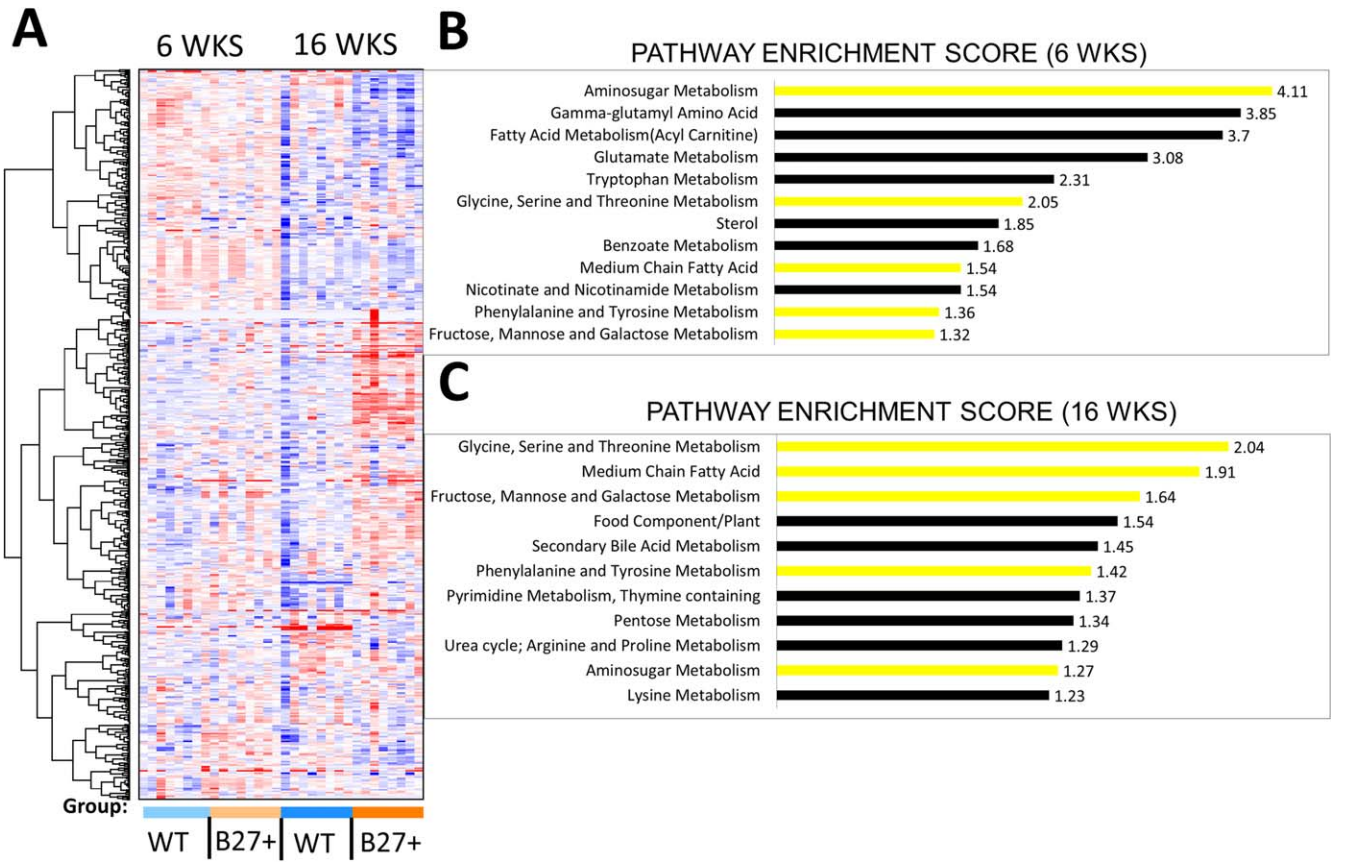

Figure 1. Significant alteration of the intestinal metabolome by HLA–B27 expression. Ultra-performance liquid chromatography tandem mass spectrometry was used to analyze the cecal metabolome of HLA–B27/β_2-microglobulin (β_2m)–transgenic rats and wild-type (WT) littermate controls either before disease onset (at 6 weeks) or during active bowel inflammation (at 16 weeks). **A,** Hierarchical cluster analysis of WT and HLA–B27/β_2m–transgenic (B27+) rats at each time point (n = 8 rats per genotype per age group). **B** and **C,** Pathway enrichment analysis of HLA–B27/β_2m–transgenic rats versus controls at 6 weeks (**B**) and 16 weeks (**C**). Yellow bars represent enrichment at both time points. Details of pathway enrichment analysis are provided in Supplementary Methods, available on the *Arthritis & Rheumatology* web site at http://onlinelibrary.wiley.com/doi/10.1002/art.40183/abstract.

up-regulated metabolites (Figure 2A) were histidine and tyrosine (amino acids), spermidine (a polyamine), *N*-acetylmuramate (a microbial cell wall component), and glycerate (a sugar). Histidine, spermidine, and glycerate were also elevated at 16 weeks (see Supplementary Figure 2A, available at http://onlinelibrary.wiley.com/doi/10.1002/art.40183/abstract), indicating that metabolomic changes detected in established disease may also be detected before disease. Interestingly, however, while *N*-acetylmuramate and tyrosine were elevated at 6 weeks in HLA–B27/β_2m–transgenic animals, they were significantly decreased once disease was established at 16 weeks (see Supplementary Figure 2).

Our subsequent analysis focused on the 16-week data set, which had a large number of individual metabolites that were significantly impacted by HLA–B27 expression (see Supplementary Table 1, available at http://onlinelibrary.wiley.com/doi/10.1002/art.40183/abstract). We have shown previously that HLA–B27 expression is accompanied by a marked expansion of the mucin-degrading bacterium *Akkermansia muciniphila* (6,7). We therefore examined the abundance of mucus components identified in our metabolomic screen.

Strikingly, the mucus carbohydrates fucose and galactose were dramatically increased in the cecum of HLA–B27/β_2m–transgenic animals (Figure 2B). The mucus aminosugar galactosamine and the sialic acids *N*-acetylneuraminate and *N*-acetylglucosamine were also increased in HLA–B27/β_2m–transgenic animals (Figure 2B). In contrast, the mucus aminosugar glucosamine was unchanged. In addition to this major host-derived microbial energy source, we also examined dietary components and their microbially derived metabolites (Figure 2C). The isoflavones daidzein, naringenin, and apigenin are flavonoid phytophenols present in soy and other plants, and they were significantly increased in

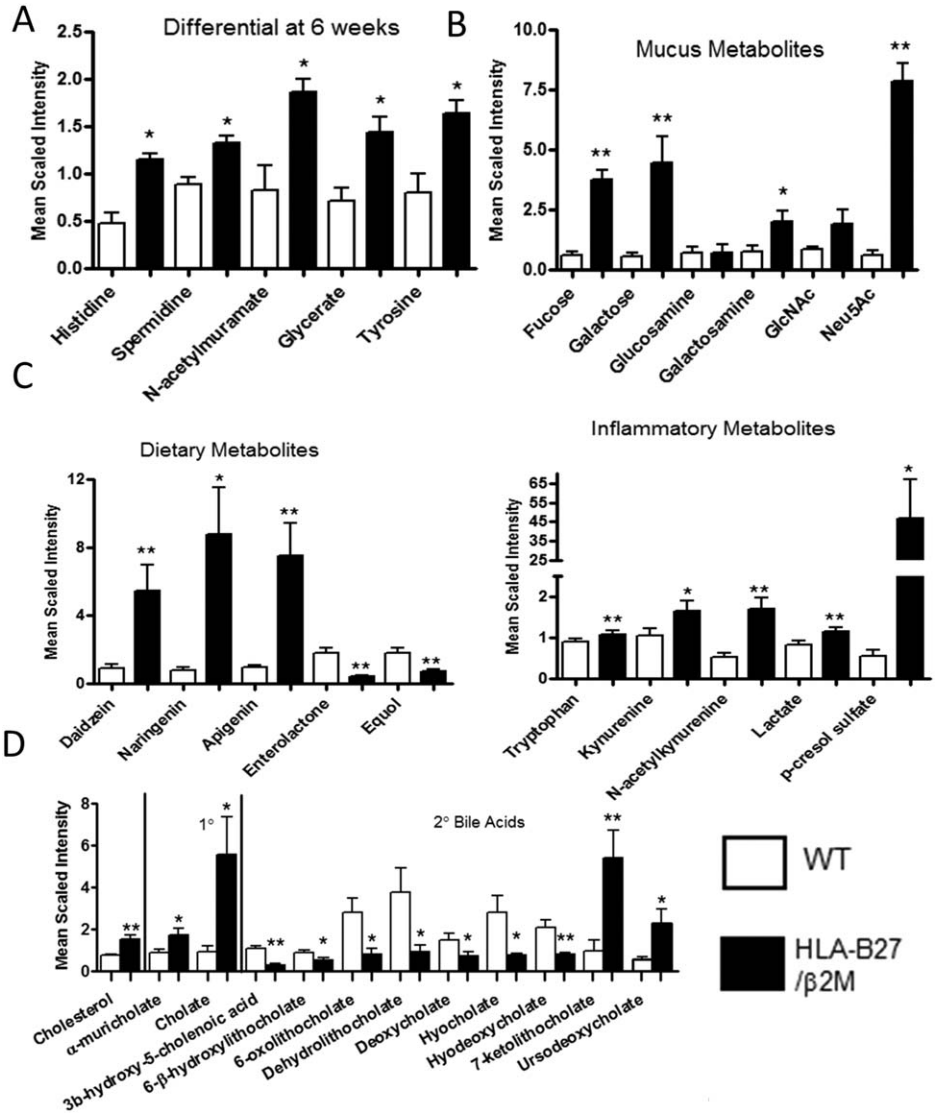

Figure 2. Significant alteration of amino acids, carbohydrates, and xenobiotics by HLA–B27 expression. The abundance of distinct metabolite classes in wild-type (WT) and HLA–B27/β_2-microglobulin (β_2m)–transgenic rats is shown, as determined by ultra-performance liquid chromatography tandem mass spectrometry and gas chromatography mass spectrometry. **A,** Significantly altered cecal metabolites in 6-week-old animals (before disease onset). **B–D,** Levels of mucus metabolites (**B**), dietary metabolites and inflammatory metabolites (**C**), and primary and secondary bile acid metabolites (**D**) in 16-week-old animals (for findings in 6-week-old animals, see Supplementary Figure 2, available on the *Arthritis & Rheumatology* web site at http://onlinelibrary.wiley.com/doi/10.1002/art.40183/abstract). Values are the mean ± SEM (n = 8 rats per group). $* = P < 0.2$; $** = P < 0.1$ versus WT rats (Benjamini-Hochberg–corrected *P* values with a false discovery rate of 0.2 instead of conventional *P* values). GlcNAc = *N*-acetylglucosamine; Neu5Ac = *N*-acetylneuraminate.

HLA–B27/β_2m–transgenic animals (Figure 2C). In contrast, equol, a microbial derivative of daidzein, was significantly decreased. Enterolactone, a mammalian lignin formed by the action of intestinal bacteria on dietary plant lignans, was also significantly decreased (Figure 2C). Taken together, the liberation of mucus components and the decrease in some plant-derived metabolites (but with increased precursors) may indicate markedly shifted metabolic function by the intestinal microbiota in HLA–B27/β_2m–transgenic animals.

We also found a number of metabolites indicative of an active inflammatory response that were significantly up-regulated in intestinal contents of HLA–B27/β_2m–transgenic animals. These included the tryptophan derivatives kynurenine and *N*-acetylkynurenine, which are downstream metabolites of indoleamine 2,3-dioxygenase activity (Figure 2C). Elevated lactate levels are

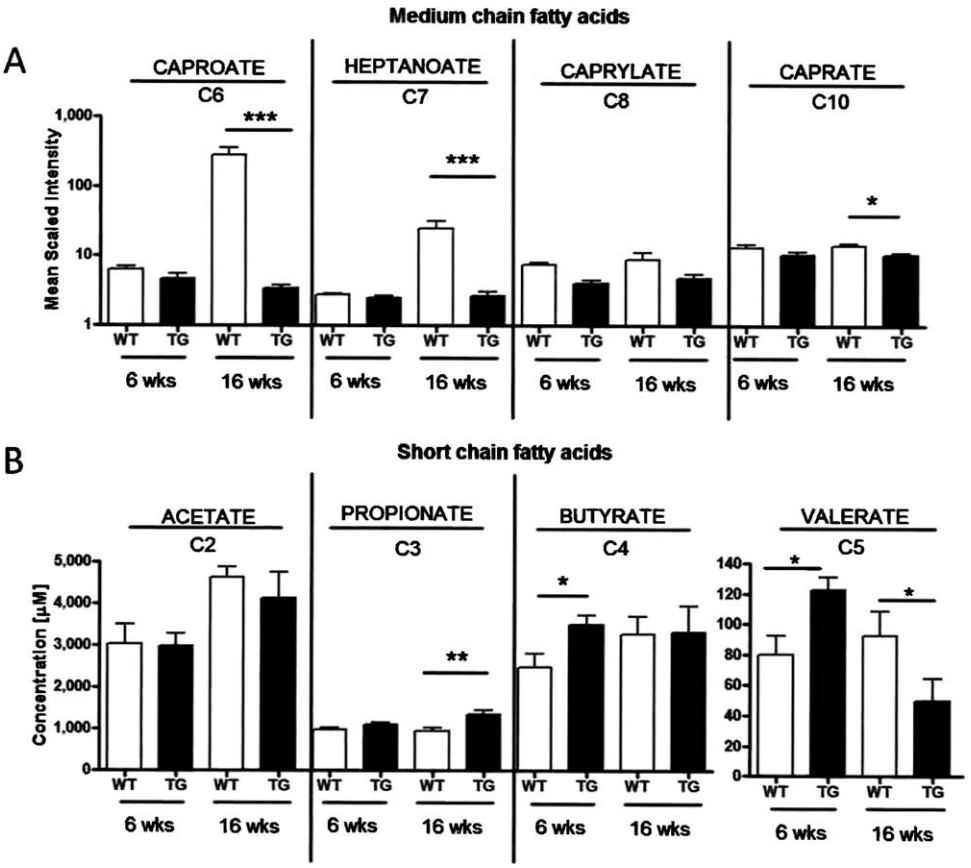

Figure 3. Significant impact of HLA–B27 expression on intestinal levels of medium-chain fatty acids (MCFAs) and short-chain fatty acids (SCFAs) at 6 weeks and 16 weeks. **A,** Levels of MCFAs in cecal contents of wild-type (WT) rats and HLA–B27/β_2-microglobulin–transgenic (TG) rats, as measured by ultra-performance liquid chromatography tandem mass spectrometry metabolomic screen. Values are the mean ± SEM (n = 8 rats per group). $* = P < 0.2$; $*** = P < 0.05$ (Benjamini-Hochberg–corrected P values with a false discovery rate of 0.2 instead of conventional P values). **B,** Cecal concentration of the SCFAs acetate, propionate, butyrate, and valerate, as determined by gas chromatography mass spectrometry. Values are the mean ± SEM (n = 6–8 rats per group). $* = P < 0.05$; $** = P < 0.01$ by Mann-Whitney U test.

also a hallmark of intestinal inflammation and were likewise significantly increased at 16 weeks in HLA–B27/β_2m–transgenic animals (Figure 2C). Interestingly, the microbial metabolite p-cresol sulfate, a product of proteolytic fermentation, was also highly increased in HLA–B27/β_2m–transgenic animals. This metabolite is associated with inflammation and oxidative stress.

Bile acid metabolism, in particular the conversion of primary to secondary bile acids, is another major functional role of the intestinal microbiota. Examination of bile acids in our metabolomic analysis determined that cholesterol and several bile acids were significantly impacted by HLA–B27 expression (Figure 2D). Interestingly, cholesterol and the primary bile acids α-muricholate and cholate were significantly increased in HLA–B27/β_2m–transgenic animals, while the secondary bile acid metabolites 3b-hydroxy-5-cholenoic acid, 6-β-hydroxylithocholate, 6-oxolithocholate, dehydrolithocholate, deoxycholate, hyocholate, and hyodeoxycholate were all significantly decreased. Only 2 bile acids, 7-ketolithocholate and ursodeoxycholate, were significantly increased in HLA–B27/β_2m–transgenic animals. Taken together, these findings further indicate that HLA–B27 expression broadly impacts the levels of microbially derived metabolites in the gut.

Association of HLA–B27 expression with altered levels of MCFAs and SCFAs. Our prior pathway enrichment analysis had identified MCFAs as one of the metabolite pathways most impacted by HLA–B27 expression in 16-week-old HLA–B27/β_2m–transgenic animals (Figure 1C). In light of this, we further examined MCFA levels in transgenic rats and WT controls (Figure 3A). Strikingly, the MCFAs caproic (C6 hexanoic) acid and enanthic (C7 heptanoic) acid were significantly reduced in HLA–B27/β_2m–transgenic animals at 16 weeks. Of note, levels of the MCFAs caprylic

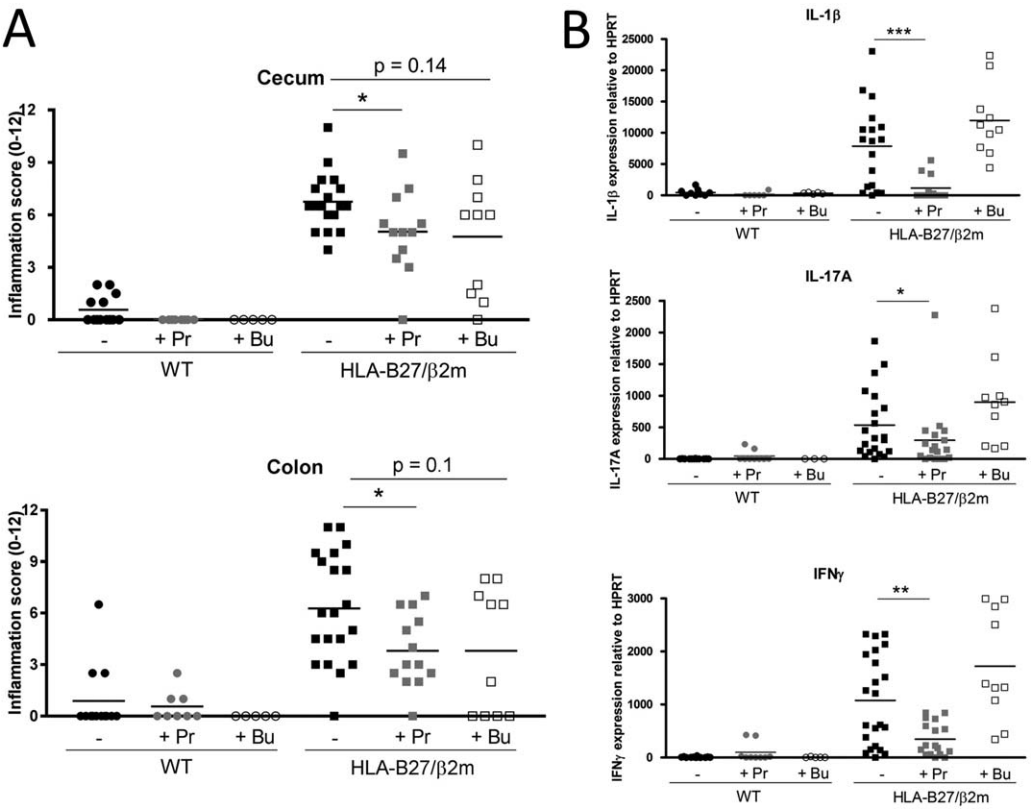

Figure 4. Administration of the short-chain fatty acid sodium propionate (Pr) significantly attenuates HLA–B27–associated immune pathology. Six-week-old HLA–B27/β_2-microglobulin (β_2m)–transgenic rats or wild-type (WT) littermate controls were left untreated (–) or were treated with either sodium propionate (150 m*M*) or sodium butyrate (Bu; 150 m*M*) in drinking water for 12 weeks. At necropsy (16 weeks), the cecum and colon were harvested for analysis of intestinal inflammation. **A,** Histologic assessment of intestinal inflammation in the cecum and colon by semiquantitative scoring system. **B,** Relative expression of mRNA for interleukin-1β (IL-1β), IL-17A, and interferon-γ (IFNγ) in colon tissue. All mRNA expression data were normalized to hypoxanthine guanine phosphoribosyltransferase (HPRT). Symbols represent individual animals; bars show the mean. Data are representative of 3 pooled independent experiments. $* = P < 0.05$; $** = P < 0.01$; $*** = P < 0.005$ by Mann-Whitney U test.

(C8 octanoic) acid and capric (C10 decanoic) acid also trended in the same direction (levels of capric acid decreased significantly prior to Benjamini-Hochberg correction for multiple comparisons). This trend toward lower MCFA levels was also seen in 6-week-old HLA–B27/β_2m–transgenic animals (Figure 3A).

SCFAs are soluble, low molecular weight metabolites that are major microbial fermentation products of dietary fiber and include acetate, propionate, butyrate, and valerate. Since these small molecules were not readily detected by our metabolomic analysis, we performed targeted GC-MS on cecal contents from HLA–B27/β_2m–transgenic and control rats to measure levels of these metabolites (Figure 3B). Validating this approach, we also confirmed that production of these metabolites was critically dependent on the gut microbiota, since antibiotic depletion of the gut microbiota with vancomycin dramatically reduced cecal SCFA levels (see Supplementary Figure 3, available on the *Arthritis & Rheumatology* web site at http://onlinelibrary.wiley.com/doi/10.1002/art.40183/abstract). Interestingly, SCFAs also showed HLA–B27–dependent differences, although with more variability than MCFAs. For instance, at 6 weeks (before disease), valerate was significantly increased in HLA–B27/β_2m–transgenic animals versus controls, although levels of valerate were significantly lower in HLA–B27/β_2m–transgenic animals than in controls at the 16-week time point (Figure 3B). Other changes observed were a significant increase in butyrate concentration at 6 weeks and a significant increase in propionate concentration at 16 weeks (Figure 3B). Taken together, these findings indicate that HLA–B27 expression leads to altered metabolism of several intestinal fatty acids.

The microbial metabolite propionate functionally impacts HLA–B27–associated inflammation. Since HLA–B27 expression clearly impacted the intestinal

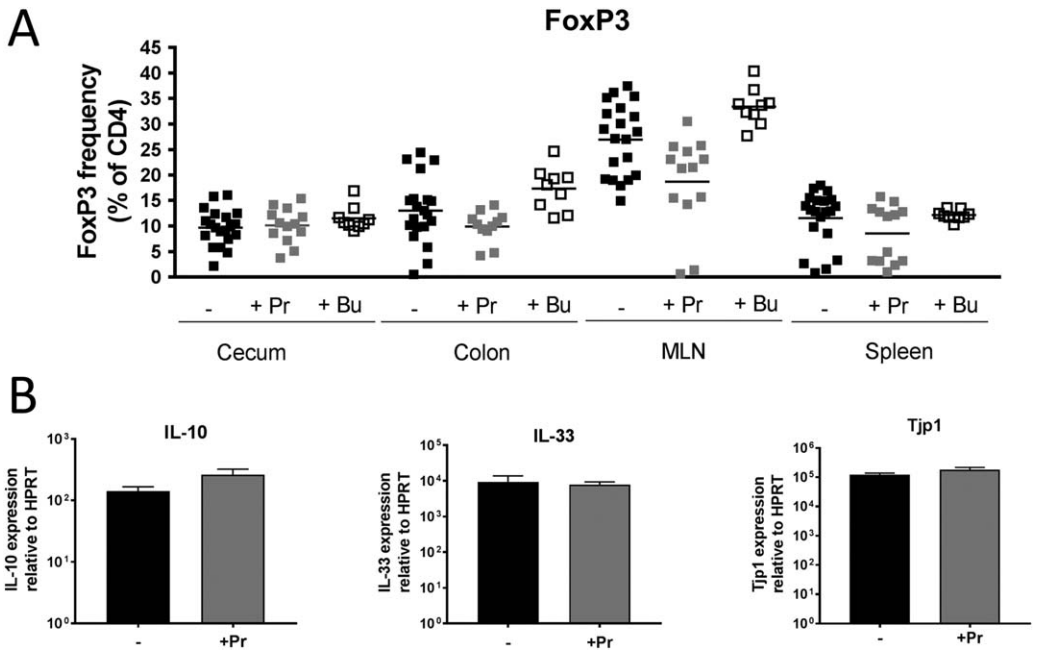

Figure 5. Administration of short-chain fatty acids does not significantly impact FoxP3+ Treg cell induction, expression of immunoregulatory cytokines, or expression of the tight junction protein zonula occludens 1 (Tjp1). Six-week-old HLA–B27/β_2-microglobulin (β_2m)–transgenic rats or wild-type (WT) littermate controls were left untreated (–) or were treated with either sodium propionate (Pr; 150 m*M*) or sodium butyrate (Bu; 150 m*M*) in drinking water for 12 weeks. **A,** Frequency of CD4+FoxP3+ T cells in the cecum, colon, mesenteric lymph nodes (MLNs), and spleen of HLA–B27/β_2m–transgenic rats (for findings in WT animals, see Supplementary Figure 5, available on the *Arthritis & Rheumatology* web site at http://onlinelibrary.wiley.com/doi/10.1002/art.40183/abstract). Symbols represent individual animals; bars show the mean. **B,** Relative colonic expression of mRNA for interleukin-10 (IL-10), IL-33, and the tight junction protein zonula occludens 1. All mRNA expression data were normalized to hypoxanthine guanine phosphoribosyltransferase (HPRT). Values are the mean ± SEM (n = 8–11 rats per group).

metabolome, we were eager to determine whether microbial metabolites specifically could modify SpA pathogenesis. In light of the large number of HLA–B27–dependent metabolites, we selected the SCFAs propionate and butyrate for in vivo functional analysis since they have low toxicity, are commercially available, and are reported to have immunomodulatory functions. We therefore administered propionate or butyrate (150 m*M*) in drinking water to 6-week-old rats (before disease) for 10 weeks, and we examined markers of HLA–B27–associated bowel inflammation (Figure 4). Strikingly, propionate significantly reduced both cecal and colonic intestinal inflammation in HLA–B27/β_2m–transgenic rats, as assessed both histologically and by expression of messenger RNA (mRNA) for the inflammatory mediators IL-1β, IL-17A, and IFNγ (Figure 4). In contrast, the effect of butyrate was more subtle, with a trend toward reduced histology scores but with no impact on inflammatory cytokine expression (Figure 4). SCFA treatment had no significant impact on body mass (see Supplementary Figure 4, available at http://onlinelibrary.wiley.com/doi/10.1002/art.40183/abstract).

The reported immunomodulatory properties of SCFAs include the induction of FoxP3+ Treg cells and the induction of immunoregulatory cytokines in the intestine. We therefore determined the frequency of CD4+FoxP3+ T cells in cecum, colon, the gut-draining MLNs, and spleen following SCFA administration in HLA–B27/β_2m–transgenic rats (Figure 5A). However, we did not observe a higher frequency of Treg cells at any of these sites following SCFA treatment. This effect was also not seen in WT animals without inflammation (see Supplementary Figure 5, http://onlinelibrary.wiley.com/doi/10.1002/art.40183/abstract). We did observe a trend toward a *reduced* frequency of Treg cells in MLNs of propionate-treated HLA–B27/β_2m–transgenic animals (Figure 5A), an observation we ascribe to the reported accumulation of Treg cells at this site, with intestinal inflammation (see ref. 7) being diminished due to less bowel inflammation in propionate-treated animals. In addition to the lack of FoxP3+ Treg cell induction, we did not observe an effect of SCFA administration on expression of intestinal mRNA for the immunomodulatory cytokines IL-10 or IL-33 or the

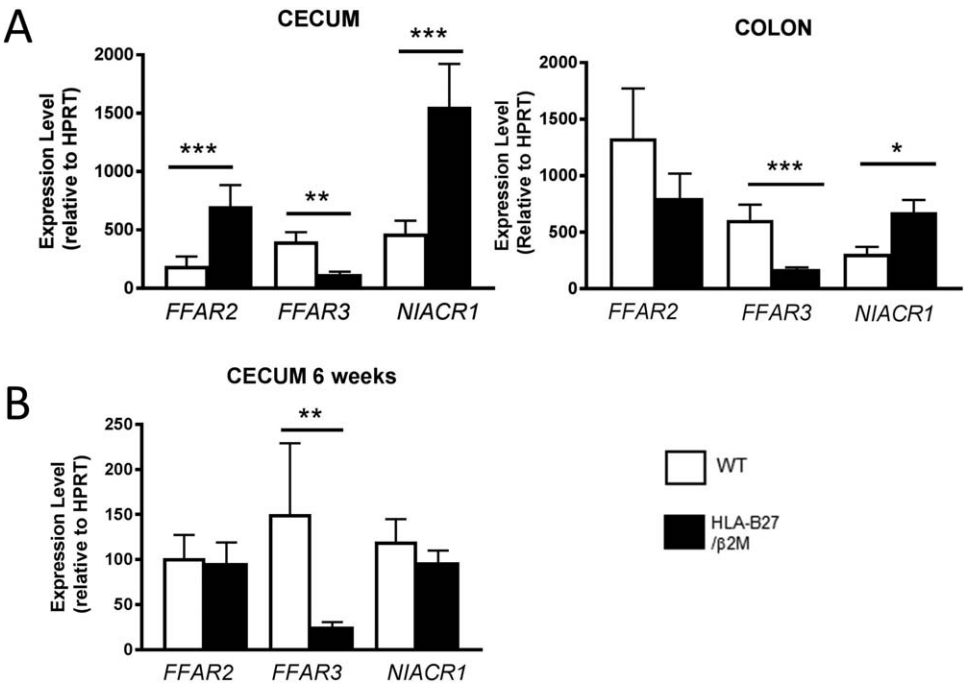

Figure 6. Significant alteration of intestinal short-chain fatty acid (SCFA) receptor expression in HLA–B27/β_2-microglobulin (β_2m)–transgenic rats. Intestinal expression of mRNA for the SCFA receptors free fatty acid receptor 2 (FFAR2), FFAR3, and niacin receptor 1 (NIACR1) in unmanipulated wild-type (WT) rats and HLA–B27/β_2m–transgenic rats was determined in samples of the cecum and colon obtained at age 16 weeks (**A**) and in samples of the cecum obtained at age 6 weeks (**B**) using quantitative reverse transcription–polymerase chain reaction analysis. All mRNA expression data were normalized to hypoxanthine guanine phosphoribosyltransferase (HPRT). Values are the mean ± SEM (n = 10–19 rats per group). * = $P < 0.05$; ** = $P < 0.01$; *** = $P < 0.005$ by Mann-Whitney U test.

tight junction protein zonula occludens 1 in HLA–B27/β_2m–transgenic rats (Figure 5B). We also did not find an obvious antimicrobial effect of SCFA administration that might lower microbial load in the gut and attenuate disease (see Supplementary Figure 6, available at http://onlinelibrary.wiley.com/doi/10.1002/art.40183/abstract).

HLA–B27 expression alters host expression of microbial metabolite receptors. In light of the beneficial effects of propionate on HLA–B27–associated inflammatory disease, despite the observation that this specific metabolite was not depleted in unmanipulated HLA–B27/β_2m–transgenic animals versus healthy controls (Figure 3), we hypothesized that HLA–B27 expression may alter host expression of SCFA receptors instead and hence disrupt this homeostatic feedback loop. We therefore examined intestinal expression of free fatty acid receptor 2 (FFAR2)/Gpr41 (a receptor that binds C2–C4 SCFAs with similar affinity), FFAR3/Gpr43 (a receptor with high affinity for propionate), and the butyrate receptor niacin receptor 1 (NIACR1)/Gpr109 (Figure 6). Strikingly, we found that HLA–B27 expression impacted intestinal expression of mRNA for several SCFA receptors, with significantly decreased cecal expression of the propionate receptor FFAR3 in contrast to increased expression of FFAR2 and NIACR1 at age 16 weeks (Figure 6A). This specific reduction in FFAR3 expression was also observed in 6-week-old (before disease) animals (Figure 6B). Significantly reduced expression of mRNA for FFAR3 was also observed in colon (see Supplementary Figure 7, available at http://onlinelibrary.wiley.com/doi/10.1002/art.40183/abstract). These findings indicate that HLA–B27 expression not only profoundly alters the intestinal metabolome, but also is associated with altered expression of host receptors that bind microbial metabolites.

DISCUSSION

Mounting evidence indicates that the intestinal microbiota may play a significant role in the pathogenesis of SpA disease. A dysbiotic or altered intestinal microbiota is observed in several forms of SpA, including psoriatic arthritis, ankylosing spondylitis (AS), and juvenile enthesitis-related arthritis (8–10), and subclinical bowel inflammation is observed in more than half of AS patients (16). Reactive arthritis following enteric infection is another prototypical SpA family member.

A dysbiotic microbiota is also observed in both the HLA–B27/β_2m–transgenic rat model of SpA and the model of curdlan-induced inflammation in ZAP-70 mutant mice (6,7,17). Depletion of the microbiota with antibiotics or the germ-free state also attenuates SpA disease in both models (17,18).

It is important to note that evidence of an altered microbiota (for example, the relative abundance or presence/absence of microbial species) does not necessarily mean that the functional potential of the microbiota is altered (19). Indeed, healthy humans exhibit a high interindividual variability in the relative abundance of microbial species in the gut but appear to select species with similar enzymatic and functional potential (19). Our study provides direct evidence, however, that the previously described dysbiotic changes observed in SpA are accompanied by functional changes in the metabolic output of the gut, including that of microbe-derived bioactive mediators such as SCFAs.

One of the major changes in the gut metabolic landscape appears to be the shift in nutrient utilization by the intestinal microbiota. For instance, microbial derivatives of plant fiber and isoflavones (such as enterolactone and equol) were decreased in HLA–B27/β_2m–transgenic animals, which indicates perturbed microbial fermentation. Interestingly, these specific microbial metabolites are estrogenic and are thought to have antiinflammatory properties (for review, see ref. 20). In contrast, we observed that several mucus components were increased. This is consistent with the increased mucus production previously reported in the HLA–B27/β_2m–transgenic rat (21), as well as with the HLA–B27–dependent expansion of *A muciniphila* (7) or other microbes that catabolize mucus. Future studies that further address the impact of altered mucus metabolism on both host immunity and the intestinal microbiota would be highly interesting in the context of SpA pathogenesis.

Strikingly, we found that multiple metabolic pathways, even before disease, were impacted by HLA–B27 expression, and we found that a number of individual metabolites were significantly up-regulated in HLA–B27/β_2m–transgenic animals compared with controls at the 6-week time point. This suggests that metabolic shifts in the gut may be a preceding event in SpA pathogenesis, rather than merely secondary to active bowel inflammation. Increased levels of tyrosine and histidine (Figure 2A) and differential usage of amino acid pathways (Figures 1B and 2A) could reflect early changes in colonic protein fermentation or utilization by the host (22). Polyamines such as spermidine are derived from amino acids (both by the host and the microbiota) and modulate enterocyte tight junction formation (23,24), secretory IgA production (25), and mucosal maturation and repair from injury (26) and thus may strongly impact intestinal homeostasis (27). Gamma glutamyl amino acids, a product of gamma glutamyl transferase that may be a marker of oxidative stress (28), also appeared up-regulated at this time point (Figure 1B; also see Supplementary Figure 1, available at http://onlinelibrary.wiley.com/doi/10.1002/art.40183/abstract). Of note, HLA–B27 misfolding triggers an unfolded protein response, which may be up-regulated in the HLA–B27/β_2m–transgenic rat and is intimately related to oxidative stress responses (29,30).

Beyond amino acid metabolites, we also observed altered levels of other biochemical classes even in animals before disease. We observed significantly increased glycerate levels at both age 6 weeks and age 16 weeks (Figure 2A; also see Supplementary Figure 2, http://onlinelibrary.wiley.com/doi/10.1002/art.40183/abstract). Glycerate is a simple sugar, derivatives of which are used in a panoply of metabolic pathways including glycolysis. *N*-acetylmuramate is a component of the microbial cell wall component peptidoglycan, and its increase may be indicative of early HLA–B27–dependent dysbiosis. Interestingly, peptidoglycan is a potent adjuvant of the innate immune system, and its systemic administration can induce both arthritis and uveitis (31).

In light of our findings that MCFAs are reduced in the HLA–B27/β_2m–transgenic rat model of SpA, it is notable that Scher et al reported reduced levels of the MCFAs heptanoate and hexanoate in the feces of psoriatic arthritis patients compared with those of healthy controls (8), an observation also made in CD (32). Indeed, the microbiota has been reported to regulate absorption of MCFAs by enterocytes and is strongly implicated in the pathogenesis of all these diseases (for review, see refs. 11 and 33). Interestingly, neither that study nor the current study found *decreased* levels of SCFAs; instead, we found that cecal propionate (at 16 weeks) and butyrate (at 6 weeks) concentrations were moderately elevated in HLA–B27/β_2m–transgenic animals (Scher et al found no change in their study [8]). This is also consistent with a previous study showing a positive correlation between cecal propionate levels and the extent of intestinal inflammation in HLA–B27/β_2m–transgenic rats (34). This is in contrast to CD, in which several groups have reported a reduction in intestinal SCFA concentrations (35–37), and indicates that canonical HLA–B27–associated spondyloarthritides may have a distinct metabolomic signature compared with

inflammatory bowel disease despite the degree of clinical overlap of these entities in bowel disease.

However, despite the lack of reduced SCFA production in HLA–B27/β_2m–transgenic rats compared with controls, we found that the SCFA propionate significantly attenuated HLA–B27–dependent intestinal inflammation. This is broadly consistent with metabolic studies in which dietary supplementation with prebiotics or dietary fiber, which increase total intestinal SCFA levels, reduces intestinal inflammation in HLA–B27/β_2m–transgenic rats (34,38,39). However, the surprising finding that propionate was elevated in luminal contents of HLA–B27/β_2m–transgenic rats compared with controls in our study (Figure 3) indicates a considerably complex picture with respect to production of SCFAs by the microbiota and their metabolism by the host. One possibility is that higher propionate levels in the gut lumen may reflect reduced SCFA absorption or consumption by colonic enterocytes during active bowel inflammation in HLA–B27/β_2m–transgenic rats, with a switch to MCFA utilization instead due to altered energy demand (40). Alternatively (or in parallel), the specific inflammatory environment of the gut in SpA may create a selective pressure favoring propionate-producing bacteria that prevent the further exacerbation of local inflammation.

Reported actions of propionate include the induction of intestinal Treg cells (12,13), induction of regulatory cytokines (13,41), and improvement of barrier function (42). However, we did not find evidence that these mechanisms were significantly impacted following propionate (or butyrate) treatment of HLA–B27/β_2m–transgenic rats, although intestinal inflammation was significantly reduced. One possibility is that this may reflect species-specific differences in propionate activity or uptake. We note, however, that doses used in our study were highly comparable to those used in murine studies. Another possibility is that regulation of colonic cytokines and tight junction proteins is post-translational, although unfortunately we were unable to obtain sufficient material for protein assays in the current study since intestinal tissue was used for other assays. A third possibility is that these mechanisms have largely been reported in healthy animals or in cell lines, and therefore they may have less effect in the context of HLA–B27–dependent inflammation. However, we did not find a significant induction of Treg cells by SCFA treatment even in WT animals (see Supplementary Figure 4, http://onlinelibrary.wiley.com/doi/10.1002/art.40183/abstract).

Thus, alternative mechanisms to identify the therapeutic mechanism of propionate administration warrant further scrutiny. We note that an examination of dose responses to SCFAs, their bioavailability, and their tissue absorption was not performed in the current study and would no doubt be of interest for further investigation. We recognize this limitation and we therefore cannot exclude the possibility that other SCFAs, such as butyrate, may also modulate HLA–B27–dependent inflammation at other doses or other routes of administration.

In summary, we found that HLA–B27 expression dramatically alters the intestinal metabolome. We also provide pivotal data that microbial metabolites significantly impact the development of HLA–B27–associated inflammatory disease. While our study examined HLA–B27–associated bowel inflammation, it would obviously be valuable to ascertain whether microbial metabolites can attenuate spondylitic and arthritic disease (an area of active research by our own group and others). Moreover, our current data set was not large enough to correlate levels of HLA–B27–associated metabolites with changes in either microbiota composition or disease activity, which likely will continue to be a fruitful avenue of research. Nonetheless, our data provide a compelling rationale to investigate whether further targeting gut microbes or gut metabolites themselves to alter the intestinal metabolome may functionally impact SpA pathogenesis and offer innovative treatment modalities for future clinical management of SpA disease.

AUTHOR CONTRIBUTIONS

All authors were involved in drafting the article or revising it critically for important intellectual content, and all authors approved the final version to be published. Dr. Asquith had full access to all of the data in the study and takes responsibility for the integrity of the data and the accuracy of the data analysis.

Study conception and design. Asquith, Rosenbaum.

Acquisition of data. Asquith, Davin, Stauffer, Janowitz, Lin, Ensign-Lewis, Koop.

Analysis and interpretation of data. Asquith, Davin, Stauffer, Michell, Kinchen, Koop, Rosenbaum.

ADDITIONAL DISCLOSURES

Author Kinchen is an employee of Metabolon, Inc.

REFERENCES

1. Petersen C, Round JL. Defining dysbiosis and its influence on host immunity and disease. Cell Microbiol 2014;16:1024–33.
2. Scher JU, Littman DR, Abramson SB. Microbiome in inflammatory arthritis and human rheumatic diseases [review]. Arthritis Rheumatol 2016;68:35–45.
3. Sharon G, Garg N, Debelius J, Knight R, Dorrestein PC, Mazmanian SK. Specialized metabolites from the microbiome in health and disease. Cell Metab 2014;20:719–30.
4. Hammer RE, Maika SD, Richardson JA, Tang JP, Taurog JD. Spontaneous inflammatory disease in transgenic rats expressing HLA-B27 and human β 2m: an animal model of HLA-B27-associated human disorders. Cell 1990;63:1099–112.

5. Taurog JD, Maika SD, Satumtira N, Dorris ML, McLean IL, Yanagisawa H, et al. Inflammatory disease in HLA-B27 transgenic rats. Immunol Rev 1999;169:209–23.
6. Lin P, Bach M, Asquith M, Lee AY, Akileswaran L, Stauffer P, et al. HLA-B27 and human β2-microglobulin affect the gut microbiota of transgenic rats. PLoS One 2014;9:e105684.
7. Asquith MJ, Stauffer P, Davin S, Mitchell C, Lin P, Rosenbaum JT. Perturbed mucosal immunity and dysbiosis accompany clinical disease in a rat model of spondyloarthritis. Arthritis Rheumatol 2016;68:2151–62.
8. Scher JU, Ubeda C, Artacho A, Attur M, Isaac S, Reddy SM, et al. Decreased bacterial diversity characterizes the altered gut microbiota in patients with psoriatic arthritis, resembling dysbiosis in inflammatory bowel disease. Arthritis Rheumatol 2015;67:128–39.
9. Costello ME, Ciccia F, Willner D, Warrington N, Robinson PC, Gardiner B, et al. Intestinal dysbiosis in ankylosing spondylitis. Arthritis Rheumatol 2015;67:686–91.
10. Stoll ML, Kumar R, Morrow CD, Lefkowitz EJ, Cui X, Genin A, et al. Altered microbiota associated with abnormal humoral immune responses to commensal organisms in enthesitis-related arthritis. Arthritis Res Ther 2014;16:486.
11. Asquith M, Elewaut D, Lin P, Rosenbaum JT. The role of the gut and microbes in the pathogenesis of spondyloarthritis. Best Pract Res Clin Rheumatol 2014;28:687–702.
12. Arpaia N, Campbell C, Fan X, Dikiy S, van der Veeken J, deRoos P, et al. Metabolites produced by commensal bacteria promote peripheral regulatory T-cell generation. Nature 2013; 504:451–5.
13. Smith PM, Howitt MR, Panikov N, Michaud M, Gallini CA, Bohlooly-Y M, et al. The microbial metabolites, short-chain fatty acids, regulate colonic Treg cell homeostasis. Science 2013;341: 569–73.
14. Uhlig HH, Coombes J, Mottet C, Izcue A, Thompson C, Fanger A, et al. Characterization of Foxp3$^+$CD4$^+$CD25$^+$ and IL-10-secreting CD4$^+$CD25$^+$ T cells during cure of colitis. J Immunol 2006;177:5852–60.
15. Brown DG, Rao S, Weir TL, O'Malia J, Bazan M, Brown RJ, et al. Metabolomics and metabolic pathway networks from human colorectal cancers, adjacent mucosa, and stool. Cancer Metab 2016;4:11.
16. De Vos M, Cuvelier C, Mielants H, Veys E, Barbier F, Elewaut A. Ileocolonoscopy in seronegative spondylarthropathy. Gastroenterology 1989;96:339–44.
17. Rehaume LM, Mondot S, Aguirre de Cárcer D, Velasco J, Benham H, Hasnain SZ, et al. ZAP-70 genotype disrupts the relationship between microbiota and host, leading to spondyloarthritis and ileitis in SKG mice. Arthritis Rheumatol 2014;66: 2780–92.
18. Taurog JD, Richardson JA, Croft JT, Simmons WA, Zhou M, Fernández-Sueiro JL, et al. The germfree state prevents development of gut and joint inflammatory disease in HLA-B27 transgenic rats. J Exp Med 1994;180:2359–64.
19. Human Microbiome Project Consortium. Structure, function and diversity of the healthy human microbiome. Nature 2012;486: 207–14.
20. Blaut M, Clavel T. Metabolic diversity of the intestinal microbiota: implications for health and disease. J Nutr 2007;137:751S–5.
21. Faure M, Moënnoz D, Mettraux C, Montigon F, Schiffrin EJ, Obled C, et al. The chronic colitis developed by HLA-B27 transgenic rats is associated with altered in vivo mucin synthesis. Dig Dis Sci 2004;49:339–46.
22. Zhao Y, Wu J, Li JV, Zhou NY, Tang H, Wang Y. Gut microbiota composition modifies fecal metabolic profiles in mice. J Proteome Res 2013;12:2987–99.
23. Guo X, Rao JN, Liu L, Zou T, Keledjian KM, Boneva D, et al. Polyamines are necessary for synthesis and stability of occludin protein in intestinal epithelial cells. Am J Physiol Gastrointest Liver Physiol 2005;288:G1159–69.
24. Guo X, Rao JN, Liu L, Zou TT, Turner DJ, Bass BL, et al. Regulation of adherens junctions and epithelial paracellular permeability: a novel function for polyamines. Am J Physiol Cell Physiol 2003;285:C1174–87.
25. Buts JP, de Keyser N, Kolanowski J, Sokal E, van Hoof F. Maturation of villus and crypt cell functions in rat small intestine: role of dietary polyamines. Dig Dis Sci 1993;38:1091–8.
26. Lux GD, Marton LJ, Baylin SB. Ornithine decarboxylase is important in intestinal mucosal maturation and recovery from injury in rats. Science 1980;210:195–8.
27. Dixon LJ, Kabi A, Nickerson KP, McDonald C. Combinatorial effects of diet and genetics on inflammatory bowel disease pathogenesis. Inflamm Bowel Dis 2015;21:912–22.
28. Lee DH, Blomhoff R, Jacobs DR Jr. Is serum γ glutamyltransferase a marker of oxidative stress? Free Rad Res 2004;38:535–9.
29. DeLay ML, Turner MJ, Klenk EI, Smith JA, Sowders DP, Colbert RA. HLA–B27 misfolding and the unfolded protein response augment interleukin-23 production and are associated with Th17 activation in transgenic rats. Arthritis Rheum 2009;60:2633–43.
30. Cao SS, Kaufman RJ. Endoplasmic reticulum stress and oxidative stress in cell fate decision and human disease. Antioxid Redox Signal 2014;21:396–413.
31. Wells A, Pararajasegaram G, Baldwin M, Yang CH, Hammer M, Fox A. Uveitis and arthritis induced by systemic injection of streptococcal cell walls. Invest Ophthalmol Vis Sci 1986;27:921–5.
32. De Preter V, Joossens M, Ballet V, Shkedy Z, Rutgeerts P, Vermeire S, et al. Metabolic profiling of the impact of oligofructose-enriched inulin in Crohn's disease patients: a double-blinded randomized controlled trial. Clin Transl Gastroenterol 2013;4:e30.
33. Semova I, Carten JD, Stombaugh J, Mackey LC, Knight R, Farber SA, et al. Microbiota regulate intestinal absorption and metabolism of fatty acids in the zebrafish. Cell Host Microbe 2012;12:277–88.
34. Koleva P, Ketabi A, Valcheva R, Gänzle MG, Dieleman LA. Chemically defined diet alters the protective properties of fructo-oligosaccharides and isomalto-oligosaccharides in HLA-B27 transgenic rats. PLoS One 2014;9:e111717.
35. Huda-Faujan N, Abdulamir AS, Fatimah AB, Anas OM, Shuhaimi M, Yazid AM, et al. The impact of the level of the intestinal short chain fatty acids in inflammatory bowel disease patients versus healthy subjects. Open Biochem J 2010;4:53–8.
36. Takaishi H, Matsuki T, Nakazawa A, Takada T, Kado S, Asahara T, et al. Imbalance in intestinal microflora constitution could be involved in the pathogenesis of inflammatory bowel disease. Int J Med Microbiol 2008;298:463–72.
37. Marchesi JR, Holmes E, Khan F, Kochhar S, Scanlan P, Shanahan F, et al. Rapid and noninvasive metabonomic characterization of inflammatory bowel disease. J Proteome Res 2007;6:546–51.
38. Rodríguez-Cabezas ME, Gálvez J, Camuesco D, Lorente MD, Concha A, Martinez-Augustin O, et al. Intestinal anti-inflammatory activity of dietary fiber (Plantago ovata seeds) in HLA-B27 transgenic rats. Clin Nutr 2003;22:463–71.
39. Hoentjen F, Welling GW, Harmsen HJ, Zhang X, Snart J, Tannock GW, et al. Reduction of colitis by prebiotics in HLA-B27 transgenic rats is associated with microflora changes and immunomodulation. Inflamm Bowel Dis 2005;11:977–85.
40. Jorgensen JR, Clausen MR, Mortensen PB. Oxidation of short and medium chain C2-C8 fatty acids in Sprague-Dawley rat colonocytes. Gut 1997;40:400–5.
41. Park J, Kim M, Kang SG, Jannasch AH, Cooper B, Patterson J, et al. Short-chain fatty acids induce both effector and regulatory T cells by suppression of histone deacetylases and regulation of the mTOR-S6K pathway. Mucosal Immunol 2015;8:80–93.
42. Suzuki T, Yoshida S, Hara H. Physiological concentrations of short-chain fatty acids immediately suppress colonic epithelial permeability. Br J Nutr 2008;100:297–305.

ARTHRITIS & RHEUMATOLOGY
Vol. 69, No. 10, October 2017, pp 1996–2005
DOI 10.1002/art.40191

The Incidence and Prevalence of Systemic Lupus Erythematosus in San Francisco County, California

The California Lupus Surveillance Project

Maria Dall'Era,[1] Miriam G. Cisternas,[2] Kurt Snipes,[3] Lisa J. Herrinton,[4] Caroline Gordon,[5] and Charles G. Helmick[6]

Objective. **Estimates of the incidence and prevalence of systemic lupus erythematosus (SLE) in the US have varied widely. The purpose of this study was to conduct the California Lupus Surveillance Project (CLSP) to determine credible estimates of SLE incidence and prevalence, with a special focus on Hispanics and Asians.**

Methods. **The CLSP, which is funded by the Centers for Disease Control and Prevention, is a population-based registry of individuals with SLE residing in San Francisco County, CA, from January 1, 2007 through December 31, 2009. Data sources included hospitals, rheumatologists, nephrologists, commercial laboratories, and a state hospital discharge database. We abstracted medical records to ascertain SLE cases, which we defined as patients who met ≥4 of the 11 American College of Rheumatology classification criteria for SLE. We estimated crude and age-standardized incidence and prevalence, which were stratified by sex and race/ethnicity.**

Results. **The overall age-standardized annual incidence rate was 4.6 per 100,000 person-years. The average annual period prevalence was 84.8 per 100,000 persons. The age-standardized incidence rate in women and men was 8.6 and 0.7 per 100,000 person-years, respectively. This rate was highest among black women (30.5), followed by Hispanic women (8.9), Asian women (7.2), and white women (5.3). The age-standardized prevalence in women per 100,000 persons was 458.1 in blacks, 177.9 in Hispanics, 149.7 in Asians, and 109.8 in whites. Capture–recapture modeling estimated 33 additional incident cases and 147 additional prevalent cases.**

Conclusion. **Comprehensive methods that include intensive case-finding provide more credible estimates of SLE in Hispanics and Asians, and confirm racial and ethnic disparities in SLE. The disease burden of SLE is highest in black women, followed by Hispanic women, Asian women, and white women.**

Historical estimates of the incidence and prevalence of systemic lupus erythematosus (SLE) in the US have varied widely (1). These differences stem from a variety of factors, including the definition of SLE used, completeness of case ascertainment, geographic area, and racial/ethnic composition of the study population. The heterogeneity of disease manifestations and the lack of an accurate, reliable diagnostic test result in substantial challenges and costs of conducting large-scale epidemiologic studies in SLE. In an effort to develop more authoritative estimates of the incidence and prevalence of SLE, the Centers for Disease Control and Prevention (CDC) initially provided funding for 2 population-based lupus surveillance registries: the Georgia Lupus Registry and the Michigan Lupus Epidemiology and Surveillance Program. These 2 registries, which were focused primarily on whites and blacks, have been successfully finished (2,3). To increase the reliability of SLE estimates in other racial/ethnic groups, the CDC funded 2 similar registries, one in California and the

The views expressed herein are those of the authors and do not necessarily represent the official position of the Centers for Disease Control and Prevention.

Supported by the CDC (National Center for Chronic Disease Prevention and Health Promotion grant A114297).

[1]Maria Dall'Era, MD: University of California, San Francisco; [2]Miriam G. Cisternas, MA: MGC Data Services, Carlsbad, California; [3]Kurt Snipes, PhD: California Department of Public Health, Sacramento; [4]Lisa J. Herrinton, PhD: Kaiser Permanente, Oakland, California; [5]Caroline Gordon, MD, FRCP: University of Birmingham, Birmingham, UK; [6]Charles G. Helmick, MD: CDC, Atlanta, Georgia.

Address correspondence to Maria Dall'Era, MD, University of California, San Francisco, 533 Parnassus Avenue, U384 Box 0633, San Francisco, CA 94143. E-mail: maria.dallera@ucsf.edu.

Submitted for publication December 20, 2016; accepted in revised form June 22, 2017.

other in New York, to focus on Hispanics and Asians, and a third registry with the Indian Health Service to focus on American Indians and Alaska Natives (4).

In collaboration with the CDC and the California Department of Public Health, we conducted the California Lupus Surveillance Project (CLSP) to determine contemporary, population-based estimates of the incidence and prevalence of SLE in San Francisco County during the period 2007 through 2009 using multiple methods of case ascertainment. A secondary goal was to describe the clinical and serologic spectrum of incident SLE in the population. To the greatest extent possible, we aligned our methodology with that of the Georgia and Michigan registries (2,3) to promote consistent data collection and optimal case ascertainment.

PATIENTS AND METHODS

The California Lupus Surveillance Project. The CLSP was conducted under the statutory authority of the California Department of Public Health (CDPH). Patients were not contacted for this study. A partnership between the CDPH and the University of California, San Francisco (UCSF), allowed medical records to be collected using the health surveillance exemption to the Health Insurance Portability and Accountability Act (HIPAA) privacy rules (45 CFR parts 160 and 164). The use of protected health information was essential in the conduct of this project in order to increase potential case-finding, perform unbiased case ascertainment, and prevent duplication of patients in the registry. The CDPH subcontracted with the UCSF to conduct this project. The State of California Institutional Review Board (IRB) granted a waiver for this public health surveillance activity, but the project was reviewed and approved by the UCSF IRB.

Source population/catchment criteria. The source population consisted of residents of San Francisco County, CA, during the period of January 1, 2007 through December 31, 2009. According to US Census estimates, the San Francisco County source population in 2007–2009 averaged 790,582 residents, 56% of whom identified themselves as white, 35% as Asian or Pacific Islander, 7% as black, and 1% as American Indian/Alaska Native (5). Of note, Hispanic ethnicity is considered a distinct concept from race and is therefore collected and reported separately from race; 15% of residents identified themselves as Hispanic ethnicity.

Case definitions. SLE is currently diagnosed in clinical practice by an expert clinician based on characteristic symptoms and signs in conjunction with supportive serologic and histologic data. For the purposes of this surveillance project in which clinical information was ascertained through review of medical records, we used various case definitions to classify a patient as having SLE. To maintain consistency with the Georgia and Michigan Lupus Registries (2,3), we report estimates using 2 case-finding definitions: the American College of Rheumatology (ACR) case definition and the combined case definition.

The ACR definition included patients who met ≥4 of the 11 ACR revised criteria for the classification of SLE as defined in 1982 and updated in 1997 (6,7). This is a standard case definition used for research. The combined definition was satisfied if a patient met any of the following 3 criteria. The patient satisfied the ACR case-finding definition as described above. The patient had documented SLE, as diagnosed by the treating rheumatologist, and met 3 of the 11 ACR classification criteria. This definition was chosen to allow for the possibility of missing data and an inability to confirm criteria in the available medical records for prevalent cases with longstanding disease. The patient had lupus-related kidney disease, as defined either by the presence of World Health Organization class II–VI lupus nephritis upon biopsy or by the presence in the medical record of a diagnosis of SLE (International Classification of Diseases, Ninth Revision, Clinical Modification [ICD-9-CM] code 710.0) along with either dialysis or renal transplantation.

Case ascertainment. The 3 primary sources of potential SLE cases were as follows: 1) community rheumatology and nephrology clinics (office-based practices), 2) community hospitals (nonacademic hospitals), and 3) integrated health care systems (integrated hospitals and clinics) within the catchment area, including the UCSF, Kaiser Permanente of Northern California, and the San Francisco Veterans Administration Medical Center (Figure 1).

We queried these sources over the period 2000–2009 using ICD-9-CM diagnostic codes 710.0 (SLE), 695.4 (discoid lupus), 710.8 (other specified connective tissue disease [CTD]), and 710.9 (unspecified CTD). A secondary source was a commercial laboratory, which we queried for the following serologic tests: antinuclear antibodies, anti–double-stranded DNA antibodies, anti-Sm antibodies, antiphospholipid antibodies, and low complement levels. Another secondary source was the California Office of Statewide Health Planning and Development (OSHPD) hospital discharge database, which we queried for discharges using the ICD-9-CM diagnostic codes 710.0 (SLE), 695.4 (discoid lupus), 710.8 (other specified CTD), and 710.9 (unspecified CTD). We added patients identified from the OSHPD query to the roster of the appropriate primary source hospitals and integrated health care systems.

After compiling a list of potential SLE patients from all sources using the queries described above, we determined catchment criteria for each patient (proof of residence in San Francisco County during the period 2007–2009). The primary methods for verifying catchment criteria were via the LexisNexis online database service, hospital billing databases, and clinic medical records. We then abstracted medical records for each of the potential SLE patients who met catchment criteria to identify those whose medical record had a physician diagnosis of SLE, possible SLE, undifferentiated/unspecified CTD, or a related connective tissue disorder, such as mixed CTD.

Data collection. Four trained field staff abstracted medical charts for each potential SLE patient who met the catchment criteria. Training of the staff included lectures by physicians, extensive reading about SLE clinical manifestations and terminology, and practice abstractions of patient charts that were then reviewed in detail by the principal investigator (MD). The field abstractors accessed all available medical records (paper charts and electronic medical records) at each source location, collecting more than 200 data elements. Laboratory records were reviewed for the presence or absence

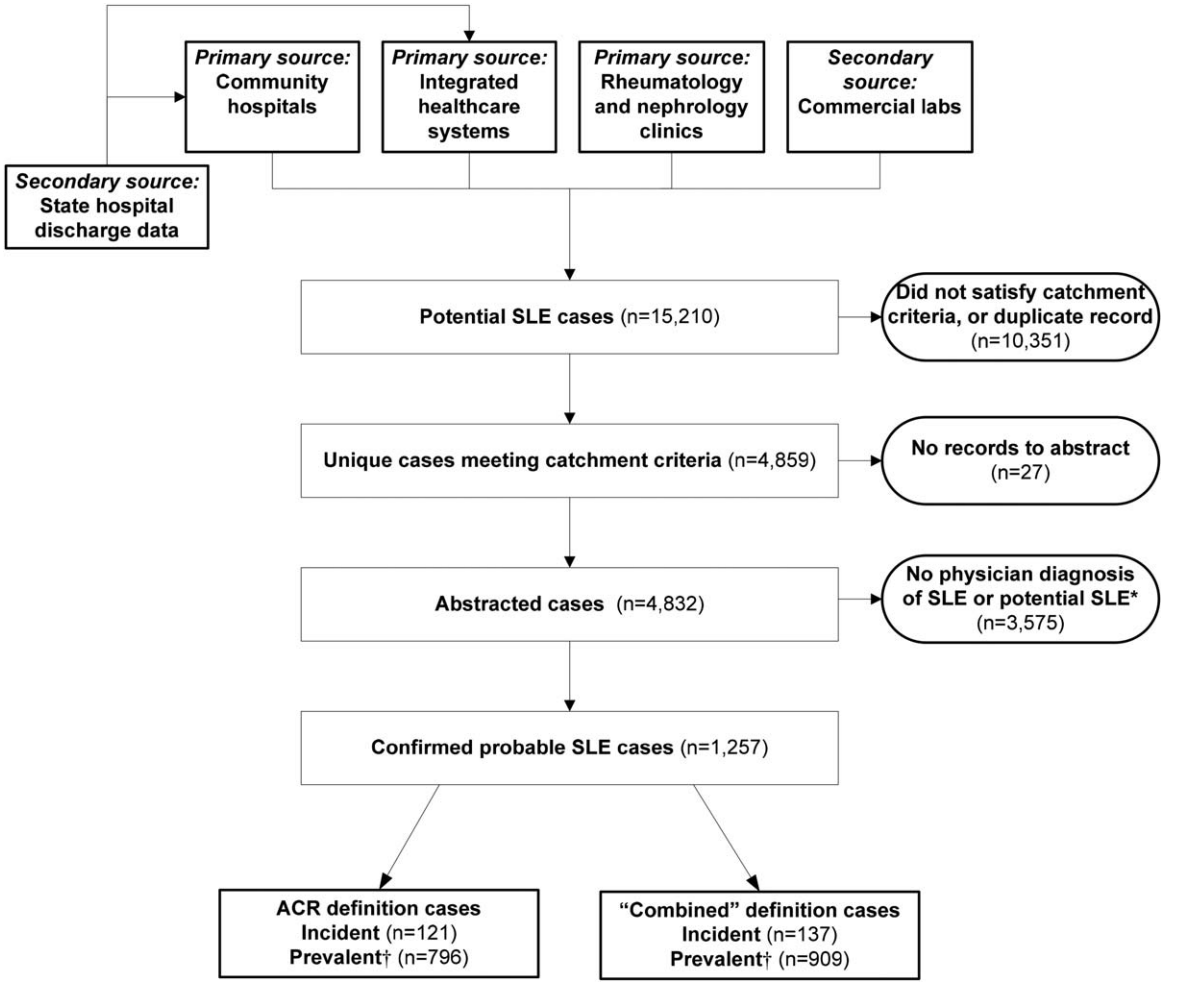

Figure 1. Flow diagram showing the case ascertainment process in San Francisco County, California, 2007–2009. Two case-finding definitions were used: the American College of Rheumatology (ACR) definition and the combined definition (see Patients and Methods for details). *Medical record diagnosis of systemic lupus erythematosus (SLE), possible SLE, undifferentiated/unspecified connective tissue disease, or related connective tissue disorder. † Prevalent cases represent unique persons over the 3-year time period.

of antibodies and for the presence or absence of low complement levels.

The abstractors recorded whether the source was a community clinic, community hospital, or integrated health care system as described above. As questions arose about the information in the medical records, the abstractors contacted the principal investigator in real time to obtain clarifications. Demographic information was obtained from the medical record. For quality control, a second field abstractor and the principal investigator reviewed 5 of every 100 charts for each abstractor, and data entry errors identified by discordant responses between abstractors were examined and corrected. Overall, we calculated 98% concordance between abstractors for the required data elements (those used to define the ACR criteria) and 93% concordance for all other data elements.

Statistical analysis. We derived all denominators for incidence and prevalence using the 2007–2009 San Francisco population estimates from the revised 2000–2009 bridged-race intercensal files (5). The average annual incidence rate (cases per 100,000 person-years) was the number of newly diagnosed SLE cases in persons residing in San Francisco County at the time of SLE diagnosis (defined as the earliest date as recorded in the medical record that the physician first stated the diagnosis of SLE, possible SLE, undifferentiated CTD, or mixed CTD) during 2007–2009 divided by the sum of the annual population of San Francisco for 2007, 2008, and 2009. We calculated the annual period prevalence (cases per 100,000 persons) for each year separately, dividing the number of SLE cases diagnosed before or during that year in persons residing in San Francisco County during the year by the San Francisco County population of that year. We then averaged the 3 annual prevalence estimates to yield the average annual prevalence for 2007–2009. Our next step was to calculate exact 95% confidence intervals (95% CIs) (8) for the incidence rate and average annual prevalence.

We calculated age-standardized incidence and prevalence using the direct method, based on the 2000 US projected population (distribution no. 2) (9). In addition, we computed

Table 1. Crude and age-standardized average annual incidence rates of systemic lupus erythematosus (overall and by race/ethnicity and sex) in the ACR case definition and combined case definition groups, San Francisco County, California, 2007–2009*

Race/ethnicity and sex	No. of person-years contributed by population	Average annual incidence rate per 100,000 person-years					
		ACR case definition			Combined case definition		
		No. of cases	Crude rate (95% CI)	Age-standardized rate (95% CI)	No. of cases	Crude rate (95% CI)	Age-standardized rate (95% CI)
Overall†	2,371,747	121	5.1 (4.3–6.1)	4.6 (3.8–5.5)	137	5.8 (4.9–6.8)	5.2 (4.3–6.2)
Women	1,170,817	112	9.6 (8.0–11.5)	8.6 (7.1–10.5)	127	10.8 (9.1–12.9)	9.8 (8.2–11.8)
Men	1,200,930	9	0.7 (0.4–1.4)	0.7 (0.4–1.4)	10	0.8 (0.5–1.5)	0.8 (0.4–1.5)
Black	170,035	27	15.9 (10.9–23.1)	15.5 (10.6–22.6)	28	16.5 (11.4–23.8)	16.0 (11.1–23.3)
Women	83,535	25	29.9 (20.3–44.2)	30.5 (20.7–44.9)	26	31.1 (21.2–45.6)	31.9 (21.8–46.5)
Men	86,500	2	2.3 (0.6–8.4)	2.1 (0.6–8.2)	2	2.3 (0.6–8.4)	2.1 (0.6–8.2)
White	1,338,200	43	3.2 (2.4–4.3)	2.8 (2.1–3.9)	50	3.7 (2.8–4.9)	3.3 (2.4–4.4)
Women	629,158	38	6.0 (4.4–8.3)	5.3 (3.8–7.5)	44	7.0 (5.2–9.4)	6.1 (4.5–8.4)
Men	709,042	5	0.7 (0.3–1.7)	0.6 (0.3–1.6)	6	0.8 (0.4–1.8)	0.8 (0.3–1.7)
Asian/Pacific Islander	840,386	39	4.6 (3.4–6.3)	4.1 (2.9–5.7)	43	5.1 (3.8–6.9)	4.6 (3.3–6.3)
Women	447,855	37	8.3 (6.0–11.4)	7.2 (5.1–10.2)	41	9.2 (6.7–12.4)	8.1 (5.8–11.2)
Men	392,531	2	0.5 (0.1–1.9)	0.6 (0.2–1.9)	2	0.5 (0.1–1.9)	0.6 (0.2–1.9)
Hispanic	347,911	17	4.9 (3.1–7.8)	4.2 (2.5–7.0)	22	6.3 (4.2–9.6)	5.6 (3.6–8.7)
Women	163,586	16	9.8 (6.0–15.9)	8.9 (5.3–14.8)	21	12.8 (8.4–19.6)	12.0 (7.7–18.6)
Men	184,325	1	0.5 (0.1–3.1)	0.3 (0.0–2.7)	1	0.5 (0.1–3.1)	0.3 (0.0–2.7)

* Age-standardized rates were age-standardized to the 2000 projected Census population. Hispanic ethnicity was recorded separately from race; therefore, persons in this ethnicity category are also represented in the race categories of black, white, and Asian/Pacific Islander. Ethnicity information was missing for 18 patients in the American College of Rheumatology (ACR) case definition group and 21 in the combined case definition (see Patients and Methods for details) group. 95% CI = 95% confidence interval.
† Represents the entire population, including persons whose race/ethnicity was not known (11 in the ACR case definition group and 15 in the combined case definition group) or was American Indian/Alaska native (1 in each case definition group).

age-specific estimates using 10-year age groups, as well as sex-specific estimates. The intercensal database of the Census Bureau codes race and Hispanic ethnicity using 2 variables. One collapses all persons into 4 mutually exclusive categories defined by bridged race, without accounting for Hispanic ethnicity: black, white, Asian/Pacific Islander, and American Indian/Alaska Native (10). The other codes Hispanic ethnicity as a separate construct.

Similar to the Georgia registry (2), we used capture–recapture methods to estimate underascertainment of cases. Specifically, we developed log-linear models that estimated the number of missing cases predicted by the overlap among the 3 primary sources (community rheumatology and nephrology clinics, community hospitals, and integrated health care systems). We evaluated the results of all log-linear models possible for a 3-source capture–recapture analysis and then chose the best-fitting model based on chi-square goodness-of-fit criteria (11). Using the estimated number of undercounted cases from the best-fitting model, we calculated the capture–recapture revised incidence and prevalence estimates for the ACR definition. *P* values less than 0.05 were considered significant.

We compared differences between estimates by case definition using the 95% CIs of the age-adjusted rates. Nonoverlapping 95% CIs were considered to be significantly different.

RESULTS

Study population. As shown in Figure 1, among 15,210 potential SLE patients identified from primary and secondary sources, 4,859 met the geographic and temporal catchment area criteria (residency in San Francisco County from 2007 through 2009). Abstraction was completed for 4,832 patients because 27 patients did not have any available medical records. Of the abstracted patients, 1,257 satisfied the catchment criteria and had a physician recorded diagnosis of SLE, possible SLE, undifferentiated/unspecified CTD, or a related connective tissue disorder such as mixed CTD in their medical record. Of these 1,257 cases, 121 incident and 796 prevalent cases met the ACR case definition while 137 incident and 909 prevalent cases met the combined case definition. All cases were confirmed using primary data sources, including those initially ascertained from state hospital discharge data. Commercial laboratory queries did not provide any additional cases.

Incidence rates according to the ACR case definition. The overall crude and age-standardized incidence rates were 5.1 (95% CI 4.3–6.1) and 4.6 (95% CI 3.8–5.5) per 100,000 person-years (Table 1). The 121 incident cases consisted of 112 women and 9 men. Race for these cases was identified as black (n = 27), white (n = 43), Asian/Pacific Islander (n = 39), and American Indian/Alaska native (n = 1); no race was identified in 11 of them. Hispanic ethnicity was identified in 17 patients; 18 had no ethnicity identified. Among the Asian/Pacific Islander subgroup, the predominant race

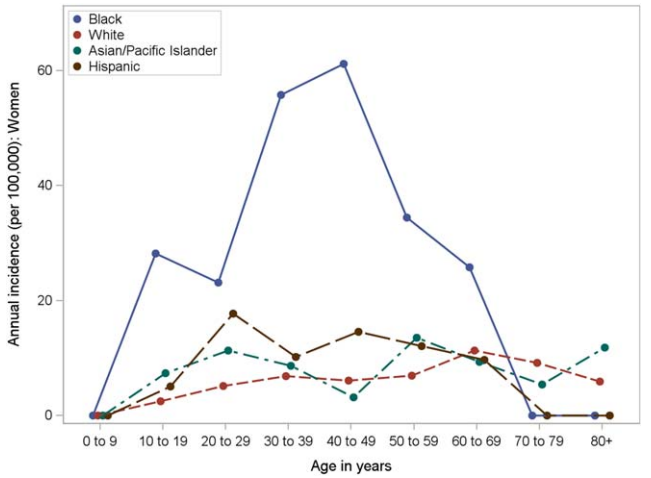

Figure 2. Average annual age-specific incidence rates of systemic lupus erythematosus (SLE) among women living in San Francisco County, California, 2007–2009, categorized by race and Hispanic ethnicity. SLE was defined according to the American College of Rheumatology criteria. The 95% confidence intervals for the incidence rates overlapped within each age group, except for the groups ages 30–39 years and 40–49 years, where the rates for black women were statistically significantly higher than those in the other racial groups or Hispanics. The race categories are mutually exclusive. Hispanic ethnicity was recorded separately from race; therefore, persons of Hispanic ethnicity are also represented in the race categories (mostly white).

was Chinese (21 patients; 17 were identified as Chinese only, with the remaining 4 including another Asian/Pacific Islander racial category) followed by Japanese (3 patients; 2 were exclusively Japanese), Filipino (2 patients; both of whom also had another Asian/Pacific Islander racial category), and 1 each of Korean, Vietnamese, Asian Indian, Samoan, and Hawaiian. The remaining 7 cases were classified as "other Asian," a category that included Burmese, Indonesian, and Asian not otherwise specified (data not shown).

The age-standardized incidence rates were about 12 times higher among women than men: 8.6 versus 0.7 per 100,000 person-years. The age-standardized incidence rate was highest among black women (30.5 [95% CI 20.7–44.9]), followed by Hispanic women (8.9 [95% CI 5.3–14.8]), Asian women (7.2 [95% CI 5.1–10.2]), and finally, white women (5.3 [95% CI 3.8–7.5]). The age-standardized incidence rate among black women was ~6 times higher than among white women.

Among black women, the age-specific incidence rate peaked at 61.2 per 100,000 women in the 40–49-year-old age group. Among the other racial/ethnic groups, incidence rates were relatively constant across the age groups (Figure 2). There were too few incident cases in men (9 cases) to enable age stratification. The overall mean age at diagnosis was 43.9 years. The mean age at diagnosis stratified by bridged race/ethnicity was 40.1 years in blacks, 46.5 years in whites, 45.1 years in Asians, and 36.6 years in Hispanics. All 95% CIs for the race/ethnicity mean age estimates overlapped (data not shown).

Our capture–recapture modeling estimated 33 (95% CI 8–130) additional incident cases in the population. This yielded a capture–recapture inflated crude rate of 6.5 per 100,000 person-years.

Incidence rates according to the combined case definition. The combined definition yielded an additional 16 cases (15 from the 3 ACR criteria plus rheumatologist diagnosis criterion and a single case from the lupus-related kidney disease criterion) for a total of 137 incident cases (Table 1). The overall crude and age-standardized incidence rates were 5.8 (95% CI 4.9–6.8) and 5.2 (95% 4.3–6.2) per 100,000 person-years. Sex and racial/ethnic disparities in the incident cases were similar to those observed in the ACR cases.

Prevalence according to the ACR case definition. The ACR definition yielded overall crude and age-standardized prevalence proportions of 96.0 (95% CI 89.4–103.1) and 84.8 (95% CI 78.6–91.5) per 100,000 persons (Table 2). The 796 unique prevalent cases over the 3-year period consisted of 708 women and 88 men. We identified race for these cases as white (n = 294), Asian/Pacific Islander (n = 290), black (n = 160), and American Indian/Alaskan native (n = 4); race was not identified in 48 patients. Hispanic ethnicity was identified for 118 patients. Similar to the incident cases, the majority of the Asian/Pacific Islander subgroup was composed of Chinese (137 patients; 101 were identified as Chinese and no other race), followed by "other Asian" (56 patients), Filipino (42 patients; 26 were not identified with any other race), Vietnamese (18 patients; 12 had no other race identified), Japanese (10 patients; 8 were not identified with any other race), Korean (5 patients; 3 had no other race identified), Thai and Pakistani (4 patients each), Asian Indian and Samoan (3 patients each), other South Asian, Cambodian, and Pacific Islander not otherwise specified (2 patients each), and Hawaiian and Laotian (1 patient each) (data not shown).

Age-standardized prevalence was about 8 times higher among women than men: 155.6 versus 19.3 per 100,000 persons. The age-standardized prevalence was highest among black women (458.1 [95% CI 385.4–544.5]), followed by Hispanic women (177.9 [95% CI 145.9–217.0]), Asian women (149.7 [95% CI 131.4–170.7]), and finally, white women (109.8 [95% CI 96.5–124.9]). The age-standardized prevalence among black women was over 4 times higher than that among white

Table 2. Crude and age-standardized average annual prevalence of systemic lupus erythematosus (overall and by race/ethnicity and sex) in the ACR case definition and combined case definition groups, San Francisco County, California, 2007–2009*

	Average annual prevalence per 100,000 persons					
	ACR case definition			Combined case definition		
Race/ethnicity and sex	No. of cases†	Crude prevalence (95% CI)	Age-standardized prevalence (95% CI)	No. of cases†	Crude prevalence (95% CI)	Age-standardized prevalence (95% CI)
Overall‡	759	96.0 (89.4–103.1)	84.8 (78.6–91.5)	869	109.9 (102.8–117.4)	96.8 (90.2–103.9)
Women	675	172.9 (160.3–186.4)	155.6 (143.7–168.5)	778	199.4 (185.9–213.9)	179.4 (166.6–193.2)
Men	84	21.1 (17.0–26.1)	19.3 (15.4–24.1)	91	22.6 (18.4–27.8)	20.6 (16.6–25.6)
Black	150	264.1 (225.1–309.8)	241.0 (203.9–284.9)	163	287.0 (246.2–334.5)	261.0 (222.3–306.5)
Women	133	476.6 (402.3–564.6)	458.1 (385.4–544.5)	145	519.7 (441.9–611.2)	498.4 (422.3–588.2)
Men	17	58.9 (36.8–94.4)	52.3 (31.7–86.2)	18	62.4 (39.5–98.6)	54.8 (33.7–89.3)
White	282	63.3 (56.3–71.1)	55.2 (48.7–62.6)	333	74.7 (67.1–83.2)	64.9 (57.8–72.8)
Women	256	121.9 (107.8–137.7)	109.8 (96.5–124.9)	303	144.6 (129.2–161.8)	130.0 (115.5–146.4)
Men	27	11.3 (7.7–16.5)	10.0 (6.7–14.9)	30	12.7 (8.9–18.1)	11.4 (7.8–16.5)
Asian/Pacific Islander	279	99.7 (88.7–112.1)	90.5 (80.0–102.3)	317	113.1 (101.4–126.3)	102.5 (91.3–115.1)
Women	247	165.2 (145.8–187.1)	149.7 (131.4–170.7)	282	189.1 (168.3–212.4)	171.0 (151.3–193.2)
Men	33	25.0 (17.7–35.1)	22.9 (16.1–32.7)	35	26.5 (19.0–36.9)	24.3 (17.2–34.3)
Hispanic	111	95.7 (79.4–115.2)	94.7 (78.5–114.1)	131	112.6 (94.9–133.6)	110.5 (93.0–131.3)
Women	98	179.0 (146.8–218.1)	177.9 (145.9–217.0)	115	211.3 (176.1–253.5)	209.9 (174.9–252.0)
Men	13	21.7 (12.8–36.9)	20.1 (11.6–34.9)	15	25.0 (15.2–41.0)	22.2 (13.1–37.5)

* Age-standardized rates were age-standardized to the 2000 projected Census population. Hispanic ethnicity was recorded separately from race; therefore, persons in this ethnicity category are also represented in the race categories. Ethnicity information was missing for 178 patients in the American College of Rheumatology (ACR) case definition group and 235 in the combined case definition (see Patients and Methods for details) group. 95% CI = 95% confidence interval.

† Average annual cases (sum of the prevalent cases for 2007–2009 divided by 3).

‡ Represents the entire population, including persons whose race/ethnicity was not known (134 in the ACR case definition group and 158 in the combined case definition group) or was American Indian/Alaska native (4 in the ACR case definition group and 6 in the combined case definition group).

women. The age-standardized prevalence among black men was over 5 times higher than among white men.

The age-specific prevalence in the ACR-defined cases was statistically significantly higher in black women compared with women of other racial groups for ages 30–59 years, with whites and Asians for ages 69–79 years, and with whites only for ages 20–29 years. Among black women, age-specific prevalence began to increase at age 20 years and peaked at 954.5 per 100,000 in the group ages 40–49 years (Figure 3). Among black men, age-specific prevalence peaked in the 50–69 year range. Age-specific prevalence was higher in black men as compared to the other racial/ethnic groups (Figure 3). Among men, 95% CIs overlapped within each age group with the following exception: among those ages 50–59 years, the prevalence in black men was statistically significantly higher than in white men.

The overall mean age at diagnosis was 34.8 years. Age at diagnosis stratified by bridged race and ethnicity was as follows: 35.5 years in blacks, 34.4 years in whites, 34.6 years in Asians, and 33.9 years in Hispanics. Once again, the 95% CIs for these estimates overlapped (data not shown).

Our capture–recapture modeling estimated 147 (95% CI 93–225) additional prevalent cases in the population. This yielded a capture–recapture inflated average annual crude prevalence of 113.7 per 100,000 persons.

Prevalence according to the combined case definition. By including an additional 113 individuals (89 based on the 3 ACR criteria plus rheumatologist diagnosis criterion and 24 based on the lupus-related kidney disease criterion), the combined definition yielded a total of 909 unique individuals over the 3-year period (Figure 1), or 869 average annual prevalent cases (Table 2). The overall crude and age-standardized prevalence proportions were 109.9 (95% CI 102.8–117.4) and 96.8 (95% 90.2–103.9) per 100,000 persons. Age-standardized prevalence proportions were 9 times higher among women than men: 179.4 versus 20.6 per 100,000 person-years. The age-standardized prevalence was highest among black women (498.4 [95% CI 422.3–588.2]), followed by Hispanic women (209.9 [174.9–252.0]), Asian/Pacific Islander women (171.0 [151.3–193.2]), and finally, white women (130.0 [115.5–146.4]). The age-standardized prevalence among black women was ~4 times higher than among white women.

Clinical manifestations. Among the incident 2007–2009 cases meeting the ACR definition, the most common manifestations were hematologic (84%),

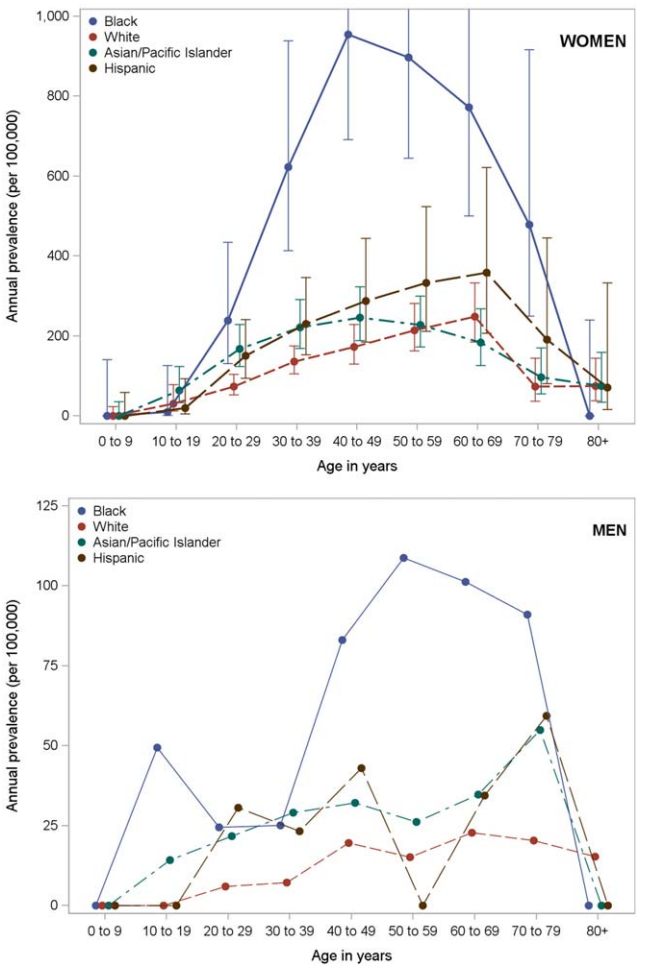

Figure 3. Average annual age-specific prevalence of systemic lupus erythematosus (SLE) among women and men living in San Francisco County, California, 2007–2009, categorized by race and Hispanic ethnicity. SLE was defined according to the American College of Rheumatology criteria. Among men, the 95% confidence intervals for prevalence overlapped within each age group, except for the group ages 50–59 years, where the prevalence in black men was statistically significantly higher than that in white men. The race categories are mutually exclusive. Hispanic ethnicity was recorded separately from race; therefore, persons of Hispanic ethnicity are also represented in the race categories (mostly white).

immunologic, (80%), arthritis (57%), renal disorder (45%), pleuritis or pericarditis (41%), and malar rash (33%) (Table 3). Neurologic disorder was the least common manifestation (8%). Renal disorder occurred more commonly in the black (52%), Asian/Pacific Islander (51%), and Hispanic (47%) patients than in the white patients (40%). Discoid rash was highest among black patients (22%) compared to the other groups and was least common in the Asian (5%) and Hispanic (0%) patients. Similar trends in the frequencies of clinical manifestations across the racial and ethnic groups were observed among the prevalent cases meeting the ACR definition (data not shown).

DISCUSSION

The California Lupus Surveillance Project had the opportunity to extend previous CDC-funded epidemiologic work to include 2 additional racial/ethnic groups and to confirm striking racial and ethnic disparities in the incidence and prevalence of SLE. San Francisco County is diverse, with substantial numbers of Asian and Hispanic patients. We found that, in addition to African Americans, Asian/Pacific Islanders and Hispanics (of any race) have been disproportionately affected by SLE as compared to whites (regardless of Hispanic ethnicity). Of the Hispanic cases included in the analyses, the majority were identified as white or had no race identified, e.g., race categories for the ACR definition of prevalent cases of Hispanic ethnicity were white (69%), no race identified (25%), Asian/Pacific Islander (5%), and black (1%).

Hispanics currently comprise 16% and Asians 5% of the US population. By 2050, these numbers are expected to rise to 30% and 8%, respectively (12). Thus, a reliable estimate of the burden of SLE in these growing populations is essential for health care planning. A major challenge to advancing knowledge in this area has been the paucity of large-scale, population-based surveillance studies with rigorously defined case definitions and case-finding procedures. Up until the recent completion of the Georgia and Michigan surveillance projects, most previous epidemiologic studies were limited by small geographic areas, homogenous populations, varying case definitions, and incomplete case ascertainment that relied on administrative codes or patient self-reported diagnosis. Such historical studies provided estimates ranging from 2.0 to 7.6 per 100,000 for the overall incidence and from 19 to 241 per 100,000 for the overall prevalence (13,14). The methods used in the CDC-funded registries, including the CLSP, have enabled us to determine more accurate and contemporary estimates of the incidence and prevalence of SLE in the US.

This study has several limitations. The first is the potential for incomplete case ascertainment. Although we used the HIPAA exemption for obtaining informed consent, each clinic and hospital had to voluntarily agree to participate in the CLSP. This issue led to the potential for incomplete case ascertainment. For example, 2 small community hospitals in San Francisco chose not to participate in the CLSP. Based on the proportion of discharges from these 2 hospitals to the total number

Table 3. ACR clinical manifestations among incident ACR-defined systemic lupus erythematosus cases, overall and by race/Hispanic ethnicity, San Francisco County, California, 2007–2009*

ACR criterion	Overall (n = 121)	Race			Hispanic ethnicity (n = 17)
		Black (n = 27)	White (n = 43)	Asian or Pacific Islander (n = 39)	
Malar rash	33.1 (24.6–41.6)	18.5 (3.7–33.4)	32.6 (18.4–46.8)	41.0 (25.4–56.7)	41.2 (17.4–64.9)
Discoid rash	12.4 (6.4–18.4)	22.2 (6.3–38.1)	16.3 (5.1–27.5)	5.1 (0.0–12.2)	0.0 (0.0–0.0)
Photosensitivity	29.8 (21.5–38.0)	25.9 (9.2–42.7)	32.6 (18.4–46.8)	25.6 (11.7–39.5)	35.3 (12.3–58.3)
Oral ulcers	19.0 (11.9–26.1)	11.1 (0.0–23.1)	16.3 (5.1–27.5)	25.6 (11.7–39.5)	23.5 (3.1–44.0)
Nonerosive arthritis	57.0 (48.1–66.0)	66.7 (48.6–84.7)	65.1 (50.7–79.6)	38.5 (23.0–53.9)	64.7 (41.7–87.7)
Pleuritis or pericarditis	40.5 (31.6–49.4)	48.1 (29.0–67.3)	39.5 (24.7–54.4)	41.0 (25.4–56.7)	58.8 (35.1–82.6)
Renal disorder	44.6 (35.6–53.6)	51.9 (32.7–71.0)	39.5 (24.7–54.4)	51.3 (35.4–67.2)	47.1 (23.0–71.1)
Neurologic disorder	8.3 (3.3–13.2)	11.1 (0.0–23.1)	9.3 (0.5–18.1)	5.1 (0.0–12.2)	11.8 (0.0–27.3)
Hematologic disorder	83.5 (76.8–90.2)	85.2 (71.6–98.8)	76.7 (63.9–89.6)	89.7 (80.1–99.4)	88.2 (72.7–100.0)
Immunologic disorder	80.2 (73.0–87.4)	88.9 (76.9–100.0)	72.1 (58.5–85.7)	84.6 (73.1–96.1)	70.6 (48.6–92.6)
Antinuclear antibody	98.3 (96.0–100.0)	96.3 (89.1–100.0)	97.7 (93.1–100.0)	100.0 (100.0–100.0)	94.1 (82.8–100.0)

* Values are the percentage (95% confidence interval). Hispanic ethnicity was recorded separately from race; therefore, persons in this ethnicity category are also represented in the race categories. Ethnicity information was missing for 18 patients in the American College of Rheumatology (ACR) case definition group and 21 in the combined case definition (see Patients and Methods for details) group. 95% CI = 95% confidence interval.

of discharges for San Francisco residents in 2007–2009 (16%) and the number of cases identified solely by community-based hospitals (9), we estimate that the lack of participation of these 2 hospitals resulted in potentially only 2 missed prevalent cases according to the ACR definition. Incomplete case ascertainment might also have occurred because we did not conduct field work in primary care clinics. Thus, it is possible that there were diagnosed cases of SLE in the community that never reached the attention of a specialist or had not been seen by a specialist for many years. Although capture–recapture analysis estimated an additional 33 incident cases and 147 prevalent cases, these estimates are imprecise, as indicated by the wide 95% CIs.

A second limitation is that data were collected from a review of the medical records rather than from direct patient interview and evaluation. The quality of medical record documentation of SLE manifestations varied widely. For longstanding, prevalent cases, it was sometimes difficult to retrieve the initial medical records that may have documented early manifestations of disease. Third, race and ethnicity were determined from the medical record and were not always well documented. This led to missing data for race and ethnicity as well as the potential for misclassification. Last, our denominator data were extracted from the US Census files, which provide population totals at the Federal Information Processing Standards level separately for race and ethnicity. Therefore, it was not possible for us to estimate the prevalence and incidence for mutually exclusive combined categories of these variables (e.g., non-Hispanic white).

One of the major strengths of the CLSP was the ability to conduct widespread case ascertainment by using a variety of sources, including university and community clinics, hospitals, regional laboratories, and state administrative databases. The abstractors comprehensively reviewed the patients' medical records, thereby minimizing underreporting bias in case ascertainment. The CDC funded this project with the specific intention of developing credible and complete estimates of the incidence and prevalence of lupus in Asians and Hispanics. Asians and Hispanics are generally smaller populations that we thought might access health care through alternative routes. To identify these patients, case-finding efforts were refined by working with physicians who were focused on those populations. For example, we partnered with a physician who cares for many of the Chinese patients in San Francisco at the Chinese Hospital. To access the Hispanic population in San Francisco, we performed extensive case-finding at San Francisco General Hospital and the associated community health network clinics. Our approach of partnering with the community and engaging culturally and linguistically concordant community members led to successful case ascertainment of these traditionally understudied populations. Had we not taken these extra steps, we would have missed SLE cases in the Asian and Hispanic populations.

SLE is a complex and heterogeneous disease for which there is no gold standard diagnostic test (15). One of the challenges of large epidemiologic studies is the need to designate a diagnosis of SLE based on documentation in the medical record without the benefit of

evaluating the patient in the clinical setting. For the purposes of the CLSP, we used case definitions identical to those utilized by other CDC-funded surveillance registries. In this way, consistent methodology across the registries was achieved. The primary case-finding definition used for the study was meeting ≥4 of the 11 revised classification criteria for SLE as defined by the ACR. Because case ascertainment relied on patients' medical records and sometimes not all medical records for a given patient were available, there was a potential for underdiagnosis of SLE if we had relied only on the ACR criteria definition. Therefore, we also used the combined case definition that was used by the Georgia Lupus Registry.

The CLSP found high age-standardized mean annual incidence rates and prevalence proportions of 4.6 and 84.8 per 100,000, respectively, for the ACR definition and 5.2 and 96.8 per 100,000, respectively, for the combined definition. The data confirmed and quantified a higher burden of SLE in women and in racial and ethnic minorities. Using the ACR definition, the age-standardized female-to-male incidence ratio was 12:1, with an 8:1 prevalence ratio. The highest age-standardized mean annual incidence rates and prevalence proportions per 100,000 were found in black women (30.5 and 458.1, respectively), followed by Hispanic women (8.9 and 177.9, respectively), Asian women (7.2 and 149.7, respectively), and white women (5.3 and 109.8, respectively). Age-specific incidence rates and prevalence proportions were highest in black women, with peak incidence and prevalence in the group ages 40–59 years. The findings confirm previous studies that showed an increased burden of SLE among black women. For example, a population-based study in Allegheny County, PA, determined a 3-fold higher incidence rate among black women compared to white women during the years 1985–1990 (16). The Georgia and Michigan registries also showed higher incidence and prevalence estimates among black women (2,3).

Interestingly, while the age-standardized incidence rate per 100,000 according to the ACR definition in CLSP was slightly lower (4.6) than those in the Georgia (5.6) and Michigan (5.5) registries, the CLSP age-standardized prevalence per 100,000 (84.8) was statistically significantly higher than that in either the Georgia (73.0) or Michigan (72.8) registries. While the reasons for the higher prevalence but lower incidence of SLE in CLSP are not clear, factors such as better access to health care and awareness of the disease in San Francisco compared to the locations of the other registries may be playing a role. Also, among black women, the age-standardized annual incidence rate and average annual prevalence per 100,000 (30.5 and 458.1) were >2 times higher in California compared to Georgia (13.4 and 196.2, respectively) and Michigan (12.8 and 186.3, respectively). Among white women, the age-standardized mean annual incidence rates were more similar among the 3 registries, although prevalence was still statistically significantly higher in the CLSP.

The reasons for the higher incidence and prevalence for black women in the CLSP compared with the other registries are not known, but may relate to several factors. With regard to the observed increased incidence, it is possible that the genetic ancestry of the black population in San Francisco is different from that in Georgia and Michigan, portending greater risk of disease. In addition, there may be environmental influences that increase the risk of SLE. Future studies will be required to address these important questions and further examine these possibilities.

There is a paucity of population-based studies estimating the incidence and prevalence of SLE among Hispanics and Asians in the US. Increased SLE disease activity and organ damage among US Hispanics versus non-Hispanic Caucasians have been previously noted by studies conducted within the LUpus in MInorities, NAture versus nurture (LUMINA) longitudinal cohort. LUMINA studies have also showed differing disease outcomes among various Hispanic subgroups, with worse outcomes occurring among Hispanics in Texas compared to Hispanics in Puerto Rico (17–19). Because of reliance on medical record documentation of ethnicity in CLSP, we were unable to differentiate various Hispanic subgroups in the incidence and prevalence estimates. Fewer studies have examined differences in SLE frequency and severity in Asian patients. One recent study from the Monash Lupus Clinic in Melbourne, Australia, showed increased disease severity and serologic activity among Asian patients compared with white patients (20). Thus, the CLSP contributes to an improved understanding of the burden of SLE among Asians and highlights the need for further work on disease phenotypes, outcomes, and drug responses which are likely to differ among patients from different racial and ethnic backgrounds.

In conclusion, the CLSP confirmed the increased burden of SLE in black, Asian, and Hispanic women compared to white women. Future studies will be necessary to broaden our understanding of the underlying etiologies for this disparity, including attempts to unravel the contributions of genetic and biologic factors versus social and environmental factors in order to improve patient outcomes.

ACKNOWLEDGMENTS

The authors wish to acknowledge and thank the following people: David Wofsy, MD, for significant contributions to the Scientific Advisory Board, Lidia Espino for administrative supervision and overall project management, Steve Lund, NP, and Crystal Warren for help with abstractor training, the team of medical abstractors (Florence Pang, Daniel Ayer, Kyle Richards, Jessica Wolf, Elizabeth Hernandez, Marilyn Foley), Valerie Shipman at CDPH, and the team of lupus surveillance investigators (Drs. Sam Lim, Cristina Drenkard, Emily Somers, Joe McCune, Peter Izmirly, and Elizabeth Ferucci). The authors also wish to acknowledge and thank the Russell/Engleman Rheumatology Research Center at UCSF.

AUTHOR CONTRIBUTIONS

All authors were involved in drafting the article or revising it critically for important intellectual content, and all authors approved the final version to be published. Dr. Dall'Era had full access to all of the data in the study and takes responsibility for the integrity of the data and the accuracy of the data analysis.

Study conception and design. Dall'Era, Snipes, Gordon, Helmick.

Acquisition of data. Dall'Era, Snipes, Herrinton.

Analysis and interpretation of data. Dall'Era, Cisternas, Herrinton, Gordon, Helmick.

REFERENCES

1. Lim SS, Drenkard C. Epidemiology of systemic lupus erythematosus: capturing the butterfly. Curr Rheumatol Rep 2008;10:265–72.
2. Lim SS, Bayakly AR, Helmick CG, Gordon C, Easley KA, Drenkard C. The incidence and prevalence of systemic lupus erythematosus, 2002–2004: the Georgia Lupus Registry. Arthritis Rheumatol 2014;66:357–68.
3. Somers EC, Marder W, Cagnoli P, Lewis EE, DeGuire P, Gordon C, et al. Population-based incidence and prevalence of systemic lupus erythematosus: the Michigan Lupus Epidemiology and Surveillance program. Arthritis Rheumatol 2014;66:369–78.
4. Ferucci ED, Johnston JM, Gaddy JR, Sumner L, Posever JO, Choromanski TL, et al. Prevalence and incidence of systemic lupus erythematosus in a population-based registry of American Indian and Alaska native people, 2007–2009. Arthritis Rheumatol 2014;66:2494–502.
5. National Vital Statistics System. National Center for Health Statistics. Centers for Disease Control and Prevention. Bridged-race population estimates: data files and documentation. URL: http://www.cdc.gov/nchs/nvss/bridged_race/data_documentation.htm.
6. Tan EM, Cohen AS, Fries JF, Masi AT, McShane DJ, Rothfield NF, et al. The 1982 revised criteria for the classification of systemic lupus erythematosus. Arthritis Rheum 1982;25:1271–7.
7. Hochberg MC, for the Diagnostic and Therapeutic Criteria Committee of the American College of Rheumatology. Updating the American College of Rheumatology revised criteria for the classification of systemic lupus erythematosus [letter]. Arthritis Rheum 1997;40:1725.
8. Newcombe RG, Altman DG. Proportions and their differences. In: Altman D, editor. Statistics with confidence: confidence intervals and statistical guidelines. 2nd ed. London: BMJ Books; 2000. p. 45–56.
9. Klein RJ, Schoenborn CA. Age adjustment using the 2000 projected U.S. population. Healthy People 2010 Stat Notes 2001;20:1–10.
10. Ingram DD, Parker JD, Schenker N, Weed JA, Hamilton B, Arias E, et al. United States Census 2000 population with bridged race categories. Vital Health Stat 2 2003:1–55.
11. Zelterman D. Advanced log-linear models using SAS. Cary (NC): SAS Institute; 2002.
12. US Census Bureau. Projected population by single year of age, sex, race, and Hispanic origin for the United States: July 1, 2000 to July 1, 2050. URL: https://www.census.gov/programs-surveys/popproj.html.
13. Lim SS, Drenkard C, McCune WJ, Helmick CG, Gordon C, DeGuire P, et al. Population-based lupus registries: advancing our epidemiologic understanding. Arthritis Rheum 2009;61:1462–6.
14. Cooper GS, Bynum ML, Somers EC. Recent insights in the epidemiology of autoimmune diseases: improved prevalence estimates and understanding of clustering of diseases. J Autoimmun 2009;33:197–207.
15. Tsokos GC. Systemic lupus erythematosus. N Engl J Med 2011;365:2110–21.
16. McCarty DJ, Manzi S, Medsger TA Jr, Ramsey-Goldman R, LaPorte RE, Kwoh CK. Incidence of systemic lupus erythematosus: race and gender differences. Arthritis Rheum 1995;38:1260–70.
17. Alarcón GS, Friedman AW, Straaton KV, Moulds JM, Lisse J, Bastian HM, et al. Systemic lupus erythematosus in three ethnic groups. Part III. A comparison of characteristics early in the natural history of the LUMINA cohort. Lupus 1999;8:197–209.
18. Fernández M, Alarcón GS, Calvo-Alén J, Andrade R, McGwin G Jr, Vilá LM, et al, for the LUMINA Study Group. A multiethnic, multicenter cohort of patients with systemic lupus erythematosus (SLE) as a model for the study of ethnic disparities in SLE. Arthritis Rheum 2007;57:576–84.
19. Pons-Estel GJ, Alarcón GS. Lupus in Hispanics: a matter of serious concern. Cleve Clin J Med 2012;79:824–34.
20. Golder V, Connelly K, Staples M, Morand E, Hoi A. Association of Asian ethnicity with disease activity in SLE: an observational study from the Monash Lupus Clinic. Lupus 2013;22:1425–30.

ARTHRITIS & RHEUMATOLOGY
Vol. 69, No. 10, October 2017, pp 2006–2017
DOI 10.1002/art.40192

The Incidence and Prevalence of Systemic Lupus Erythematosus in New York County (Manhattan), New York

The Manhattan Lupus Surveillance Program

Peter M. Izmirly,[1] Isabella Wan,[1] Sara Sahl,[1] Jill P. Buyon,[1] H. Michael Belmont,[1] Jane E. Salmon,[2] Anca Askanase,[3] Joan M. Bathon,[3] Laura Geraldino-Pardilla,[3] Yousaf Ali,[4] Ellen M. Ginzler,[5] Chaim Putterman,[6] Caroline Gordon,[7] Charles G. Helmick,[8] and Hilary Parton[9]

Objective. **The Manhattan Lupus Surveillance Program (MLSP) is a population-based registry designed to determine the prevalence of systemic lupus erythematosus (SLE) in 2007 and the incidence from 2007 to 2009 among residents of New York County (Manhattan), New York, and to characterize cases by race/ethnicity, including Asians and Hispanics, for whom data are lacking.**

Methods. **We identified possible SLE cases from hospital records, rheumatologist records, and administrative databases. Cases were defined according to the American College of Rheumatology (ACR) classification criteria, the Systemic Lupus International Collaborating Clinics (SLICC) classification criteria, or the treating rheumatologist's diagnosis. Rates among Manhattan residents were age-standardized, and capture–recapture analyses were conducted to assess case underascertainment.**

Results. **By the ACR definition, the age-standardized prevalence and incidence rates of SLE were 62.2 and 4.6 per 100,000 person-years, respectively. Rates were ~9 times higher in women than in men for prevalence (107.4 versus 12.5) and incidence (7.9 versus 1.0). Compared with non-Hispanic white women (64.3), prevalence was higher among non-Hispanic black (210.9), Hispanic (138.3), and non-Hispanic Asian (91.2) women. Incidence rates were higher among non-Hispanic black women (15.7) compared with non-Hispanic Asian (6.6), Hispanic (6.5), and non-Hispanic white (6.5) women. Capture–recapture adjustment increased the prevalence and incidence rates (75.9 and 6.0, respectively). Alternate SLE definitions without capture–recapture adjustment revealed higher age-standardized prevalence and incidence rates (73.8 and 6.2, respectively, by the SLICC definition and 72.6 and 5.0 by the rheumatologist definition) than the ACR definition, with similar patterns by sex and race/ethnicity.**

Conclusion. **The MLSP confirms findings from other registries on disparities by sex and race/ethnicity, provides new estimates among Asians and Hispanics, and provides estimates using the SLICC criteria.**

Systemic lupus erythematosus (SLE) is a potentially fatal, heterogeneous, chronic, systemic autoimmune disease of unknown etiology (1). Given widely

The views expressed herein are those of the authors and do not necessarily represent the official position of the Centers for Disease Control and Prevention.

Supported by cooperative agreements between the CDC and the New York City Department of Health and Mental Hygiene (grant U58/DP002827).

[1]Peter M. Izmirly, MD, MSc, Isabella Wan, MD, MPH, Sara Sahl, MD, MPH, Jill P. Buyon, MD, H. Michael Belmont, MD: New York University School of Medicine, New York, New York; [2]Jane E. Salmon, MD: Hospital for Special Surgery, Weill Cornell Medical College, New York, New York; [3]Anca Askanase, MD, MPH, Joan M. Bathon, MD, Laura Geraldino-Pardilla, MD, MSc: Columbia University College of Physicians and Surgeons, New York, New York; [4]Yousaf Ali, MD: Icahn School of Medicine at Mount Sinai, New York, New York; [5]Ellen M. Ginzler, MD, MPH: State University of New York Downstate College of Medicine, Brooklyn; [6]Chaim Putterman, MD: Albert Einstein College of Medicine, Bronx, New York; [7]Caroline Gordon, MD: University of Birmingham, Birmingham, UK; [8]Charles G. Helmick, MD: CDC, Atlanta, Georgia; [9]Hilary Parton, MPH: New York City Department of Health and Mental Hygiene, Long Island City, New York.

Address correspondence to Peter M. Izmirly, MD, New York University School of Medicine, Hospital for Joint Diseases, 301 East 17th Street, Room 1611B, New York, NY 10003. E-mail: Peter.Izmirly@nyumc.org.

Submitted for publication December 20, 2016; accepted in revised form June 22, 2017.

varying estimates of the incidence and prevalence of SLE in the US (2) and the absence of available data for certain demographic groups, we sought to obtain a fundamental epidemiologic understanding of SLE across racial/ethnic groups. Under the auspices of the National Arthritis Action Plan (3), the Centers for Disease Control and Prevention (CDC) funded 4 state or city health departments as well as the Indian Health Service (IHS) to more robustly define the incidence and prevalence of SLE. Results from the 2 initial sites, the Georgia Lupus Registry (GLR) and the Michigan Lupus Epidemiology and Surveillance (MILES) program, and the IHS site have been recently published (4–6). However, their estimates for Asians and Hispanics were limited. The Manhattan Lupus Surveillance Program (MLSP) was designed, along with the California Lupus Surveillance Project (CLSP), to provide estimates of the incidence and prevalence of SLE overall and specifically among Hispanic and Asian populations.

We launched the MLSP in 2009 as a collaboration between the New York City Department of Health and Mental Hygiene (DOHMH) and New York University School of Medicine (NYUSoM). Following methods similar to those used at the other CDC-funded sites (2,5,6), we designed the MLSP as a retrospective descriptive project to identify all cases of diagnosed SLE among residents of New York County (Manhattan), New York, 2007–2009, to determine the prevalence and incidence of SLE in this population.

PATIENTS AND METHODS

The Manhattan Lupus Surveillance Program. The MLSP was designed to be similar to the GLR and MILES programs and, as described elsewhere (5,6), was conducted as a public health surveillance project by the New York City DOHMH, with NYUSoM acting as a public health agent on behalf of the DOHMH. No patients were contacted for this project. Medical records were collected under the health surveillance exemption to the Health Insurance Portability and Accountability Act (HIPAA) privacy rules (45 CFR § 164.512[b]) and as authorized by New York City Charter Sections 556(c)(2) and (d)(2). The CDC deemed the MLSP to be public health practice that did not require review by the CDC Institutional Review Board (IRB). IRBs at both the New York City DOHMH and NYUSoM reviewed and deemed the MLSP to be a surveillance activity. Additional IRB applications were completed and submitted to independent case-finding sources as requested.

Study population and study period. The MLSP surveillance period was January 1, 2007 through December 31, 2009. New York County (Manhattan) was selected as the program catchment area because of its racial/ethnic diversity and because it is an island on which inhabitants largely remain for their health care, thus making access to medical records easier. We used data from lupus specialty clinics across New York City during initial planning for the MLSP and found that few Manhattan residents seek care in outer boroughs and that residents from other boroughs were more likely to seek care across a wide geographic range. Based on US Census data, there were 1,585,873 persons residing in Manhattan in 2010 (48% non-Hispanic white, 13% non-Hispanic black, 25% Hispanic, 11% non-Hispanic Asian) (7).

Case definitions. Our primary American College of Rheumatology (ACR) case definition required ≥4 of the 11 criteria for the classification of SLE (8,9). Under the ACR classification criteria, patients with evidence of lupus nephritis (by biopsy report or specific documentation by a rheumatologist and/or nephrologist) are considered to have met the renal criteria for SLE, even without information on the degree of proteinuria or a description of the sediment. We also used 2 secondary case definitions of SLE: 1) the Systemic Lupus Erythematosus Collaborating Clinics (SLICC) classification criteria, which require the presence of at least 4 of 17 criteria, at least 1 of which must be clinical and 1 immunologic, *or* requires the presence of biopsy-proven lupus nephritis as well as antinuclear antibodies or anti–double-stranded DNA antibodies (10); or 2) the treating rheumatologist's diagnosis of SLE. The SLICC case definition was included as a recently derived set of classification criteria with greater sensitivity and less specificity than the ACR classification criteria (10). The rheumatologist case definition was included because there is no gold standard for diagnosing SLE, and diagnosis is usually made by a physician who is familiar with the disease, often a rheumatologist.

Initial case-finding. We used information from administrative databases, hospitals, and private rheumatologists to identify possible cases from as far back as 2004, when records were available. Administrative databases included the State of New York Department of Health Statewide Planning and Research Cooperative System, with information on hospitalization discharges in New York State, and the New York City DOHMH Vital Records, with information on all deaths in New York City. We included only hospitals and private rheumatologists based in Manhattan. We queried these sources to identify records with International Classification of Diseases, Ninth Revision, Clinical Modification diagnosis codes indicating SLE (710.0), discoid lupus (695.4), or a related condition that may evolve into SLE or might have related symptoms (sicca syndrome [710.2], other specified connective tissue disease [CTD] [710.8], unspecified CTD [710.9]). If residence information was available from the case-finding source, we further restricted these records to include only those with evidence of Manhattan residence. Final screening of records was completed by trained MLSP abstractors to confirm physician diagnosis or suspicion of SLE or a related CTD and Manhattan residence during the surveillance period.

Data collection. After initial case-finding, abstractors collected and entered information from the medical records into a New York City DOHMH database, with database and data dictionary materials adapted from those used by the GLR. When necessary, we corroborated Manhattan residence using the LexisNexis online database service (11). Our abstractors entered any ambiguous information into open text notes, which were later reviewed with the NYUSoM principal investigator (PMI) to correctly code it in the database.

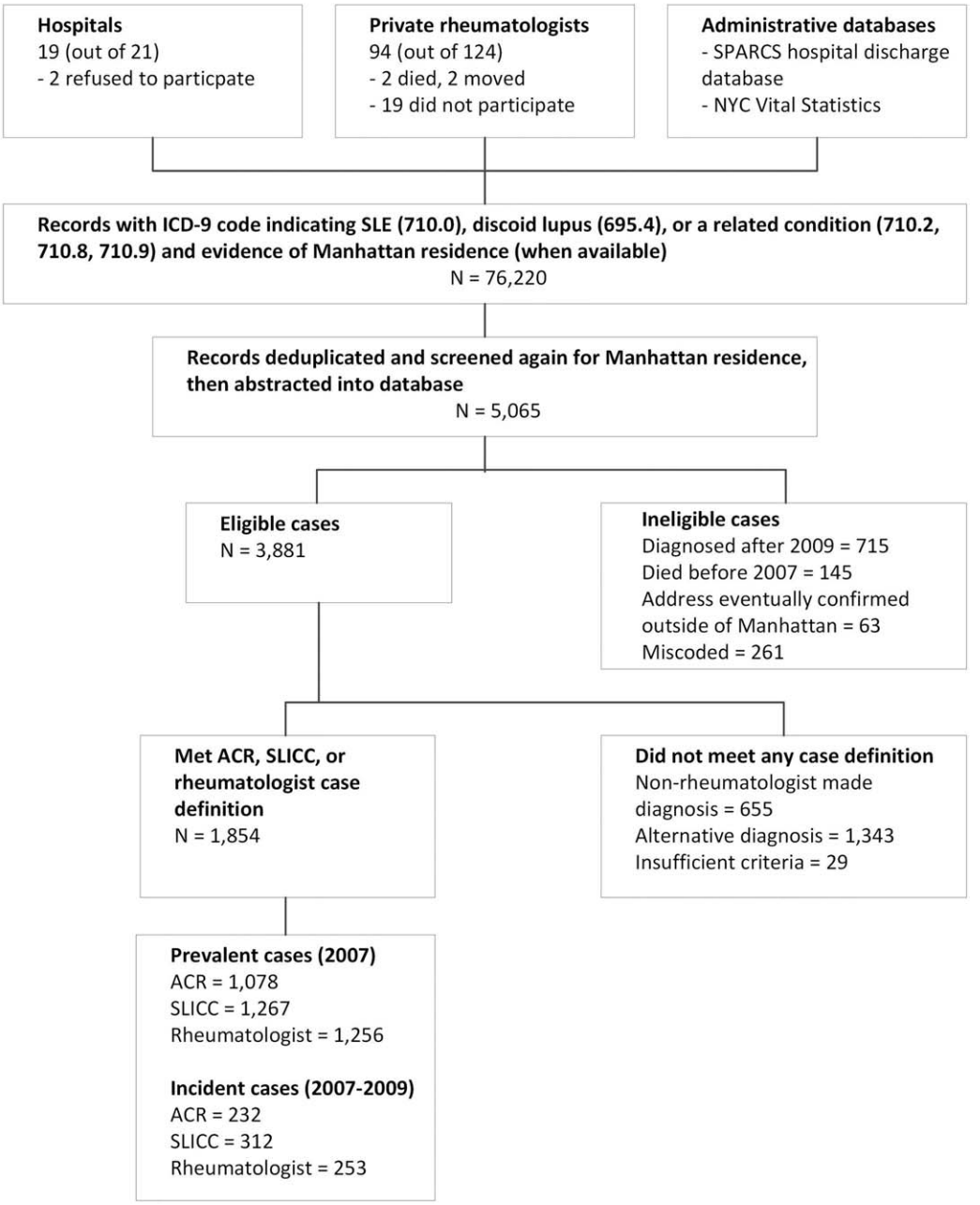

Figure 1. Flow chart showing the Manhattan Lupus Surveillance Program case-finding procedure for systemic lupus erythematosus (SLE). Cases of SLE were defined according to the American College of Rheumatology (ACR) criteria (met ≥4 of the 11 classification criteria), the Systemic Lupus International Collaborating Clinics (SLICC) criteria (met at least 4 of 17 criteria, at least 1 of which must be clinical and 1 immunologic, *or* the presence of biopsy-proven lupus nephritis as well as antinuclear antibodies or anti–double-stranded DNA antibodies), or the treating rheumatologist's diagnosis. SPARCS = Statewide Planning and Research Cooperative System (of the New York State Department of Health); NYC = New York City; ICD-9 = International Classification of Diseases, Ninth Revision Clinical Modification.

All MLSP abstractors were trained under the GLR model (5) before abstraction began and underwent routine quality assurance reviews throughout the project. These reviews provided the opportunity for abstractors and the NYUSoM principal investigator to discuss any issues arising in the field and to address questions from the abstractors. Each abstractor had a medical degree and consistently achieved the required minimum interobserver agreement of 90% on all elements and 95% on the ACR classification criteria, using as the gold standard abstraction by the NYUSoM principal investigator. The average performance of the abstractors during training and reviews was 95.6% on all elements, 97.2% on

the ACR classification criteria elements, and 97.5% on the unique elements in the SLICC classification criteria that were not already captured as part of the ACR classification criteria.

Statistical analysis. We defined prevalent cases as new or existing cases meeting the ACR, SLICC, or rheumatologist case definition and residing in Manhattan at some time from January 1, 2007 through December 31, 2007. We defined incident cases as those meeting at least 1 of the case definitions, having their first diagnosis from January 1, 2007 through December 31, 2009, and residing in Manhattan. Population denominators were taken from the New York City DOHMH–interpolated intercensal population estimates for Manhattan (12). We calculated rates overall, by sex, and by race/ethnicity per 100,000 person-years and age-standardized to the 2000 standard population of the US using 10-year age categories for each racial/ethnic group (13). Information on race was collected separately from Hispanic ethnicity during abstraction. For analysis, we assigned cases to 1 of 5 mutually exclusive race/ethnicity categories: non-Hispanic white, non-Hispanic black, Hispanic, non-Hispanic Asian, and non-Hispanic other. Non-Hispanic cases identified as >1 race were categorized as non-Hispanic other.

We conducted capture–recapture analyses (14,15) to estimate case underascertainment from our primary ACR case definition. We fit log-linear models separately for incident and prevalent cases by sex and race/ethnicity to estimate the number of cases missed in our catchment area. Specifically, we fit various models that addressed potential violation of the homogeneity assumption of capture probability and identified the best fitting model using the Akaike information criterion. We then used estimates from these models to calculate revised prevalence and incidence rates.

Chi-square tests, or Fisher's exact tests when needed, were used to assess univariate differences in SLE and ACR manifestations by race/ethnicity and sex. We compared differences between estimates by case definition using 95% confidence intervals (95% CIs) of the age-standardized rates, with non-overlapping 95% CIs considered to be significantly different. All analyses were completed using SAS version 9.3 (SAS Institute) and R version 3.3.0 (R Foundation for Statistical Computing) software.

RESULTS

Case-finding results. Case-finding and abstraction were completed in 19 of 21 hospitals (90.5%) (Figure 1), with 2 hospitals declining to participate (a cancer specialty hospital and a Veterans Affairs hospital). Case-finding and abstraction were performed from records of 94 of 124 private rheumatologists identified in the catchment area (75.8%). Of the 30 rheumatologists who did not participate, 19 did not respond to repeated requests or declined to participate, 2 died, 2 had retired and relocated, and 7 agreed to participate but abstraction could not be arranged despite repeated attempts before the data abstraction period ended.

Initial lists provided from the various case-finding sources identified 76,220 records (Figure 1). We removed duplicate records and records that did not have a Manhattan address, resulting in 5,065 possible cases with records for abstraction. During abstraction and data cleaning, we deemed 1,184 cases ineligible due to miscoded diagnosis or non-Manhattan residence. Of the remaining 3,881 possible cases, 1,854 met at least 1 of the case definitions.

Primary ACR case definition of prevalence. In 2007, a total of 1,078 cases (307 non-Hispanic white, 282 non-Hispanic black, 344 Hispanic, 111 non-Hispanic Asian, and 34 non-Hispanic other race/ethnicity) fulfilled the ACR case definition for SLE (Table 1). The overall crude and age-standardized prevalence rates were 68.2 (95% CI 64.1–72.2) and 62.2 (95% CI 58.4–66.0) per 100,000 person-years. Age-standardized rates were ~9 times higher for women compared with men (107.4 versus 12.5).

Age-standardized rates also differed by race/ethnicity among both women and men. The highest age-standardized prevalence rate was seen among non-Hispanic black women (210.9 per 100,000 person-years) followed by Hispanic women (138.3), non-Hispanic Asian women (91.2), and non-Hispanic white women (64.3). The age-standardized prevalence among men followed a similar pattern, with the highest estimate among non-Hispanic blacks (26.7) followed by Hispanics (19.4), non-Hispanic Asians (14.2), and non-Hispanic whites (3.7).

Capture–recapture estimates showed an additional 122 cases of SLE, indicating that 10.2% of cases may have been missed. Almost two-thirds (62.5%) of the estimated cases missed were non-Hispanic white women. With capture–recapture adjustment, the prevalence rate increased to 75.9 per 100,000 person-years (95% CI 70.6–81.2).

The mean ± SD age of women and men with SLE living in Manhattan in 2007 was 43.3 ± 15.5 years and 40.7 ± 16.9 years, respectively. The average age by race/ethnicity was 47.0 ± 16.5 years among non-Hispanic whites, 41.5 ± 13.7 years among non-Hispanic blacks, 42.9 ± 15.6 years among Hispanics, and 37.3 ± 15.4 years among non-Hispanic Asians. Figure 2A shows the age-specific prevalence for women by race/ethnicity. Prevalence was higher among non-Hispanic black and Hispanic women ages 20–59 years as compared to non-Hispanic white women of the same age group. Prevalence among non-Hispanic Asian women was not significantly different from that among non-Hispanic white women for any age group. Numbers among men were too small to assess age-specific rates by race/ethnicity.

Table 1. Crude and age-standardized prevalence of SLE among residents of New York County (Manhattan), New York, 2007, according to the ACR, SLICC, and rheumatologist case definitions overall and by race/ethnicity and sex*

	ACR					SLICC			Rheumatologist		
				Capture–recapture							
	No. of patients	Crude rate (95% CI)	Age-standardized rate (95% CI)	No. missed	Adjusted rate (95% CI)	No. of patients	Crude rate (95% CI)	Age-standardized rate (95% CI)	No. of patients	Crude rate (95% CI)	Age-standardized rate (95% CI)
Overall	1,078	68.2 (64.1–72.2)	62.2 (58.4–66.0)	122.4	75.9 (70.6–81.2)	1,267	80.1 (75.7–84.5)	73.8 (69.6–77.9)	1,256	79.4 (75.0–83.8)	72.6 (68.5–76.7)
Men	101	13.6 (10.9–16.2)	12.5 (10.0–15.0)	8.3	14.7 (12.5–16.9)	110	14.8 (12.0–17.6)	13.8 (11.1–16.4)	98	13.2 (10.7–16.1)	12.0 (9.7–14.7)
Women	977	116.7 (109.3–124.0)	107.4 (100.5–114.4)	114.1	130.3 (122.1–138.4)	1,157	138.2 (130.2–146.1)	128.3 (120.7–135.9)	1,158	138.3 (130.3–146.2)	127.5 (119.9–135.1)
Non-Hispanic white	307	40.5 (36.0–45.0)	34.7 (30.7–38.8)	82.4	51.4 (45.0–57.7)	373	49.2 (44.2–54.2)	42.7 (38.1–47.3)	352	46.4 (41.6–51.3)	39.7 (35.3–44.0)
Men	17	4.7 (2.7–7.5)	3.7 (2.2–6.0)	5.9	6.3 (3.2–9.4)	23	6.3 (4.0–9.5)	5.3 (3.3–8.0)	24	6.6 (4.2–9.8)	5.3 (3.4–7.8)
Women	290	73.4 (64.9–81.8)	64.3 (56.4–72.2)	76.5	92.7 (83.4–102.1)	350	88.6 (79.3–97.8)	78.2 (69.4–86.9)	328	83.0 (74.0–92.0)	72.0 (63.7–80.4)
Non-Hispanic black	282	131.4 (116.1–146.8)	124.9 (110.3–139.6)	3.6	133.1 (130.6–135.7)	326	151.9 (135.5–168.4)	144.7 (128.9–160.5)	312	145.4 (129.3–161.6)	137.7 (122.3–153.1)
Men	28	28.5 (18.9–41.2)	26.7 (17.7–38.7)	0	28.5 (28.1–28.9)	31	31.6 (21.4–44.8)	29.7 (20.2–42.3)	24	24.4 (15.7–36.4)	22.6 (14.5–33.7)
Women	254	218.4 (191.5–245.2)	210.9 (184.8–237.1)	3.6	221.4 (217.1–225.8)	295	253.6 (224.7–282.5)	244.4 (216.3–272.6)	288	247.6 (219.0–276.2)	237.2 (209.5–264.8)
Hispanic	344	84.2 (75.3–93.1)	82.8 (74.0–91.7)	1.4	84.6 (83.8–85.3)	372	91.1 (81.8–100.3)	90.2 (81.0–99.5)	396	97.0 (87.4–106.5)	96.2 (86.7–105.8)
Men	38	19.7 (13.9–27.0)	19.4 (13.6–26.9)	0.1	19.7 (19.4–20.0)	38	19.7 (13.9–27.0)	19.5 (13.7–26.9)	33	17.1 (11.8–24.0)	16.7 (11.4–23.6)
Women	306	142.1 (126.2–158.0)	138.3 (122.7–153.9)	1.3	142.7 (141.5–143.9)	334	155.1 (138.4–171.7)	151.7 (135.3–168.1)	363	168.5 (151.2–185.9)	165.3 (148.2–182.5)
Non-Hispanic Asian	111	64.0 (52.1–75.9)	56.2 (44.7–67.7)	20.0	75.5 (66.0–85.0)	145	83.6 (70.0–97.2)	75.1 (61.7–88.5)	118	68.0 (55.7–80.3)	62.2 (49.7–74.6)
Men	15	19.3 (10.8–31.9)	14.2 (7.6–24.0)	2.3	22.3 (17.0–27.6)	15	19.3 (10.8–31.9)	14.2 (7.6–24.0)	13	16.8 (8.9–28.7)	12.5 (6.2–22.6)
Women	96	100.0 (81.0–122.2)	91.2 (72.1–113.8)	17.7	118.5 (105.6–131.3)	130	135.5 (112.2–158.7)	125.9 (102.0–149.9)	105	109.4 (88.5–130.3)	103.6 (81.5–125.8)
Non-Hispanic other	34	–	–	15.0	–	51	–	–	78	–	–

* Systemic lupus erythematosus (SLE) cases were defined according to the American College of Rheumatology (ACR) criteria (met ≥4 of the 11 classification criteria), the Systemic Lupus International Collaborating Clinics (SLICC) criteria (met at least 4 of 17 criteria, at least 1 of which must be clinical and 1 immunologic, *or* the presence of biopsy-proven lupus nephritis as well as antinuclear antibodies or anti–double-stranded DNA antibodies), or the treating rheumatologist's diagnosis. Rates are per 100,000 person-years as a New York County (Manhattan) resident. Denominator data are based on 2007 intercensal population estimates from the New York City Department of Health and Mental Hygiene Bureau of Epidemiology Services (2000–2014 files). Data are standardized for age and race/ethnicity to the US standard population, 2000. Cases were assigned to 1 of 5 mutually exclusive race/ethnicity categories: non-Hispanic white, non-Hispanic black, Hispanic, non-Hispanic Asian, and non-Hispanic other. Non-Hispanic cases identified as being of >1 race were categorized as non-Hispanic other.

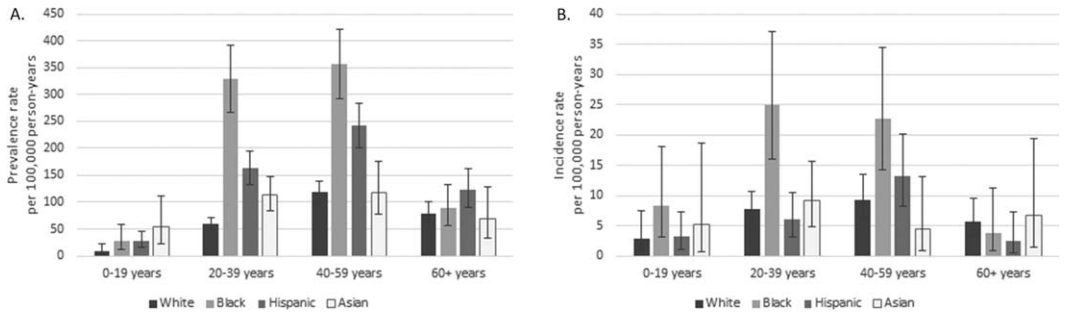

Figure 2. Age-specific prevalence and incidence rates (with 95% confidence intervals) of systemic lupus erythematosus among female residents of New York County (Manhattan) in 2007 and during 2007–2009, respectively, according to the American College of Rheumatology case definition (met ≥4 of the 11 classification criteria), categorized by age group. Cases were assigned to 1 of 5 mutually exclusive race/ethnicity categories: non-Hispanic white, non-Hispanic black, Hispanic, non-Hispanic Asian, and non-Hispanic other. Non-Hispanic cases identified as being of >1 race were categorized as non-Hispanic other and are not shown here.

Among the 344 Hispanic cases, 82.6% were also identified as white, 11.0% as black, and 6.4% as other race/ethnicity. Information on Hispanic ethnicity was often absent, with 239 (69.5%) having no further details, but Hispanic case ethnicities included Central or South American, Cuban, Dominican, Mexican, Puerto Rican, and Spanish. There were 111 non-Hispanic Asian cases as well as 5 identified as non-Hispanic other due to multiple race/ethnicity but with evidence of Asian race. More than one-fourth (26.7%) of these cases had no further classification for Asian ethnicity, but ethnicities among cases with information available included Chinese, Filipino, Hawaiian, Indian or Pakistani, Japanese, Korean, Pacific Islander not otherwise specified, South Asian, and Vietnamese.

Table 2 shows the occurrence of the 11 ACR criteria overall and by race/ethnicity among prevalent ACR cases. Renal disease was more common among non-Hispanic Asians (53.2%), non-Hispanic blacks (50.7%), and Hispanics (49.4%) compared with non-Hispanic whites (25.4%). Neurologic manifestations were more common among Hispanics (26.2%) and non-Hispanic blacks (24.5%) compared with non-Hispanic whites (16.6%). Also compared with non-Hispanic whites, discoid lesions were more commonly seen among non-Hispanic blacks (25.9% versus 8.8%) and malar rash was more commonly seen among Hispanics (50.0% versus 35.8%).

Primary ACR case definition of incidence rates. From 2007 to 2009, a total of 232 incident cases met the ACR case definition (Table 3) for SLE (92 non-Hispanic white, 62 non-Hispanic black, 49 Hispanic, 22 non-Hispanic Asian, and 7 non-Hispanic other race/ethnicity). The overall crude and age-standardized incidence rates were 4.9 (95% CI 4.3–5.5) and 4.6 (95% CI 4.0–5.2) per 100,000 person-years, respectively. Age-standardized rates differed by sex and were almost 8 times higher in women than in men (7.9 versus 1.0). Age-standardized rates also differed by race/ethnicity among both women and men. The highest age-standardized incidence rates among women were among non-Hispanic blacks (15.7) followed by non-Hispanic Asians (6.6), Hispanics (6.5), and non-Hispanic whites (6.5). Similarly, the highest age-standardized incidence rates among men were among non-Hispanic blacks (2.4) followed by Hispanics (1.3), non-Hispanic Asians (0.5), and non-Hispanic whites (0.5).

Capture–recapture adjustment estimated 284 incident cases of SLE, indicating that 18.4% of cases were missed; 67.0% of these were non-Hispanic white women. The resulting capture–recapture adjusted incidence rate increased to 6.0 per 100,000 person-years (95% CI 4.6–7.4).

The mean ± SD age at diagnosis was 40.1 ± 16.6 years among women and 42.9 ± 20.4 years among men, with values of 42.2 ± 17.7 years among non-Hispanic whites, 39.2 ± 16.3 years among non-Hispanic blacks, 39.6 ± 17.0 years among Hispanics, and 37.9 ± 16.0 years among non-Hispanic Asians. Figure 2B shows the age-specific incidence rates for women by race/ethnicity. The only age-specific difference was between non-Hispanic black and non-Hispanic white women who were 20–39 years old. Otherwise, due to small numbers within each stratum, no age-specific differences were found.

Among the 49 incident Hispanic cases, 77.6% were also identified as non-Hispanic white, 16.3% as non-Hispanic black, and 6.1% as non-Hispanic other race/ethnicity. As with the prevalent cases, Hispanic ethnicity information for incident cases was often absent, with 71.4% having no further ethnicity information available. Among the 22 incident non-Hispanic Asian cases, 32% had no further data available.

Table 2. Frequency of 11 ACR classification criteria for SLE among prevalent and incident cases defined according to the ACR case definition overall and by race/ethnicity*

ACR criterion	No. (%) of prevalent cases (2007)					No. (%) of incident cases (2007–2009)				
	Overall	Non-Hispanic white	Non-Hispanic black	Hispanic	Non-Hispanic Asian	Overall	Non-Hispanic white	Non-Hispanic black	Hispanic	Non-Hispanic Asian
Overall	1,078 (100)	307 (28.5)	282 (26.2)	344 (31.9)	111 (10.3)	232 (100)	92 (39.7)	62 (26.7)	49 (21.1)	22 (9.5)
Antinuclear antibody	996 (92.4)	284 (92.5)	262 (92.9)	316 (91.9)	103 (92.8)	213 (91.8)	82 (89.1)	58 (93.5)	47 (95.9)	22 (100)
Hematologic disorder	893 (82.8)	255 (83.1)	238 (84.4)	278 (80.8)	98 (88.3)	188 (81.0)	71 (77.2)	56 (90.3)†	37 (75.5)	19 (86.4)
Arthritis	813 (75.4)	246 (80.1)	204 (72.3)	255 (74.1)	80 (72.1)	159 (68.5)	66 (71.7)	41 (66.1)	30 (61.2)	17 (77.3)
Immunologic disorder	781 (72.4)	213 (69.4)	204 (72.3)	253 (73.5)	89 (80.2)†	170 (73.3)	66 (71.7)	46 (74.2)	37 (75.5)	18 (81.8)
Renal disorder	457 (42.4)	78 (25.4)	143 (50.7)†	170 (49.4)†	59 (53.2)†	81 (34.9)	22 (23.9)	27 (43.5)†	21 (42.9)†	10 (45.5)†
Serositis	449 (41.7)	117 (38.1)	127 (45.0)	156 (45.3)	36 (32.4)	84 (36.2)	25 (27.2)	33 (53.2)†	18 (36.7)	5 (22.7)
Malar rash	428 (39.7)	110 (35.8)	82 (29.1)	172 (50.0)†	46 (41.4)	86 (37.1)	31 (33.7)	20 (32.3)	22 (44.9)	8 (36.4)
Photo sensitivity	370 (34.3)	121 (39.4)	76 (27.0)†	132 (38.4)	30 (27.0)†	74 (31.9)	32 (34.8)	11 (17.7)†	21 (42.9)	7 (31.8)
Oral ulcers	333 (30.9)	104 (33.9)	64 (22.7)†	115 (33.4)	37 (33.3)	81 (34.9)	42 (45.7)	16 (25.8)†	12 (24.5)†	7 (31.8)
Neurologic disorder	230 (21.3)	51 (16.6)	69 (24.5)†	90 (26.2)†	11 (9.9)	43 (18.5)	15 (16.3)	15 (24.2)	11 (22.4)	1 (4.5)
Discoid rash	179 (16.6)	27 (8.8)	73 (25.9)†	58 (16.9)†	17 (15.3)	32 (13.8)	9 (9.8)	16 (25.8)†	5 (10.2)	1 (4.5)

* Systemic lupus erythematosus (SLE) cases were defined according to the American College of Rheumatology (ACR) criteria (met ≥4 of the 11 classification criteria). Cases were assigned to 1 of 5 mutually exclusive race/ethnicity categories: non-Hispanic white, non-Hispanic black, Hispanic, non-Hispanic Asian, and non-Hispanic other. Non-Hispanic cases identified as being of >1 race were categorized as non-Hispanic other.
† $P < 0.05$ versus non-Hispanic whites, by univariate logistic regression.

Table 3. Crude and age-standardized incidence rates of SLE among residents of New York County (Manhattan), New York, 2007–2009, according to the ACR, SLICC, and rheumatologist case definitions overall and by race/ethnicity and sex*

	ACR					SLICC			Rheumatologist		
				Capture–recapture							
	No. of patients	Crude rate (95% CI)	Age-standardized rate (95% CI)	No. missed	Adjusted rate (95% CI)	No. of patients	Crude rate (95% CI)	Age-standardized rate (95% CI)	No. of patients	Crude rate (95% CI)	Age-standardized rate (95% CI)
Overall	232	4.9 (4.3–5.5)	4.6 (4.0–5.2)	52.4	6.0 (4.6–7.4)	312	6.6 (5.8–7.3)	6.2 (5.5–6.9)	253	5.3 (4.7–6.0)	5.0 (4.4–5.7)
Men	23	1.0 (0.7–1.5)	1.0 (0.6–1.5)	3.3	1.2 (0.7–1.7)	38	1.7 (1.2–2.3)	1.7 (1.2–2.3)	28	1.3 (0.8–1.8)	1.2 (0.8–1.8)
Women	209	8.3 (7.2–9.4)	7.9 (6.8–9.0)	49.1	10.3 (8.0–12.5)	274	10.9 (9.6–12.2)	10.3 (9.1–11.6)	225	8.9 (7.8–10.1)	8.6 (7.4–9.7)
Non-Hispanic white	92	4.0 (3.2–4.9)	3.6 (2.8–4.5)	36.7	5.6 (4.2–7.1)	124	5.4 (4.5–6.4)	4.8 (3.9–5.8)	94	4.1 (3.3–5.0)	3.8 (3.0–4.8)
Men	7	0.6 (0.3–1.3)	0.5 (0.2–1.0)	1.6	0.8 (0.4–1.2)	13	1.2 (0.6–2.0)	1.0 (0.5–1.7)	9	0.8 (0.4–1.6)	0.7 (0.3–1.3)
Women	85	7.1 (5.7–8.8)	6.5 (5.0–8.3)	35.1	10.1 (7.7–12.5)	111	9.3 (7.6–11.1)	8.5 (6.7–10.3)	85	7.1 (5.7–8.8)	6.8 (5.2–8.6)
Non-Hispanic black	62	9.8 (7.5–12.6)	9.3 (7.1–12.0)	1.8	10.1 (9.1–11.0)	79	12.5 (9.9–15.5)	12.0 (9.5–15.0)	61	9.6 (7.4–12.4)	9.2 (7.0–11.8)
Men	7	2.4 (1.0–5.0)	2.4 (1.0–5.0)	1.0	2.8 (1.6–3.9)	11	3.8 (1.9–6.8)	3.8 (1.9–6.8)	7	2.4 (1.0–5.0)	2.3 (0.9–4.7)
Women	55	16.0 (12.1–20.9)	15.7 (11.8–20.5)	0.8	16.3 (15.5–17.0)	68	19.8 (15.4–25.1)	19.3 (14.9–24.5)	54	15.7 (11.8–20.5)	15.5 (11.6–20.3)
Hispanic	49	4.0 (3.0–5.3)	4.0 (3.0–5.4)	1.3	4.1 (3.8–4.5)	64	5.2 (4.0–6.7)	5.3 (4.1–6.7)	50	4.1 (3.0–5.4)	4.2 (3.1–5.5)
Men	7	1.2 (0.5–2.5)	1.3 (0.5–2.7)	0.4	1.3 (1.0–1.5)	8	1.4 (0.6–2.7)	1.6 (0.7–3.2)	6	1.0 (0.4–2.3)	1.1 (0.4–2.5)
Women	42	6.5 (4.7–8.8)	6.5 (4.7–8.8)	0.9	6.7 (6.2–7.1)	56	8.7 (6.6–11.3)	8.6 (6.5–11.2)	44	6.8 (5.0–9.2)	7.0 (5.1–9.4)
Non-Hispanic Asian	22	4.2 (2.6–6.3)	3.8 (2.3–6.0)	6.7	5.4 (3.3–7.5)	31	5.8 (4.0–8.3)	5.3 (3.4–7.7)	27	5.1 (3.4–7.4)	4.5 (2.9–6.9)
Men	1	0.4 (0.0–2.4)	0.5 (0.0–2.7)	0.3	0.6 (0.0–1.1)	2	0.8 (0.1–3.1)	1.0 (0.1–3.5)	2	0.8 (0.1–3.1)	1.0 (0.1–3.7)
Women	21	7.1 (4.4–10.9)	6.6 (3.8–10.5)	6.4	9.3 (6.0–12.7)	29	9.9 (6.6–14.2)	8.8 (5.6–13.1)	25	8.5 (5.5–12.6)	7.5 (4.5–11.6)
Non-Hispanic other	7			5.9		14			21		

* Systemic lupus erythematosus (SLE) cases were defined according to the American College of Rheumatology (ACR) criteria (met ≥4 of the 11 classification criteria), the Systemic Lupus International Collaborating Clinics (SLICC) criteria (met at least 4 of 17 criteria, at least 1 of which must be clinical and 1 immunologic, *or* the presence of biopsy-proven lupus nephritis as well as antinuclear antibodies or anti–double-stranded DNA antibodies), or the treating rheumatologist's diagnosis. Rates are per 100,000 person-years as a New York County (Manhattan) resident. Denominator data are based on 2007–2009 intercensal population estimates from the New York City Department of Health and Mental Hygiene Bureau of Epidemiology Services (2000–2014 files). Data are standardized for age and race/ethnicity to the US standard population, 2000. Cases were assigned to 1 of 5 mutually exclusive race/ethnicity categories: non-Hispanic white, non-Hispanic black, Hispanic, non-Hispanic Asian, and non-Hispanic other. Non-Hispanic cases identified as being of >1 race were categorized as non-Hispanic other.

Table 2 shows the occurrence of the 11 ACR criteria overall and by race/ethnicity among incident ACR cases. Evidence of renal disease was found among 34.9% of incident cases, but was more common among non-Hispanic Asians (45.5%), non-Hispanic blacks (43.5%), and Hispanics (42.9%) compared with non-Hispanic whites (23.9%). Discoid lesions were more common among non-Hispanic blacks (25.8%) compared with non-Hispanic whites (9.8%).

Secondary case definitions. Prevalence and incidence rates calculated using the SLICC case definition for SLE were significantly higher than those calculated using the primary ACR case definition. Using the SLICC case definition generated crude and age-standardized prevalence rates of 80.1 (95% CI 75.7–84.5) and 73.8 (95% CI 69.6–77.9) per 100,000 person-years, respectively, which were 17–19% higher than those calculated using the ACR case definition. The SLICC crude and age-standardized incidence rates (6.6 [95% CI 5.8–7.3] and 6.2 [95% CI 5.5–6.9], respectively) were nearly 35% higher than the ACR incidence rates.

The rheumatologist case definition yielded crude and age-standardized prevalence rates that were ~17% higher than the ACR case definition rates (79.4 [95% CI 75.0–83.8] and 72.6 [95% CI 68.5–76.7] per 100,000 person-years, respectively). Crude and age-standardized incidence rates using the rheumatologist case definition were similar to rates using the ACR case definition (5.3 [95% CI 4.7–6.0] and 5.0 [95% CI 4.4–5.7], respectively). For both secondary case definitions, differences in rates by sex and race/ethnicity were similar to those identified by the ACR case definition.

Of the 1,538 incident and prevalent cases meeting either the ACR or SLICC case definition, 75.6% met both ACR and SLICC definitions, 4.3% met only the ACR definition, and 20.2% met only the SLICC definition. Table 4 displays information on the unique SLICC criteria that are not part of the ACR classification criteria among incident and prevalent cases meeting the SLICC case definition only. The most common unique SLICC criteria among these cases were low complement levels, alopecia, and different definitions for lymphopenia. In addition, 5.5% of cases meeting the SLICC case definition had ANA or anti–double-stranded DNA antibody and biopsy findings consistent with lupus nephritis. Reasons that cases met the ACR and not the SLICC case definition were largely due to having ≥4 clinical criteria but no immunologic criteria, differences in categorization of photosensitivity and malar rash (which were separate in the ACR criteria and combined in the SLICC criteria), and differences in defining lymphopenia and anticardiolipin antibody (data not shown).

Table 4. Unique criteria among 310 incident and prevalent SLE cases meeting the SLICC, but not the ACR, case definitions*

Unique SLICC criteria	No. (%) of patients
Immunologic criteria	
Low complement levels	151 (48.7)
Anti–β_2-glycoprotein antibodies (IgG or IgM)	16 (5.2)
Positive direct Coombs' test result in the absence of hemolytic anemia	5 (1.6)
Clinical criteria	
Acute cutaneous lupus	
Bullous lupus	1 (0.3)
Toxic epidermal necrolysis variant of SLE	0 (0.0)
Maculopapular lupus rash	13 (4.2)
Subacute cutaneous lupus	4 (1.3)
Chronic cutaneous lupus	
Hypertrophic (verrucous) lupus	3 (1.0)
Lupus panniculitis (profundus)	4 (1.3)
Mucosal lupus	0 (0.0)
Lupus erythematosus tumidus	1 (0.3)
Chilblains lupus	1 (0.3)
Discoid lupus/lichen planus overlap	4 (1.3)
Nonscarring alopecia	122 (39.4)
Neurologic criteria	
Mononeuritis multiplex	3 (1.0)
Myelitis	2 (0.6)
Peripheral or cranial neuropathy	53 (17.1)
Acute confusional state	3 (1.0)
Lymphopenia	147 (47.4)
ANA or anti-dsDNA antibody and biopsy-proven lupus nephritis	17 (5.5)

* More than 1 criterion may have been manifested by a given systemic lupus erythematosus (SLE) case. Data on the IgA isotype of anti–β_2-glycoprotein I and anticardiolipin antibodies were not collected. For anti–double-stranded DNA (anti-dsDNA) determined by enzyme-linked immunosorbent assay, the results were reported as positive or negative; thus, it is possible that in some cases, this criterion was overcounted in the Systemic Lupus International Collaborating Clinics (SLICC) system if the positive result was not specifically double the upper cutoff for the negative value. Finally, CH50 was not captured, and thus, it is possible that the SLICC criterion for complement was undercounted. ACR = American College of Rheumatology; ANA- = antinuclear antibody.

DISCUSSION

Our analysis of the MLSP data provides prevalence and incidence rate estimates of SLE among Manhattan residents using methods similar to other CDC-funded SLE registries. Our analysis confirms evidence of a higher prevalence of SLE among non-Hispanic blacks compared with non-Hispanic whites and adds evidence of a higher prevalence of SLE among Hispanics and non-Hispanic Asians. The MLSP is the first among the CDC-funded SLE registries to report using the SLICC classification criteria, which were recently validated (10), to describe cases of SLE.

The age-standardized prevalence and incidence rates of SLE in Manhattan were 62.2 (95% CI 58.4–

66.0) and 4.6 (95% CI 4.0–5.2) per 100,000 person-years using the ACR case definition. Compared with previous reports by the CDC-funded sites, we estimated slightly lower overall age-standardized prevalence than did the GLR (73.0 [95% CI 68.9–77.4]) (5) and MILES (72.8 [95% CI 70.8–74.8]) studies (6), but we found similar disparities by sex and race/ethnicity for non-Hispanic whites and non-Hispanic blacks. The MLSP prevalence estimates increased with capture–recapture adjustment (75.9 [95% CI 70.6–81.2]) and were comparable to the capture–recapture–adjusted estimates from the GLR (83.0 [95% CI 78.6–87.7]). Our age-standardized incidence rates using the ACR case definition were similar to those from the GLR and MILES.

We found the highest prevalence and incidence rates among non-Hispanic blacks, consistent with the GLR and MILES studies and with preliminary data from the CLSP study. However, unlike the GLR and MILES studies, we found elevated prevalence among non-Hispanic Asians and Hispanics compared with non-Hispanic whites. Compared with preliminary crude estimates from the CLSP study (16), the MLSP showed similar elevated rates among Hispanics (84.2 [95% CI 75.3–93.1] versus 87.7 [95% CI 72.1–106.8] per 100,000 person-years) but slightly lower rates among non-Hispanic Asians (64.0 [95% CI 52.1–75.9] versus 95.8 [95% CI 84.9–108.1] per 100,000 person-years). These MLSP findings are particularly important, given the few published studies on the prevalence and incidence of SLE among Asians and Hispanics in the US. A review published in 1973 presented estimates among New York City residents from 1956 to 1965 but focused only on whites, blacks, and Puerto Ricans (17). Another study published in 2001 estimated the prevalence of SLE among Hispanics in Arizona to be 103.0 per 100,000 persons, slightly higher than the rate found by the MLSP among Hispanics in Manhattan (18). A more recent study using Medicaid data estimated an even higher prevalence of SLE among Hispanics (126.5 per 100,000 persons) with Medicaid coverage in the US from 2000 to 2004 (19).

The study using Medicaid data is one of the few to estimate rates of SLE among Asians in the US, reporting a prevalence ~3 times that estimated by the MLSP (175.1 versus 56.2 per 100,000 persons) (19). The only other studies known to assess rates of SLE among Asians in the US focused on SLE prevalence. One study identified cases in Hawaii based on physician diagnosis at 5 medical centers and outpatient practices in 1989. The overall SLE prevalence identified in that study (41.8 per 100,000 persons) was similar to the MLSP estimate for non-Hispanic Asians, and the age-standardized rates for women of specific Asian ethnic groups (Chinese, Filipino, Hawaiian, Japanese) was found to be higher compared with that among white women (20). Another study, using hospital discharge data, reported that Asian/Pacific Islander women had a lower rate of prevalent SLE compared with white women (21). Less is known about the incidence of SLE among Asians. In England, new diagnoses of SLE are more common among Asians, specifically South Asians from India and Pakistan, compared with whites (22,23), but to our knowledge, there are no other published reports on the incidence of SLE among Asians in the US.

In this analysis, we also provide information on manifestations among SLE cases. Clinical or serologic manifestations among prevalent cases approximated those from the GLR and MILES registries. The MLSP found a high burden of nephritis overall, with nearly half (42.4%) of prevalent cases developing nephritis. The proportion of those with nephritis was higher among non-white prevalent cases, specifically 50.7% among non-Hispanic blacks, 49.4% among Hispanics, and 53.2% among non-Hispanic Asians as compared with 25.4% among non-Hispanic whites, results that are consistent with those of other studies (5,6,19,24,25).

The SLICC case definition of SLE yielded higher incidence and prevalence estimates than the ACR case definition. Unique criteria which substantiated the classification of SLE based on SLICC, but not ACR, criteria included low complement levels, alopecia, and different definitions of lymphopenia (10). The small number of cases that met the ACR but not the SLICC case definition is reassuring, as it suggests that few cases met ACR criteria for SLE without the presence of autoantibodies. However, given the descriptive nature of the MLSP and the absence of a gold standard test that would unambiguously identify SLE, this project could not assess which set of classification criteria is more sensitive or specific. In addition, non-overlapping confidence intervals were used to conservatively assess differences among rates (26).

There were several limitations to this project. First, we may have underestimated cases, as 2 hospitals and one-fourth of rheumatologists in the catchment area declined to participate. Most of the practices that did not participate were in neighborhoods with a majority white population, which is consistent with our capture–recapture analysis that estimated 67.3% of prevalent cases and 70.0% of incident cases missed were non-Hispanic white. However, the exclusion of the Veterans Affairs hospital may have resulted in underidentification of men diagnosed as having SLE. We also did not include nephrology, dermatology, or primary or alternative care practices among our case-finding

sources. Though when possible we did query hospital pathology databases for relevant kidney or skin biopsies, we still may have missed milder cases that were not hospitalized or seen by a rheumatologist during the surveillance period. It is also possible that we missed cases if they lived in Manhattan but sought care in other boroughs or a neighboring state.

Second, medical systems differed tremendously, and any difficulty navigating different electronic medical records or any difficulty with the legibility of paper records could have led to missed or miscoded data. Additionally, medical records are designed for physician use, not for data abstraction and surveillance. Thus, some information of interest may have been missing or ambiguous, depending on what was collected and recorded by the case-finding source.

Third, abstracting occurred several years after the surveillance period, which could have led to missing information if records were put into storage or if data elements were lost during a facility's migration from paper to electronic records. This lag time may have also affected our ability to find cases of SLE, as some newer systems were unable to query past certain dates. Additionally, many private practices did not retain information on patients' prior addresses, so we may not have abstracted cases who moved outside of Manhattan since the surveillance period. However, when possible, the software LexisNexis was used to verify patient residence within the catchment area.

Finally, data on race and ethnicity was abstracted from administrative and medical records, which may not accurately represent the patient's own racial or ethnic identification. Additionally, information on ethnicity was often missing or did not include detail such as country of origin, which limited our ability to describe rates of SLE among specific ethnic groups. Though available information did reflect the major ethnic groups in Manhattan, ethnicity information was missing for most Hispanic cases and more than one-fourth of non-Hispanic Asian cases. Categorized broadly, Hispanic or Asian race encompasses a number of heterogeneous groups and SLE rates among them may differ. Given the already limited number of published studies on SLE among Asians and Hispanics, additional work is needed to better describe and understand the experience of SLE among specific ethnic subpopulations.

Despite these limitations, our analysis benefitted from the design and composition of the MLSP. First, the MLSP was designed as a population-based registry with methods similar to those used for 4 other CDC-funded SLE registries, which allowed us to compare rates across sites. Second, the diverse population within our catchment area allowed us to estimate rates of SLE among the major racial categories, particularly Asians and Hispanics. Third, given the recent publication of the SLICC classification criteria, we were able to estimate rates of SLE by this case definition and compare them to the ACR case definition. Fourth, the partnership with the New York City DOHMH allowed us to collect information from a number of case-finding sources and find complete clinical information on most cases. Finally, our abstractors all had a medical background, which helped during training and provided an advantage during extensive review of medical records to identify SLE criteria.

In conclusion, we found substantial disparities in prevalence, incidence, and manifestations of SLE by sex and race/ethnicity among Manhattan residents. Women consistently had higher prevalence and incidence rates of SLE compared with men, and non-Hispanic blacks, Hispanics, and non-Hispanic Asians had higher rates of diagnosed SLE and a higher proportion had lupus nephritis compared with non-Hispanic whites. The highest rates of SLE were seen among non-Hispanic black women, followed by Hispanic, non-Hispanic Asian, and non-Hispanic white women. Using the SLICC criteria for SLE provided higher prevalence and incidence rates than the ACR criteria.

ACKNOWLEDGMENTS

The authors thank all of the rheumatologists who participated in the MLSP as well as their practice managers who provided assistance. We would also like to thank all of the administrators in the medical records departments of the participating hospitals for their assistance in providing lists and obtaining medical records. We would like to acknowledge the contributions of past and current members at the New York City DOHMH, including Tamira Collins-Bowers, Manasi Joshi, Bonnie Kerker, Maushumi Mavinkurve, Angela Merges, Kyyon Nelson, Viren Shah, Joseph Slade, Lorna Thorpe, Talytha Utley, and Elizabeth Waddell. In addition, we would like to acknowledge the hard work of the MLSP abstractors, Drs. Janice McFarlane, Nick Stefanopoulos, Zahira Zahid, Rukayatu Ibrahim, Saleh Massasati, and Simone Shrestha. Finally, we would like to acknowledge the support and contributions of the principal investigators of the other CDC-funded surveillance sites, including Drs. Sam Lim, Cristina Drenkard (who each came to NYUSoM to assist in the development of the MLSP), Emily Somers, Joe McCune, Maria Dall'Era, and Elizabeth Ferucci.

AUTHOR CONTRIBUTIONS

All authors were involved in drafting the article or revising it critically for important intellectual content, and all authors approved the final version to be published. Dr. Izmirly had full access to all of the data in the study and takes responsibility for the integrity of the data and the accuracy of the data analysis.

Study conception and design. Izmirly, Askanase, Gordon, Helmick, Parton.
Acquisition of data. Izmirly, Wan, Sahl, Buyon, Belmont, Salmon, Askanase, Bathon, Geraldino-Pardilla, Ali, Ginzler, Putterman, Parton.
Analysis and interpretation of data. Izmirly, Wan, Buyon, Belmont, Gordon, Helmick, Parton.

REFERENCES

1. Rahman A, Isenberg DA. Systemic lupus erythematosus. N Engl J Med 2008;358:929–39.
2. Lim SS, Drenkard C, McCune WJ, Helmick CG, Gordon C, DeGuire P, et al. Population-based lupus registries: advancing our epidemiologic understanding. Arthritis Rheum 2009;61:1462–6.
3. Meenan RF, Callahan LF, Helmick CG. The National Arthritis Action Plan: a public health strategy for a looming epidemic. Arthritis Care Res 1999;12:79–81.
4. Ferucci ED, Johnston JM, Gaddy JR, Sumner L, Posever JO, Choromanski TL, et al. Prevalence and incidence of systemic lupus erythematosus in a population-based registry of American Indian and Alaska native people, 2007–2009. Arthritis Rheumatol 2014;66:2494–502.
5. Lim SS, Bayakly AR, Helmick CG, Gordon C, Easley KA, Drenkard C. The incidence and prevalence of systemic lupus erythematosus, 2002–2004: the Georgia Lupus Registry. Arthritis Rheumatol 2014;66:357–68.
6. Somers EC, Marder W, Cagnoli P, Lewis EE, DeGuire P, Gordon C, et al. Population-based incidence and prevalence of systemic lupus erythematosus: the Michigan Lupus Epidemiology and Surveillance program. Arthritis Rheumatol 2014;66:369–78.
7. US Census Bureau. 2010 census. Summary file 1, tables P5, P8, PCT4, PCT5, PCT8, and PCT11. URL: http://factfinder.census.gov.
8. Hochberg MC, for the Diagnostic and Therapeutic Criteria Committee of the American College of Rheumatology. Updating the American College of Rheumatology revised criteria for the classification of systemic lupus erythematosus [letter]. Arthritis Rheum 1997;40:1725.
9. Tan EM, Cohen AS, Fries JF, Masi AT, McShane DJ, Rothfield NF, et al. The 1982 revised criteria for the classification of systemic lupus erythematosus. Arthritis Rheum 1982;25:1271–7.
10. Petri M, Orbai AM, Alarcón GS, Gordon C, Merrill JT, Fortin PR, et al. Derivation and validation of the Systemic Lupus International Collaborating Clinics classification criteria for systemic lupus erythematosus. Arthritis Rheum 2012;64:2677–86.
11. LexisNexis. URL: https://www.lexisnexis.com/en-us/gateway.page.
12. New York City Department of Health and Mental Hygiene population estimates, modified from US Census Bureau intercensal population estimates, 2007–2009. Updated July 22, 2013.
13. Klein RJ, Schoenborn CA. Age adjustment using the 2000 projected U.S. population. January 2001. URL: https://www.cdc.gov/nchs/data/statnt/statnt20.pdf.
14. Hook EB, Regal RR. Capture-recapture methods in epidemiology: methods and limitations. Epidemiol Rev 1995;17:243–64.
15. Baillargeon S, Rivest LP. Rcapture: loglinear models for capture-recapture in R. J Stat Softw 2007;19:1–31.
16. Dall'Era MC, Snipes K, Cisternas M, Gordon C, Helmick CG. Preliminary population-based incidence and prevalence estimates of systemic lupus erythematosus: the California Lupus Surveillance Project [abstract]. Arthritis Rheumatol 2014;66 Suppl: S1217.
17. Siegel M, Lee SL. The epidemiology of systemic lupus erythematosus. Semin Arthritis Rheum 1973;3:1–54.
18. Balluz L, Philen R, Ortega L, Rosales C, Brock J, Barr D, et al. Investigation of systemic lupus erythematosus in Nogales, Arizona. Am J Epidemiol 2001;154:1029–36.
19. Feldman CH, Hiraki LT, Liu J, Fischer MA, Solomon DH, Alarcón GS, et al. Epidemiology and sociodemographics of systemic lupus erythematosus and lupus nephritis among US adults with Medicaid coverage, 2000–2004. Arthritis Rheum 2013;65:753–63.
20. Maskarinec G, Katz AR. Prevalence of systemic lupus erythematosus in Hawaii: is there a difference between ethnic groups? Hawaii Med J 1995;54:406–9.
21. Chakravarty EF, Bush TM, Manzi S, Clarke AE, Ward MM. Prevalence of adult systemic lupus erythematosus in California and Pennsylvania in 2000: estimates obtained using hospitalization data. Arthritis Rheum 2007;56:2092–4.
22. Johnson AE, Gordon C, Palmer RG, Bacon PA. The prevalence and incidence of systemic lupus erythematosus in Birmingham, England: relationship to ethnicity and country of birth. Arthritis Rheum 1995;38:551–8.
23. Rees F, Doherty M, Grainge M, Davenport G, Lanyon P, Zhang W. The incidence and prevalence of systemic lupus erythematosus in the UK, 1999–2012. Ann Rheum Dis 2016;75:136–41.
24. Alarcón GS, McGwin G Jr, Petri M, Reveille JD, Ramsey-Goldman R, Kimberly RP, and the PROFILE Study Group. Baseline characteristics of a multiethnic lupus cohort: PROFILE [published erratum appears in Lupus 2002;11:402]. Lupus 2002;11:95–101.
25. Hanly JG, O'Keeffe AG, Su L, Urowitz MB, Romero-Diaz J, Gordon C, et al. The frequency and outcome of lupus nephritis: results from an international inception cohort study. Rheumatology (Oxford) 2016;55:252–62.
26. Schenker N, Gentleman JF. On judging the significance of differences by examining overlap between confidence intervals. Am Stat 2001;55:182–6.

ARTHRITIS & RHEUMATOLOGY
Vol. 69, No. 10, October 2017, pp 2018–2028
DOI 10.1002/art.40181

Plasmablasts With a Mucosal Phenotype Contribute to Plasmacytosis in Systemic Lupus Erythematosus

Henrik E. Mei,[1] Stefanie Hahne,[1] Andreas Redlin,[1] Bimba F. Hoyer,[1] Kaiyin Wu,[2] Lisa Baganz,[3] Anna R. Lisney,[1] Tobias Alexander,[1] Birgit Rudolph,[2] and Thomas Dörner[1]

Objective. **To analyze the composition of known plasmacytosis in systemic lupus erythematosus (SLE) to obtain further insight into the nature of underlying mechanisms.**

Methods. **Plasmablasts from patients with active SLE, patients with inactive/treated SLE, and healthy controls were characterized by flow cytometry, enzyme-linked immunospot assay, and Transwell migration assays and compared to vaccination-induced plasmablasts. Serum cytokine levels were analyzed by Luminex assay, and histologic analysis of kidney biopsy specimens was performed.**

Results. **Circulating plasmablasts in SLE expressed markers of mucosal immune reactions. IgA, CCR10, and β7 integrin were expressed by 48%, 40%, and 38% of plasmablasts, respectively, with varying coexpression patterns. Consistent with mucosal homing, some SLE plasmablasts migrated toward the mucosal chemokine CCL28 and secreted polymeric IgA. SLE plasmablasts shared phenotypic characteristics with antigen-specific plasmablasts induced by oral, but not parenteral, vaccinations. Autoreactive antibody–secreting cells of the IgG and IgA isotypes were detectable, but only the emergence of phenotypically mucosal plasmablasts was positively associated with serum interleukin-2 and platelet-derived growth factor BB levels.**

Conclusion. **Our data suggest that distinct plasmablast differentiation pathways jointly contribute to peripheral plasmacytosis in SLE, i.e., a cytokine-amplified mucosal "steady-state" plasmablast response, and an autoreactive plasmablast response, representing conventional autoimmunity. Our results indicate an overly activated mucosal immune system in patients with SLE, with both immunologic and clinical implications.**

Systemic lupus erythematosus (SLE) is a systemic autoimmune disease that often affects multiple organs and organ systems. At the level of the immune system, it is not only characterized by a complex dysregulation of cellular and humoral adaptive immune responses, but also of innate immune functions (1). B cells, and specifically antibody-secreting plasma cells (PCs) and their immediate precursors, plasmablasts, have gained special interest in SLE since they directly cause distinctive immunologic symptoms: hypergammaglobulinemia, immune complex formation, and the production of autoantibodies. SLE patients exhibit defective B cell selection, including abnormal germinal center responses, B lymphopenia, and disturbed composition of the remaining peripheral B cells (2,3) with a marked expansion of antibody-secreting plasmablasts (2,4). Plasmablasts are positively associated with lupus disease activity, as well as with the presence of serum autoantibodies and titers (2,4), and therapeutic targeting of autoreactive PCs is discussed as a future treatment option for SLE (5).

In healthy individuals who have not been immunized recently, plasmablasts are continuously detectable in the blood at very low frequencies. Most of these plasmablasts appear to be generated in mucosal immune reactions of the gut and/or airways, as indicated by the expression of the prototypical

Supported by the DFG (grants Do 491/8-1/2 [SPP ImmunoBone], Do 491/7-2, 3, TRR130/TP24, and SFB633/TP A14) and the Berlin Senate through Charité University Medicine.

[1]Henrik E. Mei, PhD, Stefanie Hahne, Dipl.-Ing. Andreas Redlin, Bimba F. Hoyer, MD, Anna R. Lisney, Tobias Alexander, MD, Thomas Dörner, MD: Charité University Medicine Berlin and German Rheumatism Research Center Berlin, Berlin, Germany; [2]Kaiyin Wu, MD, Birgit Rudolph, MD: Charité University Medicine Berlin, Berlin, Germany; [3]Lisa Baganz, MSc: German Rheumatism Research Center Berlin, Berlin, Germany.

Dr. Hoyer has served as an expert witness on behalf of Roche. Dr. Alexander has received consulting fees and speaking fees from Pfizer and GlaxoSmithKline (less than $10,000 each).

Address correspondence to Henrik E. Mei, PhD, Deutsches Rheumaforschungszentrum Berlin, a Leibniz Institute, Charitéplatz 01, 10117 Berlin, Germany. E-mail: mei@drfz.de.

Submitted for publication February 15, 2016; accepted in revised form June 13, 2017.

immunoglobulin of mucosal immune reactions, IgA, and of the mucosal homing receptors CCR10 and $\alpha4\beta7$ integrin (6,7), as well as by secretion of polymeric IgA (8).

IgA expression results from class-switch recombination of activated B cells under the influence of transforming growth factor β (TGFβ), occurring predominantly in mucosal tissues (7), and is therefore considered a marker of mucosal B cell activation. The $\alpha4\beta7$ integrin mediates adhesion to mucosal addressin cell adhesion molecule 1 (MAdCAM-1) expressed on high endothelial venules (HEVs) of mucosal tissues of the gastrointestinal (GI) tract. Consistently, $\alpha4\beta7$ integrin–positive plasmablasts are capable of initiating homing to the gut, while $\alpha4\beta7$ integrin–negative plasmablasts can use $\alpha4\beta1$ integrin to adhere to vascular cell adhesion molecule 1–positive HEVs of the trachea and bronchoalveolar tissues (9,10). Expression of $\alpha4\beta7$ integrin in B cells is triggered by retinoic acid produced by dendritic cells (DCs) residing in gut- or airway-associated lymphoid tissue, but not other DCs (11,12), and is therefore used as a reliable identifier of not only mucosal homing, but also mucosal priming, of $\alpha4\beta7$ integrin–positive cells. The chemokine receptor CCR10 mediates plasmablast chemotaxis along gradients of CCL28, which is expressed in all mucosal tissues (13). Skin-expressed CCL27 can also bind to CCR10 (14). Unlike CCR9, which specifically mediates homing to the small intestine (7), CCR10 does not select for migration to a specific mucosal site and appears to be important for homing to the nonintestinal mucosa (15).

In mucosal PC deposits, most PCs express CCR10, $\beta7$ integrin, and IgA (15,16), including 60% coexpressing the J-chain (16) for formation of polymeric IgA that is dedicated to its secretion at mucosal surfaces (17). The $\alpha4\beta7$ integrin, IgA, and CCR10 are expressed by many but not all circulating plasmablasts specific for mucosally administered vaccines or enteric pathogens (18,19). Indeed, multiple, partially redundant molecular pathways exist that mediate plasmablast homing into different mucosal locations (7,20,21). In this study, we base our analyses on our own vaccination data, which show exclusive expression of $\beta7$ integrin and CCR10 by antigen-specific plasmablasts in blood after mucosal, but not after systemic (i.e., intramuscular or subcutaneous), vaccination.

Generally, the accumulation of plasmablasts in the blood of SLE patients is thought to result from B cell hyperactivity. Consistent with aberrant B cell stimulation by an autoantigen, autoreactive plasmablasts have been found in the blood of SLE patients (22). Despite the longstanding interest in plasmablasts as biomarkers and potential therapeutic targets, their composition and origin in SLE have not been explicitly addressed. To better understand the differentiation of plasmablasts and the mechanism(s) underlying plasmacytosis in SLE, we conducted a cross-sectional study of patients with active SLE and patients with treated, inactive SLE to investigate quantitative and qualitative characteristics of plasmablasts with a focus on mucosal traits.

PATIENTS AND METHODS

Detailed information on Patients and Methods is included in the Supplementary Methods, available on the *Arthritis & Rheumatology* web site at http://onlinelibrary.wiley.com/doi/10.1002/art.40181/abstract.

Study subjects. Blood samples were obtained from 56 SLE patients and 36 healthy controls. Additional healthy control samples were analyzed after oral cholera or intramuscular tetanus/diphtheria vaccination. Patient characteristics are summarized in Supplementary Table 1, available on the *Arthritis & Rheumatology* web site at http://onlinelibrary.wiley.com/doi/10.1002/art.40181/abstract. The ethics committee of Charité University Medicine approved the study, and informed consent was obtained from all subjects before enrollment, in accordance with the Declaration of Helsinki.

Isolation of peripheral blood mononuclear cells (PBMCs). PBMCs were isolated as previously described (23), with optional depletion of T cells and monocytes by rosetting (StemCell Technologies).

Flow cytometric analysis. Flow cytometry was performed on a FACSCanto II or LSRII flow cytometer (BD Biosciences) using fluorochrome-conjugated monoclonal antibodies. Fluorescence-labeled antigen was used to detect antigen-specific B cells (23,24).

In vitro antibody secretion and enzyme-linked immunospot (ELISpot) assay. PBMCs were incubated in media for 2 days, allowing for spontaneous antibody secretion. Detection of polymeric and monomeric IgA in PBMC supernatants was achieved by subjecting supernatants or control samples to fast-protein liquid chromatography, followed by the detection of IgA by enzyme-linked immunosorbent assay (ELISA) in the collected fractions. ELISpot assays were performed as previously described (23–25).

Cytokine quantification. Serum cytokines were quantified by ELISA and Luminex assays (Bio-Rad). In vitro chemotaxis was assessed using a Transwell migration assay as previously described (6).

Histologic analysis. Histologic analysis was performed on kidney biopsy sections by periodic acid–Schiff, IgG, and IgA staining.

Statistical analysis. Cytometric data were analyzed using FlowJo (Tree Star). ELISA data were analyzed using SoftMax Pro software version 5 (Molecular Devices). Data were statistically analyzed and displayed in GraphPad Prism. Statistical significance was calculated using the Mann-Whitney test for comparisons between patients and controls (2-tailed, 95% confidence interval), and Wilcoxon's test for paired comparisons, except where otherwise indicated. Spearman's rank correlation combined with bootstrap resampling (26) was used to correlate cytokine and cytometric data.

RESULTS

IgA+ plasmablasts contribute to the increased levels of circulating plasmablasts in SLE patients. Plasmablasts, naive B cells, and memory B cells were quantified in blood samples from 32 SLE patients and 19 healthy donors (Figure 1A). As previously reported (2), B lymphopenia in SLE affected naive B cells and memory B cells, while plasmablast numbers and frequencies were increased in SLE patients versus healthy donors (2.2-fold [$P < 0.0001$] for plasmablast numbers and 4.5-fold [$P < 0.0001$] for plasmablast frequencies) (Supplementary Figure 1 and Supplementary Table 2, available on the *Arthritis & Rheumatology* web site at http://onlinelibrary.wiley.com/doi/10.1002/art.40181/abstract). Detection of cytoplasmic Ig, CD138, and high levels of CD38 within CD19+ CD27^{high}CD20$^{-/low}$ cells confirmed the plasmablast phenotype (Figure 1C and Supplementary Figure 2, available on the *Arthritis & Rheumatology* web site at http://onlinelibrary.wiley.com/doi/10.1002/art.40181/abstract). Consistent with the inclusion of patients with largely inactive, controlled disease, the correlation between disease activity and plasmablast frequency was less striking than in previous reports (4) ($r = 0.27$, $P = 0.13$) (data not shown).

Similar proportions of plasmablasts from SLE patients and controls expressed cell-surface IgA, at median levels of 58% and 55%, respectively ($P = 0.49$). Accordingly, numbers of both IgA+ and IgA– plasmablasts were increased in SLE patients compared to healthy donors (2.5-fold [$P = 0.0003$] for IgA+ plasmablasts and 1.5-fold [$P = 0.0017$] for IgA– plasmablasts) (Figures 1A and B). Since increased frequencies of IgA+ plasmablasts were evident both in patients with high disease activity and in those with low disease activity and both in patients with high and in those with low absolute numbers of plasmablasts or plasmablast frequencies (data not shown), no association between IgA+ plasmablasts and the overall emergence of peripheral plasmablasts and SLE disease activity was established.

In an independent analysis of 4 healthy donor and 6 SLE samples, the predominance of IgA+ plasmablasts was confirmed by the detection of cytoplasmic IgA, IgG, and IgM among PBMCs. While cytoplasmic IgA–positive and cytoplasmic IgG–negative cells were detectable at comparable median frequencies among total plasmablasts in SLE patients and controls (for IgA, 66% in SLE patients and 64% in healthy donors, and for IgG, 29% in SLE patients and 23% in healthy donors), frequencies of cytoplasmic IgM–positive plasmablasts were significantly reduced in SLE patients (4% in SLE patients versus 11% in healthy donors; $P < 0.001$) (Figure 1C). These data confirm the expansion of plasmablasts in the peripheral blood of SLE patients and indicate that the expanded plasmablast

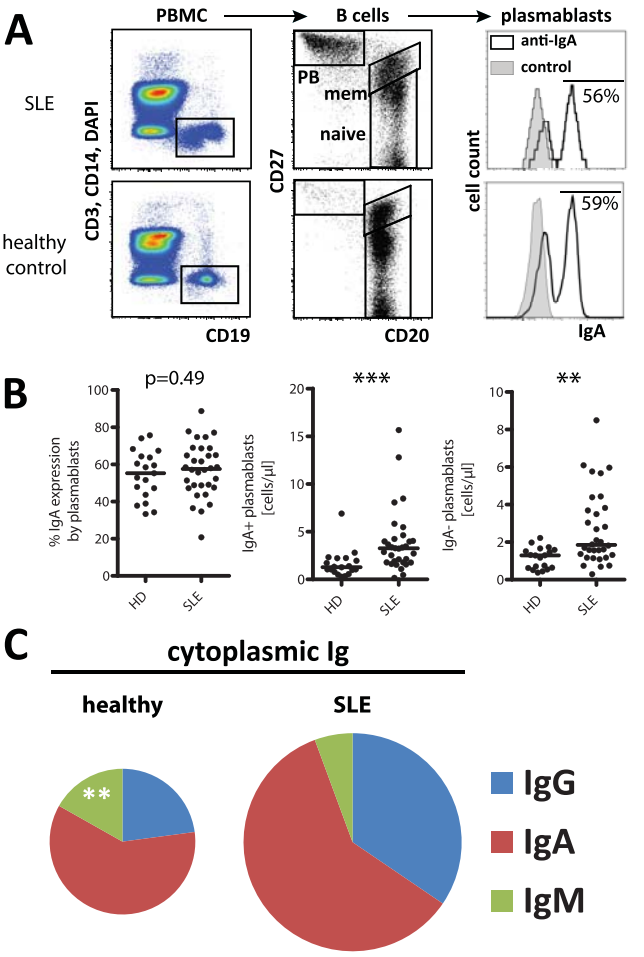

Figure 1. Increased numbers of circulating IgA-expressing and non–IgA-expressing plasmablasts (PBs) in blood samples from patients with systemic lupus erythematosus (SLE). SLE and control peripheral blood mononuclear cells (PBMCs) were analyzed by flow cytometry for the presence of IgA+ and IgA– plasmablasts among CD3–CD14–DAPI–CD19+CD27^{high}CD20$^{-/low}$ cells. **A,** Representative gating of PBMCs for IgA+ and IgA– plasmablasts. mem = memory B cell. **B,** Frequency of IgA-expressing plasmablasts, number of IgA+ plasmablasts, and number of IgA– plasmablasts in healthy donors (HDs) and SLE patients. Circles represent individual subjects; horizontal lines show the median. **C,** Cytoplasmic expression of IgA, IgG, and IgM among CD3–CD14–CD19$^{+/intermediate}$CD38^{high} PBMCs from 6 SLE patients and 4 controls. Pie charts show the mean percentage of plasmablasts expressing cytoplasmic IgG, cytoplasmic IgA, and cytoplasmic IgM. The total area of the pie reflects the median frequency of plasmablasts among PBMCs, which was 2.25-fold higher in the SLE patients than in the controls. Patients in **B** and **C** exhibited similar levels of disease activity (mean ± SD SLE Disease Activity Index 8.5 ± 2.9 and 9.7 ± 1.8, respectively). ** = $P < 0.01$; *** = $P < 0.001$ by Mann-Whitney 2-tailed test.

population consists predominantly of IgA+ plasmablasts, followed by IgG+ plasmablasts and diminished amounts of IgM+ plasmablasts.

Expression of mucosal homing receptors by circulating plasmablasts in SLE. CCR10 and β7 integrin were expressed by SLE plasmablasts at median frequencies of 40% and 38%, respectively (Figure 2A). The intestinal chemokine receptor CCR9 was not found on plasmablasts in SLE patients or controls (<1.4% of plasmablasts, except for 1 sample from a healthy donor that expressed CCR9 on 7% of plasmablasts). Likewise, SLE plasmablasts lacked expression of cutaneous lymphocyte antigen (CLA) involved in skin homing (<1.4% of plasmablasts). Frequencies of CCR10+ plasmablasts did not differ significantly between patients and healthy donors ($P > 0.05$), while frequencies of β7 integrin–positive plasmablasts were diminished in SLE patients ($P = 0.037$) (Supplementary Table 3, available on the *Arthritis & Rheumatology* web site at http://onlinelibrary.wiley.com/doi/10.1002/art.40181/abstract). Thus, CCR10+, CCR10–, and β7 integrin–negative plasmablasts clearly contributed to the expansion of plasmablasts in SLE. β7 integrin–positive plasmablasts were expanded to more than 2.2 cells/μl (a threshold set according to the maximum value in healthy donors, not considering the outlier) in a subgroup of 9 SLE patients, 6 of whom had active SLE (Figure 2A and Supplementary Table 3).

IgA, β7 integrin, and CCR10 expression were simultaneously analyzed to study their coexpression pattern on plasmablasts. CCR10 and β7 integrin were expressed by IgA+ plasmablasts but also by IgA– plasmablasts, i.e., IgM+ or IgG+ plasmablasts, indicating that a significant proportion of circulating non-IgA plasmablasts exhibit a mucosal homing phenotype in SLE (Figure 2B). In this analysis, 75% of SLE plasmablasts expressed at least IgA or 1 mucosal homing receptor (median 75% [range 57–88%] for SLE patients [n = 9] and median 81% [range 57–87%] for controls [n = 14]; $P = 0.13$) (Figure 2C). Since some IgA+ plasmablasts can also emerge from systemic immune responses (Figure 2E), we repeated the analysis without considering IgA expression. Here, 63% of control plasmablasts and 58% of SLE plasmablasts expressed β7 integrin, CCR10, or both ($P = 0.64$), confirming that at least half of the plasmablasts carry a mucosal phenotype based on their homing receptor expression. We further analyzed the composition of plasmablasts by determining the frequencies of 8 plasmablast populations defined by the expression of IgA, CCR10, and β7 integrin. This approach revealed a trend toward lower frequencies of IgA+CCR10+β7 integrin–negative plasmablasts and higher frequencies of IgA–CCR10–β7 integrin–negative plasmablasts in SLE, but the difference did not reach statistical significance (Supplementary Figure 3, available on the *Arthritis & Rheumatology* web site at http://onlinelibrary.wiley.com/doi/10.1002/art.40181/abstract).

Finally, spontaneous secretion of polymeric IgA by unstimulated SLE PBMCs in 5 of 6 samples further supported the presence of at least some IgA+ plasmablasts in SLE blood that secrete antibodies dedicated to transepithelial transport at mucosal surfaces (Figure 2D and Supplementary Figure 4, available on the *Arthritis & Rheumatology* web site at http://onlinelibrary.wiley.com/doi/10.1002/art.40181/abstract).

Next, we validated the use of IgA, CCR10, and β7 integrin expression as markers of mucosal provenance in secondary oral cholera versus systemic tetanus vaccination studies, serving as models of mucosal (GI tract) versus parenteral plasmablast responses. As previously described (6,23), tetanus toxoid (TT)–specific plasmablasts were detectable 1 week after intramuscular booster vaccination. They predominantly expressed cytoplasmic IgG (median 82%) and rarely expressed cytoplasmic IgA (9%). Few, if any, TT-specific plasmablasts expressed CCR10 (median 7%) or β7 integrin (median 6%) (Figure 2E). Cholera toxin B (CTB) subunit–specific plasmablasts peaked 4 days after secondary vaccination in both donors analyzed (Figure 2F and Supplementary Figure 5A, available on the *Arthritis & Rheumatology* web site at http://onlinelibrary.wiley.com/doi/10.1002/art.40181/abstract). The specificity of CTB-specific plasmablast detection was confirmed by blocking the staining with unlabeled antigen (Supplementary Figure 5B). CTB-specific plasmablasts expressed the phenotype IgA+/–, β7 integrin–positive, and CCR10+/– in both donors analyzed (Figure 2G). Like other vaccine-induced plasmablasts (6,27), CTB-specific plasmablasts expressed the proliferation marker Ki-67, consistent with their recent differentiation from activated B cells (Supplementary Figure 5C).

In summary, these results confirm the induction of IgA+/–, β7 integrin–positive, and CCR10+/– plasmablasts in specific mucosal immune responses. A substantial fraction of plasmablasts in SLE expressed IgA, CCR10, or β7 integrin, and thus shares similarities with plasmablasts induced by mucosal vaccination. However, IgA-expressing and CCR10-expressing plasmablasts regularly contributed to plasmacytosis in SLE, while a contribution of β7 integrin–positive plasmablasts was seen in only a few patients.

Autoreactivity of IgA+ and IgG+ plasmablasts in SLE. We next addressed whether or not autoreactivity was limited to IgG+ plasmablasts. ELISpot was used

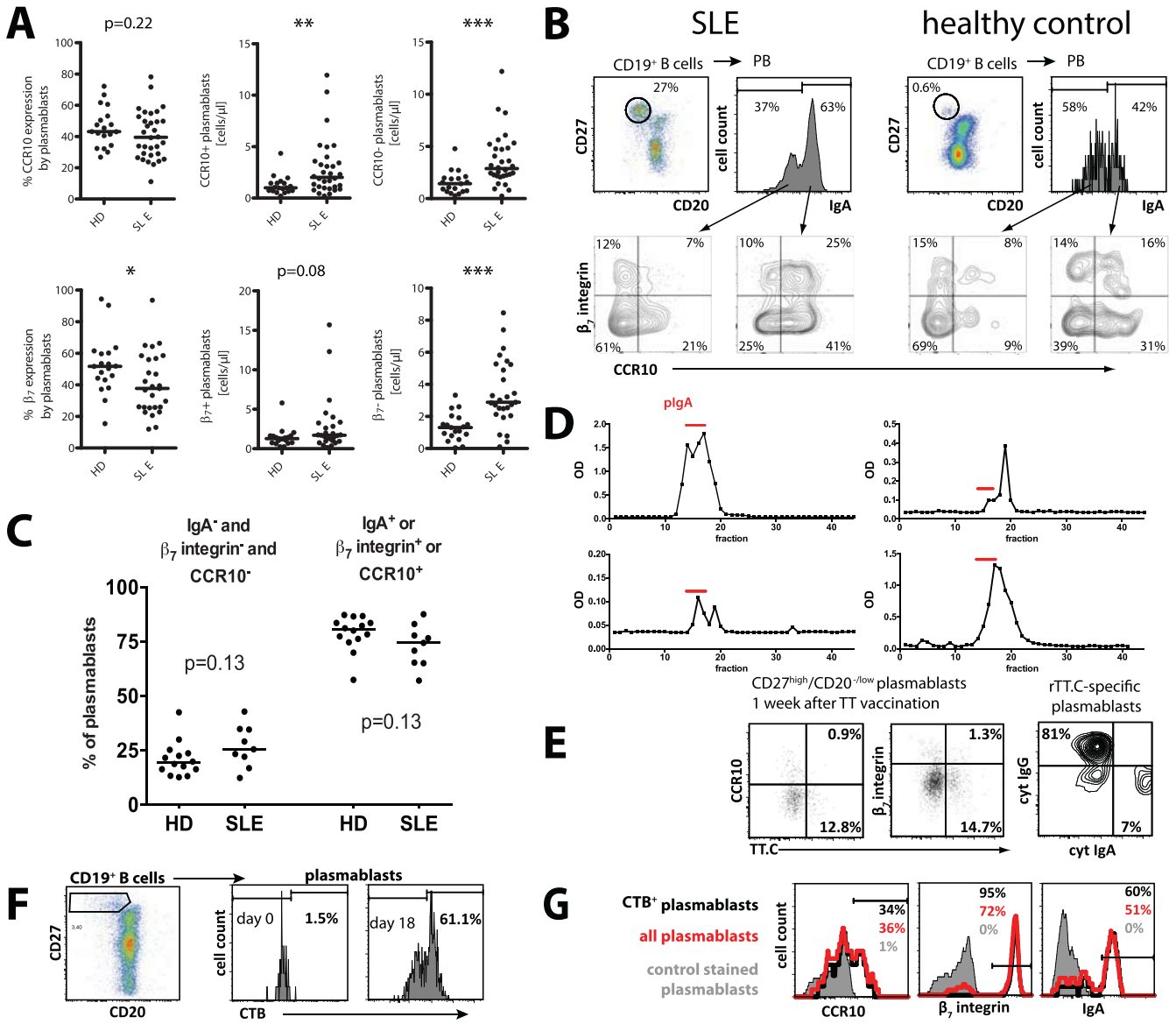

Figure 2. Mucosal phenotype of IgA+ plasmablasts (PBs) from patients with systemic lupus erythematosus (SLE). **A,** Top, Frequency of CCR10-expressing plasmablasts, number of CCR10+ plasmablasts, and number of CCR10– plasmablasts in samples from healthy donors (HDs) and SLE patients. Bottom, Frequency of $\beta 7$ integrin–expressing plasmablasts, number of $\beta 7$ integrin–positive plasmablasts, and number of $\beta 7$ integrin–negative plasmablasts in samples from healthy donors and SLE patients. Circles represent individual subjects; horizontal lines show the median. **B,** Representative gating of IgA+ and IgA– plasmablasts for coexpression of CCR10 and $\beta 7$ integrin. Contour plots (from left to right) show 1,697, 969, 107, and 150 plasmablasts, respectively. **C,** Frequencies of plasmablasts expressing neither IgA, $\beta 7$ integrin, nor CCR10 and frequencies of plasmablasts expressing at least 1 of these receptors in healthy donors and SLE patients. Circles represent individual subjects; horizontal lines show the median. *P* values were determined by Mann-Whitney test. **D,** Detection of plasmablasts secreting polymeric IgA (pIgA). Supernatants from SLE PBMCs cultured for 2 days under nonactivating conditions were subjected to size-exclusion chromatography. Fractions obtained were analyzed for IgA by enzyme-linked immunosorbent assay. Results for 4 of 6 samples analyzed are shown. Colostrum IgA was used as a reference to identify the fractions in which polymeric IgA was eluted (red bars) (see Supplementary Figure 4, available on the *Arthritis & Rheumatology* web site at http://onlinelibrary.wiley.com/doi/10.1002/art.40181/abstract). **E,** Expression of CCR10, $\beta 7$ integrin, cytoplasmic (cyt) IgG, and cytoplasmic IgA by recombinant tetanus toxin C-fragment (rTT.C)–specific plasmablasts. Dot plots show CD3–CD14–DAPI–CD19+CD27^{high}CD20$^{-/low}$ cells. Results are representative of 5 experiments. **F,** Cytometric identification of cholera toxin B (CTB) subunit–specific plasmablasts in peripheral blood after oral cholera vaccination. **G,** CCR10, $\beta 7$ integrin, and IgA expression by CTB-specific and total plasmablasts. $* = P < 0.05$; $** = P < 0.01$; $*** = P < 0.001$.

to enumerate double-stranded DNA (dsDNA)–specific IgG- and IgA-secreting blood plasmablasts from SLE patients. Both dsDNA-specific IgG+ and IgA+ plasmablasts were detectable in 5 of 5 patients with highly active disease, at frequencies between 0.03% and 3.10% among total IgG-secreting cells and between 0.01% and 1.10% among total IgA-secreting cells, corresponding to median levels of 76 and 23 cells per 1×10^6 PBMCs, respectively (Supplementary Table 4, available on the *Arthritis & Rheumatology* web site at http://onlinelibrary.wiley.com/doi/10.1002/art.40181/abstract). Thus, individual IgA+ and IgG+ plasmablasts secreted autoantibodies in SLE, indicating that autoreactivity did not spare IgA+ plasmablasts.

Association of IgA and CCR10 expression by SLE plasmablasts with serum cytokine levels. We subsequently considered the possibility that the cytokine milieu present in SLE patients accounts for the amplification of plasmablast response in an autoantigen-independent manner. We determined serum concentrations of 25 cytokines from SLE blood samples, which were simultaneously analyzed for blood plasmablast characteristics by flow cytometry. A total of 28 parameters derived from manual gating of flow cytometric plasmablast data were classified according to whether they reflected systemic or mucosal plasmablast differentiation, based on the phenotype of vaccination-induced plasmablasts. Spearman's correlation analyses and subsequent bootstrap resampling revealed a serum cytokine signature comprising interleukin-2 (IL-2), IL-6, IL-17, platelet-derived growth factor BB (PDGF-BB), and vascular endothelial growth factor (VEGF) that directly correlated with frequencies of IgA+ and/or CCR10+ plasmablasts ($r_s > 0$), but not β7 integrin–positive plasmablasts (Figure 3). Negative associations were found between levels of IL-12 and the expression of CD62L by plasmablasts. The emergence of phenotypically mucosal rather than parenteral plasmablasts was positively associated with serum cytokine levels in SLE ($P < 0.0001$ by Fisher's exact test). Few inverse correlations ($r_s < 0$) were found when features of systemic plasmablast differentiation were analyzed. These were related to frequencies of plasmablasts lacking IgA and CCR10, and to the expression of CD62L, an adhesion molecule expressed by plasmablasts induced by intramuscular vaccination (6).

A similar data set from healthy donors demonstrated a largely distinct pattern of plasmablast feature versus serum cytokine level correlations, suggesting that the pattern observed in SLE patients is associated with the disease, and not a general pattern observed in healthy individuals (data not shown).

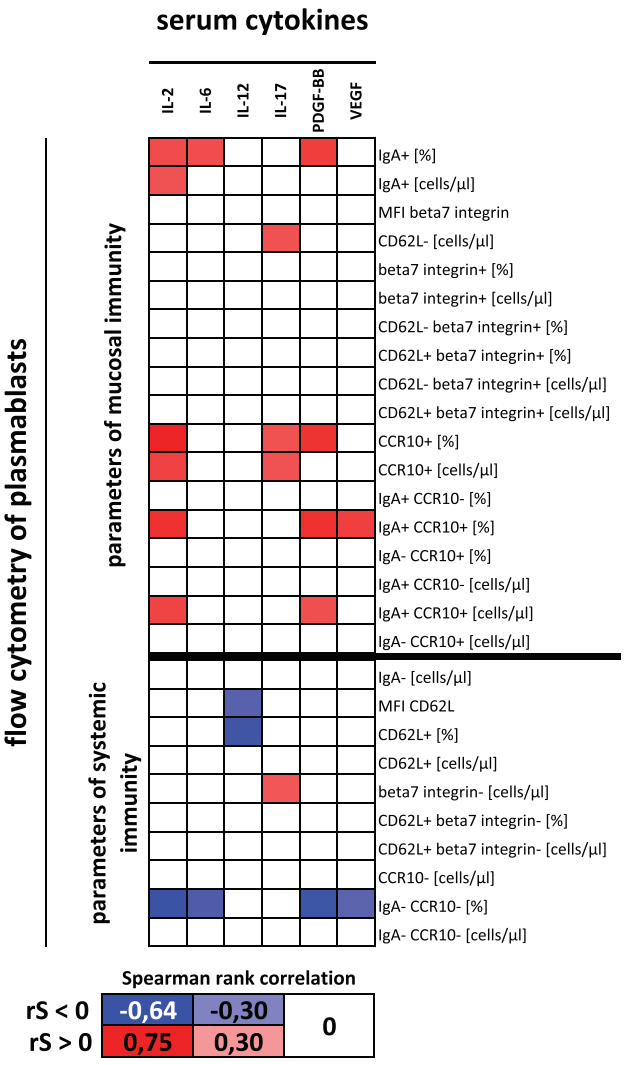

Figure 3. Correlation of measures of mucosal, but not parenteral, plasmablast differentiation with serum cytokine levels in patients with systemic lupus erythematosus (SLE). Plasmablast data from 26 SLE patients and serum concentrations of 22 cytokines, determined by bead-based multiplex assay, were analyzed using Spearman's correlation. Levels of BAFF, APRIL, and interferon-α were determined separately by enzyme-linked immunosorbent assay and did not show correlations with plasmablast data (data not shown). Serum and plasmablast analyses were performed using the same donors and time points. Sera were treated with a heterophilic binding blocker to avoid potential interference by autoantibodies (55). The matrix shows cytokines with at least 2 significant correlations ($P < 0.05$). Significant correlations confirmed by bootstrapping are shown in color according to their r_s values. IL-2 = interleukin-2; PDGF-BB = platelet-derived growth factor BB; VEGF = vascular endothelial growth factor; MFI = median fluorescence intensity.

SLE plasmablasts are migration competent. While autoreactivity of B cells and cytokines may facilitate the plasmablast expansion in SLE patients' blood

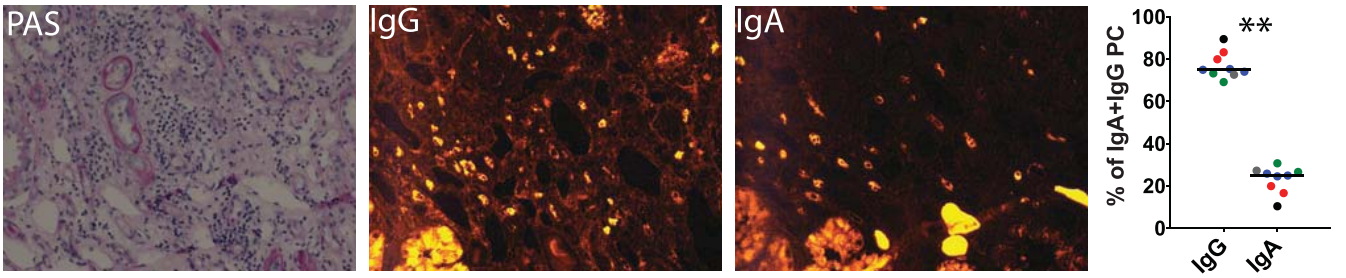

Figure 4. IgG+ plasma cells (PCs) are enriched in inflamed systemic lupus erythematosus (SLE) kidney biopsy specimens. Left, Periodic acid–Schiff (PAS), IgG, and IgA staining of representative kidney biopsy specimens containing lymphocytic infiltrates from 5 patients with SLE. PCs were detected and counted according to characteristic morphology and IgG or IgA staining. Right, Percent of IgG-expressing PCs and IgA-expressing PCs in the kidney biopsy specimens. Circles represent individual replicates; each color represents an individual patient. Horizontal lines show the median. Original magnification × 200. ** = $P < 0.01$ by Wilcoxon's test.

by enhancing plasmablast production, we additionally considered impaired plasmablast mobility as seen in the NZM mouse model of SLE (28) as a potential mechanism contributing to blood plasmacytosis in SLE. We therefore analyzed in vitro chemotaxis of plasmablasts from SLE patients and controls toward CXCL12, CCL28, and CXCL9, which have been implicated in plasmablast homing to the bone marrow, mucosal tissues, and sites of autoimmune inflammation (20,29). Like control plasmablasts, plasmablasts from SLE patients were principally competent to migrate toward the chemokines tested, with a trend for enhanced migration toward CXCL9 in individual patients and somewhat decreased migration toward CXCL12 and CCL28 (Supplementary Figure 6, available on the *Arthritis & Rheumatology* web site at http://onlinelibrary.wiley.com/doi/10.1002/art.40181/abstract). Since we found no evidence of principally impaired migration of SLE plasmablasts, plasmablasts appear to accumulate in the blood of SLE patients because of their overproduction rather than due to defective plasmablast migration.

PCs in inflamed kidneys are selected for IgG expression. Finally, we addressed whether the predominance of IgA+ plasmablasts in the peripheral blood of SLE patients is also evident at sites of chronic inflammation. We analyzed kidney biopsy specimens with lymphocytic infiltrates from 5 patients with active lupus nephritis (Supplementary Table 5, available on the *Arthritis & Rheumatology* web site at http://onlinelibrary.wiley.com/doi/10.1002/art.40181/abstract) for the presence of cytoplasmic IgA+ and cytoplasmic IgG+ cells by fluorescence microscopy. This analysis provided a numerical ratio of 3:1 for IgG:IgA PCs (Figure 4), documenting that IgG+ PCs are enriched over IgA+ PCs in inflamed kidneys in SLE. It remains unclear whether the observed kidney PCs were autoreactive or expressed mucosal homing receptor. The enrichment of IgG+ PCs in lupus nephritis supports the notion that they are more intimately involved in SLE tissue immunopathology than IgA+ PCs.

DISCUSSION

In this study, we show that major subsets of plasmablasts in the blood of SLE patients carry a phenotype reminiscent of mucosal immune reactions and that such phenotypically mucosal plasmablasts contribute to plasmablast expansion in SLE. Previous studies identified IgA+ plasmablasts as the minor (30,31) or major (32,33) plasmablast subset in SLE. In the present study, on average 58% of the plasmablasts expressed IgA, indicating the predominance of IgA+ plasmablasts in SLE, while individual patients showed rather few IgA-expressing plasmablasts, amounting to 20–40% of total plasmablasts, or in ELISpot assays, excessive amounts of IgG-secreting cells. At least some of the IgA+ plasmablasts in the blood secreted polymeric IgA, dedicated to transepithelial transport at mucosal surfaces.

By including stainings for the mucosal homing receptors β7 integrin and CCR10 in our cytometric panel, we detected additional, apparently mucosal plasmablast subsets that do not produce IgA, such as CCR10+ and/or β7 integrin–positive, IgM+, or IgG+ plasmablasts. The detection of these IgA− subsets substantiates the emergence of mucosal plasmablasts in SLE: 40% of SLE plasmablasts expressed CCR10, and 38% expressed β7 integrin. Notably, IgA, CCR10, and β7 integrin were coexpressed in different patterns, ranging from plasmablasts expressing only 1 of the receptors to cells coexpressing all 3. Seventy-five percent of plasmablasts expressed at least 1 of these molecules. Our present results confirm previous observations (23,34–36) that IgA+ plasmablasts can be byproducts of

intramuscular vaccination responses, so that IgA expression alone may not serve as an unequivocal marker of mucosally induced plasmablasts. When only the expression of CCR10 and/or β7 integrin was considered, 58% of the plasmablasts qualified as mucosal plasmablasts.

As a reference for mucosally induced plasmablasts, we studied antigen-specific plasmablasts induced by oral cholera vaccination. This analysis showed that expression of IgA, CCR10, and β7 integrin was induced in the plasmablast population resulting from oral vaccination, yet only β7 integrin was expressed by virtually all CTB-specific plasmablasts. Unlike the CTB-specific plasmablasts, which almost uniformly expressed β7 integrin, SLE plasmablasts consisted of subpopulations expressing or lacking β7 integrin. This illustrates the heterogeneity of the plasmablast response in SLE and confirms that not all SLE plasmablasts qualify as mucosal plasmablasts.

Similar heterogeneity was recently observed in a study of blood plasmablast homing receptor signatures in patient groups with different mucosal immune syndromes. For example, plasmablasts from patients with upper respiratory tract infections showed a β7 integrin–negative $CCR10^{low/+}$ phenotype, plasmablasts from patients with ulcerative colitis were β7 integrin–positive/negative and CCR10+, and plasmablasts from patients with celiac disease or symptoms of GI tract infection were β7 integrin–positive and CCR10+, besides having varying expression of additional homing receptors. Our vaccination data and the findings of Seong et al and others (18,21) support the notion that blood plasmablasts in SLE represent a mixture of plasmablasts induced in different tissues, with diverse mucosal sites contributing plasmablasts with different β7 integrin/CCR10 phenotypes. This appears to be consistent with the systemic inflammation evident in SLE, which includes mucosal tissues in some patients.

Notably, mucosal priming does not exclude homing of the resultant plasmablast to the bone marrow (37), indicating that mucosal and parenteral plasmablast migration routes are not fully separated. The absence of CLA and CCR9 expression on plasmablasts is evidence against selective intestinal and skin homing as major plasmablast migration routes in SLE.

Since an unequivocal phenotypic definition of mucosal plasmablasts is lacking, true enumeration of unambiguously mucosal plasmablasts and their assignment to specific mucosal tissues was not possible. However, our data clearly show that, unexpectedly, plasmablasts with a mucosal phenotype make up a significant fraction of total plasmablasts in SLE and that plasmablasts expressing IgA in combination with CCR10 contribute to the plasmablast expansion in SLE patients. In this study, we reproduced the typical expansion of frequencies and absolute numbers of plasmablasts in active SLE when comparing patients with active versus inactive disease using an SLE Disease Activity Index (SLEDAI) threshold of 6. However, a close and significant correlation between plasmablast numbers and disease activity could not be established in our study, possibly because of the inclusion of patients who had received previously unavailable treatments, such as anti-BAFF (belimumab) or B cell depletion, and also because patients were included from both inpatient and outpatient settings. While plasmablast expansion was detectable in patients in both groups, our prior studies on plasmablasts in SLE (2,4,38) were performed almost exclusively among hospitalized patients, who have enhanced disease activity compared to outpatients.

We found no evidence of an association between frequencies of IgA+, CCR10+, or β7 integrin–positive plasmablasts among total plasmablasts and disease activity or the overall emergence of plasmablasts. This suggested that the contribution of IgA+, CCR10+, or β7 integrin–positive plasmablasts to the overall plasmablast population in SLE is relatively stable and independent of disease activity and severity of plasmacytosis.

Unlike in blood, PCs in chronically inflamed kidneys of SLE patients were dominated by the IgG isotype in all cases analyzed, supporting the involvement of IgG-secreting cells in lupus nephritis pathology. It remained unclear whether PCs detectable in the kidneys had migrated there, were generated in situ, or were a mixture of both.

The intriguingly similar composition of SLE and control plasmablasts led us to speculate that plasmacytosis in SLE was largely due to unselective amplification of the normal steady-state plasmablast response (6). However, we detected autoreactive cells among IgG- and IgA-secreting cells, showing that at least some IgA+ plasmablasts do not belong to the homeostatic plasmablast repertoire seen in healthy controls, and peripheral blood IgA+ plasmablasts are not principally spared from autoreactivity. Our comparison of serum cytokine levels with plasmablast features indicating preferentially mucosal versus parenteral induction revealed a set of cytokines that was positively associated with the emergence of mucosal (IgA+ and/or CCR10+) plasmablasts but was not associated, or was negatively associated, with the emergence of parenteral plasmablasts. This cytokine signature included IL-2, IL-6, IL-17, PDGF-BB, and VEGF, with IL-2 and PDGF-BB having greater numbers of associations. PDGF-BB is known to be a regulator of mesangial cells and is implicated in nephropathy (39), and has also been linked to both proinflammatory and antiinflammatory roles (40,41),

although direct interactions with mature B cells or PCs have not been described.

Treg cells are candidates for a possible link between IL-2 and the emergence of mucosal plasmablasts. Treg cells produce the IgA class-switch–inducing cytokine TGFβ (42), and IL-2 therapy increases Treg cell frequencies and activation state in the blood of SLE patients (43,44). Treg cell depletion in mice decreases the amounts of lamina propria IgA+ PCs and IgA antibodies (45). Notably, serum levels of PDGF-BB and TGFβ have been found to be associated in a study of chronic pancreatitis (46). In addition, IL-2 may selectively promote differentiation of CD27+ CD25+IgA+/– memory B cells, which, when activated, likewise secrete TGFβ (47). In contrast, IL-6, which belongs to the group of inflammation-promoting cytokines, stimulates the proliferation of B cells activated by IL-2 or IL-10, promotes the survival of PCs, and likely promotes plasmablasts expressing the IL-6 receptor (48,49). Some, but not all, human blood plasmablasts express the IL-6 receptor (50), and IL-6 has been shown to be required for normal IgA production in vivo (51). A network of IL-2, TGFβ, and IL-6 appears to control Treg cells and Th17 cells (52), which are implicated in both IgA production (53) and autoimmune pathogenesis (54). However, the nature of our cytokine/plasmablast comparison is purely associative and requires further mechanistic studies.

Taken together, the cytokine signature identified is, with the exception of PDGF-BB and VEGF, consistent with the involvement of cytokine signals that either directly or via T cells can impact the quality and quantity of plasmablast responses.

Finally, we tested the hypothesis that the enrichment of plasmablasts in SLE blood might be due to a migration defect interfering with the plasmablast's exit from blood. In Transwell chemotaxis assays, SLE plasmablasts showed a somewhat enhanced response toward CXCL9 implicated in plasmablast recruitment to inflamed sites. Migration responses toward CXCL12 and CCL28, reflecting the functionality of CXCR4 and CCR10, were largely comparable to controls, and confirmed that SLE plasmablasts chemotactically respond normally, at least under in vitro conditions.

In summary, our data document the participation of mucosal plasmablasts in the exaggerated plasmablast response in SLE, reflecting an overactivation and involvement of the mucosal immune system in SLE. The heterogeneity of plasmablasts in SLE appears to be due to superimposed B cell hyperactivity driven by autoreactivity and the cytokine environment. Further studies are needed to evaluate how immune therapies influence mucosal immune activity in SLE and whether additional treatment considerations are required.

ACKNOWLEDGMENTS

We are grateful to Karin Reiter, Heidi Hecker-Kia, Heidi Schliemann, Annette Peddinghaus, and Tuula Geske for excellent technical assistance. We thank Andreas Radbruch for critical discussions.

AUTHOR CONTRIBUTIONS

All authors were involved in drafting the article or revising it critically for important intellectual content, and all authors approved the final version to be published. Dr. Mei had full access to all of the data in the study and takes responsibility for the integrity of the data and the accuracy of the data analysis.

Study conception and design. Mei, Redlin, Hoyer, Baganz, Dörner.

Acquisition of data. Mei, Hahne, Redlin, Hoyer, Wu, Lisney, Rudolph, Dörner.

Analysis and interpretation of data. Mei, Hahne, Redlin, Hoyer, Baganz, Lisney, Alexander, Dörner.

REFERENCES

1. Wahren-Herlenius M, Dörner T. Immunopathogenic mechanisms of systemic autoimmune disease. Lancet 2013;382:819–31.
2. Odendahl M, Jacobi A, Hansen A, Feist E, Hiepe F, Burmester GR, et al. Disturbed peripheral B lymphocyte homeostasis in systemic lupus erythematosus. J Immunol 2000; 165:5970–9.
3. Kaminski DA, Wei C, Qian Y, Rosenberg AF, Sanz I. Advances in human B cell phenotypic profiling. Front Immunol 2012;3: 302.
4. Jacobi AM, Odendahl M, Reiter K, Bruns A, Burmester GR, Radbruch A, et al. Correlation between circulating CD27^{high} plasma cells and disease activity in patients with systemic lupus erythematosus. Arthritis Rheum 2003;48:1332–42.
5. Hiepe F, Dörner T, Hauser AE, Hoyer BF, Mei H, Radbruch A. Long-lived autoreactive plasma cells drive persistent autoimmune inflammation. Nat Rev Rheumatol 2011;7:170–8.
6. Mei HE, Yoshida T, Sime W, Hiepe F, Thiele K, Manz RA, et al. Blood-borne human plasma cells in steady state are derived from mucosal immune responses. Blood 2009;113:2461–9.
7. Mora JR, von Andrian UH. Differentiation and homing of IgA-secreting cells. Mucosal Immunol 2008;1:96–109.
8. Kutteh WH, Prince SJ, Mestecky J. Tissue origins of human polymeric and monomeric IgA. J Immunol 1982;128:990–5.
9. Berlin C, Berg EL, Briskin MJ, Andrew DP, Kilshaw PJ, Holzmann B, et al. $\alpha4\beta7$ integrin mediates lymphocyte binding to the mucosal vascular addressin MAdCAM-1. Cell 1993;74: 185–95.
10. Briskin M, Winsor-Hines D, Shyjan A, Cochran N, Bloom S, Wilson J, et al. Human mucosal addressin cell adhesion molecule-1 is preferentially expressed in intestinal tract and associated lymphoid tissue. Am J Pathol 1997;151:97–110.
11. Mora JR, Iwata M, Eksteen B, Song SY, Junt T, Senman B, et al. Generation of gut-homing IgA-secreting B cells by intestinal dendritic cells. Science 2006;314:1157–60.
12. Ruane D, Chorny A, Lee H, Faith J, Pandey G, Shan M, et al. Microbiota regulate the ability of lung dendritic cells to induce IgA class-switch recombination and generate protective gastrointestinal immune responses. J Exp Med 2016;213:53–73.
13. Wang W, Soto H, Oldham ER, Buchanan ME, Homey B, Catron D, et al. Identification of a novel chemokine

(CCL28), which binds CCR10 (GPR2). J Biol Chem 2000; 275:22313–23.
14. Homey B, Wang W, Soto H, Buchanan ME, Wiesenborn A, Catron D, et al. The orphan chemokine receptor G protein-coupled receptor-2 (GPR-2, CCR10) binds the skin-associated chemokine CCL27 (CTACK/ALP/ILC). J Immunol 2000;164: 3465–70.
15. Kunkel EJ, Kim CH, Lazarus NH, Vierra MA, Soler D, Bowman EP, et al. CCR10 expression is a common feature of circulating and mucosal epithelial tissue IgA Ab-secreting cells. J Clin Invest 2003;111:1001–10.
16. Pabst R, Russell MW, Brandtzaeg P. Tissue distribution of lymphocytes and plasma cells and the role of the gut. Trends Immunol 2008;29:206–8.
17. Brandtzaeg P, Johansen FE. Mucosal B cells: phenotypic characteristics, transcriptional regulation, and homing properties. Immunol Rev 2005;206:32–63.
18. Jaimes MC, Rojas OL, Kunkel EJ, Lazarus NH, Soler D, Butcher EC, et al. Maturation and trafficking markers on rotavirus-specific B cells during acute infection and convalescence in children. J Virol 2004;78:10967–76.
19. Sundstrom P, Lundin SB, Nilsson LA, Quiding-Jarbrink M. Human IgA-secreting cells induced by intestinal, but not systemic, immunization respond to CCL25 (TECK) and CCL28 (MEC). Eur J Immunol 2008;38:3327–38.
20. Kunkel EJ, Butcher EC. Plasma-cell homing. Nat Rev Immunol 2003;3:822–9.
21. Seong Y, Lazarus NH, Sutherland L, Habtezion A, Abramson T, He XS, et al. Trafficking receptor signatures define blood plasmablasts responding to tissue-specific immune challenge. JCI Insight 2017;2:e90233.
22. Hanaoka H, Okazaki Y, Satoh T, Kaneko Y, Yasuoka H, Seta N, et al. Circulating anti-double-stranded DNA antibody-secreting cells in patients with systemic lupus erythematosus: a novel biomarker for disease activity. Lupus 2012;21:1284–93.
23. Odendahl M, Mei H, Hoyer BF, Jacobi AM, Hansen A, Muehlinghaus G, et al. Generation of migratory antigen-specific plasma blasts and mobilization of resident plasma cells in a secondary immune response. Blood 2005;105:1614–21.
24. Mei HE, Frolich D, Giesecke C, Loddenkemper C, Reiter K, Schmidt S, et al. Steady-state generation of mucosal IgA^+ plasmablasts is not abrogated by B-cell depletion therapy with rituximab. Blood 2010;116:5181–90.
25. Mei HE, Wirries I, Frolich D, Brisslert M, Giesecke C, Grun JR, et al. A unique population of IgG-expressing plasma cells lacking CD19 is enriched in human bone marrow. Blood 2015; 125:1739–48.
26. Carpenter J, Bithell J. Bootstrap confidence intervals: when, which, what? A practical guide for medical statisticians. Stat Med 2000;19:1141–64.
27. Wrammert J, Smith K, Miller J, Langley WA, Kokko K, Larsen C, et al. Rapid cloning of high-affinity human monoclonal antibodies against influenza virus. Nature 2008;453:667–71.
28. Erickson LD, Lin LL, Duan B, Morel L, Noelle RJ. A genetic lesion that arrests plasma cell homing to the bone marrow. Proc Natl Acad Sci U S A 2003;100:12905–10.
29. Yoshida T, Mei H, Dörner T, Hiepe F, Radbruch A, Fillatreau S, et al. Memory B and memory plasma cells. Immunol Rev 2010;237:117–39.
30. Ginsburg WW, Finkelman FD, Lipsky PE. Circulating and pokeweed mitogen-induced immunoglobulin-secreting cells in systemic lupus erythematosus. Clin Exp Immunol 1979;35:76–88.
31. Joo H, Coquery C, Xue Y, Gayet I, Dillon SR, Punaro M, et al. Serum from patients with SLE instructs monocytes to promote IgG and IgA plasmablast differentiation. J Exp Med 2012;209: 1335–48.
32. Wangel AG, Milton A, Egan JB. Spontaneous plaque forming cells in the peripheral blood of patients with systemic lupus erythematosus. Clin Exp Immunol 1982;49:41–9.
33. Saiki O, Saeki Y, Kishimoto S. Spontaneous immunoglobulin A secretion and lack of mitogen-responsive B cells in systemic lupus erythematosus. J Clin Invest 1985;76:1865–70.
34. Blanchard-Rohner G, Pulickal AS, Jol-van der Zijde CM, Snape MD, Pollard AJ. Appearance of peripheral blood plasma cells and memory B cells in a primary and secondary immune response in humans. Blood 2009;114:4998–5002.
35. Quiding-Jarbrink M, Nordstrom I, Granstrom G, Kilander A, Jertborn M, Butcher EC, et al. Differential expression of tissue-specific adhesion molecules on human circulating antibody-forming cells after systemic, enteric, and nasal immunizations: a molecular basis for the compartmentalization of effector B cell responses. J Clin Invest 1997;99:1281–6.
36. Heine G, Drozdenko G, Lahl A, Unterwalder N, Mei H, Volk HD, et al. Efficient tetanus toxoid immunization on vitamin D supplementation. Eur J Clin Nutr 2011;65:329–34.
37. Lemke A, Kraft M, Roth K, Riedel R, Lammerding D, Hauser AE. Long-lived plasma cells are generated in mucosal immune responses and contribute to the bone marrow plasma cell pool in mice. Mucosal Immunol 2016;9:83–97.
38. Jacobi AM, Mei H, Hoyer BF, Mumtaz IM, Thiele K, Radbruch A, et al. $HLA\text{-}DR^{high}/CD27^{high}$ plasmablasts indicate active disease in patients with systemic lupus erythematosus. Ann Rheum Dis 2010;69:305–8.
39. Floege J, Eitner F, Alpers CE. A new look at platelet-derived growth factor in renal disease. J Am Soc Nephrol 2008;19:12–23.
40. Rosengren S, Corr M, Boyle DL. Platelet-derived growth factor and transforming growth factor β synergistically potentiate inflammatory mediator synthesis by fibroblast-like synoviocytes. Arthritis Res Ther 2010;12:R65.
41. Tang J, Kozaki K, Farr AG, Martin PJ, Lindahl P, Betsholtz C, et al. The absence of platelet-derived growth factor-B in circulating cells promotes immune and inflammatory responses in atherosclerosis-prone ApoE−/− mice. Am J Pathol 2005;167:901–12.
42. Stavnezer J, Kang J. The surprising discovery that TGFβ specifically induces the IgA class switch. J Immunol 2009;182:5–7.
43. Von Spee-Mayer C, Siegert E, Abdirama D, Rose A, Klaus A, Alexander T, et al. Low-dose interleukin-2 selectively corrects regulatory T cell defects in patients with systemic lupus erythematosus. Ann Rheum Dis 2016;75:1407–15.
44. He J, Zhang X, Wei Y, Sun X, Chen Y, Deng J, et al. Low-dose interleukin-2 treatment selectively modulates $CD4^+$ T cell subsets in patients with systemic lupus erythematosus. Nat Med 2016;22:991–3.
45. Cong Y, Feng T, Fujihashi K, Schoeb TR, Elson CO. A dominant, coordinated T regulatory cell-IgA response to the intestinal microbiota. Proc Natl Acad Sci U S A 2009;106: 19256–61.
46. Adrych K, Smoczynski M, Stojek M, Sledzinski T, Korczynska J, Goyke E, et al. Coordinated increase in serum platelet-derived growth factor-BB and transforming growth factor-β1 in patients with chronic pancreatitis. Pancreatology 2011;11:434–40.
47. Amu S, Tarkowski A, Dörner T, Bokarewa M, Brisslert M. The human immunomodulatory $CD25^+$ B cell population belongs to the memory B cell pool. Scand J Immunol 2007;66:77–86.
48. Cassese G, Arce S, Hauser AE, Lehnert K, Moewes B, Mostarac M, et al. Plasma cell survival is mediated by synergistic effects of cytokines and adhesion-dependent signals. J Immunol 2003;171: 1684–90.
49. Jego G, Bataille R, Pellat-Deceunynck C. Interleukin-6 is a growth factor for nonmalignant human plasmablasts. Blood 2001;97:1817–22.
50. Gonzalez-Garcia I, Ocana E, Jimenez-Gomez G, Campos-Caro A, Brieva JA. Immunization-induced perturbation of human blood plasma cell pool: progressive maturation, IL-6 responsiveness, and high PRDI-BF1/BLIMP1 expression are critical

distinctions between antigen-specific and nonspecific plasma cells. J Immunol 2006;176:4042–50.
51. Ramsay AJ, Husband AJ, Ramshaw IA, Bao S, Matthaei KI, Koehler G, et al. The role of interleukin-6 in mucosal IgA antibody responses in vivo. Science 1994;264:561–3.
52. Hatton RD. TGF-β in Th17 cell development: the truth is out there. Immunity 2011;34:288–90.
53. Hirota K, Turner JE, Villa M, Duarte JH, Demengeot J, Steinmetz OM, et al. Plasticity of Th17 cells in Peyer's patches is responsible for the induction of T cell-dependent IgA responses. Nat Immunol 2013;14:372–9.
54. Martin JC, Baeten DL, Josien R. Emerging role of IL-17 and Th17 cells in systemic lupus erythematosus. Clin Immunol 2014;154:1–12.
55. Todd DJ, Knowlton N, Amato M, Frank MB, Schur PH, Izmailova ES, et al. Erroneous augmentation of multiplex assay measurements in patients with rheumatoid arthritis due to heterophilic binding by serum rheumatoid factor. Arthritis Rheum 2011;63:894–903.

ARTHRITIS & RHEUMATOLOGY
Vol. 69, No. 10, October 2017, pp 2029–2037
DOI 10.1002/art.40180

Peripheral Immunophenotyping Identifies Three Subgroups Based on T Cell Heterogeneity in Lupus Patients

Satoshi Kubo, Shingo Nakayamada, Maiko Yoshikawa, Yusuke Miyazaki, Kei Sakata, Kazuhisa Nakano, Kentaro Hanami, Shigeru Iwata, Ippei Miyagawa, Kazuyoshi Saito, and Yoshiya Tanaka

Objective. **To elucidate the diversity of systemic lupus erythematosus (SLE) based on immunophenotyping.**

Methods. **Peripheral blood mononuclear cells were obtained from 143 SLE patients and 49 healthy individuals. Circulating B, T, and dendritic cells were defined using flow cytometric analysis as recommended by the Human Immunology Project Consortium. Based on these results, immunophenotypes were distinguished by principal components analysis (PCA), and cluster analysis was used to classify SLE patients into subgroups.**

Results. **The proportions of Treg and follicular helper T (Tfh) cells were higher in SLE patients than in healthy controls, whereas Th1 and Th17 cell proportions did not differ. Proportions of class-switched memory B cells and IgD–CD27– B cells were increased in SLE patients as well. The largest difference compared to the control group was observed in the proportion of plasmablasts, which was higher in SLE patients and correlated with disease activity as assessed with the British Isles Lupus Assessment Group index. PCA indicated that the immunophenotype of SLE patients consisted of abnormalities of the T and B cell axes. Cluster analysis showed that the SLE patients could be stratified into 3 subgroups (with high proportions of plasmablasts in all groups): patients who did not show the characteristic features (T cell–independent group), patients with a high percentage of Tfh cells (Tfh-dominant group), and patients with a high percentage of memory Treg cells (Treg-dominant group). The percentage of patients whose SLE was resistant to treatment was highest among the Tfh-dominant group.**

Conclusion. **Our study indicates that patients with active SLE can be divided into 3 subgroups based on T cell heterogeneity. Further immunophenotyping studies should help elucidate the pathogenesis of SLE and provide important information for the development of new therapies.**

Systemic lupus erythematosus (SLE) is an autoimmune disease characterized by overproduction of autoantibodies by B cells and breaking self tolerance of T cells and dendritic cells (DCs). Various immunologic abnormalities are involved in the development of SLE (1). For instance, we (2,3) and others (4–7) have described characteristic abnormalities of B cells in this disease. In particular, plasmablasts play a central role in the pathogenesis of SLE, through the production of anti–double-stranded DNA (anti-dsDNA) antibody (8). CD4+ T helper cells have an important role in disease progression and pathology (9). There is evidence of a predominance of the Th1 cell subset in patients with lupus nephritis (10) and of defects in the homeostatic

Supported in part by the Ministry of Health, Labor, and Welfare of Japan (Grant-in-Aid for Scientific Research), the Ministry of Education, Culture, Sports, Science, and Technology of Japan, and the University of Occupational and Environmental Health, Japan (UOEH Grant for Advanced Research).

Satoshi Kubo, MD, PhD, Shingo Nakayamada, MD, PhD, Maiko Yoshikawa, MD, Yusuke Miyazaki, MD, Kei Sakata, MS, Kazuhisa Nakano, MD, PhD, Kentaro Hanami, MD, PhD, Shigeru Iwata, MD, PhD, Ippei Miyagawa, MD, Kazuyoshi Saito, MD, PhD, Yoshiya Tanaka, MD, PhD: University of Occupational and Environmental Health, Kitakyushu, Japan.

Dr. Kubo has received speaking fees from Bristol-Myers Squibb (less than $10,000). Dr. Tanaka has received consulting fees, speaking fees, and/or honoraria from Mitsubishi Tanabe Pharma, Eisai, Pfizer, Abbott Immunology, Janssen, Takeda Industrial Pharma, Santen, AstraZeneca, Astellas, Asahi Kasei, UCB, and GlaxoSmithKline (less than $10,000 each) and from AbbVie and Chugai (more than $10,000 each) and research grants from Bristol-Myers Squibb, Mitsubishi Tanabe, MSD, Takeda Industrial Pharma, Astellas, Eisai, Chugai, Pfizer, and Daiichi-Sankyo.

Address correspondence to Yoshiya Tanaka, MD, PhD, First Department of Internal Medicine, School of Medicine, University of Occupational and Environmental Health, 1-1 Iseigaoka, Yahata-nishi-ku, Kitakyushu, Fukuoka 807-8555, Japan. E-mail: tanaka@med.uoeh-u.ac.jp.

Submitted for publication October 16, 2016; accepted in revised form June 8, 2017.

control of Th17 and natural Treg cell subpopulations contributing to SLE pathology (11). Moreover, follicular helper T cells (Tfh cells), which are an essential helper subset for B cell maturation (12), are increased in the peripheral blood (PB) of lupus patients (13). Furthermore, plasmacytoid DCs (14) and macrophages (15), which are involved in innate immunity, contribute to the initiation and perpetuation of autoimmunity in SLE.

Taken together, the above findings suggest that SLE is molecularly heterogeneous (16). Therefore, it would be difficult to manage every case based on one kinetic molecular theory. This is evidenced by the fact that targeted therapy has not yet been established in the treatment of SLE, although it has been used in the treatment of rheumatoid arthritis for as long as 20 years.

Based on these considerations, we "took a step back" from certain molecular changes reported in previous studies (2–4,9,14,15) and tried to obtain a broader perspective on the molecular heterogeneity in SLE by immunophenotyping. The heterogeneity of SLE raises 3 clinical questions: 1) What are the differences in immunophenotype between lupus patients and healthy individuals? 2) How do the immune cell phenotypes interact? 3) Can patients be divided into subgroups by immunophenotyping? To address these questions, PB mononuclear cells (PBMCs) were obtained from 143 patients with SLE. Circulating B cells, T cells, natural killer (NK) cells, and DCs were defined based on comprehensive flow cytometric analysis for human immunophenotyping, as described by the Human Immunology Project Consortium (17).

PATIENTS AND METHODS

Patients. Patients who fulfilled the American College of Rheumatology classification criteria for SLE (18) were enrolled in this study between December 2012 and February 2016. Age- and sex-matched healthy individuals were included as controls. The Human Ethics Review Committee of our university reviewed and approved the study, including the collection of PB samples from healthy controls and SLE patients.

Clinical measurements. Disease activity at baseline was assessed using the SLE Disease Activity Index (SLEDAI) (19,20) and the British Isles Lupus Assessment Group (BILAG) index (21–23) for organ involvement. Laboratory studies included testing for anti-dsDNA, anti-Sm, IgG, CH50, and C-reactive protein (CRP) levels, erythrocyte sedimentation rate (ESR), leukocyte count, and lymphocyte count. We also collected clinical data and samples after 24 weeks of treatment. Patients who required >2 different immunosuppressive therapies in addition to glucocorticoids were considered to have treatment-resistant disease.

Flow cytometric analysis. All patients in this study were enrolled in the FLOW registry, with immunophenotyping analysis performed by multicolor flow cytometry and the results recorded in the registry. PBMCs were isolated from PB samples using lymphocyte separation medium (ICN/Cappel). Next, PBMCs were resuspended in phosphate buffered saline (PBS)/3% human IgG (Baxter) in order to block Fc receptors and prevent nonspecific antibody binding, and then incubated for 15 minutes at 4°C in the dark. The cells were then washed with PBS containing 1% bovine serum albumin. Background fluorescence was assessed using appropriate isotype- and fluorochrome-matched control monoclonal antibodies. After staining with antibodies (described in Supplementary Table 1, on the *Arthritis & Rheumatology* web site at http://onlinelibrary.wiley.com/doi/10.1002/art.40180/abstract), the cells were assessed by multicolor flow cytometry (FACSVerse; BD Biosciences) and the data analyzed with FlowJo software (Tree Star). The phenotype of immune cell subsets was defined based on the Human Immunology Project protocol of comprehensive 8-color flow cytometric analysis proposed by National Institutes of Health/Federation of Clinical Immunology Societies (17), with some modification for detecting Tfh cells. Details of the gating strategy are shown in Supplementary Figures 1 and 2 (http://onlinelibrary.wiley.com/doi/10.1002/art.40180/abstract).

Study design. Differences in immunophenotype were evaluated in 143 SLE patients and 49 healthy individuals. To elucidate the diversity among patients with active lupus, 80 patients with severe organ involvement (≥1 feature from BILAG category A or ≥2 from BILAG category B) were identified from the overall group of 143 lupus patients, for principal components analysis (PCA) and cluster analysis. These 80 patients were receiving intensive treatment, such as cyclophosphamide plus glucocorticoids, and 55 of them remained in the study for the full 24-week follow-up period. Changes after treatment were analyzed in samples obtained from these 55 patients at 24 weeks. Supplementary Figure 3 (http://onlinelibrary.wiley.com/doi/10.1002/art.40180/abstract) presents this information in flowchart format.

PCA of immunophenotyping data. For easy exploration and visualization of immunophenotyping data, which contained many items, and for estimation of the correlation between variables, we used PCA to statistically aggregate items, reducing the number of observed variables into a smaller number of principal components and reducing the dimensionality of immunophenotyping data. We selected 2 eigenvectors with the highest eigenvalues as PC1 (eigenvalue 5.6) and PC2 (eigenvalue 3.7) based on each contribution rate, although all factors aggregated in 12 eigenvectors. The values for PC1 and PC2 were also calculated in individual SLE patients.

Cluster analysis of lupus patients. Cluster analyses were performed by the Ward method (24), using the immunophenotypes of SLE patients. We determined the number of clusters based on a scree plot, which showed the sum of within-cluster dissimilarities (Supplementary Figure 4, http://onlinelibrary.wiley.com/doi/10.1002/art.40180/abstract). The ordinate is the distance that was bridged to join the clusters at each step. There was a natural break where the distance jumps up suddenly, and we defined the break as the cut point. Consequently, we judged that the appropriate number of clusters was 3 and created a tree diagram.

Statistical analysis. Continuous data were expressed as the mean ± SD, and categorical data as the number (%). The significance of differences between groups was assessed by Student's *t*-test, with chi-square test used for nominal variables. Analysis of variance was performed among 3 groups. Multiple comparisons were performed by Games-Howell test

		SLE patients (n=143)	healthy control (n=49)	p value	
				univariate	multivariate
CD4+ T cells	Naive	46.7 ± 17.7	50.3 ± 13.8	0.15	
	Central memory	29.6 ± 10.2	33.7 ± 10.7	0.02	0.75
	Effector memory	19.0 ± 12.9	13.1 ± 8.2	<0.001	0.73
	TEMRA	4.2 ± 4.9	3.0 ± 4.8	0.12	
	Activated	9.8 ± 6.6	5.3 ± 2.2	<0.001	0.74
CD8+ T cells	Naive	48.0 ± 23.1	45.8 ± 20.0	0.57	
	Central memory	10.7 ± 12.2	9.7 ± 9.8	0.60	
	Effector memory	16.1 ± 13.1	20.3 ± 13.3	0.06	
	TEMRA	24.6 ± 19.4	24.6 ± 15.2	0.99	
	Activated	21.5 ± 14.7	9.3 ± 5.9	<0.001	0.68
CD4+ T cell subsets	Th1	20.2 ± 9.4	20.8 ± 5.3	0.59	
	Activated Th1	3.2 ± 2.9	1.3 ± 0.6	<0.001	0.06
	Th17	12.1 ± 4.9	11.8 ± 5.0	0.66	
	Activated Th17	0.9 ± 0.8	0.9 ± 0.5	0.72	
	Treg	**6.5 ± 2.8**	**4.3 ± 1.3**	<0.001	0.03
	Activated Treg	2.2 ± 1.6	1.3 ± 0.7	<0.001	
	Naive Treg	2.0 ± 1.4	1.2 ± 0.8	<0.001	
	Memory Treg	4.5 ± 2.4	3.0 ± 1.1	<0.001	
	Tfh	1.1 ± 0.7	0.8 ± 0.4	0.001	
	Activated Tfh	**0.4 ± 0.3**	**0.2 ± 0.1**	<0.001	0.03
B cells	Naive	52.8 ± 22.3	58.4 ± 14.5	0.05	
	IgM memory	**13.0 ± 6.6**	**22.9 ± 8.2**	<0.001	0.001
	Class-switched	**23.6 ± 18.7**	**13.2 ± 7.2**	<0.001	0.03
	Double negative	**10.7 ± 7.0**	**5.5 ± 1.9**	<0.001	0.04
	Plasmablast	**16.2 ± 14.3**	**3.3 ± 4.3**	<0.001	0.01
Monocytes	Classical	88.5 ± 7.2	89.3 ± 5.0	0.44	
	Non classical	10.3 ± 9.2	9.4 ± 4.6	0.37	
Dendritic cells	Myeloid	**0.6 ± 0.7**	**1.1 ± 0.5**	<0.001	0.003
	Plasmacytoid	0.1 ± 0.1	0.1 ± 0.1	0.51	
NK cells	CD16+	70.3 ± 23.6	64.3 ± 40.6	0.36	
	CD16-	**28.4 ± 23.6**	**18.0 ± 18.2**	0.01	0.01

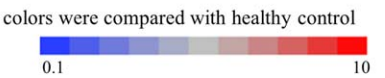

Figure 1. Differences in phenotypes of lymphocytes, monocytes, dendritic cells, and natural killer (NK) cells between patients with systemic lupus erythematosus (SLE) and age- and sex-matched healthy control subjects. Values are the mean ± SD percentage, with levels that were significantly different in the patient group compared with the healthy control group highlighted in color (blue for decreased; red for increased). *P* values in the univariate analysis were determined by Student's *t*-test. Multivariate analyses were performed using variables for which the *P* values in the univariate analysis were less than 0.05. TEMRA = terminally differentiated effector memory cells; Tfh = follicular helper T cells.

(if the samples were not homoscedastic) or Tukey's test (if the samples were homoscedastic). Pearson's correlation coefficient was used for correlation analysis. Multivariate analyses were conducted using variables that had *P* values of less than 0.05 in the univariate analysis. Paired *t*-tests were used to assess differences between baseline data and data measured at week 24 (with missing data). For assessment of statistical significance of the posttreatment data, nonparametric comparisons were used. *P* values less than 0.05 were considered significant. All analyses were conducted using JMP version 11.0 (SAS Institute) or SPSS version 22.0 (SPSS).

RESULTS

Baseline characteristics of the patients. Baseline characteristics of the study patients are shown in Supplementary Table 2 (http://onlinelibrary.wiley.com/doi/10.1002/art.40180/abstract). All were of Asian ethnicity. The mean age was 42.7 years, and most patients were women (89.5%). The mean duration of SLE was 9.5 years; mean disease activity scores at baseline were 11.0 (SLEDAI) and 11.7 (BILAG index). The proportion of patients with ≥1 BILAG category A feature or ≥2 BILAG category B features was 61.5%, although 71.3% of the patients were receiving concomitant immunosuppressive medications at baseline. Eight of the 88 patients with ≥1 BILAG category A feature or ≥2 BILAG category B features had some missing data and were not included in further analyses. Other laboratory findings included mean anti-dsDNA and IgG levels of 71.7 units/ml and 1,696 mg/dl, respectively, and a mean ESR of 49.1 mm/hour.

Peripheral immune cell phenotype in the patients with SLE. The immunophenotypes of PB from patients with SLE are shown in Figure 1. Higher proportions of effector memory and activated CD4+ T cells, and a lower proportion of central memory CD4+ T cells, were

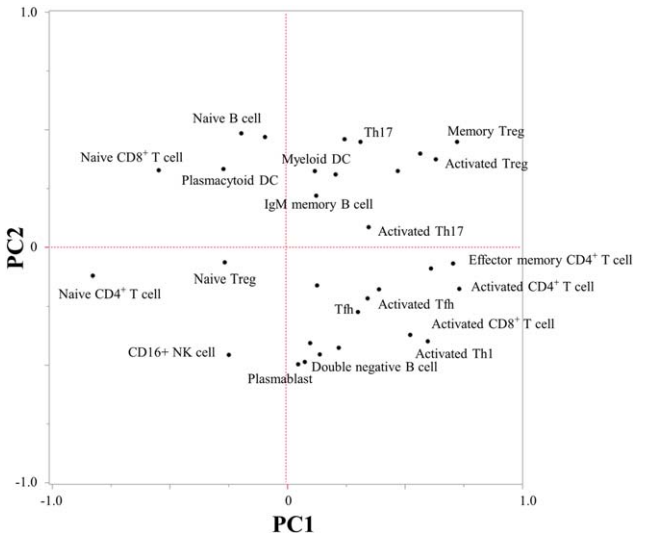

Figure 2. Results of principal components (PC) analysis based on immune cell phenotypes in patients with systemic lupus erythematosus. Each immunophenotype was visualized in 2 dimensions. DC = dendritic cells; NK = natural killer; Tfh = follicular helper T cells.

found in SLE patients compared with healthy subjects. Similarly, the proportions of activated CD8+ T cells were higher in SLE patients. We next assessed the properties of functional subsets of CD4+ T cells, such as Th1, Th17, Treg, and Tfh cells. Among them, proportions of Treg cells, Tfh cells, activated Th1 cells, activated Treg cells, and activated Tfh cells were higher in SLE patients compared with controls, but no differences in proportions of Th1 and Th17 cells were observed between groups.

Assessment of B cell subsets revealed that the proportion of IgM memory B cells was lower, while that of class-switched memory B cells and IgD–CD27– (double-negative) B cells was higher, in SLE patients than in healthy subjects. Of note, the largest difference in all immune cell phenotypes was observed in the proportion of plasmablasts (16.2% in patients and 3.3% in controls) (Figure 1).

With regard to DCs, the percentage of myeloid DCs was lower among patients compared with controls, while that of plasmacytoid DCs did not differ between the groups. For NK cells, the proportion of CD16– NK cells was higher in SLE patients, whereas the proportions of monocyte subsets did not differ.

We also investigated the correlation between various immune cells and clinical findings. The percentages of activated CD8+ T cells correlated with the SLEDAI, and the percentages of activated CD8+ T cells and plasmablasts correlated with the BILAG index. The proportion of Tfh cells correlated with serum IgG level, and the proportion of activated Tfh cells correlated with serum anti-Sm antibody level and IgG level. Detailed results are shown in Supplementary Tables 3 and 4 (http://onlinelibrary.wiley.com/doi/10.1002/art.40180/abstract).

PCA based on immunophenotype. For easier exploration and visualization of these immunophenotypes, we attempted to identify patterns using 2-dimensional PCA (Figure 2) as well as 3-dimensional PCA (Supplementary Figure 5, http://onlinelibrary.wiley.com/doi/10.1002/art.40180/abstract). Immunophenotypes were statistically aggregated to the PCs. The results showed that the first factor from the PCA (PC1) was associated with T cell phenotype. The positive side of PC1 contained effector memory CD4+ T cells, activated CD4+ T cells, and activated CD8+ T cells, while the negative side contained naive CD4+ T cells and naive CD8+ T cells. In contrast, PC2 was mainly associated with B cell phenotype. The positive side of PC2 contained naive B cells, while the negative side contained plasmablasts and double-negative B cells (Figure 2 and Supplementary Figure 6 [http://onlinelibrary.wiley.com/doi/10.1002/art.40180/abstract]).

Moreover, we were able to clarify the correlations among immunophenotypes by focusing on the distances between variables (Figure 2). Among these correlations, Th17 and Treg cells were statistically close and showed positive correlation ($P < 0.001$). Furthermore, Tfh and Th1 cells were also statistically close and showed positive correlation ($P = 0.04$). The same pattern was also noted for Tfh cells and plasmablasts ($P = 0.02$). The results of PCA indicated that the immunophenotype of SLE patients consists of T cell axis and B cell axis abnormalities.

Statistical cluster analysis based on immunophenotype in SLE. Because SLE is molecularly heterogeneous, targeting of 1 molecule is not an appropriate treatment strategy. Therefore, we next attempted to identify subgroups among the 80 SLE patients with severe organ involvement (≥1 feature in BILAG category A or ≥2 features in BILAG category B).

Cluster analysis revealed that the patients with active SLE could be classified into 3 subgroups (Figure 3A). The values in PC1, which was associated with T cell phenotype, and PC2, which was associated with B cell phenotype, in individual patients in the 3 groups are plotted in Figure 3B. The PCA score plot confirmed that SLE patients were clearly separated and localized into 3 regions according to these 2 axes. In addition, if we combined SLE patients and healthy controls in one cluster analysis, the immunophenotype of SLE formed a separate cluster from that of healthy subjects (Supplementary Figure 7, on the *Arthritis & Rheumatology* web

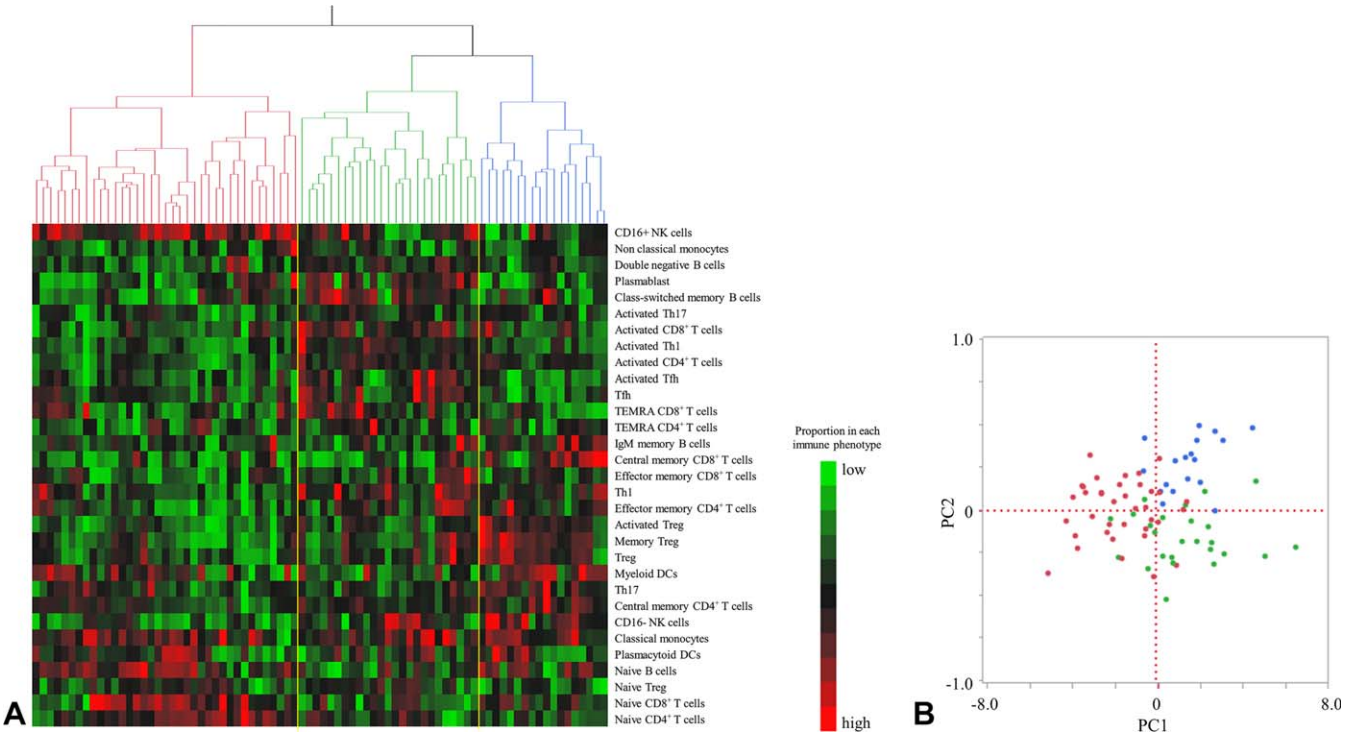

Figure 3. Results of statistical cluster analysis based on immune cell phenotypes in patients with systemic lupus erythematosus. **A,** Hierarchical statistical clustering of lupus patients. Subgroups are colored red, green, and blue. **B,** PC1 and PC2 values in individual patients in the 3 subgroups. TEMRA = terminally differentiated effector memory cells (see Figure 2 for other definitions).

site at http://onlinelibrary.wiley.com/doi/10.1002/art.40180/abstract).

Next, we explored the immunologic features of the 3 subgroups (Figure 4 and Supplementary Table 5 [http://onlinelibrary.wiley.com/doi/10.1002/art.40180/abstract]). High proportions of plasmablasts were seen in all groups, to varying extents. However, in 1 group, few changes in T cell differentiation and activation were seen. In particular, the increase in Tfh and Treg cells that was seen among the SLE patients overall was not observed in this group (termed the T cell–independent group). The second group, in which the percentage of plasmablasts was the highest, also had high percentages of Tfh and activated Tfh cells; these elevated percentages appeared in this group exclusively (termed the Tfh-dominant group). In addition, the proportion of activated Th1 cells was the highest in this group. Finally, the third group (termed the Treg-dominant group) exhibited the highest proportions of Th17, activated Treg, and memory Treg cells. Additionally, the proportion of plasmablasts was lower in this group than in either of the other SLE groups (though still increased compared with healthy controls).

Clinical features of the SLE patients in each of the subgroups identified are shown in Table 1 and Supplementary Table 6 (http://onlinelibrary.wiley.com/doi/10.1002/art.40180/abstract). There were significant differences in IgG levels (mean 1,720.5 mg/dl, 1,888.9 mg/dl, and 1,270.5 mg/dl) and leukocyte counts (mean 4,697.3/ml, 4,172.0/ml, and 7,955.6/ml among the T cell–independent group, the Tfh-dominant group, and the Treg-dominant group, respectively). However, disease activity indices, such as the SLEDAI and the BILAG index, were comparable (Table 1), as was the presence of renal and neurologic manifestations (data not shown). These findings indicate that immunologic features were different even among patients with similar clinical features. Indeed it was difficult to distinguish subgroups according to clinical features.

Effects of immunosuppressive therapy. Finally, we investigated changes in peripheral immune cell phenotypes after 24-week treatment with cyclophosphamide, mycophenolate mofetil, or calcineurin, in addition to high-dose glucocorticoids. Treatment resulted in decreases in the proportions of plasmablasts as well as double-negative B cells, activated CD8+ T cells, and Tfh cells (Supplementary Table 7 [http://onlinelibrary.wiley.com/doi/10.1002/art.40180/abstract]).

Next we assessed the effects of treatment in the 3 groups (Supplementary Figure 8 and Supplementary

		T cell independent (group red) (n=37)	Tfh dominant (group green) (n=25)	Treg dominant (group blue) (n=18)	p value	
					univariate	multivariate
CD4+ T cells	Naive	55.0 ± 16.1	40.3 ± 16.5	35.8 ± 13.5	<0.001	0.55
	Central memory	27.2 ± 9.4	30.5 ± 7.2	35.6 ± 12.7	0.01	0.82
	Effector memory	14.4 ± 10.1	25.1 ± 14.6	24.4 ± 13.5	<0.001	0.76
	TEMRA	3.4 ± 2.3	4.1 ± 2.7	3.8 ± 2.0	0.60	
	Activated	7.0 ± 3.6	**14.2 ± 6.7**	11.9 ± 5.2	<0.001	<0.001
CD8+ T cells	Naive	54.4 ± 23.0	33.1 ± 19.5	43.5 ± 16.2	<0.001	0.22
	Central memory	7.8 ± 8.7	7.7 ± 8.4	24.1 ± 17.5	<0.001	0.08
	Effector memory	13.3 ± 10.5	21.7 ± 17.2	16.1 ± 8.6	0.04	0.77
	TEMRA	24.4 ± 19.4	35.9 ± 22.2	15.9 ± 12.2	<0.001	0.69
	Activated	17.9 ± 11.1	**35.9 ± 14.7**	23.0 ± 15.6	<0.001	<0.001
CD4+ T cell subsets	Th1	16.6 ± 8.2	**25.5 ± 9.9**	22.3 ± 8.0	<0.001	0.01
	Activated Th1	2.2 ± 1.4	5.5 ± 3.8	2.6 ± 1.8	<0.001	
	Th17	11.8 ± 4.6	11.2 ± 3.5	15.9 ± 5.4	<0.001	0.06
	Activated Th17	0.7 ± 0.5	1.0 ± 0.6	1.0 ± 0.5	0.06	
	Treg	5.6 ± 2.0	7.1 ± 2.7	**9.2 ± 3.0**	<0.001	0.002
	Activated Treg	1.5 ± 0.9	2.3 ± 1.3	4.1 ± 2.2	<0.001	
	Naive Treg	2.1 ± 1.2	2.3 ± 1.3	1.4 ± 0.8	0.05	
	Memory Treg	3.5 ± 1.8	4.8 ± 2.5	7.8 ± 2.6	<0.001	
	Tfh	1.0 ± 0.5	**1.7 ± 0.9**	0.8 ± 0.5	<0.001	<0.001
	Activated Tfh	0.4 ± 0.2	0.7 ± 0.5	0.3 ± 0.2	<0.001	
B cells	Naive	59.1 ± 19.1	36.0 ± 19.9	50.5 ± 23.7	<0.001	0.74
	IgM memory	11.6 ± 5.3	12.9 ± 6.8	16.7 ± 7.7	0.03	0.08
	Class-switched	19.7 ± 14.3	38.1 ± 20.4	23.8 ± 19.7	<0.001	0.86
	Double negative	9.6 ± 7.5	12.9 ± 5.8	9.0 ± 4.3	0.08	
	Plasmablast	16.4 ± 14.7	**29.9 ± 16.5**	12.1 ± 10.4	<0.001	0.004
Monocytes	Classical	88.7 ± 8.4	89.0 ± 7.3	89.6 ± 5.2	0.90	
	Non classical	11.3 ± 14.5	9.1 ± 6.9	8.9 ± 4.8	0.64	
Dendritic cells	Myeloid	0.4±0.3	0.3±0.4	0.7±0.8	0.08	
	Plasmacytoid	0.1±0.1	0.1±0.1	0.1±0.0	0.26	
NK cells	CD16+	77.9 ± 13.6	59.0 ± 25.3	47.2 ± 25.7	<0.001	
	CD16-	20.7 ± 13.2	39.6 ± 25.1	51.4 ± 26.3	<0.001	<0.001

colors were compared with healthy control

Figure 4. Results of statistical cluster analysis based on immune cell phenotypes in patients with systemic lupus erythematosus, classified into the 3 subgroups that were identified. Baseline immunophenotypes in each group are shown. Values are the mean ± SD percentage, with levels that were significantly different in the patient group compared with the healthy control group highlighted in color (blue for decreased; red for increased). *P* values in the univariate analysis were determined by one-way analysis of variance. Multinomial logistic regression analyses were performed using variables for which the *P* values in the univariate analysis were less than 0.05. See Figure 1 for definitions.

Table 8 [http://onlinelibrary.wiley.com/doi/10.1002/art.40180/abstract]). Treatment resulted in markedly decreased proportions of plasmablasts and Tfh cells in the Tfh-dominant group, with the levels of these cells becoming comparable with those in the other groups. Other phenotypes showed the same tendency, i.e., became closer to normal after treatment. However, the features of each group were still evident (e.g., high proportion of activated Treg cells in the Treg-dominant group). Furthermore, cluster analysis revealed that the immunophenotypes of SLE patients remained different from those of healthy controls even after treatment of the patients (Supplementary Figure 9 [http://onlinelibrary.wiley.com/doi/10.1002/art.40180/abstract]). However, specific changes were not associated with specific treatments, apart from rituximab (Supplementary Figure 10 [http://onlinelibrary.wiley.com/doi/10.1002/art.40180/abstract]).

Table 2 shows the clinical changes after treatment, in the patients grouped according to SLE immunophenotype. Treatment resulted in marked improvement in disease activity indices, such as the SLEDAI and the BILAG index, and the extent of the reduction was comparable among the 3 groups. Other clinical improvements, such as changes in anti-dsDNA, IgG, CH50, and CRP levels and ESR, were also comparable. However, the proportion of SLE patients whose disease was resistant to treatment was highest among the Tfh-dominant group (Table 2).

Table 1. Baseline characteristics of the SLE patients grouped according to cluster analysis*

	T cell–independent group (n = 37)	Tfh-dominant group (n = 25)	Treg-dominant group (n = 18)	*P*	
				Univariate	Multivariate
Age, years	42.1 ± 16.9	44.4 ± 16.8	49.7 ± 17.6	0.30	
Sex, no. (%) female	36 (97.3)	20 (80.0)	15 (83.3)	0.08	
Disease duration, years	9.9 ± 11.0	7.7 ± 8.7	13.6 ± 11.7	0.19	
SLEDAI	15.8 ± 8.4	14.4 ± 8.2	13.7 ± 8.5	0.64	
BILAG	17.2 ± 9.5	17.7 ± 8.8	17.0 ± 10.2	0.97	
BILAG A1 or B2, no. (%)	37 (100)	25 (100)	18 (100)	1.00	
ANA, no. (%) positive	34 (91.9)	23 (92.0)	16 (88.9)	0.26	
Anti-dsDNA, units/ml	86.8 ± 123.8	106.3 ± 141.9	40.6 ± 54.3	0.05	0.51
Anti-dsDNA, no. (%) positive	17 (45.9)	9 (36.0)	9 (50.0)	1.00	
Anti-Sm, units/ml	78.3 ± 183.3	50.3 ± 123.4	11.3 ± 35.4	0.07	
Anti-Sm, no. (%) positive	24 (64.9)	15 (60.0)	14 (77.8)	0.31	
IgG, mg/dl	1,720.5 ± 614.8	1,888.9 ± 1,003.6	1,270.5 ± 509.7	0.03	0.05
CH50, units/ml	36.9 ± 17.1	33.3 ± 18.4	36.7 ± 15.3	0.69	
CRP, mg/dl	0.9 ± 2.1	1.3 ± 3.1	1.6 ± 4.4	0.77	
ESR, mm/hour	49.9 ± 29.5	68.5 ± 38.5	47.4 ± 30.5	0.05	0.11
Leukocyte count, /ml	4,697.3 ± 1,956.8	4,172.0 ± 2,699.3	7,955.6 ± 4,795.2	0.02	0.84
Lymphocyte count, /ml	765.8 ± 430.5	693.3 ± 512.8	815.5 ± 500.0	0.69	

* Except where indicated otherwise, values are the mean ± SD. SLE = systemic lupus erythematosus; Tfh = follicular helper T cell; SLEDAI = SLE Disease Activity Index; BILAG = British Isles Lupus Assessment Group; ANA = antinuclear antibody; anti-dsDNA = anti–double-stranded DNA; CRP = C-reactive protein; ESR = erythrocyte sedimentation rate.

DISCUSSION

In rheumatoid arthritis, targeted therapy has made it possible to induce remission in many patients, leading to a paradigm shift in treatment of that disease (25). However, there has been no published evidence of such an effect of targeted therapy in SLE. Due to the molecular heterogeneity among lupus patients, several clinical trials of potential treatments demonstrated no improvement in patients with SLE (26–29). To assess the molecular heterogeneity in SLE, we conducted the present study using PBMCs from SLE patients.

Various phenotype differences were observed among patients with SLE. In addition, there were some correlations between clinical parameters and peripheral cell phenotypes. For instance, the proportion of Tfh cells correlated with the titer of IgG, and that of activated Tfh cells correlated with anti-Sm antibody levels. This might indicate an interaction between activated Tfh and long-lived plasma cells, which promote the production of autoantibodies such as anti-Sm. Furthermore, the proportions of plasmablasts correlated with organ involvement. A landmark study investigating the blood transcriptome of 158 SLE patients identified

Table 2. Characteristics of the patients in each cluster after treatment*

	T cell–independent group (n = 24)	Tfh-dominant group (n = 10)	Treg-dominant group (n = 11)
SLEDAI	1.8 ± 3.8	2.4 ± 3.4	2.2 ± 2.6
BILAG	1.6 ± 4.0	2.1 ± 4.0	1.4 ± 1.4
BILAG A1 or B2, %	4.2	10.0	0.0
Treatment resistant, %	4.2	30.0†	0.0
Anti-dsDNA, units/ml‡	9.9 ± 11.5	8.5 ± 7.9	33.3 ± 86.6
Anti-dsDNA positive, %‡	15.0	10.0	20.0
IgG, mg/dl	977 ± 285.3	722.4 ± 174.3	919.0 ± 325.5
CH50, units/ml	54.6 ± 7.4	53.0 ± 12.2	53.7 ± 10.1
CRP, mg/dl	0.0 ± 0.1	0.2 ± 0.4	0.8 ± 1.8
ESR, mm/hour	19.2 ± 18.3	19.3 ± 15.5	25.9 ± 27.7
Leukocyte count, /ml	7,533.3 ± 2,845.2	6,320.0 ± 1,334.0	8,050.0 ± 2,099.9
Lymphocyte count, /ml	1,083.7 ± 666.8	910.7 ± 508.1	949.2 ± 595.1

* Except where indicated otherwise, values are the mean ± SD. See Table 1 for definitions.
† $P = 0.03$ versus each of the other groups, by chi-square test.
‡ Data not available for 4 patients in the T cell–independent group and 1 patient in the Treg-dominant group.

plasmablast signature as the most robust biomarker of disease activity (16). Although the methodology was different, our findings are broadly consistent with the results of that RNA transcriptome analysis.

PCA demonstrated interactions among immunophenotypes in SLE. These interactions were also described in previous reports. For example, an earlier study showed a negative correlation between proportions of Th17 and naive Treg cells (11). Our study also showed that Th17 and naive Treg cells were at opposite sites of the PCA graph (Figure 2). Meanwhile, the result that Th17 and activated Treg cells were statistically close indicates the plasticity of Th17 and Treg cells (30,31). Similar to the results of many in vivo and in vitro studies showing the importance of Tfh cells in B cell differentiation and pathogenesis of autoimmunity (12,32), our data confirmed the importance of the Tfh cell–plasmablast axis in SLE.

In this study, SLE patients could be stratified statistically by immunophenotyping, resulting in 3 immunologic subgroups (the T cell–independent group, the Tfh-dominant group, and the Treg-dominant group), although these clusters have not been validated. The finding that plasmablast proportions were elevated in all 3 groups highlights the fundamental role of plasmablasts in SLE. Further analysis of the 3 groups showed that in the first group (T cell–independent group), there were no characteristic features other than increased plasmablast proportions. Therefore, the most important factor in the pathogenesis of SLE in this group is uncertain. It is possible that neutrophils, which are not included in PBMCs and were not investigated in this study, could play a role in this group. A high percentage of Tfh cells was especially noted in the second group (Tfh-dominant group). The proportion of plasmablasts in this group was also particularly high, and almost all T cells were activated. Moreover, among patients in this group, SLE was resistant to conventional treatment. The third group (Treg-dominant group) had high proportions of activated Treg and memory Treg cells and low proportions of naive Treg cells. Thus, plasticity of Th17 and Treg cells might play an important role in the Treg-dominant group.

Our study has several limitations. First, it was exploratory and was not validated by investigation of other cohorts. Moreover, some of the patients dropped out after treatment and thus could not be included in the follow-up analyses. However, immunophenotypes that had been assessed differently at each institution were standardized through the Human Immunology Project, and this facilitated the comparison of reports from different institutions. Thus, it should be possible to conduct further studies to validate our results. Next, we did not investigate neutrophils. Although abnormality of neutrophil extracellular traps has been reported to play a role in the pathogenesis of SLE (33,34), it is difficult to study neutrophils. Finally, we did not investigate secondary lymphoid tissue or actual inflammatory lesions.

Despite these limitations, our results indicate that immunologic abnormalities are not specific in any single SLE patient. However, each abnormality was enhanced by subdividing SLE patients. In other words, the phenotype of lymphocytes was different among the patients, although these patients had similar disease activity. Accumulation of further evidence along these lines will not only contribute to the elucidation of the pathogenesis of SLE, but also help in the development of new treatments.

ACKNOWLEDGMENTS

The authors thank Ms N. Sakaguchi for excellent technical assistance and Dr. F. G. Issa (Word-Medex, Sydney, Australia) for English language proofreading.

AUTHOR CONTRIBUTIONS

All authors were involved in drafting the article or revising it critically for important intellectual content, and all authors approved the final version to be published. Dr. Kubo had full access to all of the data in the study and takes responsibility for the integrity of the data and the accuracy of the data analysis.

Study conception and design. Kubo, Nakayamada, Tanaka.

Acquisition of data. Kubo, Yoshikawa, Miyazaki, Sakata.

Analysis and interpretation of data. Kubo, Nakayamada, Yoshikawa, Miyazaki, Nakano, Hanami, Iwata, Miyagawa, Saito, Tanaka.

REFERENCES

1. Kaul A, Gordon C, Crow MK, Touma Z, Urowitz MB, van Vollenhoven R, et al. Systemic lupus erythematosus. Nat Rev Dis Primers 2016;2:16039.
2. Iwata S, Yamaoka K, Niiro H, Jabbarzadeh-Tabrizi S, Wang SP, Kondo M, et al. Increased Syk phosphorylation leads to overexpression of TRAF6 in peripheral B cells of patients with systemic lupus erythematosus. Lupus 2015;24:695–704.
3. Nakayamada S, Iwata S, Tanaka Y. Relevance of lymphocyte subsets to B cell-targeted therapy in systemic lupus erythematosus. Int J Rheum Dis 2015;18:208–18.
4. Sanz I, Lee FE. B cells as therapeutic targets in SLE. Nat Rev Rheumatol 2010;6:326–37.
5. Lipsky PE. Systemic lupus erythematosus: an autoimmune disease of B cell hyperactivity. Nat Immunol 2001;2:764–6.
6. Wei C, Anolik J, Cappione A, Zheng B, Pugh-Bernard A, Brooks J, et al. A new population of cells lacking expression of CD27 represents a notable component of the B cell memory compartment in systemic lupus erythematosus. J Immunol 2007; 178:6624–33.
7. Sanz I, Wei C, Lee FE, Anolik J. Phenotypic and functional heterogeneity of human memory B cells. Semin Immunol 2008;20: 67–82.
8. Jacobi AM, Mei H, Hoyer BF, Mumtaz IM, Thiele K, Radbruch A, et al. HLA-DR^{high}/CD27^{high} plasmablasts indicate active disease in patients with systemic lupus erythematosus. Ann Rheum Dis 2010;69:305–8.

9. Crispin JC, Kyttaris VC, Terhorst C, Tsokos GC. T cells as therapeutic targets in SLE. Nat Rev Rheumatol 2010;6:317–25.
10. Akahoshi M, Nakashima H, Tanaka Y, Kohsaka T, Nagano S, Ohgami E, et al. Th1/Th2 balance of peripheral T helper cells in systemic lupus erythematosus. Arthritis Rheum 1999;42:1644–8.
11. Yang J, Chu Y, Yang X, Gao D, Zhu L, Yang X, et al. Th17 and natural Treg cell population dynamics in systemic lupus erythematosus. Arthritis Rheum 2009;60:1472–83.
12. Craft JE. Follicular helper T cells in immunity and systemic autoimmunity. Nat Rev Rheumatol 2012;8:337–47.
13. Simpson N, Gatenby PA, Wilson A, Malik S, Fulcher DA, Tangye SG, et al. Expansion of circulating T cells resembling follicular helper T cells is a fixed phenotype that identifies a subset of severe systemic lupus erythematosus. Arthritis Rheum 2010;62:234–44.
14. Blanco P, Palucka AK, Gill M, Pascual V, Banchereau J. Induction of dendritic cell differentiation by IFN-α in systemic lupus erythematosus. Science 2001;294:1540–3.
15. Hill GS, Delahousse M, Nochy D, Remy P, Mignon F, Mery JP, et al. Predictive power of the second renal biopsy in lupus nephritis: significance of macrophages. Kidney Int 2001;59:304–16.
16. Banchereau R, Hong S, Cantarel B, Baldwin N, Baisch J, Edens M, et al. Personalized immunomonitoring uncovers molecular networks that stratify lupus patients. Cell 2016;165:551–65.
17. Maecker HT, McCoy JP, Nussenblatt R. Standardizing immunophenotyping for the Human Immunology Project. Nat Rev Immunol 2012;12:191–200.
18. Hochberg MC. Updating the American College of Rheumatology revised criteria for the classification of systemic lupus erythematosus [letter]. Arthritis Rheum 1997;40:1725.
19. Petri M, Orbai AM, Alarcon GS, Gordon C, Merrill JT, Fortin PR, et al. Derivation and validation of the Systemic Lupus International Collaborating Clinics classification criteria for systemic lupus erythematosus. Arthritis Rheum 2012;64:2677–86.
20. Bombardier C, Gladman DD, Urowitz MB, Caron D, Chang CH, and the Committee on Prognosis Studies in SLE. Derivation of the SLEDAI: a disease activity index for lupus patients. Arthritis Rheum 1992;35:630–40.
21. Symmons DP, Coppock JS, Bacon PA, Bresnihan B, Isenberg DA, Maddison P, et al, and Members of the British Isles Lupus Assessment Group (BILAG). Development and assessment of a computerized index of clinical disease activity in systemic lupus erythematosus. Q J Med 1988;69:927–37.
22. Stoll T, Stucki G, Malik J, Pyke S, Isenberg DA. Further validation of the BILAG disease activity index in patients with systemic lupus erythematosus. Ann Rheum Dis 1996;55:756–60.
23. Isenberg DA, Rahman A, Allen E, Farewell V, Akil M, Bruce IN, et al. BILAG 2004: development and initial validation of an updated version of the British Isles Lupus Assessment Group's disease activity index for patients with systemic lupus erythematosus. Rheumatology (Oxford) 2005;44:902–6.
24. Ward JH. Hierarchical grouping to optimize an objective function. J Am Stat Assoc 1963;58:236–44.
25. Scott DL, Wolfe F, Huizinga TW. Rheumatoid arthritis. Lancet 2010;376:1094–108.
26. Merrill JT, Neuwelt CM, Wallace DJ, Shanahan JC, Latinis KM, Oates JC, et al. Efficacy and safety of rituximab in moderately-to-severely active systemic lupus erythematosus: the Randomized, Double-Blind, Phase II/III Systemic Lupus Erythematosus Evaluation of Rituximab trial. Arthritis Rheum 2010;62:222–33.
27. Rovin BH, Furie R, Latinis K, Looney RJ, Fervenza FC, Sanchez-Guerrero J, et al. Efficacy and safety of rituximab in patients with active proliferative lupus nephritis: the Lupus Nephritis Assessment with Rituximab study. Arthritis Rheum 2012;64:1215–26.
28. Cardiel MH, Tumlin JA, Furie RA, Wallace DJ, Joh T, Linnik MD, et al. Abetimus sodium for renal flare in systemic lupus erythematosus: results of a randomized, controlled phase III trial. Arthritis Rheum 2008;58:2470–80.
29. Merrill JT, Burgos-Vargas R, Westhovens R, Chalmers A, D'Cruz D, Wallace DJ, et al. The efficacy and safety of abatacept in patients with non–life-threatening manifestations of systemic lupus erythematosus: results of a twelve-month, multicenter, exploratory, phase IIb, randomized, double-blind, placebo-controlled trial. Arthritis Rheum 2010;62:3077–87.
30. Koenen HJ, Smeets RL, Vink PM, van Rijssen E, Boots AM, Joosten I. Human $CD25^{high}Foxp3^{pos}$ regulatory T cells differentiate into IL-17-producing cells. Blood 2008;112:2340–52.
31. Kleinewietfeld M, Hafler DA. The plasticity of human Treg and Th17 cells and its role in autoimmunity. Semin Immunol 2013;25:305–12.
32. Linterman MA, Rigby RJ, Wong RK, Yu D, Brink R, Cannons JL, et al. Follicular helper T cells are required for systemic autoimmunity. J Exp Med 2009;206:561–76.
33. Villanueva E, Yalavarthi S, Berthier CC, Hodgin JB, Khandpur R, Lin AM, et al. Netting neutrophils induce endothelial damage, infiltrate tissues, and expose immunostimulatory molecules in systemic lupus erythematosus. J Immunol 2011;187:538–52.
34. Kaplan MJ. Role of neutrophils in systemic autoimmune diseases. Arthritis Res Ther 2013;15:219.

ARTHRITIS & RHEUMATOLOGY
Vol. 69, No. 10, October 2017, pp 2038–2051
DOI 10.1002/art.40182

Increased CCL25 and T Helper Cells Expressing CCR9 in the Salivary Glands of Patients With Primary Sjögren's Syndrome

Potential New Axis in Lymphoid Neogenesis

Sofie L. M. Blokland,[1] Maarten R. Hillen,[1] Aike A. Kruize,[1] Stephan Meller,[2] Bernhard Homey,[2] Glennda M. Smithson,[3] Timothy R. D. J. Radstake,[1] and Joel A. G. van Roon[1]

Objective. **Follicular helper T (Tfh) cells play a critical role in germinal center formation and B cell activation, both of which are hallmarks of primary Sjögren's syndrome (SS). CCR9-expressing T helper cells have "Tfh-like" characteristics and their numbers are increased at mucosa-associated sites in several inflammatory conditions. Because the characteristics of these cells are unique and evaluation has been limited, this study was undertaken to investigate the local and systemic CCL25/CCR9 axis in patients with primary SS.**

Methods. **Levels of CCL25 protein and messenger RNA (mRNA) and CCR9+ T helper cells were evaluated in the labial salivary glands (LSGs) of patients with primary SS and patients with sicca syndrome without a diagnosis of primary SS (non-SS sicca controls). CCL25 levels were assessed for correlation with parameters of inflammation and clinical features. Circulating CCR9+ and CXCR5+ T helper cells were compared on the basis of phenotypic and functional properties.**

Results. **CCL25 protein and mRNA levels were elevated in the LSGs of patients with primary SS as compared to non-SS sicca controls. Increased levels of CCL25 were associated with B cell hyperactivity, autoimmunity, and levels of interleukin-21 (IL-21) and soluble IL-7 receptor α-chain (IL-7Rα). Furthermore, the frequency of CCR9-expressing cells in the LSGs was increased and levels of circulating CCR9+ T helper cells expressing programmed death 1 and inducible T cell costimulator were elevated in patients with primary SS. CCR9+ T helper cells displayed higher expression of IL-7Rα and secreted higher levels of interferon-γ, IL-17, IL-4, and IL-21 as compared to CXCR5+ T helper cells, ex vivo and upon triggering with antigen or IL-7. Both CCR9+ and CXCR5+ T helper cells induced IgG production by B cells more potently than that induced in the cultures with CCR9−CXCR5− T helper cells.**

Conclusion. **Enhanced expression of CCL25 in LSGs of patients with primary SS can facilitate attraction of CCR9+ T helper cells, and these cells secrete high levels of proinflammatory cytokines when triggered with antigen or IL-7. The observed associations with B cell hyperactivity, autoimmunity, and markers of lymphoid neogenesis indicate that the CCL25/CCR9 axis plays a significant role in the immunopathology of primary SS, suggesting that this axis could represent a novel therapeutic target for the disease.**

Primary Sjögren's syndrome (SS) is characterized by inflammation of the exocrine glands, with features mainly involving dryness of the eyes and mouth. A hallmark feature of primary SS is B cell hyperactivity, which is reflected by production of autoantibodies, elevated levels of serum IgG, and an increased risk of lymphoma

Supported by Takeda Pharmaceuticals.
[1]Sofie L. M. Blokland, MD, Maarten R. Hillen, PhD, Aike A. Kruize, MD, PhD, Timothy R. D. J. Radstake, MD, PhD, Joel A. G. van Roon, PhD: University Medical Center Utrecht, Utrecht, The Netherlands; [2]Stephan Meller, MD, Bernhard Homey, MD, PhD: University of Düsseldorf, Düsseldorf, Germany; [3]Glennda M. Smithson, PhD: Takeda Pharmaceuticals International, Chicago, Illinois.

Address correspondence to Timothy R. D. J. Radstake, MD, PhD or Joel A. G. van Roon, PhD: University Medical Center Utrecht, Heidelberglaan 100, 3584 CX, Utrecht F02.127, The Netherlands. E-mail: T.R.D.J.Radstake@umcutrecht.nl or J.vanRoon@umcutrecht.nl.

Submitted for publication October 18, 2016; accepted in revised form June 13, 2017.

development (in ~10% of patients) (1,2). Both the presence of germinal centers (GCs) and a high number of lymphocytic infiltrates in the salivary glands are associated with lymphoma development (3,4).

Follicular helper T (Tfh) cells are potent B cell–stimulating cells and reside in GCs in the lymph nodes. Tfh cells are characterized by expression of Bcl-6, CXCR5, inducible T cell costimulator (ICOS), programmed death 1 (PD-1), and cytokines such as interleukin-21 (IL-21), IL-4, and CXCL13, which attracts CXCR5+ Tfh cells and CXCR5+ B cells (5,6). Tfh cells are elevated in the peripheral blood of patients with primary SS, and the frequency of Tfh cells correlates with autoantibody production, disease severity, and presence of aberrant memory B cell and plasma cell subsets. Expression of IL-21, IL-4, and CXCL13 as well as the numbers of Tfh cells are increased in the salivary glands of patients with primary SS (7–10).

McGuire et al recently described a novel CD4+ T helper cell subset that has characteristics similar to those of Tfh cells, including the production of IL-21, expression of ICOS and Bcl-6, and expression of the chemokine receptor CCR9, but not CXCR5. These CCR9+ T helper cells are therefore called "Tfh-like" cells (11). Both in mice and in humans, CCR9+ T helper cells are present in secondary lymphoid organs (12,13). In humans, CCR9+ T helper cells produce high levels of interferon-γ (IFNγ) in addition to high levels of IL-17, IL-10, and IL-4. Moreover, these cells induce robust B cell responses (12,14,15). They specifically migrate to mucosal sites in response to the chemokine CCL25 (also known as thymus-expressed chemokine, or TECK) (16,17). CCR9+ T helper cells are important for the maintenance of mucosal immune homeostasis, but also may have a function in mucosal inflammation, potentially contributing to inflammatory bowel disease (IBD) and primary sclerosing cholangitis (18–20). Increased numbers of CCR9-expressing cells have been found in the peripheral blood and inflamed intestinal tissue of patients with Crohn's disease, and elevated production of CCL25 has also been observed at sites of inflammation (21,22). Inhibition of CCR9 decreased intestinal inflammation in a mouse model of ileitis. In patients with Crohn's disease, inconsistent results with regard to the inhibition of CCR9 have been demonstrated, possibly because the pharmacokinetic properties of this small-molecule therapy are poor (23–25).

Recently, in NOD mice, CCR9+ T cells were also shown to mediate immunopathologic processes in mucosa-associated tissue from accessory organs of the digestive tract, including the pancreas and salivary glands. The NOD mice spontaneously developed primary SS–like symptoms and exhibited infiltration of IL-21–expressing CCR9+ T helper cells in the salivary glands (11).

CCL25 messenger RNA (mRNA) is not detectable in healthy human salivary gland tissue, but is up-regulated during oral inflammation (26). Reduced methylation of the CCL25 gene is found in gingival tissue of patients with periodontitis (27). In mice, CCL25 gene expression is up-regulated in the oral mucosa upon triggering with antigen and during wound healing (28,29).

Apart from demonstrating a pivotal role for CCR9+ T helper cells in experimental SS-like disease, McGuire and colleagues found that CCR9+ T helper cells are enriched in the circulation of patients with primary SS (11), indicating that these cells might play a role in the disease. In the present study, we confirmed these findings and further characterized the role of CCR9+ T helper cells in primary SS. We investigated the presence of CCR9+ T helper cells and its specific ligand, CCL25, in the labial salivary glands (LSGs) of patients with primary SS. In addition, the phenotypic and functional properties of circulating CCR9+ T helper cells were studied in comparison to CXCR5+ T helper cells.

PATIENTS AND METHODS

Patients and controls. All patients with primary SS were classified according to the American-European Consensus Group (AECG) criteria for SS (30). Patients with sicca syndrome who did not fulfill the AECG criteria for SS were defined as non-SS sicca disease controls. In both groups, autoantibody status and LSG biopsy samples were assessed. All patients, disease controls, and healthy volunteers were from the University Medical Center (UMC) Utrecht. The demographic and clinical characteristics of the patients and controls are shown in Table 1. The UMC Utrecht ethics committee approved the study, and all participants gave written informed consent.

Analyses of CCL25 and CCR9 expression. CCL25 and CCR9 mRNA expression levels in the LSG biopsy tissue were assessed by quantitative reverse transcription–polymerase chain reaction; *18S* was used as a housekeeping gene. The expression of mRNA was calculated using the $2^{-\Delta\Delta C_t}$ method, with values normalized against the median value of the disease control group. To detect the secretion of CCL25 by LSG tissue, the LSGs were thoroughly rinsed directly after the biopsy procedure and incubated in 200 μl of saline for 1 hour at room temperature. The tissue supernatant was then frozen. Levels of CCL25 as well as IFNγ, IL-17, IL-4, IL-21, IL-7, soluble IL-7 receptor α-chain (sIL-7Rα), and CXCL13 were measured using a Luminex multianalyte assay, as previously described (31).

Immunohistochemical analysis was performed to detect CCR9 expression in the LSG samples. Frozen tissue sections were incubated with an anti-CCR9 monoclonal antibody; control incubations involved a mouse IgG2a isotype or omission of the first antibody. Antigen–antibody complexes

Table 1. Characteristics of the patients with primary SS, non-SS sicca controls, and healthy controls according to sample availability in each tested group*

	Serum analysis		LSG biopsy supernatant analysis		Immunohistochemical analysis		Gene expression analysis		Flow cytometry analysis	
	Healthy controls (n = 5)	Primary SS (n = 12)	Non-SS sicca controls (n = 34)	Primary SS (n = 26)	Non-SS sicca controls (n = 9)	Primary SS (n = 10)	Non-SS sicca controls (n = 9)	Primary SS (n = 9)	Healthy controls (n = 9)	Primary SS (n = 12)
Female sex, no. (%)	5 (100)	9 (75)	30 (88)	23 (88)	9 (100)	9 (90)	8 (89)	8 (89)	8 (89)	12 (100)
Age, mean ± SD years	58.2 ± 5.8	50.0 ± 11.1	50.3 ± 15.6	52.6 ± 13.8	45.8 ± 15.5	48.2 ± 12.8	53.3 ± 7.5	43.7 ± 19.7	43.6 ± 14.1	54.1 ± 14.5
Anti-Ro/SSA positive, no. (%)	–	8 (67)	10 (29)	18 (69)	1 (11)	9 (90)	2 (22)	9 (100)	–	11 (92)
Anti-La/SSB positive, no. (%)	–	3 (25)	0 (0)	5 (19)	1 (11)	5 (50)	0 (0)	3 (33)	–	7 (58)
ANA positive, no. (%)	–	10 (83)	10 (29)	19 (73)	2 (22)	7 (70)	1 (11)	7 (78)	–	10 (83)
RF positive, no. (%)	–	4 (33)	1 (3)	10 (38)	1 (11)	3 (30)	1 (11)	3 (33)	–	3 (25)
Lymphocytic focus score, median (IQR) foci/4 mm^2	–	1.5 (1.0–2.4)	0.0 (0.0–0.1)	1.7 (1.0–2.7)	0 (0–0)	4.5 (3.0–6.0)	0 (0–0)	3.0 (1.5–5.0)	–	2.0 (1.6–2.8)
IgA+ plasma cells, median (IQR) %	–	50 (46–60)	75 (70–80)	59 (47–65)	85 (51–89)	40 (15–50)	>70	43 (16–50)	–	40 (15–59)
Schirmer's test, median (IQR) mm/5 minutes	–	8.5 (1.0–27.5)	5.3 (2.3–12.1)	7.0 (3.0–10.0)	0.0 (0.0–14.0)	3.5 (0–13.8)	1.5 (1.0–5.0)	4.0 (0.8–17.0)	–	4.5 (0.3–12.5)
Serum IgG, median (IQR) gm/liter	–	15.3 (10.3–20.4)	10.6 (8.1–12.8)	14.0 (10.8–19.7)	11.5 (9.8–12.8)	15.1 (12.7–24.6)	11.4 (11.0–2.4)	17.4 (10.4–28.5)	–	16.5 (11.8–18.1)
ESR, median (IQR) mm/hour	–	16 (7–25)	7 (6–14)	16 (7–28)	22 (13–28)	27 (10–56)	6 (3–21)	14 (10–52)	–	27 (12–33)
ESSDAI score, median (IQR) (scale 0–123)	–	2.5 (2.0–6.5)	–	3.0 (0.5–5.5)	–	–	–	–	–	6.0 (5.0–9.0)
ESSPRI score, median (IQR) (scale 0–10)	–	5.7 (2–7.7)	–	5.3 (2.3–6.0)	–	–	–	–	–	5.0 (5.0–7.0)
Immunosuppressant drugs, no.	–	3	3	3	5	4	1	2	–	1
Hydroxychloroquine	–	1	2	0	0	0	0	0	–	1
NSAIDs daily	–	0	0	0	5	2	1	1	–	1
Other	–	2	1	3	0	2	0	1	–	0

* SS = Sjögren's syndrome; LSG = labial salivary gland; ANA = antinuclear antibody; RF = rheumatoid factor; IQR = interquartile range; ESR = erythrocyte sedimentation rate; ESSDAI = EULAR Sjögren's Syndrome Disease Activity Index; ESSPRI = EULAR Sjögren's Syndrome Patient Reported Index; NSAIDs = nonsteroidal antiinflammatory drugs.

were visualized using a BrightVision poly–horseradish peroxidase detection system.

For immunofluorescence staining to assess colocalization, anti-CCR9, anti-CD3, anti-CD4, and anti-ICOS antibodies were used along with Alexa Fluor 488–labeled and Alexa Fluor 555–labeled secondary antibodies. Details on the gene expression and immunohistochemical analyses are provided in Supplementary Materials and Methods (available on the *Arthritis & Rheumatology* web site at http://onlinelibrary.wiley.com/doi/10.1002/art.40182/abstract).

Isolation of cells. Peripheral blood mononuclear cells (PBMCs) were isolated by density-gradient centrifugation using Ficoll-Paque. Monocytes, CD19+ B cells, and CD4+ T cells were isolated from the PBMCs using an autoMACS system. To compare the functional characteristics of CCR9+ T helper cells to those of CXCR5+ T helper cells, 5–12 $\times$ 10^7 PBMCs from patients and healthy controls were obtained, and each cell subset was sorted using a BD FACSAria III flow cytometer. The cells were sorted for the expression of CD3, CD4, CXCR5, and CCR9, after which they were cultured.

Flow cytometric analysis. To characterize CCR9+ T helper cells, 1 $\times$ 10^6 PBMCs from patients and healthy controls were stained for the expression of CD3, CD4, CD45RO, CXCR5, CCR9, CD127 (IL-7Rα), ICOS, and PD-1. For intracellular cytokine staining, 1 $\times$ 10^6 CD4+ T cells per milliliter were stimulated with phorbol myristate acetate (PMA) and ionomycin in the presence of brefeldin A for 4 hours at 37°C. Thereafter, the cells were fixed, permeabilized, and stained for the expression of CD3, CD4, CD45RO, CD27, CXCR5, CCR9, CD127, IFNγ, IL-17A, IL-4, IL-21, and IL-10. Details on the flow cytometry analyses are shown in Supplementary Materials and Methods (available on the *Arthritis & Rheumatology* web site at http://onlinelibrary.wiley.com/doi/10.1002/art.40182/abstract).

Cell culture. For analysis of cytokine secretion, 2 $\times$ 10^4 CCR9+ T helper cells or CXCR5+ T helper cells were cultured with 5 $\times$ 10^3 monocytes for 3 days with 10 ng/ml IL-7 or 0.1 ng/ml superantigen (*Staphylococcus* enterotoxin B [SEB]) and restimulated with PMA and ionomycin for 24 hours. For analysis of B cell stimulation, 2 $\times$ 10^4 CCR9+, CXCR5+, or CCR9−CXCR5− T helper cells were cultured with 2 $\times$ 10^5 B cells and 5 $\times$ 10^3 monocytes for 12 days, along with 1 ng/ml IL-7 or 0.01 ng/ml SEB superantigen. IgG production was measured by enzyme-linked immunosorbent assay (Human IgG Quantification Kit; Bethyl Laboratories) in accordance with the manufacturer's instructions.

Statistical analysis. Statistical analyses were performed in Prism version 6 and SPSS software. Student's *t*-test, a paired parametric *t*-test, Mann-Whitney U test, and nonparametric Wilcoxon's paired test were used as appropriate. For assessment of correlations with disease parameters, Pearson's correlation coefficient and Spearman's rho were used as appropriate. Differences and correlations were considered statistically significant at *P* values less than 0.05.

RESULTS

Correlation of increased levels of CCL25 in LSG tissue with B cell hyperactivity and factors associated with lymphoid neogenesis in primary SS. Levels of serum CCL25 were not significantly different in patients with primary SS (n = 12) as compared to healthy controls (n = 5) (median 2,748 pg/ml, interquartile range [IQR] 2,056–3,748 versus median 1,992 pg/ml, IQR 1,904–2,449; $P = 0.064$). No significant correlations of the CCL25 serum levels with clinical parameters were found.

In the LSG biopsy samples, expression of CCL25 mRNA was significantly increased in patients with primary SS as compared to non-SS sicca controls (Figure 1A). In most individuals, expression of CCR9 mRNA in this tissue was not detectable or was very low.

Furthermore, CCL25 protein levels were significantly increased in the LSG biopsy supernatants from patients with primary SS as compared to non-SS sicca controls (Figure 1B). In addition, CCL25 protein levels were found to be elevated in anti-Ro/SSA–positive patients with primary SS as compared to those negative for anti-Ro/SSA (Figure 1C).

In LSG supernatants from all patients with sicca syndrome, the levels of CCL25 correlated with the lymphocytic focus score. In LSG supernatants from patients with primary SS, the CCL25 protein levels significantly correlated with an increased percentage of IgM-expressing and IgG-expressing plasma cells and increased serum IgG levels (Figure 1D). No significant correlations were found between the levels of CCL25 in LSGs and Schirmer's test results for eye dryness, the EULAR Sjögren's Syndrome Disease Activity Index, or the EULAR Sjögren's Syndrome Patient Reported Index (data not shown).

In view of the potential role of CCL25 in attracting CCR9+ T helper cells, we assessed whether CCL25 protein expression in the tissue supernatants was associated with LSG expression of cytokines that are typically associated with Tfh cells and lymphoid neogenesis, including IL-21, CXCL13, IL-7, and sIL-7Rα (6,32). In addition, the major Th1-, Th2-, and Th17-defining cytokines IFNγ, IL-4, and IL-17 were assessed. IFNγ, IL-4, IL-17, and IL-7 were detectable in a minority of the LSG samples, which hampered the assessment of correlations with CCL25 protein expression (data not shown). Levels of IL-21 and sIL-7Rα, however, were significantly increased in patients with primary SS compared to non-SS sicca controls, and the levels of both cytokines correlated robustly with the levels of CCL25 (Figure 1E). Furthermore, CXCL13 levels were significantly increased in patients with primary SS as compared to non-SS sicca controls, but this did not correlate with the levels of CCL25 (Figure 1E).

Enhanced numbers of CCR9-expressing cells in primary SS LSGs. We confirmed the findings reported by McGuire et al (11), observing that the frequency of

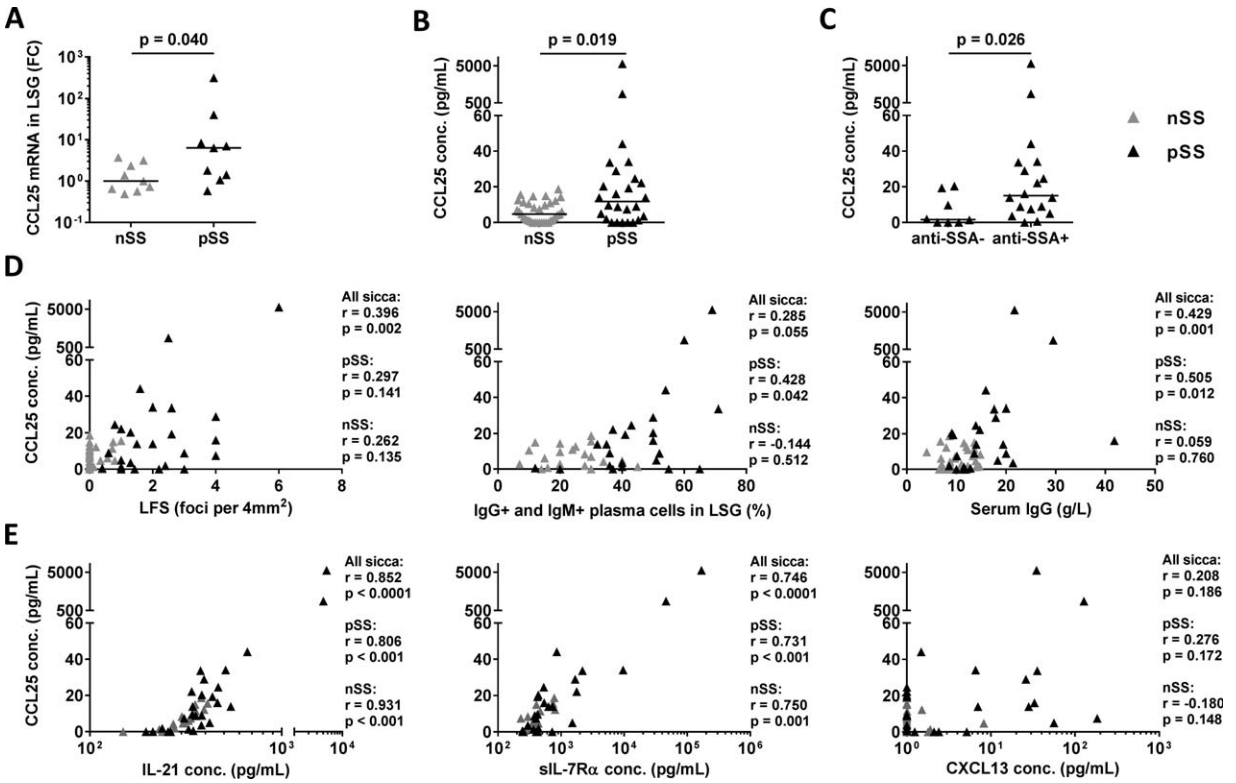

Figure 1. Elevated expression of CCL25 in the labial salivary glands (LSGs) of patients with primary Sjögren's syndrome (pSS) is associated with autoimmunity and B cell hyperactivity. **A,** CCL25 mRNA expression in LSG tissue was compared between patients with primary SS (n = 9) and control sicca syndrome patients without a diagnosis of primary SS (nSS) (n = 9). Relative expression was calculated with values normalized against the median value in the non-SS sicca controls; *18S* was used as a housekeeping gene. FC = fold change. **B** and **C,** CCL25 protein concentrations (conc.) in LSG biopsy supernatants were compared between patients with primary SS (n = 26) and non-SS sicca controls (n = 34) (**B**) and between patients with primary SS who were positive for anti-Ro/SSA autoantibodies and those who were negative for anti-Ro/SSA (**C**). Symbols in **A–C** represent individual patients; horizontal lines indicate the median. **D** and **E,** CCL25 concentrations in LSG biopsy supernatants from all patients with sicca syndrome (primary SS and non-SS sicca), patients with primary SS, and non-SS sicca controls were assessed for correlations with the lymphocytic focus score (LFS), percentage of IgM-expressing and IgG-expressing plasma cells, and serum IgG levels (**D**) and for levels of interleukin-21 (IL-21), soluble IL-7 receptor α-chain (sIL-7Rα; a marker of the IL-7/IL-7Rα pathway), and CXCL13 (**E**). Spearman's correlation coefficients were used.

CCR9+CD4+ T cells was increased in the peripheral blood of patients with primary SS as compared to healthy controls (mean ± SD 3.0 ± 1.3% versus 2.4 ± 0.9%; $P = 0.041$). In addition, we extended these findings by evaluating the numbers of CCR9+ cells upon immunohistochemical staining of the LSG biopsy tissue. The numbers of CCR9+ cells were increased in the LSGs of patients with primary SS as compared to non-SS sicca controls (Figures 2A and B), and the presence of these cells largely colocalized with CD3 and CD4 (Figure 2C). In addition, 41.4 ± 15.7% of the CCR9+ cells expressed ICOS in the LSGs of patients with primary SS (n = 4) (Figure 2D), thus confirming the presence of functional molecules associated with B cell activation.

CCR9+ cells were found mostly near epithelial cells, in and around lymphocytic infiltrates. No significant correlations of CCR9+ cell numbers with the lymphocytic focus score, percentage of IgG+IgM+ plasma cells, or serum IgG levels were found (data not shown).

High expression levels of IL-7Rα in circulating CCR9+ T helper cells compared to CXCR5+ T helper cells, and elevated proportions of circulating CCR9+ T helper cells coexpressing ICOS and PD-1 in primary SS. Since the IL-7/IL-7Rα pathway plays an important role in the pathogenesis of primary SS (8,33–37) and in (ectopic) GC formation, including that occurring in LSGs, expression of IL-7Rα on circulating CCR9+ and CXCR5+ T helper cells from patients with primary SS and healthy controls was studied (32,38,39). CCR9+ T helper cells showed a higher median fluorescence intensity of IL-7Rα expression as compared to CXCR5+ T helper cells, both in patients with primary SS and in healthy controls (Figures 3A–C).

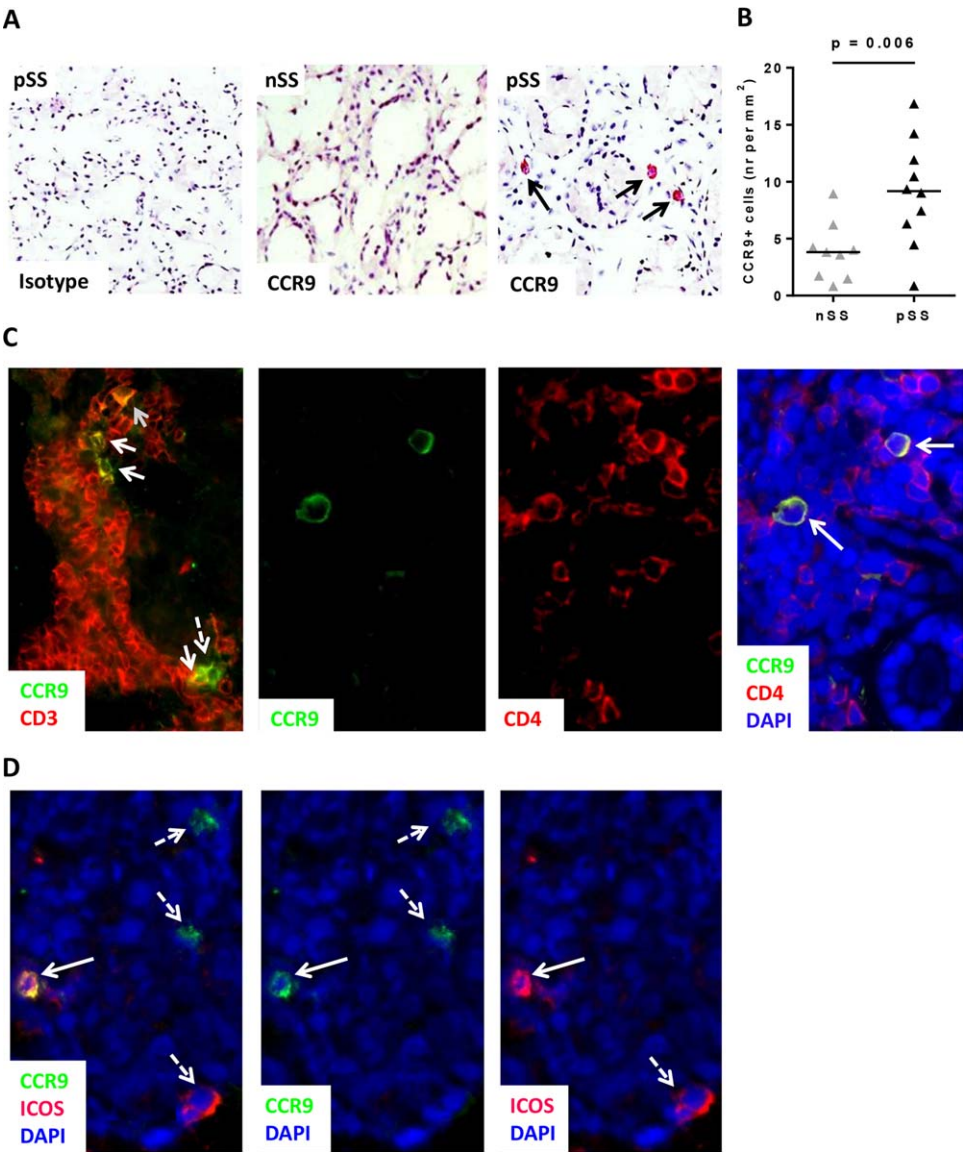

Figure 2. Levels of CCR9-expressing T cells are increased in the salivary glands of patients with primary SS. **A,** Representative images of immunohistochemical staining for CCR9 (red) in LSG tissue from a patient with primary SS and a non-SS control patient with sicca syndrome are shown, along with a mouse IgG2a isotype control. **Arrows** indicate CCR9+ cells. **B,** Levels of CCR9-expressing cells in LSG tissue were compared between patients with primary SS (n = 10) and non-SS sicca controls (n = 9). Symbols represent individual patients; horizontal lines indicate the median. **C,** Representative immunofluorescence images demonstrate that in a CD3 (red) T cell–rich lymphoid aggregate, the majority of CCR9+ cells coexpress CD3 and CD4 (yellow/orange). **Solid arrows** indicate colocalization, and **dashed arrow** indicates CD3−CCR9+ cells (green). **D,** Representative immunofluorescence images of the LSGs of a patient with primary SS demonstrate the presence of CCR9+ cells (green) that are positive for inducible T cell costimulator (ICOS) (red) (counterstained with DAPI [blue]). **Solid arrows** indicate colocalization, and **dashed arrows** indicate single expression of CCR9 or ICOS. Original magnification × 200 in **A**; × 400 in **C** and **D**. See Figure 1 for other definitions.

As CCR9+ T helper cells share many features with Tfh cells, it was of particular interest to compare them to CXCR5+ T helper cells. Expression of ICOS and PD-1, both of which are activation markers characteristically expressed on Tfh cells, was assessed (6). Since the majority of PD-1 and ICOS in both cell subsets was expressed on the CD45RO+ effector memory cells and central memory cells, CD45RO+CCR9+ and CD45RO+CXCR5+ T helper cells from patients with primary SS were compared to those from healthy controls (40,41). Patients with primary SS displayed significantly increased numbers of ICOS and PD-1–coexpressing cells in the CCR9+ T helper cell subset compared to that from healthy controls; this was not

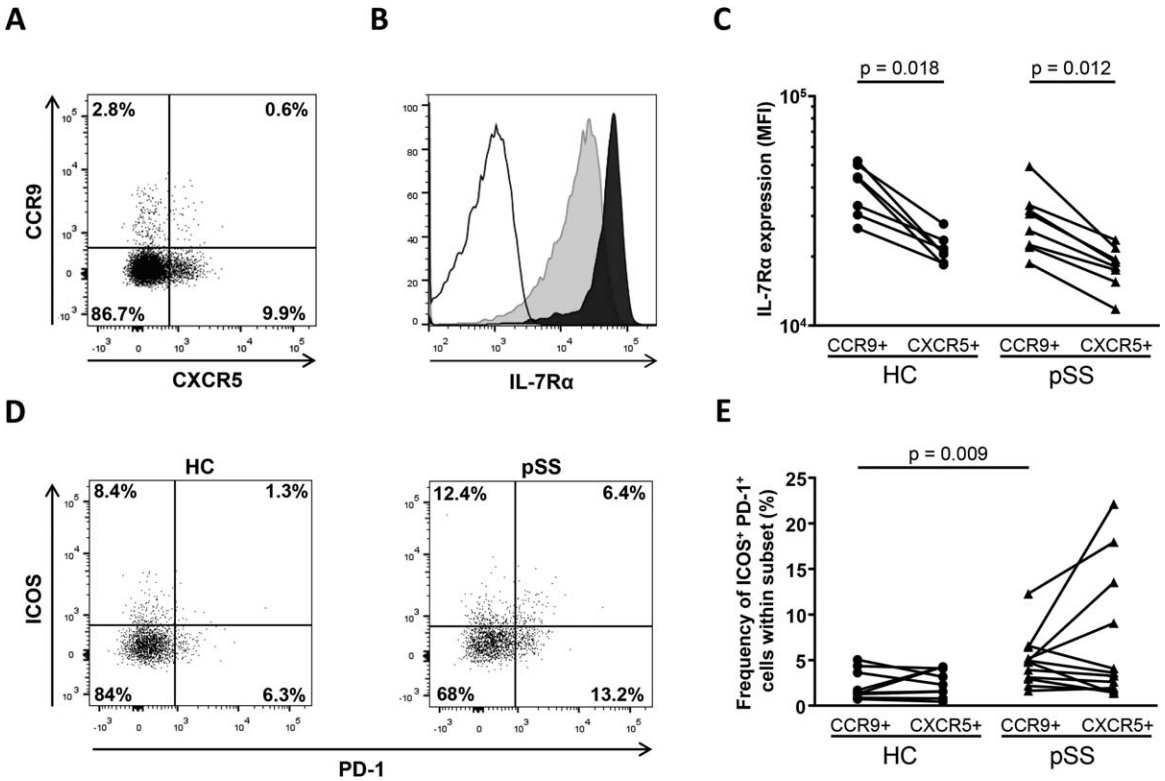

Figure 3. CCR9+ T helper cells are characterized by high levels of IL-7Rα and increased coexpression of inducible T cell costimulator (ICOS) and programmed death 1 (PD-1) in patients with primary SS. **A,** The representative flow cytometry dot plot identifies distinct CCR9-expressing and CXCR5-expressing CD4+ T cells. **B,** The representative histograms show IL-7Rα expression by CCR9+ T helper cells (solid) compared to CXCR5+ T helper cells (gray shaded) and the unstained control (open). **C,** Expression of IL-7Rα by CCR9+ and CXCR5+ T helper cells was compared between healthy controls (HC) (n = 7) and patients with primary SS (n = 8). Symbols represent individual subjects, with results expressed as the median fluorescence intensity (MFI). **D,** Representative dot plots show the expression of ICOS and PD-1 by CCR9+ T helper cells from a healthy individual and a patient with primary SS. **E,** The percentages of ICOS and PD-1–coexpressing CCR9+ and CXCR5+ T helper cells were compared between healthy controls (n = 9) and patients with primary SS (n = 12). Symbols represent individual subjects. See Figure 1 for other definitions.

observed in CXCR5+ T helper cells. Among patients with primary SS or healthy controls, no statistically significant differences were seen in the percentage of ICOS+PD-1+ cells, either in the CCR9+ T helper cell subset or in the CXCR5+ T helper cell subset (Figures 3D and E).

Higher proportions of circulating CCR9+ T helper cells producing IL-21 and IL-10 and expressing a Th1/Th17.1 phenotype as compared to CXCR5+ T helper cells. Intracellular cytokine staining was performed to characterize the polarization of T helper cells ex vivo among total peripheral blood CCR9+ and CXCR5+ T helper cells from patients with primary SS compared to healthy controls (representative images from fluorescence-activated cell sorting analysis are shown in Figure 4A). Both in patients with primary SS and in healthy controls, higher percentages of CCR9+ T helper cells produced IFNγ (Th1 cells, not expressing IL-4 or IL-17) as compared to CXCR5+ T helper cells (mean ± SD 54.9 ± 21.1% versus 12.8 ± 4.5%; $P < 0.001$). In addition, the proportion of IFNγ+ cells coexpressing IL-17, a typical cytokine profile for proinflammatory Th17.1 cells (42), was elevated in the CCR9+ T helper cell subpopulation (mean ± SD 0.8 ± 0.6% versus 0.1 ± 0.1% of CXCR5+ cells; $P < 0.001$). Furthermore, the percentages of CCR9+ T helper cells producing IL-21 and IL-10 were increased (for IL-21, 3.8 ± 1.6% versus 2.3 ± 1.3% of CXCR5+ cells [$P = 0.003$]; for IL-10, 2.2 ± 1.4% versus 1.1 ± 1.1% of CXCR5+ cells [$P = 0.002$]). The percentages of Th17 cells (IL-17–producing T helper cells, not producing IFNγ or IL-4) and Th2 cells (IL-4–producing T helper cells, not producing IFNγ or IL-17) did not differ significantly between the CCR9+ and CXCR5+ cell subsets (for Th17, 1.1 ± 0.6% versus 0.8 ± 0.6%; for Th2, 1.3 ± 0.7% versus 1.0 ± 1.0%). Within the group of patients

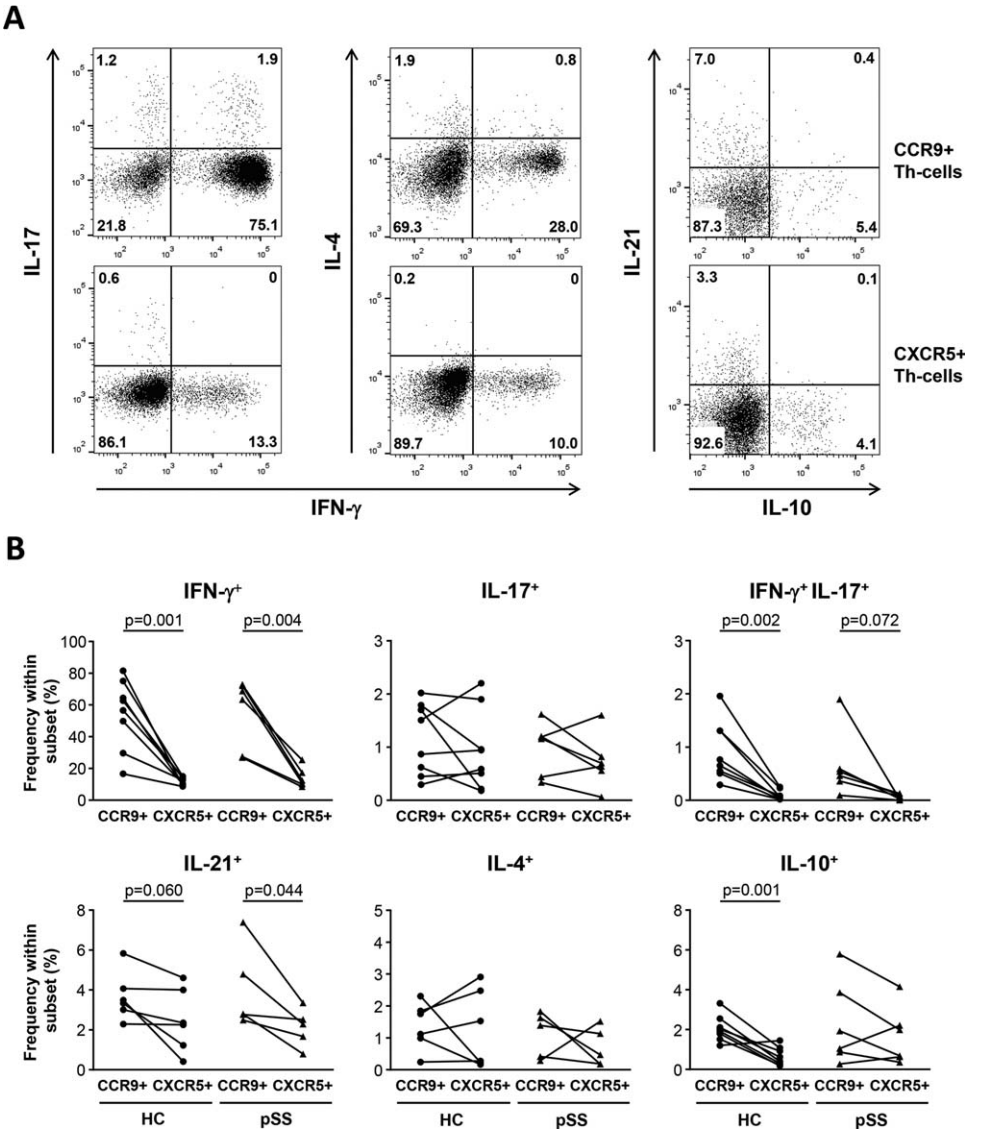

Figure 4. Enhanced proportions of ex vivo peripheral blood CCR9+ T helper cells produce IL-21 and IL-10 and have a more robust Th1 phenotype (interferon-γ positive [IFNγ+]) and Th17.1 phenotype (IFNγ+IL-17+) compared to CXCR5+ T helper cells. **A,** The representative flow cytometry dot plots show the expression of IL-17, IFNγ, IL-4, IL-21, and IL-10 by CCR9+ T helper cells as compared to CXCR5+ T helper cells. Values in each quadrant are percentages of cells. **B,** The percentages of CCR9+ and CXCR5+ T helper cells secreting IFNγ, IL-17, both IFNγ and IL-17, IL-21, IL-4, and IL-10 were determined in healthy controls (HC) (n = 8; for IL-21 staining, n = 6) and patients with primary SS (n = 6; for IL-21 staining, n = 5). Symbols represent individual subjects. See Figure 1 for other definitions.

with primary SS and the healthy control group, no significant differences in circulating T helper cell subset polarization were found for either CCR9+ T helper cells or CXCR5+ T helper cells (Figure 4B).

Naive, effector, effector memory, and central memory T helper cells were expected to produce different levels of cytokines. Therefore, the frequencies of these subsets within the CCR9+ and CXCR5+ T helper cell populations were assessed, showing that the CCR9+ T helper cell subset contained a higher frequency of effector and effector memory cells, and the CXCR5+ T helper cell subset contained a higher frequency of central memory cells (see Supplementary Figure 1, available on the *Arthritis & Rheumatology* web site at http://onlinelibrary.wiley.com/doi/10.1002/art.40182/abstract). These subsets were distinguished on the basis of the expression of CD45RO and CD27.

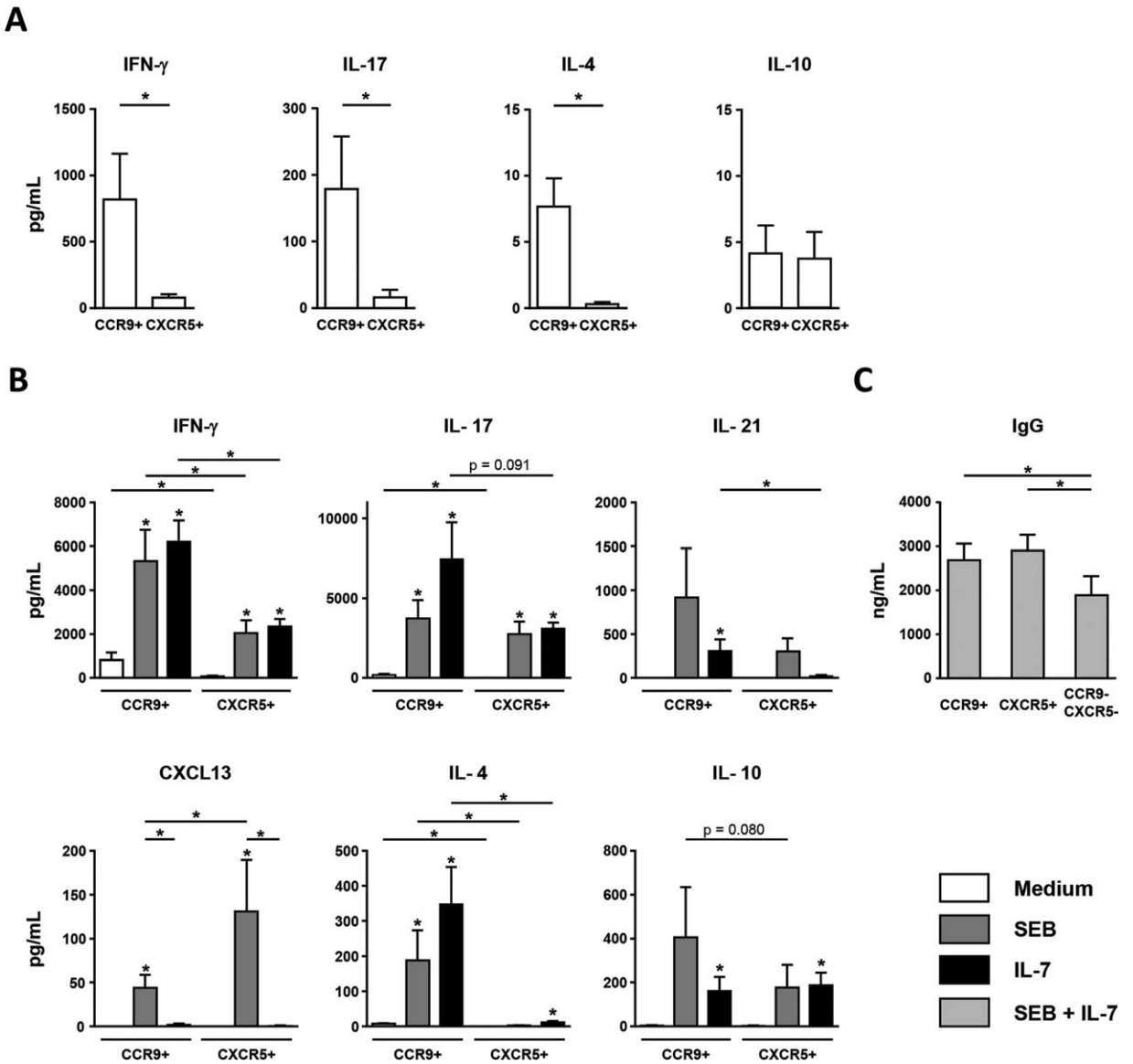

Figure 5. CCR9+ T helper cells robustly produce interferon-γ (IFNγ), IL-17, IL-4, and IL-21 upon challenge with antigen or IL-7, while antigen-triggered CXCR5+ T helper cells more potently produce CXCL13. Both CCR9+ and CXCR5+ T helper cells have increased capacity to stimulate IgG production. **A,** CCR9+ and CXCR5+ T helper cells (2×10^4) (n = 4 healthy controls and n = 3 patients with primary SS) were cocultured with monocytes (5×10^3) for 3 days and restimulated with phorbol myristate acetate and ionomycin. Culture of CCR9+ T helper cells without stimuli showed increased production of IFNγ, IL-17, and IL-4 as compared to CXCR5+ T helper cells. **B,** CXCR5+ T helper cells stimulated with superantigen (*Staphylococcus* enterotoxin B [SEB]) (n = 3 healthy controls and n = 2 patients with primary SS) produced significantly more CXCL13 than CCR9+ T helper cells. However, in response to SEB, CCR9+ T helper cells produced higher levels of IFNγ and IL-4. Stimulation with IL-7 (n = 4 healthy controls and n = 3 patients with primary SS) induced CCR9+ T helper cells to produce significantly more IFNγ, IL-21, and IL-4 as compared to CXCR5+ T helper cells. **C,** CCR9+, CXCR5+, and CCR9−CXCR5− T helper cells (2×10^4) (n = 6 healthy controls) were cocultured with B cells (2×10^5) and monocytes (5×10^3) for 12 days in the presence of IL-7 and SEB. IgG levels were measured in the supernatants. In the cultures with CCR9+ and CXCR5+ T helper cells, IgG production was significantly higher as compared to cultures with CCR9−CXCR5− T helper cells. Results are the mean ± SEM. $* = P < 0.05$ for the indicated comparisons or for cells stimulated with SEB or IL-7 alone versus cells cultured in medium alone. See Figure 1 for other definitions.

We subsequently assessed cytokine production in these cell subsets, and found that cytokine production differed between the subsets, as had also been observed in total CD4+ T cells. Frequencies of IFNγ+ cells were increased in all CCR9+ T helper subsets, while the frequencies of IFNγ+IL-17+ cells and IL-10+ cells were increased in the naive, effector memory, and central memory CCR9+ T helper subsets, and the frequency of IL-21+ cells was increased in the naive and central memory CCR9+ T helper cell subset (see

Supplementary Figure 2, available on the *Arthritis & Rheumatology* web site at http://onlinelibrary.wiley.com/doi/10.1002/art.40182/abstract).

Both CCR9+ and CXCR5+ memory T helper cells showed higher IL-7Rα expression and higher percentages of ICOS+PD-1+ cells than did CCR9−CXCR5− naive T helper cells (see Supplementary Figure 3, available on the *Arthritis & Rheumatology* web site at http://onlinelibrary.wiley.com/doi/10.1002/art.40182/abstract). Furthermore, CCR9+ and CXCR5+ T helper cells that consisted primarily of central memory cells (Supplementary Figure 1) showed higher percentages of cytokine-secreting cells (producing IL-21, IFNγ, IL-17, IL-4, and IL-10) as compared to CCR9−CXCR5− T helper cells that mainly consisted of naive T helper cells (see Supplementary Figure 4, available on the *Arthritis & Rheumatology* web site at http://onlinelibrary.wiley.com/doi/10.1002/art.40182/abstract).

Robust production of IFNγ, IL-4, IL-17, and IL-21 by antigen- and IL-7–triggered CCR9+ T helper cells, compared to antigen-driven production of CXCL13 by CXCR5+ T helper cells. In view of their crucial role in immunopathology, the function of CCR9+ T helper cells from patients with primary SS and healthy controls were studied in cocultures with monocytes (43). No significant differences in in vitro cytokine production were found between cocultures with primary SS patient cells and cocultures with healthy control cells. Therefore, the data on in vitro cytokine production were pooled together to compare the function of CCR9+ and CXCR5+ T helper cells. Upon restimulation, CCR9+ T helper cells showed elevated production of IFNγ, IL-17, and IL-4 as compared to CXCR5+ T helper cells (Figure 5A). Production of IL-21 and CXCL13 under the same conditions was very low or undetectable (data not shown), and IL-10 production was not different between CCR9+ and CXCR5+ T helper cell cultures (Figure 5A).

To investigate T cell receptor–triggered T cell activation, which is expected to occur in the target organs when T helper cells enter the tissue, CCR9+ and CXCR5+ T helper cells were cultured in the presence of SEB antigen. Interestingly, CXCR5+ T helper cells, when stimulated with SEB superantigen, produced levels of CXCL13 that were significantly higher than that produced by CCR9+ T helper cells ($P = 0.043$). In contrast, CCR9+ T helper cells, in response to stimulation with SEB, produced higher levels of IFNγ and IL-4 as compared to CXCR5+ T helper cells (both $P = 0.043$). In addition, CCR9+ T helper cells produced higher levels of IL-17, IL-21, and IL-10 as compared to CXCR5+ T helper cells, although this difference did not reach statistical significance (Figure 5B). IL-7Rα–mediated stimulation of the cells was also investigated, because it is known to play a role in the immunopathology of primary SS (8,33–37). A strong correlation of sIL-7Rα levels with CCL25 levels was observed in CCR9+ T helper cells, and expression of IL-7Rα on CCR9+ T helper cells was high. Stimulation with IL-7 induced CCR9+ T helper cells to produce significantly higher amounts of IFNγ, IL-21, and IL-4 as compared to that produced by CXCR5+ T helper cells ($P = 0.018$, $P = 0.018$, and $P = 0.028$, respectively). In addition, a trend toward increased production of IL-17 by CCR9+ T helper cells was found ($P = 0.091$). Production of CXCL13 was not significantly induced by IL-7, and production of IL-10 did not significantly differ between CCR9+ T helper cells and CXCR5+ T helper cells upon stimulation with IL-7 (Figures 5A and B).

Potent induction of IgG production by B cells in the presence of CCR9+ and CXCR5+ T helper cells as compared to CCR9−CXCR5− T helper cells. Since both CCR9+ and CXCR5+ T helper cells have been described to potently induce the antibody responses of B cells, coculture of these cells with B cells was performed (6,14). Stimulation with IL-7 and SEB was performed to activate each subset of T helper cells. Both CCR9+ and CXCR5+ T helper cells induced B cell production of IgG, the levels of which were significantly increased as compared to that induced in the presence of CCR9−CXCR5− T helper cells ($P = 0.025$ and $P = 0.013$, respectively) (Figure 5C).

DISCUSSION

The present study demonstrates, for the first time, increased levels of CCL25 and elevated numbers of CCR9-expressing cells in the salivary glands of patients with primary SS. Elevated CCL25 levels correlated with lymphocytic focus scores, B cell hyperactivity, autoimmunity (presence of anti-Ro/SSA autoantibodies), and expression of mediators potentially involved in lymphoid neogenesis (IL-21 and sIL-7Rα). Circulating CCR9+ T helper cells from patients with primary SS displayed increased expression of ICOS and PD-1. In addition, we demonstrated that CCR9+ T helper cells, as compared to CXCR5+ T helper cells, had increased IL-7Rα expression, and increased proportions of CCR9+ T helper cells, ex vivo and in response to stimulation with antigen and IL-7, produced higher levels of IFNγ, IL-4, IL-17, and IL-21. The CXCR5+ T helper cell subset, in turn, produced more CXCL13. Both CCR9+ and CXCR5+ T helper cells stimulated IgG production by B cells more potently than that by CCR9−CXCR5− T helper cells. Taken together, these findings suggest a role for the CCL25/CCR9 axis in the pathogenesis of primary SS, in a

manner that is distinct from that of CXCR5+ T helper cells.

CCR9-expressing T helper cells both from patients with primary SS and from healthy controls were found to migrate in response to CCL25 (16,26,44). CCL25 is found in the intestinal mucosa of patients with IBD as well as in healthy individuals, and is primarily produced by epithelial cells (21,26). However, CCL25 expression has not been detected in the LSGs of healthy individuals (26). We show herein that expression of CCL25 mRNA and protein was increased in the salivary glands of patients with primary SS as compared to non-SS sicca controls. Moreover, consistent with the production of CCL25 by epithelial cells, we observed CCR9+ cells mainly in the vicinity of epithelial cells. Although the trigger for CCL25 induction in the salivary glands of patients with primary SS is unknown, studies in cell lines and mice have demonstrated that viral and bacterial infections and tissue damage can up-regulate CCL25 expression in mucosal tissue (28,29,45–48).

We and others have shown that incubation of CCR9+ T helper cells with CCL25 dramatically reduces CCR9 cell surface expression (44,49). This might explain the findings of a low frequency of CCR9+ T helper cells at the site of inflammation without a significant correlation with the lymphocytic focus score. The lack of detection of CCR9 mRNA expression may be attributable to the characteristics of chemokine receptor expression. Since chemokine receptor genes are known to be low copy number genes and because the chemokine receptor proteins are recycled on the cell membrane, the expression of chemokine receptor mRNAs tends to be low and is often not directly correlated with the levels of protein present (50). In support of a role for the CCL25/CCR9 axis in primary SS, we demonstrated significant correlations of CCL25 in LSG supernatants with the lymphocytic focus score, B cell hyperactivity, and autoimmunity in patients with primary SS. Consistent with this finding, increased expression of PD-1 and ICOS on CCR9+ T helper cells in patients with primary SS was observed, indicating activation and potentially superior interaction with B cells.

Finally, in this study, we demonstrated the strong capability of CCR9+ T helper cells to produce high levels of IFNγ, IL-4, IL-10, IL-17, and IL-21 and to stimulate increased IgG production by B cells. Taken together, these findings suggest that these cells play a role in activation of B cells in primary SS. Expression of ICOS and PD-1 and production of the cytokines IL-4 and IL-21 by Tfh cells have been shown to play important roles in GC processes that induce long-term, high-affinity B cell responses (5,6). The Tfh-like role for CCR9+ T helper cells is supported by the finding that they are potent inducers of antibody production (14). A role for the CCL25/CCR9 T helper cell axis in autoimmunity and the immunopathology of primary SS is further supported by the increased frequencies of CCR9+ T helper cells in the blood of patients with primary SS and by the capacity of CCR9+ T helper cells to induce experimental sialadenitis, glandular disease, and autoimmunity (11). Thus, despite their low numbers, increased numbers of CCR9+ T cells in the salivary glands are shown to play a pivotal role in autoimmunity via the production of high levels of cytokines and the capacity to stimulate B cells (14).

Corresponding to the findings of previous studies that focused on CCR9+ T helper cells in healthy controls, ex vivo studies in patients with primary SS showed that CCR9+ T helper cells produced high levels of the Th1 and Th17 cytokines IFNγ and IL-17 as compared to CXCR5+ T helper cells (14,15). In addition, we demonstrated that CCR9+ T helper cells producing IL-10 were enriched in patients with primary SS (14). Herein we demonstrate, for the first time, that human CCR9+ T helper cells encompass enriched proportions of IL-21–producing cells, as well as the proinflammatory Th17.1 cell subset that produces both IFNγ and IL-17.

In vitro, CCR9+ T helper cells were superior producers of IFNγ, IL-4, IL-17, and IL-21 as compared to CXCR5+ T helper cells, depending on the stimulus. Upon triggering of the T cell receptor, elevated production of IFNγ and IL-4 by CCR9+ T helper cells was found, but CXCR5+ T helper cells were superior producers of CXCL13. Interestingly, IL-7–induced activation caused strong up-regulation of all of the cytokines measured, except for CXCL13, and CCR9+ T helper cells produced significantly elevated levels of IFNγ, IL-4, and IL-21 compared to CXCR5+ T helper cells. In addition, we demonstrated a strong correlation of CCL25 levels with sIL-7Rα levels, which recently was shown to strongly enhance IL-7–induced immune activation in vivo (51). Considering these findings and the pivotal role of the IL-7/IL-7Rα pathway in lymphoid neogenesis in salivary glands, IL-7–driven activation of CCR9+ T helper cells may play a pivotal role in this process (32).

Our results showed that CCL25 levels did not correlate with CXCL13 levels in the LSGs, and that CCR9+ T helper cells did not produce high levels of CXCL13 as compared to CXCR5+ T helper cells. In addition, CCR9+ T helper cells were much more potent cytokine producers in response to IL-7 than CXCR5+ T helper cells. These findings, in combination with the Tfh-like characteristics of CCR9+ T helper cells, indicate a distinct role for the IL-7/IL-7R–associated CCL25/CCR9 axis as compared to the CXCL13/CXCR5 axis in B

cell activation and lymphocyte infiltration, including GC-like structure formation, in patients with primary SS.

Both in the ex vivo and in vitro experiments, we demonstrated equally potent cytokine production by CCR9+ T helper cells from patients with primary SS and healthy controls. In view of the increased expression of PD-1 and ICOS on CCR9+ T helper cells from patients with primary SS, this finding is still unexplained. Currently, we are investigating coexpression of other chemokine receptors on CCR9+ T helper cells to support the hypothesis that subsets of CCR9+ T helper cells migrate in response to coexpressed chemokine receptors, which would thus explain the lack of increased circulating cytokine-secreting cells.

In conclusion, elevated expression of CCL25 and increased numbers of CCR9+ cells in the LSGs of patients with primary SS correlate with clinical features, including lymphocytic infiltration in the LSGs, B cell hyperactivity, and autoimmunity. Peripheral blood CCR9+ T helper cells from patients with primary SS displayed increased expression of ICOS and PD-1. When compared to CXCR5+ T helper cells, the CCR9+ T helper cells were found to be IL-7Rα^{high} and produced elevated levels of IFNγ, IL-4, IL-17, and IL-21, especially upon IL-7R–mediated stimulation. Considering the pivotal role of CCR9+ T cells in an experimental SS-like disease model, our findings suggest an important role for the CCL25/CCR9 axis in the immunopathology of primary SS, thus representing a novel therapeutic target in this disease.

ACKNOWLEDGMENTS

We would like to thank M. Wenting-van Wijk, Dr. B. Giovannone, and R. Broekhuizen for assistance with development of the immunohistochemical analyses and immunofluorescence assays, Dr. T. van den Broek and Dr. N. J. G. Jansen for providing human thymus tissue, A. Kislat for performing the quantitative polymerase chain reaction, A. P. Pinheiro-Lopes for performing the intracellular fluorescence-activated cell sorter staining, T. S. van Kempen for advice regarding culture experiments, the Flow Cytometry Core Facility (UMC Utrecht) for performing the cell sorting, and the Multiplex Core Facility of the Laboratory for Translational Immunology (UMC Utrecht) for performing the in-house–developed and validated multiplex immunoassay.

AUTHOR CONTRIBUTIONS

All authors were involved in drafting the article or revising it critically for important intellectual content, and all authors approved the final version to be published. Drs. Radstake and van Roon had full access to all of the data in the study and take responsibility for the integrity of the data and the accuracy of the data analysis.

Study conception and design. Blokland, Kruize, Homey, Radstake, van Roon.

Acquisition of data. Blokland, Hillen, Meller.

Analysis and interpretation of data. Blokland, Homey, Smithson, Radstake, van Roon.

ROLE OF THE STUDY SPONSOR

This study was funded by Takeda Pharmaceuticals. Takeda had no role in the study design or in the collection, analysis, or interpretation of the data, the writing of the manuscript, or the decision to submit the manuscript for publication. Publication of this article was approved by Takeda.

REFERENCES

1. Fox RI. Sjögren's syndrome. Lancet 2005;366:321–31.
2. Kroese FG, Abdulahad WH, Haacke E, Bos NA, Vissink A, Bootsma H. B-cell hyperactivity in primary Sjögren's syndrome. Expert Rev Clin Immunol 2014;10:483–99.
3. Theander E, Vasaitis L, Baecklund E, Nordmark G, Warfvinge G, Liedholm R, et al. Lymphoid organisation in labial salivary gland biopsies is a possible predictor for the development of malignant lymphoma in primary Sjögren's syndrome. Ann Rheum Dis 2011;70:1363–8.
4. Risselada AP, Kruize AA, Goldschmeding R, Lafeber FP, Bijlsma JW, van Roon JA. The prognostic value of routinely performed minor salivary gland assessments in primary Sjögren's syndrome. Ann Rheum Dis 2014;73:1537–40.
5. Nurieva R, Yang XO, Martinez G, Zhang Y, Panopoulos AD, Ma L, et al. Essential autocrine regulation by IL-21 in the generation of inflammatory T cells. Nature 2007;448:480–3.
6. Crotty S. T follicular helper cell differentiation, function, and roles in disease. Immunity 2014;41:529–42.
7. Li XY, Wu ZB, Ding J, Zheng ZH, Li XY, Chen LN, et al. Role of the frequency of blood $CD4^+$ $CXCR5^+$ $CCR6^+$ T cells in autoimmunity in patients with Sjögren's syndrome. Biochem Biophys Res Commun 2012;422:238–44.
8. Jin L, Yu D, Li X, Yu N, Li X, Wang Y, et al. $CD4^+CXCR5^+$ follicular helper T cells in salivary gland promote B cells maturation in patients with primary Sjögren's syndrome. Int J Clin Exp Pathol 2014;7:1988–96.
9. Gong YZ, Nititham J, Taylor K, Miceli-Richard C, Sordet C, Wachsmann D, et al. Differentiation of follicular helper T cells by salivary gland epithelial cells in primary Sjögren's syndrome. J Autoimmun 2014;51:57–66.
10. Szabo K, Papp G, Barath S, Gyimesi E, Szanto A, Zeher M. Follicular helper T cells may play an important role in the severity of primary Sjögren's syndrome. Clin Immunol 2013;147:95–104.
11. McGuire HM, Vogelzang A, Ma CS, Hughes WE, Silveira PA, Tangye SG, et al. A subset of interleukin-21^+ chemokine receptor $CCR9^+$ T helper cells target accessory organs of the digestive system in autoimmunity. Immunity 2011;34:602–15.
12. Saruta M, Yu QT, Avanesyan A, Fleshner PR, Targan SR, Papadakis KA. Phenotype and effector function of CC chemokine receptor 9-expressing lymphocytes in small intestinal Crohn's disease. J Immunol 2007;178:3293–300.
13. Lee HS, Kim HR, Lee EH, Jang MH, Kim SB, Park JW, et al. Characterization of CCR9 expression and thymus-expressed chemokine responsiveness of the murine thymus, spleen and mesenteric lymph node. Immunobiology 2012;217:402–11.
14. Papadakis KA, Landers C, Prehn J, Kouroumalis EA, Moreno ST, Gutierrez-Ramos JC, et al. CC chemokine receptor 9 expression defines a subset of peripheral blood lymphocytes with mucosal T cell phenotype and Th1 or T-regulatory 1 cytokine profile. J Immunol 2003;171:159–65.
15. Rampal R, Awasthi A, Ahuja V. Retinoic acid-primed human dendritic cells inhibit Th9 cells and induce Th1/Th17 cell differentiation. J Leukoc Biol 2016;100:111–20.
16. Papadakis KA, Prehn J, Nelson V, Cheng L, Binder SW, Ponath PD, et al. The role of thymus-expressed chemokine and its receptor CCR9 on lymphocytes in the regional specialization of the mucosal immune system. J Immunol 2000;165:5069–76.
17. Kunkel EJ, Campbell DJ, Butcher EC. Chemokines in lymphocyte trafficking and intestinal immunity. Microcirculation 2003; 10:313–23.

18. Eksteen B, Grant AJ, Miles A, Curbishley SM, Lalor PF, Hubscher SG, et al. Hepatic endothelial CCL25 mediates the recruitment of $CCR9^+$ gut-homing lymphocytes to the liver in primary sclerosing cholangitis. J Exp Med 2004;200:1511–7.
19. Hart AL, Ng SC, Mann E, Al-Hassi HO, Bernardo D, Knight SC. Homing of immune cells: role in homeostasis and intestinal inflammation. Inflamm Bowel Dis 2010;16:1969–77.
20. Singh UP, Singh NP, Murphy EA, Price RL, Fayad R, Nagarkatti M, et al. Chemokine and cytokine levels in inflammatory bowel disease patients. Cytokine 2016;77:44–9.
21. Papadakis KA, Prehn J, Moreno ST, Cheng L, Kouroumalis EA, Deem R, et al. CCR9-positive lymphocytes and thymus-expressed chemokine distinguish small bowel from colonic Crohn's disease. Gastroenterology 2001;121:246–54.
22. Arijs I, de Hertogh G, Machiels K, van Steen K, Lemaire K, Schraenen A, et al. Mucosal gene expression of cell adhesion molecules, chemokines, and chemokine receptors in patients with inflammatory bowel disease before and after infliximab treatment. Am J Gastroenterol 2011;106:748–61.
23. Walters MJ, Wang Y, Lai N, Baumgart T, Zhao BN, Dairaghi DJ, et al. Characterization of CCX282-B, an orally bioavailable antagonist of the CCR9 chemokine receptor, for treatment of inflammatory bowel disease. J Pharmacol Exp Ther 2010;335: 61–9.
24. Keshav S, Vanasek T, Niv Y, Petryka R, Howaldt S, Bafutto M, et al. A randomized controlled trial of the efficacy and safety of CCX282-B, an orally-administered blocker of chemokine receptor CCR9, for patients with Crohn's disease. PLoS One 2013;8: e60094.
25. Feagan BG, Sandborn WJ, D'Haens G, Lee SD, Allez M, Fedorak RN, et al. Randomised clinical trial: vercirnon, an oral CCR9 antagonist, vs. placebo as induction therapy in active Crohn's disease. Aliment Pharmacol Ther 2015;42:1170–81.
26. Kunkel EJ, Campbell JJ, Haraldsen G, Pan J, Boisvert J, Roberts AI, et al. Lymphocyte CC chemokine receptor 9 and epithelial thymus-expressed chemokine (TECK) expression distinguish the small intestinal immune compartment: epithelial expression of tissue-specific chemokines as an organizing principle in regional immunity. J Exp Med 2000;192:761–8.
27. Schulz S, Immel UD, Just L, Schaller HG, Glaser C, Reichert S. Epigenetic characteristics in inflammatory candidate genes in aggressive periodontitis. Hum Immunol 2016;77:71–5.
28. McGrory K, Flaitz CM, Klein JR. Chemokine changes during oral wound healing. Biochem Biophys Res Commun 2004;324: 317–20.
29. Otten K, Dragoo J, Wang HC, Klein JR. Antigen-induced chemokine activation in mouse buccal epithelium. Biochem Biophys Res Commun 2003;304:36–40.
30. Vitali C, Bombardieri S, Jonsson R, Moutsopoulos HM, Alexander EL, Carsons SE, et al. Classification criteria for Sjögren's syndrome: a revised version of the European criteria proposed by the American-European Consensus Group. Ann Rheum Dis 2002;61: 554–8.
31. De Jager W, te Velthuis H, Prakken BJ, Kuis W, Rijkers GT. Simultaneous detection of 15 human cytokines in a single sample of stimulated peripheral blood mononuclear cells. Clin Diagn Lab Immunol 2003;10:133–9.
32. Meier D, Bornmann C, Chappaz S, Schmutz S, Otten LA, Ceredig R, et al. Ectopic lymphoid-organ development occurs through interleukin 7-mediated enhanced survival of lymphoid-tissue-inducer cells. Immunity 2007;26:643–54.
33. Bikker A, Kruize AA, Wenting M, Versnel MA, Bijlsma JW, Lafeber FP, et al. Increased interleukin (IL)-7Rα expression in salivary glands of patients with primary Sjögren's syndrome is restricted to T cells and correlates with IL-7 expression, lymphocyte numbers and activity. Ann Rheum Dis 2012;71:1027–33.
34. Bikker A, van Woerkom JM, Kruize AA, Wenting-van Wijk M, de Jager W, Bijlsma JW, et al. Increased expression of interleukin-7 in labial salivary glands of patients with primary Sjögren's syndrome correlates with increased inflammation. Arthritis Rheum 2010;62:969–77.
35. Hillen MR, Blokland SL, Risselada AP, Bikker A, Lauwerys BR, Kruize AA, et al. High soluble IL-7 receptor expression in Sjögren's syndrome identifies patients with increased immunopathology and dryness. Ann Rheum Dis 2016;75:1735–6.
36. Jin JO, Kawai T, Cha S, Yu Q. Interleukin-7 enhances the Th1 response to promote the development of Sjögren's syndrome–like autoimmune exocrinopathy in mice. Arthritis Rheum 2013; 65:2132–42.
37. Van Roon JA, Kruize AA, Radstake TR. Interleukin-7 and its receptor: the axis of evil to target in Sjögren's syndrome? [editorial]. Arthritis Rheum 2013;65:1980–4.
38. Seo YB, Im SJ, Namkoong H, Kim SW, Choi YW, Kang MC, et al. Crucial roles of interleukin-7 in the development of T follicular helper cells and in the induction of humoral immunity. J Virol 2014;88:8998–9009.
39. Timmer TC, Baltus B, Vondenhoff M, Huizinga TW, Tak PP, Verweij CL, et al. Inflammation and ectopic lymphoid structures in rheumatoid arthritis synovial tissues dissected by genomics technology: identification of the interleukin-7 signaling pathway in tissues with lymphoid neogenesis. Arthritis Rheum 2007;56: 2492–502.
40. Szodoray P, Gal I, Barath S, Aleksza M, Horvath IF, Gergely P Jr, et al. Immunological alterations in newly diagnosed primary Sjögren's syndrome characterized by skewed peripheral T-cell subsets and inflammatory cytokines. Scand J Rheumatol 2008; 37:205–12.
41. Breitfeld D, Ohl L, Kremmer E, Ellwart J, Sallusto F, Lipp M, et al. Follicular B helper T cells express CXC chemokine receptor 5, localize to B cell follicles, and support immunoglobulin production. J Exp Med 2000;192:1545–52.
42. Maggi L, Santarlasci V, Capone M, Rossi MC, Querci V, Mazzoni A, et al. Distinctive features of classic and nonclassic (Th17 derived) human Th1 cells. Eur J Immunol 2012;42:3180–8.
43. Manoussakis MN, Boiu S, Korkolopoulou P, Kapsogeorgou EK, Kavantzas N, Ziakas P, et al. Rates of infiltration by macrophages and dendritic cells and expression of interleukin-18 and interleukin-12 in the chronic inflammatory lesions of Sjögren's syndrome: correlation with certain features of immune hyperactivity and factors associated with high risk of lymphoma development. Arthritis Rheum 2007;56:3977–88.
44. Zabel BA, Agace WW, Campbell JJ, Heath HM, Parent D, Roberts AI, et al. Human G protein-coupled receptor GPR-9–6/CC chemokine receptor 9 is selectively expressed on intestinal homing T lymphocytes, mucosal lymphocytes, and thymocytes and is required for thymus-expressed chemokine-mediated chemotaxis. J Exp Med 1999;190:1241–56.
45. Mukherjee S, Vipat VC, Chakrabarti AK. Infection with influenza A viruses causes changes in promoter DNA methylation of inflammatory genes. Influenza Other Respir Viruses 2013;7:979–86.
46. Feng N, Jaimes MC, Lazarus NH, Monak D, Zhang C, Butcher EC, et al. Redundant role of chemokines CCL25/TECK and CCL28/MEC in IgA^+ plasmablast recruitment to the intestinal lamina propria after rotavirus infection. J Immunol 2006;176:5749–59.
47. Foster R, Segers I, Smart D, Adriaenssens T, Smitz J, Arce JC, et al. A differential cytokine expression profile is induced by highly purified human menopausal gonadotropin and recombinant follicle-stimulating hormone in a pre- and postovulatory mouse follicle culture model. Fertil Steril 2010;93:1464–76.
48. Ekhlassi S, Scruggs LY, Garza T, Montufar-Solis D, Moretti AJ, Klein JR. Porphyromonas gingivalis lipopolysaccharide induces tumor necrosis factor-α and interleukin-6 secretion, and CCL25 gene expression, in mouse primary gingival cell lines: interleukin-6-driven activation of CCL2. J Periodontal Res 2008; 43:431–9.

49. Uehara S, Grinberg A, Farber JM, Love PE. A role for CCR9 in T lymphocyte development and migration. J Immunol 2002; 168:2811–9.
50. Bennett LD, Fox JM, Signoret N. Mechanisms regulating chemokine receptor activity. Immunology 2011;134:246–56.
51. Lundstrom W, Highfill S, Walsh ST, Beq S, Morse E, Kockum I, et al. Soluble IL7Rα potentiates IL-7 bioactivity and promotes autoimmunity. Proc Natl Acad Sci U S A 2013;110: E1761–70.

DOI:10.1002/art.40162

Clinical Images: Carpal tunnel biopsy identifying transthyretin amyloidosis

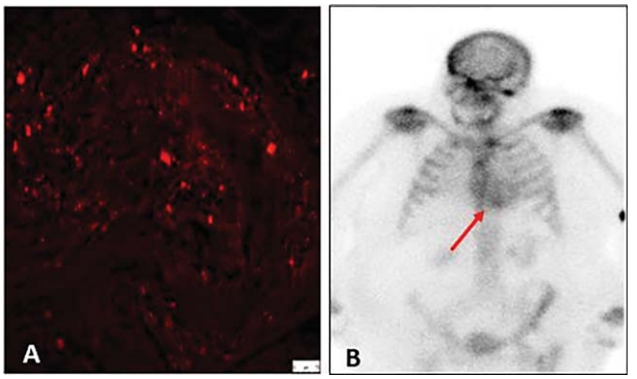

The patient, an 86-year-old woman, underwent routine decompression for carpal tunnel syndrome (CTS). A sample of tenosynovium was examined histologically, and amyloid deposits were identified (Congo red staining under polarized light) (**A**). Immunohistochemical staining confirmed that the amyloid deposits were transthyretin type. The patient was referred to us for further evaluation, at which time she described a recent hospital admission for unexplained dyspnea. Echocardiography showed normal systolic function but a thickened intraventricular septum along with an impaired global strain rate (–15.7%) and a strain pattern consistent with cardiac amyloidosis. Scintigraphy with ^{99m}Tc-3,3-diphosphono-1,2-propanodicarboxylic acid (^{99m}Tc–DPD) revealed Perugini grade 2 uptake of tracer (**B**) (**arrow**). Gene sequencing revealed no mutations in the transthyretin gene. Wild-type ATTR (ATTRwt) amyloidosis was diagnosed. CTS is a common early clinical manifestation of wild-type transthyretin amyloidosis, also known as senile systemic or cardiac amyloidosis. Of the patients with cardiac ATTRwt amyloidosis who have been treated at our institution, 98% showed evidence of median nerve entrapment on neurophysiologic studies, and 48% had a history of carpal tunnel decompression as many as 12 years prior to presentation, with advanced heart failure symptoms. Cardiac ATTRwt amyloidosis is currently diagnosed in only ~150 individuals in the UK each year, but postmortem studies indicate that ATTRwt amyloid deposits are present in up to 30% of men older than age 80 years (1). Repurposing of ^{99m}Tc–DPD bone scintigraphy largely abrogates the need for diagnostic cardiac biopsy, showing substantial cardiac uptake in nearly all cases (2). Carpal tunnel biopsy can readily identify ATTR amyloid deposition and may identify individuals at risk of developing cardiac ATTR amyloidosis, for which specific therapies are now being studied in clinical trials (3).

1. Pinney JH, Whelan CJ, Petrie A, Dungu J, Banypersad SM, Sattianayagam P, et al. Senile systemic amyloidosis: clinical features at presentation and outcome. J Am Heart Assoc 2013;2: e000098.
2. Gillmore JD, Maurer MS, Falk RH, Merlini G, Damy T, Dispenzieri A, et al. Nonbiopsy diagnosis of cardiac transthyretin amyloidosis. Circulation 2016;133:2404–12.
3. Hawkins PN, Ando Y, Dispenzeri A, Gonzalez-Duarte A, Adams D, Suhr OB. Evolving landscape in the management of transthyretin amyloidosis. Ann Med 2015;47:625–38.

Taryn Youngstein, MD
Janet A. Gilbertson, CSCI, FIMBS
David F. Hutt, BAppSc
Mark R. E. Coyne, PhD
Tamer Rezk, MD
Richa Manwani, MD
Candida C. Quarta, PhD
Helen J. Lachmann, PhD
Julian D. Gillmore, PhD
National Amyloidosis Centre
University College of London
Huw Beynon, MD
Nicholas Goddard, MD
Royal Free Hospital
Philip N. Hawkins, PhD, FMedSci
National Amyloidosis Centre
University College of London
London, UK

49. Uehara S, Grinberg A, Farber JM, Love PE. A role for CCR9 in T lymphocyte development and migration. J Immunol 2002; 168:2811–9.
50. Bennett LD, Fox JM, Signoret N. Mechanisms regulating chemokine receptor activity. Immunology 2011;134:246–56.
51. Lundstrom W, Highfill S, Walsh ST, Beq S, Morse E, Kockum I, et al. Soluble IL7Rα potentiates IL-7 bioactivity and promotes autoimmunity. Proc Natl Acad Sci U S A 2013;110: E1761–70.

DOI:10.1002/art.40162

Clinical Images: Carpal tunnel biopsy identifying transthyretin amyloidosis

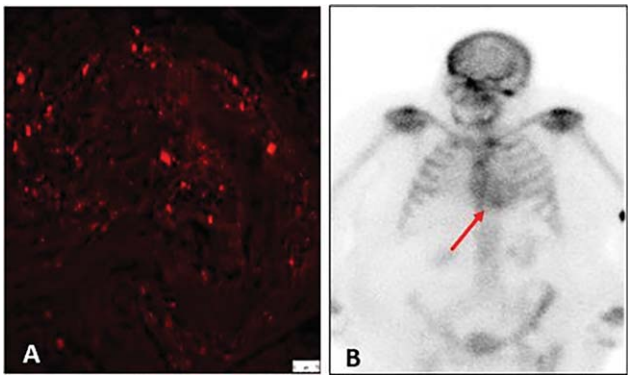

The patient, an 86-year-old woman, underwent routine decompression for carpal tunnel syndrome (CTS). A sample of tenosynovium was examined histologically, and amyloid deposits were identified (Congo red staining under polarized light) (**A**). Immunohistochemical staining confirmed that the amyloid deposits were transthyretin type. The patient was referred to us for further evaluation, at which time she described a recent hospital admission for unexplained dyspnea. Echocardiography showed normal systolic function but a thickened intraventricular septum along with an impaired global strain rate (–15.7%) and a strain pattern consistent with cardiac amyloidosis. Scintigraphy with ^{99m}Tc-3,3-diphosphono-1,2-propanodicarboxylic acid (^{99m}Tc–DPD) revealed Perugini grade 2 uptake of tracer (**B**) (**arrow**). Gene sequencing revealed no mutations in the transthyretin gene. Wild-type ATTR (ATTRwt) amyloidosis was diagnosed. CTS is a common early clinical manifestation of wild-type transthyretin amyloidosis, also known as senile systemic or cardiac amyloidosis. Of the patients with cardiac ATTRwt amyloidosis who have been treated at our institution, 98% showed evidence of median nerve entrapment on neurophysiologic studies, and 48% had a history of carpal tunnel decompression as many as 12 years prior to presentation, with advanced heart failure symptoms. Cardiac ATTRwt amyloidosis is currently diagnosed in only ~150 individuals in the UK each year, but postmortem studies indicate that ATTRwt amyloid deposits are present in up to 30% of men older than age 80 years (1). Repurposing of ^{99m}Tc–DPD bone scintigraphy largely abrogates the need for diagnostic cardiac biopsy, showing substantial cardiac uptake in nearly all cases (2). Carpal tunnel biopsy can readily identify ATTR amyloid deposition and may identify individuals at risk of developing cardiac ATTR amyloidosis, for which specific therapies are now being studied in clinical trials (3).

1. Pinney JH, Whelan CJ, Petrie A, Dungu J, Banypersad SM, Sattianayagam P, et al. Senile systemic amyloidosis: clinical features at presentation and outcome. J Am Heart Assoc 2013;2: e000098.
2. Gillmore JD, Maurer MS, Falk RH, Merlini G, Damy T, Dispenzieri A, et al. Nonbiopsy diagnosis of cardiac transthyretin amyloidosis. Circulation 2016;133:2404–12.
3. Hawkins PN, Ando Y, Dispenzeri A, Gonzalez-Duarte A, Adams D, Suhr OB. Evolving landscape in the management of transthyretin amyloidosis. Ann Med 2015;47:625–38.

Taryn Youngstein, MD
Janet A. Gilbertson, CSCI, FIMBS
David F. Hutt, BAppSc
Mark R. E. Coyne, PhD
Tamer Rezk, MD
Richa Manwani, MD
Candida C. Quarta, PhD
Helen J. Lachmann, PhD
Julian D. Gillmore, PhD
National Amyloidosis Centre
University College of London
Huw Beynon, MD
Nicholas Goddard, MD
Royal Free Hospital
Philip N. Hawkins, PhD, FMedSci
National Amyloidosis Centre
University College of London
London, UK

ARTHRITIS & RHEUMATOLOGY
Vol. 69, No. 10, October 2017, pp 2052–2061
DOI 10.1002/art.40195

Major Histocompatibility Complex Class II Alleles Influence Induction of Pathogenic Antiphospholipid Antibodies in a Mouse Model of Thrombosis

Elizabeth Papalardo,[1] Zurina Romay-Penabad,[1] Rohan Willis,[1] Premkumar Christadoss,[1] Ana Laura Carrera-Marin,[1] Elba Reyes-Maldonado,[2] Rajani Rudrangi,[1] Silvana Alfieri-Papalardo,[1] Ethel Garcia-Latorre,[2] Miri Blank,[3] Silvia Pierangeli,† Allan R. Brasier,[1] and Emilio B. Gonzalez[1]

Objective. **Both environmental and genetic factors are important in the development of antiphospholipid antibodies (aPL) in patients with antiphospholipid syndrome (APS). Currently, the only available data on predisposing genetic factors have been obtained from epidemiologic studies, without mechanistic evidence. Therefore, we studied the influence of major histocompatibility complex (MHC) class II alleles on the production of aPL in a mouse model of APS.**

Methods. **Three groups of mice, MHC class II–deficient ($MHCII^{-/-}$) mice, $MHCII^{-/-}$ mice transgenic for human HLA–DQ6 (DQ6), DQ8, or DR4 alleles, and the corresponding wild-type (WT) mouse strains were immunized; half were immunized with human β_2-glycoprotein I (β_2GPI), and the other half were immunized with control ovalbumin (OVA) protein. Thrombus formation in vivo, tissue factor activity in carotid and peritoneal macrophages, and serum levels of tumor necrosis factor (TNF), IgG anticardiolipin (aCL), antibodies, and anti-OVA antibodies were determined.**

Results. **Immunization with β_2GPI induced significant production of aCL and anti-β_2GPI in WT mice compared with control mice immunized with OVA ($P < 0.001$) but diminished aCL ($P < 0.001$) and anti-β_2GPI ($P = 0.016$) production in $MHCII^{-/-}$ mice. Anti-β_2GPI production was fully restored in DQ6 and DQ8 mice, while levels of anti-β_2GPI in DR4 mice and aCL in all transgenic lines were only partially restored ($P < 0.001$ to $P < 0.046$). Thrombus size in WT mice was twice that in $MHCII^{-/-}$ mice ($P < 0.001$) but similar to that in all transgenic lines. Carotid and peritoneal macrophage tissue factor levels decreased by >50% in $MHCII^{-/-}$ mice compared with wild-type B6 mice and were restored in DQ8 mice but not DR4 mice or DQ6 mice. TNF levels decreased 4-fold in $MHCII^{-/-}$ mice ($P < 0.001$) and were not restored in transgenic mice.**

Conclusion. **Our mechanistic study is the first to show that MHC class II alleles influence not only quantitative aPL production but also the pathogenic capacity of induced aPL.**

Antiphospholipid syndrome (APS) is an autoimmune disease of unknown etiology that is characterized by persistent antiphospholipid antibodies (aPL) with associated thrombosis and/or adverse obstetric events (1,2). Antiphospholipid antibodies represent a large, heterogeneous group of autoantibodies that target anionic phospholipids such as phosphatidylserine and cardiolipin as well as proteins such as β_2-glycoprotein I (β_2GPI) and prothrombin. Beta$_2$-GPI has been recognized as one of the main antigenic targets of aPL and has an important pathogenic role in the development of

Drs. Gonzalez and Blank's work was supported by the United States–Israel Binational Science Foundation (grant 2009099). Dr. Willis' work was supported by a Mallinckrodt-Questcor Fellowship grant.

[1]Elizabeth Papalardo, MSc, Zurina Romay-Penabad, PhD, Rohan Willis, MBBS, DM, Premkumar Christadoss, MD, Ana Laura Carrera-Marin, PhD, Rajani Rudrangi, MD, Silvana Alfieri-Papalardo, Allan R. Brasier, MD, Emilio B. Gonzalez, MD: University of Texas Medical Branch, Galveston; [2]Elba Reyes-Maldonado, PhD, Ethel Garcia-Latorre, PhD: Instituto Politécnico Nacional, Mexico City, Mexico; [3]Miri Blank, PhD: Sheba Medical Center, Tel-Aviv University, Tel-Aviv, Israel.

† Dr. Pierangeli is deceased.

Address correspondence to Emilio B. Gonzalez, MD, Antiphospholipid Standardization Laboratory, Division of Rheumatology, Department of Internal Medicine, University of Texas Medical Branch, 122 6th Street, 2.108 Brackenridge Hall, Galveston, TX 77555. E-mail: ebgonzal@utmb.edu.

Submitted for publication February 16, 2017; accepted in revised form June 27, 2017.

thrombosis in patients with systemic lupus erythematosus (SLE) and those with APS (3,4).

Dysregulated activation of platelets, endothelial cells, and monocytes occurs in conjunction with disruption of natural anticoagulant and fibrinolytic systems in response to pathogenic aPL and results in a procoagulant phenotype in patients with APS (5). Endothelial cells activated by pathogenic aPL, particularly anti-β_2GPI–β_2GPI complexes, express significantly greater amounts of adhesion molecules promoting leukocyte adhesion and transformation (6,7). This is accompanied by up-regulation of tissue factor and tumor necrosis factor (TNF) gene expression and secretion in both endothelial cells and monocytes, resulting in a proinflammatory vascular environment (8–10). This proinflammatory environment is key to the pathophysiology of thrombosis in APS, which is a highly heterogeneous and multifaceted process that is linked to a variety of different genes and acquired factors (5).

Similar to most autoimmune diseases, APS is believed to occur as a result of a complex interaction between environmental and genetic factors, and current evidence suggests that pathogenic aPL are produced by exposure to certain viral or bacterial products containing sequences similar to those contained in host antigens, thus inducing a break in tolerance (11). These environmental antigens are believed to be phospholipid-binding proteins with structural similarity to β_2GPI that induce aPL production through activation of cross-reacting T cells (12). There is also evidence that environmental antigens can interact with β_2GPI to reveal cryptic epitopes and in so doing activate epitope-specific autoreactive T cells and B cells (13). Previous studies have demonstrated that active immunization of mice and rabbits with β_2GPI, or portions of the protein, induces production of pathogenic anticardiolipin antibodies (aCL) and anti-β_2GPI that are capable of causing intrauterine fetal death, thrombocytopenia, and thrombosis (12,14–16).

Familial and nonfamilial population studies in different ethnic groups of patients with primary or secondary APS have shown multiple associations of HLA–DR and HLA–DQ with the occurrence of APS and the development of aPL. Loci that are relevant in conferring susceptibility to the development of APS and aPL include HLA–DR4, DR7, DR9, DR13, DR53, DQ6, DQ7, and DQ8 major histocompatibility complex (MHC) class II alleles (17). The most consistently reported HLA associations with APS across several ethnic groups appeared to be with HLA–DR4 and HLA–DRw53. These haplotypes are thought to be efficient at presentation of antigens relevant to the development of APS. However, these epidemiologic associations have not been proven mechanistically in an experimental model. As such, we studied the in vivo involvement of human HLA–DR4, DQ6, and DQ8 MHC class II alleles in the production of pathogenic aPL.

MATERIALS AND METHODS

Mice. Mice with a homozygous null mutation for MHC class II genes (B6.129-H2dl$^{AB\text{-}EaAbl}$ [MHCII$^{-/-}$] mice) and unique transgenic strains of MHCII$^{-/-}$ mice that solely express functional human HLA–DQ8 (HLA–DQA1*0301/DQB1*0302 [DQ8+]), HLA–DQ6 (HLA–DQA1*0103/DQB1*0601) [DQ6+]), or HLA–DR4 (DRB1*0401) [DR4+]) up to 16 weeks of age were kindly provided by Dr. Chella David (Mayo Clinic, Rochester, MN). Generation of knockout and transgenic mice was achieved as previously described (18,19). Corresponding wild-type (WT) strains for MHCII$^{-/-}$ mice (C57BL/6J) [B6]) and transgenic mice (C57BL/10J [B10]) ranged from age 8 weeks to age 12 weeks and were obtained from The Jackson Laboratory. All animals were housed in the viral antibody–free barrier facility at the University of Texas Medical Branch (UTMB).

Reagents. Beta$_2$-GPI was isolated from pooled normal human sera, as described in detail elsewhere (3). Briefly, human β_2GPI was purified using perchloric acid precipitation and affinity chromatography on a heparin–Sepharose column (GE Healthcare), and purified mouse β_2GPI (R&D Systems) and cardiolipin from bovine heart were purchased from Sigma-Aldrich. All preparations were determined to be free of endotoxin contamination, using a *Limulus* amebocyte cell lysate assay (E-Toxate; Sigma-Aldrich) (assay sensitivity <0.06 IU/ml).

Immunization scheme and experimental groups. The DQ6+ mice (n = 12), DQ8+ mice (n = 12), DR4+ mice (n = 6), B6 mice (n = 6), B10 mice (n = 6), and MHCII$^{-/-}$ mice (n = 6) were injected intraperitoneally at time 0 with either a 1-ml preparation containing 150 μg/ml of human β_2GPI and 200 μg/ml of adjuvant (AdjuPrime, Immune Modulator; Pierce) or ovalbumin (OVA) (Sigma-Aldrich) and adjuvant, at the same concentrations. In each group of mice, half were immunized with β_2GPI and the other half with the control protein OVA. Each mouse received 2 subsequent booster injections with the same antigen that was given at the start of the immunization schedule, using the same technique. The second injection was given 8 days after the first injection, and the third injection was given 15 days after the first injection. Animal use and care were performed according to the guidelines established by the UTMB Institutional Animal Care and Use Committee.

Determination of aCL, anti-β_2GPI, and anti-OVA antibodies. To monitor the production of IgG anti-β_2GPI and aCL, blood samples were obtained from each mouse weekly over the course of 4 weeks on days 7, 14, 21, and 28 after the first injection was given. The serum level of IgG anti-OVA antibodies was determined on day 28 of the immunization schedule. IgG aCL, anti-β_2GPI, and anti-OVA antibodies were determined using in-house enzyme-linked immunosorbent assays (ELISAs) according to a standardized protocol, as previously described (14). Murine β_2GPI (2 μg/ml) instead of human β_2GPI was used as the coating antigen in a

modified anti-β_2GPI assay to identify antibodies with specific affinity for murine β_2GPI. To examine the cofactor dependency of induced aCL, we carried out the aCL assay in the presence of increasing concentrations of purified human β_2GPI to a maximum of 10 μg/ml in the reaction well, and the results were compared with those obtained in the absence of β_2GPI, as previously described (20). To avoid the influence of β_2GPI external to the assay system, both blocking and assay buffers were serum free (2% bovine serum albumin [BSA]/phosphate buffered saline [PBS]). In addition, the serum samples to be tested were obtained on day 28 from 3 mice in each WT group (i.e., high-titer antibody levels) and diluted 1:200 with assay diluent.

Inhibition studies. The inhibition studies were performed as previously described (14). A 1:100 dilution of mouse sera obtained on day 28 (in 2% BSA/PBS) was preincubated overnight with PBS solutions containing purified human β_2GPI or cardiolipin vesicles of increasing concentrations, up to maximums of 3.4 mg/ml and 2.0 mg/ml, respectively. The sera were then tested for aCL or anti-β_2GPI activity by ELISA, as described above. Each serum sample was preincubated with only PBS solution to serve as a baseline control, with the results expressed as the percent inhibition compared with baseline.

Assessment of the thrombogenicity of aPL. The thrombogenicity of induced aPL in the mice was assessed using a mouse model of induced thrombosis. Thrombus dynamics were assessed on day 28 after the first immunization, as described previously (16). Briefly, the mice were anesthetized, the right femoral vein was exposed for observation, and an ~0.5-mm segment was transilluminated using a microscope equipped with a closed circuit video system. The isolated vein was pinched to introduce a standardized injury, and thrombus formation and dissolution were then visualized and recorded. Three thrombi per animal were each measured 5 times, and the mean values were calculated.

Determination of cytokines in serum, peritoneal macrophages, and carotid homogenates. Measurements of TNF in serum from the mice were assessed on day 28, using a commercial ELISA (R&D Systems) performed according to the manufacturer's instructions. On day 28, tissue factor activity in peritoneal macrophages and carotid homogenates was determined using a commercial chromogenic assay (Actichrome Tissue Factor; American Diagnostica) that measures the conversion of factor X into factor Xa after activation by the tissue factor–factor VII complex, as described previously (21). Briefly, peritoneal macrophages were generated by flushing the peritoneal cavity, followed by centrifugation, resuspension, and sonication of the cell pellet in a Tris–saline buffer to obtain lysates, which were stored at −70°C. Pieces (~5 mm) of uninjured carotid were dissected from both sides in each animal, homogenized, and stored at −70°C. The tissue factor activity in peritoneal macrophage lysates and carotid homogenates for each mouse group treated with β_2GPI was expressed as the fold increase above levels in the corresponding OVA-treated control group.

Statistical analysis. Data are presented as the mean ± SD, as appropriate. One-way analysis of variance followed by Tukey's multicomparison test was used to compare differences between groups. The association between variables was evaluated using Pearson's correlation test and a multivariate linear regression model of best fit. P values less than 0.05 were considered significant.

RESULTS

Induction of aPL in β_2GPI-immunized WT mice. Compared with control mice treated with OVA, β_2GPI-immunized B6 (mean ± SD 1.42 ± 0.40 versus 0.31 ± 0.04 optical density [OD]; $P < 0.001$) and B10 mice produced significantly higher anti-β_2GPI levels by week 1, and levels remained significantly elevated over the entire 4-week period ($P < 0.001$). The maximum anti-β_2GPI level was attained by week 2 in B10 mice (mean ± SD 2.75 ± 0.16 OD) and by week 3 in B6 mice (mean ± SD 2.90 ± 0.27 OD) (Figure 1A). Anticardiolipin antibody levels in β_2GPI-immunized B6 and B10 mice were also significantly elevated compared with those in the corresponding OVA-immunized mice (mean ± SD

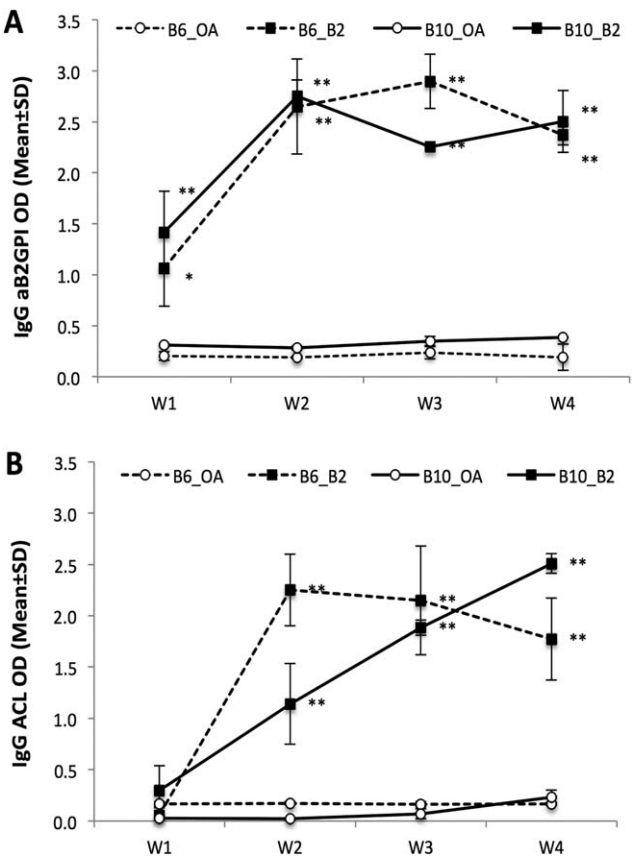

Figure 1. Titers of autoantibodies induced in immunized wild-type C57BL/6J (B6) and C57BL/10J (B10) mice. Wild-type mice immunized with β_2-glycoprotein I (β_2GPI; B2) produced significantly higher titers of anti-β_2GPI antibodies (**A**) and anticardiolipin antibodies (aCL) (**B**) over the 4-week period compared with corresponding ovalbumin (OVA; OA)–immunized controls. * = $P < 0.05$; ** = $P < 0.001$ versus OVA-immunized control mice.

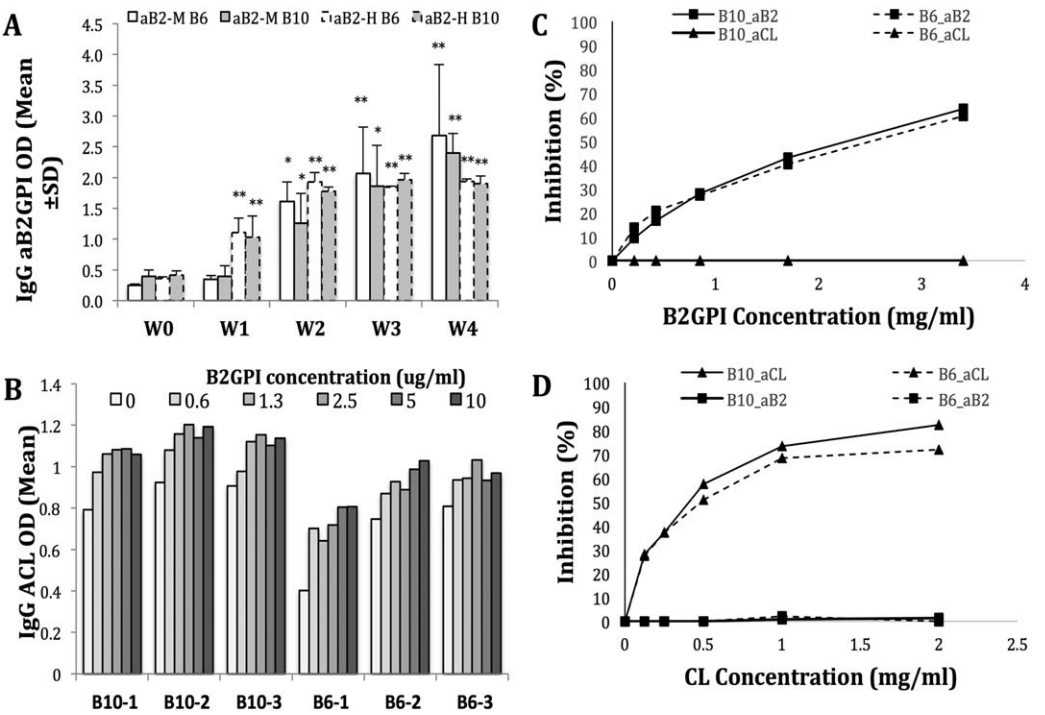

Figure 2. Binding characteristics of autoantibodies induced in immunized wild-type mice. **A,** Anti-β_2GPI antibodies with affinity for human anti-β_2GPI (aβ_2-H) were the first type to be produced, while production of antibodies with affinity for mouse anti-β_2GPI (aβ_2-M) occurred later in the time course of the study. Ultimately, aβ_2-M levels continued to increase, while aβ_2-H levels stabilized by weeks 3–4. **B–D,** While induced aCL demonstrated cofactor dependency, with increased activity relative to the increase in β_2GPI (**B**), inhibition studies indicated that induced anti-β_2GPI (**C**) and aCL (**D**) were not cross-reactive. $* = P < 0.05$; $** = P < 0.001$ versus corresponding mice at week 0. See Figure 1 for other definitions.

2.25 ± 0.35 OD versus 0.17 ± 0.02 and 1.14 ± 0.39 versus 0.02 ± 0.01 OD, respectively; $P < 0.001$/ for both) but not until week 2. Anticardiolipin antibody levels remained significantly elevated in these mice over the remainder of the 4-week period ($P < 0.001$) (Figure 1B).

Binding characteristics of induced aPL in mice immunized with β_2GPI. In order to evaluate the binding characteristics of induced aPL in mice treated with β_2GPI, the affinity of induced aPL for mouse versus human β_2GPI as well as the cofactor dependency of induced aCL were determined. In both B6 and B10 mice, although the levels of aPL against human β_2GPI (aβ_2-H) were increased by week 1 (mean $\pm$ SD 1.10 ± 0.24 OD in B6 mice [$P < 0.001$] and 1.03 ± 0.35 OD in B10 mice [$P < 0.001$]), aPL against mouse β_2GPI (aβ_2-M) did not attain significantly elevated levels until week 2 (mean $\pm$ SD 1.61 ± 0.32 OD in B6 mice [$P = 0.009$] and 1.26 ± 0.49 OD in B10 mice [$P = 0.04$]). Interestingly, although the increase in aβ_2-H stabilized during the last 2 weeks, aβ_2-M values increased consistently throughout the 4-week period (Figure 2A). In our aCL cofactor dependency assay, the cardiolipin binding activity of mouse sera was elevated in a dose-dependent manner with sequentially higher levels of β_2GPI. The maximum increase in OD varied from 27% to 100% with the addition of β_2GPI, indicating that the induced aCL are cofactor dependent (Figure 2B). The results of cross-inhibition studies using cardiolipin vesicles and β_2GPI demonstrated the presence of at least 2 separate, non–cross-reacting populations of antibodies (i.e., aCL-specific and anti-β_2GPI–specific) (Figures 2C and D).

Necessity of MHC class II alleles for complete production of aPL. Maximum anti-β_2GPI levels in β_2GPI-immunized MHCII$^{-/-}$ mice were approximately half those in the corresponding WT B6 mice (mean $\pm$ SD 1.29 ± 0.50 versus 2.90 ± 0.27 OD; $P = 0.016$). Surprisingly, maximum anti-β_2GPI levels in MHCII$^{-/-}$ mice immunized with β_2GPI were significantly higher than those in control mice immunized with OVA (mean $\pm$ SD 1.29 ± 0.50 versus 0.30 ± 0.02 OD; $P < 0.001$). In MHCII$^{-/-}$ mice, however, a longer period of time was required to attain anti-β_2GPI levels significantly greater than those in OVA-treated controls

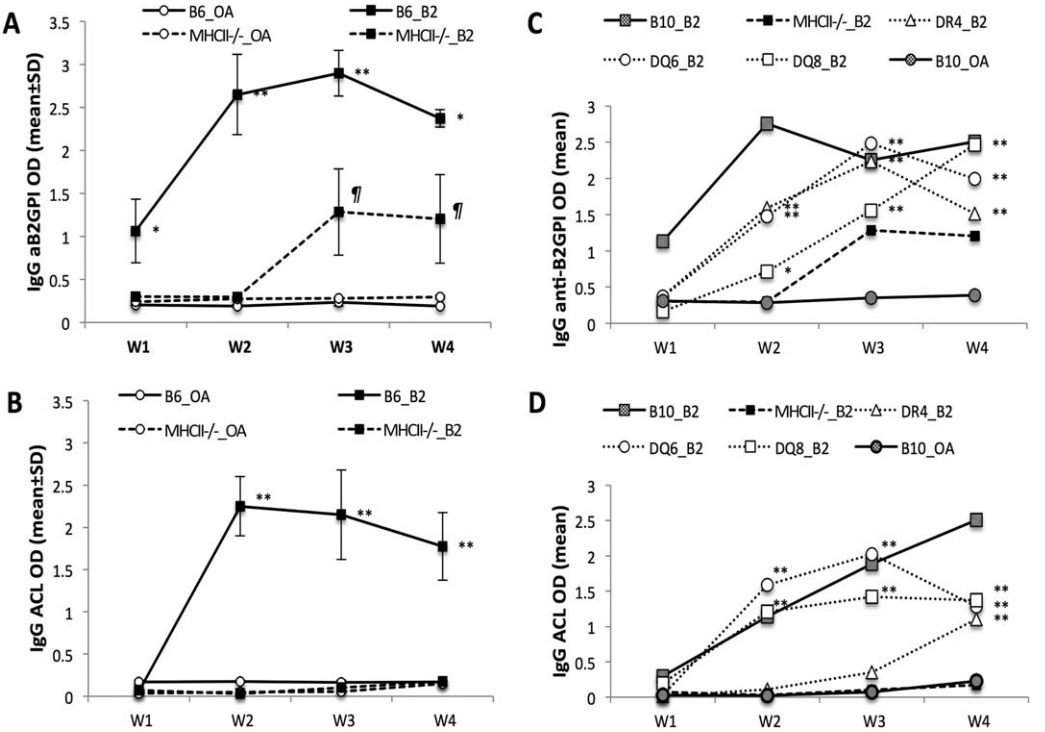

Figure 3. Effect of major histocompatibility complex (MHC) class II–knockout and transgenic DR4, DQ6, and DQ8 alleles on autoantibody production in immunized mice. MHCII$^{-/-}$ mice immunized with β_2GPI produced lower levels of anti-β_2GPI (**A**) with delayed induction and no aCL (**B**) over the 4-week period compared with wild-type (WT) mice. Transgenic DR4, DQ6 and DQ8 mice immunized with β_2GPI had variable restoration of anti-β_2GPI (**C**) and aCL (**D**) production compared with WT mice. $* = P < 0.05$; $** = P < 0.001$, β_2GPI-immunized transgenic mice versus corresponding mice (**A** and **B**) and versus corresponding ovalbumin-immunized control mice (**C** and **D**). $¶ = P < 0.001$, β_2GPI-immunized MHCII$^{-/-}$ mice versus corresponding ovalbumin-immunized MHCII$^{-/-}$ mice. Note that values for transgenic mice immunized with ovalbumin are not shown in **C** and **D**. See Figure 1 for other definitions.

(21 days in MHCII$^{-/-}$ mice and 7 days in B6 mice) (Figure 3A).

In contrast, the β_2GPI-immunized MHCII$^{-/-}$ mice failed to produce significant amounts of aCL, with maximum levels in B6 mice being more than 10 times higher than those in MHCII$^{-/-}$ mice (mean ± SD 2.25 ± 0.35 versus 0.17 ± 0.06 OD; $P < 0.001$). There was no significant difference between the aCL levels in β_2GPI-immunized MHCII$^{-/-}$ mice compared with those in OVA-immunized mice ($P = 0.563$) (Figure 3B).

Variable restoration of aPL induction by DR4, DQ6, and DQ8 MHC class II alleles. Maximum anti-β_2GPI levels in transgenic DR4+ mice (mean ± SD 2.24 ± 0.22 OD; $P < 0.001$), transgenic DQ6+ mice (2.49 ± 0.20 OD; $P < 0.001$), and transgenic DQ8+ mice (2.47 ± 0.46 OD; $P < 0.001$) immunized with β_2GPI were significantly higher than those in β_2GPI-immunized MHCII$^{-/-}$ mice (mean ± SD 1.29 ± 0.50 OD). Significantly elevated anti-β_2GPI levels were achieved in DR4+, DQ6+, and DQ8+ mice by day 14, compared with day 21 in β_2GPI-immunized MHCII$^{-/-}$ mice. Interestingly, anti-β_2GPI production in DQ6+ mice ($P = 0.550$) and DQ8+ mice ($P = 0.392$) was restored to levels comparable with those in WT B10 mice (mean ± SD 2.75 ± 0.16 OD), but the levels in DR4+ mice were only partially restored ($P = 0.022$) (Figure 3C). The time line of anti-β_2GPI production also varied among β_2GPI-immunized DR4+, DQ6+, and DQ8+ mice. In all transgenic lines, there was no anti-β_2GPI induction during week 1, but by day 14 there was significant anti-β_2GPI production, with levels in DQ8+ mice being approximately half those in DR4+ and DQ6+ mice ($P < 0.001$). By day 21, maximum levels were attained in DR4+ and DQ6+ mice, with waning until day 28, while maximum levels were attained in DQ8+ mice on day 28 (Figure 3C).

Similarly, there was partial restoration of maximum aCL production in β_2GPI-immunized DR4+ mice (mean ± SD 1.10 ± 0.26 OD; $P < 0.001$), DQ6+ mice (2.02 ± 0.49 OD; $P = 0.046$), and DQ8+ mice (1.42 ± 0.14 OD; $P < 0.001$) compared with WT mice (2.51 ± 0.10 OD). Significant aCL production was seen by day 14 in both DQ6+ and DQ8+ mice, while this did

Table 1. Serum levels of anti-OVA antibodies on day 28 in mice immunized with OVA or β_2GPI*

Mice	Immunization with OVA	Immunization with β_2GPI	P
B6	0.94 ± 0.28	0.35 ± 0.17	<0.001
B10	1.05 ± 0.19	0.23 ± 0.08	<0.001
MHCII$^{-/-}$	0.13 ± 0.02	0.25 ± 0.14	0.999
DR4	0.29 ± 0.14	0.28 ± 0.14	1.000
DQ6	0.28 ± 0.14	0.28 ± 0.11	1.000
DQ8	1.09 ± 0.42	0.34 ± 0.09	<0.001

* Values are the mean ± SD OD. Anti-OVA = anti-ovalbumin; β_2GPI = β_2-glycoprotein I; MHCII$^{-/-}$ = major histocompatibility complex class II–deficient.

not occur until day 28 in DR4+ mice. Interestingly, aCL production in DQ6+ and DQ8+ mice waned between week 3 and week 4 (Figure 3D).

Effect of MHC class II knockout and transgenic human DR4, DQ6, and DQ8 on anti-OVA production. Immunization of WT mice with OVA induced anti-OVA antibody production similar to that of aPL induction following β_2GPI immunization. On day 28, anti-OVA antibody levels in B6 mice and B10 mice immunized with OVA (mean ± SD 0.94 ± 0.28 and 1.05 ± 0.19 OD, respectively) were significantly higher ($P < 0.001$) than levels in the corresponding mice immunized with β_2GPI (mean ± SD 0.35 ± 0.17 and 0.23 ± 0.08 OD, respectively). MHCII$^{-/-}$ mice immunized with OVA failed to produce significant amounts of anti-OVA antibodies compared with B6 mice immunized with OVA (mean ± SD 0.13 ± 0.02 versus 0.94 ± 0.28 OD; $P < 0.001$). There was no significant difference in anti-OVA antibody levels in OVA-immunized MHCII$^{-/-}$ mice compared with control β_2GPI-immunized B6 mice ($P = 0.717$). Interestingly, although there was complete restoration of anti-OVA in OVA-immunized DQ8+ mice compared with WT mice (mean ± SD 1.09 ± 0.42 versus 1.05 ± 0.19 OD; $P = 1.000$), there was no production in OVA-immunized DQ6+ mice (mean ± SD 0.28 ± 0.14 OD; $P < 0.001$) and DR4+ mice (0.29 ± 0.14 OD; $P < 0.001$) (Table 1).

Thrombotic properties of induced aPL. Levels of both aCL ($r = 0.688$, $P < 0.001$) and anti-β_2GPI ($r = 0.853$, $P < 0.001$) were positively associated with thrombus size, while anti-OVA antibodies ($r = -0.409$, $P = 0.018$) were negatively associated. It is important to note that anti-β_2GPI was positively correlated with aCL ($r = 0.746$, $P < 0.001$) and negatively correlated with anti-OVA antibodies ($r = -0.365$, $P = 0.037$). In a multivariate linear regression best-fit model, the maximum anti-β_2GPI level ($\beta = 0.651$, $P < 0.001$) was the strongest and only significant predictor of thrombus size. The contribution of maximum levels of aCL ($\beta = 0.192$, $P = 0.203$) and anti-OVA ($\beta = -0.160$, $P = 0.105$) was not significant. The overall fit of the model (R^2) was 0.753.

Both B6 (mean ± SD 2,978.5 ± 501.3 μm^2) and B10 (2,267.0 ± 539.0 μm^2) WT mice immunized with β_2GPI produced thrombi ~5 times larger than those in their corresponding control OVA-immunized mice (mean ± SD 615.0 ± 169.3 and 460.7 ± 15.3 μm^2, respectively; $P < 0.001$ for both). β_2GPI-immunized MHCII$^{-/-}$ mice (mean ± SD 1,470 ± 242.0 μm^2) produced thrombi half the size of those in β_2GPI-immunized WT B6 mice ($P < 0.001$). The full thrombogenic effect was restored in transgenic DR4+ mice (mean ± SD 2,100.7 ± 507.6 μm^2; $P = 1.000$), DQ8+ mice (1,936.8 ± 634.3 μm^2; $P = 0.993$), and DQ6+ mice (1,936.0 ± 501.3 μm^2; $P = 0.993$) compared with WT B10 mice. Interestingly, although the mean thrombus size in transgenic DR4+, DQ6+, and DQ8+ mice was 1.3–1.5 times as large as that in MHCII$^{-/-}$ mice, the difference was not statistically significant ($P = 0.492$) (Figure 4).

Proinflammatory properties of induced aPL. Tissue factor levels in the carotid of MHCII$^{-/-}$ mice treated with β_2GPI (1.7-fold increase compared with OVA-treated controls) were significantly lower than those in the corresponding WT B6 mice (3.7-fold; $P = 0.024$). Although carotid tissue factor activity in DQ8+ mice treated with β_2GPI was restored to the levels in WT B10 mice (3.1-fold versus 4.6-fold increase above the level in control mice; $P = 0.171$), those in DR4+ mice (1.6-fold; $P = 0.024$) and DQ6+ mice (1.6-

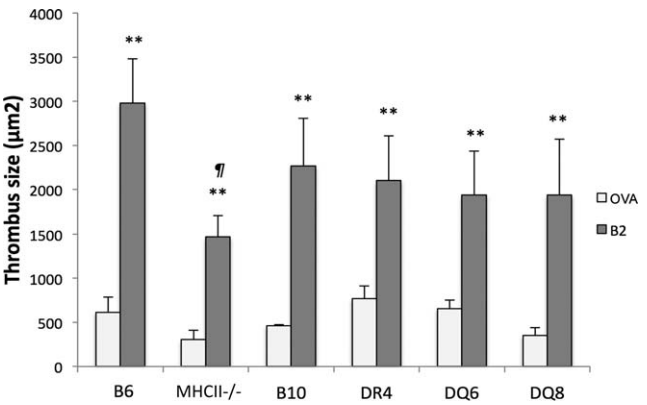

Figure 4. Thrombus size in all groups of immunized mice. In wild-type (WT) mice immunized with β_2-glycoprotein I (β_2GPI; B2), thrombi were significantly larger than those in the corresponding major histocompatibility complex (MHC) class II–knockout mice. In transgenic DR4, DQ6, and DQ8 mice immunized with β_2GPI, thrombi were similar in size to those in the corresponding WT mice. Values are the mean ± SD. ** = $P < 0.001$ versus corresponding ovalbumin (OVA)–immunized control mice; ¶ = $P < 0.001$ versus β_2GPI-immunized B6 mice.

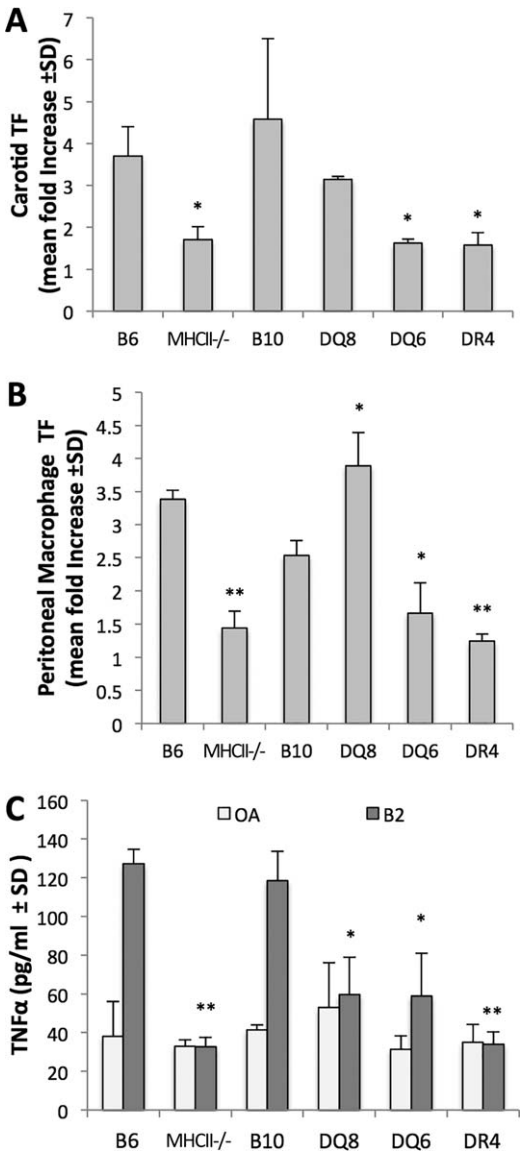

Figure 5. Carotid tissue factor (TF) levels (**A**), peritoneal macrophage tissue factor levels (**B**), and tumor necrosis factor (TNF) levels (**C**) in immunized mice. Both carotid and peritoneal macrophage tissue factor levels decreased significantly in MHCII$^{-/-}$ mice compared with WT mice. Although tissue factor activity in transgenic DQ8 mice was restored, tissue factor levels in DR4 and DQ6 mice remained low. While TNF levels decreased in MHCII$^{-/-}$ mice compared with WT mice, there was no restoration of TNF activity in the transgenic mice. Values in **A** and **B** are the fold increase above levels in the corresponding OVA-immunized mice on day 28. Values in **C** are the levels in OVA-immunized mice and β_2GPI-immunized mice. $* = P < 0.05$; $** = P < 0.001$ versus levels in WT B6 or B10 mice. See Figure 4 for other definitions.

fold; $P = 0.026$) were significantly lower (Figure 5A). A similar pattern was observed for tissue factor levels in MHCII$^{-/-}$mice. Peritoneal macrophage tissue factor activity in B6, MHCII$^{-/-}$, B10, DQ8+, DQ6+, and DR4+ mice immunized with β_2GPI was increased over that in OVA-immunized controls by 3.4-, 1.4-, 2.5-, 3.9-, 1.7-, and 1.2-fold, respectively (Figure 5B).

TNF levels in MHCII$^{-/-}$ mice treated with β_2GPI (mean ± SD 32.7 ± 4.8 pg/ml) were 4 times lower than the levels in corresponding WT B6 mice (127.3 ± 7.4 pg/ml; $P < 0.001$). TNF production was not restored in transgenic DR4+ mice (34.0 ± 6.4 pg/ml; $P < 0.001$), transgenic DQ6+ mice (58.9 ± 22.2 pg/ml; $P = 0.004$), or transgenic DQ8+ mice (59.7 ± 19.2 pg/ml; $P = 0.006$) compared with levels in WT B10 mice (118.6 ± 15.1 pg/ml) (Figure 5C).

DISCUSSION

Several epidemiologic studies have highlighted associations of HLA–DR and HLA–DQ with the occurrence of aPL, but to our knowledge, this is the first mechanistic study to evaluate these associations in vivo. The development of aPL in our WT mice indicates the normal pattern for a T cell–dependent primary immune response of conventional B2 cells to an antigen. Indeed, there is reported evidence suggesting a role of Th1 CD4+ T cells in the production of aCL and anti-β_2GPI in patients with APS (22,23). We have shown that immunization of mice with human β_2GPI first leads to the production of antibodies reactive with human β_2GPI followed by the appearance of autoantibodies reactive with mouse (self) β_2GPI; this sequence of events was noted in previous experiments (24).

This break in tolerance to mouse β_2GPI is likely attributable to the high structural homology between human and mouse β_2GPI (25). Furthermore, the development of aCL in response to β_2GPI immunization occurred in a manner suggestive of epitope spreading, a mechanism that is important in the progression of autoimmune responses (26). Several epitopes on β_2GPI have been identified as being cross-reactive with aCL (27,28), and protein–lipid complexes containing β_2GPI and cardiolipin occur with enough frequency (29) that epitope spreading with increased reactivity to cardiolipin is very likely. The absence of aCL activity in immunized MHCII$^{-/-}$ mice strongly suggests that the increase in aCL titers in this animal model is likely a result of epitope spreading in a T cell–dependent manner requiring antigen presentation.

Quite surprisingly, our expectation that all autoantibody production would be completely abolished in the MHCII$^{-/-}$ mice was overturned by the development of anti-β_2GPI in these mice, albeit at significantly lower titers and on a delayed time line. We surmise that

although the major pathway for the production of autoreactive aPL requires T cell–dependent B cell activation, which in turn is dependent on MHC class II presentation of antigenic peptides from β_2GPI or structural homologs to autoreactive T cells, aPL production can seemingly occur through T cell–independent mechanisms as well. The activation of B1 cells rather than direct stimulation of B2 cells is more likely to occur in this regard, and there is some evidence that B1 cells may contribute to the development of systemic autoimmune diseases such as SLE (30).

It is important to note, however, that the exact role of B1 cells in autoimmunity has not been clearly defined, and there are conflicting data regarding their importance (31). An interesting feature of the typical autoimmune response observed with B1 cells is that autoantibodies produced in this manner do not tend to facilitate epitope spreading (30,31). The delayed induction of aCL and its dependency on anti-β_2GPI coupled with the non–cross-reactivity of the antibody populations may also point to development of aCL by epitope spreading. Further research is necessary to make a definitive determination of the potential role of B1 cells and epitope spreading in the development of APS.

As outlined previously, both familial and nonfamilial population studies in APS indicate a definite genetic component in the development of disease. Key alleles associated with aCL include DRB1*04 (DR4), DQB1*0302 (DQ8), DRB1*07 (DR7), DRB1*09 (DR9), DRw53, and DQw3 (32–34), and those associated with lupus anticoagulant include DR4, DR7, and DQB1*0301 (DQ7) (35–37). Anti-β_2GPI production has been linked to DQ8, DR4, DRB1*0604/05 (DQ6), and DRB1*1302 (DR13) (33,34,38,39), while APS disease manifestations have been linked to DR4, DRw53, DQw7, DR7, DQ6, and DQ8 (38,40–42). Given these associations, it is not surprising that the introduction of human DR4 (DRB1*0401), DQ6 (DQA1*0103/DQB1*0601), and DQ8 (DQA1*0301/DQB1*0302) molecules in MHCII$^{-/-}$ mice restored production of anti-β_2GPI and aCL in the APS model, albeit with varying effect. The variation in titer and the time line of autoantibody development in these transgenic mice is likely an indication of the relative efficiency of these alleles in presenting β_2GPI-like epitopes relevant to the production of autoimmune aPL. Interestingly, induction of anti-OVA antibodies was abolished in MHCII$^{-/-}$ mice and restored in transgenic DQ8 mice but not in DR4 or DQ6 mice, highlighting the notion that these MHC class II alleles do vary in their ability to bind and present antigens. Despite such variation, however, all 3 are seemingly able to bind and present antigenic epitopes relevant to the induction of an autoimmune aPL response.

Perhaps one of the most interesting findings in the current study is variation in the pathogenicity of induced aPL in the different mouse groups. The titer of induced anti-β_2GPI was the most important predictor of thrombus size; this explains the observation that the MHCII$^{-/-}$ mice, which had lower levels of anti-β_2GPI, had significantly smaller thrombi compared with WT mice. Accordingly, the thrombus size in transgenic mice was similar to that in WT type mice, due to the restoration of anti-β_2GPI production. However, although the tissue factor activity in MHCII-knockout mice was diminished, as expected, this activity was restored only in transgenic DQ8 mice and not in transgenic DQ6 or DR4 mice. Furthermore, TNF levels were not restored in any of the transgenic mice (DR4, DQ6, and DQ8).

Tissue factor plays a major role in the progression of both thrombotic and obstetric disorders in patients with APS (8), and although the contribution of TNF to APS pathogenesis is less certain, there is some evidence that it has a role in obstetric APS (43). Therefore, one would expect that restoration of aPL production in transgenic mice would result in the restoration of both tissue factor and TNF activity. It is noteworthy that the absence of tissue factor in particular did not unduly affect the ability of aPL to induce thrombosis, suggesting the importance of other cytokine pathways in this regard. Therefore, induced aPL likely vary in their pathogenic capacity as it relates to the induction of cytokine production, and this capacity may be traced to the epitopes against which these aPL are reactive. Supportive evidence for this theory is provided by several studies that highlight the ability of aPL to activate distinct intracellular signaling pathways, the corollary of which is the development of different clinical manifestations of APS (5,44).

We are aware that our model of aPL induction using heterologous β_2GPI does not provide a complete approximation of the spontaneous development of APS, which is true of all animal models of APS developed to date. However, we submit that the development of mouse self-reactive anti-β_2GPI with the ability to induce thrombosis and cytokine production indicates that this model at the very least provides insight into the role of these MHC class II alleles in the break in tolerance necessary for the development of pathogenic autoreactive anti-β_2GPI. Transgenic animals with MHC class II alleles that are not associated with APS were not available to us; therefore, we were unable to compare their ability to produce aPL in response to β_2GPI immunization.

A priority for future studies is development of transgenic mice with nonsusceptible MHC CLASS II alleles, to confirm that these alleles are less permissive of a break in tolerance to β_2GPI. Because our knockout and transgenic mice were compared with WT mice from different sources and were not littermates, it is difficult to state with absolute certainty that the MHC CLASS II differences were solely responsible for the observed effects on antibody production and pathogenicity. However, previous studies have shown that in B6.129-H2dl$^{AB\text{-}EaAbl}$ (MHCII$^{-/-}$) mice, all immune parameters not directly connected to the MHC CLASS II genes appeared normal, including T cell differentiation to the CD8 lineage, B cell differentiation, peripheral B cell populations, and immunoglobulin levels (18). Similarly, the introduction of human MHC class II alleles into the MHCII$^{-/-}$ mice led to the selection and restoration of a peripheral CD4+ T cell compartment, which was directly related to the generation of mouse collagen-reactive autoantibodies in a model of human polyarthritis when compared with transgene-negative littermates (18,19).

Despite these limitations, our study does provide some tantalizing insights into the process of autoimmune aPL induction in APS. As we expected, a lack of MHC class II alleles resulted in diminished aPL production; however, aPL production was not completely abolished. This indicates that both T cell–dependent and T cell–independent mechanisms are likely to play a role in aPL production, but further research into these possible mechanisms is necessary. We also conclude that both the titer and pathogenic ability of aPL produced during the progression of APS appear to be dependent on the expression of relevant MHC class II alleles. Therefore, our findings provide direct mechanistic evidence that APS susceptibility may be linked to the efficiency with which MHC class II alleles present antigens with structural similarity to the main antigen in APS, i.e., β_2GPI, as indicated previously in epidemiologic studies. Given that MHC class II is one of the most polymorphic gene groups, additional studies are needed to more fully elucidate the relative efficiency of these alleles in presenting specific β_2GPI epitopes and the pathogenic effects of aPL that are produced as a result.

ACKNOWLEDGMENTS

This work is dedicated to the memory of Dr. Silvia Pierangeli, who contributed significantly to the development of this project. We thank Dr. Chella David at the Mayo Clinic for kindly providing knockout and transgenic mice. We also thank the teams at the Antiphospholipid Standardization Laboratory and the Institute for Translational Sciences at the University of Texas Medical Branch for assistance with funding, assay development, and manuscript review.

AUTHOR CONTRIBUTIONS

All authors were involved in drafting the article or revising it critically for important intellectual content, and all authors approved the final version to be published. Dr. Gonzalez had full access to all of the data in the study and takes responsibility for the integrity of the data and the accuracy of the data analysis.

Study conception and design. Papalardo, Romay-Penabad, Willis, Reyes-Maldonado, Garcia-Latorre, Pierangeli, Brasier, Gonzalez.

Acquisition of data. Papalardo, Romay-Penabad, Willis, Christadoss, Carrera-Marin, Rudrangi, Alfieri-Papalardo, Blank, Pierangeli.

Analysis and interpretation of data. Papalardo, Romay-Penabad, Willis, Reyes-Maldonado, Garcia-Latorre, Pierangeli, Brasier, Gonzalez.

REFERENCES

1. Harris EN. Syndrome of the black swan. Br J Rheumatol 1987; 26:324–6.
2. Miyakis S, Lockshin MD, Atsumi T, Branch DW, Brey RL, Cervera R, et al. International consensus statement on an update of the classification criteria for definite antiphospholipid syndrome (APS). J Thromb Haemost 2006;4:295–306.
3. McNeil HP, Simpson RJ, Chesterman CN, Krilis SA. Anti-phospholipid antibodies are directed against a complex antigen that includes a lipid-binding inhibitor of coagulation: β 2-glycoprotein I (apolipoprotein H). Proc Natl Acad Sci U S A 1990;87:4120–4.
4. Galli M, Comfurius P, Maassen C, Hemker HC, de Baets MH, van Breda-Vriesman PJ, et al. Anticardiolipin antibodies (ACA) directed not to cardiolipin but to a plasma protein cofactor. Lancet 1990;335:1544–7.
5. Willis R, Harris EN, Pierangeli SS. Pathogenesis of the antiphospholipid syndrome. Semin Thromb Hemost 2012;38:305–21.
6. Pierangeli SS, Espinola RG, Liu X, Harris EN. Thrombogenic effects of antiphospholipid antibodies are mediated by intercellular cell adhesion molecule-1, vascular cell adhesion molecule-1, and P-selectin. Circ Res 2001;88:245–50.
7. Pierangeli SS, Colden-Stanfield M, Liu X, Barker JH, Anderson GL, Harris EN. Antiphospholipid antibodies from antiphospholipid syndrome patients activate endothelial cells in vitro and in vivo. Circulation 1999;99:1997–2002.
8. Redecha P, Tilley R, Tencati M, Salmon JE, Kirchhofer D, Mackman N, et al. Tissue factor: a link between C5a and neutrophil activation in antiphospholipid antibody induced fetal injury. Blood 2007;110:2423–31.
9. Sorice M, Longo A, Capozzi A, Garofalo T, Misasi R, Alessandri C, et al. Anti–β_2-glycoprotein I antibodies induce monocyte release of tumor necrosis factor α and tissue factor by signal transduction pathways involving lipid rafts. Arthritis Rheum 2007;56:2687–97.
10. Cuadrado MJ, Buendía P, Velasco F, Aguirre MA, Barbarroja N, Torres LA, et al. Vascular endothelial growth factor expression in monocytes from patients with primary antiphospholipid syndrome. J Thromb Haemost 2006;4:2461–9.
11. De Groot PG, Urbanus RT. Antiphospholipid syndrome: not a noninflammatory disease. Semin Thromb Hemost 2015;41:607–14.
12. Gharavi AE, Pierangeli SS, Espinola RG, Liu X, Colden-Stanfield M, Harris EN. Antiphospholipid antibodies induced in mice by immunization with a cytomegalovirus-derived peptide cause thrombosis and activation of endothelial cells in vivo. Arthritis Rheum 2002;46:545–52.
13. Van Os GM, Meijers JC, Agar Ç, Seron MV, Marquart JA, Åkesson P, et al. Induction of anti-β2-glycoprotein I autoantibodies

in mice by protein H of Streptococcus pyogenes. J Thromb Haemost 2011;9:2447–56.
14. Gharavi AE, Sammaritano LR, Wen J, Elkon KB. Induction of antiphospholipid autoantibodies by immunization with β2 glycoprotein I (apolipoprotein H). J Clin Invest 1992;90:1105–9.
15. Gharavi AE, Pierangeli SS, Colden-Stanfield M, Liu XW, Espinola RG, Harris EN. GDKV-induced antiphospholipid antibodies enhance thrombosis and activate endothelial cells in vivo and in vitro. J Immunol 1999;163:2922–7.
16. Pierangeli SS, Liu SW, Anderson G, Barker JH, Harris EN. Thrombogenic properties of mouse anti-cardiolipin antibodies induced by β2 glycoprotein 1 and human immunoglobulin G antiphospholipid antibodies. Circulation 1996;94:1746–51.
17. Sebastiani GD, Iuliano A, Cantarini L, Galeazzi M. Genetic aspects of the antiphospholipid syndrome: an update. Autoimmun Rev 2016;15:433–9.
18. Madsen L, Labrecque N, Engberg J, Dierich A, Svejgaard A, Benoist C, et al. Mice lacking all conventional MHC class II genes. Proc Natl Acad Sci U S A 1999;96:10338–43.
19. Nabozny GH, Baisch JM, Cheng S, Cosgrove D, Griffiths MM, Luthra HS, et al. HLA-DQ8 transgenic mice are highly susceptible to collagen-induced arthritis: a novel model for human polyarthritis. J Exp Med 1996;183:27–37.
20. Hashimoto Y, Kawamura M, Ichikawa K, Suzuki T, Sumida T, Yoshida S, et al. Anticardiolipin antibodies in NZW x BXSB F1 mice: a model of antiphospholipid syndrome. J Immunol 1992; 149:1063–8.
21. Romay-Penabad Z, Aguilar-Valenzuela R, Urbanus RT, Derksen RH, Pennings MT, Papalardo E, et al. Apolipoprotein E receptor 2 is involved in the thrombotic complications in a murine model of the antiphospholipid syndrome. Blood 2011;117:1408–14.
22. Tolomeo T, Rico De Souza A, Roter E, Dieudé M, Amireault P, Subang R, et al. T cells demonstrate a Th1-biased response to native β_2-glycoprotein I in a murine model of anti-phospholipid antibody induction. Autoimmunity 2009;42:292–5.
23. Blank M, Krause I, Lanir N, Vardi P, Gilburd B, Tincani A, et al. Transfer of experimental antiphospholipid syndrome by bone marrow cell transplantation: the importance of the T cell. Arthritis Rheum 1995;38:115–22.
24. Tincani A, Gilburd B, Abu-Shakra M, Blank M, Allegri F, Ottaviani R, et al. Immunization of naive BALB/c mice with human β_2-glycoprotein I breaks tolerance to the murine molecule. Arthritis Rheum 2002;46:1399–404.
25. Matsuura E, Igarashi M, Igarashi Y, Nagae H, Ichikawa K, Yasuda T, et al. Molecular definition of human β2-glycoprotein I (β2-GPI) by cDNA cloning and inter-species differences of β2-GPI in alternation of anticardiolipin binding. Int Immunol 1991;3:1217–21.
26. Cornaby C, Gibbons L, Mayhew V, Sloan CS, Welling A, Poole BD. B cell epitope spreading: mechanisms and contribution to autoimmune diseases. Immunol Lett 2015;163:56–68.
27. Koike T, Ichikawa K, Kasahara H, Atsumi T, Tsutsumi A, Matsuura E. Epitopes on β2-GPI recognized by anticardiolipin antibodies. Lupus 1998;7 Suppl 2:S14–7.
28. Kasahara H, Matsuura E, Kaihara K, Yamamoto D, Kobayashi K, Inagaki J, et al. Antigenic structures recognized by anti-β2-glycoprotein I auto-antibodies. Int Immunol 2005;17:1533–42.
29. Levy Y, Sherer Y, Mathieu A, Cauli A, Passiu G, Sanna G, et al. Anti-cardiolipin antibody from a patient with antiphospholipid syndrome (APS) recognizes only an epitope expressed by cardiolipin/β2-glycoprotein-I (β2GPI) complex and induces APS. Clin Exp Rheumatol 2000;18:479–84.
30. Youinou P, Renaudineau Y. The antiphospholipid syndrome as a model for B cell-induced autoimmune diseases. Thromb Res 2004;114:363–9.
31. Duan B, Morel L. Role of B-1a cells in autoimmunity. Autoimmun Rev 2006;5:403–8.
32. Dagenais P, Urowitz MB, Gladman DD, Norman CS. A family study of the antiphospholipid syndrome associated with other autoimmune diseases. J Rheumatol 1992;19:1393–6.
33. Galeazzi M, Sebastiani GD, Tincani A, Piette JC, Allegri F, Morozzi G, et al. HLA class II alleles associations of anticardiolipin and anti-β2GPI antibodies in a large series of European patients with systemic lupus erythematosus. Lupus 2000;9: 47–55.
34. Hashimoto H, Yamanaka K, Tokano Y, Iida N, Takasaki Y, Kabasawa K, et al. HLA-DRB1 alleles and β2 glycoprotein I-dependent anticardiolipin antibodies in Japanese patients with systemic lupus erythematosus. Clin Exp Rheumatol 1998; 16:423–7.
35. Rouget JP, Goudemand J, Montreuil G, Cosson A, Jaillard J. Lupus anticoagulant: a familial observation. Lancet 1982;2:105.
36. Mackie IJ, Colaco CB, Machin SJ. Familial lupus anticoagulants. Br J Haematol 1987;67:359–63.
37. Arnett FC, Olsen ML, Anderson KL, Reveille JD. Molecular analysis of major histocompatibility complex alleles associated with the lupus anticoagulant. J Clin Invest 1991;87:1490–5.
38. Caliz R, Atsumi T, Kondeatis E, Amengual O, Khamashta MA, Vaughan RW. HLA class II gene polymorphisms in antiphospholipid syndrome: haplotype analysis in 83 Caucasoid patients. Rheumatology (Oxford) 2001;40:31–6.
39. Arnett FC, Thiagarajan P, Ahn C, Reveille JD. Associations of anti–β_2-glycoprotein I autoantibodies with HLA class II alleles in three ethnic groups. Arthritis Rheum 1999;42:268–74.
40. May KP, West SG, Moulds J, Kotzin BL. Different manifestations of the antiphospholipid antibody syndrome in a family with systemic lupus erythematosus. Arthritis Rheum 1993;36:528–33.
41. Bertolaccini ML, Atsumi T, Caliz AR, Amengual O, Khamashta MA, Hughes GR, et al. Association of antiphosphatidylserine/prothrombin autoantibodies with HLA class II genes. Arthritis Rheum 2000;43:683–8.
42. Asherson RA, Doherty DG, Vergani D, Khamashta MA, Hughes GR. Major histocompatibility complex associations with primary antiphospholipid syndrome. Arthritis Rheum 1992;35: 124–5.
43. Berman J, Girardi G, Salmon JE. TNF-α is a critical effector and a target for therapy in antiphospholipid antibody-induced pregnancy loss. J Immunol 2005;174:485–90.
44. Lambrianides A, Carroll CJ, Pierangeli SS, Pericleous C, Branch W, Rice J, et al. Effects of polyclonal IgG derived from patients with different clinical types of the antiphospholipid syndrome on monocyte signaling pathways. J Immunol 2010;184:6622–8.

ARTHRITIS & RHEUMATOLOGY
Vol. 69, No. 10, October 2017, pp 2062–2068
DOI 10.1002/art.40193

BRIEF REPORT

Association of Elevated Adipsin Levels With Pulmonary Arterial Hypertension in Systemic Sclerosis

Benjamin D. Korman, Roberta Goncalves Marangoni, Monique Hinchcliff, Sanjiv J. Shah, Mary Carns, Aileen Hoffmann, Rosalind Ramsey-Goldman, and John Varga

Objective. **Adipose tissues secrete adipokines, peptides with potent effects modulating fibrosis, inflammation, and vascular homeostasis. Dysregulated adipose tissue biology and adipokine balance have recently been implicated in systemic sclerosis (SSc). This study was undertaken to determine whether altered circulating adipokine levels correlate with SSc disease subsets or clinical manifestations.**

Methods. **Multiplex assays were used to measure circulating adipokine levels in 198 patients with SSc and 33 healthy controls. Data were evaluated for correlations between serum adipokine levels and demographic and clinical features, including pulmonary arterial hypertension (PAH). To assess the relevance of adipsin, an adipokine involved in complement pathway activation, in SSc, we analyzed publicly available genetic and transcriptomic data.**

Results. **Levels of adiponectin and adipsin differed significantly between controls and patients. Adipsin was significantly elevated in patients with limited cutaneous SSc (odds ratio [OR] 28.3 [95% confidence interval (95% CI) 7.0–113.8]; $P < 0.0001$), and its levels were associated with serum autoantibody status, pulmonary function and cardiovascular parameters, and PAH (OR 3.3 [95% CI 1.3–8.7]; $P = 0.02$). Elevated adipsin was more strongly associated with PAH than B-type natriuretic peptide was. Moreover, in SSc patients, adipsin gene single-nucleotide polymorphisms were associated with PAH. Transcriptome data set analysis demonstrated elevated adipsin expression in patients with SSc-related PAH.**

Conclusion. **We identify adipsin as a novel adipose tissue–derived marker of SSc-related PAH. Circulating adipsin levels might serve as predictive biomarkers in SSc. Mechanistically, adipsin might represent a pathogenic link between adipocyte dysfunction and complement pathway activation and play an important role in the pathogenesis of SSc-related PAH.**

Systemic sclerosis (SSc) is a devastating multisystem disorder that causes significant organ dysfunction, has no approved therapy, and has the highest mortality rate of any connective tissue disease. A hallmark of SSc is its marked heterogeneity, with substantial patient-to-patient variations in clinical manifestations, autoantibody patterns, and disease outcomes. The pathogenesis of SSc is driven by autoimmunity, vascular damage, and tissue fibrosis. Skin fibrosis and Raynaud's phenomenon are the most common disease manifestations, while interstitial lung disease (ILD) and pulmonary arterial hypertension (PAH) are leading causes of death (1). The prognosis of SSc-related PAH is worse than that of idiopathic and other forms of PAH (2).

Recent studies highlight an emerging role for adipose tissue and fat cells (adipocytes) in modulating fibrosis (3). Patients with SSc have markedly attenuated intradermal white adipose tissue, and attrition of this adipose depot correlates inversely with increased skin fibrosis (4). Adipokines, including leptin, adiponectin, resistin, visfatin, and adipsin, are peptides secreted from adipose tissue that have systemic paracrine and autocrine effects and play key roles in health and disease (5). These adipokines modulate immune cell activation, vascular function, and fibrogenesis, processes that are central to SSc pathogenesis (6).

Supported by the NIH (Eunice Kennedy Shriver National Institute of Child Health and Human Development grant K12-HD-055884 and National Institute of Arthritis and Musculoskeletal and Skin Diseases grant 5R03-AR-066343-02) and the Northwestern University Clinical and Translational Sciences Institute (Dixon Young Investigator Award).

Benjamin D. Korman, MD, Roberta Goncalves Marangoni, MD, PhD, Monique Hinchcliff, MD, Sanjiv J. Shah, MD, Mary Carns, MS, Aileen Hoffmann, MS, Rosalind Ramsey-Goldman, MD, DrPH, John Varga, MD: Northwestern University, Chicago, Illinois.

Address correspondence to Benjamin D. Korman, MD, Northwestern University, Rheumatology, 240 East Huron Street, McGaw M-230, Chicago, IL 60611. E-mail: benjamin-korman@northwestern.edu.

Submitted for publication October 6, 2016; accepted in revised form June 22, 2017.

Previous studies have revealed alterations in circulating adipokine levels in SSc patients (7). However, to date only leptin and adiponectin have been thoroughly investigated, and the results have been variable. Moreover, the association of altered adipokine levels with SSc organ involvement has not been comprehensively assessed. In the present study, we tested the hypothesis that adipokines are dysregulated in SSc, that they are associated with clinical features, and that their levels may have prognostic value as biomarkers.

Our initial studies led us to focus on adipsin (also known as complement factor D), which was elevated in a subset of patients with limited cutaneous SSc (lcSSc), especially those with prevalent PAH. To assess a potential pathogenic role of adipsin in SSc, we queried adipsin genetic and gene expression data from SSc patients with and those without PAH. Our results identify adipsin as a potential biomarker for SSc-related PAH, and provide evidence suggesting that by linking adipose tissue dysfunction and complement pathway activation, it may play a role in the pathogenesis of SSc and SSc-related PAH.

PATIENTS AND METHODS

Patients. The study sample consisted of 198 patients with SSc evaluated at a single center. Patients were classified as having lcSSc (n = 116) or diffuse cutaneous SSc (dcSSc; n = 82) based on criteria proposed by LeRoy et al (8). All patients fulfilled the American College of Rheumatology/European League Against Rheumatism 2013 classification criteria (9). Thirty-three healthy controls were also included. Patients underwent baseline clinical evaluation, pulmonary function testing, and echocardiograms, which were completed within 12 months of serum collection. Pulmonary hypertension (PH) was assessed both by echocardiography (echocardiography-proven PH was defined as systolic pulmonary artery pressure [PAP] >35 mm Hg) and by hemodynamic measures (PAH was defined as mean PAP ≥25 mm Hg, pulmonary capillary wedge pressure ≤15 mm Hg, and pulmonary vascular resistance >3 Wood units). Demographic and clinical characteristics of the patients are shown in Table 1. Further descriptions of the patients and assessments are included in the Supplementary Methods, available on the *Arthritis & Rheumatology* web site at http://onlinelibrary.wiley.com/doi/10.1002/art.40193/abstract.

Determination of serum adipokine levels. Serum was collected during a standard-of-care blood draw. Levels of leptin, resistin, visfatin, adipsin, and adiponectin were determined using multiplex assay kits (Bio-Rad) according to the manufacturer's protocol. Samples were run in duplicate, and the

Table 1. Clinical characteristics of the SSc patients*

	SSc (n = 198)	dcSSc (n = 82)	lcSSc (n = 116)	*P*†
Age, years	52.6 ± 11.4	50.1 ± 11.2	54.3 ± 11.3	0.66
BMI, kg/m^2	26.2 ± 5.5	26.0 ± 5.1	26.4 ± 5.8	0.20
Sex, % female	83.3	77.3	87.9	0.05
ANA positive, %	95.8	97.6	94.4	0.03
ACA positive, %	20.0	5.0	30.9	<0.0001
Antitopo positive, %	27.5	29.3	26.0	0.63
RNAP III positive, %	27.4	43.4	11.3	<0.0001
Disease duration, years	9.2 ± 8.1	3.6 ± 4.2	13.2 ± 7.0	<0.0001
Immunomodulatory treatment, %	32.9	59.8	21.4	<0.0001
MRSS	10.4 ± 9.9	16.4 ± 12.1	4.7 ± 3.8	<0.0001
FVC, % predicted	79.9 ± 19.3	75.1 ± 18.7	83.4 ± 19.3	0.003
DLCO, % predicted	60.2 ± 20.0	60.2 ± 20.6	60.2 ± 19.9	0.99
Systolic PAP, mm Hg	33.4 ± 10.7	33.2 ± 13.3	32.0 ± 7.5	0.85
TAPSE, cm	2.1 ± 0.5	2.2 ± 0.5	2.1 ± 0.5	0.80
Left ventricular mass, gm	77.7 ± 20.2	80.7 ± 24.0	76.0 ± 17.6	0.18
E′ lateral velocity, cm/second	12.0 ± 3.7	12.2 ± 3.4	12.0 ± 3.3	0.62
Left ventricular ejection fraction, %	62.0 ± 5.4	60.5 ± 4.0	62.2 ± 5.0	0.12
Precapillary PAH, %	13.2	3.7	19.0	0.001
Adiponectin, μg/ml	7.16 ± 7.32	3.41 ± 3.21	9.16 ± 8.09	<0.0001
Adipsin, μg/ml	1.18 ± 1.04	0.71 ± 0.22	1.51 ± 1.25	<0.0001
Leptin, ng/ml	15.38 ± 26.83	8.35 ± 10.09	20.38 ± 33.19	0.002
Resistin, ng/ml	18.39 ± 5.76	16.97 ± 4.52	19.60 ± 6.40	0.002
Visfatin, ng/ml	6.99 ± 10.75	7.15 ± 13.49	6.89 ± 8.34	0.32

* Except where indicated otherwise, values are the mean ± SD. SSc = systemic sclerosis; dcSSc = diffuse cutaneous SSc; lcSSc = limited cutaneous SSc; BMI = body mass index; ANA = antinuclear antibody; ACA = anticentromere antibody; antitopo = antitopoisomerase antibody; RNAP III = RNA polymerase III; MRSS = modified Rodnan skin thickness score; FVC = forced vital capacity; DLCO = diffusing capacity for carbon monoxide; PAP = pulmonary artery pressure; TAPSE = tricuspid annular plane systolic excursion; PAH = pulmonary arterial hypertension.
† Patients with dcSSc versus patients with lcSSc.

coefficient of variation for adipsin was 6.7%. Measurement was performed on a Luminex 100 platform.

Evaluation of correlation of serum adipokine levels with clinical parameters. We first compared clinical characteristics and levels of each adipokine in lcSSc versus dcSSc subgroups using chi-square and Fisher's exact tests (for categorical variables) and the Mann-Whitney U test (for continuous variables). In addition, we further subdivided lcSSc patients into those with high and those with low adipsin levels, with the cutoff value for high adipsin level defined as 2 SD above the mean in the control group. Next, we performed a multivariable logistic regression analysis to determine the independent association between adipsin and PAH. For additional description of the statistical methods used, see Supplementary Methods, available on the *Arthritis & Rheumatology* web site at http://onlinelibrary.wiley.com/doi/10.1002/art.40193/abstract.

Assessment of adipsin genetic polymorphisms and gene expression. Adipsin gene single-nucleotide polymorphisms (SNPs) were assessed using publicly available data from a genome-wide association study (GWAS) that included SSc patients with and SSc patients without PH determined by echocardiography (systolic PAP >40 mm Hg) (clinical data obtained with authorized access from dbGaP, accession no. phs000357.v1.p1). SNPs associated with SSc-related PAH were then assessed for the presence of expression quantitative trait loci (eQTLs) using expression data from the GTEx portal (www.gtexportal.org). Additionally, adipsin expression was assessed using publicly available data from both peripheral blood mononuclear cells (PBMCs) and lung tissue from SSc patients with and SSc patients without PAH (GEO accession nos. GSE19617and GSE22356). Further descriptions of the data sets and methods of analysis used are presented in the Supplementary Methods.

RESULTS

Adipokine levels in SSc. Compared to patients with dcSSc, patients with lcSSc had significantly higher levels of adiponectin (mean ± SD 9.16 ± 8.09 μg/ml versus 3.41 ± 3.21 μg/ml; $P < 0.0001$), adipsin (mean ± SD 1.51 ± 1.25 μg/ml versus 0.71 ± 0.22 μg/ml; $P < 0.0001$), leptin (mean ± SD 20.38 ± 33.19 ng/ml versus 8.35 ± 10.09 ng/ml; $P = 0.002$), and resistin (mean ± SD 19.60 ± 6.40 ng/ml versus 16.97 ± 4.52 ng/ml; $P = 0.002$) (Table 1). Similar differences in adipokine levels were noted between lcSSc patients and controls. After correction for multiple hypothesis testing and adjustment for age, sex, race, body mass index (BMI), and disease duration (defined as the interval between the first non-Raynaud's phenomenon SSc symptom and serum collection), only levels of adiponectin ($P = 0.003$) and adipsin ($P = 0.001$) remained significantly different between the lcSSc and dcSSc subsets (Supplementary Table 1, available on the *Arthritis & Rheumatology* web site at http://onlinelibrary.wiley.com/doi/10.1002/art.40193/abstract). Further analysis focused on adipsin, also known as complement factor D, which has been implicated in the alternative complement pathway, but has not previously been linked to SSc.

Stratification of adipsin levels. Adipsin was substantially elevated in a subset of SSc patients, almost exclusively those with lcSSc (Figure 1A). Using a cutoff of 1.49 μg/ml (Figure 1B), 25.8% of the patients with lcSSc (30 of 116), but only 1.2% of the patients with dcSSc (1 of 82) and 6.1% of the controls (2 of 33) had elevated adipsin levels (odds ratio [OR] for lcSSc 28.3 [95% confidence interval (95% CI) 7.0–113.8]; $P < 0.0001$ and OR for dcSSc 38.2 [95% CI 4.1–333.3]; $P = 0.001$ after adjustment for clinical covariates). Moreover, elevated adipsin levels were associated with a greater frequency of anticentromere antibodies (OR 2.85 [95% CI 1.25–6.51]; $P = 0.01$), and a lower frequency of anti–Scl-70 antibodies (OR 0.09 [95% CI 0.01–0.69]; $P = 0.004$) (Figures 1C and D). The difference in adipsin levels in SSc patients overall versus controls was not significant ($P = 0.66$) (Supplementary Table 1, available on the *Arthritis & Rheumatology* web site at http://onlinelibrary.wiley.com/doi/10.1002/art.40193/abstract), largely reflecting the bimodal distribution in which adipsin was increased in lcSSc patients and decreased in dcSSc patients as compared to controls.

Lack of association between adipsin levels and markers of fibrosis in SSc. Adipsin was assessed for association with severity of SSc-related skin and lung disease. These analyses showed no association between the levels of adipsin (or any other adipokines) and the modified Rodnan skin thickness score (MRSS), radiographically defined ILD, or pulmonary function parameters (forced vital capacity [FVC], forced expiratory volume in 1 second [FEV_1], or total lung capacity) (Supplementary Figure 1, available on the *Arthritis & Rheumatology* web site at http://onlinelibrary.wiley.com/doi/10.1002/art.40193/abstract).

Association of adipsin levels with PAH in SSc. High adipsin levels were significantly associated with PH, as determined by echocardiography (OR 4.6 [95% CI 1.8–11.3]; $P = 0.001$), and with PAH, as defined by invasive hemodynamic testing (OR 3.3 [95% CI 1.3–8.7]; $P = 0.02$) (Figures 1E and F). After adjustment for age, sex, BMI, disease duration, and disease subtype, the association between adipsin levels and echocardiography-proven PH remained significant (OR 7.7 [95% CI 2.1–21.0]; $P < 0.001$), but the association between adipsin level and PAH did not (OR 2.7 [95% CI 0.8–8.9]; $P = 0.10$). Elevated adipsin levels were also associated with a reduction in diffusing capacity for carbon monoxide (DL_{CO}), an increased ratio of FVC to DL_{CO}, and lower values of tricuspid annular plane systolic excursion (TAPSE) and Doppler E′ lateral velocity, which are indicative of right ventricular dysfunction and diastolic dysfunction, respectively (Figures 1G–J). Patients

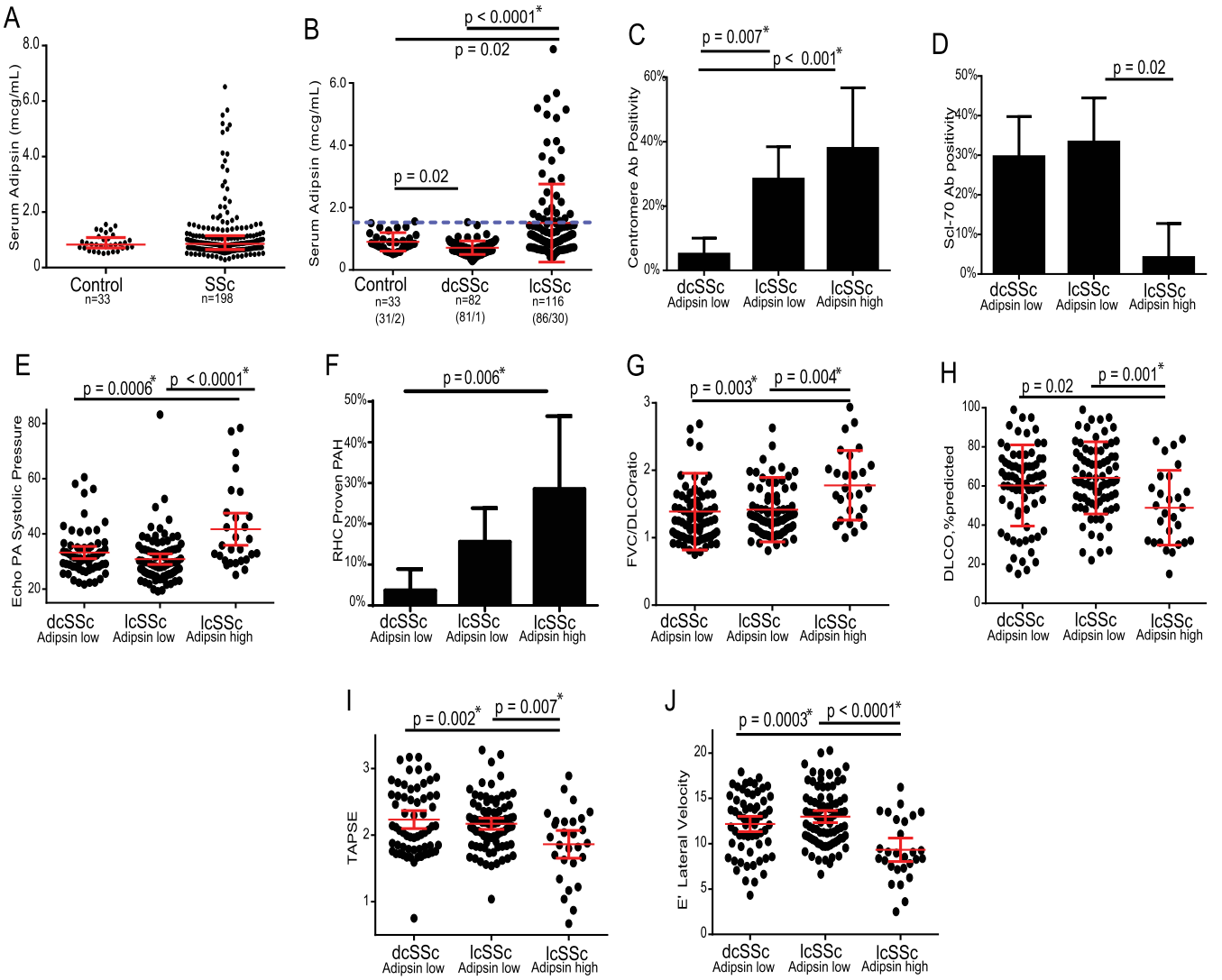

Figure 1. Association of serum adipsin levels with limited cutaneous systemic sclerosis (lcSSc) and pulmonary arterial hypertension (PAH). **A**, Serum levels of adipsin in controls and SSc patients. There was no significant difference between the 2 groups. **B**, Higher adipsin levels in patients with lcSSc than in controls or patients with diffuse SSc (dcSSc). The broken line represents the upper cutoff value for adipsin. **C–J**, Association of SSc groups stratified by limited or diffuse cutaneous status and adipsin level with anticentromere antibodies (Ab) (**C**), anti–Scl-70 antibodies (**D**), pulmonary artery (PA) systolic pressure measured by echocardiography (**E**), PAH proven by right-sided heart catheterization (RHC) (**F**), ratio of forced vital capacity (FVC) to diffusing capacity for carbon monoxide (DLco) (**G**), DLco (**H**), tricuspid annular plane systolic excursion (TAPSE) (**I**), and E′ lateral velocity (**J**). In **A**, **B**, **E**, and **G–J**, symbols represent individual subjects; horizontal lines and error bars show the mean and 95% confidence interval. In **C**, **D**, and **F**, bars show the mean ± SD. In **C–J**, n = 82 patients (81 with low adipsin) in the dcSSc group, n = 86 patients in the lcSSc adipsin low group, and n = 30 patients in the lcSSc adipsin high group. *P* values were determined by Mann-Whitney test. * = $P < 0.01$.

with elevated adipsin levels had increased frequency of both right ventricular dysfunction (TAPSE <1.5 cm) (OR 19.9 [95% CI 3.8–104.5]; $P < 0.001$), and left ventricular diastolic dysfunction (OR 5.1 [95% CI 2.1–12.4) (Figures 1I and J).

Stronger association between adipsin levels and SSc-related PAH than between B-type natriuretic peptide (BNP) levels and SSc-related PAH. BNP is widely used as a biomarker for SSc-related PAH (10). Serum levels of BNP were elevated (>100 pg/ml) in 21% of SSc patients, while levels of adipsin were elevated in 16%. Elevated BNP was not significantly associated with PH defined by echocardiography ($P = 0.91$) or PAH defined by invasive hemodynamic assessment ($P = 0.23$), in contrast to elevated adipsin levels, which were significantly associated with both echocardiography-proven PH ($P < 0.0001$) and PAH defined by invasive hemodynamic assessment ($P = 0.001$). High adipsin levels were more

A

ID	Alleles	MAF SSc no PH (n=167)	MAF SSc -PH (n=91)	p-value no PH vs PH
rs1651895	T/C	0.247	0.326	0.061
rs13090	A/C	0.267	0.335	0.09
rs1683591	C/T	0.326	0.365	**0.037**
rs2241623	A/G	0.293	0.313	0.639
rs2365702	G/A	0.357	0.272	**0.045**
rs1060442	C/T	0.335	0.456	**0.007**
rs2965292	T/C	0.247	0.333	**0.044**

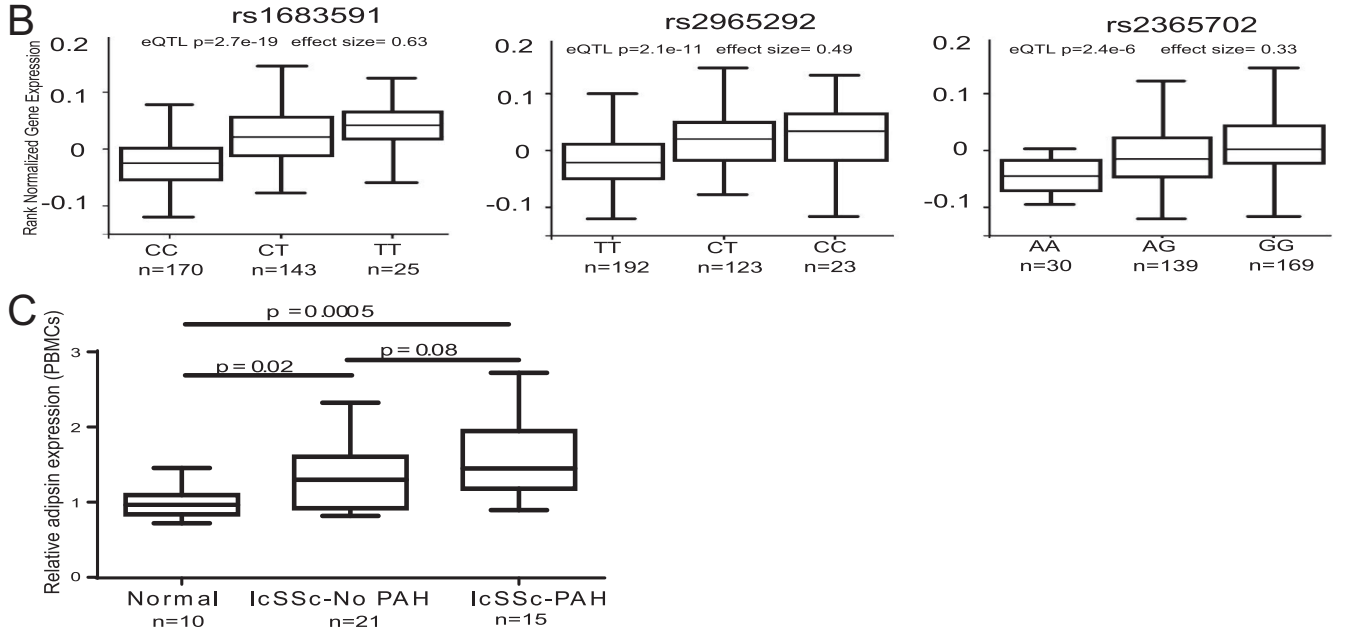

Figure 2. Genetic and expression studies demonstrating dysregulated adipsin in systemic sclerosis (SSc)–associated pulmonary arterial hypertension (PAH). **A**, List of 7 single-nucleotide polymorphisms (SNPs) in the adipsin (complement factor D) region on chromosome 19 genotyped in an SSc genome-wide association study (dbGAP accession no. phs000357.v1.p1). Minor allele frequencies (MAFs) for patients with SSc without pulmonary hypertension (PH) (systolic pulmonary artery pressure [PAP] >40 on echocardiography) and patients with SSc with PH (systolic PAP <40 on echocardiography) are shown. Note that 4 of 7 SNPs in the region are associated with SSc-related PAH. Data were derived from dbGaP accession no. phs000357.v1.p1. **B**, Whole blood expression quantitative trait loci (eQTLs) SNPs. **C**, Elevated adipsin expression in peripheral blood mononuclear cells (PBMCs) from patients with limited cutaneous SSc (lcSSc) and patients with lcSSc with PAH (data derived from GEO accession no. GSE19617). In **B** and **C**, data are shown as box plots. Each box represents the 25th to 75th percentiles. Lines inside the boxes represent the median. Lines outside the boxes represent the maximum and minimum range.

specific for PAH than BNP levels (specificity of 85% versus 57% for PAH defined by invasive hemodynamic assessment), and receiver operating curve analysis demonstrated that adipsin had a greater area under the curve (AUC) than BNP for both echocardiography-proven PH and PAH proven by invasive hemodynamic assessment (AUC of 0.73 versus 0.51 for systolic PAP >35 by echocardiography and 0.65 versus 0.62 for PAH proven by right-sided heart catheterization) (Supplementary Figure 2, available on the *Arthritis & Rheumatology* web site at http://onlinelibrary.wiley.com/doi/10.1002/art.40193/abstract).

Adipsin gene variants are associated with SSc-related PAH and modulate gene expression. To investigate whether elevated adipsin levels may be genetically determined in SSc-related PAH, we evaluated the association of polymorphisms in the *CFD* (adipsin) gene with SSc-related PAH using GWAS data (dbGAP phs000357.v1.p1). We analyzed data from 7 SNPs in the *CFD* region and assessed SNP allele frequencies in patients classified as having normal systolic PAP (<40 mm Hg; n = 167) or elevated systolic PAP (>40 mm Hg; n = 91) as determined by echocardiography. This strategy revealed that 4 of 7 *CFD* region SNPs (rs1683591, rs2365702, rs106044, and rs2965292) were associated with elevated PAP (Figure 2A). To determine the potential functional consequences of the genetic association between *CFD* and PAH, we queried the GTEx portal. This analysis showed a significant eQTL effect in whole blood, with individuals carrying the minor allele of the PAH-associated SNPs showing increased adipsin expression (Figure 2B).

Increased adipsin expression in lcSSc patients with SSc-related PAH. Next, to determine if the genetic association of *CFD* SNPs with SSc-related PAH leads to dysregulated adipsin expression in tissue, we analyzed

data from publicly available PBMCs and lung tissue microarrays. Data from 2 independent SSc cohorts (GEO accession nos. GSE19617 and GSE22356) demonstrated that circulating PBMCs from SSc patients with PAH had higher adipsin expression compared to patients without PAH (Figure 2C and Supplementary Figure 3, available on the *Arthritis & Rheumatology* web site at http://onlinelibrary.wiley.com/doi/10.1002/art.40193/abstract). In lung tissue obtained at the time of lung transplant, patients who received a transplant for SSc-related PAH also demonstrated elevated adipsin expression when compared to those who received a transplant for SSc-related ILD (accession no. GSE48149; data not shown).

DISCUSSION

We found that levels of multiple adipokines were significantly dysregulated in SSc. Our detailed analysis focused on adipsin for a number of reasons. First, the largest difference in adipsin levels was seen between lcSSc and dcSSc patients. Second, adipsin, which is also known as complement factor D, has not previously been associated with SSc or vascular disease. Most intriguing, adipsin has a unique role in linking adipose tissue function and complement pathway activation. In this analysis, we uncovered a robust association between elevated circulating levels of adipsin and SSc-associated PAH.

Patients with elevated adipsin levels were more likely to have the limited cutaneous form of SSc and were at significantly increased risk of PAH and related cardiac dysfunction. The association with PAH was confirmed by both echocardiography and hemodynamic data and further bolstered by associations with DLCO, the FVC:DLCO ratio, and measures of right ventricular function. While levels of leptin, resistin, and adiponectin were also elevated in lcSSc patients, they were not significantly associated with clinical markers of fibrosis or vascular disease, suggesting that while multiple adipokines are dysregulated in SSc, adipsin may be unique in its relationship with vascular outcomes such as PAH.

To begin to explore a potential involvement of adipsin in SSc pathogenesis, we queried publicly available data sets. The results indicate that adipsin gene variants are associated with increased PAH susceptibility. Moreover, SNPs associated with SSc-related PAH were associated with increased adipsin expression, SSc patients (particularly those with lcSSc) had elevated adipsin expression compared to controls, and patients with SSc-related PAH showed increased adipsin expression compared to SSc patients without PAH. Taken together, these findings suggest that elevated adipsin production may play a pathogenic role in SSc-related PAH. While we are unaware of studies evaluating adipsin in PAH, an intriguing study showed that a protease implicated in the pathogenesis of monocrotaline-induced PAH in rats is related to adipsin (11).

Our analyses have certain limitations. First, in view of its cross-sectional design, the study is limited in its ability to assess the prognostic significance of adipsin. Future studies are planned to examine the prognostic value of baseline adipsin levels for predicting future outcomes such as clinical worsening, development of PAH, and the implications of changes in adipsin over time. Because the results of this study are Luminex based, future studies might use confirmatory enzyme-linked immunosorbent assay or other sensitive assays. Additionally, while we studied a relatively large and well-characterized cohort of SSc patients, the association of serum adipsin with SSc-related PAH will need to be validated in independent SSc cohorts. Moreover, the relatively small number of controls included in the present study ($n = 33$) limits the power to detect adipokine differences between SSc patients and controls. Although genetic and gene expression data support a possible mechanistic relationship between adipsin, SSc, and PAH, functional studies will be required to demonstrate the role of adipsin in disease pathogenesis.

In contrast to adipokines such as leptin and adiponectin, adipsin has not been well studied, and its role in autoimmune/inflammatory/fibrotic disease has not been evaluated. Adipsin is one of the major adipocyte products and was the first adipokine described (12). Subsequently, it was recognized to function as the serine protease complement factor D, which catalyzes the rate-limiting step of the alternative complement pathway, promotes the formation of the membrane-attack complex, and generates complement-signaling molecules, including the anaphylatoxins C3a and C5a (13). Serum levels of adipsin decline in obesity, pregnancy, and type 2 diabetes mellitus, while elevated levels are seen in preeclampsia, but adipsin levels have not previously been assessed in patients with SSc or other rheumatic diseases (12).

The pathogenic role of the complement cascade remains incompletely characterized in SSc. However, previous studies have described dysregulated complement activity in a subset of patients, particularly those with vascular disease. SSc patients have increased complement activation (14), and activated complement complex C5b–9 and CD46 are present on arterioles in SSc skin biopsy specimens (15). Moreover, SSc patients with vascular damage have elevated circulating levels of complement C3f desarginine (DRC3f) which enhances endothelial cell proliferation (16).

Importantly, adipsin and complement cascade activation represent potential drug targets. In particular, lampalizumab, a pharmacologic inhibitor of adipsin, is currently in phase III clinical trials for macular degeneration, while eculizumab, a terminal complement inhibitor, has been approved for the treatment of paroxysmal nocturnal hemoglobinuria and atypical hemolytic uremic syndrome (HUS). Remarkably, eculizumab has been reported to induce remission in scleroderma renal crisis (a thrombotic microangiopathy that resembles atypical HUS), and to ameliorate pulmonary hypertension in patients with paroxysmal nocturnal hemoglobinuria (17). If adipsin-mediated activation of the alternative complement pathway is shown to be pathogenic in SSc, in addition to marking a set of patients with severe vascular manifestations, this work may also identify a novel personalized and much needed treatment approach for this set of patients.

We demonstrate that circulating adipsin levels are elevated in patients with lcSSc and identify a significant association between elevated adipsin levels and PAH in this population. Genetic variants of adipsin are associated with SSc-related PAH, and adipsin gene expression was elevated in patients with SSc-related PAH. Taken together, these findings suggest a previously unrecognized pathogenic role for adipsin in SSc and SSc-related PAH and highlight adipsin as a novel marker of vascular manifestations with important prognostic and potentially therapeutic value. Moreover, in light of the essential role of adipsin in modulating complement pathway activity, our results implicate the complement system in SSc-related PAH.

ACKNOWLEDGMENTS

We graciously thank the members of the Scleroderma Program (Northwestern University), including Kathleen Aren, Esperanza Arroyo, and Lauren Beussink-Nelson, for their help with clinical, echocardiographic, and serum data collection. We thank the Northwestern Metabolic Hormone Core for performing Luminex assays.

AUTHOR CONTRIBUTIONS

All authors were involved in drafting the article or revising it critically for important intellectual content, and all authors approved the final version to be published. Dr. Korman had full access to all of the data in the study and takes responsibility for the integrity of the data and the accuracy of the data analysis.

Study conception and design. Korman, Marangoni, Hinchcliff, Shah, Ramsey-Goldman, Varga.

Acquisition of data. Korman, Marangoni.

Analysis and interpretation of data. Korman, Carns, Hoffmann, Varga.

REFERENCES

1. Allanore Y, Simms R, Distler O, Trojanowska M, Pope J, Denton CP, et al. Systemic sclerosis. Nat Rev Dis Primers 2015;1:15002.
2. Campo A, Mathai SC, Le Pavec J, Zaiman AL, Hummers LK, Boyce D, et al. Hemodynamic predictors of survival in scleroderma-related pulmonary arterial hypertension. Am J Respir Crit Care Med 2010;182:252–60.
3. Rodriguez A, Ezquerro S, Mendez-Gimenez L, Becerril S, Fruhbeck G. Revisiting the adipocyte: a model for integration of cytokine signaling in the regulation of energy metabolism. Am J Physiol Endocrinol Metab 2015;309:E691–714.
4. Marangoni RG, Korman BD, Wei J, Wood TA, Graham LV, Whitfield ML, et al. Myofibroblasts in murine cutaneous fibrosis originate from adiponectin-positive intradermal progenitors. Arthritis Rheumatol 2015;67:1062–73.
5. Falcao-Pires I, Castro-Chaves P, Miranda-Silva D, Lourenco AP, Leite-Moreira AF. Physiological, pathological and potential therapeutic roles of adipokines. Drug Discov Today 2012;17:880–9.
6. Ezure T, Amano S. Negative regulation of dermal fibroblasts by enlarged adipocytes through release of free fatty acids. J Invest Dermatol 2011;131:2004–9.
7. Lakota K, Wei J, Carns M, Hinchcliff M, Lee J, Whitfield ML, et al. Levels of adiponectin, a marker for PPAR-γ activity, correlate with skin fibrosis in systemic sclerosis: potential utility as biomarker? Arthritis Res Ther 2012;14:R102.
8. LeRoy EC, Black C, Fleischmajer R, Jablonska S, Krieg T, Medsger TA Jr, et al. Scleroderma (systemic sclerosis): classification, subsets, and pathogenesis. J Rheumatol 1988;15:202–5.
9. Van den Hoogen F, Khanna D, Fransen J, Johnson SR, Baron M, Tyndall A, et al. 2013 classification criteria for systemic sclerosis: an American College of Rheumatology/European League Against Rheumatism collaborative initiative. Arthritis Rheum 2013;65:2737–47.
10. Mathai SC, Bueso M, Hummers LK, Boyce D, Lechtzin N, Le Pavec J, et al. Disproportionate elevation of N-terminal pro-brain natriuretic peptide in scleroderma-related pulmonary hypertension. Eur Respir J 2010;35:95–104.
11. Zhu L, Wigle D, Hinek A, Kobayashi J, Ye C, Zuker M, et al. The endogenous vascular elastase that governs development and progression of monocrotaline-induced pulmonary hypertension in rats is a novel enzyme related to the serine proteinase adipsin. J Clin Invest 1994;94:1163–71.
12. Cook KS, Min HY, Johnson D, Chaplinsky RJ, Flier JS, Hunt CR, et al. Adipsin: a circulating serine protease homolog secreted by adipose tissue and sciatic nerve. Science 1987;237:402–5.
13. Xu Y, Ma M, Ippolito GC, Schroeder HW Jr, Carroll MC, Volanakis JE. Complement activation in factor D-deficient mice. Proc Natl Acad Sci U S A 2001;98:14577–82.
14. Senaldi G, Lupoli S, Vergani D, Black CM. Activation of the complement system in systemic sclerosis: relationship to clinical severity. Arthritis Rheum 1989;32:1262–7.
15. Sprott H, Muller-Ladner U, Distler O, Gay RE, Barnum SR, Landthaler M, et al. Detection of activated complement complex C5b-9 and complement receptor C5a in skin biopsies of patients with systemic sclerosis (scleroderma). J Rheumatol 2000;27:402–4.
16. Xiang Y, Matsui T, Matsuo K, Shimada K, Tohma S, Nakamura H, et al. Comprehensive investigation of disease-specific short peptides in sera from patients with systemic sclerosis: complement C3f-des-arginine, detected predominantly in systemic sclerosis sera, enhances proliferation of vascular endothelial cells. Arthritis Rheum 2007;56:2018–30.
17. Hill A, Rother RP, Wang X, Morris SM Jr, Quinn-Senger K, Kelly R, et al. Effect of eculizumab on haemolysis-associated nitric oxide depletion, dyspnoea, and measures of pulmonary hypertension in patients with paroxysmal nocturnal haemoglobinuria. Br J Haematol 2010;149:414–25.

ARTHRITIS & RHEUMATOLOGY
Vol. 69, No. 10, October 2017, pp 2069–2080
DOI 10.1002/art.40170

Myeloperoxidase/HLA Class II Complexes Recognized by Autoantibodies in Microscopic Polyangiitis

Ryosuke Hiwa,[1] Koichiro Ohmura,[2] Noriko Arase,[3] Hui Jin,[4] Kouyuki Hirayasu,[5] Masako Kohyama,[4] Tadahiro Suenaga,[4] Fumiji Saito,[3] Chikashi Terao,[2] Tatsuya Atsumi,[6] Hirotsugu Iwatani,[3] Tsuneyo Mimori,[2] and Hisashi Arase[4]

Objective. **Autoantibodies against myeloperoxidase (MPO) that are expressed in neutrophils play an important role in the pathogenesis of microscopic polyangiitis (MPA). We recently observed that misfolded cellular proteins are transported to the cell surface by HLA class II molecules and are targeted by autoantibodies in patients with rheumatoid arthritis or antiphospholipid syndrome, suggesting that HLA class II molecules play an important role in autoantibody recognition. The aim of this study was to address the role of HLA class II molecules in the cell surface expression of MPO in patients with MPA.**

Methods. **The association of MPO with HLA–DR was analyzed using MPO and HLA–DR transfectants as well as neutrophils from healthy donors and patients with MPA. Autoantibody binding to the MPO/HLA–DR complex was analyzed by flow cytometry. The association of MPO with HLA–DR was assessed using the immunoprecipitation technique. The function of MPO–antineutrophil cytoplasmic antibody (ANCA) was assessed using a neutrophil-like cell line expressing HLA–DR and MPO.**

Results. **MPO protein was detected on the cell surface in the presence of HLA–DR, and the MPO/HLA–DR complex was recognized by MPO-ANCA. A competitive inhibition assay suggested that MPO associated with HLA–DR expresses cryptic autoantibody epitopes for MPO-ANCA. Autoantibody binding to the MPO/HLA–DR complex was correlated with disease susceptibility conferred by each HLA–DR allele, suggesting that the MPO/HLA–DR complex is involved in the pathogenicity of MPA. Indeed, MPO–HLA class II complexes were detected in neutrophils from a patient with MPA as well as in cytokine-stimulated neutrophils from healthy donors. Moreover, MPO-ANCA stimulated MPO/HLA–DR complex–expressing HL-60 cells.**

Conclusion. **Our findings suggest that MPO complexed with HLA class II molecules is involved in the pathogenesis of MPA as a target for MPO-ANCA.**

Microscopic polyangiitis (MPA) is a type of systemic small vessel vasculitis that affects multiple organs (1). It is categorized as an antineutrophil cytoplasmic antibody (ANCA)–associated vasculitis (1). Approximately 70% of patients with MPA possess myeloperoxidase (MPO)–ANCAs (2) that recognize MPO expressed in neutrophils (3). Although MPO is not expressed on the cell surface of neutrophils in a steady state, it is transported to the cell surface via cytokine stimulation, which enables MPO-ANCAs to bind to the cell surface of neutrophils (4,5). ANCAs bind to and stimulate neutrophils (4,6–8) and cause vasculitis in small vessels (9,10). A mouse model of MPA has demonstrated that the transfer of anti-MPO antibodies causes vasculitis (11), suggesting that MPO-ANCAs are directly involved in the pathogenesis of MPA

Supported in part by the Japan Society for the Promotion of Science (KAKENHI grant 15H02545), the Japan Agency for Medical Research and Development (Practical Research Project for Allergic Diseases and Immunology), the Mochida Memorial Foundation for Medical and Pharmaceutical Research, the Uehara Memorial Foundation, Bristol-Myers K.K. (BRAVE RA Clinical Investigation grant), the Terumo Life Science Foundation, and the Tokyo Biochemical Research Foundation.

[1]Ryosuke Hiwa, MD: World Premier International Immunology Frontier Research Center and Osaka University, Suita, Japan, and Kyoto University, Kyoto, Japan; [2]Koichiro Ohmura, MD, PhD, Chikashi Terao, MD, PhD, Tsuneyo Mimori, MD, PhD: Kyoto University, Kyoto, Japan; [3]Noriko Arase, MD, PhD, Fumiji Saito, PhD, Hirotsugu Iwatani, MD, PhD (current address: Osaka National Hospital, Osaka, Japan): Osaka University, Suita, Japan; [4]Hui Jin, PhD, Masako Kohyama, PhD, Tadahiro Suenaga, MD, PhD, Hisashi Arase, MD, PhD: World Premier International Immunology Frontier Research Center and Osaka University, Suita, Japan; [5]Kouyuki Hirayasu, PhD: World Premier International Immunology Frontier Research Center, Suita, Japan; [6]Tatsuya Atsumi, MD, PhD: Hokkaido University Graduate School of Medicine, Sapporo, Japan.

Address correspondence to Hisashi Arase, MD, PhD, Department of Immunochemistry, Research Institute for Microbial Diseases, Osaka University, 3-1 Yamadaoka, Suita, Osaka 565-0871, Japan. E-mail: arase@biken.osaka-u.ac.jp.

Submitted for publication February 20, 2017; accepted in revised form June 1, 2017.

(12,13). However, it has not been fully elucidated how MPO is transported to the cell surface of neutrophils after cytokine stimulation.

We previously observed that misfolded endoplasmic reticulum (ER) proteins are transported to the cell surface, without processing to peptides, by HLA class II molecules. This occurs when misfolded proteins are associated with the peptide-binding groove of HLA class II molecules instead of the invariant chain (14). Furthermore, misfolded proteins that were transported to the outside of the cell by HLA class II molecules were efficiently recognized by autoantibodies from patients with rheumatoid arthritis (RA) or the antiphospholipid syndrome (15–17). More importantly, autoantibody binding to the IgG heavy chain/HLA class II complex is strongly associated with susceptibility to RA conferred by each HLA–DR allele, suggesting that the IgG heavy chain/HLA class II complex is involved in the pathogenesis of RA (15). Although HLA class II expression is generally limited to certain cell populations, such as dendritic cells and B cells, HLA class II expression is induced on a variety of cells upon stimulation by cytokines, such as interferon-γ (IFNγ). Therefore, certain types of inflammation or infection would induce expression of HLA class II molecules. Because the antigenicity of misfolded proteins seems to be different from that of normally folded proteins, we hypothesized that the misfolded proteins that are transported to the cell surface by these HLA class II molecules might be involved in the pathogenesis of autoimmune diseases (18).

Resting neutrophils do not express HLA class II molecules. However, HLA class II expression is induced in neutrophils by cytokine stimulation (19,20). In addition, a recent genome-wide association study (GWAS) revealed that susceptibility to MPA is associated with polymorphisms in HLA class II genes (21). In Japanese individuals, MPA is significantly associated with HLA–DRB1*09:01 (22,23). However, the role of HLA class II molecules expressed on neutrophils in the pathogenesis of MPA has remained unknown. In this study, we addressed the role of HLA class II molecules in the cell surface expression of MPO in patients with MPA. Our findings provide new insight into the role of HLA class II molecules in the pathogenesis of MPO-ANCAs in patients with MPA.

PATIENTS AND METHODS

Patient samples. Sera, peripheral blood neutrophils, and DNA from patients with MPA were collected from Kyoto University, Hokkaido University, and Osaka University. Diagnoses of MPA were based on the European Medicines Agency algorithm–based criteria (24) and the Chapel Hill Consensus Conference definition (1). Human peripheral blood neutrophils were obtained from healthy volunteers or patients with MPA, using the Ficoll-dextran method (25). IgG was purified from the plasma of MPA patients or healthy donors by affinity chromatography using protein G–Sepharose, as described previously (26).

Study approval. The protocol for the collection and use of human sera, peripheral blood cells, and DNA was approved by the institutional review boards (IRBs) of Kyoto University (E458, G1006–1), Hokkaido University (010–0326), and Osaka University (25–2, 12246). Written informed consent in accordance with the Declaration of Helsinki was obtained from all participants according to the relevant guidelines of the IRBs.

Plasmids. Complementary DNAs (cDNAs) for different HLA class II alleles and the invariant chain (accession no. NM_004355.2) were prepared as previously described (14–16). Human MPO (accession no. NC_000017.11) was cloned from cDNA prepared from human bone marrow total RNA (Clontech). Some HLA–DR alleles were generated using QuikChange multimutagenesis kits (Agilent) from HLA genes with similar sequences. All cDNA sequences for HLA were based on information in the IMGT/HLA Database (www.ebi.ac.uk/imgt/hla/index.html). The nucleotide sequences of all of the constructs were confirmed by DNA sequencing (ABI 3130xl DNA Sequencer; Applied Biosciences). HLA–DRB1*01:01 containing a covalently attached transferrin receptor peptide (TfRpep–HLA–DRB1*01:01) and HLA–DRB1*04:04 containing a covalently attached HLA–Cw3 peptide (HLA–Cw3–pep–HLA–DRB1*04:04) were generated as previously described (27).

Antibodies. Anti–HLA–DR monoclonal antibody (L243; American Type Culture Collection) was used for the detection of HLA–DR by flow cytometry and immunoprecipitation (IP) of HLA–DR proteins. Anti–HLA–DR/DP monoclonal antibody (HL-38; Sigma-Aldrich) was used for IP detected by flow cytometry. Anti-human MPO monoclonal antibody (16E3; GeneWay Research) was used for flow cytometry. Anti-DYKDDDDK–tagged (clone L5) monoclonal antibody (BioLegend) was used for IP. Rabbit anti–HLA–DRα antibody (FL-254; Santa Cruz Biotechnology), anti-FLAG monoclonal antibody (clone M2; Sigma-Aldrich), and anti-human MPO polyclonal antibody (HPA021147; Sigma-Aldrich) were used for Western blotting.

Cell lines. HEK 293T cells (RCB2202) were purchased from the RIKEN BioResource Center (Tsukuba, Japan). HL-60 cells (JCRB0085) were purchased from the Japanese Collection of Research Bioresources Cell Bank (JCRB) (Osaka, Japan). We used polymerase chain reaction to confirm that the cells were negative for mycoplasma contamination. Expression plasmids containing each cDNA were transfected into cells, using Polyethylenimine Max (Polysciences).

Flow cytometric analysis. Cells were incubated with mouse primary monoclonal antibodies (anti–HLA–DRα antibody [L243] or anti-human MPO antibody [16E3]), followed by allophycocyanin (APC)–conjugated anti-mouse IgG antibody (Jackson ImmunoResearch). For intracellular staining, cells were fixed and permeabilized with Fixation/Permeabilization solution (BD Biosciences). Intracellular MPO was detected with anti-human MPO followed by APC-conjugated anti-mouse IgG antibody. Stained cells were analyzed using a FACSCalibur (Becton Dickinson) or FACSVerse cytometer (Becton Dickinson).

Analysis of autoantibody binding to the MPO/HLA–DR complex. Human MPO was cotransfected together with HLA–DRα and green fluorescent protein (GFP). The transfectants were mixed with sera (dilution 1:300) from patients with MPA, followed by APC-labeled anti-human IgG Fc antibody

(Jackson ImmunoResearch). To determine specific autoantibody titers against MPO/HLA–DR complex, the mean fluorescence intensity (MFI) of autoantibody binding to HLA–DR9 alone transfectants was subtracted from the MFI of autoantibody binding to HLA–DR9 and human MPO transfectants. Anti–MPO/HLA–DR complex antibody titers were calculated based on the MFI of IgG autoantibody binding to MPO/HLA–DR9 cotransfectants, using a standard MPA serum for which the MPO-ANCA titer (720 units/ml) is known, as determined by enzyme-linked immunosorbent assay (ELISA).

Immunoprecipitation and immunoblotting. Cells were lysed in lysis buffer (10 m*M* Tris, 150 m*M* NaCl, pH 7.5) containing 0.5% Nonidet P40 (Sigma). HLA–DR and human MPO were precipitated with anti–HLA–DR monoclonal antibody (L243) and protein G–Sepharose (GE Healthcare) or anti-DYKDDDDK monoclonal antibody (L5) and protein G–Sepharose. Mouse IgG2a (BD Biosciences) was used as an isotype-matched control. The immunoprecipitates were eluted by boiling with sodium dodecyl sulfate–polyacrylamide gel electrophoresis sample buffer, separated on 10% (weight/volume) polyacrylamide gels (Atto), and transferred onto PVDF membranes (Millipore). The membranes were incubated with anti–HLA–DRα antibody (FL-254) or anti-human MPO antibody (HPA021147), followed by horseradish peroxidase (HRP)–conjugated anti-rabbit IgG (Thermo Fisher Scientific). The membranes were also incubated with anti-FLAG antibody (M2), followed by HRP-conjugated anti-mouse IgG antibody (Jackson ImmunoResearch). Peroxidase activity was detected with SuperSignal reagent (Thermo Fisher Scientific).

HLA–DRB1 genotyping and ELISA. HLA–DRB1 alleles were determined as previously described (28). Briefly, a WAKFlow system (Wakunaga Pharmaceutical) was used for the HLA–DRB1 typing.

MPO protein purified from human neutrophils (Sigma-Aldrich) was coated onto 96-microwell plates (3690; Costar), and IgG bound to the plates was detected by HRP-conjugated donkey anti-human IgG antibody (Jackson ImmunoResearch). Peroxidase activity was detected using an OptEIA kit (BD Biosciences). Anti-MPO antibody titers were calculated using standard serum from a patient with MPA, for which the MPO-ANCA titer is known (720 units/ml). Interleukin-8 (IL-8) expression in the culture supernatant was determined by ELISA (eBioscience).

Competitive inhibition assay. Sera from MPA patients were mixed with various concentrations of MPO protein purified from human neutrophils (Sigma) and incubated overnight at 4°C. Anti–MPO/HLA–DR complex antibodies and anti-MPO antibodies were detected using flow cytometry and ELISA, respectively. Anti–MPO/HLA–DR complex antibody titers and anti-MPO antibody titers were calculated using a standard MPA serum, as described above. The percent inhibition was defined as 100 – (titer of inhibited serum/titer of noninhibited serum) $\times$ 100.

Immunoprecipitation detected by flow cytometry (IP-FCM). For the IP-FCM assay, we used a modified version of the protocol described by Schrum et al (29). Anti–HLA–DRα monoclonal antibody HL-38 was coupled to Aldehyde/Sulfate Latex Beads (Life Technologies). The beads were washed twice with MES buffer. Anti–HLA–DRα monoclonal antibody (HL-38) was mixed with the beads and shaken at room temperature overnight. The antibody-coupled beads were then washed 3 times and suspended in phosphate buffered saline (PBS) containing 0.1% glycine and 0.1% NaN_3. Next, the antibody-coupled beads were mixed with cell lysate at 4°C for 1 hour. The beads were subsequently stained with biotinylated primary antibody, followed by APC–streptavidin (Jackson ImmunoResearch). Finally, the stained beads were analyzed using a FACSVerse system (Becton Dickinson).

Stimulation of neutrophils. Isolated neutrophils were resuspended with RPMI 1640 medium containing 10% autologous serum. Neutrophils (1×10^7) were cultured for 48 hours in the presence of IFNγ (final concentration 100 units/ml) plus autologous serum in a 6-well plate. Thereafter, neutrophils were stained with anti–HLA–DR or anti-MPO antibody and analyzed by flow cytometry.

Stimulation of HLA–DR–transfected HL-60 cells. HLA–DR9 was stably transfected into HL-60 cells using a Platinum-E (Plat-E) system (30). HLA–DR9 and an amphotropic envelope were transfected into Plat-E cells. Culture supernatant containing a retroviral vector was collected 2 days after replacement and added to medium for the HL-60 cells. HLA–DR–positive cells were then sorted with a Sony SH800 cell sorter. GFP was stably transfected into HL-60 cells in the same manner, and these were used as mock cells. HL-60 cells were cultured in medium containing 10 μM all-*trans*-retinoic acid for 5 days in order to differentiate into neutrophil-like cells (31,32). Next, 20 μg/ml IgG purified from plasma was coated onto a 96-well plate. After incubation at 4°C overnight, the plate was washed twice with PBS. A total of 100 μl of 1×10^6 cells/ml of differentiated HL-60 cells was cultured with the precoated plate for 3 hours. The IL-8 concentration in culture supernatant was determined by ELISA.

Statistical analysis. Pearson's product-moment correlation coefficient was used to assess the significance of correlations, and the correlation coefficient and *P* value of the linear regression line were calculated. Mann-Whitney U test, Student's *t*-test, or one-way analysis of variance with Tukey's post hoc test was used to determine the significance of differences. The odds ratios (ORs) for the association between different HLA–DRB1 alleles and MPA were log-transformed to normalize the distribution. HLA–DRB1 alleles with a frequency of >2% in MPA patients were analyzed for their association with autoantibody binding to the MPO/HLA–DR complex. *P* values less than 0.05 were considered significant.

RESULTS

MPO expression on the cell surface in association with HLA class II molecules. In order to address the role of HLA class II molecules in the cell surface expression of MPO, we transfected human MPO with MPA-susceptible HLA–DR9 (HLA–DRA*01:01/DRB1*09:01) (22) into HEK 293T cells and used flow cytometry to analyze the cell surface expression of MPO. Cell surface expression of MPO was low when MPO alone was transfected. However, when MPO and HLA–DR9 were cotransfected, the cell surface expression of MPO was markedly increased; the intracellular level of MPO was not affected by HLA–DR9 expression (Figure 1A). We then investigated whether MPO-ANCAs could bind to cell surface–expressed MPO induced by HLA–DR. IgG autoantibodies from an MPA patient bound to MPO induced on the cell surface by HLA–

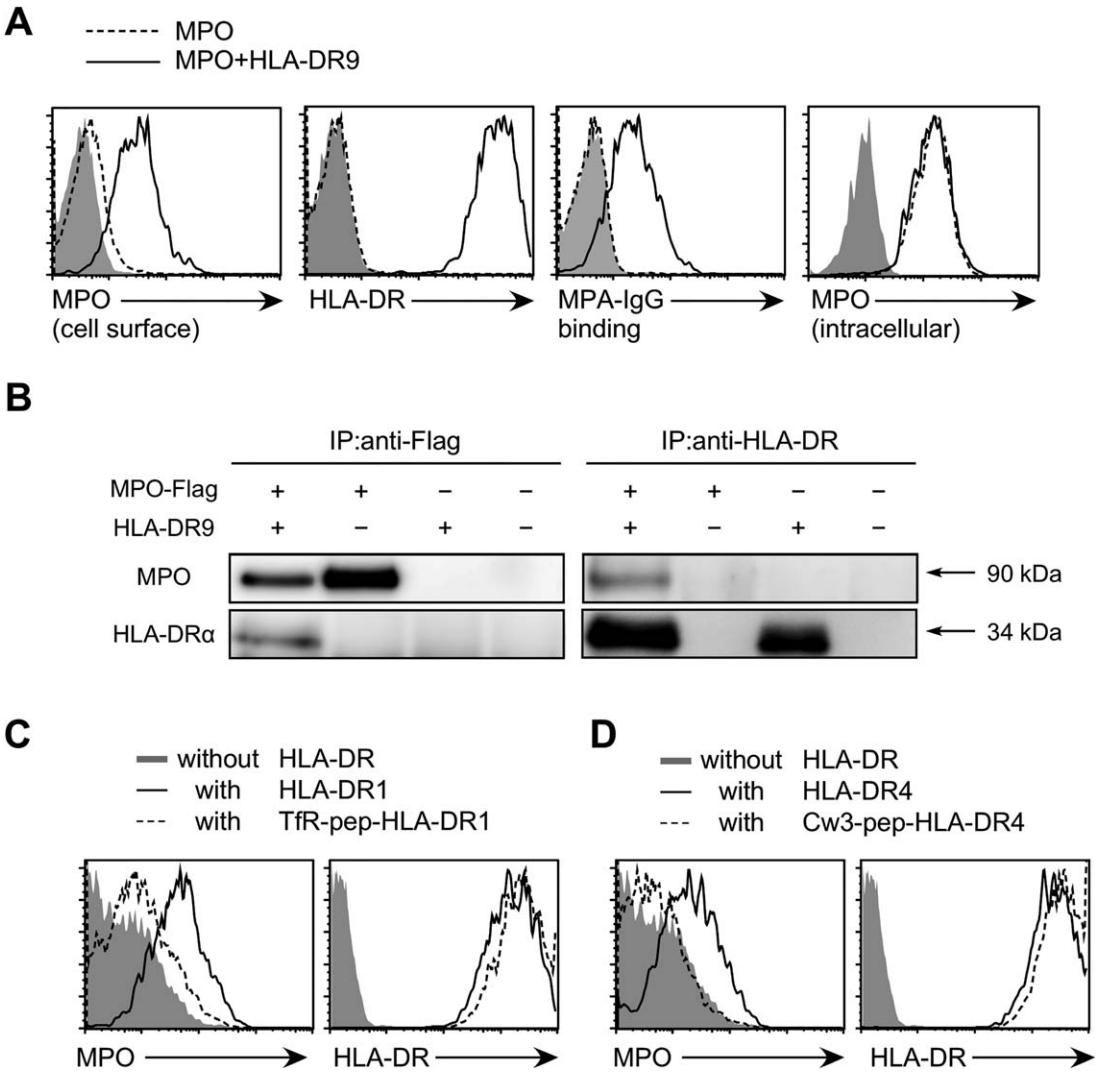

Figure 1. Myeloperoxidase (MPO) is expressed on the cell surface in association with HLA–DR. **A,** MPO and green fluorescent protein (GFP) were transfected into HEK 293T cells with (solid line) or without (broken line) HLA–DRA*01:01 and HLA–DRB1*09:01 (HLA–DR9). The transfectants were stained with anti-MPO antibodies, anti–HLA–DR antibodies, or serum from a patient with microscopic polyangiitis (MPA-IgG). Intracellular MPO was also stained. Antibody binding to GFP-expressing cells is shown. Cells transfected with GFP alone were stained as a control (shaded histograms). **B,** MPO protein was coimmunoprecipitated with HLA–DR9. HLA–DR9 and/or MPO was transfected into HEK 293T cells. Cell lysates were immunoprecipitated (IP) with anti-FLAG or anti–HLA–DR antibody. Immunoprecipitates were blotted with anti-FLAG, anti-MPO, or anti–HLA–DRα antibodies. **C,** HLA–DR1 (solid lines), HLA–DRB1*01:01 containing a covalently attached transferrin receptor peptide (TfRpep–HLA–DR1) (broken lines), or control plasmids (shaded histograms) were cotransfected with MPO and GFP. Cell surface expression of MPO and HLA–DR on GFP-positive cells is shown. **D,** HLA–DR4 (solid lines), HLA–DRB1*04:04 containing a covalently attached HLA–Cw3 peptide (HLA–Cw3–pep–HLA–DR4) (broken lines), or control plasmids (shaded histograms) were cotransfected with MPO and GFP. Cell surface expression of MPO and HLA–DR on GFP-positive cells is shown. Results are representative of at least 3 independent experiments.

DR. In contrast, MPO-ANCAs did not bind to the cells that were transfected with MPO alone.

Next, we used an IP assay to investigate whether full-length MPO is associated with HLA–DR. Full-length 90-kd MPO protein was coimmunoprecipitated with HLA–DR9, whereas MPO was not detected in the absence of HLA–DR9, indicating that full-length but not fragmented MPO is associated with HLA–DR (Figure 1B). Our group previously showed that various misfolded proteins are associated with the peptide-binding groove of major histocompatibility complex (MHC) class II molecules (14–16). To test the possibility that MPO also is

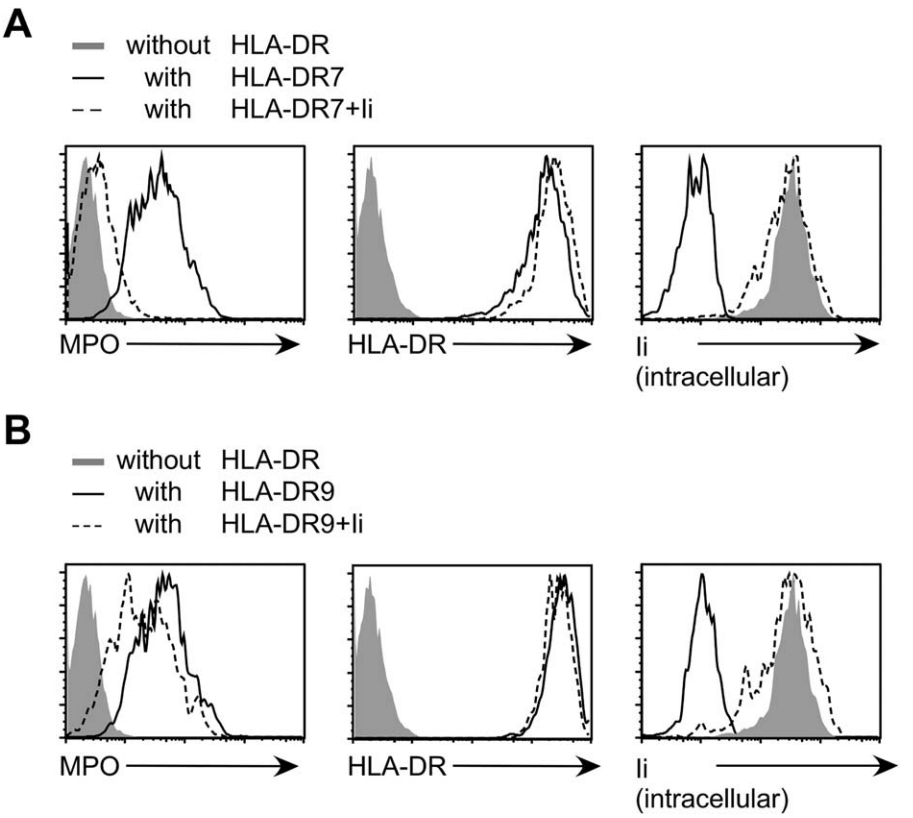

Figure 2. Cell surface expression of MPO induced by HLA–DR with an MPA-susceptible allele is less affected by the invariant chain (Ii) than by an MPA-nonsusceptible allele (HLA–DR7). MPO and GFP were cotransfected with HLA–DR into HEK 293T cells in the presence (broken lines) or absence (solid lines) of the invariant chain. Cell surface expression of HLA–DR and MPO on GFP-positive cells was analyzed. Cells transfected without HLA–DR were stained as a control (shaded histograms). Expression of the invariant chain was analyzed by intracellular staining. **A,** MPO was transfected with HLA–DR7. **B,** MPO was transfected with HLA–DR9. Results are representative of at least 3 independent experiments. See Figure 1 for other definitions.

associated with the peptide-binding groove of HLA–DR, we measured MPO cell surface expression using HLA–DR1 that was covalently attached to a transferrin receptor peptide, which reportedly binds to the peptide-binding groove of HLA–DR1 with relatively high affinity (14,27,33). We also used HLA–DR4 that was covalently attached to a HLA–Cw3 peptide, which also binds to the peptide-binding groove of HLA–DR4 (15,34). When covalently attached to a peptide, both HLA–DR1 and HLA–DR4 transported less MPO to the cell surface than did wild-type HLA–DR (Figures 1C and D). These findings indicate that full-length MPO is associated with the peptide-binding groove of HLA class II molecules.

The invariant chain binds to the peptide-binding groove of newly synthesized MHC class II molecules at the ER and transports them to the endolysosomal pathway. In addition, the invariant chain inhibits the binding of certain proteins to MHC class II molecules at the ER (35). We investigated the effect of the invariant chain on the association of MPO with HLA–DR. In the absence of the invariant chain, HLA–DR7, an allele not associated with susceptibility to MPA, transported MPO to the cell surface in a manner similar to that of HLA–DR9 (Figures 2A and B). In the presence of the invariant chain, the cell surface expression of MPO induced by HLA–DR7 was clearly inhibited (Figure 2A). On the other hand, inhibition of MPO cell surface expression by the invariant chain was low when HLA–DR9 was transfected (Figure 2B). Therefore, the affinities of HLA class II molecules to the invariant chain and MPO differed depending on the alleles of HLA class II molecules that were expressed.

Binding of autoantibodies from MPA patients to MPO complexed with MHC. We determined the anti–MPO/HLA–DR complex antibody titers in sera obtained from patients with MPA at the time of disease onset as well as those in sera obtained from healthy controls. Anti–MPO/HLA–DR complex antibodies were detected in 87.5% of patients with MPA when the cutoff

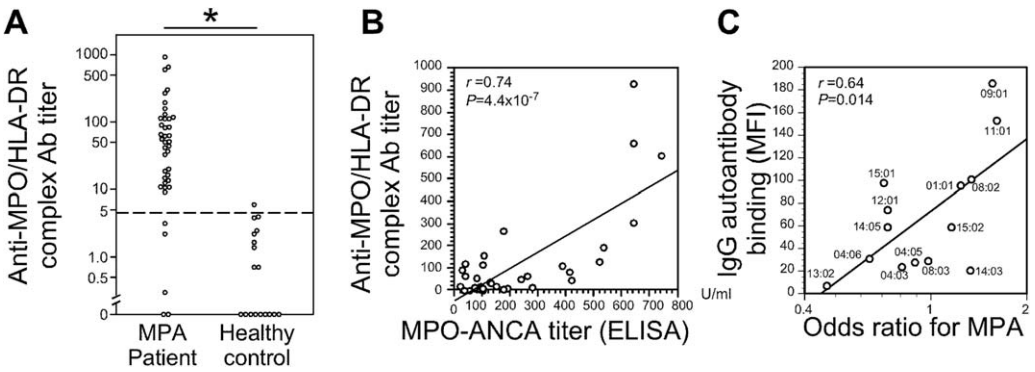

Figure 3. Autoantibodies from MPA patients bind to MPO complexed with HLA–DR. **A,** Anti–MPO/HLA–DR complex antibody (Ab) titers were determined in sera obtained from patients with MPA (n = 40) and from healthy controls. The cutoff value was defined as the mean + 2SD of the titers in healthy controls. Differences between anti–MPO/HLA–DR complex antibody titers in patients with MPA and healthy controls were analyzed by Mann-Whitney U test. Each data point represents an individual subject; the horizontal line shows the cutoff value. $* = P < 0.05$. **B,** MPO–antineutrophil cytoplasmic antibody (ANCA) titers in serum samples from 40 MPA patients were plotted in relation to IgG autoantibody titers in each serum to MPO complexed with HLA–DR9 (anti–MPO/HLA–DR antibody titer). **C,** MPO was cotransfected with HLA–DRA*01:01 in combination with each HLA–DRB1 allele indicated, and the mean fluorescence intensity (MFI) of binding of autoantibodies from an MPA patient to MPO complexed with HLA–DR was plotted against the odds ratio for MPA susceptibility for each HLA–DRB1 allele. The odds ratios for the association between different HLA–DRB1 alleles and MPA were log-transformed to normalize the distribution. In **B** and **C,** Pearson's product-moment correlation coefficient was used for the analysis. Results are representative of at least 3 independent experiments. ELISA = enzyme-linked immunosorbent assay (see Figure 1 for other definitions).

value was defined as the mean +2SD of the titers in healthy controls. The titers of anti–MPO/HLA–DR complex antibody in patients with MPA were significantly higher than those in healthy controls (Figure 3A). This finding suggests that the MPO/HLA–DR complex is recognized by autoantibodies from patients with MPA. We next analyzed whether anti–MPO/HLA–DR complex antibody titers were correlated with MPO-ANCAs detected by conventional ELISA. The anti–MPO/HLA–DR complex antibody titer was significantly correlated with the MPO-ANCA titer determined by ELISA (Figure 3B). These results imply that MPO/HLA–DR complexes are targets for MPO-ANCAs in patients with MPA.

We investigated the effects of the HLA–DR of different alleles on the transport of MPO to the cell surface. MPO was transfected into HEK 293T cells with different HLA–DR alleles, and its cell surface expression was analyzed (Figure 3C). The results indicated that the cell surface expression of MPO differed depending on the HLA–DR alleles. As observed in other autoimmune diseases, susceptibility to MPA is associated with certain HLA–DRB1 alleles (22,23). The ORs for the association between MPA and each HLA–DR allele were plotted against autoantibody binding to the MPO/HLA–DR complex for each allele (Figure 3C). There was a significant positive correlation between autoantibody binding to the MPO/HLA–DR complex and the OR for the correlation conferred by each HLA–DR allele ($r = 0.64$, $P = 0.014$). These findings suggest that the MPO/HLA–DR complex is involved in the pathogenesis of MPA.

Cryptic autoantibody epitopes expressed by MPO associated with HLA–DR. Because the structure of the proteins associated with HLA–DR differs from that of native proteins (14–16), there is a possibility that cryptic autoantibody epitopes that are not exposed on the surface of native MPO proteins are exposed on MPO by association with HLA–DR. To test this possibility, we neutralized patient sera containing MPO-ANCAs using native MPO protein purified from human neutrophils. Anti–native MPO antibody titers detected by ELISA were decreased in the presence of native MPO proteins, in a dose-dependent manner (Figure 4). In contrast, autoantibodies against the MPO/HLA–DR complex were still detected in sera from MPA patients even after neutralization with native MPO proteins (Figure 4). In particular, there was a significant difference between the anti–MPO/HLA–DR antibody titer and the anti-MPO antibody titer after neutralization with 3.16 μg/ml native MPO. These results suggest that MPO associated with HLA–DR might express cryptic autoantibody epitopes that are not exposed on native MPO.

Formation of the MPO/HLA–DR complex in neutrophils stimulated with IFNγ. The presence of autoantibodies specific to MPO complexed with HLA–DR suggests that under certain conditions, MPO is associated with HLA–DR in neutrophils. Although neutrophils

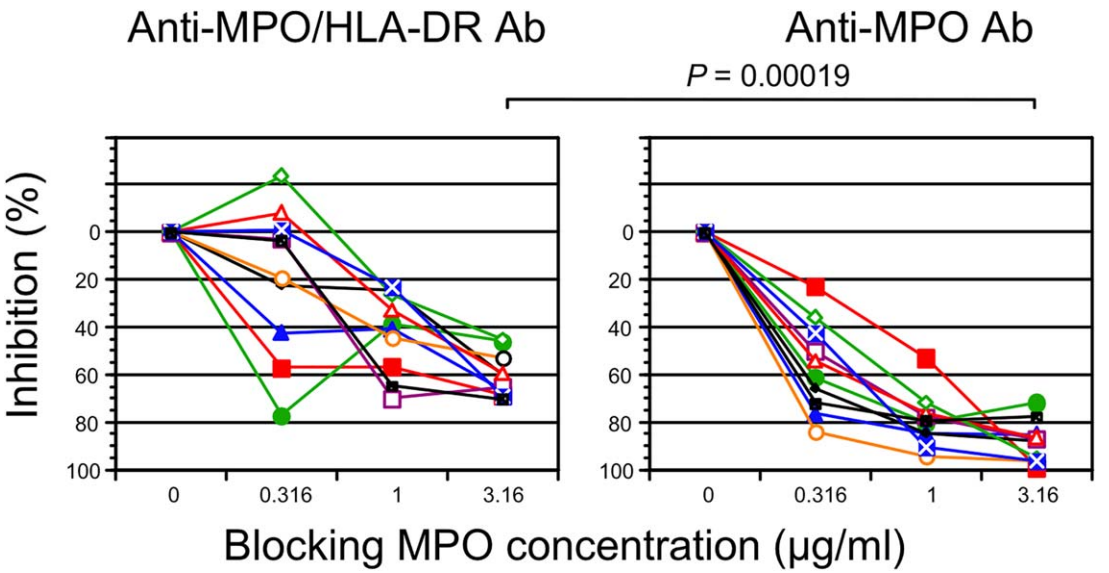

Figure 4. Cryptic autoantibody epitopes on myeloperoxidase (MPO) are exposed by association with HLA–DR. Serum samples from patients with microscopic polyangiitis (MPA) (n = 10) were mixed with various concentrations of MPO protein purified from human neutrophils and incubated overnight at 4°C. After incubation, anti–MPO/HLA–DR complex antibodies (Ab) were detected using flow cytometry, and anti-MPO antibodies were determined using enzyme-linked immunosorbent assay. Autoantibody titers were calculated using standard serum. Inhibition (%) was defined as 100 – (titer of inhibited serum/titer of noninhibited serum) × 100. Results are representative of at least 3 independent experiments. Student's *t*-test was used to analyze the difference between the anti–MPO/HLA–DR antibody titer and the anti-MPO antibody titer after incubation with MPO at a concentration of 3.16 μg/ml native MPO. Lines connect the data points for each subject. Each patient was distinguished using different colors and symbols.

contain high levels of intracellular MPO, resting neutrophils express few HLA class II molecules. However, it has been reported that human neutrophils express HLA class II molecules after stimulation with IFNγ (19,20). We thus analyzed HLA–DR expression on the surface of neutrophils isolated from healthy donors, following IFNγ stimulation (Figure 5A). As reported previously, neutrophils expressed HLA–DR following stimulation with IFNγ.

When HLA–DR was immunoprecipitated from the cell lysates of neutrophils from healthy donors, MPO was coprecipitated with HLA–DR from the cell lysates of IFNγ-stimulated neutrophils with MPA-susceptible HLA–DRB1*09:01, but not from those of unstimulated neutrophils. In addition, MPO was not coprecipitated with HLA–DR from the cell lysates of IFNγ-stimulated neutrophils with MPA-nonsusceptible HLA–DRB1*12:01/15:02 (Figure 5B). These findings indicate that MPO can be complexed with HLA class II molecules in neutrophils, under pathophysiologic conditions.

Detection of the MPO/HLA–DR complex in neutrophils isolated from a patient with MPA. We next analyzed neutrophils obtained from a patient with a diagnosis of MPA. The patient, a 75-year-old female, had an MPO-ANCA titer of 220 units/ml. She had a fever and interstitial pneumonia but no glomerulonephritis or neuropathy. We isolated neutrophils from her peripheral blood at onset and after immunosuppressive therapy and analyzed them using flow cytometry. A small but significant amount of HLA–DR was expressed on the surface of neutrophils at onset, but this decreased after treatment (Figure 5C). We next investigated whether the MPO/HLA–DR complex was present in the patient's neutrophils, using the IP-FCM method, which is much more sensitive for the detection of molecular interactions compared with conventional methods using IP and Western blotting (29,36). The association of MPO with HLA–DR was detected in neutrophil cell lysates obtained from the patient at onset (Figure 5D). The amount of MPO complexed with HLA–DR decreased after treatment. In contrast, the association of MPO with HLA–DR was not detected in cell lysates from healthy donors. These results indicate that MPO forms a complex with HLA–DR in the neutrophils of MPA patients.

Activation of neutrophil-like cell lines by MPO-ANCA autoantibodies. Next, we investigated the pathophysiologic function of the MPO/HLA–DR complex on the surface of neutrophils. We hypothesized that MPO-ANCAs activate neutrophils through MPO/HLA–DR complexes. However, in vitro functional analyses of the MPO/HLA–DR complex on IFNγ-stimulated neutrophils were not successful, because resting peripheral neutrophils are nonspecifically activated by IFNγ. Accordingly, we stably transfected

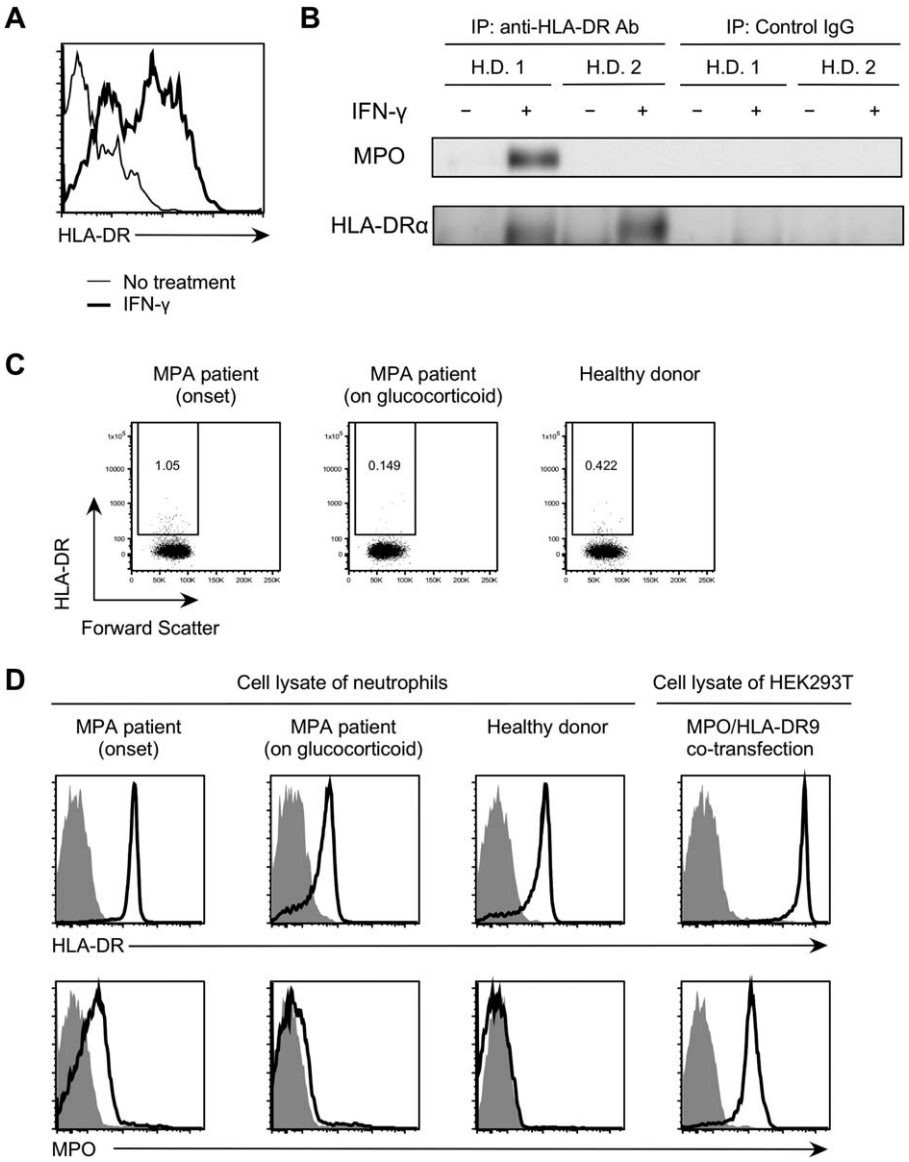

Figure 5. The MPO/HLA–DR complex is detected in neutrophils stimulated with interferon-γ (IFNγ) and neutrophils isolated from patients with MPA. **A,** Neutrophils from healthy donors (HDs) were isolated and incubated for 2 days in the presence or absence of IFNγ. After stimulation, neutrophils were stained with anti–HLA–DR antibody (Ab). The expression of HLA–DR on neutrophils with (thick line) or without (thin line) stimulation by IFNγ is shown. **B,** MPO protein was coimmunoprecipitated with HLA–DR9. After stimulation with IFNγ, cell lysates were immunoprecipitated with anti–HLA–DR or isotype-matched control IgG antibody. Immunoprecipitates were blotted with anti-MPO or anti–HLA–DR antibody. HD 1 = a donor carrying HLA–DRB1*09:01/09:01; HD 2 = a donor carrying HLA–DRB1*12:01/15:02. Results are representative of at least 3 independent experiments. **C,** Neutrophils were isolated from a patient with MPA at disease onset and after immunosuppressive therapy. Freshly isolated neutrophils were stained with anti–HLA–DR antibody. Numbers in the boxes are the proportions of HLA–DR–positive cells. **D,** Anti–HLA–DR antibody–coupled beads were mixed with cell lysates of neutrophils obtained from a patient with MPA and shaken at 4°C for 1 hour. The beads were stained with biotinylated anti–HLA–DR or anti-MPO antibody, followed by allophycocyanin–streptavidin. Staining of isotype-matched control IgG-coupled beads is shown as shaded histograms. Results are representative of at least 3 independent experiments. See Figure 4 for other definitions.

HLA–DR9 into HL-60 cells, which constitutively express MPO and differentiate into mature neutrophil-like cells upon stimulation with all-*trans*-retinoic acid (31,32). Intrinsic MPO expressed in HL-60 cells was expressed on the cell surface in the presence of HLA–DR9, suggesting that MPO formed a complex with HLA–DR (Figure 6A). HL-60 cells were differentiated into neutrophil-like cells by stimulation with all-*trans*-retinoic acid and then were stimulated with

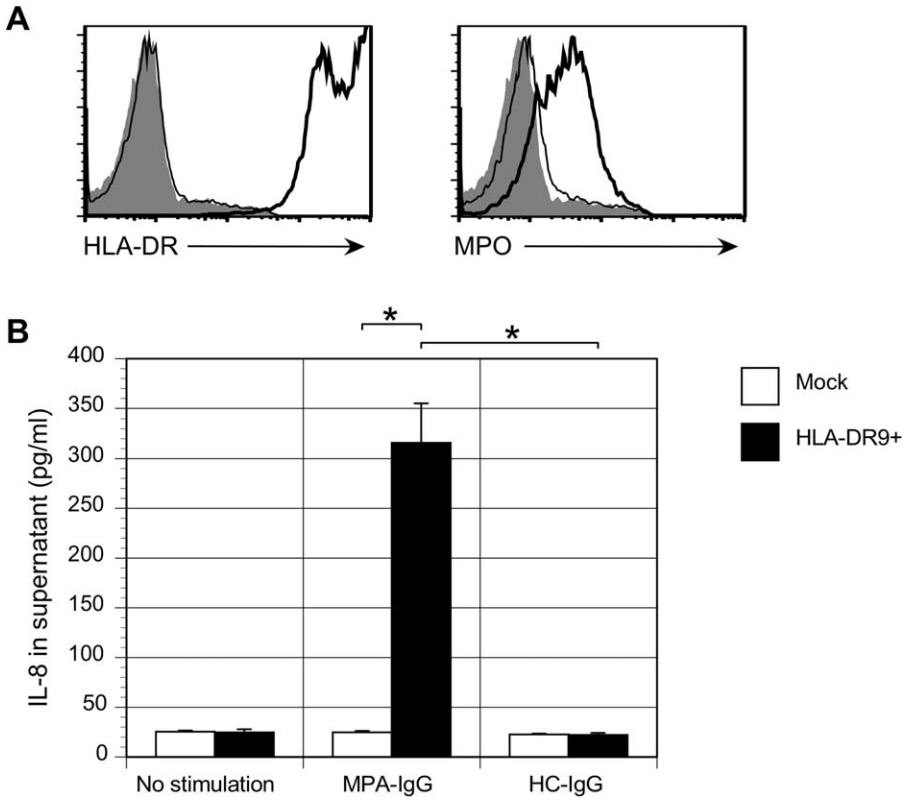

Figure 6. MPO–antineutrophil cytoplasmic antibodies activate the HL-60 neutrophil-like cell line expressing MPA-susceptible HLA–DR. **A,** HLA–DR9 was stably transfected into HL-60 cells via a retroviral vector. HLA–DR–positive cells were sorted. The sorted cells (thick lines) and mock cells (thin lines) were stained with anti-MPO antibody or anti–HLA–DR antibody. Shaded histograms represent control staining. Results are representative of at least 3 independent experiments. **B,** HLA–DR–transfected HL-60 cells were differentiated into neutrophil-like cells with all-*trans*-retinoic acid. Cells were stimulated with plate-bound IgG purified from a patient with MPA or a healthy control (HC). The interleukin-8 (IL-8) concentration of culture supernatants was determined using enzyme-linked immunosorbent assay. Values are the mean ± SD of triplicate experiments. $* = P < 0.05$ by one-way analysis of variance and Tukey's post hoc test. See Figure 4 for other definitions.

IgG purified from the sera of MPA patients or healthy donors. IL-8 was secreted by HLA–DR9–expressing HL-60 cells upon stimulation with IgG from MPA patients, but not with IgG from healthy donors (Figure 6B). These results suggest that the MPO-ANCAs stimulate neutrophils through the MPO/HLA–DR complex.

DISCUSSION

In the current study, we demonstrated that intracellular MPO is transported to the cell surface by HLA class II molecules with an MPA-susceptible allele. MPO expressed on the cell surface by HLA class II molecules was recognized by MPO-ANCAs, which was involved in neutrophil activation by MPO-ANCAs. These findings suggest that HLA class II molecules are involved in the pathogenesis of MPA by direct association with MPO.

The major function of HLA class II molecules is to present antigenic peptides to T cells. However, it has remained unclear how HLA class II molecules control susceptibility to autoimmune diseases. However, we have observed that misfolded ER proteins are transported to the cell surface by MHC class II molecules without processing to peptides when they are associated with MHC class II molecules (14,18). In the current study, we demonstrated that MPO proteins are also transported to the cell surface by associating with HLA–DR. Although mature MPO consists of a heavy subunit (60 kd) and a light subunit (12 kd), the MPO protein that coimmunoprecipitated with HLA–DR was 90 kd, which is a molecular weight compatible with apopro-MPO or pro-MPO (37). Because both ends of the peptide-binding groove of HLA class II are open (38–40), it is possible (structurally) that the peptide-like structure exposed on full-length MPO proteins binds to the peptide-binding groove. Although we cannot determine the conformation of MPO proteins that are bound to HLA class II molecules, it is likely that MPO proteins associated with HLA class II molecules are

structurally different from native MPO proteins, because only misfolded proteins are associated with HLA class II molecules and are transported to the cell surface (14,15). Indeed, native MPO protein efficiently blocked anti–native MPO autoantibodies, whereas autoantibodies against the MPO/HLA–DR complex were not completely blocked by native MPO protein. These results suggest that cryptic autoantibody epitopes on MPO might be exposed by an association with HLA–DR. These findings are consistent with our hypothesis that MPO associated with HLA–DR is structurally altered compared with native MPO protein.

The ORs for the association between each HLA–DRB1 allele and MPA were significantly correlated with autoantibody binding to MPO complexed with HLA–DR for each allele. This is the first study to show a molecular mechanism that is associated with MPA susceptibility conferred by each HLA–DR allele. HLA–DR of MPA-susceptible alleles efficiently transported MPO to the cell surface, suggesting a relatively high affinity for MPO. The invariant chain binds to newly synthesized HLA class II molecules at the ER and blocks the binding of ER proteins to HLA class II molecules (35). Interestingly, the effect of the invariant chain on the binding of MPO to HLA–DR was lower for susceptible alleles than for nonsusceptible alleles. The affinities of MPO to HLA–DR seem to be higher than the affinities of the invariant chain to HLA–DR in the case of MPA-susceptible HLA–DR alleles.

Significant associations of HLA–DRB1*09:01 with MPA and MPO-ANCA–positive vasculitis in Japanese patients have been reported (22,23). HLA–DRB1*09:01 is the most common HLA–DRB1 allele in Japanese individuals but is rare in Caucasians (Allele*Frequencies in Worldwide Populations [http://www.allelefrequencies.net/]) (41). Our results demonstrating the efficient binding of MPO protein with HLA–DRB1*09:01 might explain why MPA is more common than granulomatosis with polyangiitis (Wegener's) (GPA) in Japan, while GPA is more common in Europe (42). A previous GWAS demonstrated that positivity for MPO-ANCAs, not susceptibility to MPA, is significantly associated with a single-nucleotide polymorphism (rs5000634) in the HLA–DQ region (21). Because the HLA–DR region was not included in the GWAS, and there is strong linkage disequilibrium between HLA–DQ and HLA–DR, HLA–DR is also a possible candidate gene. Because HLA–DRB1*09:01 is a dominant allele in Japan, the high frequency of MPO-ANCAs in Japanese individuals (43), unlike that in Caucasians, might be a result of the high-affinity binding between MPO and HLA–DR9.

The presence of autoantibodies against MPO/HLA–DR complexes suggested that MPO/HLA–DR complexes are generated in vivo. Neutrophils possess high levels of MPO but express very few HLA–DR molecules in a steady state. Previous studies have shown that HLA–DR molecules are induced on neutrophils after stimulation with cytokines such as IFNγ (20,44). Indeed, it has been reported that neutrophils isolated from patients with GPA express MHC class II molecules (45,46). Similarly, we showed that neutrophils from MPA patients express HLA–DR. In addition, we demonstrated that HLA–DR9–positive neutrophils but not HLA–DR12–positive or HLA–DR15–positive neutrophils from healthy donors produce MPO/HLA–DR complexes following stimulation with IFNγ. Therefore, in certain pathologic conditions such as viral infections in which various cytokines are produced, HLA–DR induced by cytokines forms a complex with MPO. Indeed, MPO/HLA–DR complexes were detected in freshly isolated neutrophils from MPA patients. These results imply that the MPO/HLA–DR complex is involved in the pathogenesis of MPA.

We demonstrated that MPO-ANCAs activated HL-60 cells that expressed the MPO/HLA–DR complex. Pathologic conditions in which cytokines such as IFNγ are overproduced might lead to cell surface expression of the MPO/HLA–DR complex in neutrophils, which could be a target for MPO-ANCAs. Several studies have demonstrated that HLA class II molecules transduce activating signals in MHC class II–expressing cells such as dendritic cells and B cells (47–50). Although the precise mechanism of neutrophil activation by autoantibodies is unclear, it is possible that HLA–DR complexed with MPO transduces activating signals in neutrophils by MPO-ANCAs.

The mechanism by which MPO-ANCAs are produced in patients with MPA remains unclear. The presence of autoantibodies against the MPO/HLA–DR complex suggests that MPO proteins complexed with HLA–DR are the targets of autoantibodies against MPO. It is possible that structurally altered MPO proteins that are associated with HLA–DR could be recognized as "altered-self" or "neo-self" antigens by immune cells and initiate autoantibody production (18). Indeed, misfolded protein–HLA class II complexes stimulate antigen-specific B cells (14). At present, it remains unclear how T cells are involved in the production of autoantibodies against the complex. Considering that IgG autoantibodies are the most common, T cells must be involved in production of autoantibodies against the misfolded protein–HLA class II complexes. Further analyses are necessary to elucidate how autoantibodies against MPO/HLA class II complexes are produced.

ACKNOWLEDGMENTS

We thank K. Shida, S. Matsuoka, K. Furuno, and M. Matsumoto for providing technical assistance and C. Kita for providing secretarial assistance. We also thank N. Tsuchiya for

granting permission to use data about the HLA–DRB1 allele frequency in MPA.

AUTHOR CONTRIBUTIONS

All authors were involved in drafting the article or revising it critically for important intellectual content, and all authors approved the final version to be published. Dr. Hiwa had full access to all of the data in the study and takes responsibility for the integrity of the data and the accuracy of the data analysis.

Study conception and design. Hiwa, Ohmura, N. Arase, Hirayasu, Kohyama, Suenaga, Atsumi, Mimori, H. Arase.

Acquisition of data. Hiwa, Ohmura, N. Arase, Jin, Saito, Terao, Atsumi, Iwatani.

Analysis and interpretation of data. Hiwa, Ohmura, N. Arase, Jin, Hirayasu, Kohyama, Suenaga, Saito, Terao, Atsumi, Iwatani, Mimori, H. Arase.

REFERENCES

1. Jennette JC, Falk RJ, Bacon PA, Basu N, Cid MC, Ferrario F, et al. 2012 revised International Chapel Hill Consensus Conference nomenclature of vasculitides. Arthritis Rheum 2013;65:1–11.
2. Guillevin L, Durand-Gasselin B, Cevallos R, Gayraud M, Lhote F, Callard P, et al. Microscopic polyangiitis: clinical and laboratory findings in eighty-five patients. Arthritis Rheum 1999;42:421–30.
3. Falk RJ, Jennette JC. Anti-neutrophil cytoplasmic autoantibodies with specificity for myeloperoxidase in patients with systemic vasculitis and idiopathic necrotizing and crescentic glomerulonephritis. N Engl J Med 1988;318:1651–7.
4. Falk RJ, Terrell RS, Charles LA, Jennette JC. Anti-neutrophil cytoplasmic autoantibodies induce neutrophils to degranulate and produce oxygen radicals in vitro. Proc Natl Acad Sci U S A 1990;87:4115–9.
5. Huugen D, Xiao H, van Esch A, Falk RJ, Peutz-Kootstra CJ, Buurman WA, et al. Aggravation of anti-myeloperoxidase antibody-induced glomerulonephritis by bacterial lipopolysaccharide. Am J Pathol 2005;167:47–58.
6. Kettritz R, Jennette JC, Falk RJ. Crosslinking of ANCA-antigens stimulates superoxide release by human neutrophils. J Am Soc Nephrol 1997;8:386–94.
7. Kessenbrock K, Krumbholz M, Schonermarck U, Back W, Gross WL, Werb Z, et al. Netting neutrophils in autoimmune small-vessel vasculitis. Nat Med 2009;15:623–5.
8. Nakazawa D, Shida H, Tomaru U, Yoshida M, Nishio S, Atsumi T, et al. Enhanced formation and disordered regulation of NETs in myeloperoxidase-ANCA-associated microscopic polyangiitis. J Am Soc Nephrol 2014;25:990–7.
9. Ewert BH, Jennette JC, Falk RJ. Anti-myeloperoxidase antibodies stimulate neutrophils to damage human endothelial cells. Kidney Int 1992;41:375–83.
10. Lu X, Garfield A, Rainger GE, Savage CO, Nash GB. Mediation of endothelial cell damage by serine proteases, but not superoxide, released from antineutrophil cytoplasmic antibody–stimulated neutrophils. Arthritis Rheum 2006;54:1619–28.
11. Xiao H, Heeringa P, Hu P, Liu Z, Zhao M, Aratani Y, et al. Antineutrophil cytoplasmic autoantibodies specific for myeloperoxidase cause glomerulonephritis and vasculitis in mice. J Clin Invest 2002;110:955–63.
12. Kallenberg CG, Stegeman CA, Abdulahad WH, Heeringa P. Pathogenesis of ANCA-associated vasculitis: new possibilities for intervention. Am J Kidney Dis 2013;62:1176–87.
13. Jennette JC, Falk RJ. Pathogenesis of antineutrophil cytoplasmic autoantibody-mediated disease. Nat Rev Rheumatol 2014;10:463–73.
14. Jiang Y, Arase N, Kohyama M, Hirayasu K, Suenaga T, Jin H, et al. Transport of misfolded endoplasmic reticulum proteins to the cell surface by MHC class II molecules. Int Immunol 2013;25:235–46.
15. Jin H, Arase N, Hirayasu K, Kohyama M, Suenaga T, Saito F, et al. Autoantibodies to IgG/HLA class II complexes are associated with rheumatoid arthritis susceptibility. Proc Natl Acad Sci U S A 2014;111:3787–92.
16. Tanimura K, Jin H, Suenaga T, Morikami S, Arase N, Kishida K, et al. β2-Glycoprotein I/HLA class II complexes are novel autoantigens in antiphospholipid syndrome. Blood 2015;125:2835–44.
17. Arase N, Tanimura K, Jin H, Yamaoka T, Kishibe M, Nishioka M, et al. Novel autoantibody against the β2-glycoprotein I/HLA-DR complex in patients with refractory cutaneous ulcers. Br J Dermatol 2017. E-pub ahead of print.
18. Arase H. Rheumatoid rescue of misfolded cellular proteins by MHC class II molecules: a new hypothesis for autoimmune diseases. Adv Immunol 2016;129:1–23.
19. Gosselin EJ, Wardwell K, Rigby WF, Guyre PM. Induction of MHC class II on human polymorphonuclear neutrophils by granulocyte/macrophage colony-stimulating factor, IFN-γ, and IL-3. J Immunol 1993;151:1482–90.
20. Fanger NA, Liu C, Guyre PM, Wardwell K, O'Neil J, Guo TL, et al. Activation of human T cells by major histocompatibility complex class II expressing neutrophils: proliferation in the presence of superantigen, but not tetanus toxoid. Blood 1997;89:4128–35.
21. Lyons PA, Rayner TF, Trivedi S, Holle JU, Watts RA, Jayne DR, et al. Genetically distinct subsets within ANCA-associated vasculitis. N Engl J Med 2012;367:214–23.
22. Tsuchiya N, Kobayashi S, Kawasaki A, Kyogoku C, Arimura Y, Yoshida M, et al. Genetic background of Japanese patients with antineutrophil cytoplasmic antibody-associated vasculitis: association of HLA-DRB1*0901 with microscopic polyangiitis. J Rheumatol 2003;30:1534–40.
23. Kawasaki A, Hasebe N, Hidaka M, Hirano F, Sada KE, Kobayashi S, et al. Protective role of HLA-DRB1*13:02 against microscopic polyangiitis and MPO-ANCA-positive vasculitides in a Japanese population: a case-control study. PLoS One 2016;11:e0154393.
24. Watts R, Lane S, Hanslik T, Hauser T, Hellmich B, Koldingsnes W, et al. Development and validation of a consensus methodology for the classification of the ANCA-associated vasculitides and polyarteritis nodosa for epidemiological studies. Ann Rheum Dis 2007;66:222–7.
25. Weinrauch Y, Drujan D, Shapiro SD, Weiss J, Zychlinsky A. Neutrophil elastase targets virulence factors of enterobacteria. Nature 2002;417:91–4.
26. Andrew SM, Titus JA. Purification and fragmentation of antibodies. Curr Protoc Immunol 19972.7.1–2.7.12.
27. Scott CA, Peterson PA, Teyton L, Wilson IA. Crystal structures of two I-Ad-peptide complexes reveal that high affinity can be achieved without large anchor residues. Immunity 1998;8:319–29.
28. Terao C, Ohmura K, Kochi Y, Ikari K, Maruya E, Katayama M, et al. A large-scale association study identified multiple HLA-DRB1 alleles associated with ACPA-negative rheumatoid arthritis in Japanese subjects. Ann Rheum Dis 2011;70:2134–9.
29. Schrum AG, Gil D, Dopfer EP, Wiest DL, Turka LA, Schamel WW, et al. High-sensitivity detection and quantitative analysis of native protein-protein interactions and multiprotein complexes by flow cytometry. Sci STKE 2007;2007:pl2.
30. Morita S, Kojima T, Kitamura T. Plat-E: an efficient and stable system for transient packaging of retroviruses. Gene Ther 2000;7:1063–6.
31. Millius A, Weiner OD. Chemotaxis in neutrophil-like HL-60 cells. Methods Mol Biol 2009;571:167–77.
32. Breitman TR, Selonick SE, Collins SJ. Induction of differentiation of the human promyelocytic leukemia cell line (HL-60) by retinoic acid. Proc Natl Acad Sci U S A 1980;77:2936–40.

33. Chicz RM, Urban RG, Lane WS, Gorga JC, Stern LJ, Vignali DA, et al. Predominant naturally processed peptides bound to HLA-DR1 are derived from MHC-related molecules and are heterogeneous in size. Nature 1992;358:764–8.
34. Hayden JB, McCormack AL, Yates JR III, Davey MP. Analysis of naturally processed peptides eluted from HLA DRB1*0402 and *0404. J Neurosci Res 1996;45:795–802.
35. Neefjes J, Jongsma ML, Paul P, Bakke O. Towards a systems understanding of MHC class I and MHC class II antigen presentation. Nat Rev Immunol 2011;11:823–36.
36. Schrum AG. Visualization of multiprotein complexes by flow cytometry. Curr Protoc Immunol 2009;Chapter 5:Unit5 9.
37. Andersson E. The role of the propeptide for processing and sorting of human myeloperoxidase. J Biol Chem 1998;273:4747–53.
38. Stern LJ, Brown JH, Jardetzky TS, Gorga JC, Urban RG, Strominger JL, et al. Crystal structure of the human class II MHC protein HLA-DR1 complexed with an influenza virus peptide. Nature 1994;368:215–21.
39. Ghosh P, Amaya M, Mellins E, Wiley DC. The structure of an intermediate in class II MHC maturation: CLIP bound to HLA-DR3. Nature 1995;378:457–62.
40. Fremont DH, Hendrickson WA, Marrack P, Kappler J. Structures of an MHC class II molecule with covalently bound single peptides. Science 1996;272:1001–4.
41. Gonzalez-Galarza FF, Takeshita LY, Santos EJ, Kempson F, Maia MH, da Silva AL, et al. Allele frequency net 2015 update: new features for HLA epitopes, KIR and disease and HLA adverse drug reaction associations. Nucleic Acids Res 2015;43:D784–8.
42. Fujimoto S, Watts RA, Kobayashi S, Suzuki K, Jayne DR, Scott DG, et al. Comparison of the epidemiology of anti-neutrophil cytoplasmic antibody-associated vasculitis between Japan and the U.K. Rheumatology (Oxford) 2011;50:1916–20.
43. Sada KE, Yamamura M, Harigai M, Fujii T, Dobashi H, Takasaki Y, et al. Classification and characteristics of Japanese patients with antineutrophil cytoplasmic antibody-associated vasculitis in a nationwide, prospective, inception cohort study. Arthritis Res Ther 2014;16:R101.
44. Kambayashi T, Laufer TM. Atypical MHC class II-expressing antigen-presenting cells: can anything replace a dendritic cell? Nat Rev Immunol 2014;14:719–30.
45. Hansch GM, Radsak M, Wagner C, Reis B, Koch A, Breitbart A, et al. Expression of major histocompatibility class II antigens on polymorphonuclear neutrophils in patients with Wegener's granulomatosis. Kidney Int 1999;55:1811–8.
46. Iking-Konert C, Vogt S, Radsak M, Wagner C, Hansch GM, Andrassy K. Polymorphonuclear neutrophils in Wegener's granulomatosis acquire characteristics of antigen presenting cells. Kidney Int 2001;60:2247–62.
47. Al-Daccak R, Mooney N, Charron D. MHC class II signaling in antigen-presenting cells. Curr Opin Immunol 2004;16:108–13.
48. Haylett RS, Koch N, Rink L. MHC class II molecules activate NFAT and the ERK group of MAPK through distinct signaling pathways in B cells. Eur J Immunol 2009;39:1947–55.
49. Nagaraj S, Nelson A, Youn JI, Cheng P, Quiceno D, Gabrilovich DI. Antigen-specific CD4+ T cells regulate function of myeloid-derived suppressor cells in cancer via retrograde MHC class II signaling. Cancer Res 2012;72:928–38.
50. Lang P, Stolpa JC, Freiberg BA, Crawford F, Kappler J, Kupfer A, et al. TCR-induced transmembrane signaling by peptide/MHC class II via associated Ig-α/β dimers. Science 2001;291:1537–40.

Errata

DOI 10.1002/art.40317

In the article by Roman-Blas et al in the January 2017 issue of *Arthritis & Rheumatology* (pages 77–85), there were some errors regarding the format in which the VAS global pain score was presented, and an error in the footnote of Table 2. In the abstract, the first sentence of the Results paragraph (page 77) should have read "Intriguingly, in the modified intent-to-treat (mITT) population, CS/GS combination therapy was inferior to placebo in the reduction of joint pain (mean ± SEM change in VAS global pain score over 6 months −11.8 ± 2.4 mm [19% reduction] in patients receiving CS plus GS versus −20.5 ± 2.4 mm [33% reduction] in patients receiving placebo; peak between-group difference in global pain score at 6 months 8.7 mm [14.2%], $P < 0.03$), but no between-group differences were seen in the per-protocol completers." In the "Statistical analysis" section under Patients and Methods (page 79), the first sentence of the fifth paragraph should have read "Continuous variables were summarized using the mean ± SD, unless otherwise indicated." In the "Efficacy results" section under Results (page 80), the third sentence of the first paragraph should have read "Indeed, at this interim time point, in the mITT population, there was a mean ± SEM reduction in the VAS global pain score from baseline to 6 months of 20.5 ± 2.4 mm (33% reduction) in the placebo group compared to 11.8 ± 2.4 mm (19% reduction) in the active treatment group." In the legend to Figure 2 (page 80), the second sentence should have read "Results are the mean ± SEM." In the first footnote of Table 2 (page 81), the first sentence of the first footnote should have read "Values are the mean ± SEM change in score (on 100-mm visual analog scale)."

DOI 10.1002/art.40318

In the article by Kalampokis et al in the January 2017 issue of *Arthritis & Rheumatology* (pages 225–238), information on support from 2 NIH grants was omitted from the first paragraph of the footnotes on page 225. That paragraph should have read "Supported by the Arthritis Foundation (Clinical to Research Transition Award, project 5577), the Rheumatology Research Foundation (Scientist Development Award), and the NIH (grants 5R01-AI-100147, UL1-TR-001117, and 5R01-HL-129061, and Duke Rheumatology 32 Training Grant from the National Institute of Arthritis and Musculoskeletal and Skin Diseases)."

We regret the errors.

33. Chicz RM, Urban RG, Lane WS, Gorga JC, Stern LJ, Vignali DA, et al. Predominant naturally processed peptides bound to HLA-DR1 are derived from MHC-related molecules and are heterogeneous in size. Nature 1992;358:764–8.
34. Hayden JB, McCormack AL, Yates JR III, Davey MP. Analysis of naturally processed peptides eluted from HLA DRB1*0402 and *0404. J Neurosci Res 1996;45:795–802.
35. Neefjes J, Jongsma ML, Paul P, Bakke O. Towards a systems understanding of MHC class I and MHC class II antigen presentation. Nat Rev Immunol 2011;11:823–36.
36. Schrum AG. Visualization of multiprotein complexes by flow cytometry. Curr Protoc Immunol 2009;Chapter 5:Unit5 9.
37. Andersson E. The role of the propeptide for processing and sorting of human myeloperoxidase. J Biol Chem 1998;273:4747–53.
38. Stern LJ, Brown JH, Jardetzky TS, Gorga JC, Urban RG, Strominger JL, et al. Crystal structure of the human class II MHC protein HLA-DR1 complexed with an influenza virus peptide. Nature 1994;368:215–21.
39. Ghosh P, Amaya M, Mellins E, Wiley DC. The structure of an intermediate in class II MHC maturation: CLIP bound to HLA-DR3. Nature 1995;378:457–62.
40. Fremont DH, Hendrickson WA, Marrack P, Kappler J. Structures of an MHC class II molecule with covalently bound single peptides. Science 1996;272:1001–4.
41. Gonzalez-Galarza FF, Takeshita LY, Santos EJ, Kempson F, Maia MH, da Silva AL, et al. Allele frequency net 2015 update: new features for HLA epitopes, KIR and disease and HLA adverse drug reaction associations. Nucleic Acids Res 2015;43:D784–8.
42. Fujimoto S, Watts RA, Kobayashi S, Suzuki K, Jayne DR, Scott DG, et al. Comparison of the epidemiology of anti-neutrophil cytoplasmic antibody-associated vasculitis between Japan and the U.K. Rheumatology (Oxford) 2011;50:1916–20.
43. Sada KE, Yamamura M, Harigai M, Fujii T, Dobashi H, Takasaki Y, et al. Classification and characteristics of Japanese patients with antineutrophil cytoplasmic antibody-associated vasculitis in a nationwide, prospective, inception cohort study. Arthritis Res Ther 2014;16:R101.
44. Kambayashi T, Laufer TM. Atypical MHC class II-expressing antigen-presenting cells: can anything replace a dendritic cell? Nat Rev Immunol 2014;14:719–30.
45. Hansch GM, Radsak M, Wagner C, Reis B, Koch A, Breitbart A, et al. Expression of major histocompatibility class II antigens on polymorphonuclear neutrophils in patients with Wegener's granulomatosis. Kidney Int 1999;55:1811–8.
46. Iking-Konert C, Vogt S, Radsak M, Wagner C, Hansch GM, Andrassy K. Polymorphonuclear neutrophils in Wegener's granulomatosis acquire characteristics of antigen presenting cells. Kidney Int 2001;60:2247–62.
47. Al-Daccak R, Mooney N, Charron D. MHC class II signaling in antigen-presenting cells. Curr Opin Immunol 2004;16:108–13.
48. Haylett RS, Koch N, Rink L. MHC class II molecules activate NFAT and the ERK group of MAPK through distinct signaling pathways in B cells. Eur J Immunol 2009;39:1947–55.
49. Nagaraj S, Nelson A, Youn JI, Cheng P, Quiceno D, Gabrilovich DI. Antigen-specific CD4+ T cells regulate function of myeloid-derived suppressor cells in cancer via retrograde MHC class II signaling. Cancer Res 2012;72:928–38.
50. Lang P, Stolpa JC, Freiberg BA, Crawford F, Kappler J, Kupfer A, et al. TCR-induced transmembrane signaling by peptide/MHC class II via associated Ig-α/β dimers. Science 2001;291:1537–40.

Errata

DOI 10.1002/art.40317

In the article by Roman-Blas et al in the January 2017 issue of *Arthritis & Rheumatology* (pages 77–85), there were some errors regarding the format in which the VAS global pain score was presented, and an error in the footnote of Table 2. In the abstract, the first sentence of the Results paragraph (page 77) should have read "Intriguingly, in the modified intent-to-treat (mITT) population, CS/GS combination therapy was inferior to placebo in the reduction of joint pain (mean ± SEM change in VAS global pain score over 6 months −11.8 ± 2.4 mm [19% reduction] in patients receiving CS plus GS versus −20.5 ± 2.4 mm [33% reduction] in patients receiving placebo; peak between-group difference in global pain score at 6 months 8.7 mm [14.2%], $P < 0.03$), but no between-group differences were seen in the per-protocol completers." In the "Statistical analysis" section under Patients and Methods (page 79), the first sentence of the fifth paragraph should have read "Continuous variables were summarized using the mean ± SD, unless otherwise indicated." In the "Efficacy results" section under Results (page 80), the third sentence of the first paragraph should have read "Indeed, at this interim time point, in the mITT population, there was a mean ± SEM reduction in the VAS global pain score from baseline to 6 months of 20.5 ± 2.4 mm (33% reduction) in the placebo group compared to 11.8 ± 2.4 mm (19% reduction) in the active treatment group." In the legend to Figure 2 (page 80), the second sentence should have read "Results are the mean ± SEM." In the first footnote of Table 2 (page 81), the first sentence of the first footnote should have read "Values are the mean ± SEM change in score (on 100-mm visual analog scale)."

DOI 10.1002/art.40318

In the article by Kalampokis et al in the January 2017 issue of *Arthritis & Rheumatology* (pages 225–238), information on support from 2 NIH grants was omitted from the first paragraph of the footnotes on page 225. That paragraph should have read "Supported by the Arthritis Foundation (Clinical to Research Transition Award, project 5577), the Rheumatology Research Foundation (Scientist Development Award), and the NIH (grants 5R01-AI-100147, UL1-TR-001117, and 5R01-HL-129061, and Duke Rheumatology 32 Training Grant from the National Institute of Arthritis and Musculoskeletal and Skin Diseases)."

We regret the errors.

ARTHRITIS & RHEUMATOLOGY
Vol. 69, No. 10, October 2017, pp 2081–2091
DOI 10.1002/art.40179

Musculoskeletal Disease in MDA5-Related Type I Interferonopathy

A Mendelian Mimic of Jaccoud's Arthropathy

Luciana Martins de Carvalho,[1] Gonza Ngoumou,[2] Ji Woo Park,[3] Nadja Ehmke,[4] Nikolaus Deigendesch,[2] Naoki Kitabayashi,[5] Isabelle Melki,[6] Flávio Falcäo L. Souza,[1] Andreas Tzschach,[7] Marcello H. Nogueira-Barbosa,[1] Virgínia Ferriani,[1] Paulo Louzada-Junior,[1] Wilson Marques Jr.,[1] Charles M. Lourenço,[1] Denise Horn,[2] Tilmann Kallinich,[2] Werner Stenzel,[2] Sun Hur,[8] Gillian I. Rice,[9] and Yanick J. Crow[10]

Objective. **To define the molecular basis of a multisystem phenotype with progressive musculoskeletal disease of the hands and feet, including camptodactyly, subluxation, and tendon rupture, reminiscent of Jaccoud's arthropathy.**

Methods. **We identified 2 families segregating an autosomal-dominant phenotype encompassing musculoskeletal disease and variable additional features, including psoriasis, dental abnormalities, cardiac valve involvement, glaucoma, and basal ganglia calcification. We measured the expression of interferon (IFN)–stimulated genes in the peripheral blood and skin, and undertook targeted Sanger sequencing of the *IFIH1* gene encoding the cytosolic double-stranded RNA (dsRNA) sensor melanoma differentiation–associated protein 5 (MDA-5). We also assessed the functional consequences of *IFIH1* gene variants using an in vitro IFNβ reporter assay in HEK 293T cells.**

Results. **We recorded an up-regulation of type I IFN–induced gene transcripts in all 5 patients tested and identified a heterozygous gain-of-function mutation in *IFIH1* in each family, resulting in different substitutions of the threonine residue at position 331 of MDA-5. Both of these variants were associated with increased IFNβ expression in the absence of exogenous dsRNA ligand, consistent with constitutive activation of MDA-5.**

Conclusion. **These cases highlight the significant musculoskeletal involvement that can be associated with mutations in MDA-5, and emphasize the value of testing for up-regulation of IFN signaling as a marker of the underlying molecular lesion. Our data indicate that both Singleton-Merten syndrome and neuroinflammation described in the**

Dr. Ehmke's work was supported by the Clinician Scientist Program funded by the Charité–Universitätsmedizin Berlin and the Berlin Institute of Health. Dr. Crow's work was supported by the European Research Council (grant GA309449) and a state subsidy managed by the National Research Agency, France (Investments for the Future grant ANR-10-IAHU-01).

[1]Luciana Martins de Carvalho, MD, PhD, Flávio Falcäo L. Souza, MD, Marcello H. Nogueira-Barbosa, MD, PhD, Virgínia Ferriani, MD, PhD, Paulo Louzada-Junior, MD, PhD, Wilson Marques Jr., MD, PhD, Charles M. Lourenço, MD, PhD: Ribeirão Preto Medical School, University of São Paulo, São Paulo, Brazil; [2]Gonza Ngoumou, MD, Nikolaus Deigendesch, MD, PhD, Denise Horn, MD, Tilmann Kallinich, MD, Werner Stenzel, MD: Charité–Universitätsmedizin Berlin, Berlin, Germany; [3]Ji Woo Park: Boston College, Chestnut Hill, Massachusetts; [4]Nadja Ehmke, MD: Charité–Universitätsmedizin Berlin and Berlin Institute of Health, Berlin, Germany; [5]Naoki Kitabayashi, BSc: INSERM UMR 1163, Laboratory of Neurogenetics and Neuroinflammation and Paris Descartes University, Sorbonne Paris Cité, Institut Imagine, Paris, France; [6]Isabelle Melki, MD: INSERM UMR 1163, Laboratory of Neurogenetics and Neuroinflammation, Paris Descartes University, Sorbonne Paris Cité, Institut Imagine, Hôpital Robert Debré, AP-HP Paris, and Hôpital Necker-Enfants Malades, AP-HP Paris, Paris, France; [7]Andreas Tzschach, MD: Technische Universität Dresden, Dresden, Germany; [8]Sun Hur, PhD: Harvard Medical School, Boston, Massachusetts; [9]Gillian I. Rice, PhD: University of Manchester, Manchester Academic Health Science Centre, Manchester, UK; [10]Yanick J. Crow, MD, PhD: INSERM UMR 1163, Laboratory of Neurogenetics and Neuroinflammation, Paris Descartes University, Sorbonne Paris Cité, Institut Imagine, and Hôpital Necker Enfants Malades, AP-HP Paris, Paris, France, and University of Manchester, Manchester Academic Health Science Centre, Manchester, UK.

Drs. de Carvalho, Ngoumou, and Ehmke and Mr. Park contributed equally to this work.

Address correspondence to Yanick J. Crow, MD, PhD, Institut Imagine, Laboratory of Neurogenetics and Neuroinflammation, 24 Boulevard du Montparnasse, Paris 75015, France. E-mail: yanickcrow@mac.com.

Submitted for publication March 16, 2017; accepted in revised form June 8, 2017.

context of MDA-5 gain-of-function constitute part of the same type I interferonopathy disease spectrum, and provide possible novel insight into the pathology of Jaccoud's arthropathy.

The type I interferonopathies represent discrete examples of a disturbance of the homeostatic control of type I interferon (IFN) signaling due to Mendelian mutations, where constitutive up-regulation of type I IFN activity is considered directly relevant to pathogenesis. Definition of the type I interferonopathies has emphasized involvement of the central nervous system and the skin as primary clinical characteristics (1). The recent observation of mutations in *IFIH1*, encoding the cytosolic double-stranded RNA (dsRNA) sensor melanoma differentiation–associated protein 5 (MDA-5), has highlighted the possibility of joint disease in this context also (2,3). In this report we describe 2 families segregating autosomal-dominant mutations in MDA-5 where musculoskeletal involvement demonstrating overlap with Jaccoud's arthropathy was a major clinical feature. We also provide a brief overview of joint disease so far described in the broader type I interferonopathy grouping, the recognition of which may become of increasing importance as anti-IFN therapies are developed.

PATIENTS AND METHODS

Study participants. Clinical and molecular data were ascertained through direct clinical contact. Written informed consent was obtained from participating family members. The study was approved by the Comité de Protection des Personnes (ID-RCB/EUDRACT: 2014-A01017-40) and the Leeds (East) Research Ethics Committee (reference number 10/H1307/132). Clinical and radiologic features of each patient are listed in Table 1.

IFN score. The IFN scoring method has been described in detail elsewhere (4). Whole blood was collected into PAXgene tubes, total RNA was extracted using a PreAnalytiX RNA isolation kit, and RNA concentration was assessed by spectrophotometry (FLUOstar Omega; Labtech). Quantitative reverse transcription–polymerase chain reaction (PCR) analysis was performed using TaqMan Universal PCR Master Mix (Applied Biosystems) and complementary DNA (cDNA) derived from 40 ng of total RNA. Using TaqMan probes for *IFI27* (Hs01086370_m1), *IFI44L* (Hs00199115_m1), *IFIT1* (Hs00356631_g1), *ISG15* (Hs00192713_m1), *RSAD2* (Hs01057264_m1), and *SIGLEC1* (Hs00988063_m1), the relative abundance of each target transcript was normalized to the expression levels of *HPRT1* (Hs03929096_g1) and *18S* (Hs999999001_s1), and assessed with Applied Biosystems StepOne software version 2.1 and DataAssist software version 3.01. For each of the 6 probes, individual data were expressed relative to a single calibrator. Relative quantification is equal to $2^{-\Delta\Delta C_t}$, i.e., the normalized fold change relative to the control data. The median fold change of the 6 genes compared to the median in 29 previously assessed healthy controls is used to create an IFN score for each individual, with an abnormal IFN score being defined as greater than 2SD above the mean of the control group, i.e., an IFN score of >2.466 was considered abnormal.

Mutation analysis. Primers were designed to amplify the coding exons of *IFIH1* (sequences available upon request from the corresponding author). Purified PCR amplification products were sequenced using BigDye Terminator chemistry and an ABI 3130 DNA sequencer. The mutation description is based on the reference cDNA sequence NM_022168, with nucleotide numbering beginning from the first A in the initiating ATG codon. Variants were assessed using the in silico programs SIFT (http://sift.jcvi.org) and PolyPhen-2 (http://genetics.bwh.harvard.edu/pph2/), and population allele frequencies were obtained from the ExAC database (http://exac.broadinstitute.org).

IFN reporter assay. The pFLAG-CMV4 plasmid encoding IFN-induced helicase C domain–containing protein 1 (IFIH-1) has been described elsewhere (5). The mutations indicated were introduced using KAPA HiFi DNA polymerase. HEK 293T cells (ATCC) were maintained in 48-well plates in Dulbecco's modified Eagle's medium (Cellgro) supplemented with 10% heat-inactivated fetal calf serum and 1% L-glutamine. At ~80% confluence, cells were cotransfected with pFLAG-CMV4 plasmids encoding wild-type or mutant IFIH-1 (10 ng, unless indicated otherwise), IFNβ promoter–driven firefly luciferase reporter plasmid (100 ng), and a constitutively expressed *Renilla* luciferase reporter plasmid (pRL-CMV, 10 ng) by using Lipofectamine 2000 (Life Technologies) according to the manufacturer's protocol. The medium was changed 6 hours after transfection, and cells were subsequently stimulated with poly(I-C) (0.5 μg/ml; InvivoGen) or with in vitro–transcribed 162-bp dsRNA (0.5 μg/ml) using Lipofectamine 2000. Cells were lysed 16 hours after stimulation, and IFNβ promoter activity was measured using a Dual-Luciferase Reporter Assay (Promega) and a Synergy 2 plate reader (BioTek). Firefly luciferase activity was normalized to *Renilla* luciferase activity.

Histopathologic analysis. Snap-frozen skin samples from family 1972 patient 2 and a control subject without any obvious rheumatic or inflammatory skin disease were obtained by open biopsy. Cryostat sections (7 μm) were stained with hematoxylin and eosin and by immunohistochemistry with the following antibodies: IFN-stimulated gene 15 (ISG-15) (clone ab14374; 1:50) (Abcam), sialic acid–binding Ig-like lectin 1 (Siglec-1) (clone HSn7D2; Novus Biologicals), CD45 (clone 2B11; Dako), and CD3 (rabbit polyclonal; Dako). Staining was performed using a Ventana iVIEW DAB Detection Kit. Appropriate biotinylated secondary antibodies were used, and visualization of the reaction product was carried out on a Benchmark XT immunostainer (Ventana).

RESULTS

Family 1938. *Family 1938 patient 1.* The proband of family 1938, who was 18 years old at the time of this study, is a female born to nonconsanguineous parents of Brazilian ancestry. She was delivered at 32 weeks gestation by cesarean section indicated because of placental abruption. A gluteal fistula, diagnosed at age 2 months, necessitated multiple surgical interventions between the ages of 2 and 7 years. She sat at 5 months of age (adjusted for gestation at birth), and walked independently at 24 months of age. At 4 years of age muscle weakness and

Table 1. Summary of the clinical and radiologic features observed in MDA5 mutation–positive patients from families 1938 and 1972*

	Family 1938 patient 1	Family 1938 patient 2	Family 1938 patient 3	Family 1972 patient 1	Family 1972 patient 2
Mutation	c.992C>T/p.Thr331Ile	c.992C>T/p.Thr331Ile	c.992C>T/p.Thr331Ile	c.992C>G/p.Thr331Arg	c.992C>G/p.Thr331Arg
Sex	Female	Female	Female	Female	Male
Age at onset, years	Early infancy	6	3	8	11
Current age, years	18	45	27	9	47
Height at last contact, cm/age, years/SD of mean height	146/18/–2	145/45/–3	144/27/–3	125/9/0	NR
Features at presentation	Gluteal fistula, muscle weakness, joint pain	Joint pain	Joint pain	Muscle weakness and leg pain	Glaucoma
Acro-osteolysis	Yes	Yes	Yes	Yes	Yes
Joint subluxation	Yes	Yes	Yes	No	Yes
Tendon rupture	No	No	No	No	Yes (quadriceps, bilateral, at ages 34 and 35 years)
Periarticular calcifications	Yes	Yes	Yes	No	No
Abnormal dentition	Yes (delayed eruption of primary and secondary dentition)	Yes (loss of teeth in adolescence leading to use of prosthesis)	Yes (loss of teeth in adolescence leading to use of prosthesis)	Delayed eruption of secondary dentition	Yes (delayed tooth eruption and early loss of secondary dentition with resorption of dental roots)
Glaucoma (age at diagnosis, years)	No	No	No	No	Yes (11)
Aortic/cardiac valve calcification	No	Yes	Yes	No	NA
Cardiac status	Hypertension, concentric LVH, mild left atrial and aortic root dilation with aortic valve insufficiency	Hypertension, LVH, aortic valve stenosis	Aortic valve calcification	No abnormalities	NA
Psoriasiform rash (age at onset, years)	Yes (13)	No	Yes (21)	No	Yes (early adulthood)
Multiple lentigines	Yes	Yes	No	No	Yes
Basal ganglia calcification	Yes	Yes	Yes	No cerebral imaging	No cerebral imaging
High hairline/broad forehead	Yes	Yes	Yes	Yes	Yes
Prominent muscle weakness	Yes, as infant with myopathic changes on muscle biopsy	No	No	Yes, as infant	No
IFN score (age, years)†	29.7 (18)	15.1 (45)	16.9 (27)	14.0 (9)	18.8 (47)
Markers of inflammation/ autoantibodies	ESR and CRP normal; autoantibody (ANA and anti-dsDNA) and RF negative; HLA–B27 positivity; C3 and C4 normal	ESR and CRP normal; autoantibody (ANA, anti-dsDNA, Sm/RNP, and Scl-70) and RF negative; C3 and C4 normal	NR	ESR and CRP normal; mildly elevated anti-dsDNA antibodies on 1 occasion; ANA, anti-MDA5 and anti-CCP antibodies negative; RF negative; monocyte CD169/Siglec-1 expression increased; C3 slightly reduced, C4 normal	ESR and CRP normal; RF increased; elevated ANA, anti-CCP, anti-SSA/Ro, and anti–angiotensin II type 1 antibodies; anti-dsDNA antibodies normal; monocyte CD169/Siglec-1 expression increased; C3 and C4 normal

* NR = not recorded; NA = not assessed; LVH = left ventricular hypertrophy; ESR = erythrocyte sedimentation rate; CRP = C-reactive protein; ANA = antinuclear antibody; anti-dsDNA = anti–double-stranded DNA; RF = rheumatoid factor; anti-CCP = anti–cyclic citrullinated peptide; Siglec-1 = sialic acid–binding Ig-like lectin 1.
† Interferon (IFN) scores of >2.466 are considered abnormal.

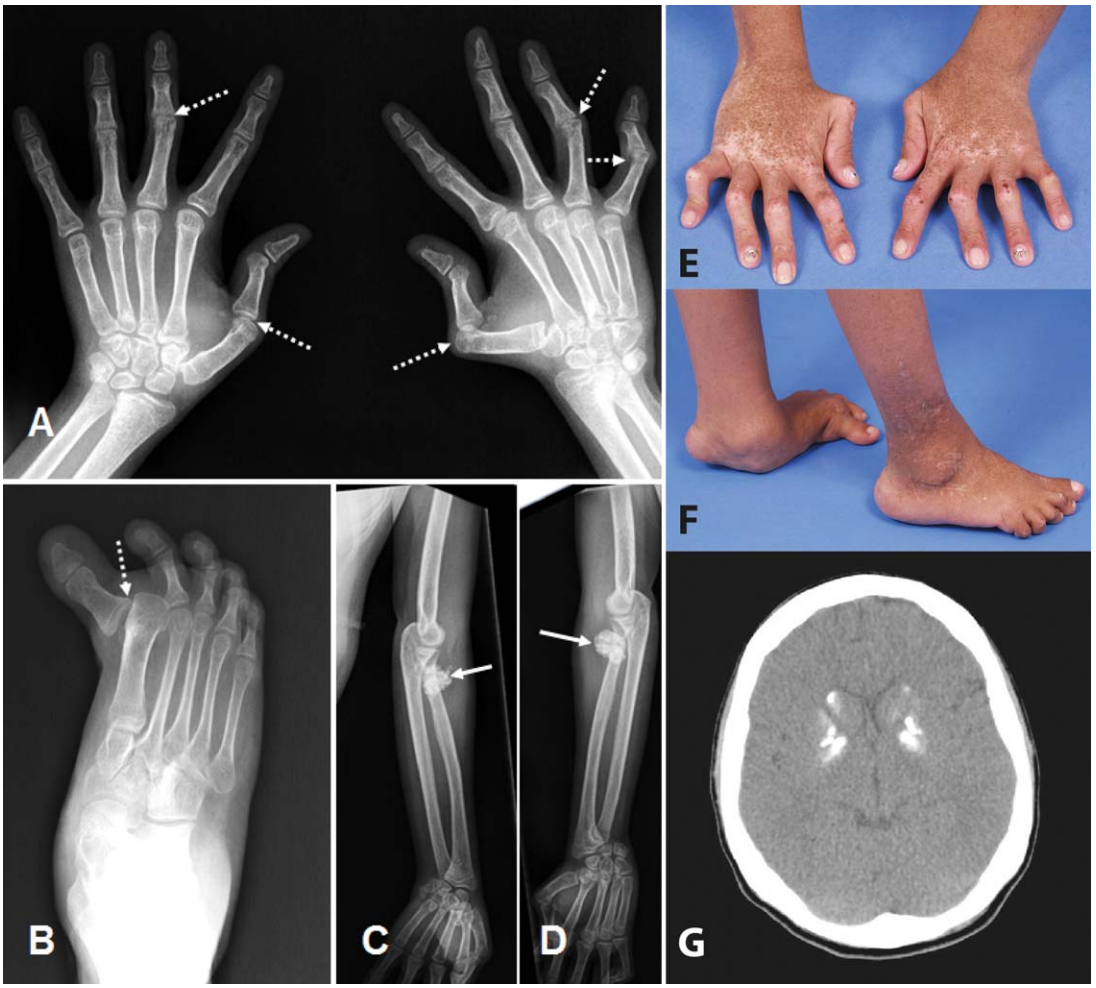

Figure 1. Radiologic and clinical features of patient 1 of family 1938. **A–D**, Radiographs of the hands (**A**), right foot (**B**), and upper limbs (**C** and **D**) at age 18 years, demonstrating subluxations (**broken arrows**), with well-preserved joint spaces and articular surfaces, and dense calcifications of tendon insertions at the elbows (**solid arrows**), which were not palpable. **E** and **F**, Photographs of the hands (**E**) and feet (**F**) at age 18 years, demonstrating camptodactyly, subluxation, and plantar collapse. Note the pigmentary abnormalities on the hands. **G**, Computed tomography image of the brain at age 18 years, demonstrating dense calcification of the basal ganglia (in the absence of any neurologic signs or symptoms).

difficulties with climbing stairs were noted. Electromyography results were suggestive of a myopathic process, and a muscle biopsy showed striated muscle fibers with discrete irregularity of myofibril diameter and peripheral nuclei in a subsarcolemmal distribution. Creatine kinase levels measured on multiple occasions were consistently normal.

Beginning at the age of 2 years she reported joint pain, and subsequently developed progressive deformities of the hands and feet. Rheumatologic review at 7 years of age revealed significant deformities of both feet, and limitation of movement of the cervical spine, elbows, wrists, hands, knees, and ankles (Figures 1A–F). There was no obvious muscle weakness at that time. She was noted to have dry skin, multiple lentigines, and hypochromic macular lesions (Figure 1E). She was diagnosed as having juvenile idiopathic arthritis (JIA) and started on methotrexate and, subsequently, the tumor necrosis factor (TNF) inhibitor etanercept. At age 12 years, considering the degree of joint damage and poor response to etanercept, a putative diagnosis of psoriatic arthritis was made, and treatment with infliximab was initiated but was stopped after 7 months, following an infusion reaction. Due to pain at the injection site, a subsequent course of adalimumab was also stopped. After the appearance of diffuse cutaneous guttate psoriatic lesions at age 13 years, etanercept treatment was started again in combination with leflunomide, with equivocal therapeutic benefit. The erythrocyte sedimentation rate (ESR) and C-reactive protein (CRP)

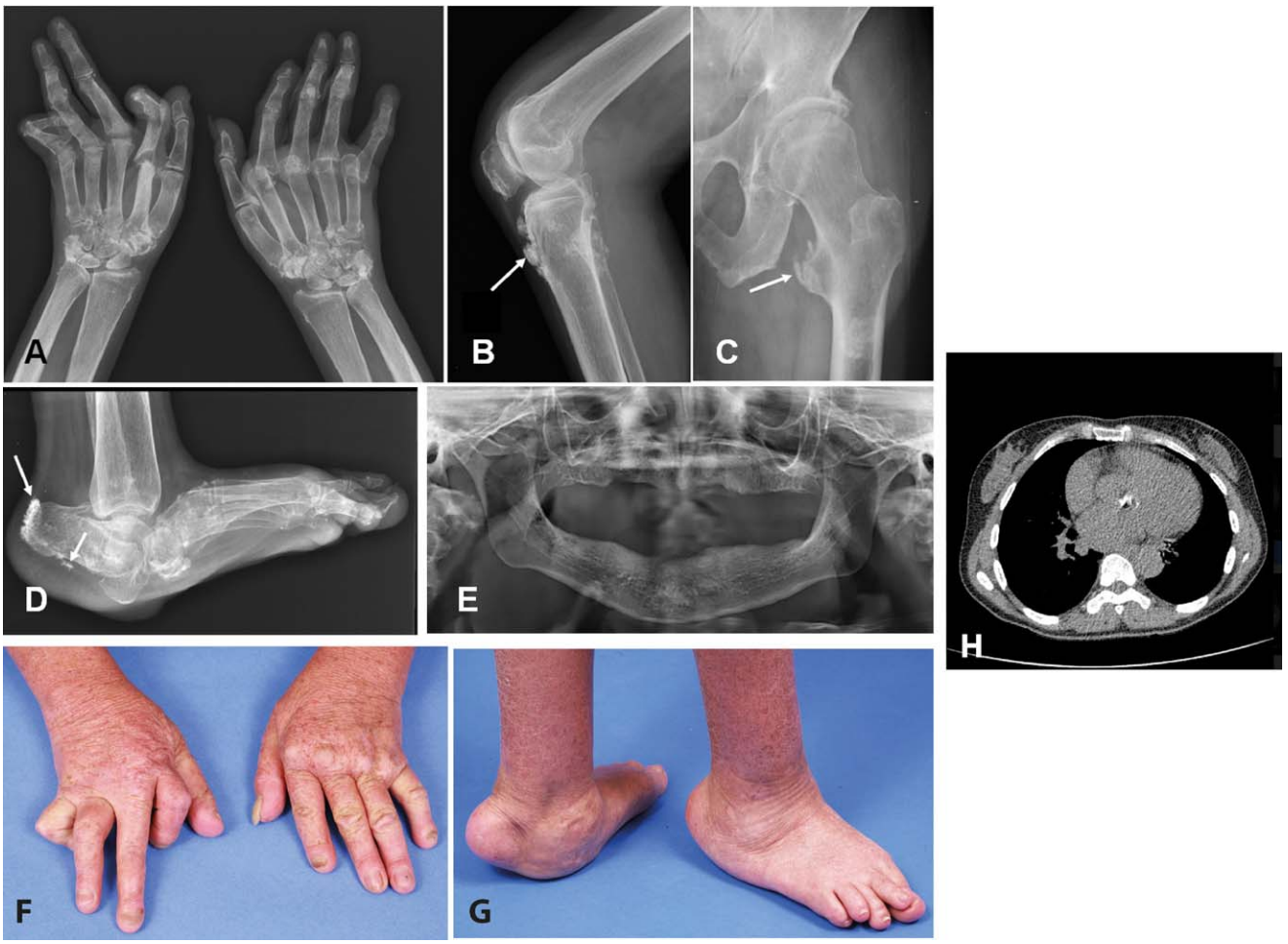

Figure 2. Radiologic and clinical features of patient 2 of family 1938. **A–D**, Radiographs of the hands (**A**), left knee (**B**), left femur and hip (**C**), and left foot (**D**) at age 45 years, demonstrating significant deformities and ectopic calcification at the sites of tendon insertions (**arrows**). **E**, Radiograph of the jaw, demonstrating a complete absence of teeth. **F** and **G**, Photographs of the hands (**F**) and feet (**G**) at age 45 years, demonstrating musculoskeletal deformities. **H**, Transverse computed tomography image of the chest, demonstrating dense ectopic calcification of the aortic valve. Color figure can be viewed in the online issue, which is available at http://onlinelibrary.wiley.com/doi/10.1002/art.40179/abstract.

level have been consistently normal, and the patient has always been negative for autoantibodies.

In addition, this patient was noted to have experienced delayed eruption of her primary and secondary dentition. During adolescence she was found to have hypertension, and echocardiography revealed concentric left ventricle hypertrophy, left atrial dilation, and aortic root dilation with aortic valve insufficiency. There was no evidence of aortic calcification.

At the age of 18 years her height was 146 cm (2 SD below the mean). There was no evidence of glaucoma. Dense calcification of the basal ganglia was observed on cranial computed tomography (CT) imaging (Figure 1G), in the absence of overt neurologic features.

Family 1938 patient 2. The proband's mother was initially evaluated at 35 years of age because of a deforming polyarthritis of the hands and feet. Joint involvement was reported to have started at 6 years of age. She lost almost all of her teeth during adolescence and early adulthood, necessitating the use of a dental prosthesis. She was diagnosed as having psoriatic arthropathy, and treatment with methotrexate and the TNF inhibitor infliximab was initiated at age 44 years, with apparently limited efficacy.

At the time of this study, the patient was 45 years of age and had a height of 145 cm (3 SD below the mean), dry skin, and lentigines. She had subluxation, camptodactyly, and ulnar deviation in the hands, with plantar arch collapse, valgus deformity, and bilateral plantar callosities of the feet (Figures 2A–D, F, and G). There was also a reduction in the range of motion at the elbows, and valgus orientation of the knees. Radiologic evaluation demonstrated

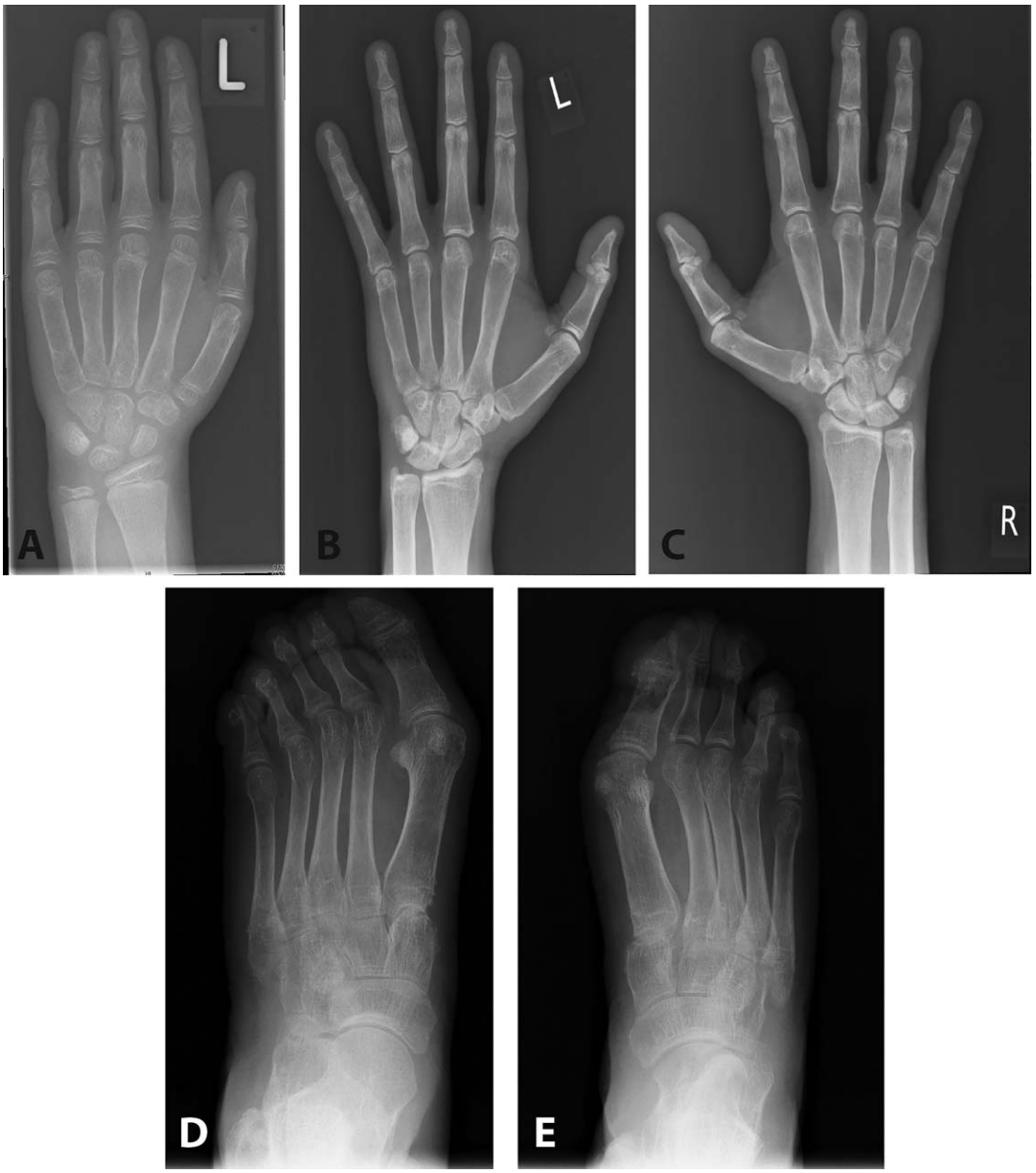

Figure 3. Radiologic features of patients 1 and 2 of family 1972. **A**, Radiograph of the left hand of patient 1 of family 1972 at age 8 years. There were no major radiologic changes other than slight osteopenia. **B–E**, Radiographs of the hands (**B** and **C**) and feet (**D** and **E**) of her father, patient 2 of family 1972, at age 47 years. Bilateral subluxation of the thumbs and hallux deformity of the large toes can be seen. Note a suggestion of acro-osteolysis of the phalanges in **B** and **C**.

acro-osteolysis, joint subluxation, and tendon insertion calcification. Imaging of her jaw confirmed complete loss of her teeth (Figure 2E). She was found to have hypertension, and echocardiography revealed left ventricular hypertrophy with moderate aortic insufficiency and aortic stenosis. Calcification of the aortic valve was observed on chest CT (Figure 2H), and calcification of the basal ganglia was seen on cranial CT in the absence of neurologic signs.

Family 1938 patient 3. A maternal aunt to the proband was evaluated at age 27 years, with a height of 144 cm (3 SD below the mean). She reported the loss of almost all of her teeth during adolescence, necessitating the use of a dental prosthesis beginning at age 15 years.

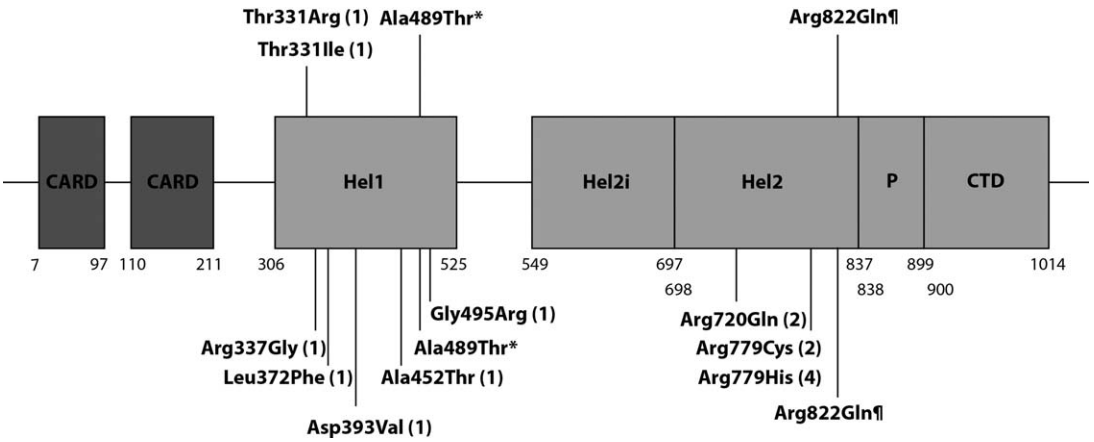

Figure 4. Schematic illustration of melanoma differentiation–associated protein 5 (MDA-5) and disease-associated mutations. The protein domains and their amino acid boundaries within the 1,025–amino acid protein MDA-5 are shown. Hel1 and Hel2 are the 2 conserved core helicase domains, and Hel2i is an insertion domain that is conserved in the retinoic acid–inducible gene 1–like helicase family. P denotes the pincer or bridge region that connects Hel2 to the C-terminal domain (CTD) involved in binding double-stranded RNA. Mutations shown above the line have been recorded in patients with a Singleton-Merton syndrome phenotype. Mutations shown below the line have been identified in patients with a neurologic phenotype. Numbers in parentheses are the numbers of families with each mutation described in the literature. Asterisk denotes a variant identified in 3 members of the same family, 2 with a neurologic phenotype and 1 with a Singleton-Merten syndrome phenotype (3). ¶ denotes a variant identified in 3 families segregating a Singleton-Merten syndrome phenotype (7), an individual with predominant neurologic involvement more consistent with Aicardi-Goutières syndrome (13), and a further family including a patient with features of Singleton-Merten syndrome, spastic paraparesis, and systemic lupus erythematosus (12). CARD = caspase activation recruitment domain.

There was a history of arthralgia of the wrists, metacarpophalangeal and interphalangeal joints, elbows, knees, and ankles, with progressive deformation starting at age 3 years. Radiography revealed diffuse osteopenia, acro-osteolysis, and calcifications at tendon insertions and of the plantar fascia. She had a 6-year history of guttate psoriasis. Chest CT demonstrated calcification of the aortic valve, and calcification of the basal ganglia was observed on cranial CT in the absence of overt neurologic disease.

Other patients in family 1938. The family history indicated that a maternal uncle was evaluated at 24 years of age with a history of a deforming arthropathy beginning at age 12 years. He exhibited features of acro-osteolysis of the hands with metacarpophalangeal subluxations. There were scaly erythematous plaques involving the trunk, scalp, limbs, and buttocks. Lesional biopsy findings were compatible with psoriasis vulgaris with hyperkeratosis and accumulation of neutrophils in the corneal layer, acanthosis with scarce granulosa layer, and mild spongiosis associated with microabscesses. He was treated with methotrexate with good response of the cutaneous features, but with no apparent effect on his joint disease. He was subsequently lost to follow-up. It was reported that the proband's maternal grandmother and another maternal aunt also exhibited a deforming arthropathy, cutaneous lesions, and cardiac valvulopathy of which they both died. The aunt had 2 children, also described to have severe arthropathy. None of these individuals were available for clinical or molecular evaluation.

Family 1972. *Family 1972 patient 1.* The proband of family 1972 is a girl, age 9 years at the time of this study, who was born to nonconsanguineous parents of Caucasian ancestry. She presented to the rheumatology service at age 8 years with muscle weakness and pain in her legs. At that time her height was 125 cm (the median for her age). She was noted to have short distal phalanges of the hands and feet, and hallux valgus deformity of both feet. Radiography showed wide medullary cavities of the metacarpal bones and the proximal phalanges of the hands (Figure 3A), and acro-osteolysis of the distal phalanges of the feet. There were no skin abnormalities, ophthalmologic examination identified no evidence of glaucoma, and there was no calcification of the aorta or cardiac valves. Her developmental history was normal. She had delayed eruption of secondary dentition, having lost her first tooth at age 8 years. Laboratory studies showed normal levels of antinuclear antibodies. The ESR and CRP level were consistently normal. Levels of antibodies against double-stranded DNA (dsDNA) were elevated (30.8 units/ml; normal <20), and the expression of CD169/Siglec-1 on monocytes was increased (5).

Family 1972 patient 2. The father of the proband was 47 years old at the time of this study. He reported a history of joint pain without evidence of arthritis, beginning at age 20 years. He experienced delayed tooth eruption, and

the early loss of secondary dentition with resorption of the dental roots. He was diagnosed as having glaucoma at age 11 years, and as having psoriasis as a young adult. There was a history of rupture of both quadriceps tendons at ages 34 and 35 years. At the time of this study, he had multiple lentigines with hypochromic macules, and deformations of the hands and feet with acro-osteolysis of the phalanges and osteopenia seen on radiography (Figures 3B–E). Laboratory studies showed elevated rheumatoid factor and elevated levels of antinuclear (1:2,560), anti-SSA/Ro, and anti–angiotensin II receptor type 1 antibodies, while levels of antibodies against dsDNA were normal. Expression of CD169/Siglec-1 on monocytes was increased. A lesional skin biopsy demonstrated orthokeratosis and parakeratosis with a markedly thickened epithelial layer and prominent dermal papillae (results available upon request from the corresponding author). The epidermal layer showed strong immunoreactivity for ISG-15, and numerous Siglec-1–positive macrophages and dendritic cells were seen in inflammatory subepidermal foci and epithelial infiltrates (results available upon request from the corresponding author). There was a prominent CD45+ leukocytic infiltrate composed of macrophages and T cells (results available upon request from the corresponding author), while B cells were absent.

Other patients in family 1972. The paternal grandmother of the proband was reported to have experienced delayed tooth eruption and early loss of secondary dentition, as well as osteopenia, bilateral hallux valgus, thickening of the Achilles tendons, and cervical myelopathy. Other family members were also reported to have glaucoma and bone and dental abnormalities, but no further details were available.

Molecular data. In family 1938 all 3 patients tested were heterozygous for missense variant c.992C>T/p.Thr331Ile in *IFIH1*, while in family 1972 the 2 patients sampled were heterozygous for missense variant c.992C>G/p.Thr331Arg in the same gene (Figure 4). The threonine at position 331 is highly conserved to baker's yeast (data available upon request from the corresponding author). Both substitutions are predicted by in silico programs to be damaging, and neither is annotated in the ExAC database. Mapping of the Thr331 residue onto the crystal structure of the 2CARD deletion construct (Δ2CARD) demonstrated that the residue lies within the Hel1 domain, one of two highly conserved core helicase domains responsible for binding RNA and RNA-dependent ATP hydrolysis (results available upon request from the corresponding author).

IFN signature. All 5 individuals tested from both families demonstrated a marked up-regulation of IFN-induced gene transcripts. The IFN scores for family 1938 were 29.7 in patient 1 at age 18 years, 15.1 in patient 2 at age 45 years, and 16.8 in patient 3 at age 27 years (normal ≤2.466). The IFN scores for family 1972 were 14.0 in patient 1 at age 9 years and 18.8 in patient 2 at age 47 years (Figure 5A).

IFN reporter activity. IFNβ reporter stimulatory activity of wild-type and mutant MDA-5 in HEK 293T cells was also assessed (Figure 5B). HEK 293T cells express low levels of endogenous viral RNA receptors, including IFIH-1, as evidenced by low IFN production upon stimulation with dsRNA, allowing comparison of the signaling activity of ectopically expressed receptors. Wild-type MDA-5 was induced only upon stimulation with poly(I-C), a long (>1-kb) dsRNA, and not upon stimulation with short (162-bp) dsRNA, and activity was negligible in the absence of exogenous RNA. In contrast, as in previously described disease-associated mutations (6), basal levels of IFN signaling were markedly increased with the 2 p.Thr331 mutant constructs in the absence of exogenous RNA.

DISCUSSION

We describe 5 individuals from 2 families demonstrating progressive joint disease of the hands and feet consequent to heterozygous gain-of-function mutations in MDA-5. Musculoskeletal involvement began in infancy or early adulthood and was severely deforming in the 4 oldest patients ascertained. Contractures, subluxations, tendon rupture, and tendon insertion calcification were major features, becoming more prominent over time. Joint swelling, effusion, and synovial thickening were absent clinically and on radiologic imaging. In 1 patient, patient 1 of family 1938, the degree of joint involvement prompted a diagnosis of JIA and of psoriatic arthritis, leading to the use of TNF antagonists with minimal efficacy. Her more severely affected mother, patient 2 of family 1938, was also treated with disease-modifying antirheumatic drugs, again with little effect. All 5 individuals experienced significant dental problems, with a variable defect of primary exfoliation and abnormal permanent dentition leading to premature tooth loss. Furthermore, 3 patients were diagnosed as having psoriasis, 2 as having cardiac valve calcification, and 1 as having glaucoma.

Singleton-Merten syndrome is an autosomal-dominant trait characterized by bone disease particularly affecting the hands and feet, abnormal tooth development, and aortic and cardiac valve calcification associated with a considerable risk of mortality (7,8). Additional features include glaucoma, psoriasis, and poorly defined muscle weakness. A possibly characteristic facies with broad forehead has been reported in certain cases. In 2015, a p.Arg822Gln (c.2456G>A) heterozygous gain-of-function

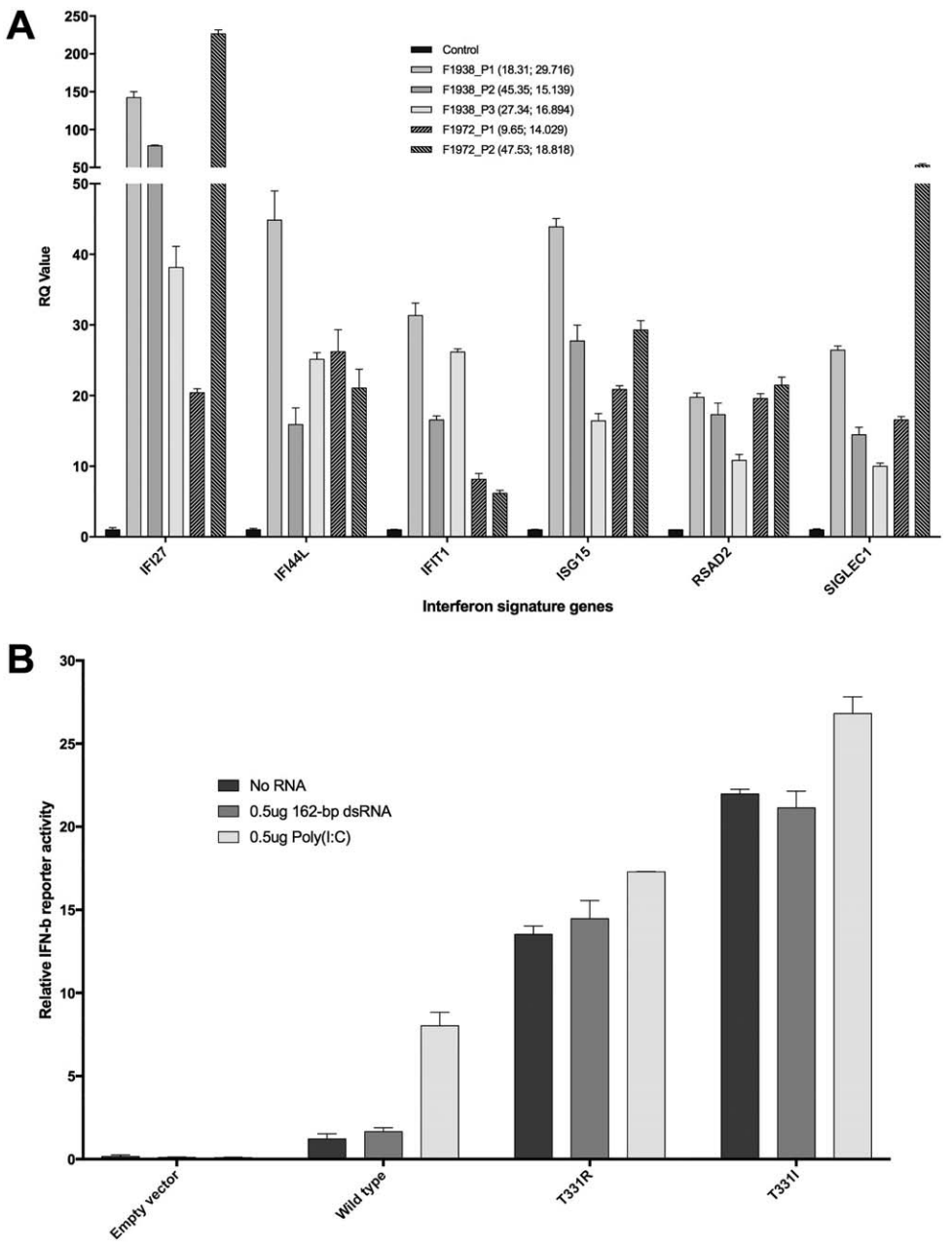

Figure 5. Type I interferon (IFN) status in families 1938 (F1938) and 1972. **A**, Expression of 6 IFN-stimulated genes. Values in parentheses are the patient's age (years); IFN score. Scores of >2.466 are considered abnormal. RQ = relative quantification. **B**, IFNβ reporter activity in Flag-tagged wild-type and mutant IFN-induced helicase C domain–containing protein 1 (IFIH-1) left unstimulated, stimulated with 162-bp double-stranded RNA (dsRNA), or stimulated with poly(I-C) in HEK 293T cells. IFIH-1 mutants activated the IFN signaling pathway more efficiently than did wild-type IFIH-1. Bars show the mean ± SD of 3 independent experiments.

mutation in MDA-5 was identified to segregate with the Singleton-Merten syndrome phenotype in 2 families comprising multiple affected individuals, and in an isolated patient in whom the mutation occurred de novo (2).

Findings in the 2 families described here conform to previous descriptions of Singleton-Merten syndrome. However, their disease is not due to the recurrent p.Arg822Gln mutation identified by Rutsch et al (2), indicating that Singleton-Merten syndrome–like features are not exclusively associated with that particular amino acid substitution. In further support of this suggestion, Bursztejn et al described a 41-year-old man with

camptodactyly of the fifth fingers, bilateral hallux valgus, and loss of permanent teeth after adolescence, whose disease was due to a p.Ala489Thr MDA-5 substitution (3).

Gain-of-function mutations in MDA-5 have also been described in a broad range of neuroimmunologic phenotypes, encompassing the early-onset encephalopathy Aicardi-Goutières syndrome (AGS), isolated spastic paraparesis, and spastic paraparesis with systemic lupus erythematosus (SLE) (6,9–12). Interestingly, all 3 members of family 1938 exhibited calcification of the basal ganglia, a cardinal sign of AGS, in the absence of any neurologic features. Calcification of the basal ganglia and abnormalities of the white matter were also recorded in the adult male patient described by Bursztejn et al (3), again in the absence of overt neurologic disease. These observations indicate that the Singleton-Merten syndrome and neuroinflammatory phenotypes seen in the context of MDA-5 gain-of-function constitute part of the same disease spectrum. Indeed, we note that case 2 described by Singleton and Merten in 1973 developed a fever and lost the ability to walk at the age of 14 months, after a previously unremarkable neonatal period (8). Furthermore, and effectively conclusive in support of this point, Buers et al (13) very recently reported the previously described p.Arg822Gln Singleton-Merten syndrome–associated mutation in a child with an AGS-like phenotype, while Pettersson et al (12) described a female patient with SLE and spastic paraparesis in association with the same mutation.

The type I interferonopathies represent a set of diseases grouped on the premise of a shared pathogenic role of up-regulated type I IFN signaling. A recent review suggested that this grouping currently comprises 18 distinct genotypes including *IFIH1* (1). MDA-5, encoded by *IFIH1*, recognizes viral RNA in the cytosol, leading to the induction of a type I IFN–mediated immune response. All of the *IFIH1* mutations so far characterized confer a gain of function on MDA-5, resulting in constitutive activation of the receptor and enhanced type I IFN signaling. Consistent with published data on a large cohort of patients with MDA-5 mutations (2,3,14), all 5 affected individuals tested in the present study exhibited a marked up-regulation of type I IFN signaling. As such, an IFN signature clearly represents a useful indicator of MDA-5–related pathology.

The nature of the musculoskeletal disease associated with mutations in MDA-5, and the role of type I IFN in this process, remain undefined. We note the frequent observation of psoriasis in the context of Singleton-Merten syndrome (ref. 8 and 3 patients in the present study), and that variants in *IFIH1* have been associated with an increased risk of psoriasis (15). We also note a lack of consistent autoantibody production in Singleton-Merten syndrome (2,7), the absence of elevated levels of inflammation markers (ESR and CRP), and the limited therapeutic efficacy of anti-TNF agents in 2 patients in family 1938. Although bone changes have been described in Singleton-Merten syndrome, in particular widened medullary cavities of the metacarpal bones and acro-osteolysis, joint spaces are well preserved without any obvious erosions or involvement of the epiphyses/metaphyses, and with no evidence of an increased fracture risk. Musculoskeletal disease seems mainly limited to the hands and feet, with an absence of obvious joint swelling. Muscle weakness has been described in a number of patients with Singleton-Merten syndrome reported in the literature, as in patient 1 in family 1938 in this study, but this is not a universal feature, and investigations do not support a specific neuromuscular disturbance or myositis.

Jaccoud's arthropathy has been described as a deforming arthropathy of the hands and feet, seen most commonly in the context of SLE. Importantly, there is an absence of cartilage loss or erosion of juxtaarticular bone on radiography (16,17). The pathogenesis of Jaccoud's arthropathy is unknown, but is thought to involve tendon inflammation, with an animal model suggesting a possible link with enhanced IFN signaling (18). Tendon rupture, as previously described in Singleton-Merten syndrome (7) and as recorded in patient 2 of family 1972 in this study, has been reported to frequently co-occur with Jaccoud's arthropathy in SLE patients (19). Taking these features into account, we suggest that MDA-5–related musculoskeletal disease might be considered to be a Mendelian mimic of Jaccoud's arthropathy, providing possible clues to the underlying pathogenesis.

The prominent joint disease observed in the Singleton-Merten syndrome phenotype indicates a particular association with mutations in *IFIH1* compared to other type I interferonopathy genotypes (20). However, arthropathy has been noted in individual reports of patients with dysfunction of SAM domain and HD domain–containing protein 1 (21–24), 3′ repair exonuclease 1 (25,26), stimulator of IFN genes (27,28), retinoic acid–inducible gene 1 (29), and proteasome subunit β type 8 (30) (results available upon request from the corresponding author), providing possible evidence of for a shared underlying pathology related to enhanced type I IFN signaling. If this is proven to be the case, the identification of such IFN-associated phenotypes will be of increasing clinical relevance as anti-IFN treatments become available (31).

AUTHOR CONTRIBUTIONS

All authors were involved in drafting the article or revising it critically for important intellectual content, and all authors approved the final version to be published. Dr. Crow had full access to all of the data in the

study and takes responsibility for the integrity of the data and the accuracy of the data analysis.

Study conception and design. De Carvalho, Ehmke, Melki, Stenzel, Crow.

Acquisition of data. De Carvalho, Ngoumou, Park, Ehmke, Deigendesch, Kitabayashi, Souza, Tzschach, Nogueira-Barbosa, Ferriani, Marques, Lourenço, Horn, Kallinich, Stenzel, Hur, Rice, Crow.

Analysis and interpretation of data. De Carvalho, Ngoumou, Park, Kitabayashi, Melki, Ferriani, Louzada-Junior, Kallinich, Stenzel, Hur, Rice, Crow.

REFERENCES

1. Rodero MP, Crow YJ. Type I interferon-mediated monogenic autoinflammation: the type I interferonopathies, a conceptual overview. J Exp Med 2016;213:2527–38.
2. Rutsch F, MacDougall M, Lu C, Buers I, Mamaeva O, Nitschke Y, et al. A specific IFIH1 gain-of-function mutation causes Singleton-Merten syndrome. Am J Hum Genet 2015;96:275–82.
3. Bursztejn AC, Briggs TA, del Toro Duany Y, Anderson BH, O'Sullivan J, Williams SG, et al. Unusual cutaneous features associated with a heterozygous gain-of-function mutation in IFIH1: overlap between Aicardi–Goutières and Singleton–Merten syndromes. Br J Dermatol 2015;173:1505–13.
4. Rice GI, Forte GM, Szynkiewicz M, Chase DS, Aeby A, Abdel-Hamid MS, et al. Assessment of interferon-related biomarkers in Aicardi-Goutières syndrome associated with mutations in TREX1, RNASEH2A, RNASEH2B, RNASEH2C, SAMHD1, and ADAR: a case-control study. Lancet Neurol 2013;12:1159–69.
5. Li Y, Lee PY, Kellner ES, Paulus M, Switanek J, Xu Y, et al. Monocyte surface expression of Fcγ receptor RI (CD64), a biomarker reflecting type-I interferon levels in systemic lupus erythematosus. Arthritis Res Ther 2010;12:R90.
6. Rice GI, del Toro Duany Y, Jenkinson EM, Forte GM, Anderson BH, Ariaudo G, et al. Gain-of-function mutations in IFIH1 cause a spectrum of human disease phenotypes associated with upregulated type I interferon signaling. Nat Genet 2014;46:503–9.
7. Feigenbaum A, Muller C, Yale C, Kleinheinz J, Jezewski P, Kehl HG, et al. Singleton-Merten syndrome: an autosomal dominant disorder with variable expression. Am J Med Genet A 2013;161A:360–70.
8. Singleton EB, Merten DF. An unusual syndrome of widened medullary cavities of the metacarpals and phalanges, aortic calcification and abnormal dentition. Pediatr Radiol 1973;1:2–7.
9. Oda H, Nakagawa K, Abe J, Awaya T, Funabiki M, Hijikata A, et al. Aicardi–Goutières syndrome is caused by IFIH1 mutations. Am J Hum Genet 2014;95:121–5.
10. Crow YJ, Zaki MS, Abdel-Hamid MS, Abdel-Salam G, Boespflug-Tanguy O, Cordeiro NJ, et al. Mutations in ADAR1, IFIH1, and RNASEH2B presenting as spastic paraplegia. Neuropediatrics 2014;45:386–93.
11. Van Eyck L, de Somer L, Pombal D, Bornschein S, Frans G, Humblet-Baron S, et al. IFIH1 mutation causes systemic lupus erythematosus with selective IgA deficiency. Arthritis Rheumatol 2015;67:1592–7.
12. Pettersson M, Bergendal B, Norderyd J, Nilsson D, Anderlid BM, Nordgren A, et al. Further evidence for specific IFIH1 mutation as a cause of Singleton-Merten syndrome with phenotypic heterogeneity. Am J Med Genet A 2017;173:1396–9.
13. Buers I, Rice GI, Crow YJ, Rutsch F. MDA5-associated neuroinflammation and the Singleton-Merten syndrome: two faces of the same type I interferonopathy spectrum. J Interferon Cytokine Res 2017;37:214–9.
14. Rice GI, Melki I, Fremond ML, Briggs TA, Rodero MP, Kitabayashi N, et al. Assessment of type I interferon signaling in pediatric inflammatory disease. J Clin Immunol 2016:1–10.
15. Genetic Analysis of Psoriasis Consortium, the Wellcome Trust Case Control Consortium, Strange A, Capon F, Spencer CC, Knight J, et al. A genome-wide association study identifies new psoriasis susceptibility loci and an interaction between HLA-C and ERAP1. Nat Genet 2010;42:985–90.
16. Santiago MB. Miscellaneous non-inflammatory musculoskeletal conditions: Jaccoud's arthropathy. Best Pract Res Clin Rheumatol 2011;25:715–25.
17. Santiago MB. Jaccoud's arthropathy: proper classification criteria and treatment are still needed. Rheumatol Int 2013;33:2953–4.
18. Mensah KA, Mathian A, Ma L, Xing L, Ritchlin CT, Schwarz EM. Mediation of nonerosive arthritis in a mouse model of lupus by interferon-α–stimulated monocyte differentiation that is nonpermissive of osteoclastogenesis. Arthritis Rheum 2010;62:1127–37.
19. Alves EM, Macieira JC, Borba E, Chiuchetta FA, Santiago MB. Spontaneous tendon rupture in systemic lupus erythematosus: association with Jaccoud's arthropathy. Lupus 2010;19:247–54.
20. Crow YJ, Chase DS, Lowenstein Schmidt J, Szynkiewicz M, Forte GM, Gornall HL, et al. Characterization of human disease phenotypes associated with mutations in TREX1, RNASEH2A, RNASEH2B, RNASEH2C, SAMHD1, ADAR, and IFIH1. Am J Med Genet A 2015;167:296–312.
21. Dale RC, Gornall H, Singh-Grewal D, Alcausin M, Rice GI, Crow YJ. Familial Aicardi–Goutières syndrome due to SAMHD1 mutations is associated with chronic arthropathy and contractures. Am J Med Genet A 2010;152A:938–42.
22. Ramantani G, Kohlhase J, Hertzberg C, Innes AM, Engel K, Hunger S, et al. Expanding the phenotypic spectrum of lupus erythematosus in Aicardi-Goutières syndrome. Arthritis Rheum 2010;62:1469–77.
23. Xin B, Jones S, Puffenberger EG, Hinze C, Bright A, Tan H, et al. Homozygous mutation in SAMHD1 gene causes cerebral vasculopathy and early onset stroke. Proc Natl Acad Sci U S A 2011;108:5372–7.
24. Yarbrough K, Danko C, Krol A, Zonana J, Leitenberger S. The importance of chilblains as a diagnostic clue for mild Aicardi–Goutières syndrome. Am J Med Genet A 2016;170:3308–12.
25. Rice G, Newman WG, Dean J, Patrick T, Parmar R, Flintoff K, et al. Heterozygous mutations in TREX1 cause familial chilblain lupus and dominant Aicardi-Goutières syndrome. Am J Hum Genet 2007;80:811–5.
26. Sugiura K, Takeichi T, Kono M, Ito Y, Ogawa Y, Muro Y, et al. Severe chilblain lupus is associated with heterozygous missense mutations of catalytic amino acids or their adjacent mutations in the exonuclease domains of 3′-repair exonuclease 1. J Invest Dermatol 2012;132:2855–7.
27. Liu Y, Jesus AA, Marrero B, Yang D, Ramsey SE, Montealegre Sanchez GA, et al. Activated STING in a vascular and pulmonary syndrome. N Engl J Med 2014;371:507–18.
28. Jeremiah N, Neven B, Gentili M, Callebaut I, Maschalidi S, Stolzenberg MC, et al. Inherited STING-activating mutation underlies a familial inflammatory syndrome with lupus-like manifestations. J Clin Invest 2014;124:5516–20.
29. Jang MA, Kim EK, Now H, Nguyen NT, Kim WJ, Yoo JY, et al. Mutations in DDX58, which encodes RIG-I, cause atypical Singleton-Merten syndrome. Am J Hum Genet 2015;96:266–74.
30. Garg A. Lipodystrophies: genetic and acquired body fat disorders. J Clin Endocrinol Metab 2011;96:3313–25.
31. Fremond ML, Rodero MP, Jeremiah N, Belot A, Jeziorski E, Duffy D, et al. Efficacy of the Janus kinase 1/2 inhibitor ruxolitinib in the treatment of vasculopathy associated with TMEM173-activating mutations in 3 children. J Allergy Clin Immunol 2016;138:1752–5.

ARTHRITIS & RHEUMATOLOGY
Vol. 69, No. 10, October 2017, pp 2092–2096

LETTERS

DOI 10.1002/art.40214

Methodologic questions regarding study of the efficacy of chondroitin sulfate/glucosamine treatment of knee osteoarthritis: comment on the article by Roman-Blas et al

To the Editor:

I read with interest the article by Roman-Blas et al describing a randomized, double-blind, placebo-controlled clinical trial of combined treatment with chondroitin sulfate (CS) and glucosamine sulfate (GS) in patients with knee osteoarthritis (1). While the results presented are very intriguing, I would like to point out some critical flaws in the reported study methodology that render the findings inconclusive and doubtful.

First, intragroup variability was extremely low. The authors and reviewers should have observed this, considering that a common standard deviation of 30 was one of the study assumptions, whereas the reported result was ~2.4—much lower than that in any recently published similar clinical trials and 10 times lower than expected. This artificially low estimation of the standard deviation consequently makes it possible to mistakenly establish statistically significant differences. When assessing differences, both the magnitude of the effect and its precision matter; if the precision is very high (low variability) it is easy to establish as significant, small differences, which may not even be clinically relevant. The low variability estimated from the analysis using the mixed model for repeated measurements (MMRM) method to impute missing values should be the first sign that something did not function properly and that the statistical analysis was likely not correct.

Second, a high percentage of the initially enrolled study subjects dropped out before completion of the trial (~30% of those in the active treatment group), thereby making interpretation problematic. Missing data were ignored in this study, which could potentially bias the results. In fact, given that the study was discontinued prematurely, the proportion of missing data is unusually high, as many patients did not attend the final assessment visit.

Third, in the primary analysis for the primary efficacy end point the authors used MMRM, which assumes that data are missing at random and that findings among dropouts would be similar to those among other patients in the same treatment group, had they not dropped out. The absolute change from baseline was calculated for each visit without imputing any missing values before applying the MMRM. This seems to be the root of the problem. As seen in the reported study results, the standard deviation was extraordinarily low in comparison to that in other similar studies of CS plus GS (for example, the Glucosamine/Chondroitin Arthritis Intervention Trial [GAIT] [2] or the Multicentre Osteoarthritis Intervention Trial With SYSADOA [MOVES] [3]). This is most likely due to the application of MMRM without imputing missing values. Considering the premature ending of the study, it is fairly likely that most patients did not attend the final visit, which resulted in the use of MMRM with an extraordinarily high proportion of missing data. Obviously, this makes the estimation of the model effect have a much smaller artificial variability than it should have had with all available data. Therefore, it may produce false findings. Furthermore, considering the low mean estimated difference, with the correct variability, such as the one in GAIT or MOVES, it seems unlikely that the study would have been halted.

Fourth, results in the modified intent-to-treat (mITT) population were different from those in the per-protocol (PP) population. Although the data trended in the same direction, the primary end point was significant in the mITT population but not in the PP population. This is likely due to the large amount of missing data. If the interest is in the effectiveness of the assigned treatment in all randomized subjects, whether or not they complied with the protocol (i.e., the intent-to-treat estimate), then the primary analysis assumes that among patients who dropped out early, the observed early treatment effect was maintained after they discontinued treatment. This assumption is not scientifically plausible for this study because CS plus GS treats symptoms, and therefore any benefits of treatment will not be retained after the treatment stops. Additionally, it is not scientifically plausible that virtually all patients would experience improvement in all symptomatic parameters measured, as depicted in Table 2 of the article (1).

Finally, the calculation of sample size was based on a 10-mm decrease from baseline on a visual analog scale (VAS). However, several peer-reviewed reports indicate that this decrease is not a clinically relevant change. Tubach et al (4) defined a 19.9-mm change in VAS-reported pain (41%) from baseline to follow-up as a clinically important within-group change. Dworkin et al (5), on behalf of the Initiative on Methods, Measurement, and Pain Assessment in Clinical Trials group, recommended provisional benchmarks for interpreting the clinical importance of treatment outcomes in studies of patients with chronic pain: "moderately important" and "substantial" improvement were defined, respectively, as ≥30% and ≥50% reduction in pain intensity. Similarly, Farrar and colleagues (6) recommended a 30% improvement from baseline as the threshold for clinical importance in pain studies.

Overall, based on the above-mentioned considerations, I believe the study results described by Roman-Blas et al may be misleading. Therefore, I would suggest that the conclusions discussed in the article be interpreted with caution.

Maritza Quintero, MD, MSc, PhD
University of Los Andes
Mérida, Venezuela

1. Roman-Blas JA, Castañeda S, Sánchez-Pernaute O, Largo R, Herrero-Beaumont G, and the CS/GS Combined Therapy Study Group. Combined treatment with chondroitin sulfate and glucosamine sulfate shows no superiority over placebo for reduction of joint pain and functional impairment in patients with knee osteoarthritis: a six-month multicenter, randomized, double-blind, placebo-controlled clinical trial. Arthritis Rheumatol 2017;69:77–85.
2. Clegg DO, Reda DJ, Harris CL, Klein MA, O'Dell JR, Hooper MM, et al. Glucosamine, chondroitin sulfate, and the two in combination for painful knee osteoarthritis. N Engl J Med 2006;354:795–808.

3. Hochberg MC, Martel-Pelletier J, Monfort J, Möller I, Castillo JR, Arden N, et al. Combined chondroitin sulfate and glucosamine for painful knee osteoarthritis: a multicentre, randomised, double-blind, non-inferiority trial versus celecoxib. Ann Rheum Dis 2016;75:37–44.
4. Tubach F, Ravaud P, Baron G, Falissard B, Logeart I, Bellamy N, et al. Evaluation of clinically relevant changes in patient reported outcomes in knee and hip osteoarthritis: the minimal clinically important improvement. Ann Rheum Dis 2005;64:29–33.
5. Dworkin RH, Turk DC, McDermott MP, Peirce-Sandner S, Burke LB, Cowan P, et al. Interpreting the clinical importance of group differences in chronic pain clinical trials: IMMPACT recommendations. Pain 2009;146:238–44.
6. Farrar JT, Young JP Jr, LaMoreaux L, Werth JL, Poole RM. Clinical importance of changes in chronic pain intensity measured on an 11-point numerical pain rating scale. Pain 2001;94:149–58.

DOI 10.1002/art.40212

Reply

To the Editor:

We thank Dr. Quintero for her interest in this intricate field of statistics applied to osteoarthritis (OA) clinical trials, and in particular in our recent publication. Precisely due to the difficulties in protocol design that are usually encountered in studies of this disease, we also would like to stress once more the necessity of independent analysis and critique.

First, we apologize for a typographical error in our manuscript, which appears to have prompted Dr. Quintero's reply. Specifically, data on the primary end point, reduction in the VAS global pain score at 6 months (mentioned in the abstract, Results section, Figure 2, and Table 2 of our article), should be shown as the mean ± SEM rather than the mean ± SD (1). This being stated, in our study a sensitivity analysis was carried out in order to select the best method for imputation of missing values in the primary efficacy analysis. Of them, a multiple assignment based on an MMRM method was the one used, as it can be regarded as the most conservative for the analysis. The other methods that were considered but not used were last observation carried forward and baseline observation carried forward.

As Dr. Quintero rightly points out, it is critical to address the threshold for clinical relevance of improvement in knee OA pain in clinical trials. This issue was underscored by a European panel of experts and regulators on OA clinical trials (Reginster et al [2]) in a 2015 update of the European Medicines Agency 2010 guideline on clinical investigation of medicinal products used in the treatment of OA. However, a clear cutoff value has not been provided so far, and remains a matter of controversy, particularly with regard to trials of symptomatic slow-acting drugs in OA (SySADOAs). Dr. Quintero suggests that a 20-mm improvement on a VAS would be needed for clinical relevance. This is in sharp contrast to the consensus reported by Reginster and colleagues (2), who concluded that a difference between placebo and active treatment groups of ≥5 mm on a 100-mm VAS could be taken as a clinically relevant cutoff for SySADOAs. This threshold was proposed because most published clinical trials of SySADOAs show pain improvement in the 5–6-mm range (2). In our study, we calculated sample size taking 10 mm as clinically relevant improvement, i.e., a bit higher than that usually established. Accordingly, our sample size allowed for detection of differences in the VAS global pain score between mean values in the placebo and active treatment groups of ≥10 mm at the end of the study. It is important to note that this end point measure, and not a 10-mm decrease from baseline in the VAS, as mistakenly stated by Dr. Quintero, was used for sample size calculation.

In the same way, a dropout rate of 20% was taken for calculation of the sample size. It is true that the final dropout count was slightly greater than predicted, and this issue was discussed with the statisticians, who found it of little relevance for the analysis. All patients attended an "early termination visit."

We disagree with Dr. Quintero in that missing data were not ignored as explained above, nor was the study halted prematurely. Conversely, a data and safety monitoring board was instituted to ensure the ongoing safety of participants and the accurate, bias-free gathering of data. Since this was a placebo-controlled study, the protocol established beforehand that an interim analysis would be performed when 50% of the estimated sample had reached the point of 6-month follow-up. If conclusive results were obtained at that time the trial would be stopped and the code broken, thereby avoiding further placebo treatment in more patients. This was actually the case, and the result quite unexpectedly showed that the effect on the primary end point was greater in the placebo group than in the active treatment group.

Dr. Quintero's concern that the primary end point was significant for the mITT population but not for PP completers is unjustified. Rather, the statistical significance of the primary end point was similar with both approaches. Often, the mITT population is chosen for analysis because this tends to avoid overoptimistic estimates of efficacy drawn by PP analysis. It is thought that including noncompleters in the full analysis set diminishes the overestimation of improvement. It is not uncommon that mITT and PP analyses yield different results, but, as Dr. Quintero notes, this was not the case in our study. The lower improvement in pain severity observed with active treatment as compared to placebo could derive from a larger number of patients with abdominal discomfort in the CS plus GS treatment group, potentially accounting for the skewing of results toward higher self-reported pain improvement in the placebo group.

The experts who carried out the statistical analysis were from Pivotal (Madrid, Spain), a leading full-service contract research organization with substantial experience in the design of clinical trials, most of which have been published in highly respected journals. To date, none of these trials have received any negative criticism, although it should also be taken into account, that unlike our study, all showed positive results (3).

In summary, we understand that our study is complex and it can take time to understand its methodology. We were, in fact, the first to be intrigued by the results of this clinical trial, since our previous experimental studies had shown that high doses of intraperitoneal CS improved chronic arthritis and prevented atherosclerosis in rabbits (4,5). Similarly, GS has been shown to exert similar effects in in vitro and animal models, as well as exhibiting a modest analgesic effect in human OA (6). We therefore expected that the combination of these 2 agents would be efficacious. We conclude that, even considering the important hurdles that are encountered in placebo-controlled clinical trials in OA, our study shows a consistent lack of superiority of CS plus GS over placebo for reduction of joint pain and functional impairment. This type of negative result needs to be reported in a neutral, unbiased manner.

Jorge A. Roman-Blas, MD
Olga Sánchez-Pernaute, MD, PhD
Raquel Largo, PhD
Gabriel Herrero-Beaumont, MD, PhD
Fundación Jiménez Díaz
Madrid, Spain

1. Erratum. Arthritis Rheumatol 2017;69:2080.
2. Reginster JY, Reiter-Niesert S, Bruyère O, Berenbaum F, Brandi ML, Branco J, et al. Recommendations for an update of the 2010 European regulatory guideline on clinical investigation of medicinal products used in the treatment of osteoarthritis and reflections about related clinically relevant outcomes: expert consensus statement. Osteoarthritis Cartilage 2015;23:2086–93.
3. Navarro-Sarabia F, Coronel P, Collantes E, Navarro FJ, Rodriguez de la Serna A, Naranjo A, et al. A 40-month multicentre, randomised placebo-controlled study to assess the efficacy and carry-over effect of repeated intra-articular injections of hyaluronic acid in knee osteoarthritis: the AMELIA project. Ann Rheum Dis 2011;70:1957–62.
4. Herrero-Beaumont G, Marcos ME, Sánchez-Pernaute O, Granados R, Ortega L, Montell E, et al. Effect of chondroitin sulphate in a rabbit model of atherosclerosis aggravated by chronic arthritis. Br J Pharmacol 2008;154:843–51.
5. Largo R, Roman-Blas J, Moreno-Rubio J, Sánchez-Pernaute O, Martínez-Calatrava MJ, Castañeda S, et al. Chondroitin sulfate improves synovitis in rabbits with chronic antigen-induced arthritis. Osteoarthritis Cartilage 2010;18 Suppl 1:S17–23.
6. Largo R, Martínez-Calatrava MJ, Sánchez-Pernaute O, Marcos ME, Moreno-Rubio J, Aparicio C, et al. Effect of a high dose of glucosamine on systemic and tissue inflammation in an experimental model of atherosclerosis aggravated by chronic arthritis. Am J Physiol Heart Circ Physiol 2009;297:H268–76.

DOI 10.1002/art.40209

Rituximab for antineutrophil cytoplasmic antibody–associated vasculitis—not everything in the garden is rosy: comment on the article by Cortazar et al

To the Editor:

Rituximab is a well-studied biologic agent that is used to treat antineutrophil cytoplasmic antibody (ANCA)–associated vasculitis (AAV). However, new data continue to emerge. In a large cohort of patients with AAV, Cortazar et al showed that remission induction treatment with rituximab resulted in a preferential decline in ANCA titers relative to total IgG levels (47–48% per month versus 6% per month, respectively) (1). Furthermore, IgG levels remained essentially stable during prolonged maintenance therapy. Serious infections were associated with hypogammaglobulinemia (<4 gm/liter), but the latter was a rare finding (4.6%). During maintenance therapy with relatively high rituximab exposure (1,000-mg dose every 4 months for 2 years, followed by 1,000 mg every 6 months), only 5 patients (2.1%) required treatment with intravenous immunoglobulin (IVIG) for recurrent infections. A preferential decline in rheumatoid factor and antibodies to cyclic citrullinated peptide compared to total immunoglobulin levels has also been shown in patients with rheumatoid arthritis (2).

However, we should not assume that everything in the garden is rosy. Cortazar and colleagues cite another retrospective study that evaluated rituximab administered for a median of 42 months in 243 patients with autoimmune diseases (AAV was the most common diagnosis) (3). Moderate or severe hypogammaglobulinemia (IgG <5 gm/liter) occurred in 26% of the patients. It was transient and improved spontaneously in approximately half of the cases. Nevertheless, IVIG replacement was initiated in 12 patients (4.9%) because of recurrent infections. Later-onset hypogammaglobulinemia after rituximab treatment was more likely to be sustained and could persist for years, e.g., only 2 of 12 patients showed IgG recovery and were able to discontinue replacement therapy (after 48 months and 90 months, respectively). Ten patients were still receiving immunoglobulin at last follow-up (IVIG or switched to subcutaneous immunoglobulin). These data suggest that permanent IVIG treatment may be required in a proportion of patients with sustained hypogammaglobulinemia.

Administration of rituximab in lower doses may improve its safety profile. Currently, there is a lack of data on the comparative efficacy of different regimens of rituximab for maintenance therapy in patients with AAV (e.g., 1,000 mg versus 500 mg every 6 months). However, in the Comparison Study of Two Rituximab Regimens in the Remission of ANCA Associated Vasculitis, more patients with AAV had sustained remission at month 28 with rituximab (500 mg on days 0 and 14 and at months 6, 12, and 18) than with azathioprine (4). Major relapses occurred only in 3 patients in the rituximab group (5%). The authors did not report any cases of severe hypogammaglobulinemia, and no significant between-group differences or decreases in total immunoglobulin, IgG, or IgM levels were observed throughout the trial. However, the number of patients in the rituximab arm was relatively small ($n = 57$), and we therefore cannot conclude that hypogammaglobulinemia can be avoided with administration of rituximab in low doses. The total dose of rituximab did not influence the nadir serum IgG concentration in that study (4). Furthermore, there was only a weak effect of previous cyclophosphamide treatment on the nadir IgG level, in contrast to previous reports of stronger associations.

We prescribed rituximab as maintenance therapy in 111 patients with AAV. Eighty-two of them were treated with 1,000 mg every 6 months for 164 patient-years, while 29 patients received a lower dose (500 mg every 6 months for 33 patient-years). The incidence of hypogammaglobulinemia (<5 gm/liter) was similar in the 2 groups of patients (6.1 per 100 patient-years and 5.9 per 100 patient-years, respectively). The incidence of infections was also comparable. Four patients developed severe sustained hypogammaglobulinemia (<3 gm/liter) that persisted for at least 2 years after the last dose of rituximab. Notably, one-third of patients were treated with rituximab in combination with standard immunosuppressive agents (azathioprine, methotrexate, or mycophenolate mofetil).

It appears that rituximab in any dose, and even 1 infusion, can induce hypogammaglobulinemia. In our opinion, an additive effect of cumulative cyclophosphamide dose cannot be completely ruled out. Corticosteroids may also contribute to the increased risk of hypogammaglobulinemia after rituximab administration. Marco et al showed a weak but statistically significant negative correlation ($r = -0.17$, $P = 0.02$) between total oral prednisolone exposure after initial rituximab treatment and IgG levels in patients with various autoimmune diseases (5). Hypogammaglobulinemia developed in 49% of

patients (28 of 57) who received at least 1 dose of intravenous methylprednisolone following rituximab, compared to 28% (34 of 120) of those who did not ($P = 0.011$). There was a positive correlation between cumulative oral prednisolone exposure and the occurrence of infection. However, no correlation between the risk of infection and cumulative rituximab exposure or prior cumulative cyclophosphamide exposure was observed.

In summary, the results of the study by Cortazar et al are encouraging and support the positive risk/benefit ratio of rituximab in patients with AAV. The use of rituximab in lower doses or as-needed administration may further improve the favorable safety profile of biologic therapy. However, in real-life clinical practice, hypogammaglobulinemia is not so uncommon, can be associated with recurrent infections, and can require prolonged or even permanent IVIG treatment. On the other hand, hypogammaglobulinemia after rituximab treatment, even when severe, is frequently transient and self-limited and does not always necessitate cessation of treatment. Immunoglobulin levels should be regularly monitored during rituximab therapy. The indications for IVIG replacement in patients with rituximab-induced hypogammaglobulinemia should be defined more clearly by experts.

Pavel Novikov, MD
Leonid Strizhakov, MD
Sergey Moiseev, MD
Sechenov First Moscow State Medical University
Moscow, Russia

1. Cortazar FB, Pendergraft WF III, Wenger J, Owens CT, Laliberte K, Niles JL. Effect of continuous B cell depletion with rituximab on pathogenic autoantibodies and total IgG levels in antineutrophil cytoplasmic antibody–associated vasculitis. Arthritis Rheumatol 2017;69:1045–53.
2. Cambridge G, Leandro MJ, Edwards JC, Ehrenstein MR, Salden M, Bodman-Smith M, et al. Serologic changes following B lymphocyte depletion therapy for rheumatoid arthritis. Arthritis Rheum 2003;48:2146–54.
3. Roberts DM, Jones RB, Smith RM, Alberici F, Kumaratne DS, Burns S, et al. Rituximab-associated hypogammaglobulinemia: incidence, predictors and outcomes in patients with multi-system autoimmune disease. J Autoimmun 2015;57:60–5.
4. Guillevin L, Pagnoux C, Karras A, Khouatra C, Aumaître O, Cohen P, et al. Rituximab versus azathioprine for maintenance in ANCA-associated vasculitis. N Engl J Med 2014;371:1771–80.
5. Marco H, Smith RM, Jones RB, Guerry MJ, Catapano F, Burns S, et al. The effect of rituximab therapy on immunoglobulin levels in patients with multisystem autoimmune disease. BMC Musculoskelet Disord 2014;15:178.

DOI 10.1002/art.40210

Reply

To the Editor:

Dr. Novikov and colleagues stress that the complications of hypogammaglobulinemia must be carefully considered in patients treated with rituximab. We agree. Our analysis, however, assists in identifying the subgroup of patients in whom closer monitoring is warranted due to their increased risk. The largest decline in IgG levels occurs following the first dose of rituximab, as short-lived antibody-producing cells that require repletion from the B cell pool are eliminated. Other medications used for remission induction (i.e., prednisone and cyclophosphamide) also contribute to this effect. In our cohort, the mean within-person decrease in IgG level from the beginning of induction therapy to the beginning of maintenance therapy was 226 mg/dl (95% confidence interval [95% CI] 155, 298). Thereafter, the IgG level changed little despite ongoing rituximab-induced continuous B cell depletion, with a mean decrease of 0.6% per year (95% CI −0.2, 1.4). Of the 161 patients in the top 3 baseline IgG quartiles (IgG ≥560 mg/dl) upon entry into the maintenance cohort, none developed significant hypogammaglobulinemia (IgG ≤400 mg/dl) despite some patients having received rituximab every 4–6 months for 7 years. Thus, the baseline IgG level at the commencement of maintenance rituximab therapy can be used to identify patients who are at very low risk of significant hypogammaglobulinemia and those who should be closely monitored or treated with a different agent.

Novikov et al cite a retrospective study by Roberts et al (1) to suggest an increased rate of moderate-to-severe hypogammaglobulinemia (26%) with rituximab treatment. This proportion, however, includes patients who had moderate-to-severe hypogammaglobulinemia prior to initiation of rituximab treatment (7%) and also was derived using a different definition of hypogammaglobulinemia than in our study (500 mg/dl versus 400 mg/dl). The rate of new-onset severe hypogammaglobulinemia (IgG <300 mg/dl) reported by Roberts and colleagues was 3%. In addition, Novikov et al highlight the higher proportion of patients requiring IVIG (4.9%) in that study (1) compared with our cohort (2.1%). This is an unreliable metric for comparison given that in the absence of clear evidence, the threshold for treatment with IVIG is based on clinician judgment and there is likely to be significant variation between centers. We agree that further investigation is needed to define evidence-based indications for the use of IVIG in this population.

The rituximab dosing regimen that optimally balances maintenance of remission with development of hypogammaglobulinemia and other treatment-related complications remains unknown. It is unlikely that administering rituximab every 6 months at a lower dose (e.g., 500 mg) will circumvent the issue of hypogammaglobulinemia given that the cumulative dose of rituximab did not influence the rate of hypogammaglobulinemia in our analysis and in others (1,2). It is possible that increasing the dosing interval, thereby allowing periods of B cell reconstitution, will mitigate the complications of long-term rituximab therapy. To address this issue, we designed the Maintenance of ANCA Vasculitis Remission by Intermittent Rituximab Dosing Trial (NCT02749292), whereby patients in whom remission has been maintained for at least 2 years with fixed-interval rituximab (i.e., every 4–6 months) stop scheduled treatment and are randomized to 2 different dosing strategies: 1) re-dosing based on B cell reconstitution, and 2) re-dosing based on a specified rise in ANCA titer. We hope this study and others will bring us closer to the optimal strategy to prevent relapse while minimizing treatment-related adverse events.

Frank B. Cortazar, MD
John L. Niles, MD
Massachusetts General Hospital
Boston, MA

1. Roberts DM, Jones RB, Smith RM, Alberici F, Kumaratne DS, Burns S, et al. Rituximab-associated hypogammaglobulinemia: incidence, predictors and outcomes in patients with multi-system autoimmune disease. J Autoimmun 2015;57:60–5.

2. Van Vollenhoven RF, Emery P, Bingham CO III, Keystone EC, Fleischmann R, Furst DE, et al. Longterm safety of patients receiving rituximab in rheumatoid arthritis clinical trials. J Rheumatol 2010;37:558–67.

DOI: 10.1002/art.40153

Clinical Images: Livedoid vasculopathy

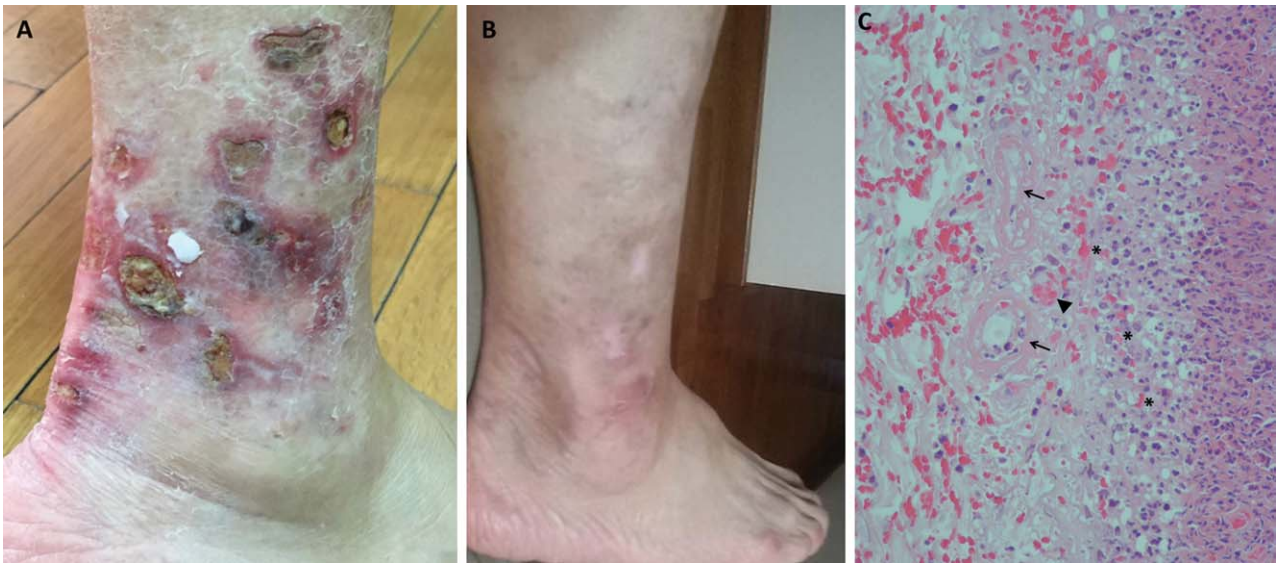

The patient was a 55-year-old woman who, during the past year, had developed tender, coalescent, purpuric papules on her lower legs, which evolved into deep and painful ulcers. She began an immunosuppressive treatment regimen as is used for vasculitis, but without benefit. At presentation, multiple well-demarcated ulcers on a livedoid base, surrounded by atrophic white-ivory skin and areas of hyperpigmentation, were evident (**A**). Doppler ultrasound of the legs revealed no venous insufficiency, thrombi, or peripheral arterial disease. Serum protein electrophoresis and cryoglobulin, autoantibody, complement, and acute-phase reactant measurements all yielded normal results. Skin biopsy (**C**) (hematoxylin and eosin stained; original magnification × 400) revealed fibrinoid material and mid-dermis segmental thickening of the vessel wall (**arrows**), as well as vessel occlusion with hyaline microthrombi (**arrowhead**) and extravasated erythrocytes without features of inflammation (**asterisks**). These findings are compatible with livedoid vasculopathy (LV). LV is seen mostly in middle-aged women and was originally described as a form of vasculitis. However, decreased fibrinolytic activity and defective release of tissue plasminogen activator leading to noninflammatory thrombosis of dermal vessels are now considered to be the pathogenetic factors (1). LV can be idiopathic or secondary. It may include features of vasculitides and numerous other conditions that should be considered in the differential diagnosis. Skin biopsy is diagnostic and should be performed to avoid unnecessary immunosuppressive treatment. The characteristic fibrin occlusion and thrombus formation involve the upper- and mid-dermal capillaries. In contrast to vasculitis, perivascular neutrophil infiltrates and leukocytoclasia are absent. Our patient was prescribed antiplatelet agents, with complete resolution of the ulcerations in the form of white atrophic scars after 6 months (**B**). This provided additional evidence that LV was the correct diagnosis.

1. Alavi A, Hafner J, Dutz JP, Mayer D, Sibbald RG, Criado PR, et al. Livedoid vasculopathy: an in-depth analysis using a modified Delphi approach. J Am Acad Dermatol 2013;69:1033–42.

Evangelia Zampeli, MD
Institute of Autoimmune Systemic and Neurological Diseases
Haralampos M. Moutsopoulos, MD, FACP, FRCP (hc), Master ACR
Institute of Autoimmune Systemic and Neurological Diseases, Academy of Athens and National and Kapodistrian University of Athens
Athens, Greece